



New Methods for the Construction of Selectively Difluorinated Carbocycles

Adam William McCarter

Submitted in partial fulfilment of the requirements of the degree of
Doctor of Philosophy

April 2018

Academic Supervisor: **Dr. Craig Jamieson** (Pure and Applied Chemistry)

Industrial Supervisor: **Dr. David J. Hirst** (GlaxoSmithKline)

Internal Examiner: **Prof. Nick C. O. Tomkinson** (Pure and Applied
Chemistry)



THE CARNEGIE TRUST
FOR THE UNIVERSITIES OF SCOTLAND

Declaration

‘This thesis is the result of the author’s original research. It has been composed by the author and has not been previously submitted for examination which has led to the award of a degree’

‘The copyright of this thesis belongs to the author under the terms of the United Kingdom Copyright Acts as qualified by the University of Strathclyde Regulation 3.50. Due acknowledgement must always be made of the use of any material contained in, or derived from, this thesis.’

Signed: 

Print: ADAM MCCARTER

Date: April 2018

*'Education is an admirable thing,
but it is well to remember from time to time
that nothing that is worth knowing
can be taught.'*

Oscar Wilde

Acknowledgements

I would like to thank Prof. Jonathan Percy for providing me with the opportunity to undertake this research project and for his continual support and guidance up until his retirement. I would also like to thank Dr. Craig Jamieson for taking over supervision of the project and for providing further guidance and assistance. Dr. David Nelson is also thanked for allowing me to continue working in his laboratory as well as for useful discussions.

Dr. David Hirst (GlaxoSmithKline, Stevenage) is thanked for his continual interest in the project and advice throughout. His organisation and planning of my industrial CASE Placement was very much appreciated as well as his supervision throughout the 3 months at Stevenage.

I would also like to thank members of the Percy group, past and present, for helpful discussions throughout the years. I would also like to thank the Jamieson research group for warmly accepting me and for providing many useful ideas and new perspectives throughout my final year.

Special thanks go to Magdalena Sommer for working on the gold chemistry. The work she conducted was invaluable towards the success of the project.

The academic and technical staff at the University of Strathclyde has supported much of the work. Dr Alan Kennedy is thanked for providing invaluable X-ray crystallographic analysis. Craig Irving has been immensely helpful with providing assistance in running NMR experiments and is thanked. Pat Keating is thanked for her assistance with mass spectrometry. Gavin Bain is thanked for all his assistance with maintaining and designing technical equipment and performing KF titrations. All three are thanked for providing some light relief in the way of 'informal' discussions. Alex Clunie is thanked for CHN microanalysis and the EPSRC NMSCC team in Swansea for accurate mass and MS analysis.

The Carnegie Trust for the Universities of Scotland and GlaxoSmithKline (specifically Dr. Vipulkumar Patel) are thanked for their financial support.

Finally, my deepest thanks go to my parents, brother Paul and sister Katherine, their continued love and support throughout my undergraduate and postgraduate studies will never be forgotten and I would certainly not be in the place I am today without them.

Abstract

The design and synthesis of geminal difluoromethylated compounds is extremely important owing to their unique biological properties, such as enzyme inhibition, pKa modulation and improving metabolic stability. However, efficient methods, starting from sustainable low cost starting materials, for the introduction of the *gem*-difluoromethylene group into cyclic molecules are still scarce. Work towards developing the *de novo* synthesis of difluorinated sugar analogues by using trifluoroethanol as an inexpensive building block is presented.

The Saegusa-Ito cyclisation was utilised for the construction of selectively fluorinated carbocycles. Difluorinated silyl enol ether precursors were prepared in two synthetic steps from commercially available trifluoroethanol. Protection with diethylcarbamoyl chloride was followed by dehydrofluorination/lithiation, under cryogenic conditions, and the metalated enol carbamate generated *in situ* trapped with either a ketone or aldehyde electrophile. Following transacylation, the enolate species could be trapped with chlorotriethylsilane to afford silyl enol ethers in good yield. Cyclisations ensued smoothly under mild conditions. A combination of copper(I) chloride and Pd(OAc)₂ in acetonitrile at 70 °C proved the most effective catalytic system. α,α -Difluoroketones were often isolated as mixtures of ketone and the corresponding hydrate; however, these mixtures could be efficiently dried in a vacuum oven to deliver pure ketones.

The cyclisation of difluorinated enol acetals as alternative cyclisation mediators was investigated. These precursors were also synthesised in two steps from trifluoroethanol using cryogenic lithium based chemistry. Using a catalytic 1:1 mixture of 1,3-bis(2,6-diisopropylphenyl-imidazol-2-ylidene)gold(I) chloride and silver hexafluoroantimonate(V), the intramolecular carbocyclisation of difluorinated enol acetals has been achieved. Difluorinated enol acetals bearing a pendant alkene group can be cyclised and reduced *in situ* using tetrabutylammonium borohydride in one pot to form fluorinated diol motifs. Alternatively, the cyclisation of terminal alkynes allows for the concise synthesis of fluorinated pyran scaffolds. Both cyclisation processes can be performed under mild conditions allowing for the construction of complex difluorinated cyclic systems.

Contents

1. Abbreviations.....	1
2. Chapter 1: Introduction.....	5
2.1 Carbohydrate- structure	5
2.2 Carbohydrates – Function	6
2.3 Carbohydrates as drug targets and glycomimetics	7
2.4 Carbohydrate Mimics – Carbasugars and Fluorocarbasugars	9
2.5 Biological properties of fluorine.....	14
2.6 Synthesis of fluorocarbasugars.....	26
2.6.1 Synthesis of fluorocarbasugars from carbohydrate precursors	26
2.6.2 Synthesis of fluorocarbasugars starting from fluorinated building blocks.....	35
Aims	44
3. Chapter 2: Saegusa-Ito Cyclisation of Difluorinated Silyl Enol Ethers	46
3.1 Saegusa-Ito Cycloalkenylation	46
3.1.1 Discovery and Application.....	46
3.1.2 Mechanism of action	48
3.2 Palladium(II) Oxidation Chemistry.....	51
3.2.1 Background	51
3.2.2 Reoxidation of Pd(0).....	52
3.2.3 Intramolecular oxidative carbocyclisations involving alkene-alkene coupling	57
3.3 Initial Objectives.....	62
3.4 Results and Discussion	63
3.4.1 Cyclisation Precursor Preparation	63
3.4.2 Work up and isolation modifications	71
3.4.3 Substrate scope	78
3.4.3.1 The Thorpe-Ingold Effect	80
3.4.3.2 Attempts to synthesise 113b	81
3.4.3.3 Attempts to synthesise 113i	91

3.4.4	<i>Copper/Palladium Screening Experiments</i>	93
3.5	Conclusions	105
4.	Chapter 3: Difluorinated Enol Acetals in Difluorinated Carbocycle Synthesis	108
4.1	Introduction	108
4.1.1	<i>Difluorinated Enol Acetals</i>	108
4.1.2	<i>Palladium(II) catalysis</i>	113
4.1.3	<i>Gold(I) catalysis</i>	114
4.1.4	<i>Carbocyclisations of enol species onto gold(I) activated alkenes</i>	116
4.2	Results and Discussion	118
4.2.1	<i>Palladium Catalysis</i>	118
4.2.2	<i>Gold Cyclisation Studies</i>	126
4.2.3	<i>Developing a one-pot process</i>	137
4.2.4	<i>Substrate Scope – Allylic Alcohols</i>	143
4.2.5	<i>Substrate Scope – Difluorinated Diols</i>	146
4.2.6	<i>Difluorinated Pyran Synthesis and Optimisation.</i>	160
4.2.7	<i>Difluorinated Pyran Substrate Scope</i>	163
4.2.8	<i>Allylic Amination</i>	167
4.3	Conclusions.....	169
4.4.	<i>Overall Conclusions and Future Work</i>	173
4.4.1	<i>Conclusions</i>	173
4.4.2	<i>Future Work</i>	176
6.	Chapter 4: Experimental	180
6.1	General Experimental	180
6.2	Compounds from Chapter 1.....	182
6.2.1	Preparation of electrophiles	182
6.2.2	General Procedure A – Silyl Enol Ether Preparation.....	189
6.2.3	General procedure B: Preparation of α,α -difluoroketones.....	199
6.2.4	Synthesis of reverse Wacker oxidation product.....	211

6.2.5 Synthesis of 1-chloro-1,1-difluoro-2-oxo-3-(<i>N,N</i> -diethylcarbamoyloxy)-hepta-1,6-diene (157).....	212
6.2.6 Synthesis of rearrangements products.....	213
6.2.7 Synthesis of 1-Chloro-1,1-difluoro 3-(<i>N,N</i> -diethylcarbamoyloxy)-3-methylhepta-1,6-dien-2-one (164)	214
6.3 Compounds from Chapter 2.....	215
6.3.1 General Procedure C – Allylic Alcohol Preparation.....	215
6.3.2 Synthesis of difluoromethylketone 147b	217
6.3.3 Synthesis of monofluorinated enone 193.....	218
6.3.4 Synthesis of Wacker oxidation product 195aa and 195ab	219
6.3.5 Synthesis of α -hydroxy ketone 200aa and hydrate 202	221
6.3.6 Synthesis of tricyclic acetal 203.....	223
6.3.7 General Procedure D – Difluorinated Diol Preparation.....	225
6.3.8 Preparation of electrophiles	228
6.3.9 Preparation of allylic alcohols to investigate scope of cyclisation/reduction	231
6.3.10 Scope of cyclisation/reduction methodology	241
6.3.11 Synthesis of non-fluorinated pyran 209	259
6.3.11 Preparation of allylic alcohols to investigate scope of alkyne cyclisation..	261
6.3.12 General Procedure E – Propargyl Ether Preparation	267
6.3.13 General Procedure F – Difluorinated Pyran Preparation	273
6.3.14 Synthesis of morpholine derivative 228.....	281
7. References	283

1. Abbreviations

AD	Asymmetric Dihydroxylation
API	Active Pharmaceutical Ingredient
Arg	Arginine
Asn	Asparagine
Asp	Aspartic Acid
bpy	2,2'-Bipyridine
CA-II	Carbonic Anhydrase II
CAN	Ceric Ammonium Nitrate
CDFMK	Chlorodifluoromethyl Ketone
CETP	Cholesteryl Ester Transfer Protein
CSA	Chemical Shift Anisotropy
DAST	Diethylaminosulfur Trifluoride
DCE	Dichloroethane
DCM	Dichloromethane
DEC	<i>N,N</i> -Diethylcarbamoyloxy
DEIPS	Diethyl <i>isopropyl</i> silyl
DCD	Dewar-Chatt-Duncanson
DFMK	Difluoromethyl Ketone
DFT	Density Functional Theory
DMAP	4-Dimethylaminopyridine
DMDO	Dimethyl dioxirane
DMF	Dimethylformamide

DMSO	Dimethyl Sulfoxide
DNP	Dinitrophenyl
ETM	Electron Transfer Mediator
FMO	Frontier Molecular Orbital
GC-MS	Gas Chromatography – Mass Spectrometry
Gln	Glutamine
Gly	Glycine
GOase	Galactose Oxidase
GT	Glycosyltransferase
HA	Haemagglutinin
HIV	Human Immunodeficiency Virus
HMPT	Hexamethylphosphorous Triamide
HMBC	Heteronuclear Multiple Bond Correlation
HOESY	Heteronuclear Nuclear Overhauser Effect Spectroscopy
HSQC	Heteronuclear Single Quantum Coherence Spectroscopy
IgM	Immunoglobulin M
IMes	1,3- <i>bis</i> -(2,4,6-trimethylphenyl)imidazol-2-ylidene
IPr	1,3- <i>bis</i> -(2,6-diisopropylphenyl)imidazol-2-ylidene
KIE	Kinetic Isotope Effect
KSP	Kinesin Spindle Protein
LDA	Lithium Diisopropylamide
LUMO	Lowest Unoccupied Molecular Orbital
mCPBA	<i>meta</i> -Chloroperoxybenzoic acid
MEM	Methoxyethoxymethyl Ether

MOM	Methoxymethyl Acetal
NDP	Nucleoside-Diphosphate
NGP	Neighbouring Group Participation
NHC	<i>N</i> -Heterocyclic Carbene
NMI	<i>N</i> -Methylimidazole
NMR	Nuclear Magnetic Resonance
NOE	Nuclear Overhauser Effect
NOESY	Nuclear Overhauser Effect Spectroscopy
PCC	Pyridinium Chlorochromate
PTSA	<i>p</i> -Sulphonic Acid Monohydrate
RCM	Ring Closing Metathesis
SEE	Silyl Enol Ether
SPM32	3-Mercaptopropyl Ethyl Sulfide Silica
STA3	Triamine Ethyl Sulfide Amide Silica
TBDMS	tert-Butyldimethylsilyl
TBDPSCI	tert-Butyl(chloro)diphenylsilane
TEMPO	(2,2,6,6-Tetramethyl-piperidin-1-yl)oxyl
TES	Triethylsilyl
TES-Cl	Chlorotriethylsilane
TFA	Trifluoroacetic Acid
TFDO	(trifluoromethyl)dioxirane
THF	Tetrahydrofuran
TIBAL	Triisobutylaluminium
TIPS	Triisopropylsilyl

TLC	Thin Layer Chromatography
TMEDA	Tetramethylethylenediamine
TMS	Trimethylsilyl
TMS-Cl	Chlorotrimethylsilane
Trp	Tryptophan
VT	Variable Temperature
XRD	X-Ray Diffraction

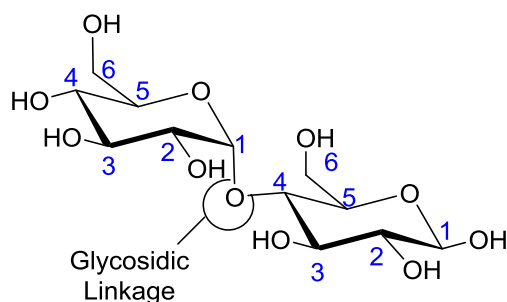


Figure 1 – Glycosidic linkage between two glucose molecules to form the disaccharide β -maltose.

The terminal sugar unit has the potential to form further glycosidic bonds and can therefore generate carbohydrates (polysaccharides) more complex than the simple monosaccharide and disaccharide shown above in **Scheme 1** and **Figure 1**, respectively. **Figure 2** displays an example of the glucose polymer amylose, one of the major components of starch.

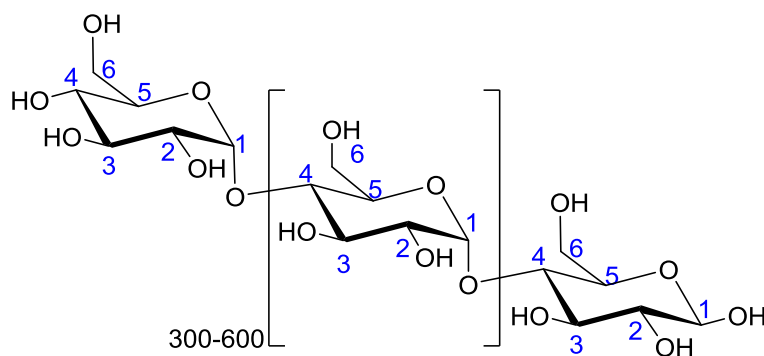


Figure 2 – Structure of polysaccharide amylose.

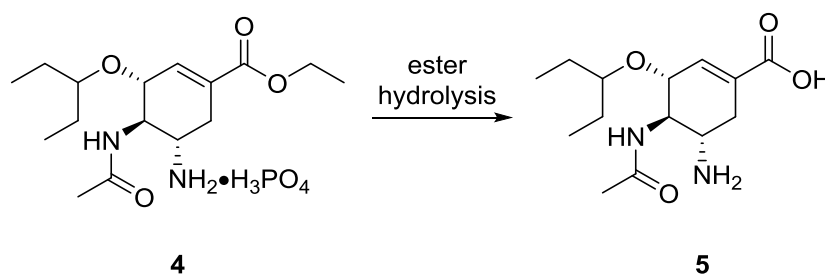
2.2 Carbohydrates – Function

The introduction of glycans (oligosaccharides) onto proteins is carried out by the post translational modification reaction known as glycosylation. The idea that carbohydrates were purely energy sources changed when Goldstein *et al.* highlighted the ability of carbohydrate residues on the surface of glycoproteins phytohemagglutinin and monoclonal IgM to interact with the protein Concanavalin A.⁵ Following this discovery, the importance of cell surface glycans in biological systems has been demonstrated by the role they play in crucial physiological processes such as cell-cell recognition, cell signalling, host-pathogen interactions, host immune responses and plasma membrane stability.¹ Their involvement in these processes may be explained by the fact that the surface carbohydrates come together to form a layer known as the glycocalyx which extends much further out into the extracellular matrix than the proteins located in the

lipid bilayer.⁶ This allows these sugar species to enter into interactions with extracellular entities when they first approach the cell.

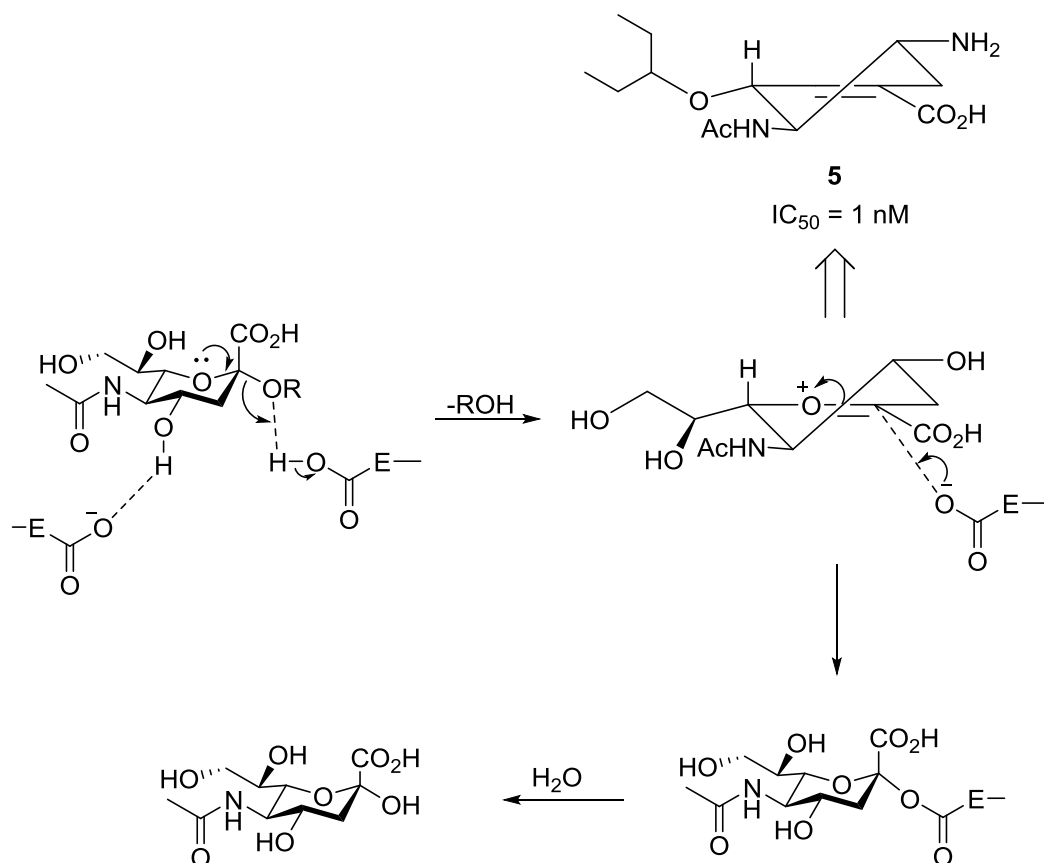
2.3 Carbohydrates as drug targets and glycomimetics

The composition of cell surface carbohydrates can vary significantly between those located on healthy and diseased cells. In particular, unique glycan markers can be found on diseased cells.⁷ Carbohydrate-based pharmaceuticals could potentially be used to target these glycoproteins and inhibit interactions with their natural binding partner or ligands. However the number of carbohydrate-derived drugs on the market remains low due to unfavourable pharmacokinetic properties linked with carbohydrates, such as poor oral bioavailability and rapid renal excretion.⁸ To tackle the issues associated with carbohydrate derived drugs a new class of therapeutics, known as glycomimetics, was developed. These small molecules resemble the structure, size and shape of the parent carbohydrate thereby ‘mimicking’ their interaction with the natural binding substrate whilst possessing vastly improved pharmacokinetic and physicochemical properties over their carbohydrate counterparts.⁸ Oseltamivir (Tamiflu) developed by Kim *et al.*, is an example, and is of one of the most successful glycomimetic drugs; it is used for the treatment of influenza.⁹ Oseltamivir is often administered in the form of an oral prodrug **4** (oseltamivir phosphate) which is readily metabolized to the active metabolite **5** *in vivo*.¹⁰



Scheme 2 – Structure of Oseltamivir phosphate **4** (prodrug) and Oseltamivir carboxylate **5** the active form of the influenza neuraminidase inhibitor.

Oseltamivir carboxylate **5** inhibits the enzyme neuraminidase, a surface glycosidase expressed by both influenza A and B. This protein is known to catalyse the cleavage of terminal sialic acids bound to the HA receptor of infected cells which, in turn, releases the virus back into the extracellular environment (**Scheme 3**).¹¹



Scheme 3: Hydrolysis of sialic acid by the glycosidase protein neuraminidase and rationale design of Oseltamivir as an oxacarbenium transition state analogue.

Metabolite **5** acts by mimicking the oxacarbenium transition state structure, a key intermediate in the hydrolysis of sialic acid by neuraminidase. The flat oxonium cation intermediate is similar in shape to an alkenyl group so the cyclohexene scaffold in **5** keeps conformational changes to a minimum, a feature which is important for maintaining biological activity.⁹ Analysis of the ligand-bound neuraminidase crystal structure reveals multiple strong binding interactions responsible for the high antiviral potency observed for Oseltamivir (**Figure 3**). The carboxylate functionality of the inhibitor is held in place through strong salt contacts with three arginine residues as well as hydrogen bonding interactions between the C₃ amino group and Glu119 and Asp151. However, in order to accommodate the large 3-pentyl group of **5** the carboxylate group of Glu276 is forced to project out of the hydrophobic pocket. This leads to an increased number of hydrophobic interactions between the 3-pentyl group and the amino acid residues within the active site, further increasing potency.

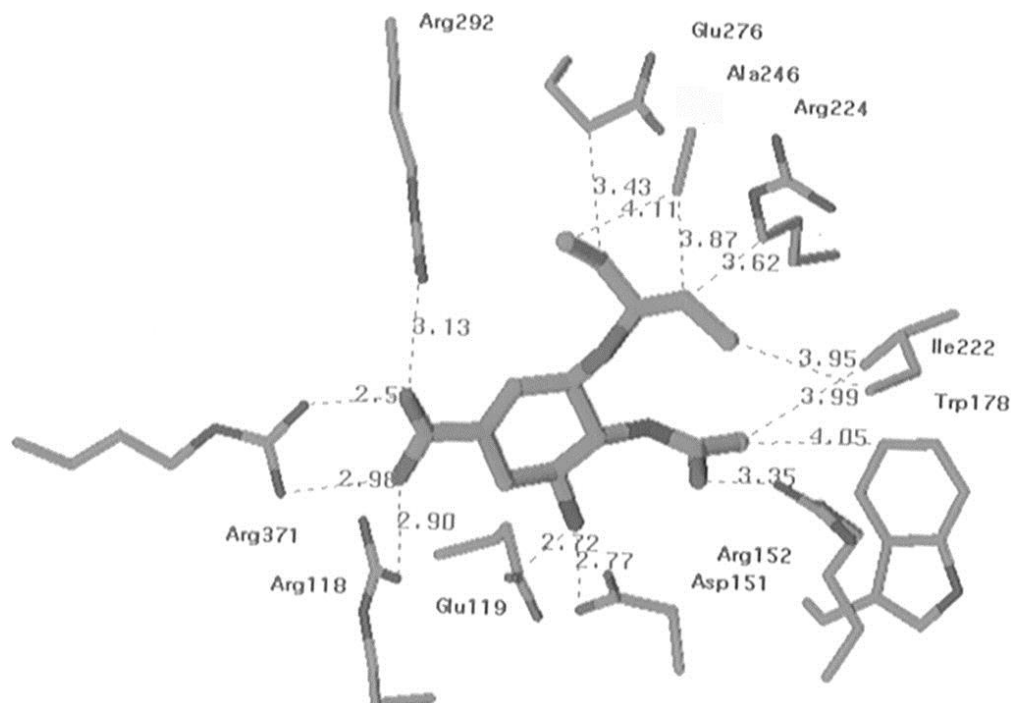
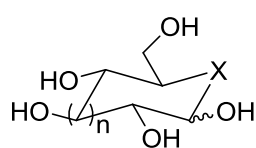


Figure 3: X-Ray structure of **5** bound to influenza neuraminidase.⁹

A specific class of carbohydrate mimics known as carbasugars have attracted considerable interest within the scientific community as potential glycosidase inhibitors and much effort has been devoted to the synthesis and application of these molecules.¹² However, the number of selectively fluorinated carbasugar analogues that exist remains relatively low and the application of this new class of glycomimetic is still very much in its infancy.

2.4 Carbohydrate Mimics – Carbasugars and Fluorocarbasugars

Carbasugars are sugar analogues in which the endocyclic oxygen in the natural sugar has been replaced by a methylene group (**Figure 4**).



$n = 5-8$

$X = O$ **6a**

$X = CH_2$ **6b**

$X = CHF$ **6c**

$X = CF_2$ **6d**

Figure 4 – Generic structure of naturally occurring sugars (**6a**), carbasugars (**6b**) and fluorocarbasugars (**6c** and **6d**).

Carbasugars are frequently based on five- and six-membered rings; however, there has been increasing interest in the preparation of seven- and eight- membered carbasugar analogues.¹³ The different spatial distribution of hydroxyl groups and the increased conformational flexibility of larger rings could produce sugar analogues which are more

adaptable to fit into the active site of carbohydrate processing enzymes. Sinaý *et al.* have reported the synthesis of both cycloheptane¹⁴ and cyclooctane¹⁵ ring cyclitols (**Figure 5**).

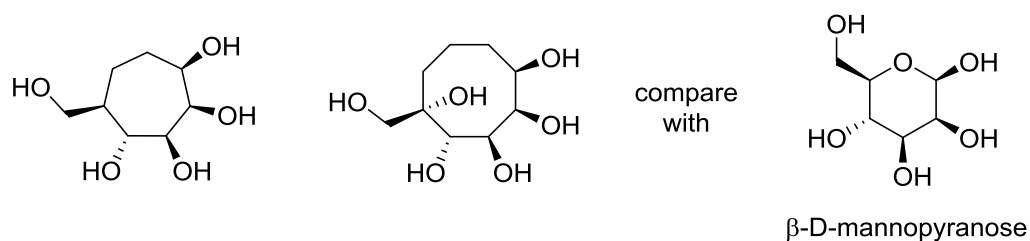


Figure 5: Cycloheptanic and cyclooctanic mimetics.

The occurrence of these compounds in nature is sparse; Miller *et al.* were the first group to report the isolation of ‘true’ carbasugar **7b** from nature.¹⁶ 5a-Carba-α-D-galactopyranose **7b** was isolated from the gram positive bacteria *Streptomyces sp.* MA-4145 and was found to have weak antibacterial properties against *Klebsiella pneumonia*, MB-1264. (**Figure 6**).

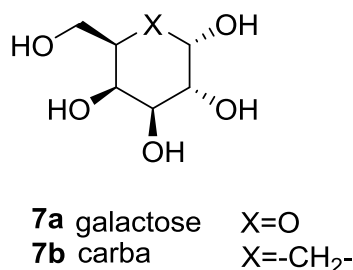


Figure 6– Galactose sugar and related 5a-Carba-α-D-galactopyranose **7a** and **7b** respectively.

Curiously, McCasland *et al.* had synthesised carbasugar **7b** 7 years prior to its discovery in nature.¹⁷ Replacement of the endocyclic oxygen with a CH₂ renders the molecule inert to hydrolysis and markedly improves metabolic stability. This is because such a substitution removes the ability to form an oxacarbenium cation, a key intermediate in sugar hydrolysis (**Scheme 3**).¹⁸ A number of drugs which belong to this family of glycomimetics have now come to market; these include Acarbose and Voglibose, both of which are glucosidase inhibitors used for the treatment of diabetes (**Figure 7**).

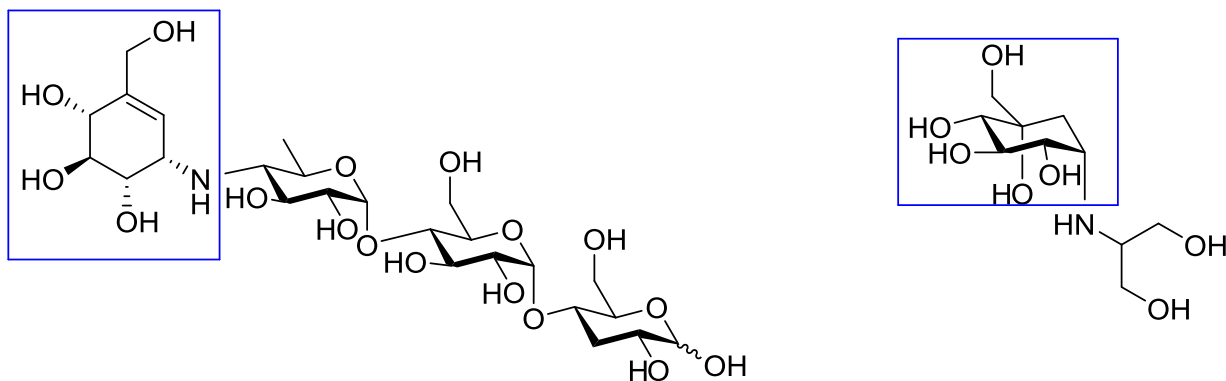
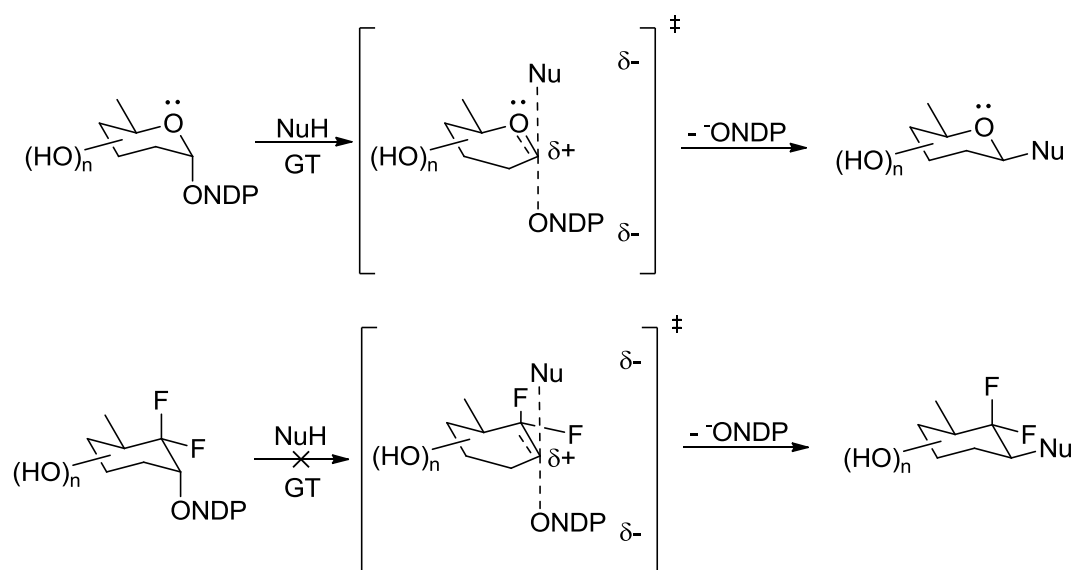


Figure 7: Marketed carbasugar based drugs Acarbose (left) and Voglibose (right). The carbasugar component of each drug is highlighted.

The use of a fluoroalkyl group could potentially provide surrogates (**6c** and **6d** in **Figure 4**) with much improved physicochemical properties over ‘classical’ carbasugars; however, the biological applications of these specific classes of glycomimetic structures are yet to be realised. Given that such species are also inert to hydrolysis this feature could be utilised in the design of biological probes for enzymes such as glycosyltransferases (**Scheme 4**).^{19,20}



GT = Glycosyltransferase
NDP = Nucleoside-diphosphate

Scheme 4: Stability of difluorinated carbasugars to glycosyltransferases.¹⁹

Another important feature of difluorinated carbasugars is that their stereoelectronic properties more closely resemble those of a natural glycoside motif compared to non-fluorinated analogues. This is due to the *exo*-anomeric effect, and is crucial for improving their mimicking ability. The origins of this effect lies in the favourable interaction that exists between the lone pair of the exocyclic anomeric oxygen and the larger σ^*_{C1-O5} orbital. This stabilizing interaction therefore results in reduced conformational interconversion. By removing the anomeric oxygen (this being the case

in classical carbasugars) the exocyclic O-C bond becomes more flexible and this increases the population of unnatural conformers (**Figure 8**).²¹

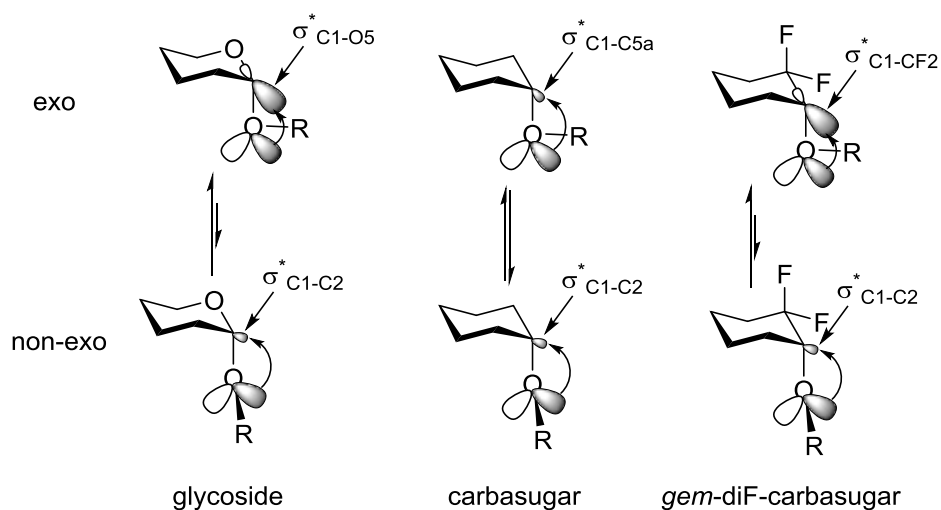
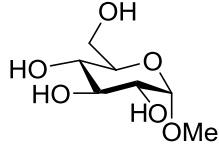
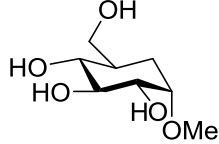
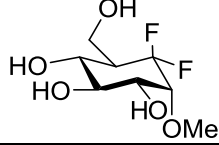


Figure 8 – Lone pair interactions responsible for the *exo*-anomeric effect.²¹

This could potentially be detrimental to small molecule protein binding because of the entropic penalty that it induces. However, replacement of the endocyclic oxygen with a CF₂ should effectively maintain the polarisation at the C1 position and restore the *exo*-anomeric effect. Indeed, Xu *et al.* have performed electronic structure calculations and NMR studies to show that this is the case with CF₂ which is intermediate in nature between O and CH₂ (**Table 1**).²¹

Table 1: Stabilization energy between donor and acceptor orbitals in natural sugar, carbasugar and difluorinated carbasugar

Molecule	Stabilization Energy (E^2) through <i>exo</i> -anomeric effect, kcal mol ⁻¹ ^a
	$n_{O_{exo}} \rightarrow \sigma^*_{C1-O_{endo}}$ 17.39
	$n_{O_{exo}} \rightarrow \sigma^*_{C1-C5a}$ 0.84
	$n_{O_{exo}} \rightarrow \sigma^*_{C1-C5a}$ 9.24

^a $E^{(2)}$ represents the second-order interaction energy between intramolecular donor and acceptor orbitals.

To validate this *in silico* model the authors synthesised *gem*-difluorocarbadisaccharide **8** and carbasugar analogue **9** and investigated their conformations through NMR NOESY and HOESY experiments (¹H-¹H and ¹⁹F-¹H).

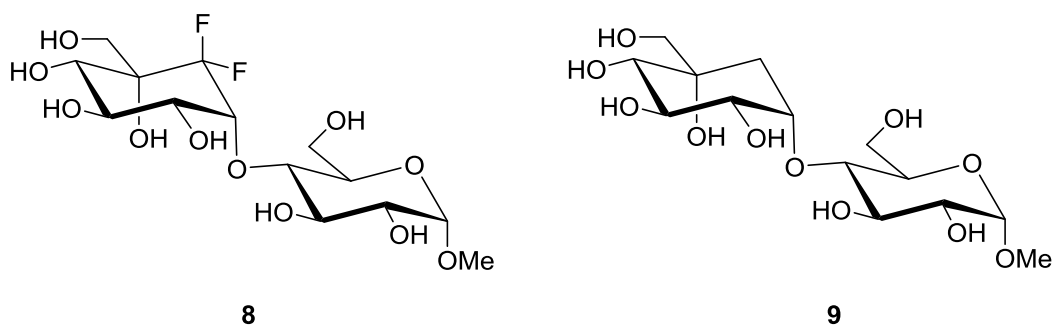


Figure 9: Disaccharides used in NMR studies to validate the *exo*-anomeric effect.

In the case of difluorocarbasugar analogue **8** the *exo*- Φ /*syn* Ψ conformation was favoured exclusively. In contrast, carbasugar **9** exhibited conformational interconversion between three different conformers (*exo*- Φ /*syn* Ψ , *exo*- Φ /*anti* Ψ and non *exo*- Φ /*syn* Ψ) in solution. The results of these experiments demonstrate the ability to restore the anomeric effect when substituting an oxygen atom with a CF₂ group.

Whilst these fluorinated sugars appear to have a number of attractive properties, the potential of such species to serve as effective glycomimetics has still to be sufficiently

investigated. This may be attributed to the fact that a paucity of synthetic pathways exist to provide access to such molecules.²²

2.5 Biological properties of fluorine

As fluorine is the most abundant halogen in the Earth's crust, it is surprising that nature produces very few fluorine-containing organic compounds. To date, only 13 naturally occurring organofluorine molecules, 8 of which are ω -fluorinated fatty acids derived from the same plant species, have been reported.²³ In contrast to such scarcity in nature it is estimated that up to 20% of prescribed therapeutics and up to 30% of the leading 30 'blockbuster drugs' contain one or more fluorine atoms.²⁴ In 2012, Advair developed by GlaxoSmithKline, and Lipitor®, developed by Warner-Lambert, were among two of the top 20 bestselling drugs worldwide, grossing \$3.2 billion and \$7.9 billion, respectively (**Figure 10**).²⁵

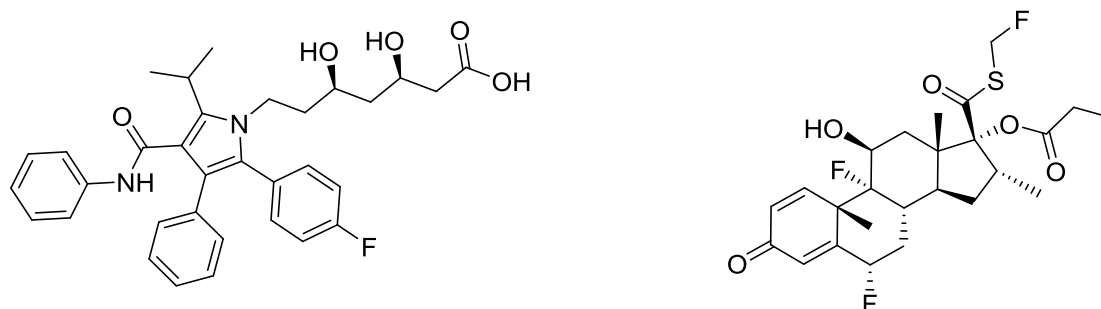


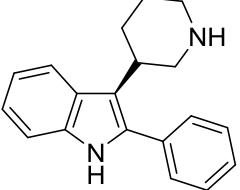
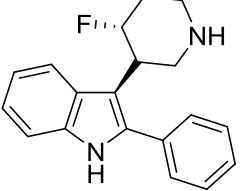
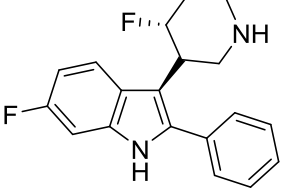
Figure 10: Lipitor® (left) and fluticasone propionate component of Advair (right).

It would not be an over-exaggeration to state that most drug discovery programmes will at some stage explore the use of fluorinated compounds as potential drug candidates. This is in a large part due to the unique physicochemical properties and stereoelectronic effects imparted by fluorine atom incorporation.²⁶ The powerful electron withdrawing capability of the fluorine atom means that its incorporation into a drug molecule can have a drastic effect on important physicochemical properties such as bioavailability.

Rowley *et al.* utilised this feature to attenuate the basicity of the piperidyl fragment in a series of 2-phenyl-3-(3-piperidyl)indoles.²⁷ In this case the introduction of fluorine decreased the basicity of the piperidyl nitrogen by two orders of magnitude and subsequently improved oral bioavailability by decreasing the concentration of protonated species *in vivo* and improving cellular absorption (**Table 2**). Furthermore, fluorinated analogues exhibited improved selectivity for 5-HT_{2A} receptors over the IKr potassium channel (hERG), a factor which is critical for avoiding potential QT interval

prolongation. This decreased hERG activity is likely to be driven through modification of the pK_a value.

Table 2 – Changes in pK_a and bioavailability upon addition of fluorine.

Indole	5-HT _{2A} ^a	pK _a	F (%) ^b
	0.99	10.4	Poor
	0.43	8.5	18
	0.06	-	80

^a Affinities at human cloned 5-HT_{2A} receptor (nM). ^b Bioavailability calculated from dosing at 0.5-2 mg/kg in rat.

The authors note that the indole was prone to aromatic hydroxylation at the C-6 position but introduction of a second fluorine atom inhibited metabolism by P450 enzymes at this site and further improved bioavailability. This so called ‘block effect’ is used quite often as a technique in medicinal chemistry to prevent the deactivation of biologically active species.²⁸ The enhanced metabolic stability can be explained by the differences in the bond dissociation energies of C-F and C-H bonds which are 105.4 kcal/mole and 98.8 kcal/mole, respectively.²⁹

As well as influencing bioavailability, the perturbation of pK_a can also modify the binding affinity of a particular pharmaceutical agent strongly. Conroy *et al.* found that a linear relationship existed between pK_i and pK_a for a series of carbonic anhydrase II (CA-II) inhibitors whereby pK_i increased as pK_a decreased (**Figure 11**).³⁰

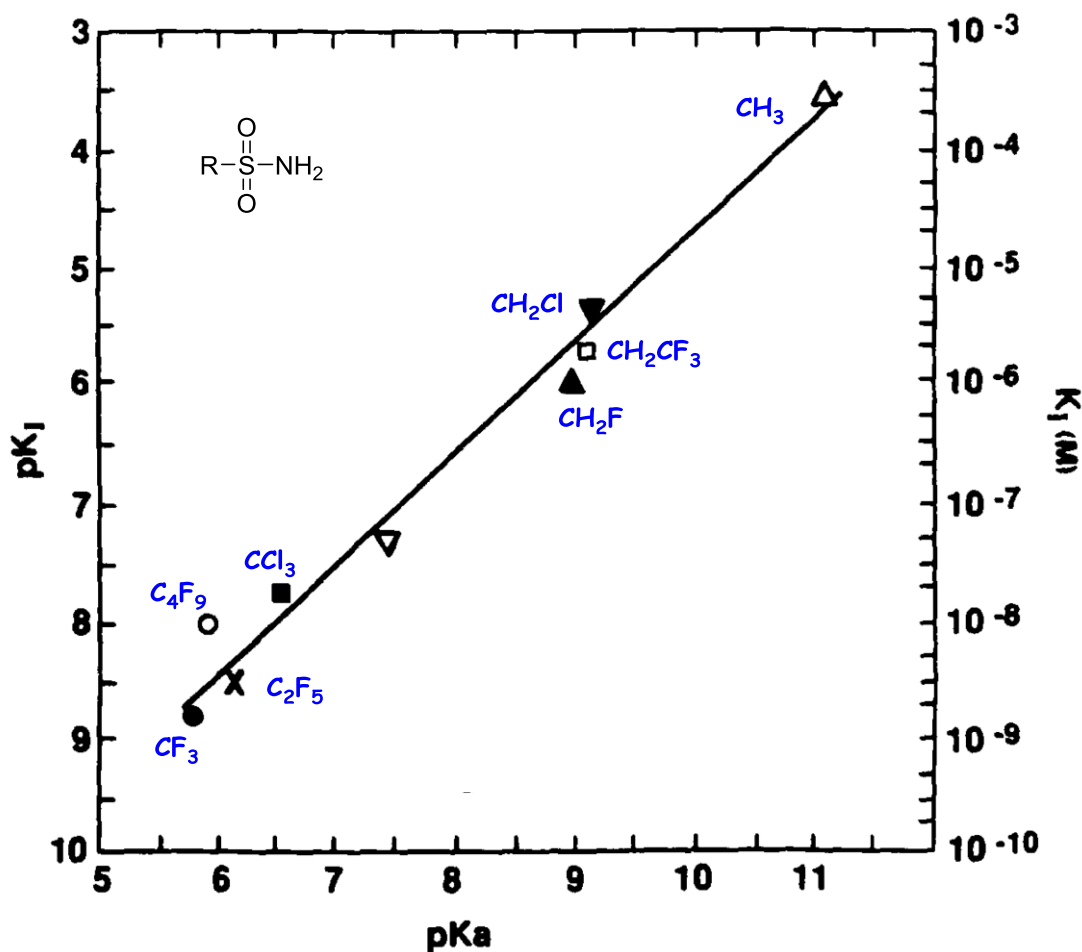


Figure 11: Linear relationship between dissociation constants of sulfonamide-CA II (K_i) and pK_a .³⁰

By replacing the CH_3 group ($pK_a = 10.5$) with CF_3 ($pK_a = 5.8$) an increase in potency of up to five orders of magnitude was observed, $K_i = 320 \mu M$ and $2nM$, respectively. This dramatic increase in binding affinity was attributed to the increased electronegativity on the sulfonamide nitrogen at physiological pH (4% $CF_3SO_2NH_2$ unionized) which binds tighter to the zinc ion within the active site of CA-II. The membrane permeability of ionised $CF_3SO_2NH_2$ was twenty fold less than that of the unionised form; however, both the ionised and unionised forms were found to penetrate red blood cells and rapidly saturate CA-II.

Care must be exercised when using fluorine as a pK_a modulator in drug molecules because of the potential to generate highly toxic fluorinated metabolites *in vivo*. Inhibition of kinesin spindle protein (KSP) has been shown to be effective in the treatment of taxane-refractory cancer and optimal profiles are observed for compounds with a pK_a between 6.5 and 8.³¹ Cox *et al.* found that β -fluorination modulated the pK_a of the piperidine nitrogen in KSP inhibitor **10** so that it fell within this optimal range (Figure 12).³¹

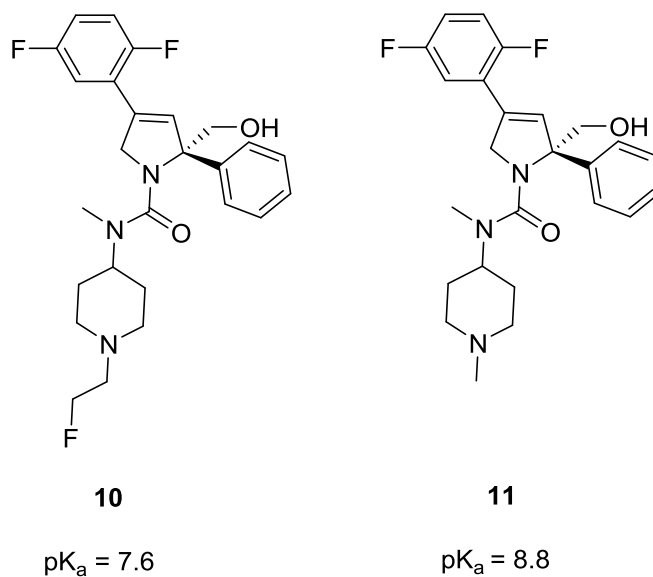


Figure 12: pK_a values of KSP inhibitors **10** and **11**.

However, fluorinated analogue **10** was found to be acutely toxic and mortality was found in two thirds of rat subjects twelve hours after dosage. It was found that *N*-dealkylation in rat hepatocytes resulted in the formation of *N*-dealkylated analogue **12** and fluoroacetate **13**, a known toxin in mammals (**Figure 13**).³²

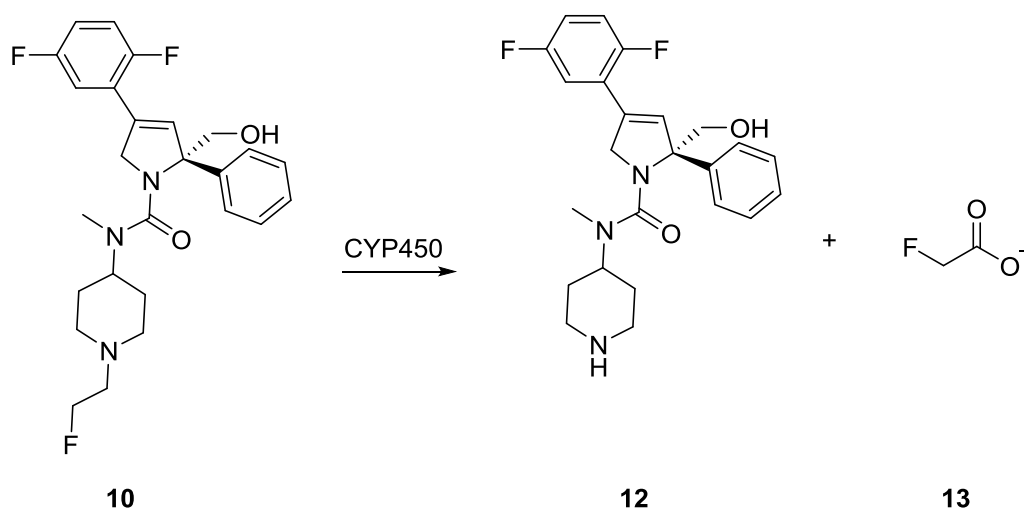


Figure 13: Metabolism of **10** in rat hepatocytes affording toxic **13**.

To overcome this issue the authors found that fluorination of the piperidine ring at the 3 position afforded an analogue with similar pharmacokinetic properties yet suppressed the formation of toxic fluorinated acid by-products.

Considering the electronegativity of the fluorine atom, it would be reasonable to assume that the C-F motif behaved much like the corresponding C-O and C-N fragments in terms of hydrogen bond accepting ability. However, because the C-F bond is weakly polarisable, this reduces the hydrogen bond accepting ability of organic fluorine drastically.^{33,34} Having stated this, fluorine can participate in electrostatic interactions. Indeed, there are a number of examples whereby the introduction of fluorine into a small molecule improves potency. This is likely attributable to the dipolar interactions which can exist between fluorine and the amide backbone of a protein within its active site.³⁵ In their development of a number thrombin inhibitors, Olsen *et al.* demonstrated this effect particularly well.³⁶ The binding mode of the fluorinated thrombin inhibitor was revealed by X-ray crystallography and was similar to that of previously reported non-fluorinated inhibitors.³⁷ However, the authors discovered the D-pocket of the thrombin active site to accommodate a fluorine atom and that a simple switch from hydrogen to fluorine brought about a six fold increase in binding affinity for the target protein (**Figure 14**).

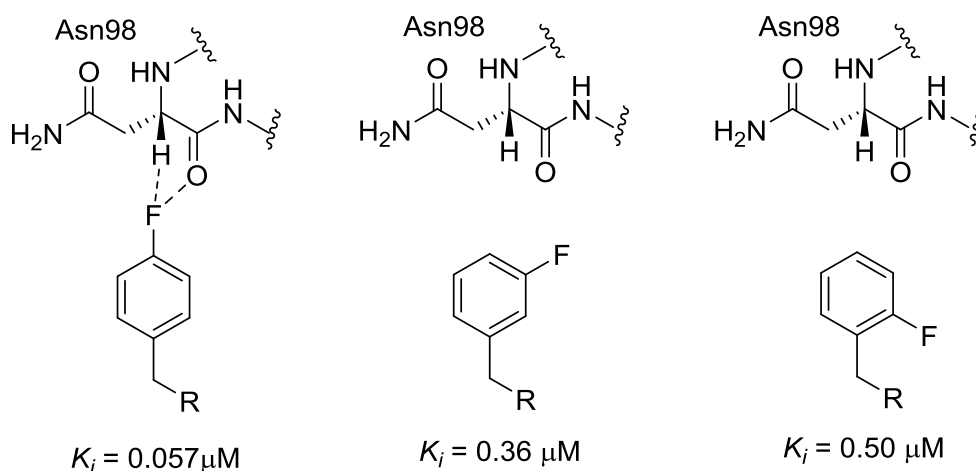


Figure 14: Importance of fluorine in 4-position for interaction with amide backbone in the active site of a series of thrombin inhibitors.³⁶

The fluorine atom present in the inhibitor was within close proximity to the polarised H-C α -C=O fragment of Asn98 resulting in attractive interactions between the two moieties.³⁸ The strength of these interactions are reflected in the binding affinity, K_i , with the fluorinated analogue displaying a K_i value of 0.057 μM whilst the non-fluorinated counterpart has a K_i value of 0.31 μM . Goldstein *et al.* also found that a similar interaction was responsible for an eight fold increase in potency in a series of fluorinated p38 α kinase inhibitors.³⁹ There are some interesting features about these interactions which should be noted. In the context of ligand-protein binding such C-F \cdots C=O interactions are quite rare. The weak nature of such an interaction has prevented its

energetic quantification in bimolecular systems; however, Fischer *et al.* calculated the interaction free enthalpy between a CF₃ group and a spatially close amide group in an extended indole to lie between -0.8 and -1.2 kJ mol⁻¹ (**Figure 15**).⁴⁰

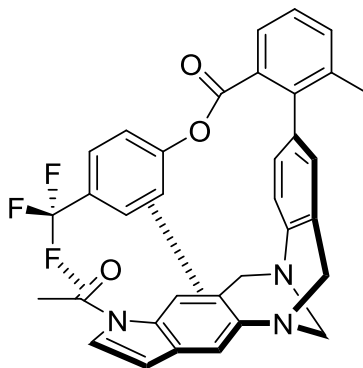


Figure 15: Representative intramolecular orthogonal polar interaction between -CF₃ and amide group.

Although fluorine acts only as a weak H-bond acceptor, C-F \cdots H-C interactions have been reported to play an important role in the crystal packing of fluorobenzenes, as well as in base stacking of fluorinated ribonucleosides.^{41,42}

The ability for fluorine to act only as a hydrogen bond acceptor has been used in studying carbohydrate chemistry to enable distinction between the roles of donor and/or acceptor for a given substrate hydroxyl group. The significance of individual hydrogen bonds for the kinetics of binding can then be assessed in specific carbohydrate-protein interactions. Westwood *et al.* have demonstrated this during a study of yeast galactokinase.⁴³ The hydrogen bond accepting/donating of specific hydroxyl functionalities was elucidated by comparison of the kinetic parameters obtained for the 2-deoxy and isomeric 2-deoxyfluoro-D-galactopyranoses analogues (**Figure 16**).

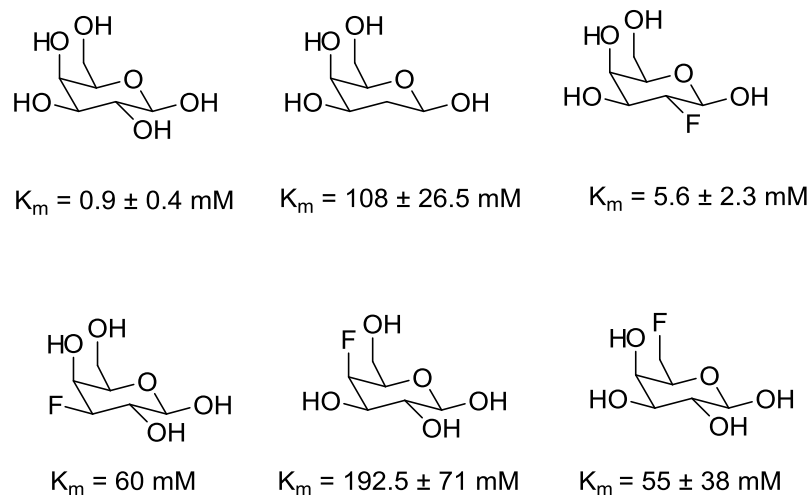


Figure 16: Analysis of hydrogen bond donating/accepting ability of the hydroxyl groups in D-galactose.

From these results it appears that the role of OH-2 is to act as a H-bond acceptor whereas OH-3, OH-4 and OH-6 are involved in the binding to galactokinase as hydrogen bond donors. However, a more recent study by Linclau *et al.* found that fluorine is acting as an isostere and substitution at the OH-3 position of D-galactose had no detrimental effect on binding to galactose oxidase (GOase).⁴⁴ Despite the loss of hydrogen bond donating capacity the K_m value of fluorinated galactose analogue **14** was found to be equivalent to that of the natural substrate (**Figure 17**).

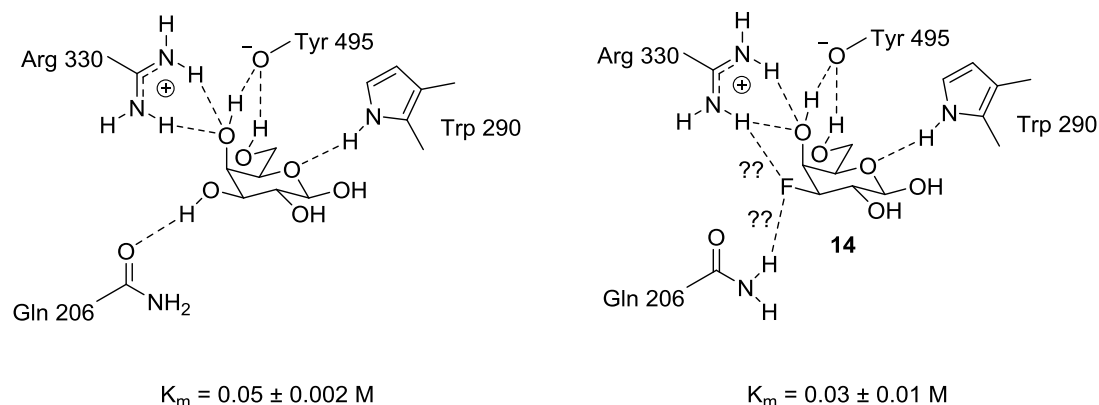
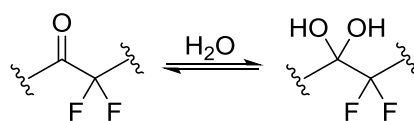


Figure 17: Binding modes of D-galactose and fluorinated analogue **14** in active site of GOase.

This indicates that an even stronger Gln206 NH \cdots F interaction might exist or that the 3-fluoro group is now involved in an attractive interaction with the guanidinium group in Arg330.

Fluorine can also heavily influence the properties of nearby functional groups. The introduction of fluorine on a carbon adjacent to a carbonyl group is known to enhance

the tendency of ketones to add nucleophiles. In aqueous solution water can readily hydrate carbonyl groups bearing α,α -fluorine substituents (**Scheme 5**).



Scheme 5: Ketone/hydrate equilibrium.

This particular feature has been used in the design of protease inhibitors. This is due to the fact that hydrated ketones closely resemble the tetrahedral adduct formed when H_2O adds to the carbonyl group of a peptide substrate, and therefore can be regarded as transition state analogue inhibitors (**Figure 18**).



Figure 18: Natural tetrahedral intermediate in peptide hydrolysis of phenylalanine residue (left) and potential transition state mimic (right).

Angiotensin is an enzyme which catalyses the hydrolysis of Angiotensin I to Angiotensin II, the latter being a potent vasoconstrictor. Antagonists of this enzyme are therefore likely candidates for antihypertension pharmaceuticals. Abeles *et al.* demonstrated the effectiveness of fluorine in the design of inhibitors of the zinc metalloprotease Angiotensin.⁴⁵ The trifluoromethylketone proline analogue **15** was three hundred fold more potent than its methyl ketone counterpart **16** highlighting the significance of fluorine substitution adjacent to a carbonyl group (**Figure 19**).

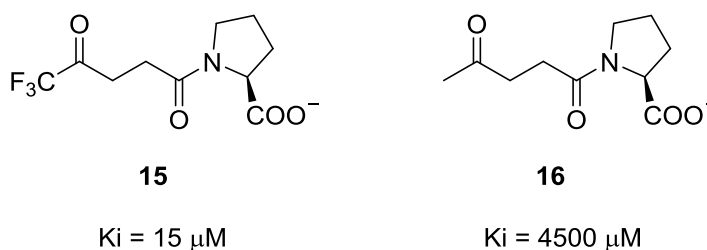
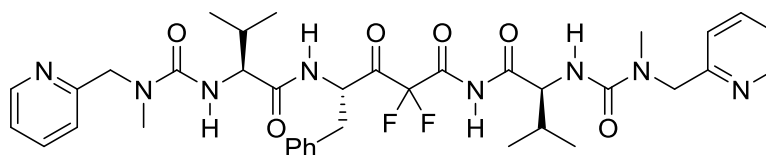


Figure 19: Angiotensin converting enzyme inhibitors.

Erickson *et al.* successfully modelled the complex of HIV-1 protease with inhibitor **17** in performing a series of vigorous *ab initio* calculations (**Figure 20**).⁴⁶



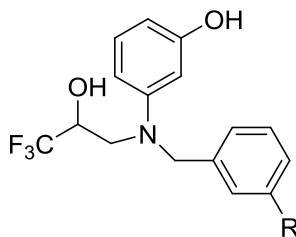
17

Ki = 22 pM

Figure 20: HIV-1 protease inhibitor.

The calculations revealed that the difluoroketone core is hydrated and in a *gauche* conformation within the enzyme active site. The high activity of **17** was attributed to its ability to mimic a peptide bond that has undergone carbonyl hydration.

Another interesting feature is the conformational change that can potentially occur upon incorporating fluorine into a molecule. Usually the substitution of H with F imposes only a minor additional steric demand; the van der Waals radii of hydrogen and fluorine atoms are 1.20 Å and 1.47 Å, respectively. However, the replacement of a methyl group with a trifluoromethyl group can drastically alter the conformation. This is because the volume of a trifluoromethyl group is approximately twice that of a methyl group, comparable to an isopropyl substituent. In a comparison of anisole with trifluoromethoxybenzene, Klocker *et al.* performed quantum mechanical calculations to show that whereas it is energetically favourable for the methoxy group to lie within the plane of the phenyl ring in anisole, the trifluoromethoxy group must lie orthogonal to it in trifluoromethoxybenzene.⁴⁷ This effect could have significant biological consequences. Massa *et al.* have highlighted the significance molecular geometry can have on protein binding affinity by comparing the potencies of two CETP (cholesteryl ester transfer protein) inhibitors (**Figure 21**).⁴⁸



18: R = OCF₂CF₂H IC₅₀ = 0.2 μM

19: R = OCH₂CH₃ IC₅₀ = 1.6 μM

Figure 21: CETP inhibitors **18** and **19** with corresponding IC₅₀ values.⁴⁸

Ab initio calculations showed that the 3-tetrafluoroethoxy substituent lies out of the plane of the phenyl ring, whereas the nonfluorinated ethoxy group lies in plane. The

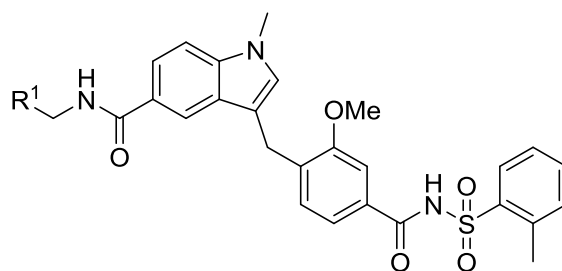
eight fold lower potency of the ethoxy analogue was attributed to this effect. The fluorine atom therefore cannot be considered simply as an isosteric replacement for hydrogen with spatial considerations having to be taken into account during molecular design.

One of the most important physicochemical properties associated with orally administered drugs is lipophilicity. A drug's lipophilicity is quantified by its partition coefficient ($\log P$ value) which is a measure of the molecule's relative affinities for octanol and water. A molecule with a high $\log P$ value would be considered as highly lipophilic whereas one with a lower $\log P$ value would be considered as highly polar. In 1997, Lipinski *et al.* developed a set of rules (Lipinski's rule of 5) which could be used to evaluate the suitability of a drug for oral administration.⁴⁹ One of the rules states that any molecule with a $\log P$ value greater than five or less than zero could potentially have issues with membrane permeability. This is because a drug which is too lipophilic could become trapped upon traversing the lipid bilayer of a cell whereas one which is too polar would not be absorbed at all. It has since been demonstrated that the introduction of fluorine into molecules can tune the $\log P$ value for a given compound (**Table 3**).⁵⁰ This is a result of the polar hydrophobicity of the C-F bond associated with the high electronegativity and small size of the fluorine atom as well the low polarisability of the C-F bond.

Table 3-Effects of fluorine introduction on $\log P$.⁵⁰

Compound	$\log P$ (octanol-water)
C ₆ H ₆	2.1
C ₆ H ₅ F	2.3
C ₆ H ₅ CH ₃	2.1
C ₆ H ₅ CF ₃	3.0

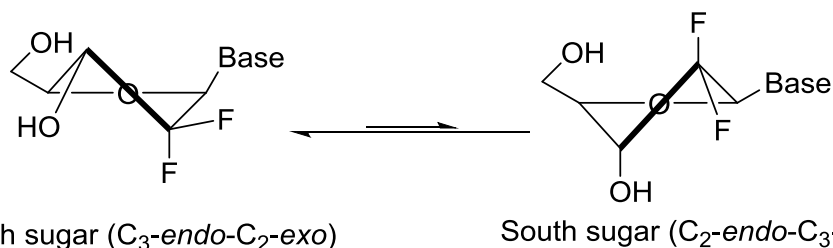
In their development of orally active antagonists of the Leukotrienes D₄ and E₄, Jacobs *et al.* observed that indolecarboxamide analogues with greater lipophilic character showed markedly improved potencies.⁵¹ Attempts to further increase lipophilicity by extending the amide substituent (R¹) carbon chain length beyond six carbons resulted in decreased target affinity. The authors overcame this issue by introducing fluorine into their systems. This effectively increased drug lipophilicity and potency whilst at the same time retaining receptor affinity (**Table 4**).

Table 4: Fluorinated indolecarboxamides: comparison to non-fluorinated analogues.⁵¹

R ¹	poED ₅₀ (μmol/kg)	Log P
	14.73	6.29
	2.64	6.45
	19.96	5.85
	1.44	6.18

Consequently, because of their highly lipophilic nature these potential drug candidates suffered from poor oral bioavailability *in vivo* (12-38% in dog, guinea pig and rat) which may be attributed to hepatic clearance.

Fluorine can also be a useful NMR biomarker *in vivo* for the analysis of proteins because the sensitivity of the ¹⁹F nucleus is high and the absence of natural abundance background greatly simplifies data analysis.⁵² Moreover, NMR analysis can be used to elucidate the structural conformation of small biological molecules. An excellent example of this is demonstrated by Thibaudeau *et al.* who developed a novel Karplus-type equation which effectively correlates ³J_{H-H} and ³J_{H-F} values with the corresponding Φ_{HF} torsion angle. This simplifies structural elucidation and allows for the effective conformational analysis of fluorinated nucleoside analogues, **20a-20d**.⁵³ Compounds **20a-20d** are important anti-cancer compounds; however, their biological activity is greatly influenced by their conformation. In solution the pentafuranosyl moiety can undergo pseudorotation whereby the cyclopentane ring is involved in continuous interconversions of puckered forms. For nucleosides this process exists preferentially in a two-state dynamic equilibrium where the ring is found to populate primarily the North (N-type) and South (S-type) conformations (**Figure 22**).⁵⁴



Base = adenine-9-yl (**20a**), guanine-9-yl (**20b**), cytosine-1-yl (**20c**), thymine-1-yl (**20d**)

Figure 22: Dynamic pseudorotational equilibrium of nucleosides.

Therefore, robust conformational analysis techniques are required in order to fully understand structure activity relationships for **20a-20d** both in the presence and absence of target enzymes. Using a combination of both $^3J_{H-H}$ and $^3J_{H-F}$ coupling constants it was revealed that their conformational equilibria greatly favoured the N-type conformation. Their geometry was characterised by P (phase angle of pseudorotation) values in the range from 61° to 76° and Ψ_M (puckering amplitude) values in the range from 35° and 46° where P defines the part of the ring which is most puckered and Ψ_m the extent of the puckering. The range of P values calculated indicates a preference for the puckering between the C_4' -exo and O_4' -endo- C_4' -exo forms for all four difluorinated nucleosides.

From the various examples detailed above, the dramatic effects fluorine can impart on the physical properties of small molecules and its importance in medicinal chemistry are apparent. The remainder of this review will highlight successes in the synthesis of fluorinated sugar analogues, and the ongoing research within our laboratories to develop new synthetic routes using a modular, building block approach.

2.6 Synthesis of fluorocarbasugars

There are two main strategies for the preparation of *gem*-difluoro-carbasugars. The first involves manipulation of natural carbohydrate precursors by treatment with nucleophilic or electrophilic fluorinating agents while the second involves construction of the carbocyclic skeleton from fluorinated small molecule precursors *via* building block (or *de novo*) routes.²²

2.6.1 Synthesis of fluorocarbasugars from carbohydrate precursors

The treatment of aldehyde and ketone functional groups (which can be readily introduced in sugars through oxidative manipulations) with fluorinating agents has been utilised in the formation of *gem*-difluoro compounds.⁵⁵ Selectfluor® **21** is an an electrophilic fluorinating agent whereas DAST **22** and Deoxo-Fluor® **23** are both examples of nucleophilic fluorinating agents (**Figure 23**).

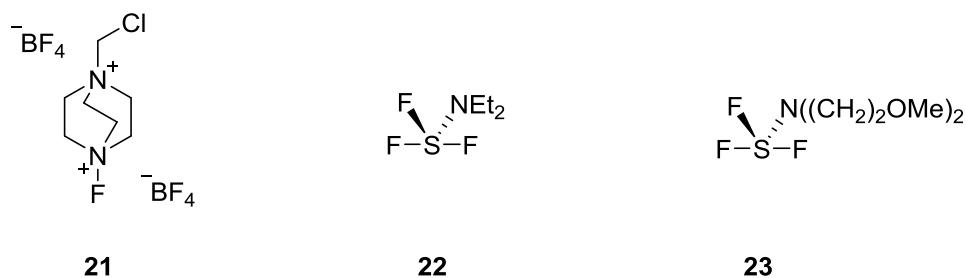
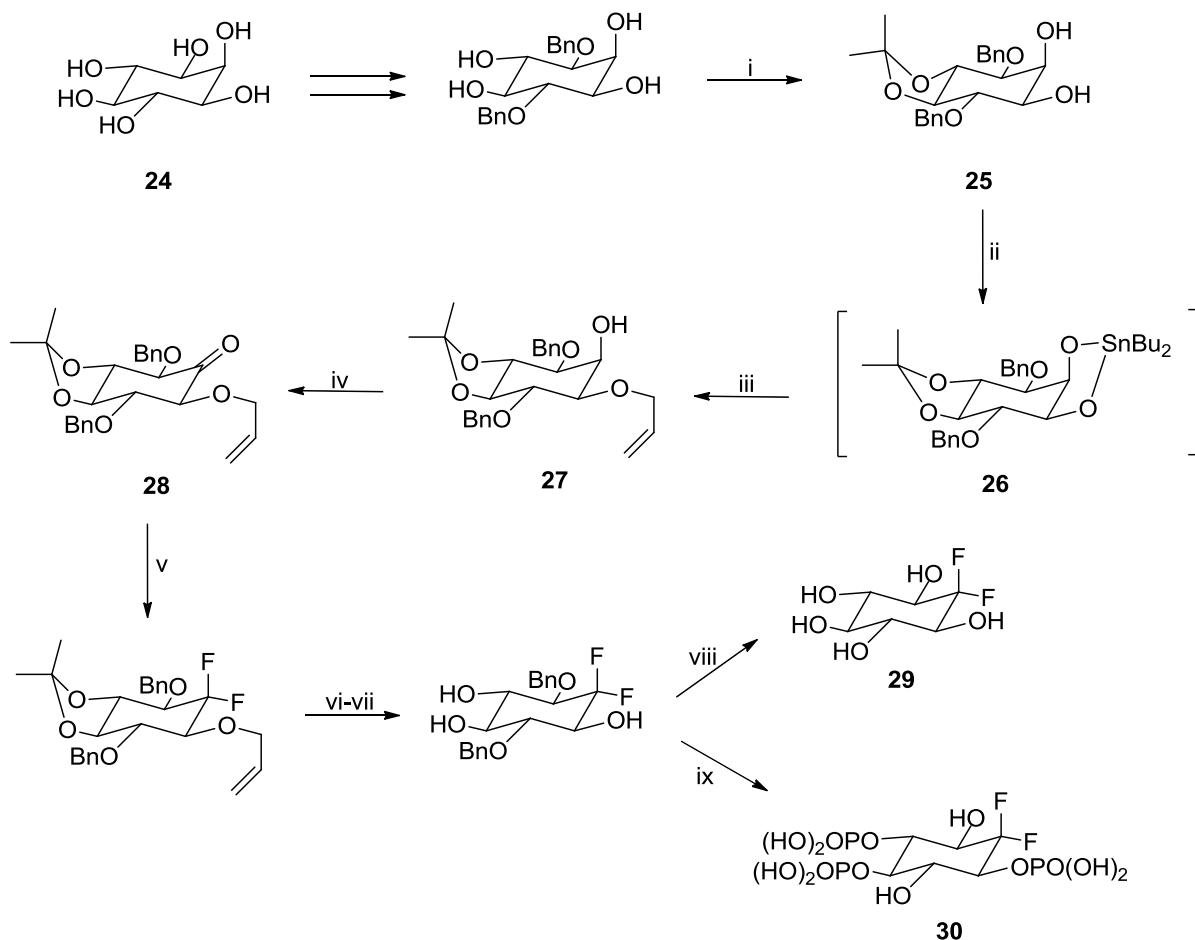


Figure 23- Common fluorinating agents Selectfluor® (**21**) DAST (**22**) and Deoxo-Fluor® (**23**).

Sawyer and Potter were able to successfully synthesise difluorinated analogues of inositol **29** and inositol 1,4,5-triphosphate **30** starting from *myo*-inositol **24** using DAST as the fluorinating agent (**Scheme 6**).⁵⁶ Initial benzylation followed by selective diol protection of the starting carbohydrate **24** affords the acetonide **25**. Treatment of **25** with Bu₂SnO generates the stannylene acetal **26** *in situ* which undergoes selective *O*-allylation to afford **27**. Selective oxidation of the C-2 hydroxyl group delivered ketone **28**. Treatment of the ketone with four equivalents of DAST, followed by further protecting group manipulation led to the target compounds **29** and **30**.

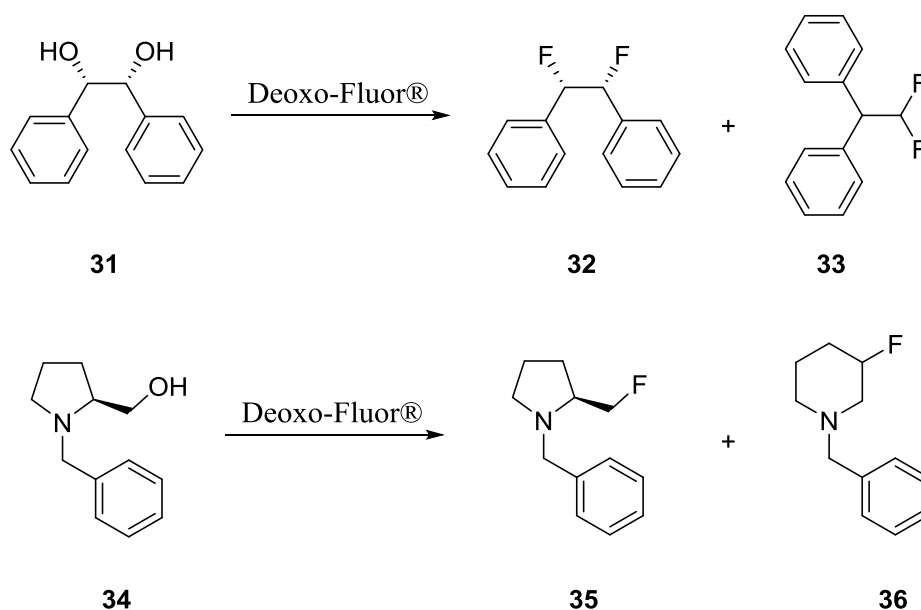
A major problem that arises during the synthesis of fluorocarbasugars from carbohydrate precursors, which is highlighted in **Scheme 6**, is that a large number of protection/deprotections together with oxidation state manipulations may be required prior to the use of the fluorinating agent.⁵⁷ Carbohydrate precursors possess a number of hydroxyl functionalities which obviously poses an issue when oxidation of a specific –OH to the corresponding aldehyde or ketone is required as shown in **Scheme 6**. The

requirement for a large number of protecting group manipulations can therefore compromise synthetic efficiency.⁵⁸



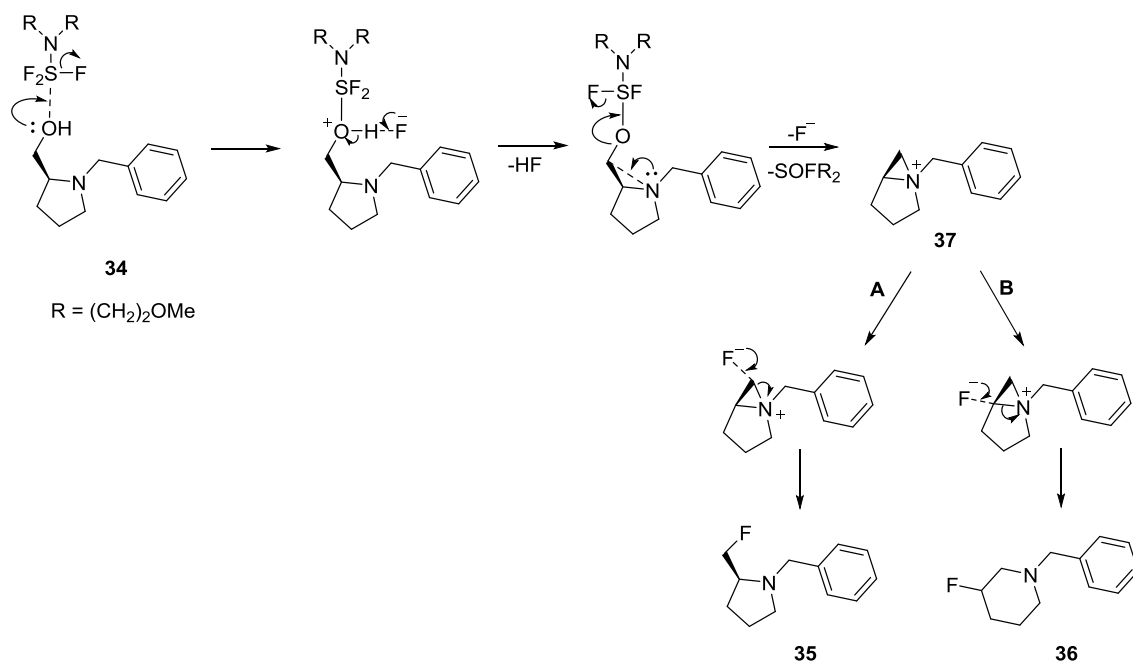
Scheme 6 – Sawyer and Potter's synthesis of difluorinated analogues of *myo*-inositol.^{56,59} i) DMSO, 2,2-dimethoxypropane, PTSA 60%; ii) dibutyltin oxide, benzene iii) DMF, Allyl Bromide, 62% iv) DMSO, Ac₂O, NaHCO₃ 80%; v) DAST (4 mol equiv.), DCM, rt, 5 hours, 79%; vi) 1,4-diazabicyclo[2.2.2]octane, RhCl(PPh₃)₃, 75%; vii) HCl/MeOH, 86% viii) 10% Pd/C, H₂, EtOH/AcOH, 50 psi, 3 days, 71%; ix) *bis*-(2-cyanoethyl)-(N,N-diisopropylamino)phosphoramidite, tetrazole, 70% *t*-BuOOH, Na, NH_{3(l)}, -78 °C, 15 min, 67%. Overall yield of **29** and **30** ≈ 11% and 10%, respectively from **24**.

However, the main problem associated with fluorinating agents is their rather capricious nature. Ye *et al.* have shown that in a number of cases the treatment of 2-amino alcohols and 1,2-diols with Deoxo-Fluor® produces both the fluorinated product, as well as a rearrangement side product (**Scheme 7**).⁶⁰



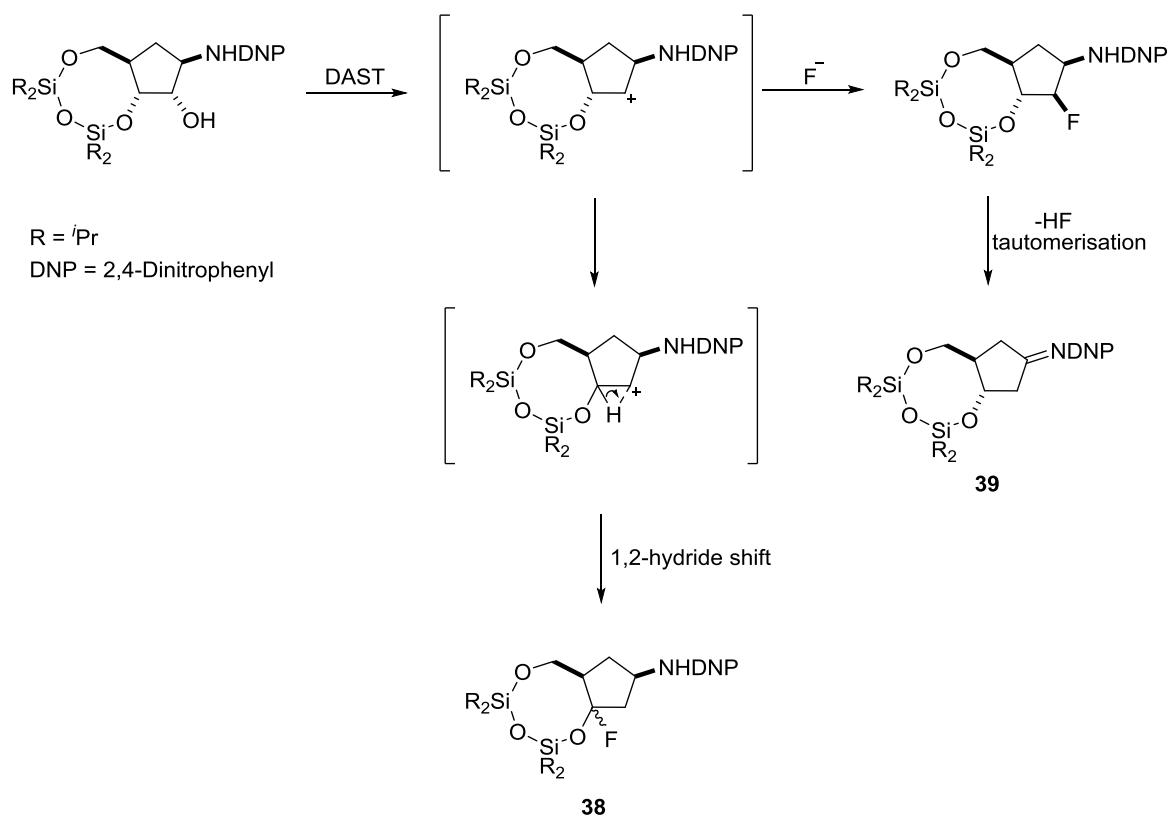
Scheme 7: Product mixture from treatment of diol, **31**, and amino alcohol **34** with Deoxo-Fluor® (product ratio 3:2 and 1:2 respectively).

The authors postulate that the formation of *gem*-difluoride **33** occurs *via* a rearrangement analogous to that of a pinacol rearrangement, with the resulting aldehyde reacting with Deoxo-Fluor® to deliver the *gem*-difluoride species. The reaction of aminosulfur trifluorides with alcohols that can form stable carbocations often proceed through an S_N1-like pathway.⁶¹ Intermediates with high carbenium ion character can be activated towards neighbouring group participation (NGP). The authors suggest that such NGP is the cause of the formation of the major side product **36** which passes through an aziridinium intermediate **37** (**Scheme 8**). Strain relief from ring opening of the cyclopropane ring by nucleophilic attack of the fluoride ion affords the monofluorinated piperidine **36**.



Scheme 8: Mechanism for fluorination of **34** with aminosulfurane Deoxo-Fluor® to give the desired fluorinated product (Pathway A) and the undesired ring expanded product **36** (Pathway B).

Another issue with some fluorinating agents is their hazardous nature. Deoxo-Fluor® is severely toxic and reacts violently with water, therefore extreme care must be taken during handling.⁶² Additionally, DAST has a propensity to explode upon heating, and accordingly, there is a desire to move away from such precarious reagents.⁶³ Fluorinations that involve the use of DAST and Deoxo-Fluor® can also result in the production of both rearrangement and elimination side products. The formation of such side products can often complicate purification resulting in diminished reaction yields. During the preparation of fluorinated nucleoside analogues, Youds *et al.* reported the formation of two significant side products.⁶⁴ The first was a product resulting from the elimination of HF and the second the result of a 1,2-hydride shift (**Scheme 9**).



Scheme 9: Rearrangement **38** and elimination **39** side products formed from DAST fluorination.

Recently, the synthesis of novel fluorinating agents such as XtalFluor-E **40** and Xtalfluor-M **41** (**Figure 24**) has allowed some of the issues associated with DAST and Deoxo-Fluor® to be overcome; these include improved selectivity and limiting the formation of corrosive HF.⁶⁵ Handling of these materials is also simplified due to the fact they are crystalline weighable solids.

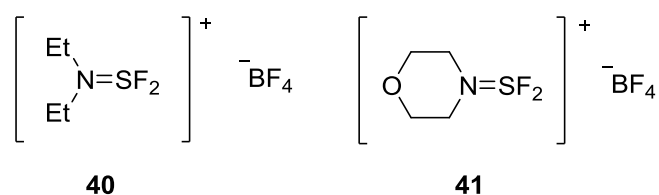
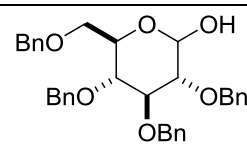
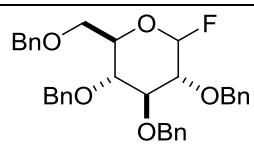


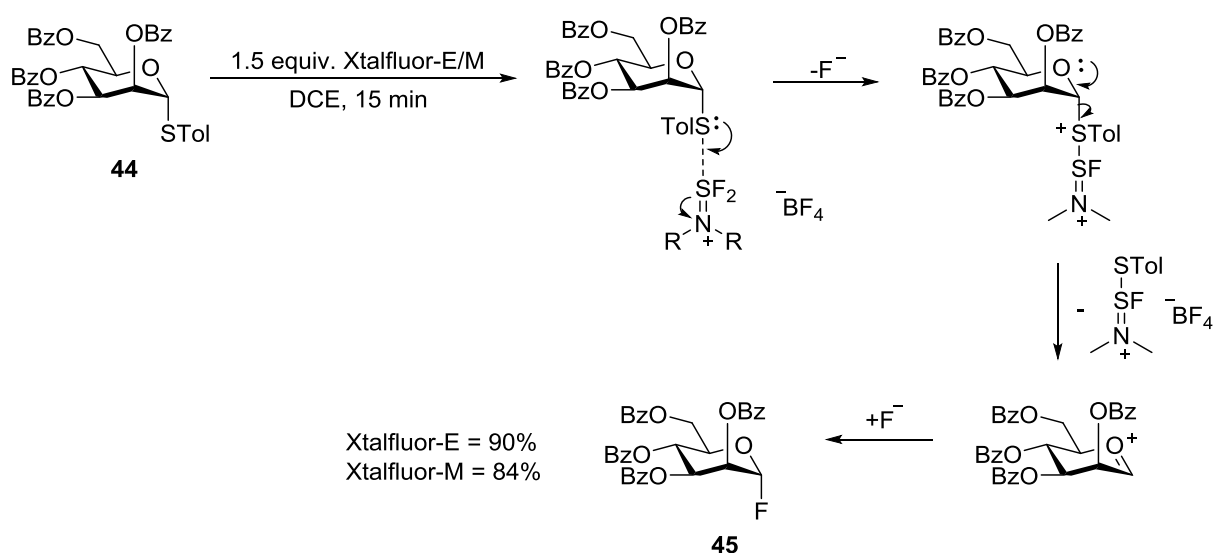
Figure 24: Fluorinating agents XtalFluor-E, **40**, and Xtalfluor-M, **41**.⁶⁵

These aminodifluorosulfonium salts have been successfully applied in carbohydrate based chemistry for the monofluorination of 2,3,4,6-tetra-*O*-benzyl-*D*-glucose **42** to afford glycosyl fluoride **43** in near quantitative yield (**Table 5**).⁶⁵

Table 5: Deoxofluorination of protected carbohydrate substrate.

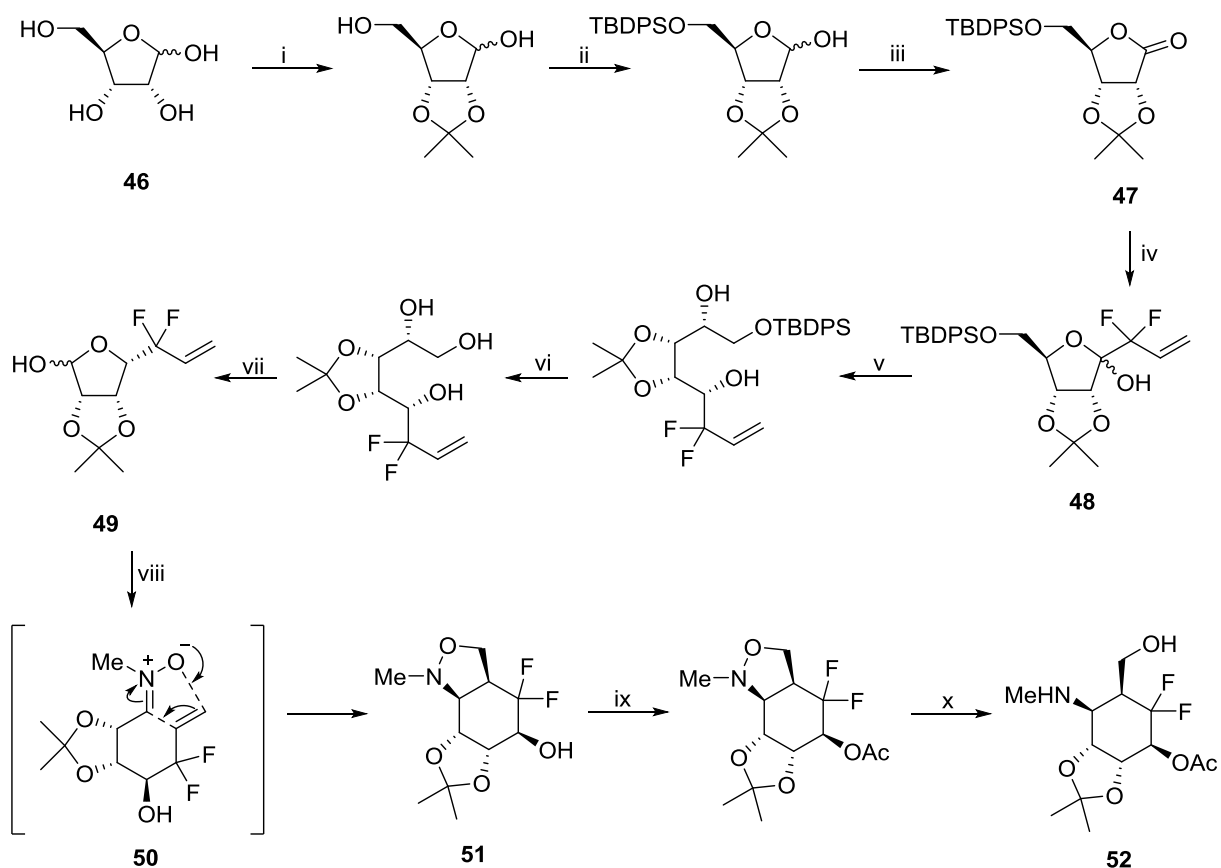
Starting material	Reagent	Additive	Temp (°C)	Time (h)	Yield (%)	Product
	XtalFluor-E	TEA·3HF	rt	3	99	
42	XtalFluor-M	TEA·3HF	rt	1.5	90	

Unlike DAST, the XtalFluor-E and -M reagents have been described as ‘fluorine starved’ and require the use of additives such as Et₃N·3HF to provide a nucleophilic fluoride source. However, Tsegay *et al* have reported the conversion of aryl thiomannoside **44** to glycosyl fluoride **45** without the requirement of additional additives (**Scheme 10**).⁶⁶

**Scheme 10:** Fluorination with Xtalfluor-E/M without use of additives.

However, the reactivity of these reagents towards more challenging substrates which are unable to form stabilised intermediates is yet to be demonstrated. An alternative method for introducing fluorine into sugar-type species also involves starting from carbohydrate precursors; however, this time, the fluorine atoms are introduced through the use of building blocks rather than fluorinating agents. Jiang *et al.* have reported a method for the formation of a difluoroaminocarbasugar starting from D-ribose which utilised an intramolecular nitronc cycloaddition as the key ring forming reaction (**Scheme 11**).⁶⁷ Lactone **47** can be delivered from D-ribose **46** through protection and oxidation. It is at this point that the *gem*-difluoro moiety is introduced into the molecule; 3,3-difluoro-3-bromopropene undergoes metal-halogen exchange in the presence of *n*-BuLi. The

organolithium species generated *in situ* then goes on to react with the carbonyl group of the lactone to give difluorinated species **48**. Further protecting group manipulation and reduction delivered the rearrangement precursor **49** existing predominantly as the α -anomer. Treatment of **49** with *N*-methylhydroxylamine hydrochloride generated the nitron species **50** *in situ* which underwent cyclisation from the least hindered face to deliver isoxazolidine **51**. This species was then acetylated and reduced to afford difluorinated carbasugar **52**. One of the drawbacks in the route described by Jiang and co-workers is the lengthy synthetic sequence, a consequence of which is reflected in the low overall yield of the reaction (2.2%).

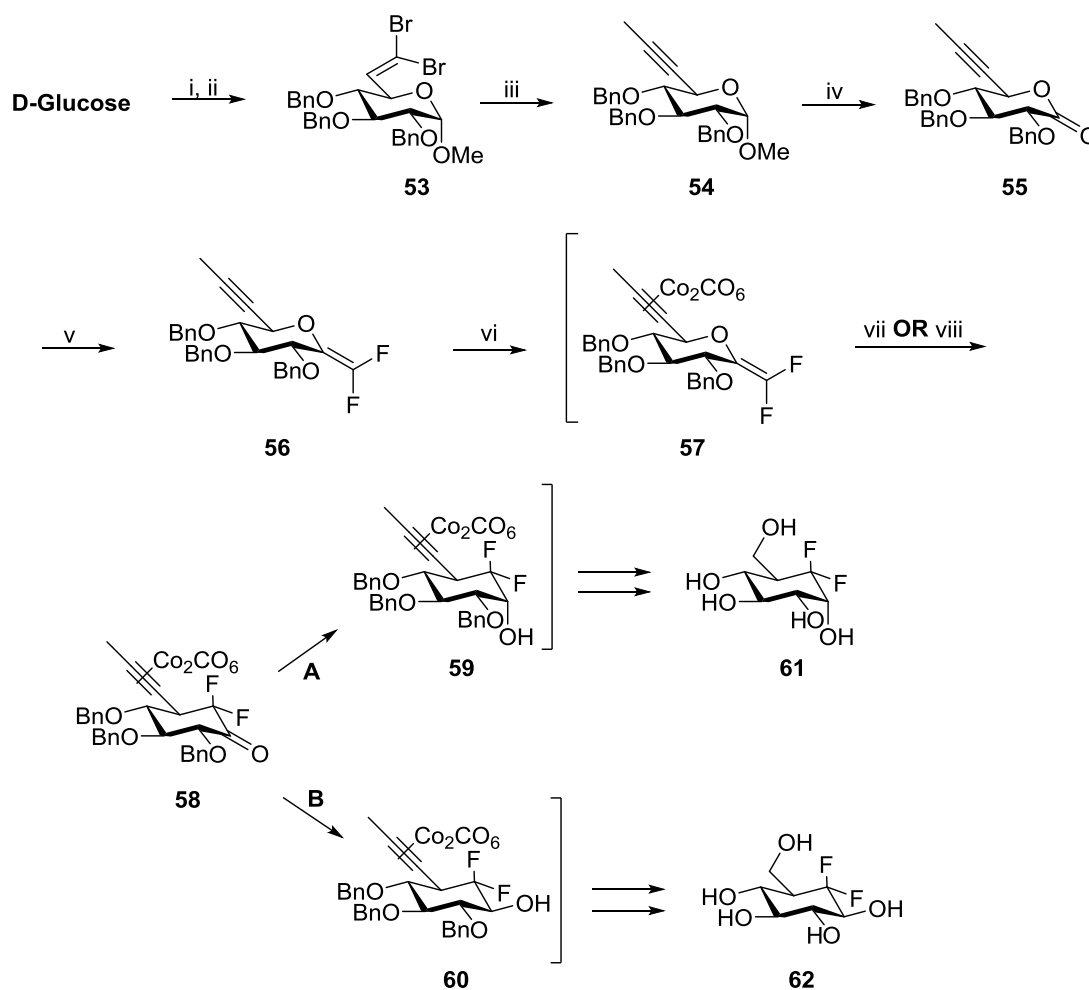


Scheme 11: Synthesis of *gem*-dimethylaminocarbasugar **52**.⁶⁷ i) , acetone, aq. HCl (37%, cat.), rt, 4 h (90%); ii, TBDPSCl, Et₃N, DMAP (cat.), CH₂Cl₂, rt, 3 h (98%); iii, KMnO₄, acetone, 60 °C, 2 h (74%); iv, 3,3-difluoro-3-bromopropene, *n*-BuLi, THF–ether–pentane (5:1:1), –100 °C, 2.5 h (82%); v, NaBH₄, MeOH, reflux, 5 h (66%); vi, *n*-Bu₄NF, THF, rt, 6 h (84%); vii, NaIO₄, H₂O, rt, 1 h (95%); viii, MeNH₂·HCl, pyridine, rt, 12 h (85%); ix, Ac₂O, DMAP (cat.), pyridine, rt, 12 h (100%); x, Pd(OH)₂-C (20%), H₂ (5 atm), EtOH, rt, 19 h (92%). Overall yield ≈ 2.2% from **46**.

Furthermore, 3,3-difluoro-3-bromopropene is an expensive building block and its synthesis is not trivial. The synthesis of this halide precursor, BrCH₂CH₂CF₂Br, requires

specialised high pressure equipment for the reaction between dibromodifluoromethane and ethylene.⁶⁸

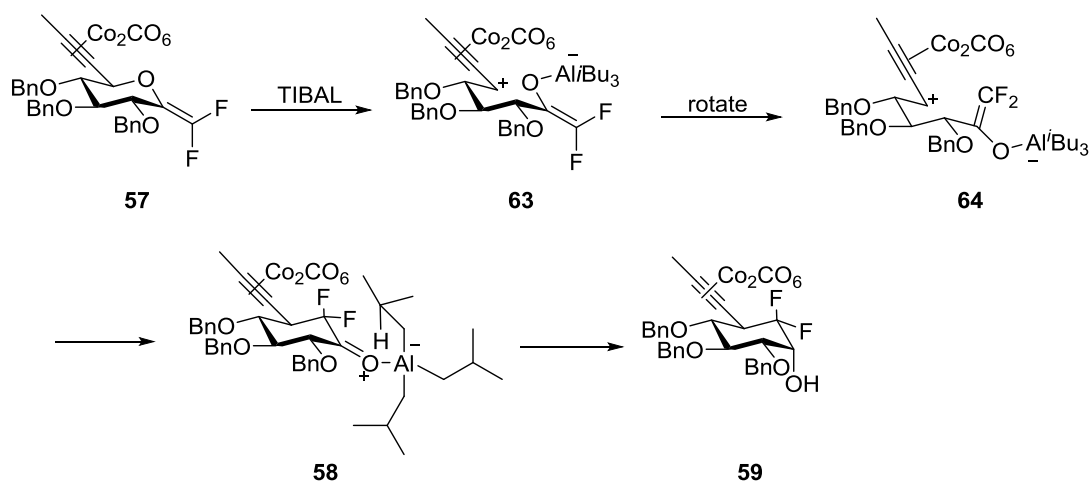
Deleuze *et al.* reported the synthesis of both *gem*-difluorinated α - and β -D-glucopyranoses for the first time by employing either a TIBAL or Cl_3TiOiPr based O-C rearrangement (**Scheme 12**).⁶⁹



Scheme 12: Deleuze's rearrangement chemistry to difluorinated glucopyranoses **61** and **62**.⁶⁹ i) Swern oxidation; ii) CBr_4 , PPh_3 ; iii) $n\text{-BuLi}$ (2.1 equiv.), MeI , HMPT , -78°C , 75% over three steps; iv) a) Ac_2O , H_2SO_4 (1 equiv.), 0°C , 75%; b) MeONa (4 equiv.), MeOH , 0°C , 90%; c) PCC (3 equiv.), 4 \AA molecular sieves (3 equiv.), DCM , rt , 74%; v) HMPT (10 equiv.), CBr_2F_2 (5 equiv.), THF , rt vi) $[\text{Co}_2(\text{CO})_8]$ (1.5 equiv.), DCM rt ; vii) TIBAL (5 equiv.), toluene, rt (**Path A**); viii) Cl_3TiOiPr (2 equiv.), DCM -78°C , Et_3BHLi (2 equiv.) (**Path B**); Overall Yield $\approx 16\%$ and 18% for **61** and **62**, respectively over 16 steps from **53**.

Protection of the appropriate hydroxyl groups in D-glucose followed by oxidation and a Ramirez-Corey-Fuchs reaction afforded alkyne **54**. A one pot procedure, whereby acetylation at the anomeric position followed by hydrolysis and oxidation delivers lactone

55. Difluorinated species **56** was prepared according to the procedure reported by Motherwell *et al.*,⁷⁰ which utilises dibromodifluoromethane as a building block and reacts with HMPT to generate a difluorinated ylide *in situ*. This species reacts with the lactone in a Wittig reaction to afford **56**. The addition of dicobalt octacarbonyl generates the Nicholas complex **57** *in situ*. At this point, depending on the target compound, O-C rearrangement can be mediated either by the addition of TIBAL or Cl_3TiOiPr with both transformations progressing through the common intermediate ketone **58**. This key metal mediated rearrangement is equivalent to the Ferrier carbocyclization reaction. In this case however rearrangement of the difluoro enol ether pyran **57** does not require the addition of mercury salts, as is usually required.⁷¹ The initial addition of TIBAL results in ring opening to form the propargylic cation **63** (Scheme 13). The stability of this dicobalt hexacarbonyl species lies in the ability to delocalise the positive charge onto the $\text{Co}_2(\text{CO})_6$ moiety.⁷²



Scheme 13: TIBAL induced O-C rearrangement mechanism followed by stereoselective TIBAL reduction.²²

The long lived nature of **63** allows for bond rotation to occur followed by ring closure to afford ketone **58**. In the case of the TIBAL induced rearrangement pathway, selective reduction of ketone **58** occurs with delivery of hydride from the less hindered equatorial position to give alcohol **59** (Scheme 13). Path B represents the Cl_3TiOiPr mediated rearrangement and in this case addition of a reducing agent, LiEt_3BH , is required. Whilst the selectivity for TIBAL reduction was based on steric grounds, selectivity for hydride delivery from the axial position using LiEt_3BH is controlled by electronic effects where hydride adds to be antiperiplanar relative to the axial C-F bond.⁷³ Alcohols **59** and **60** were then subjected to CAN (ceric ammonium nitrate) oxidation, to remove the cobalt complex, reduction, ozonolysis, further reduction, and finally benzyl group deprotection

to afford enantiopure *gem*-difluorinated α - and β -D-glucopyranose, **61** and **62**, respectively. The group has used the same TIBAL-reduction rearrangement to produce *gem*-difluorinated analogues of mannopyranose, **65a** and **65b**, and galactopyranose, **66a** and **66b**, (Figure 25).⁷⁴

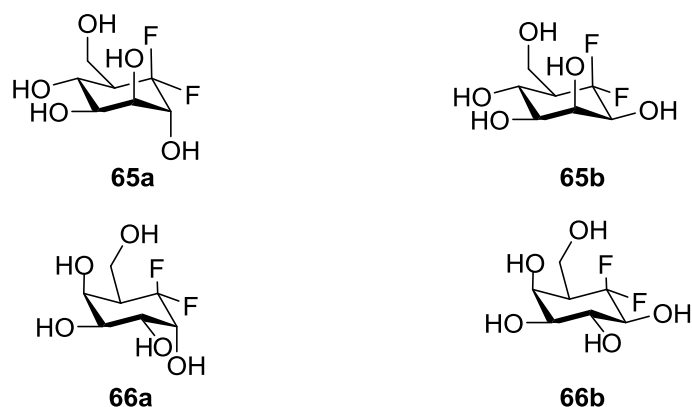


Figure 25: Difluorinated sugar analogues synthesised by Sardinha *et al.*: *gem*-difluorocarba- α -D-mannopyranose, **65a**; *gem*-difluorocarba- β -D-mannopyranose, **65b**; *gem*-difluorocarba- α -D-galactopyranose, **66a**; *gem*-difluorocarba- β -D-galactopyranose, **66b**.⁷⁴

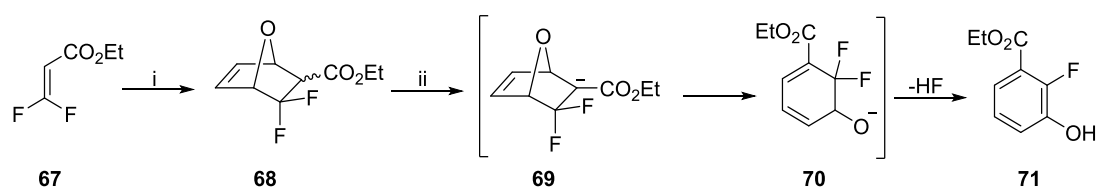
Ultimately, whether it be through the use of fluorinating agents or *via* intramolecular rearrangements, all the methods described required the use of carbohydrate precursors to produce difluorinated cyclitol analogues. The abundance of naturally occurring cyclitol starting materials is limited and this restricts the diversity of difluorinated analogues which can be accessed; a different starting material and often a different route is required for each novel target. To overcome this problem, synthetic chemists have designed building block approaches starting from fluorinated small molecule precursors to allow access to an array of sugar analogues. Not only do these approaches provide the possibility of accessing a range of analogues, but they also allow for the possibility of controlling product stereochemistry.⁷⁵

2.6.2 Synthesis of fluorocarbasugars starting from fluorinated building blocks

The necessity to overcome the issues associated with fluorinating agents has inspired chemists to explore new synthetic routes to fluorinated sugar analogues. Successful examples in the literature for the formation of the *gem*-difluoromethylene carbocycle skeletons utilise either one of two major transformations: cycloadditions or ring closing metathesis.²²

2.6.2.1 Cycloadditions

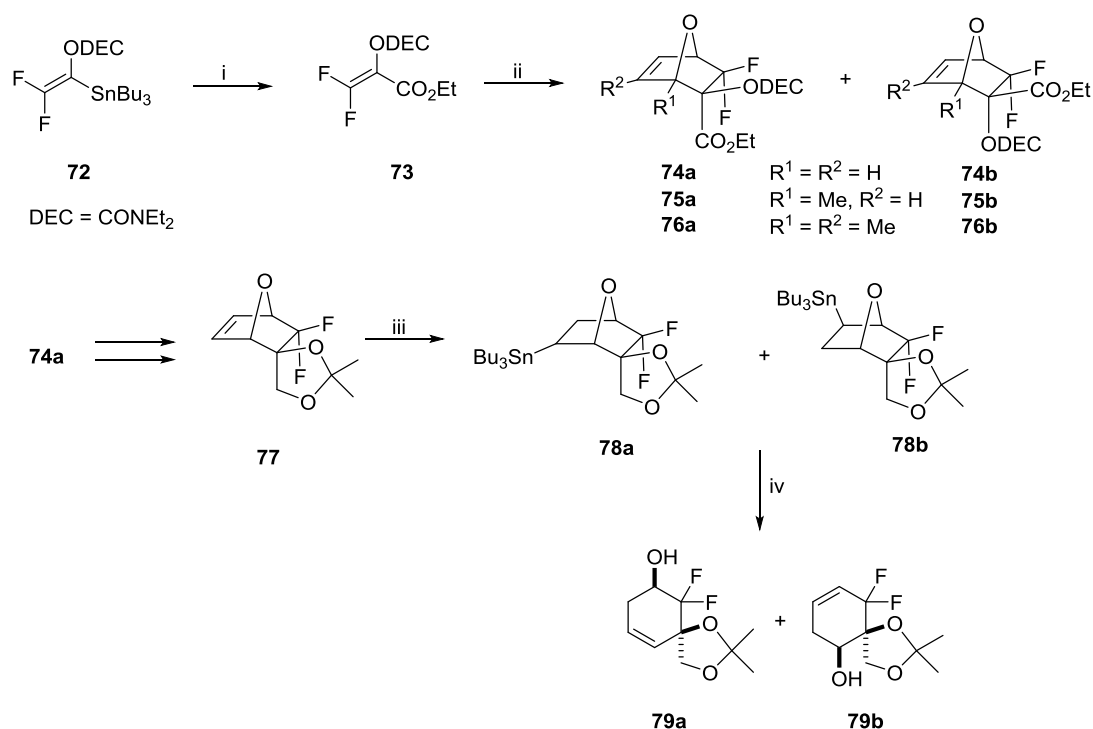
One particularly useful method for the formation of difluorinated cyclohexane derivatives involves a Diels-Alder [4+2] cycloaddition. The LUMO energy of fluorinated dienophiles are thought to be very similar to those of their defluorinated counterparts, an effect known as the perfluoro effect. From an FMO perspective, desfluorinated and difluorinated derivatives could therefore behave similarly in cycloadditions.⁷⁶ Wakselman *et al.* were the first to attempt this, reacting ethyl 3,3-difluoroacrylate **67** with furan (**Scheme 14**).⁷⁷



Scheme 14: Wakselman's cycloaddition and attempted ring opening.⁷⁷ i) Furan, ZnI₂, hydroquinone, 80 °C; ii) Tetrabutylammonium fluoride trihydrate.

The cycloaddition was successful, with the authors reporting a 40% isolated yield of **68** as a mixture of *endo/exo* (4:1) epimers. Base induced ring opening of **68** however did not deliver the desired diene **70**. Instead the reaction afforded phenol **71** which was produced through the loss of HF from **70** following ring opening.

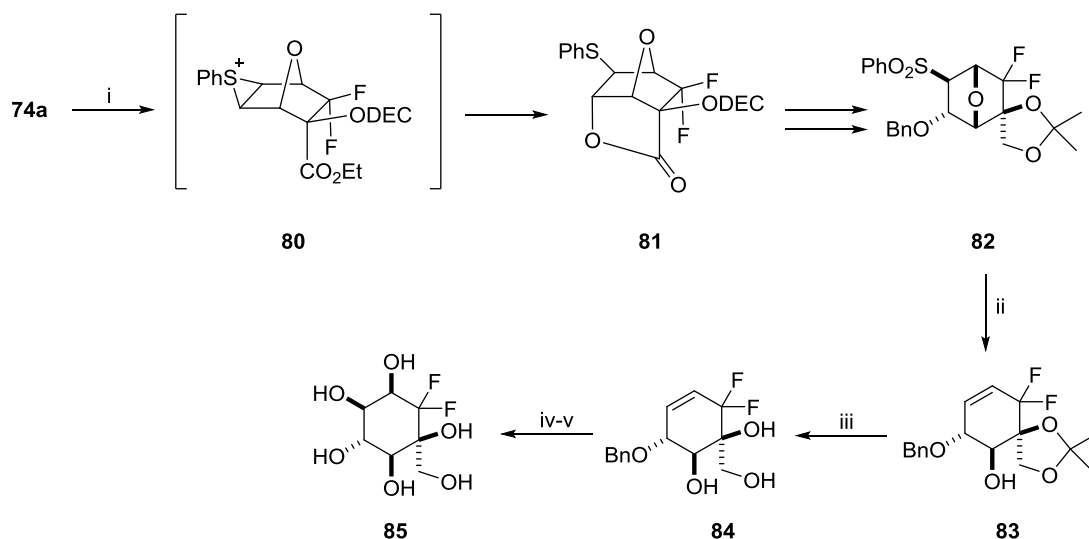
Arany *et al.* subsequently developed a methodology that could successfully ring open the product of cycloaddition using Bu₃SnH followed by MeLi·OEt₂.⁷⁸ Initial reaction of furan, 2-methylfuran and 2,3-dimethylfuran with alkenoate **73** successfully afforded a mixture of *endo* and *exo* cycloadducts **74-76**, respectively (**Scheme 15**).



Scheme 15: Preparation of difluorinated cyclohexenols via a Diels Alder reaction.⁷⁸ i) ClCO₂Et, Pd(OAc)₂, CuI, Ph₃P, THF, 60 °C, 2h, 70%; ii) furan, 2-methylfuran or 2,3-dimethylfuran, SnCl₄, DCM, rt or 0 °C, 53% **74a**, and 14% **74b** from **72**, 93% inseparable mixture of **75a** and **75b** from **72**, 53% **76b** from **72**; iii) Bu₃SnH, Pd₂dba₃.CHCl₃, PPh₃, PhMe, rt, 16h, 57% mixture of regioisomers; iv) MeLi·OEt₂, THF, 0 °C, **79a** = 71%, **79b** = 40%.

Taking **74a** as an example, hydrostannylation was non-regioselective and instead afforded a 1:1 mixture of stannanes **78a** and **78b**. It was therefore impossible to provide either one of cyclohexenols **79a** or **79b** exclusively without careful separation of the regioisomeric stannane mixture. Despite the inability to control regiochemistry and the use of highly toxic tin species, this was the first time difluorinated cyclohexenols had been prepared *via* a cycloaddition route.

This same methodology was utilised by Crowley *et al.* who managed to overcome the major issues regarding regioselective ring opening (**Scheme 16**).⁷⁹



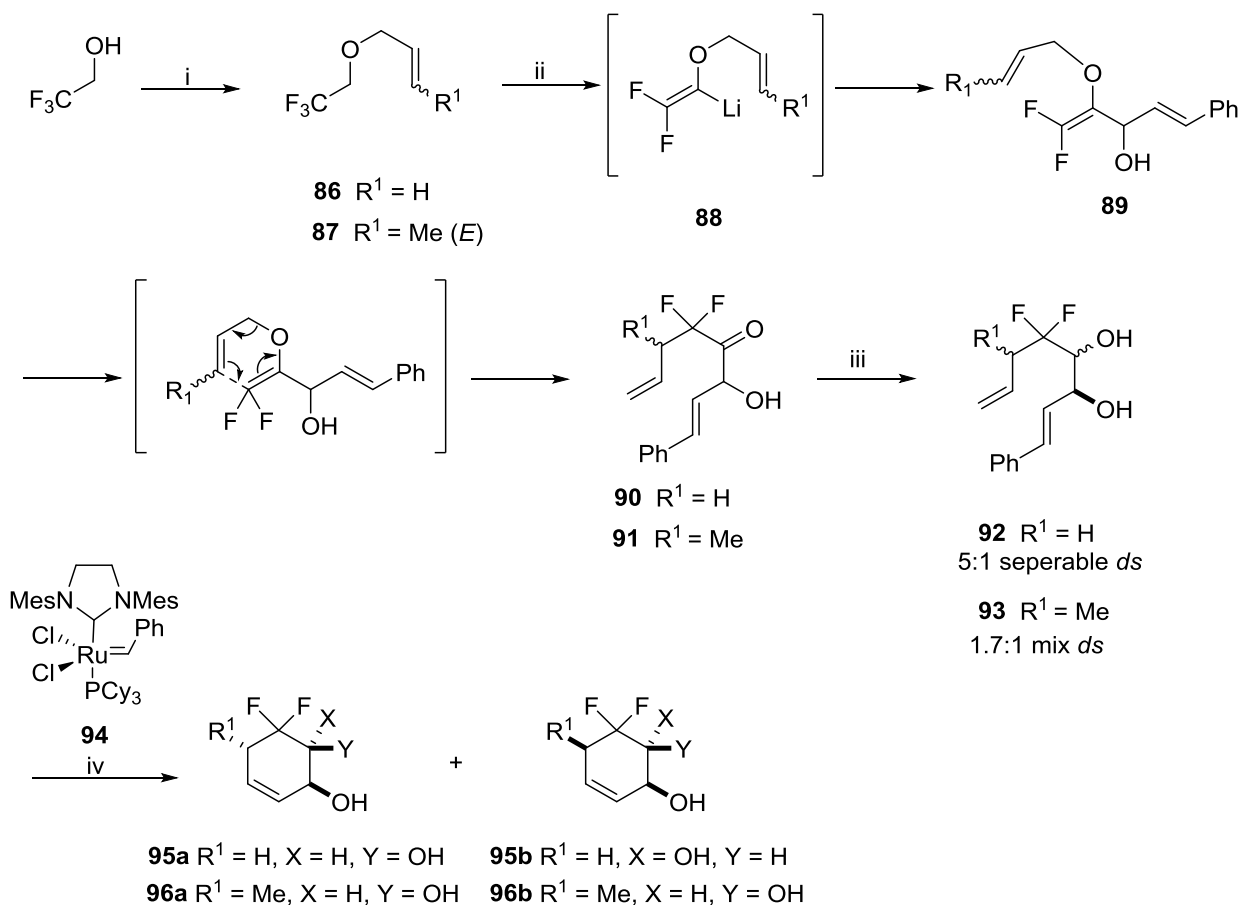
Scheme 16: Regiochemical control for synthesis of fluorinated cyclohexane derivatives **85**. i) PhSCL, CHCl₃, rt, 89%; ii) Mg, HgCl₂, EtOH, 0 °C, 50%; iii) Amberlyst-15, MeOH, 85%;; iv) OsO₄, NMO, *t*-BuOH-acetone-water, 63%; v) H₂, 5% Pd/C, EtOH, 100%. ⁷⁹

The same Diels-Alder cycloaddition conditions were used to deliver the cycloadducts **74-76**. However, instead of employing a hydrostannylation/stannate ring opening procedure, the episulfonium intermediate **80** was generated by reaction of **74a** with phenylsulfenyl chloride. The formation of this intermediate *in situ* allows neighbouring group participation of the ester functionality to deliver lactone **81**, with the thiophenyl group residing exclusively on C-6. Reduction followed by protection could deliver the difluorinated cyclitol species **82**. Reductive desulfonative ring opening with HgCl₂ and Mg afforded the difluorinated cyclohexene **83** which could be dihydroxylated and deprotected to deliver the densely functionalised polyol **85**. This synthesis provides a concise regiocontrolled route to difluorinated cyclitol species **85**. One major problem however is that the initial [4 + 2] cycloaddition often produces a mixture of endo/exo cycloadducts which require careful separation by chromatography. In some instances the diastereomers were inseparable and the cycloadducts were progressed as an isomeric mixture. Moreover, the synthesis of **85** is lengthy requiring various protection/deprotection steps which ultimately has a detrimental effect on overall yield (approximately 5% **85** over eight steps). The synthesis also necessitates the use of highly toxic SnCl₄ in the initial cycloaddition.

2.6.2.2 Ring Closing Metathesis (RCM)

Audouard *et al.* developed a method to access difluorocyclitol analogues starting from inexpensive and readily available starting materials. Construction of the carbocyclic skeleton was achieved by applying Grubbs 2nd generation catalyst **94** in a ring closing metathesis reaction (**Scheme 17**).⁸⁰ Treatment of trifluoroethanol with the appropriate

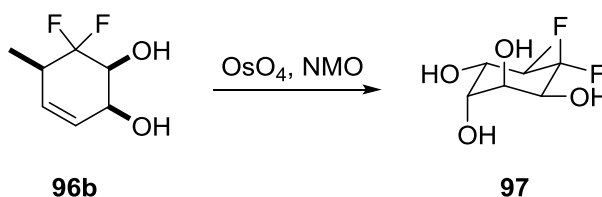
allyl halide delivered the allyl ethers **86** and **87** in good yield (99% and 87%, respectively).



Scheme 17: Formation of racemic difluorinated cyclohexene diols **95a-96b**.⁸⁰ i) KOH, allyl halide, 99% for **86** and 87% for **87**; ii) a) 2.2 equiv. *t*-BuLi, 0.9 equiv. cinnamaldehyde; iii) 3.0 equiv. NaBH₄ for **90**, 2.0 equiv. NaBH₄ for **91**, 57% major diastereoisomer and 11% minor diastereoisomer of **92**, 51% mix of diastereoisomers of **93**; iv) 1 mol % **94**; *cis*-**95a** (86%), *trans*-**95b** (82%), *cis,trans*-**96a** (33%) and *all cis*-**96b** (15%).

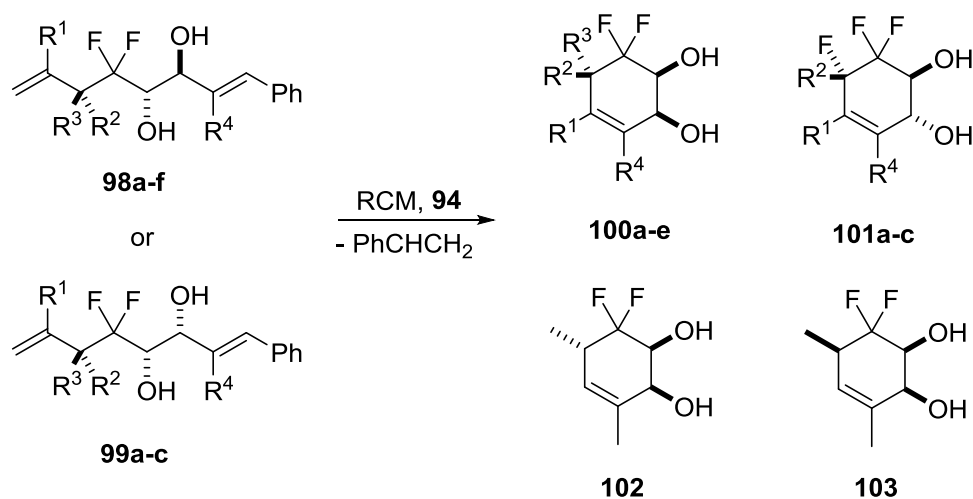
The next step in the reaction involved a dehydrofluorination/metallation process with the lithiated enol ether species **88** generated *in situ* reacting upon addition of the electrophile, cinnamaldehyde. When *n*-BuLi was used as the base and acrolein as the electrophile, the products from the reaction with ether **86** proved to be volatile and extremely difficult to handle. Moreover, a significant by-product from this reaction was hept-1-en-3-ol formed from the direct addition of *n*-BuLi to acrolein. However, by using *t*-BuLi as the base and cinnamaldehyde as the electrophile this side reaction was completely suppressed. Allylic alcohol **89** then underwent a [3,3]-Claisen rearrangement to afford dienes **90** and **91**. Diene **90** could be reduced with NaBH₄ to obtain a diastereomeric mixture of diols **92** which could be separated by flash chromatography. Both the *syn*- and *anti*- 1,2-diastereoisomers of diol **92** could undergo RCM to give a

racemic mixture of cyclohexene diols **95a** and **95b**, respectively. Unfortunately, the *syn*- and *anti*- diastereoisomers of monomethylated diol **93** could not be separated and subsequent reaction of the mixture delivered the diastereomerically pure compounds **96a** and **96b** in poor yield (33% and 15%, respectively). Formation of the olefin-containing cyclohexene diols **95a-96b** meant that they could be subject to stereoselective transformations such as the case for **96b** which was transformed to tetrol **97** by Upjohn dihydroxylation, **Scheme 18**.



Scheme 18: Asymmetric dihydroxylation of *cis*-**96b**. i) 5 mol % OsO₄, 2.0 equiv. NMO, *t*-BuOH, Acetone, H₂O, rt, 79%.

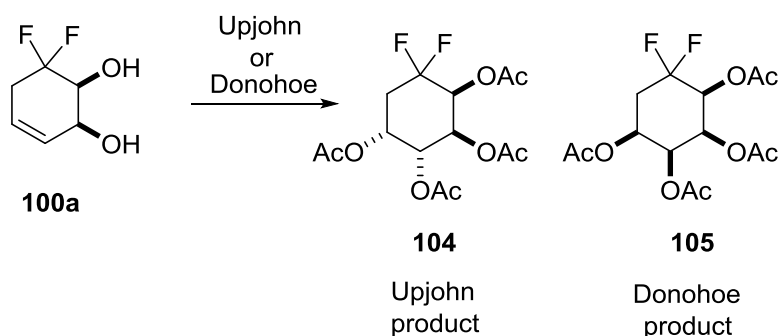
K  rour  dan then explored the scope of this reaction by using the same conditions to prepare a small library of cyclic diols from diols **98a-99c**, with results of these RCM reactions displayed in **Table 6**.¹⁹ Unfortunately, in the cases of **98d**, and **98f** pre-catalyst loading had to be increased to 8.5 mol %.

Table 6: Isolated yields of racemic mixtures of cyclic diols **100-103**.¹⁹

Diol	R ¹	R ²	R ³	R ⁴	% 94	Time ^a (h)	Product	Yield (%) ^b
98a	H	H	H	H	0.5	0.75	100a	76
99a	H	H	H	H	0.5	0.75	101a	81
98b	Me	H	H	H	4	30	100b	79
99b	Me	H	H	H	5	48	101b	90
98c	H	H	H	Me	2.5	48	100c	77
98d	Me	H	H	Me	8.5	48	100d	81
98e	H	Me	Me	H	5	5	100e	83
99c	H	Me	Me	H	5	18	101c	80
<i>anti</i> - 98f ^c	H	H	Me	Me	8.5	48	102	61
<i>syn</i> - 98f ^c	H	Me	H	Me	8.5	48	103	20

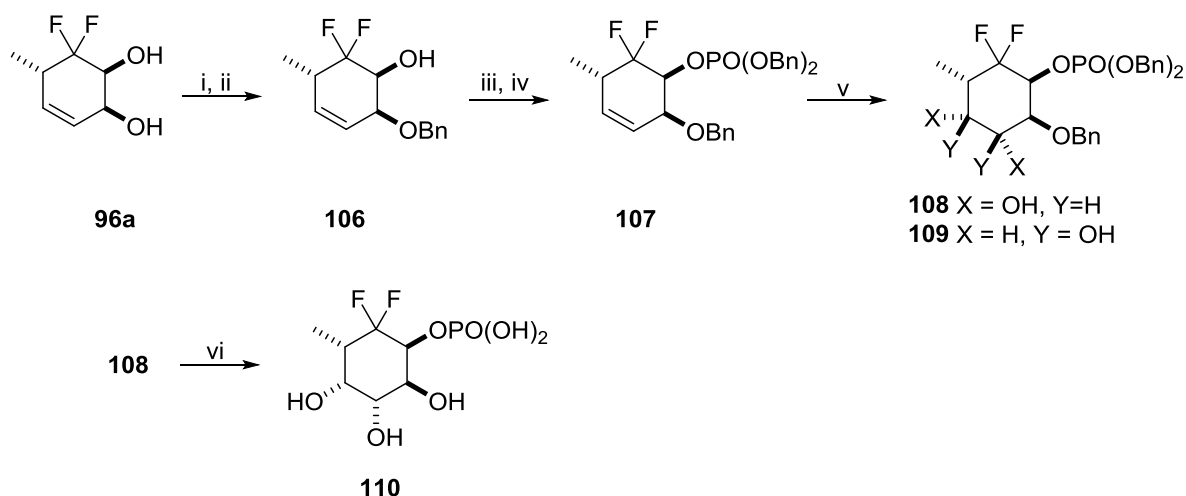
^a Time taken for 100% conversion of acyclic diol; ^b Yield of isolated purified material ^c An inseparable mixture of diastereoisomers

Treatment of cyclohexene diol derivatives **100-103** by two different dihydroxylation protocols (Upjohn or Donohoe)^{81,82} allows for rapid diversification with the ability to access two different tetrol series, **104** and **105**, respectively, from a common starting material (**Scheme 19**).¹⁹ This obviously has a significant advantage over synthesis from carbohydrate precursors where access to these series would require two separate synthetic routes using two different starting materials. Despite the high toxicity and cost of OsO₄ the reagent can be used in catalytic quantities when employed alongside a co-oxidant.⁸³



Scheme 19: Access to tetrols **104** and **105** from **100a**.¹⁹ Upjohn conditions- OsO₄, NMO, *t*-BuOH, acetone, H₂O, 58%; Donohoe conditions- OsO₄, TMEDA, DCM, 48%.

Anderl *et al.* further developed the scope of the reaction by accessing difluorinated carbasugar phosphate analogues.⁸⁴ Selective benzylation and phosphorylation could deliver cyclohexene **107** which was treated under Upjohn dihydroxylation conditions. The difluorinated cyclohexane diols **108** and **109** could be separated by careful flash column chromatography. Using **108** as an example this could undergo global deprotection to afford phosphate analogue **110** (Scheme 20).^{80,84}



Scheme 20: Synthesis of difluorinated cyclohexane phosphates.⁸⁴ i) *n*-Bu₂Sn(OMe)₂; ii) BnBr, Bu₄NI; iii) NaH; iv) [(BnO)₂PO]₂O; v) OsO₄, NMO; vi) H₂, Pd/C.

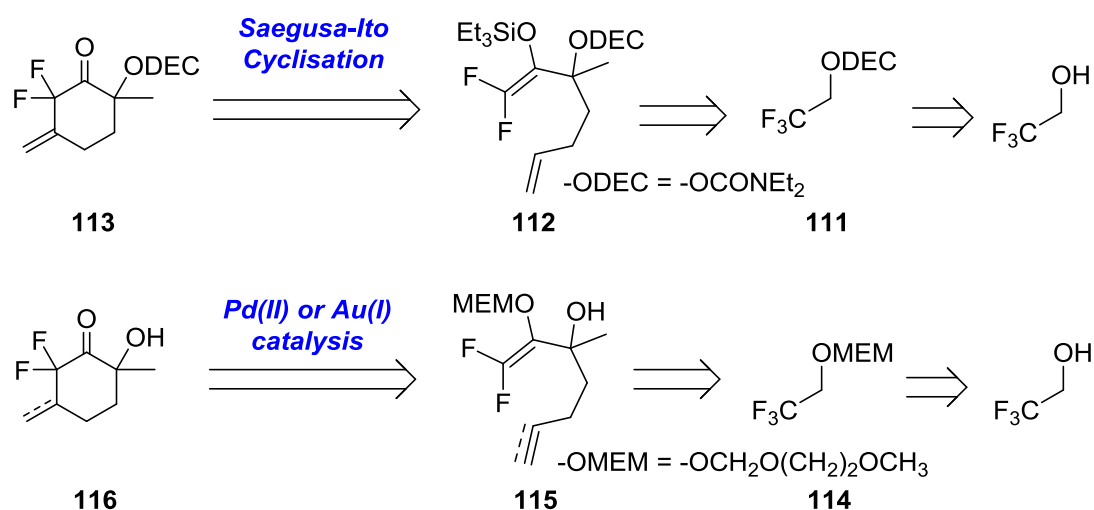
The RCM route described has a number of significant advantages. Starting from readily available and inexpensive trifluoroethanol, access to fluorinated carbasugars can be achieved in no more than four steps with minimal isolation and purification of products required. The synthesis also avoids the problem associated with starting from carbohydrate precursors in that it negates the need for a number of protecting group manipulations with each reaction being a constructive bond forming step. The olefin moiety also gives rise to a number of possible transformations on top of the Upjohn

hydroxylation, including stereoselective epoxidation and stereoselective nucleophilic epoxide opening reactions.⁸⁵

Due to the specificity of organofluorine compounds, their synthesis and reactivity can often provide a significant challenge for the synthetic chemist. Fluorinating agents are limited by their hazardous nature, poor selectivity and ability to trigger undesirable side reactions. These unappealing features have made building block methodology an attractive alternative method for the synthesis of elaborated molecules containing one or more fluorine atoms in their scaffold.

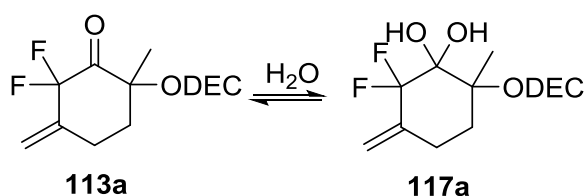
Aims

Difluorinated carbasugars constitute a unique class of carbohydrate analogue; however, there are few examples in the literature describing the *de novo* synthesis of these molecules. The work reported in this thesis has two main aims; the first is to develop the Saegusa-Ito cyclisation of difluorinated silyl enol ethers **112** as a method for the construction of cyclic difluoroketones **113**. The second is to investigate an alternative cyclisation strategy which utilises difluorinated enol acetals **115** in a novel ring closing reaction to synthesise cyclic α -hydroxy ketones **116** (Scheme 21).



Scheme 21: Retrosynthesis of cyclic difluoroketones **113** and **116**.

Whilst a successful proof of concept had been previously demonstrated for the Saegusa-Ito cyclisation the method still suffered from a number of limitations.⁸⁶ The initial yields reported for the reaction ranged from moderate (49%) to poor (22%). Moreover, the products isolated often existed as mixtures of the desired ketone and the corresponding hydrate (**Scheme 22**). Consequently, no reliable yields for pure ketones had been reported.



Scheme 22: Ketone/hydrate mixtures typically isolated from cyclisation.

Successfully isolating pure α,α -difluoroketones and significantly improving reaction yields formed the two major initial goals of the project. Achieving these goals were of critical importance if the current methodology was to represent a tractable and efficient route to difluorosugar analogues. Furthermore, the ability to effectively isolate and

understand the behaviour of these cyclic difluoroketones would serve as an excellent platform for future work within the study.

The substrate scope of the cyclisation will also be examined with the aim of expanding upon the current library of α,α -difluoroketones.

A range of copper(I) and copper(II) salts will be screened in order to gain further understanding into the influence of palladium catalyst and copper salt on the current redox system along with various Pd(II) sources. The co-catalysts to be investigated include CuCl, CuCl₂, CuOAc, Cu(OAc)₂ in combination with either Pd(OAc)₂ or PdCl₂.

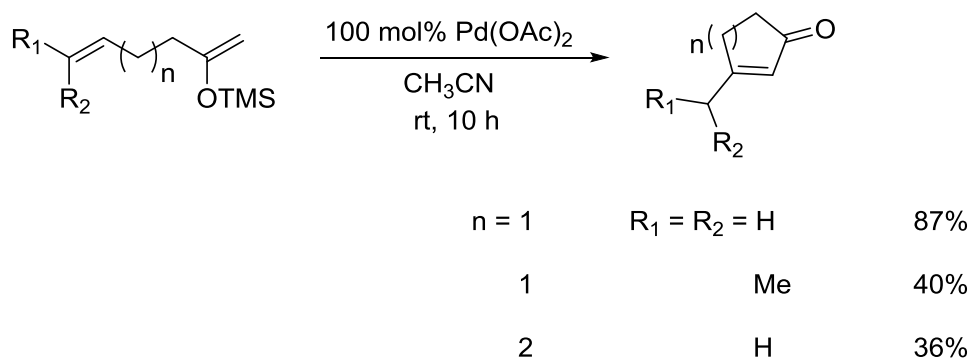
Once the Saegusa-Ito methodology has been successfully established the focus of the project will shift towards developing a novel synthetic route into difluorinated carbocycles, based on difluorinated enol derivatives **115**. These substrates are of interest as they potentially allow for a more atom efficient synthesis of cyclic difluoroketones. Initial investigations will focus on attempting to translate the oxidative palladium(II) chemistry developed for the Saegusa-Ito precursors across to these nucleophilic surrogates. If unsuccessful we will look to explore alternative transition metals, namely gold(I), to achieve the desired carbocyclisation. Gold(I) catalysis also provides a further opportunity for diversification as, depending on the choice of substrate, this would allow access to cyclic molecules bearing either an exocyclic alkene or exocyclic methyl group.

3. Chapter 2: Saegusa-Ito Cyclisation of Difluorinated Silyl Enol Ethers

3.1 Saegusa-Ito Cycloalkenylation

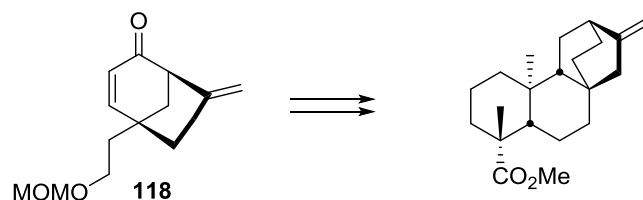
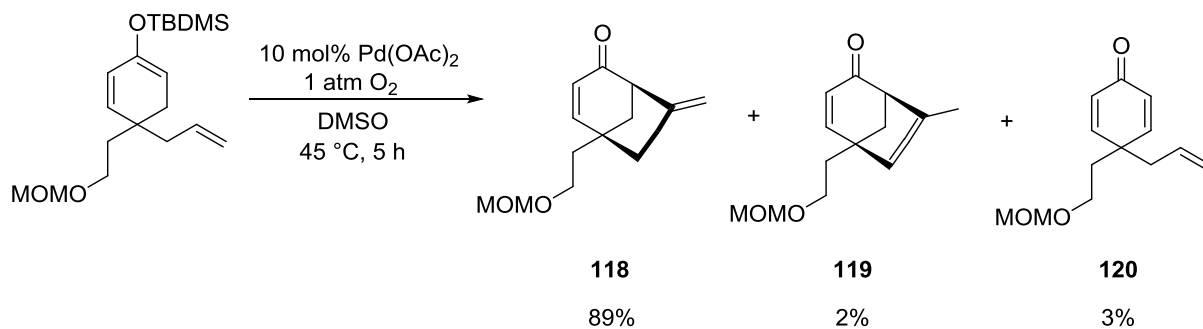
3.1.1 Discovery and Application

In their seminal publication Saegusa *et al.* described the Pd(II)-catalysed transformation of silyl enol ethers of alkenyl methyl ketones into cyclic α,β -unsaturated ketones (**Scheme 23**).⁸⁷



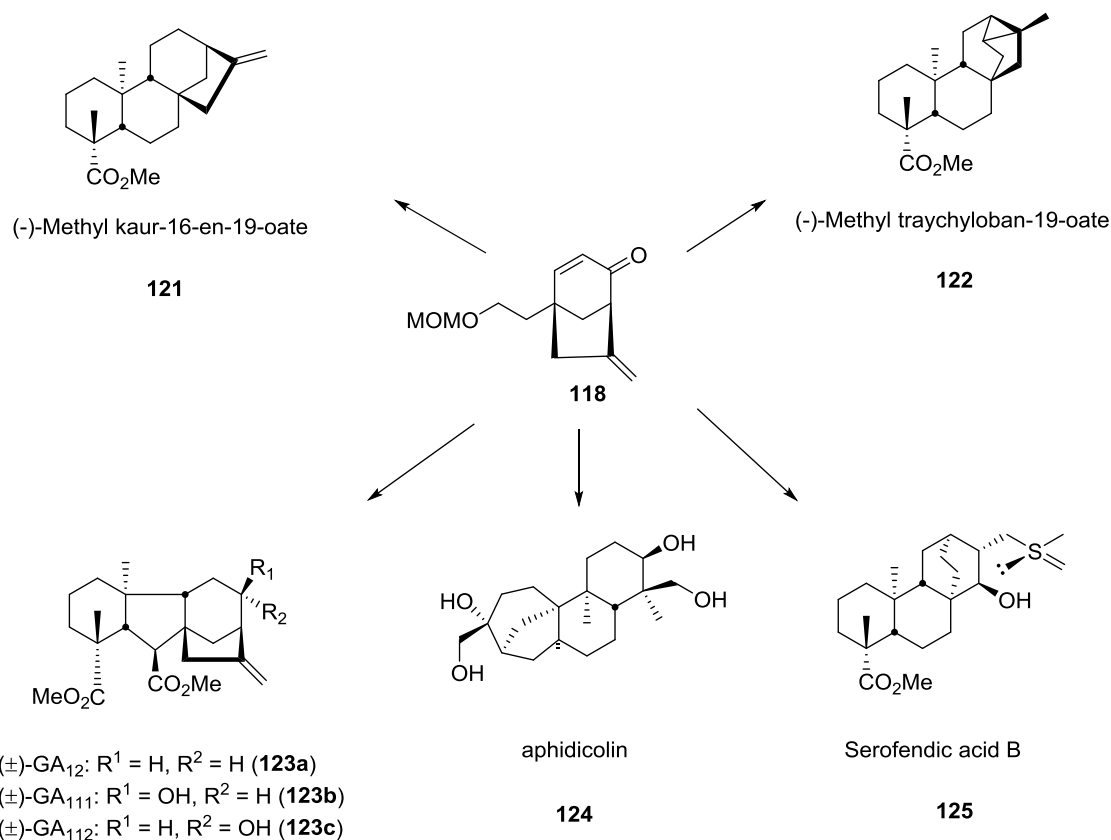
Scheme 23: Saegusa's cycloalkenylation of trimethylsilyl enol ethers.

A number of α,β -cyclopentenone derivatives were successfully synthesised using stoichiometric quantities of palladium. Although 5-membered rings were readily accessible with this methodology, 6- and 7-membered ring formation, and cyclisations onto di or trisubstituted alkenes proved to be less efficient. The reaction has been employed many times since its first publication in the formation of a number of natural products containing complex carbocyclic skeletons.⁸⁸ Remarkably, no efficient catalytic version of the reaction was disclosed until 1998. Toyota *et al.* described a palladium catalysed cycloalkenylation reaction of cross conjugated silyl enol ethers in the total synthesis of (\pm)-methyl atis-16-en-19-oate (**Scheme 24**).⁸⁹ The synthesis of bicyclo[3.2.1]octane derivative **118** was achieved in excellent yield under fairly mild conditions with **118** being a key intermediate in the overall synthetic pathway.



Scheme 24: Toyota and Ihara's palladium catalysed cycloalkenylation towards the synthesis of diterpenoid (±)-Methyl Atis-16-en-19-oate.

The bicyclo[3.2.1]octane motif has since been used by Ihara and Toyota in the synthesis of a range of natural products including (-)-methyl kaur-16-en-19-oate (**121**), (-)-methyl trachyloban-19-oate (**122**), C₂₀ gibberellins (**123a-c**) and more recently (±)-aphidicolin (**124**) and serofendic acids (**125**) (Scheme 25).^{90,91}



Scheme 25- Natural products synthesised from **118**.

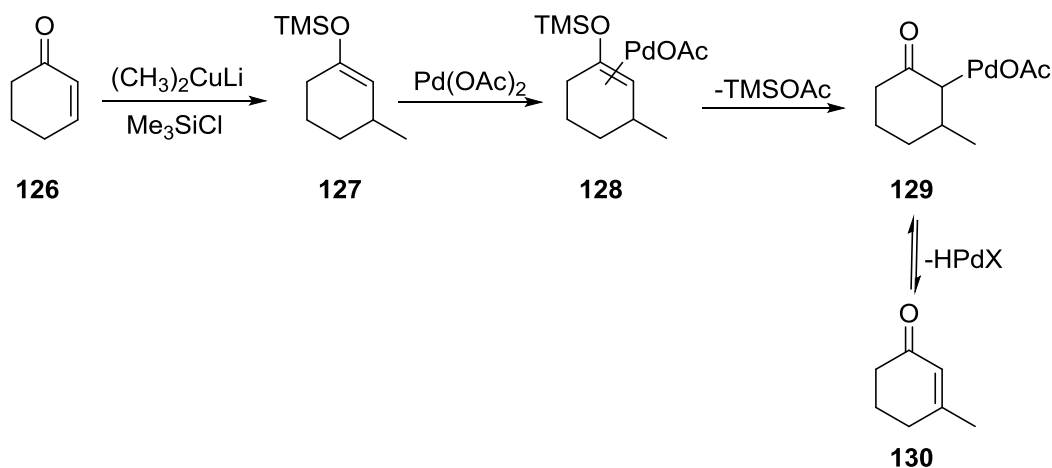
Successful cycloalkenylations required the use of bulky *t*-butyldimethylsilyl enol ethers. The product of competitive dehydrosilylation **120** was more readily observed when the

related trimethylsilyl- and triethylsilyl enol ethers were used.⁸⁹ Interestingly, and in contrast to the observations reported by Saegusa, it is the exocyclic alkene which is the most thermodynamically stable product on this template, with only trace amounts of internal alkene detected (**Scheme 24**).

There has been some debate concerning the mechanism of the Saegusa-Ito cyclisation with two different mechanistic pathways having been proposed to explain the formation of the adducts.

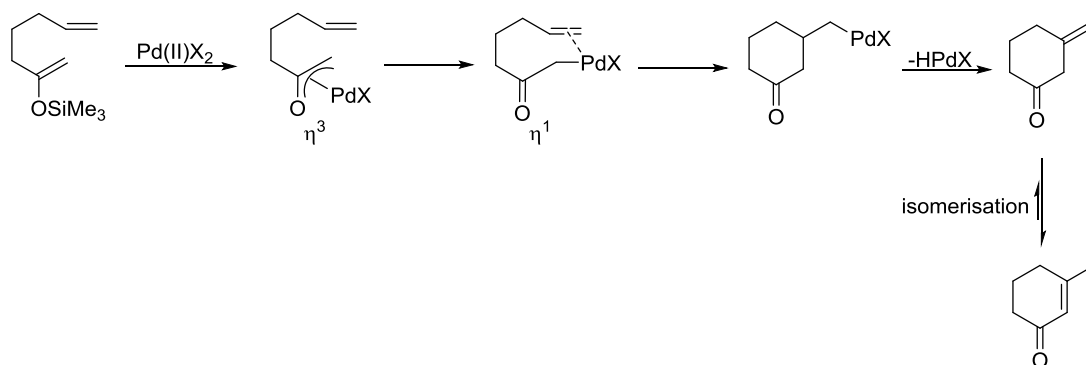
3.1.2 Mechanism of action

The mechanism of action of the Saegusa-Ito cyclisation is closely related to that of Saegusa-Ito oxidation which converts silyl enol ethers to enones (**Scheme 26**).⁹²



Scheme 26 General Saegusa-Ito oxidation.

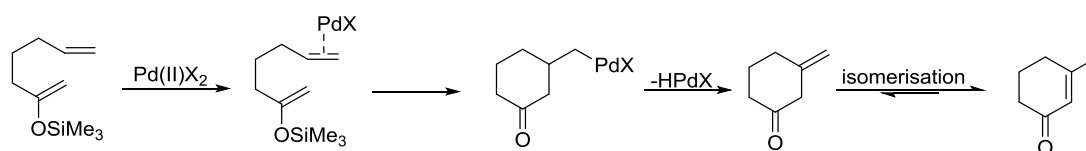
Initial 1,4-conjugate addition of lithium dialkylcuprate to enone **126** followed by the addition of TMS-Cl affords the silyl enol ether **127**. Addition of Pd(OAc)₂ initially produces the palladium-olefin coordinated species **128**. Loss of the trialkylsilyl group delivers the σ -alkylpalladium intermediate **129** which undergoes β -hydride elimination to afford enone **130**. The difference between this mechanism and the cyclisation is that in the presence of a terminal alkene moiety the oxo- π -allylpalladium(II) species can undergo carbopalladation before β -hydride elimination (**Scheme 27**).



Scheme 27: Saegusa's proposed mechanism for cyclisation henceforth referred to as the 'oxo- π -allylpalladium' mechanism.

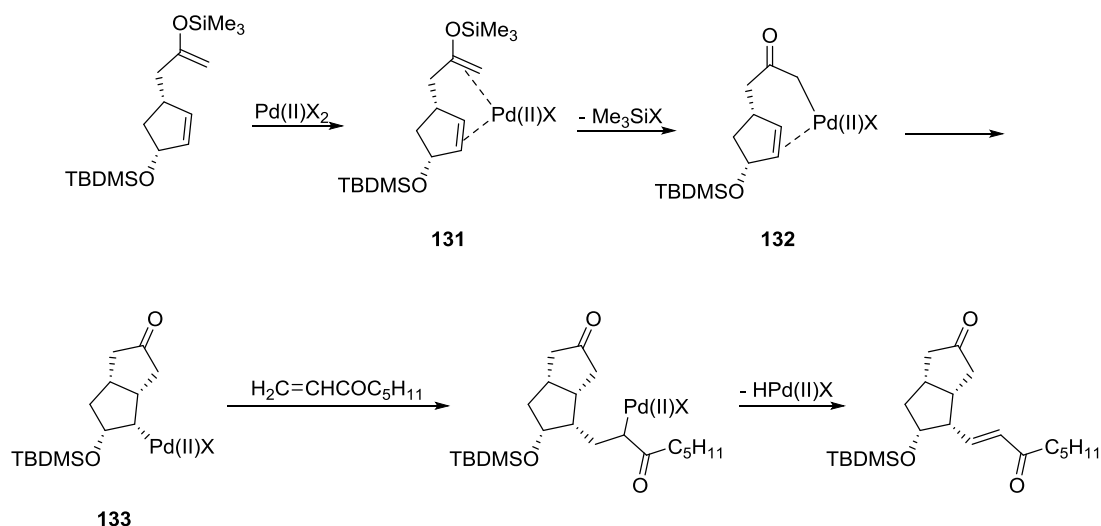
The mechanism of the Saegusa-Ito cyclisation has been debated between various research groups since its discovery in 1979. In their initial publication, Saegusa *et al.* postulated that the reaction proceeded through an η^3 oxo- π -allylpalladium(II) intermediate (**Scheme 27**).⁸⁷

Kende *et al.* have contested this proposed mechanism and argued against the formation of oxo- π -allylpalladium(II) intermediates in both cyclisation and enone formation (**Scheme 28**).⁹³ Instead they believed that initial coordination of the Pd(II) species to the terminal olefin is followed by intramolecular nucleophilic attack from the opposite face by the silyl enol ether nucleophile.



Scheme 28: Kende's proposed mechanism for cycloalkenylation *trans* to Pd.

However, in their synthesis of carbacyclin analogues *via* a palladium promoted tandem alkene insertion, Larock and Lee were in agreement with Saegusa *et al.* with regards to the formation of an oxo- π -allylpalladium(II) intermediate and ruled out the mechanism postulated by Kende based upon the stereochemical outcome of the cyclisation (**Scheme 29**).⁹⁴

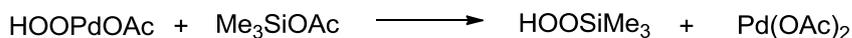
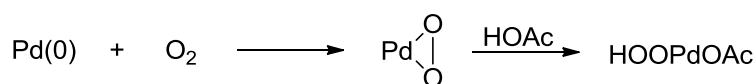


Scheme 29: Larock's stereoselective synthesis towards prostaglandin analogues.

The authors believed that Pd initially coordinates to both the silyl enol ether alkene and also the cyclopentene olefin **131**. Transformation of this species to either a σ -bonded or oxa- π -allylic palladium complex **132** is thought to occur before facile cyclisation to the all-*cis* bicycle **133**.

Toyota and Ihara have since demonstrated that the mechanistic pathway and product outcome is very much dependent on substrate and reaction conditions.⁹⁰ For example the use of bulky silanes such as TBDMS will favour nucleophilic attack *trans* to Pd whereas use of the smaller TMS enol ether will favour the 'oxo- π -allylpalladium' mechanistic pathway. Solvent choice also appears to be critical in determining the outcome of the reaction. The use of DMSO as a solvent will lead to a mixture of cyclised product and uncyclised enone due to the Lewis basic sulfur strongly coordinating to Pd(II). This slows down carbopalladation and therefore makes the process competitive with β -hydride elimination. The use of acetonitrile however overcomes this problem by acting as a more labile ligand and avoids the extensive formation of mixtures.

Larock *et al.* have also reported the use of catalytic amounts of Pd(OAc)₂ by using oxygen as the oxidant, and DMSO as the essential solvent.⁹⁵ The mechanism which they proposed for the oxidation of Pd(0) back to Pd(II) is shown in **Scheme 30**.



Scheme 30: Oxidation of Pd(0) to Pd(II) using molecular oxygen as the primary oxidant.

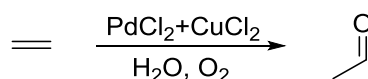
Because the concentrations of HOOPdOAc and Me₃SiOAc in solution are low, the rate at which active Pd(II) is regenerated is also low. The use of DMSO as a solvent however is sometimes not particularly viable if the substrate molecules are particularly lipophilic. It has also been reported that the solubility of oxygen gas in DMSO is relatively poor.⁹⁶

Palladium(II)-catalysed carbocyclisations such as the Saegusa-Ito reaction involving C-C bond formation by means of carbopalladation constitute an extremely useful class of reaction. Critical to the success of such cyclisation strategies is the ability to efficiently recycle palladium(II) within an appropriate redox system. Oxidative Pd(II) redox chemistry underpins much of the work detailed within this first chapter and a greater appreciation of this method of catalysis is therefore important to fully contextualise the current study. Further aspects of Pd(II)/Pd(0) oxidation chemistry and its application in the carbocyclisation of alkenes involving β-hydride elimination shall now be briefly discussed.

3.2 Palladium(II) Oxidation Chemistry

3.2.1 Background

One of the first palladium(II) catalysed processes to be reported was the Wacker process in 1959 (**Scheme 31**).⁹⁷



Scheme 31: Palladium (II) catalysed Wacker process.

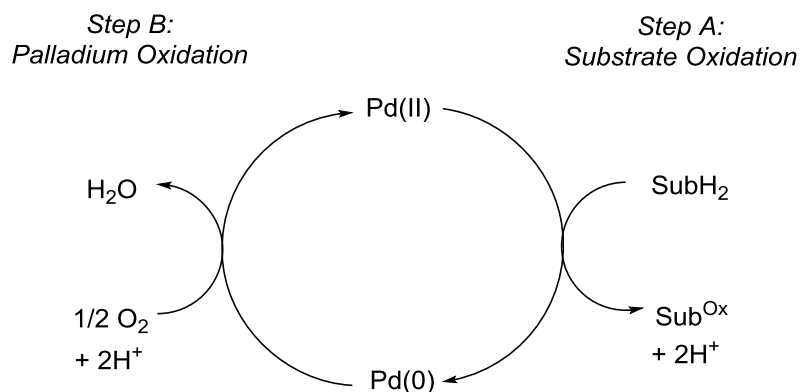
The industrially significant process involves the transformation of ethylene to acetaldehyde in the presence of catalytic quantities of PdCl₂ together with a CuCl₂ co-oxidant and molecular oxygen.⁹⁸ This initial discovery played a decisive and fundamental role in shaping modern organic synthesis by initiating an era of intense research into palladium-mediated processes. These are now essential tools with very

many applications in the syntheses of natural products, agrochemicals and pharmaceuticals.^{99,100}

The versatility of palladium in catalysis is ensured by its ability to readily interconvert between the oxidation states 0 and +2. Pd(0) complexes have d^{10} configuration and are nucleophilic at palladium whereas Pd(II) species which have d^8 configuration are more electrophilic. In recent years, considerable attention has also focussed towards Pd(IV) catalysis, in particular for the formation of carbon heteroatom bonds via C-H activation.¹⁰¹ The relatively 'soft' character of palladium gives the metal a higher affinity towards 'soft' σ and π donors compared to 'harder' groups like alcohols. As a result, palladium can readily coordinate with a host of functional groups including alkenes, alkynes and allenes.¹⁰² The bonding between a nucleophilic alkene and an electrophilic Pd(II) species leaves the olefin susceptible to nucleophilic attack. This is because of the instability associated with Pd(II)-alkene complexes due to insufficient overlap between the d-orbitals of Pd and the π^* orbitals of the alkene.¹⁰³ This feature means that Pd(II)-alkene complexes can act as catalytic species in a variety of reactions. In addition, palladium can form complexes with a variety of ligands such as *N*-heterocyclic carbenes (NHCs) and phosphines. The use of ligands in palladium catalysis is quite common practice and can be used to optimise reactions by finely tuning the electronic properties of the palladium centre.¹⁰⁴ The choice of ligand can also have major effects on the outcome of a reaction and can completely alter the reaction pathway in some cases.¹⁰⁵

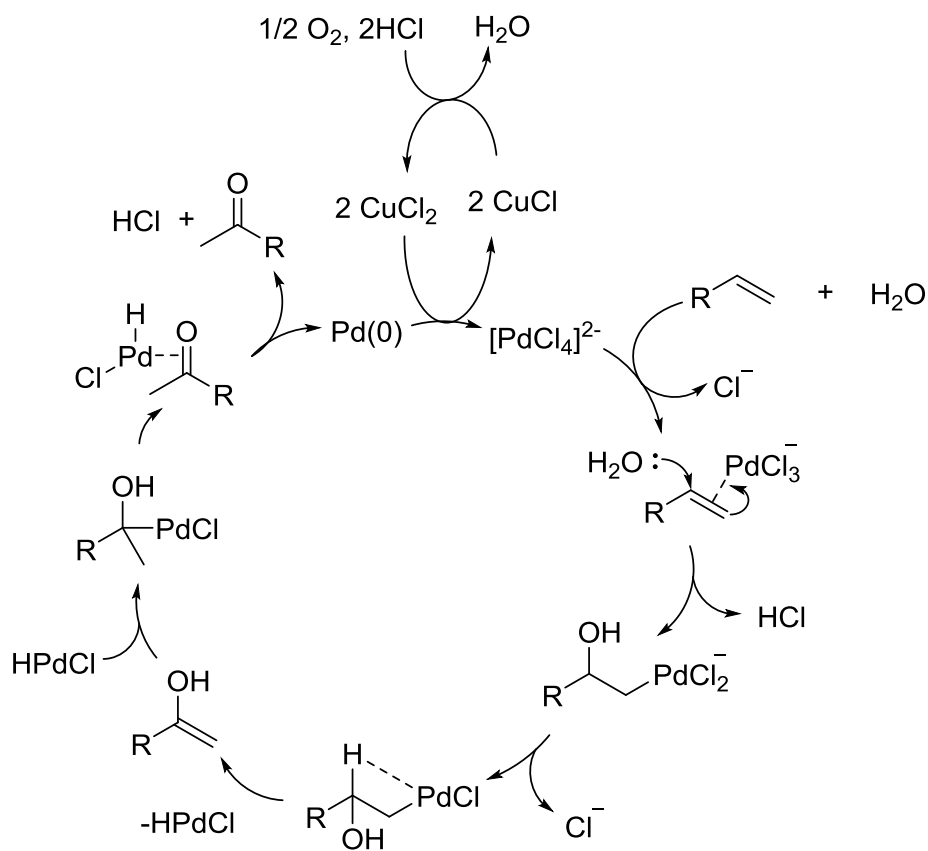
3.2.2 Reoxidation of Pd(0)

Palladium(II)-catalysed oxidation reactions are considered extremely useful methods for the selective oxidation of organic molecules. For such a process to be catalytic, the Pd(0) produced must be efficiently reoxidized back to Pd(II) to ensure turnover and to prevent precipitation of Pd black (**Scheme 32**).¹⁰⁶



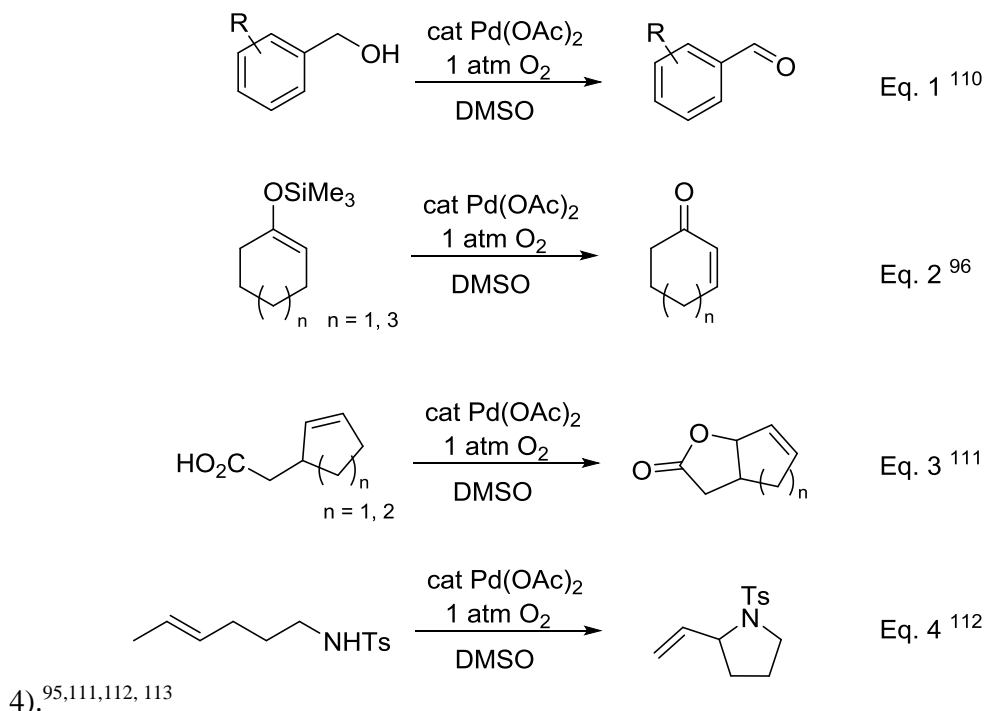
Scheme 32: Simplified catalytic cycle for palladium catalyzed aerobic oxidation reactions.

Although the majority of palladium-mediated carbon-carbon bond forming reactions are non-oxidative palladium(0) catalyzed processes, there has been revitalized interest within recent years with regards to Pd(II) catalyzed processes under oxidative conditions.^{107,108} However, one of the main problems which has hindered the development of Pd(II) methodology lies in identifying suitable reoxidation systems. Using the Wacker process as an example, the overall effect of passing through one cycle is the generation of Pd(0) (**Scheme 33**).¹⁰⁹



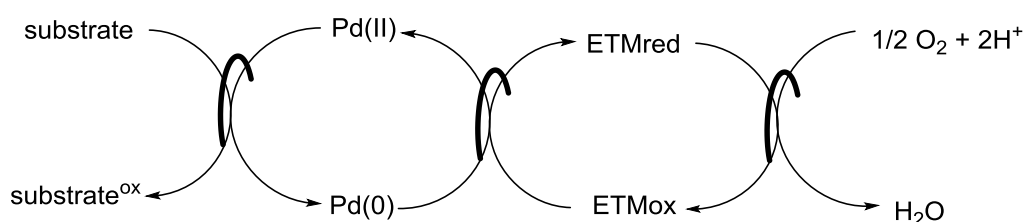
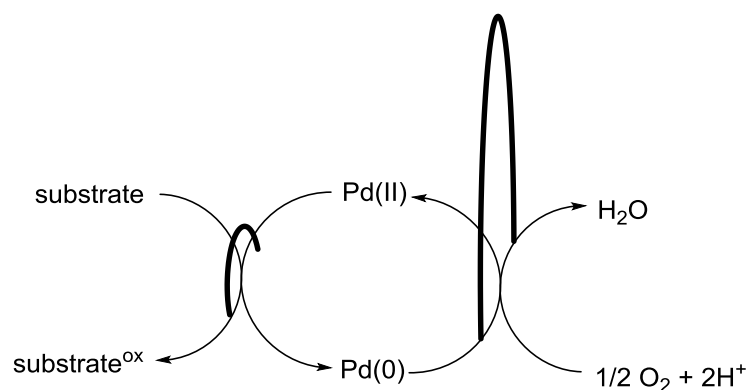
Scheme 33: Mechanism of Wacker Process.¹⁰⁹

However, finding a redox system compatible with both substrate and product is arguably one of the biggest challenges in oxidation chemistry. With its low cost and lack of environmentally hazardous by-products, molecular oxygen as a sole oxidant would be highly advantageous.¹¹⁰ There are a number of examples in the literature where molecular oxygen alone has shown to provide catalytic turnover of Pd(II), particularly in the areas of alcohol oxidation and oxidative heterocyclisations (**Scheme 34**, Eq 1-



Scheme 34: Oxidative Pd catalyzed reactions using O₂ as the sole oxidant.

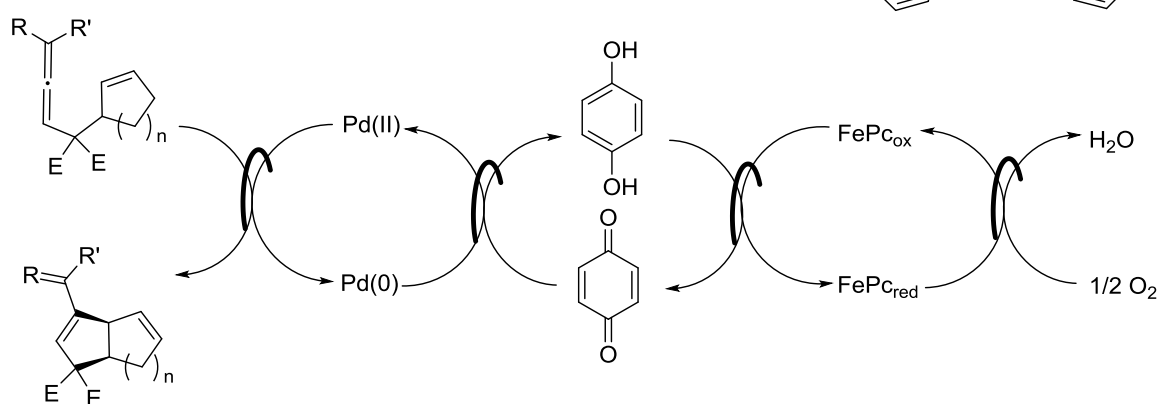
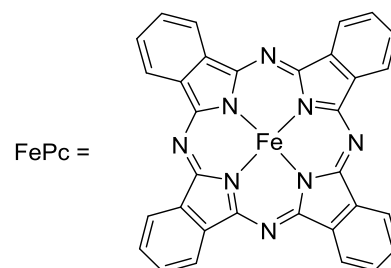
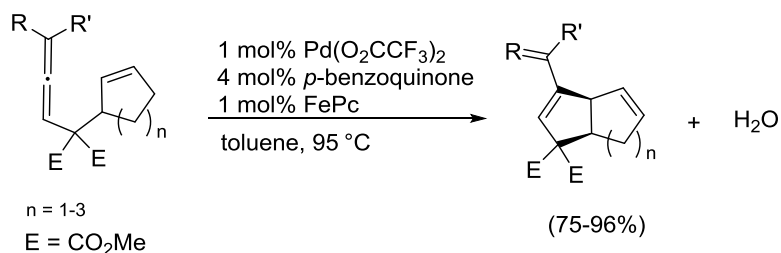
It is important to note that the use of DMSO (**Scheme 34**, Equiv. 1-4) as the solvent is critical for catalytic turnover. Stahl *et al.* have reported that DMSO coordinates strongly to Pd(II) through sulfur.¹¹⁴ The ‘softer’ character of Pd(0) relative to Pd(II) suggests that DMSO will coordinate in a similar manner *via* sulfur. It is proposed that DMSO coordinates and stabilises the Pd(0) intermediate by inhibiting its aggregation into Pd black and promoting reoxidation of the catalyst by O₂.^{96,114,115,116} Unfortunately, this approach fails in many cases because the electron transfer process between Pd(0) and O₂ is slow and aggregation of the catalyst into bulk metal is kinetically competitive.¹¹⁷ One method that chemists have used to overcome this issue uses electron transfer mediators (ETM’s). ETM’s, or co-oxidants, work by facilitating electron transfer from Mⁿ to the oxidant *via* a low energy pathway thus competing kinetically with any side reactions of the reduced form of the metal (**Scheme 35**).¹¹⁸



Scheme 35: Influence of ETM on energy barrier of electron transfer for Pd catalysed oxidative processes.

The Wacker process provides an excellent illustrative example of the principle of using an ETM with the requirement of CuCl_2 to promote $\text{Pd}(0)$ oxidation. It is proposed that an interaction between palladium and copper chloride via bridged chlorides aids in the oxidation of Pd by $\text{Cu}(\text{II})$.¹¹⁹ The CuCl produced is then readily oxidized by air back into CuCl_2 .¹²⁰ Some of the most commonly used ETM's include copper salts, MnO_2 , quinones,¹²¹ TEMPO,¹¹⁸ peroxides,¹²² and various hypervalent periodinanes.¹²³ One of the major problems associated with such oxidants however is the requirement to use stoichiometric quantities resulting in decreased atom efficiency and increasing overall waste production. Replacement of these oxidants however is far from trivial as they may also act as essential co-factors or ligands in specific transformations, removal of which may perturb the catalytic system.

A successful alternative co-factor modulated oxidation based on a novel biomimetic approach has been pioneered by Bäckvall.¹²⁴ The process has been termed biomimetic because of its similarities to enzyme mediated electron transfer processes in biological systems.¹²⁵ In their oxidative carbocyclisations of various allene substituted olefins the authors employ a triple coupled catalytic system for the aerobic allylic oxidation (**Scheme 36**).



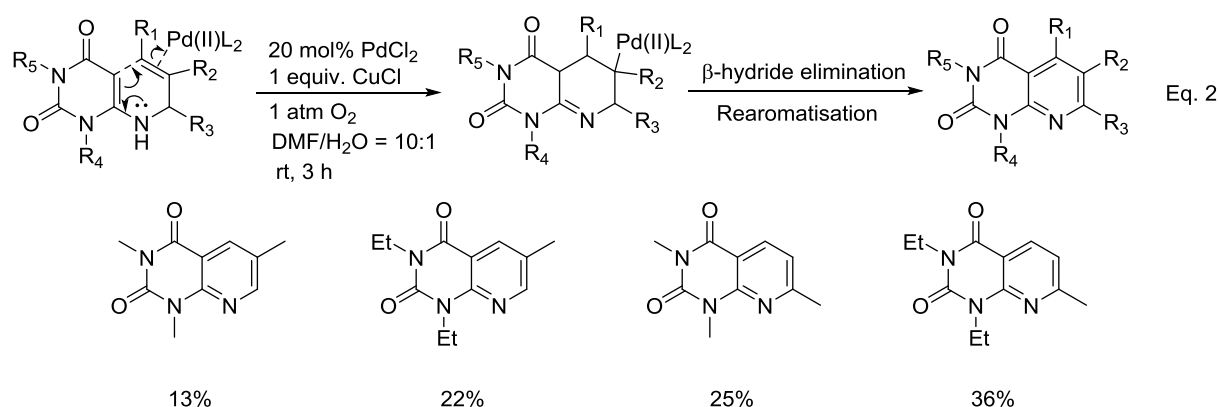
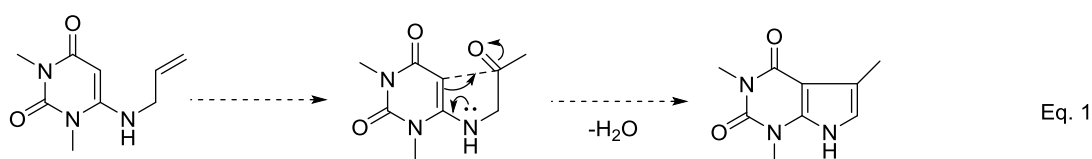
Scheme 36: Bäckvall's Biomimetic strategy.

Incorporation of an oxygen-activating macrocyclic iron(II) phthalocyanine metal complex (FePc) was essential in order for low loadings of catalyst and co-oxidants to be used. The authors went on to demonstrate the recycling potential of this metal complex by immobilising the catalyst onto a resin which could be used up to five times without any detectable loss in activity. This biomimetic approach had been used previously by Bäckvall in the allylic oxidation of olefins.¹²⁶ However, the ability for this technique to be translated across to a carbon-carbon bond forming method is especially appealing from a synthetic perspective. In fact, the number of oxidative Pd(II) catalysed carbon-carbon bond forming reactions reported in the literature is limited, particularly when compared to Pd(0) methods. The lack of Pd(II) methodology could be as a result of the problems which can arise when carbon nucleophiles are employed under oxidative conditions. Firstly, carbanions, even those which are stabilized, are susceptible to oxidation, a consequence of which is the formation of carbon radicals and subsequent side reactions.¹²⁷ Another potential problem is that the carbon nucleophile itself could reduce the catalytically active Pd(II) species to produce inactive Pd(0).¹²⁸ A number of successful examples have been reported despite these issues. The rest of this section will

now highlight successful Pd(II) oxidative carbocyclisation strategies of alkenes involving β -H elimination.

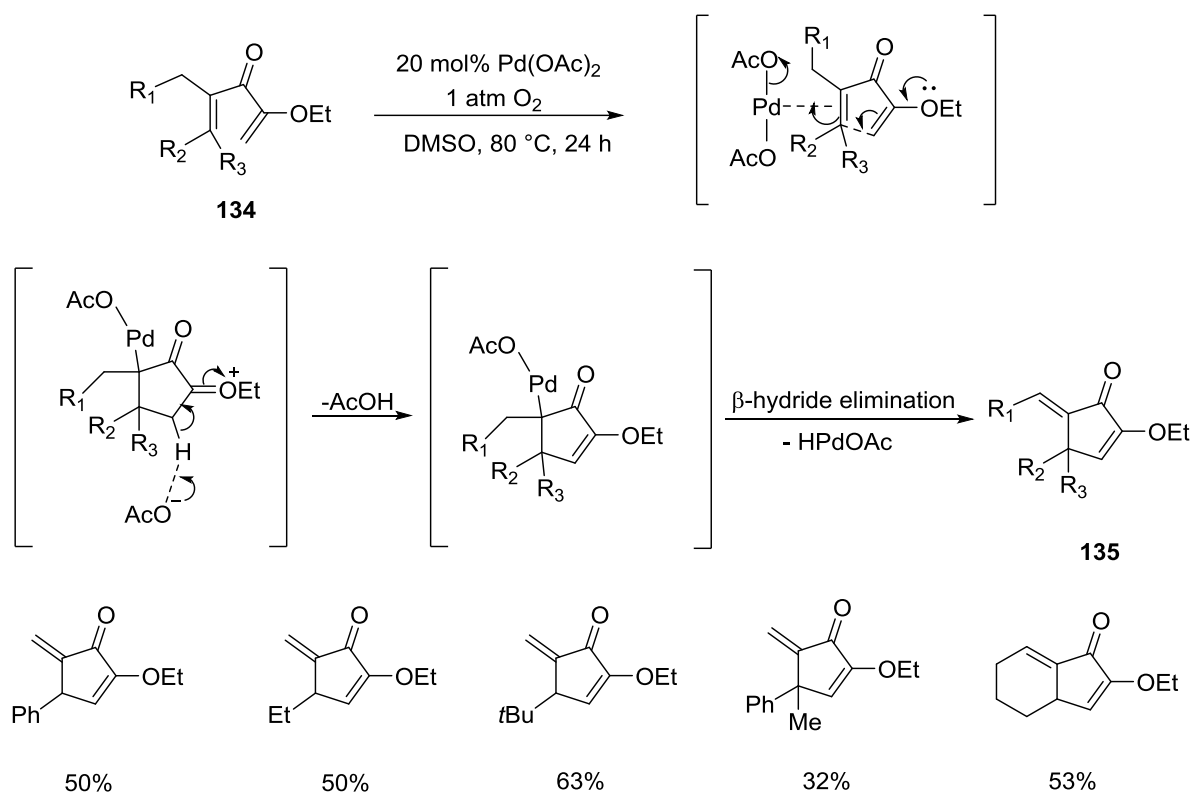
3.2.3 Intramolecular oxidative carbocyclisations involving alkene-alkene coupling

In 1985 Itoh and co-workers described a Pd(II) catalyzed oxidative cyclisation of 6-(substituted allyl)aminouracils (Eq 2, **Scheme 37**).¹²⁹ The authors had initially aimed to prepare 7-deazacaffeine derivatives from these precursors by employing Wacker conditions followed by an intramolecular cyclisation (Equiv. 1, **Scheme 37**). The outcome of the reaction however afforded the 1,3-dialkylpyrido[2,3-*d*]pyrimidines as the sole products.



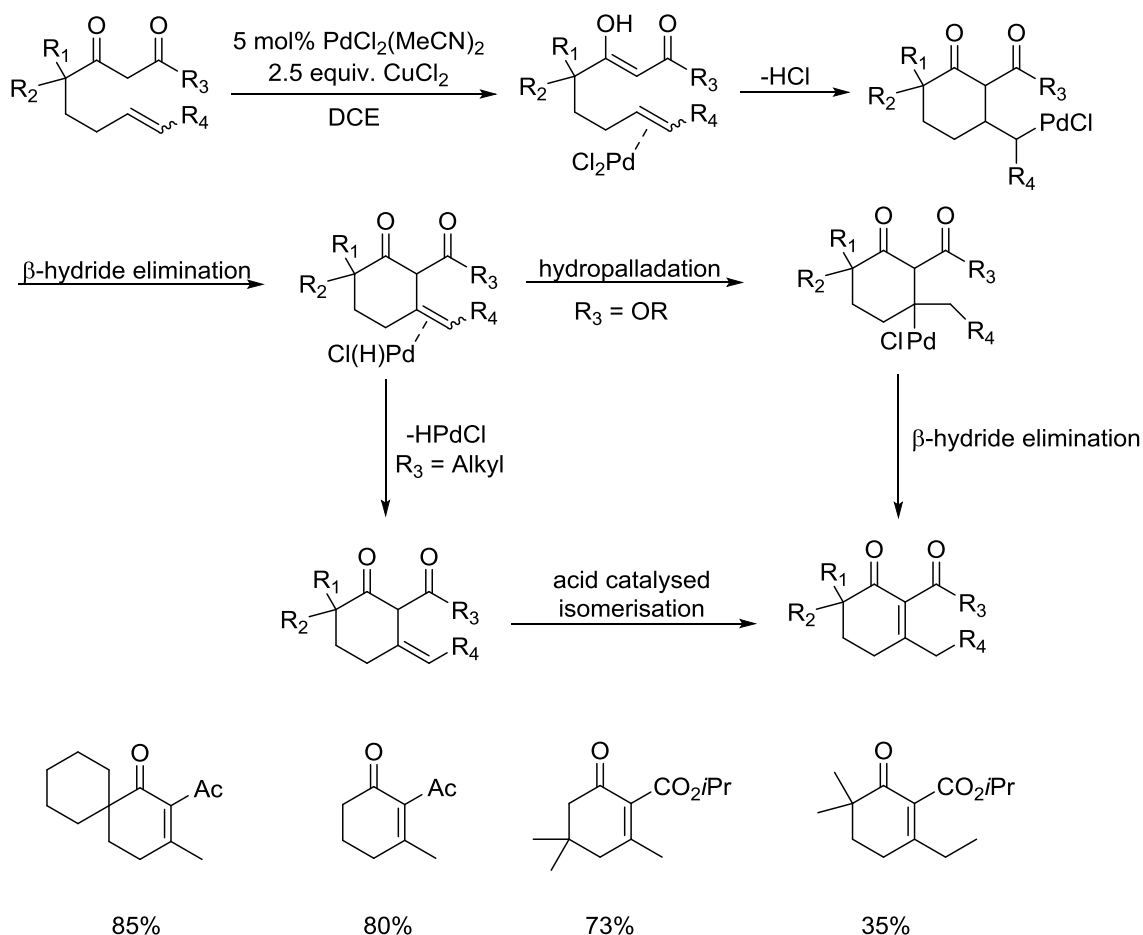
Scheme 37: Eq 1. Proposed synthetic strategy; Equiv. 2. Observed reaction outcome.

A number of highly substituted aromatic heterocycles were prepared in only 2 synthetic steps using this catalytic system. Unfortunately the reaction proved to be low yielding despite the use of stoichiometric copper and high catalyst loadings. In 2003, Tius *et al* developed an oxidative palladium catalysed Nazarov-type reaction which involved the formation of cross conjugated cyclopentenones **135** from α -alkoxydienones **134** (**Scheme 38**).¹³⁰



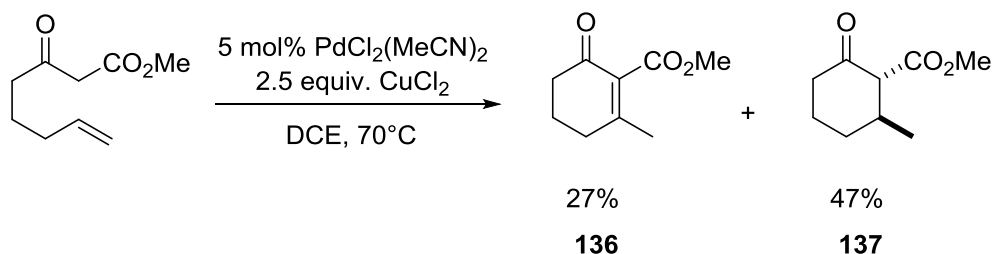
Scheme 38: Pd(II) catalysed Nazarov-type cyclisation.

The authors suggested that the electron deficient olefin is further activated by coordination to palladium; intramolecular attack of the electron rich vinyl ether followed by β -hydride elimination afforded the desired products. This methodology also required high palladium loadings and afforded only moderate yields of cyclopentenones. Widenhoefer used a similar approach in the synthesis of cyclohexenones by utilising the nucleophilic capability of the enolic carbon in a number of stabilised carbon nucleophiles (**Scheme 39**).^{131,132}



Scheme 39. Widenhoefer's oxidative alkylation of stabilised carbon nucleophiles.

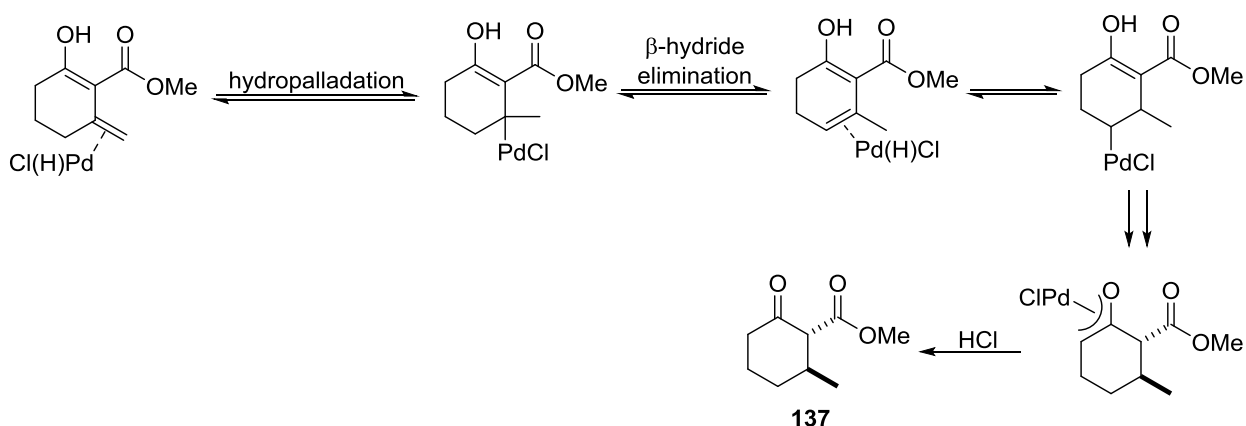
A number of stabilized carbon nucleophiles were tolerated and successfully cyclised under the reaction conditions including some which possessed substitution at the pendant olefin, though these reacted in only modest yield. However, the substrate scope was limited to that of stabilized carbon nucleophiles with enolization of the β -diketones and β -ketoesters critical for reactivity. An interesting observation reported was that unsubstituted β -diketones could undergo a competing hydroalkylation pathway (**Scheme 40**).



Scheme 40: Competing oxidative hydroalkylation pathway for unsubstituted β -ketoesters.

The authors propose that this competing pathway arises following hydropalladation where subsequent migration of palladium to the C6 carbon atom of the cyclohexanone

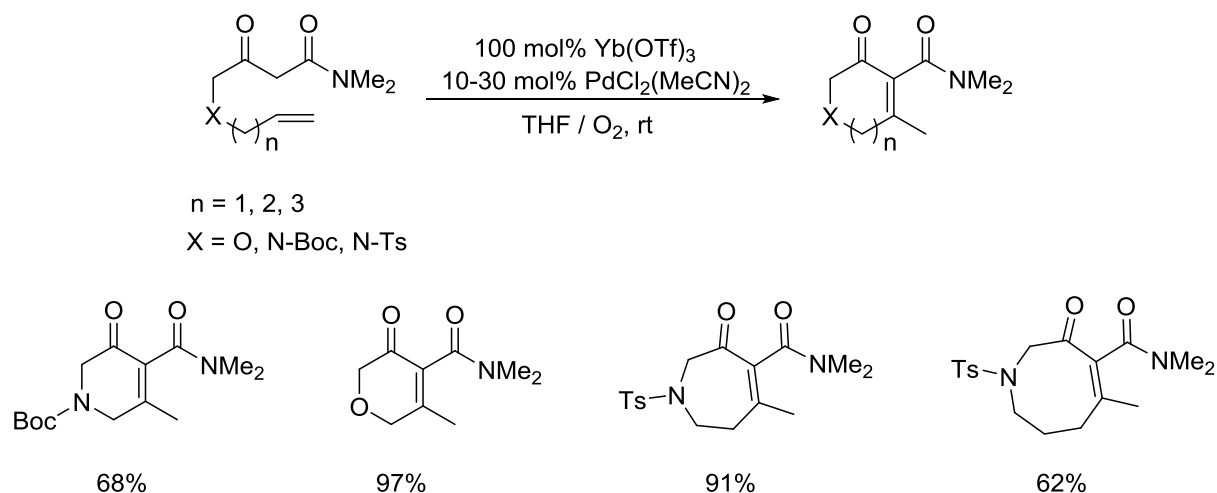
ring generates a palladium enolate. Subsequent protonolysis of this species delivers the cyclohexanone **137** (Scheme 41).



Scheme 41: Formation of cyclohexanone product of hydroalkylation.

Gem-dialkyl substitution along the 4-pentenyl chain of the cyclisation precursor prevents formation of the requisite enolate complex by preventing palladium migration. Substituted β -ketoesters are therefore not susceptible to this competing mechanism.¹³² β -Diketones also favoured oxidative alkylation over competing hydroalkylation. This was attributed to the fact that β -diketones possess a more favourable $K_{enol/ketone}$ than β -keto esters.¹³³ The formation of enol intermediates during the cyclisation was thought to destabilize the palladium olefin interaction, thereby increasing the rate of alkene displacement compared to hydropalladation.¹³²

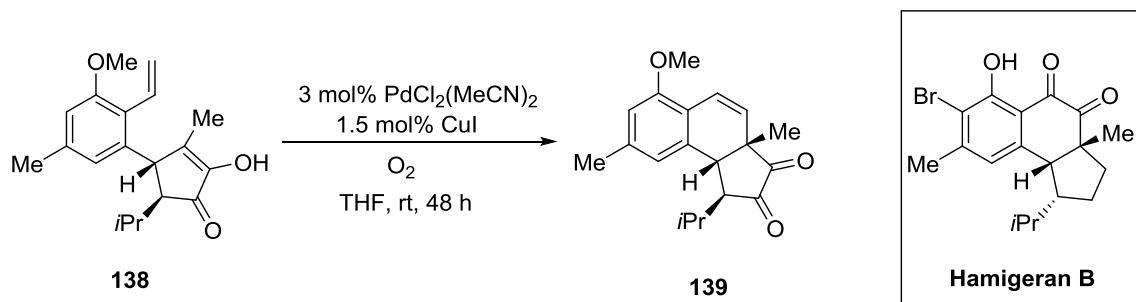
Following on from this work Yang *et al* developed a similar strategy, this time involving the oxidative cyclisation of β -ketoamides under mild conditions (Scheme 42).¹³⁴



Scheme 42: Yang's oxidative carbocyclisation of β -ketoamides.

A number of *N*- and *O*- heterocycles were synthesised in good to excellent yields including seven and eight membered rings which had been inaccessible with previous methodology. A further attractive feature of this protocol is the use of molecular oxygen as the sole oxidant. This overcomes the issues associated with copper salts by improving atom efficiency and reducing reaction waste. The difference between Yang and Widenhoefer's work is the requirement of a highly oxophilic Lewis acid, Yb(OTf)₃. The authors state that this is critical for promoting enolisation and nucleophilic attack of the terminal alkene. Unfortunately in a number of cases, including the synthesis of the seven and eight membered heterocycles, palladium loading had to be increased to as much as 30%.

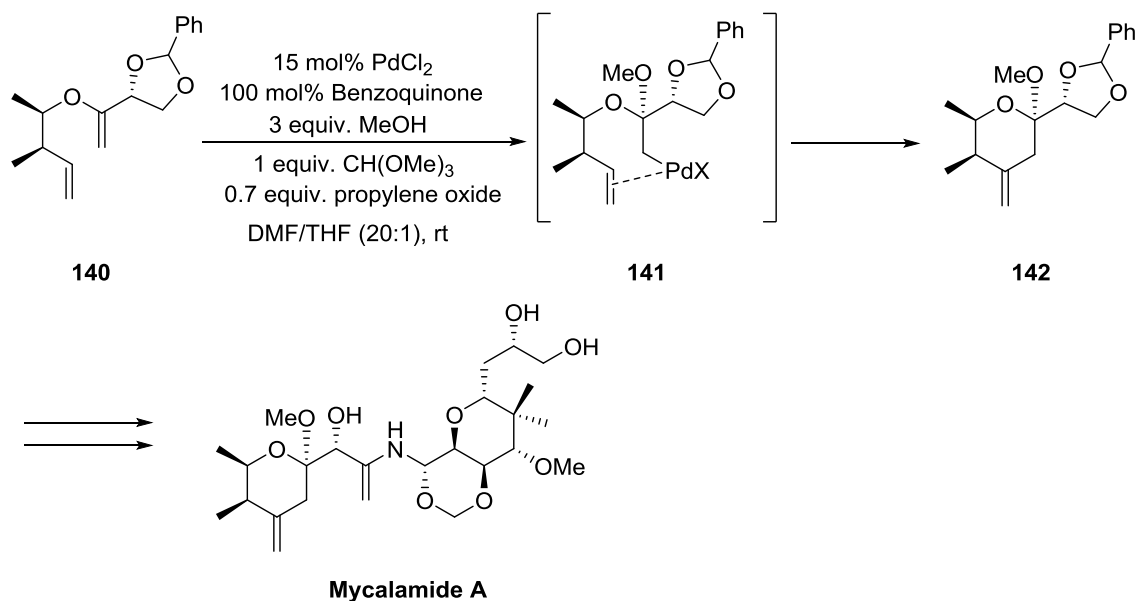
Palladium(II)-catalysed oxidative carbocyclisations have also featured as key steps in the synthesis of a number of natural products. Inspired by the work of Widenhoefer, Cai *et al.* worked towards the synthesis of Hamigeran B (**Scheme 43**).¹³⁵ In this instance the α -hydroxyenone **138** was utilised as a nucleophile, and under the given redox conditions, the subsequent cyclisation proceeded smoothly to afford α -diketone **139** in 87% yield.



Scheme 43. Towards the synthesis of Hamigeran B

Impressively, catalyst and co-oxidant loadings could be lowered to as little as 3 mol % and 1.5 mol% respectively whilst still achieving catalytic turnover and excellent product yield.

A further example where a Pd(II)-catalysed cyclisation process has been employed is in the total synthesis of Mycalamide A (**Scheme 44**).¹³⁶



Scheme 44: Palladium (II) catalysed cyclisation step in the synthesis of Mycalamide A.

Interestingly the reaction slightly differs from the previously described palladium(II) catalysed processes in that the palladium is not merely activating the alkene towards nucleophilic attack. The reaction proceeds *via* a palladium-catalysed tandem cyclisation sequence where an initial Wacker-type reaction generates the σ -alkylpalladium species **141**. This electrophilic Pd(II) species accepts the terminal alkene as a ligand and subsequent carbopalladation affords the exocyclic double bond containing pyran ring **142** in a good yield of 78%. It could be argued, however, that one of the drawbacks of this process is the requirement of higher palladium loadings.

3.3 Initial Objectives

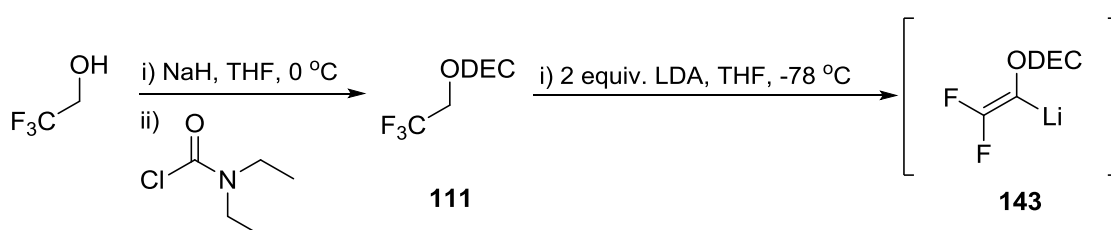
The aim of the current study was to provide a novel approach to construct difluorinated carbocycles by utilising a Pd(II) catalysed intramolecular cyclisation. Whilst there is precedent for catalytic oxidative Pd(II) cyclisation strategies there are no reports of applying this method for the synthesis of selectively fluorinated carbocycles.¹²⁷ The design and synthesis of geminal difluoro compounds is an extremely important objective in medicinal chemistry owing to their unique biological properties, such as enzyme inhibition, pKa modulation and improving metabolic stability.²⁶ The proposed route would overcome some of the issues associated with existing methodologies such as the use of costly and hazardous reagents. Moreover, Pd(II) catalysis offers advantages over Pd(0) methodology such as circumvention of the necessity of an inert atmosphere.¹³⁸

The work detailed in this chapter will focus primarily on the application of difluorinated silyl enol ethers in a Saegusa-Ito cycloalkenylation, features of which include; expanding substrate scope; understanding and controlling product formation; improving overall product yields and attempting to understand the effects of altering the redox system on reactivity.

3.4 Results and Discussion

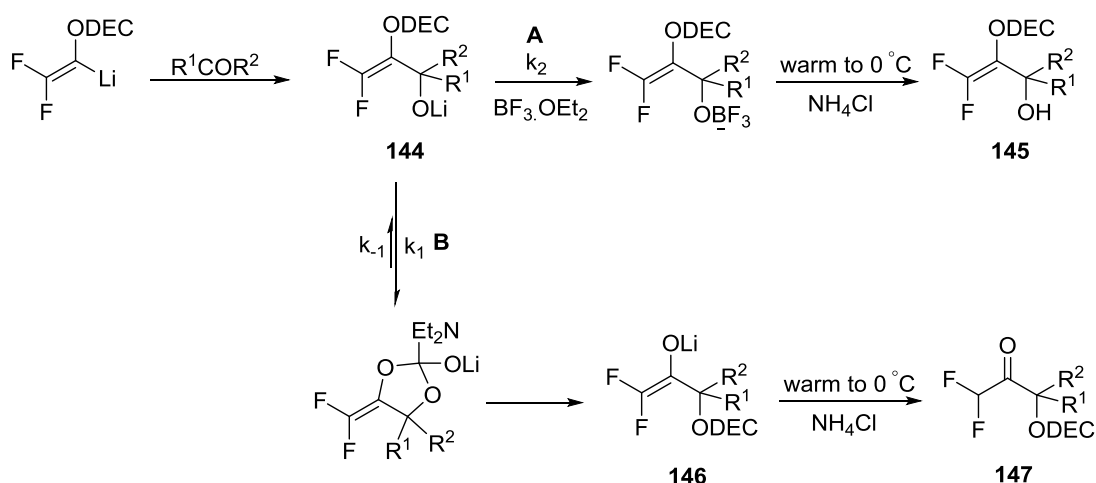
3.4.1 Cyclisation Precursor Preparation

Trifluoroethanol is an inexpensive, commercially available and extremely versatile feedstock used in the synthesis of a range of fluorinated molecules. It is this particular building block which underpins much of the chemistry detailed within this thesis. Initial protection of trifluoroethanol affords carbamate **111** which undergoes dehydrofluorination/lithiation *via* an E2 elimination in the presence of two equivalents of lithium diisopropylamide (LDA). This process generates organometallic intermediate **143** (Scheme 45).¹³⁹



Scheme 45: Trifluoroethanol protection followed by carbamate dehydrofluorination/lithiation.

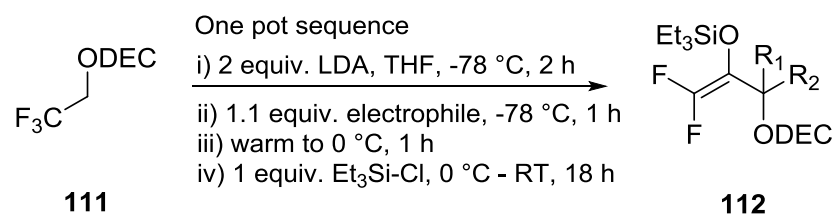
Addition of either an aldehyde or ketone electrophile generates lithium alkoxide **144** which can go down either of two pathways (Scheme 46).¹⁴⁰



Scheme 46: Generation of allylic alcohols, and difluoromethyl ketones (DFMK) through a competing transacylation pathway.

The first pathway involves trapping the alkoxide with $\text{BF}_3 \cdot \text{OEt}_2$ followed by aqueous workup to afford difluoroallylic alcohols **145** (Scheme 46, path A). The second and competitive pathway consists of a cyclisation process followed by ring opening (transacylation), the driving force being formation of the thermodynamically more favourable enolate species **146** ($\text{pK}_a^{\text{E}}(\text{OH}) \approx 10-11$ in water *cf.* alkoxide oxygen alcohol

$pK_a \approx 16-18$ in water).¹⁴¹ Protonation of these enolates affords the corresponding difluoromethyl ketones **147** (Scheme 46, path B). Such a process has now been utilised in the preparation of cyclisation precursors by instead trapping enolate **146** with a hard silicon electrophile to afford silyl enol ethers (SEE) **112** (Scheme 47).



Scheme 47: Preparation of SEE's.

Investigations had previously been performed to determine the effects of varying the degree of trialkylsilyl substitution on the enol ether starting material (Figure 26).⁸⁶

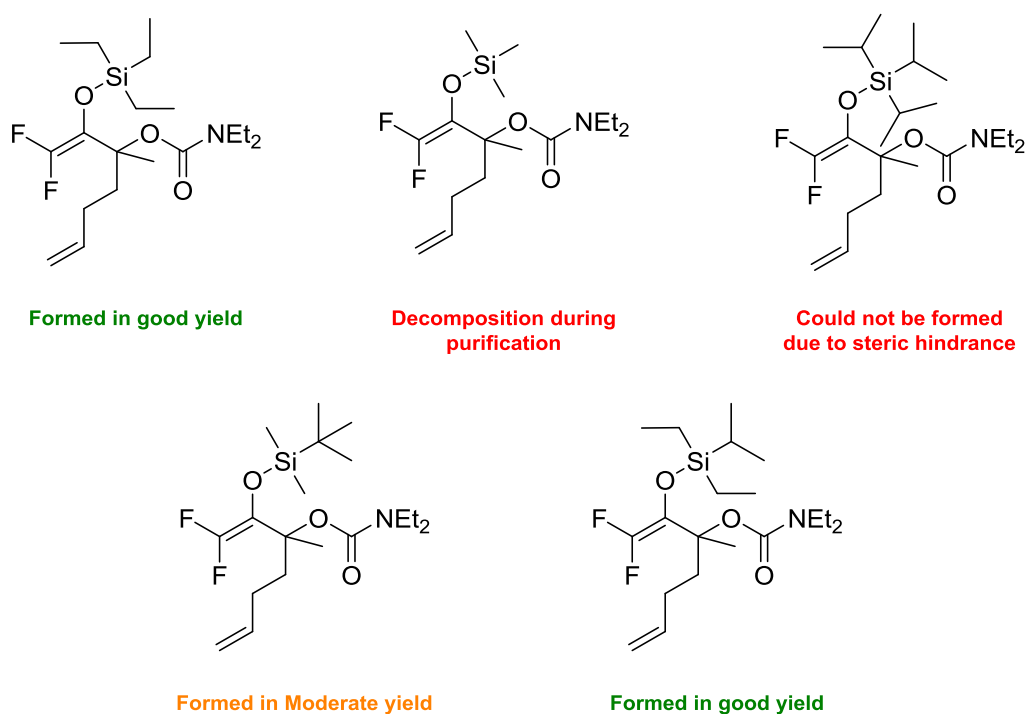
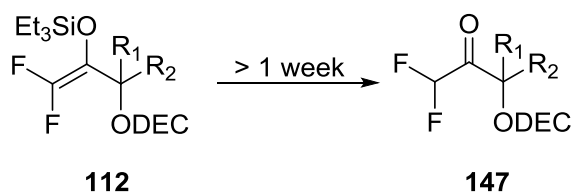


Figure 26: Properties of various SEE's.

The corresponding *tert*-butyldimethylsilyl (TBDMS-), triethylsilyl- (TES-) and diethylisopropylsilyl- (DEIPS-) enol ethers were synthesised successfully using 5-hexen-2-one as a standard electrophile. The attempted synthesis of triisopropylsilyl (TIPS-) enol ethers was unsuccessful whereas the purification of trimethylsilyl- (TMS-) enol ethers proved problematic. The failure of the former to react was attributed to steric repulsion between the triisopropyl groups of the silane and the adjacent carbamate.¹⁴² While enolate **146** reacted successfully with TMS-Cl, the resulting TMS-enol ethers were extremely sensitive, decomposing on silica during column chromatography. The

TBDMS- and DEIPS- enol ethers could be isolated successfully; however, these proved to be ineffective substrates for cyclisation compared to the TES- analogue. The DEIPS- and TBDMS- species were consumed less fully in the cyclisation reactions (details of the cyclisation procedure will be discussed in further detail in *Section 3.4.4*). Chlorotriethylsilane (TES-Cl) was therefore the preferred choice of electrophile in the current work and was used to synthesise the SEE's from a range of aldehydes and ketones in good to moderate yield (**Table 7**). In the case of **112g**, it was possible to separate the *cis*- and *trans*- diastereoisomeric adducts chromatographically. It should be noted that these difluorinated silyl enol ethers have a limited shelf life (approximately one week storage in the refrigerator). After this time, slow decomposition of the silyl enol ether to the corresponding difluoromethyl ketone **147** (DFMK) was observed (**Scheme 48**).



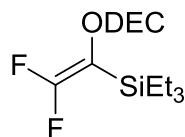
Scheme 48: Decomposition of **112** to **147**.

Table 7: Difluorinated silylenol ethers **112** prepared from **111**.^a

Electrophile	Product	Yield	dr ^b
<p>One pot sequence</p> <p>i) 2 equiv. LDA, THF, -78 °C, 2 h</p> <p>ii) 1.1 equiv. electrophile, -78 °C, 1 h</p> <p>iii) warm to 0 °C, 1 h</p> <p>iv) 1 equiv. Et₃Si-Cl, 0 °C - RT, 18 h</p>			
		112a	67% ^c
		112b	63% ^d
		112c	67%
		112d	61%
		112e	38%
		112f	71% ^e
		112g	43% ^f
		112h	57% ^e
		112i	69% ^e
		112j	25% ^e

^a All reactions were carried out with 5 mmol of **111** unless otherwise stated ^b dr determined by ¹⁹F NMR spectroscopy ^c 10 mmol scale (68%), at 40 mmol scale (70%) ^d 10 mmol scale ^e Isolated as a mixture of *cis*- and *trans*- diastereoisomers, major isomer shown. ^f 6.5 mmol scale, *cis*- and *trans*-diastereoisomers could be separated chromatographically.

It is also worth noting that in the preparation of SEE derivatives a slight excess of electrophile is used to ensure that **111** is trapped fully and to attenuate the formation of vinyl silane **148** (Figure 27).



148

Figure 27: Vinyl silane side product observed in preparation of silyl enol ethers.

In an earlier attempt to synthesize **112c** examination of the ^{19}F NMR of the crude reaction mixture (**Figure 28**) showed four distinct peaks. The doublet at -103.7 ($^2J_{\text{F-F}} = 77.2$ Hz) and doublet of doublets at -114.6 ppm ($^2J_{\text{F-F}} = 77.7$ Hz, $^4J_{\text{F-H}} = 2.9$ Hz) correspond to **112c** whilst the two doublets at -80.6 ppm ($^2J_{\text{F-F}} = 47.8$ Hz) and -102.6 ($^2J_{\text{F-F}} = 47.8$ Hz) are associated with **148**.

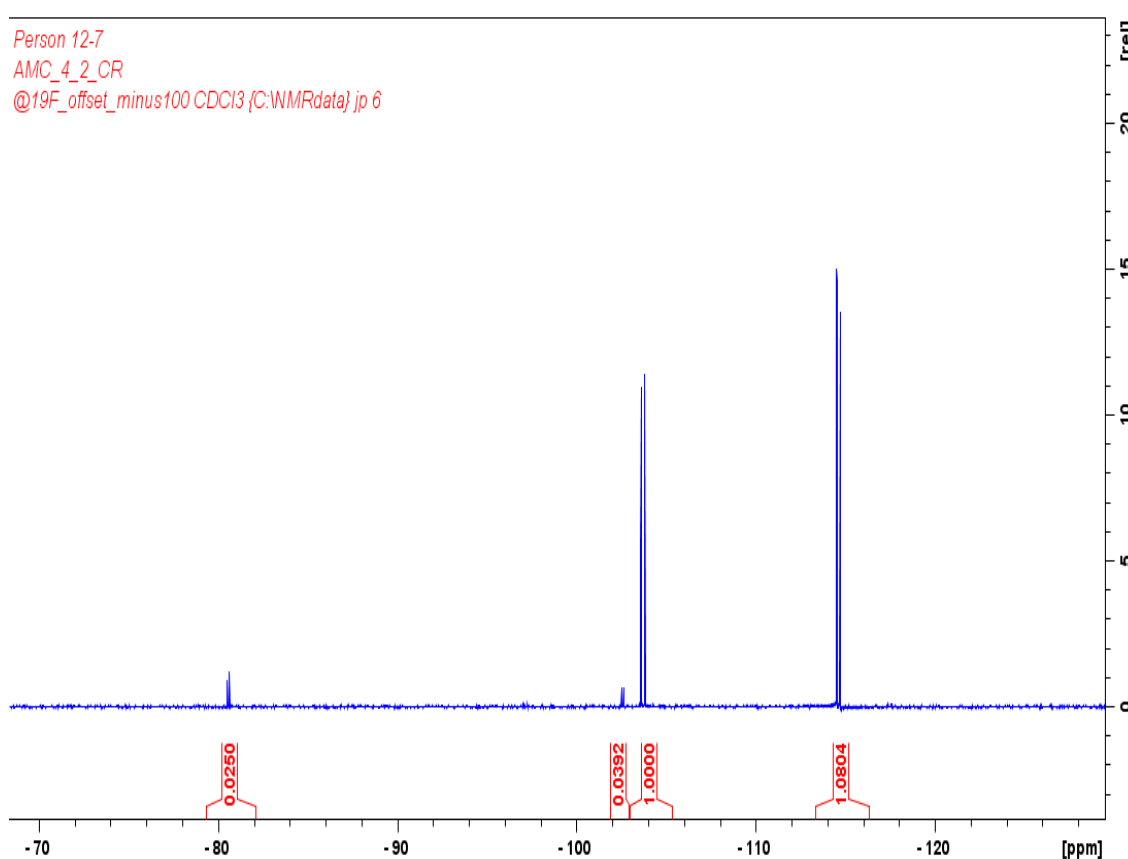
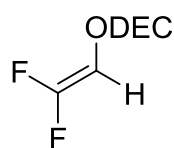


Figure 28: ^{19}F NMR spectrum of crude reaction mixture in preparation of **112c**.

Though only trace amounts of **148** were detected (97:3 **112c**:**148** by ^{19}F NMR), it was not possible to separate the vinyl silane from the desired product by chromatography. The formation of this species can be associated with an incorrect reaction stoichiometry

indicating that an insufficient amount of electrophile had been added to the reaction mixture. Although the use of excess electrophile might appear wasteful and less cost-effective, it is important to ensure that products are free from vinyl silane which appears to impede cyclisation.⁸⁶

One of the lowest SEE yields to be recorded was that of sulfone **112j**. On inspection of the ¹⁹F NMR of the crude reaction mixture it appeared that the reaction contained predominantly enol carbamate (**Figure 29**).¹⁴³



149

Figure 29: Enol carbamate detected in crude reaction mixture in preparation of **112j**.

The presence of enol carbamate indicates that either ‘wet’ electrophile was added to the reaction mixture or that lithiated enol carbamate **143** had deprotonated the sulfone electrophile. However, because a C-H bond adjacent to a sulfone functionality is less acidic than a C-H bond adjacent to a carbonyl group the formation of **149** was attributed to the former explanation (**Figure 30**).¹⁴⁴

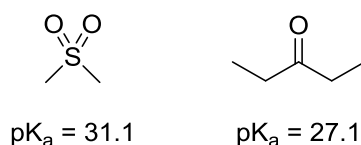


Figure 30: pKa values of C-H bonds adjacent to carbonyl and sulfone groups in DMSO.

The sulfone electrophile was formed by oxidation of the corresponding sulfide and was the only electrophile to exist as a solid. Despite vigorous attempts to dry the material by storing in a vacuum oven for one week (40 °C/0.75 mmHg), significant amounts of enol carbamate were returned from the reaction (**Figure 31**).

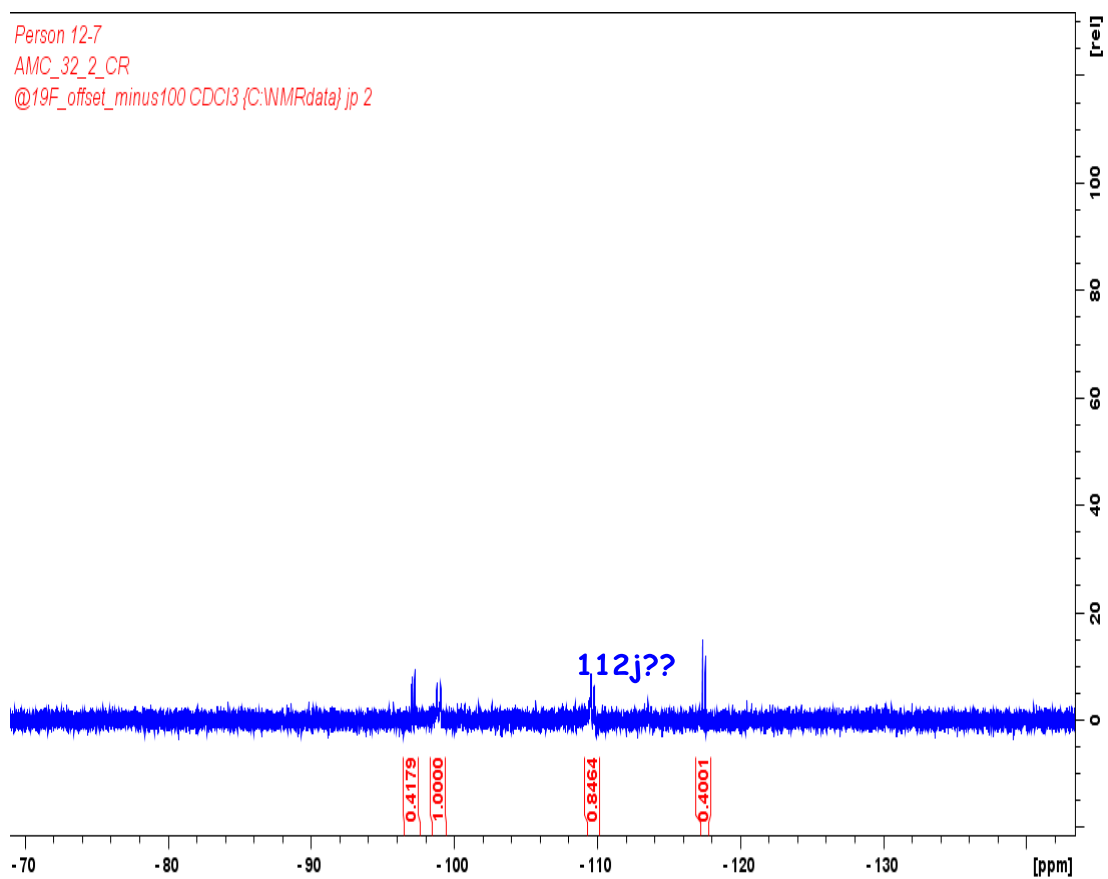


Figure 31: ^{19}F NMR spectrum of crude reaction mixture in preparation of **112j**.

Initially, it was unclear whether or not the weaker broad signals at -98.9 and -109.9 ppm did in fact represent the desired product. Annelative precursors often existed as a mixture of *cis*- and *trans*- diastereoisomers represented as 4 distinct signals by ^{19}F NMR.

Following purification of the crude reaction mixture, variable temperature (VT) ^{19}F NMR experiments were conducted which revealed the desired product as a mixture of *cis*- and *trans*-diastereoisomers (**Figure 32**).

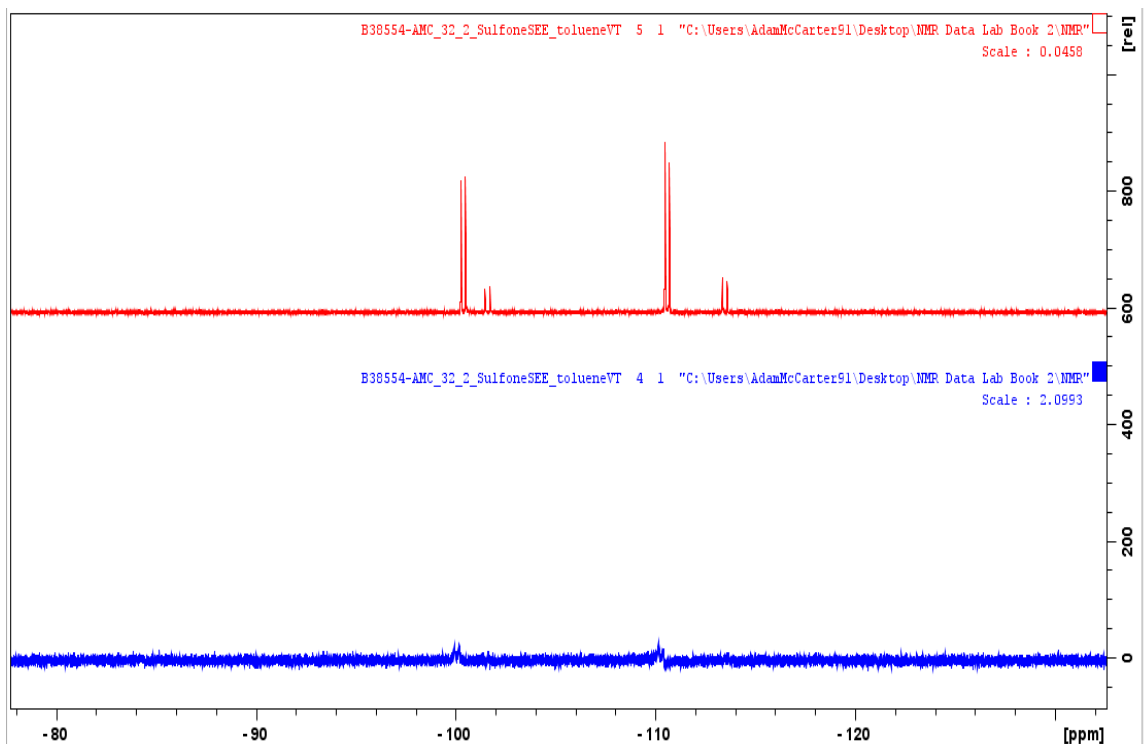


Figure 32: ^{19}F VT-NMR experiment of **112j** revealing the desired product as a mixture of *cis*- and *trans*- diastereoisomers.

Interestingly, ^1H and ^{13}C NMR spectra were sharp, therefore it was only the ^{19}F nucleus which suffered from this extreme line broadening at room temperature. One possible explanation for this phenomenon lies in the relationship between fluorine chemical shift anisotropy (CSA) and the T_2 relaxation time. This is represented by Equiv. 1 where T_2 represents the spin-spin relaxation time, $\sigma_{\parallel} - \sigma_{\perp}$ the shielding anisotropy, ω_{F} the chemical shift frequency of the free species in solution and τ_c the correlation time.

$$\text{Equiv. 1} \quad \frac{1}{T_2} = \frac{2}{15} (\sigma_{\parallel} - \sigma_{\perp})^2 \omega_{\text{F}}^2 \tau_c \left\{ \frac{2}{3} + \frac{1}{2} \frac{1}{(1 + \omega_{\text{F}}^2 \tau_c^2)} \right\}$$

The shielding anisotropy is often relatively small for the ^1H nucleus ($\sigma_{\parallel} - \sigma_{\perp} \approx 5$ ppm) but can be much larger for heavier elements such as ^{19}F ($\sigma_{\parallel} - \sigma_{\perp} \approx 1000$ ppm).¹⁴⁵ Because there is an inverse relationship between ^{19}F CSA and T_2 , the value of T_2 will decrease as the value of the CSA increases. The spin-spin relaxation time is also related to peak linewidth ($W_{1/2}$) by the following equation:

$$\text{Equiv. 2} \quad W_{1/2} = \frac{1}{\pi T_2}$$

A lower T_2 will generate resonance signals with extremely broad lineshapes in the resulting 1D ^{19}F NMR spectrum. Equation 1 also highlights the principles of VT NMR in

which heating molecules in solution will result in a decreased correlation time (τ_c) and therefore a larger T_2 value resulting in well resolved signals in the 1D NMR spectrum.

With the cyclisation precursors in hand, the first goal was to try and isolate pure α,α -difluoroketones. Secondly, if hydrate formation could be understood, it might be possible to improve the overall reaction yields.

3.4.2 Work up and isolation modifications

The reaction conditions that currently existed for the cyclisation procedure had previously been established following a preliminary optimisation process (**Scheme 49**).⁸⁶



Scheme 49: Optimised reaction conditions for cyclisation of **112a**.

However, in order for the Saegusa-Ito methodology to become a more effective and attractive synthetic protocol, two aspects required improvement; the isolation of pure α,α -difluoroketones was essential and higher overall yields were sought.

The cyclisation of **112a** was chosen as a standard protocol to investigate these issues before utilising different silyl enol ethers (*vide supra*) in the cyclisation.

The cyclisation of **112a** under the optimised conditions resulted in an extremely clean reaction. The ^{19}F NMR spectrum of the crude reaction mixture contained two doublets at -103.8 and -117.5 ppm with large coupling constants ($^2J_{\text{F-F}} = 251$ Hz), characteristic of geminal F-F coupling in cyclic compounds (A in **Figure 33**).¹⁴⁶

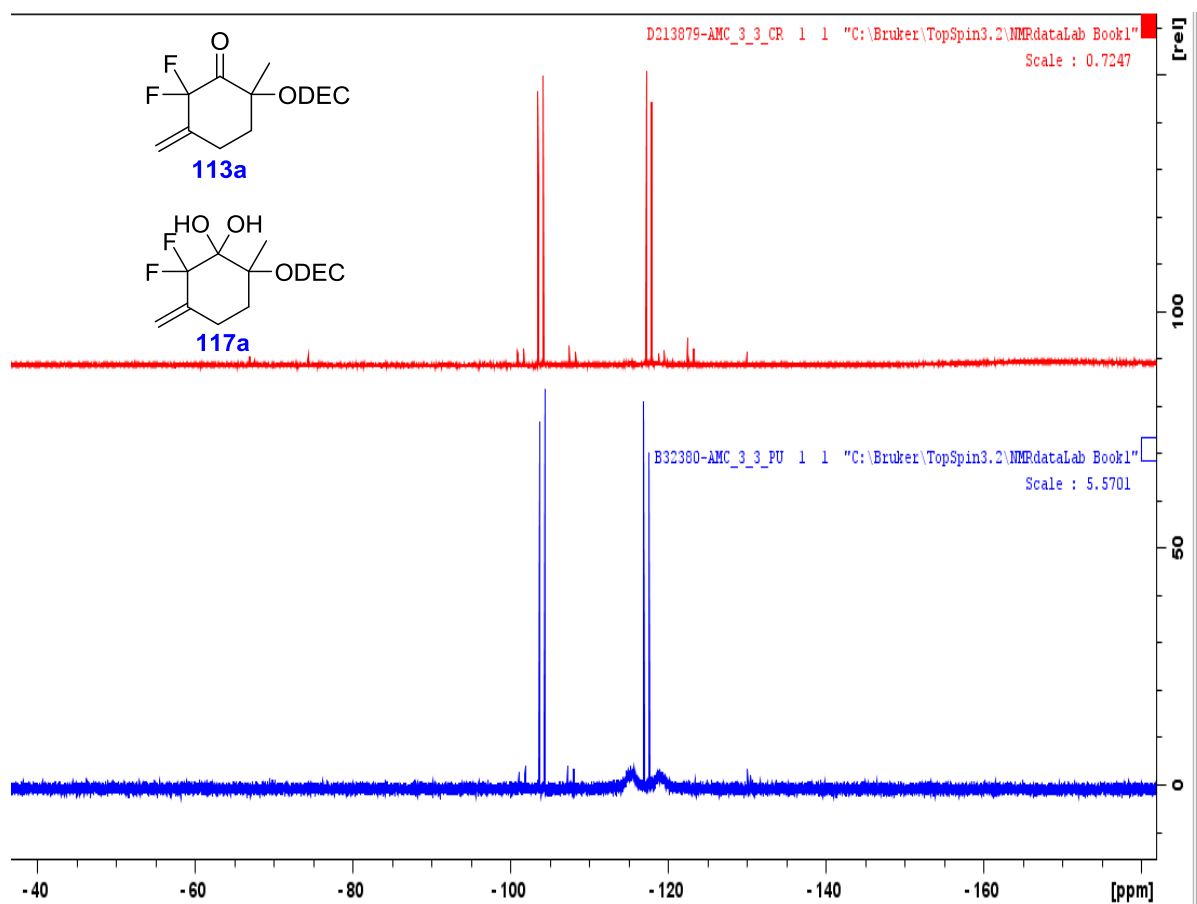


Figure 33: A) ^{19}F NMR spectrum of crude mixture of cyclisation of **139a** B) ^{19}F NMR spectrum following flash column chromatography.

However, a second broad set of signals at -115.2 and -118.9 ppm appeared following purification of the crude material by flash column chromatography (B in **Figure 34**). These signals have since been attributed to the hydrate and while the ^{19}F NMR spectrum is ambiguous because of the presence of such broad signals, the ^{13}C NMR spectrum of the mixture shows two complete sets of signals associated with the ketone and corresponding hydrate.

The mixture was isolated as an oil following chromatography; however, the hydrate had previously been crystallised and its identity confirmed by XRD and microanalysis. It was not possible to obtain NMR data of the pure hydrate as crystals of the hydrate equilibrated to the mixture when taken up in CDCl_3 .

The hydration of α,α -difluoroketones is well documented and has been attributed to the effects imposed by the adjacent fluorine substituents. These highly electronegative atoms are less destabilising on a less electronegative sp^3 carbon centre than on a more electronegative sp^2 carbon centre. This makes the carbonyl carbon more susceptible to nucleophilic attack by water and is the driving force for hydration.¹⁴⁷ The dramatic effects of fluorine substitution on the hydration equilibrium constant ($K_{\text{hydr}} =$

[hydrate]/[ketone]) becomes apparent when the values of K_{hydr} for acetone, α -fluoroacetone and α,α,α -trifluoroacetone are compared (**Table 8**).¹⁴⁸

Table 8: Equilibrium constants for covalent hydration of selected carbonyl compounds.

Compound	K_{hydr}
acetone	0.0014
α -fluoroacetone	0.17
α,α,α -trifluoroacetone	32.36

The tendency of difluoroketones to hydrate readily can play an important role in medicinal chemistry. In a biological context, hydration can generate species with increased aqueous solubility as well as imparting a tetrahedral geometry at the newly formed sp^3 centre which can mimic tetrahedral intermediates involved in peptide hydrolysis.^{149,150} However, despite the potentially useful applications of hydrated difluoroketones, mixtures of difluoroketones and hydrated difluoroketones were not desired. Combined with the electrophilic nature of the carbonyl group in **113a** and the use of potentially wet silica gel it is not surprising that hydrate formation during the purification process is observed.

Given that both ketone and hydrate are in equilibrium it should be possible to drive the equilibrium towards the ketone through the removal of water (**Figure 34**).

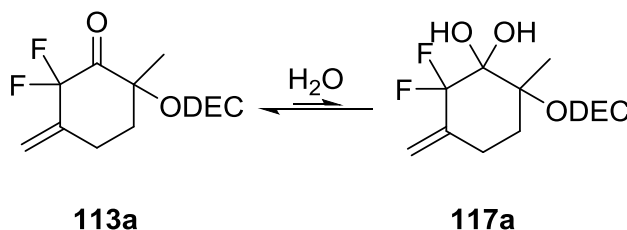


Figure 34: Ketone hydrate equilibrium.

Initial attempts to achieve this by removing water through evaporation of toluene solutions of the mixture proved to be successful with the broad signals associated with **117a** collapsing in the ^{19}F NMR spectrum (B in **Figure 35**).

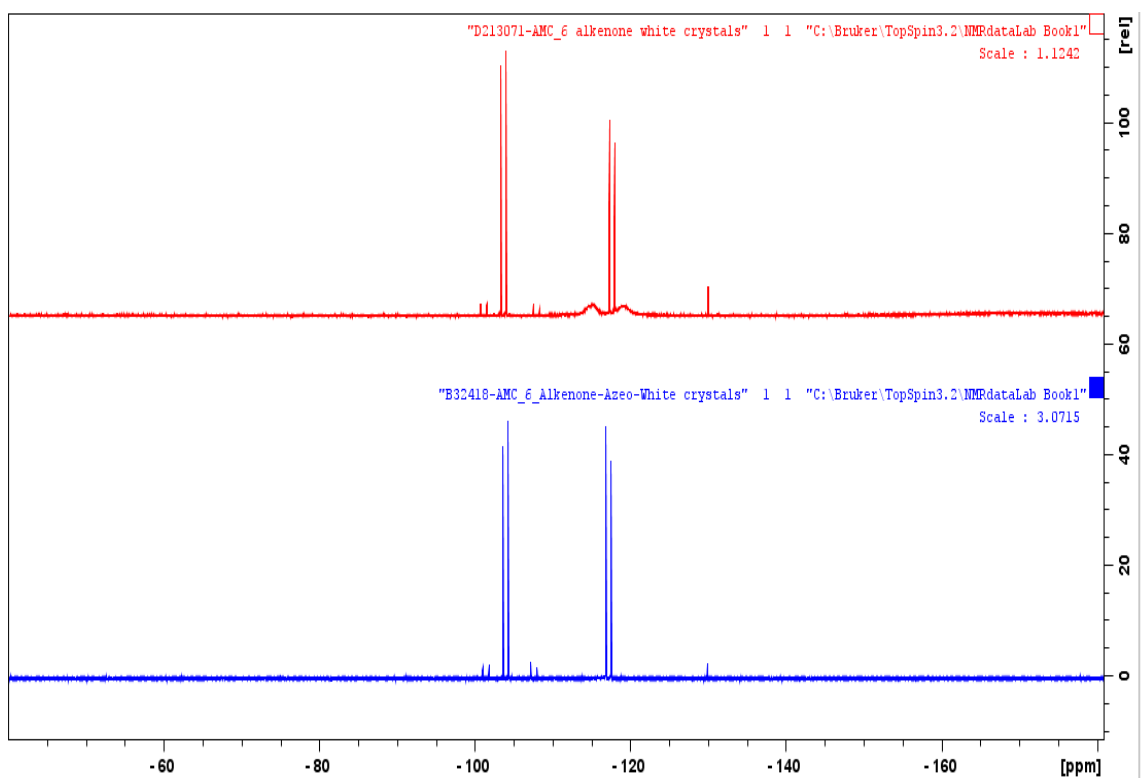


Figure 35: A) ^{19}F NMR spectrum of ketone/hydrate mixture **113a/117a**. B) ^{19}F NMR spectrum of **113a/117a** following evaporation of toluene solutions.

This technique for removing water afforded the desired ketone as an oil; however, it was possible to convert it into a solid simply by triturating the oil with pentane. The solid material was bench stable and could be stored at room temperature without observation of any product decomposition. However, following a prolonged period of time (1 month) traces of hydrate could be detected by ^{19}F NMR. Rather than subjecting the solid mixture to the azeotroping procedure it was instead placed inside a vacuum oven at 40 °C and 1 mbar for 48 hours. Analysis of the solid after this time revealed that the solid ketone/hydrate mixture had been converted fully to the α,α -difluoroketone **113a**. This method of drying was much more attractive as it did not require the use of solvent and was more practical than the azeotroping method.

An attempt to convert **113a** fully to the hydrate was made by stirring **113a** in a 1:1 mixture of water and tetrahydrofuran (THF) for 48 hours (spectrum B in **Figure 36**).

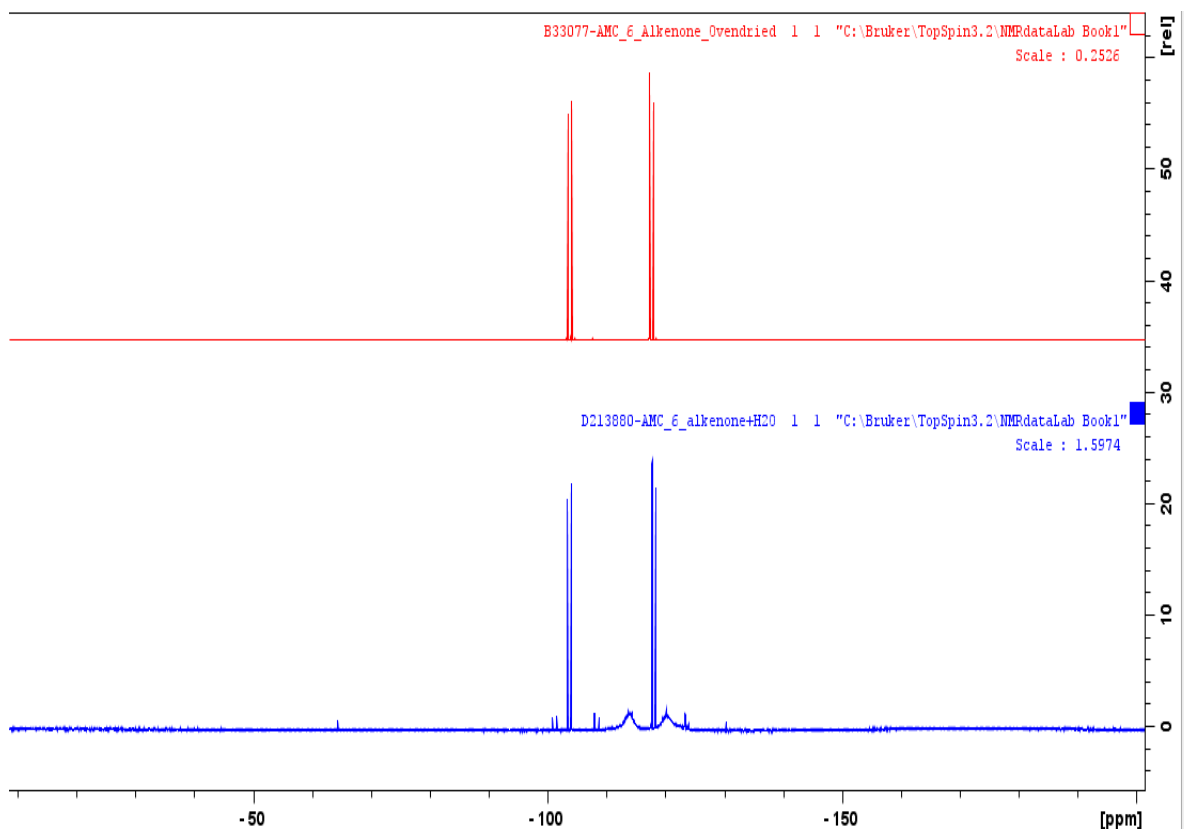


Figure 36: A) ^{19}F NMR spectrum of α,α -difluoroketone **113a** B) ^{19}F NMR spectrum of crude reaction mixture.

Though increased levels of hydrate were observed a significant amount of ketone remained in the reaction mixture and no further attempts to synthesise the pure hydrate were made.

With access to this oven drying procedure, it was then possible to isolate and characterise pure ketones with improved and reliable yields compared to previous attempts (**Figure 37**).⁸⁶

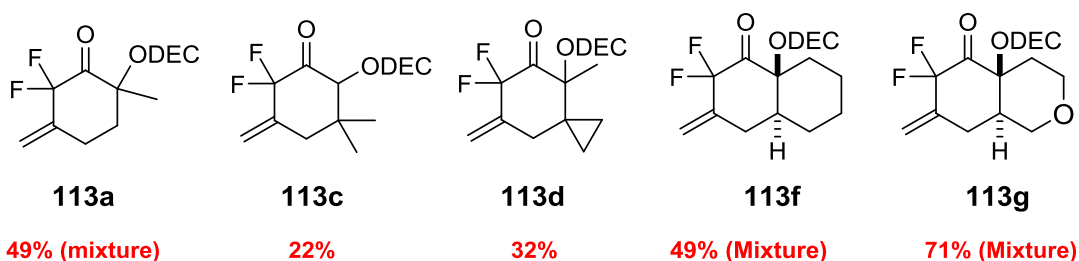


Figure 37: Previously reported yields of α,α -difluoroketones and mixtures of hydrate and ketone.⁸⁶

Furthermore, the hydration of α,α -difluoroketones was not universal and it would appear that the inductively electron-withdrawing effect of fluorine may not be the only factor in determining ketone hydration. On comparison of the crystal structures of the monomethylated hydrate **117a** and the gem-dimethyl ketone **113c** it is clear that the

(*N,N*-diethylcarbamoyloxy) (DEC) group occupies a different position in each case (Figure 38).⁸⁶ For **117a** the DEC group lies in the *pseudo*-axial position whereas in **113c** it adopts the equatorial position.

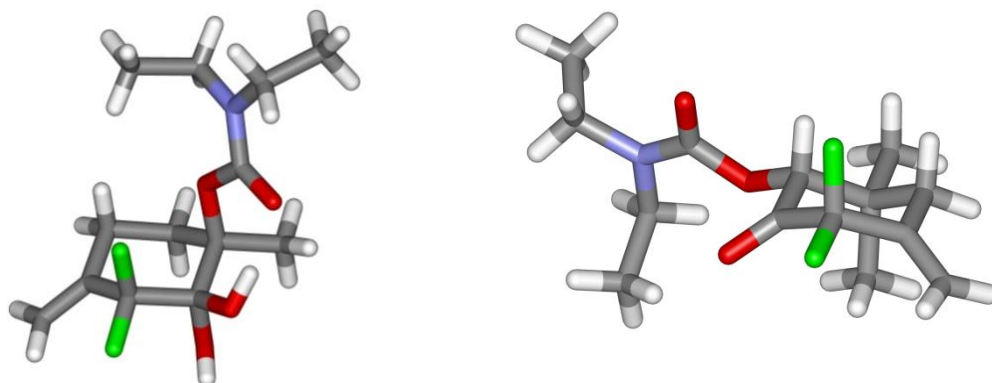


Figure 38: X ray crystal structure of hydrate **117a** (left) and ketone **113c** (right).

In the *pseudo*-axial position there is clear potential for hydrogen bonding interactions between the carbonyl functionality of the DEC group and the hydroxyl groups of the hydrate. However, distance constraints would prevent these interactions when the DEC group lies in the equatorial position, as is the case for **113c**. The availability of the DEC group to stabilise the hydrate form may therefore play an influential role in determining the ease of hydrate formation. However, though species **113c** and **113d** resist hydration the previously reported yields were still low.⁸⁶ To address these poor yields, the work up and purification procedure was revisited.

The original work up and purification procedure consisted of concentrating the reaction mixture onto silica, then dry loading the material onto a silica plug and eluting with a chosen solvent system before finally purifying the crude material by flash column chromatography. However, avoiding silica altogether might inhibit hydration and aid in the isolation of pure ketones.

Following completion, the reaction mixture was filtered through a plug of celite to remove insoluble metal salts and eluted with diethyl ether. The filtrate was concentrated to afford the crude product as a dark brown oil which, although clean by ¹⁹F NMR, was contaminated with palladium and copper residues. The presence of these metals was suggested by extensive streaking of the crude product on silica plates. Removal of these metal contaminants was essential in order to afford clean product. This issue is one commonly faced within the pharmaceutical industry in the synthesis of active pharmaceutical ingredients (APIs). In medicinal chemistry, palladium catalysed

reactions such as Negishi and Suzuki cross couplings are often key transformations towards the synthesis of new APIs. The problem with employing such metal-catalysed chemistry is that expensive and extremely toxic metal residues may contaminate the API. With strict European guidelines on the allowable limits of metal contaminants associated with APIs (<10 ppm for Pd), the discovery of efficient methods of removing these contaminants is of fundamental importance.¹⁵¹

In recent years the emergence and development of metal scavenging kits have helped to address this issue. Silica-based metal scavengers developed by PhosphonicS Ltd. have been shown to have useful binding affinities to palladium in various oxidation states (**Figure 39**).¹⁵² As well as palladium, these scavengers are also known to bind to a host of other metals including copper, ruthenium and nickel.

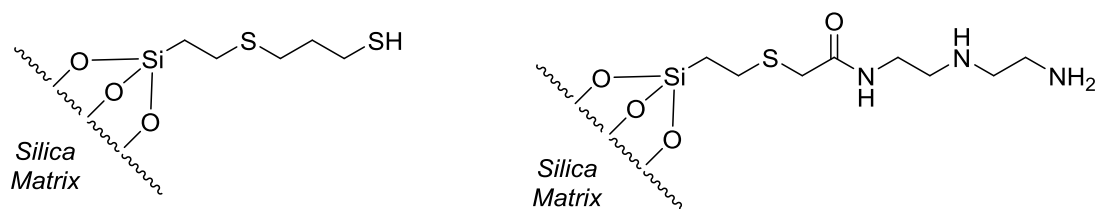


Figure 39: 3-Mercaptopropyl ethyl sulfide Silica (SPM32, left) and Triamine ethyl sulfide amide Silica (STA3, right) metal scavenging silica developed by PhosphonicS Ltd.

These functionalised materials incorporate multidentate functional groups which can bind with sufficiently high affinity to palladium (**Figure 40**).¹⁵³

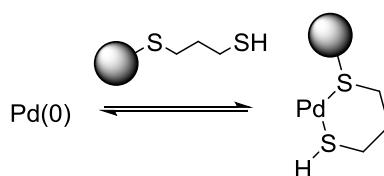


Figure 40: Chelation of sulfur based metal scavenger with palladium (0) species.

The SPM32 and STA3 metal scavengers were implemented in the new work up procedure in the hope of simplifying purification. An instant colour change from colourless to black was observed in the solid support when it was added to the crude reaction mixture in diethyl ether. The mixture was stirred for thirty minutes, then the silica was filtered off and the filtrate was concentrated to afford a colourless oil. On closer inspection it was apparent that the oil contained a small amount of solid. This solid was not present in the crude mixture before being scavenged and only appeared following effective sequestration of the metal contaminants. Trituration of this oil with pentane afforded ketone **113a** as a colourless solid (**Figure 41**).

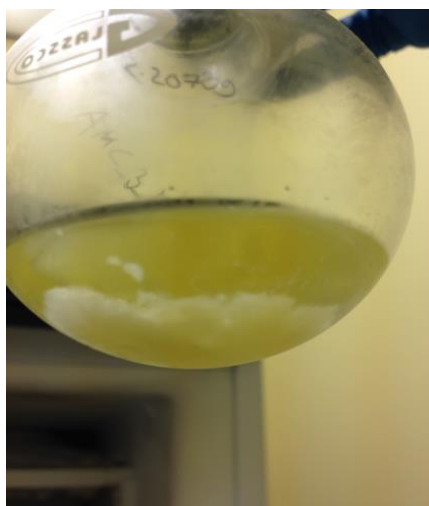


Figure 41: Solid ketone **113a** formed following addition of pentane to crude reaction mixture post-scavenge.

This material proved to be of high purity; a satisfactory CHN analysis was obtained, and no further purification was required. The importance of the metal scavenger cannot be overstated as its use allows the desired products to be isolated without chromatography. With this new work up and ketone isolation procedure in place, the generality of this method was tested by synthesising a range of α,α -difluoroketones.

3.4.3 Substrate scope

It was then possible to isolate a range of ketones in good to excellent yields (**Table 9**) following successful cyclisations using the scavenger method. When the ketone was susceptible to hydration, trituration would afford a solid mixture consisting of ketone and hydrate. However, in such cases, the material could be converted fully to the ketone by drying in a vacuum oven.

The annulative cyclisations of **113f-h** and **113j** were successful using only 5 mol % palladium however most annulations, with the exception of **113c**, required higher palladium loadings (10 mol %). This feature could be attributed to the lower reaction entropies associated with the annulative processes; the presence of a pre-formed ring system reduces the number of degrees of freedom available to the cyclisation precursor resulting in a lower loss of entropy in the rate-determining step.

Table 9: Palladium catalysed cycloalkenylation of silyl enol ethers.^[a]



SEE	Product	Pd (mol %)	Yield (%)	Previous yield (%) ⁸⁶	
		113a	10	52 ^[b]	49 ^[c]
		113b	50	0 ^[f]	-
		113c	5	72 ^[d]	22
		113d	10	67 ^[d]	32
		113e	10	72 ^[e]	-
		113f	5	71 ^[g]	49
		113g	5	90	71
		113h	5	73	-
		113i	5	0 ^[h]	-
		113j	5	44 ^[i]	-

[a] Unless otherwise stated all reactions were carried out with 1.0 mmol of SEE. [b] At 3 mmol scale (68%), at 10 mmol scale (70%) [c] mixture of ketone and hydrate [d] 1.23 mmol scale. [e] 0.91 mmol scale. [f] Only enal **150** could be isolated cleanly from the reaction. [g] 1.22 mmol scale [h] The reaction time was 144 h [i] Isolated as a mixture of *trans*- and *cis*- bicyclic ketones (*trans*:*cis* 87:13).

Previously reported yields⁸⁶ were improved and three novel ketones were also formed including spirocycle **113e**, *N*-heterocycle **113h** and sulfone heterocycle **113j**.

3.4.3.1 The Thorpe-Ingold Effect

An interesting comparison from **Table 9** is between the cyclisation of the cyclopropane substituted SEE **112d** with that of the corresponding *gem*-dimethyl **112c**. The former annulation required a palladium catalyst loading of 10 mol % whereas the latter required only 5 mol % Pd(OAc)₂. Attempts to cyclise **112d** at lower catalyst loadings (5 mol %) returned only starting material, even after stirring at 70 °C for one week. The slower reaction profile attributed to the cyclopropyl analogue may have been caused by a reverse Thorpe-Ingold effect. The origins of the Thorpe-Ingold effect (or *gem*-dialkyl effect) lie in the correlation between distance between reactive termini (dictated by changes in the bond angles between the carbons of an open chain structure) and relative rate of cyclisation (**Figure 42**).¹⁵⁴

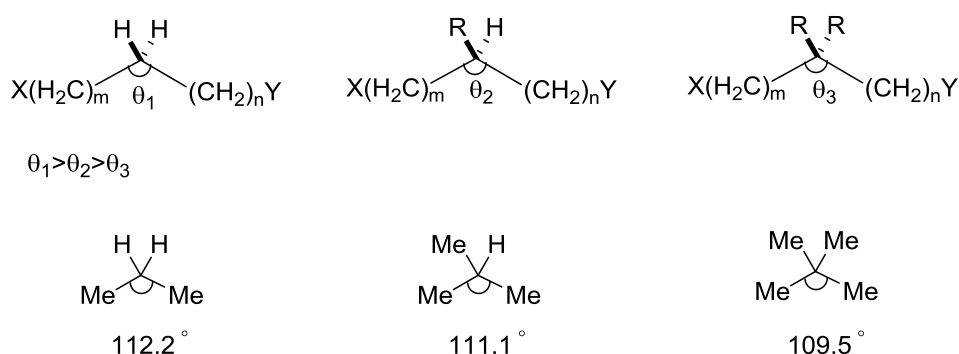


Figure 42: Origins of the Thorpe-Ingold effect.

The rate enhancement of ring closing reactions from the replacement of hydrogen atoms on the carbon tethering two reacting centres with alkyl substituents has been well documented.^{155,156} However, in the case of cyclopropane substitution the geometric demands of the cyclopropane ring cause the angle between reactive termini to increase and therefore lower the rate of cyclisation.^{156,157}

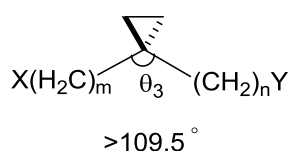
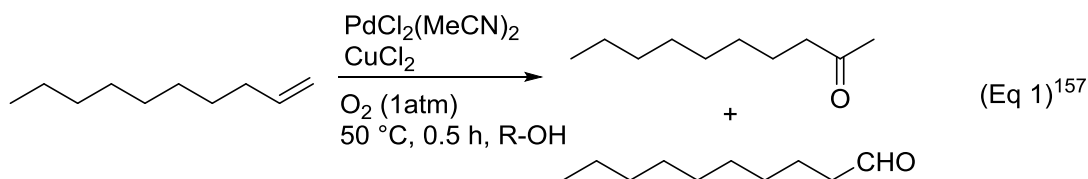
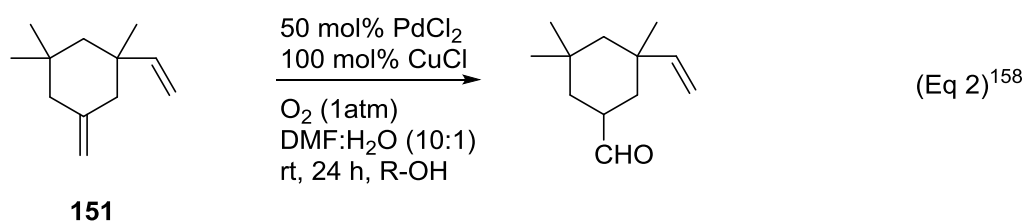


Figure 43: Angle constraints imposed by cyclopropane ring.

Replacement of the cyclopropane ring in **112d** with cyclopentane should theoretically decrease the bond angle in the alkyl backbone and, if the Thorpe-Ingold effect is playing an important role, lead to an increased reaction rate for **112e**. Indeed, when the



R	Yield (%)	Ketone:Aldehyde
Me	26%	97:3
Et	22%	84:16
<i>i</i> -Pr	11%	58:42
<i>t</i> -Bu	7%	16:84

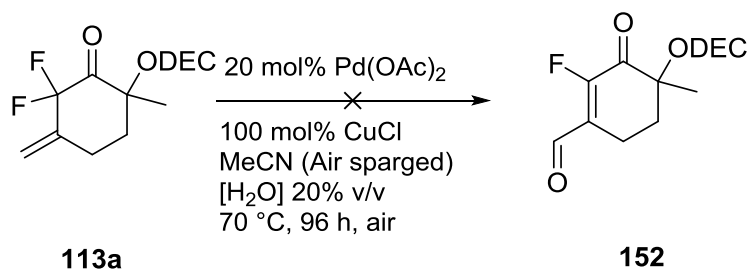


Scheme 51: Examples of reversed Wacker regiochemistry.

It is worth noting that the unique nature of the substrates and reaction systems highlighted in **Scheme 51** are what is responsible for the observed selectivity. The oxidation of 1-decene (Eq 1) required the use of a bulky alcohol in order to achieve selectivity for the aldehyde, a feature which is absent in the Saegusa reaction conditions.¹⁵⁸ Although selectivity is observed, the reaction is extremely inefficient and only a 7% yield of the corresponding aldehyde is reported.

Whilst diene **151** (**Scheme 51**) is structurally similar to α,α -difluoroketone **113b** (presumably the precursor to enal **150**), the authors believe that the presence of the monosubstituted terminal olefin is what drives aldehyde selectivity.¹⁵⁹

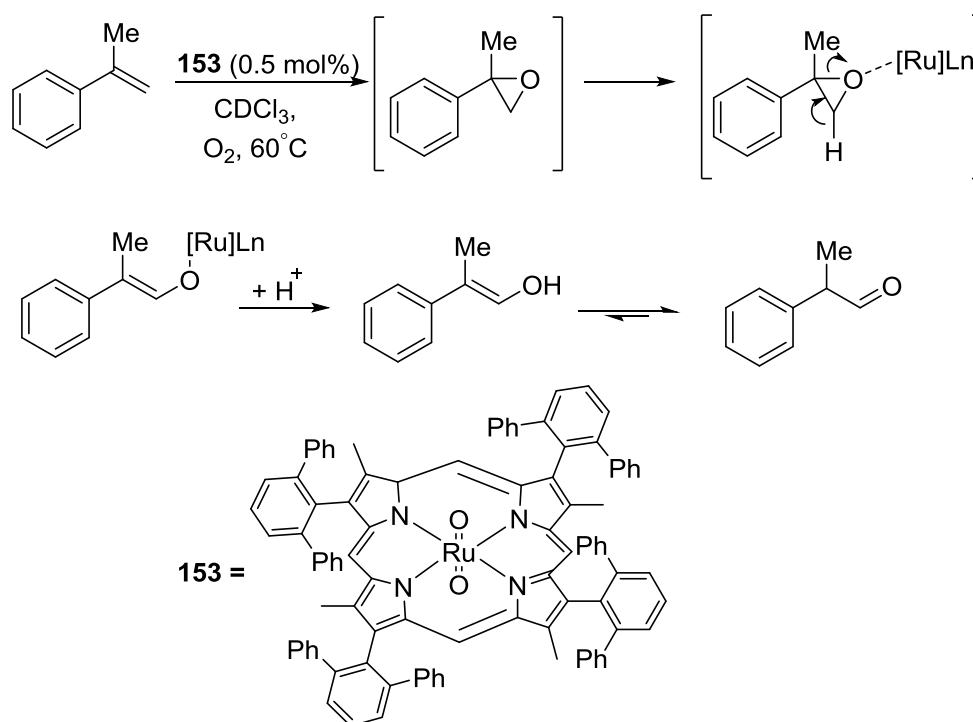
To confirm if a Wacker oxidation was occurring, monomethylated α,α -difluoroketone **113a** was subjected to the cyclisation conditions (**Scheme 52**). The palladium loading was increased to 20 mol %, the reaction time extended and the solvent system now consisted of acetonitrile saturated with 20% v/v water. If a palladium catalysed Wacker-type process was occurring, these conditions were expected to favour formation of the corresponding enal **152** (**Scheme 52**).



Scheme 52: Attempted formation of enal **152**.

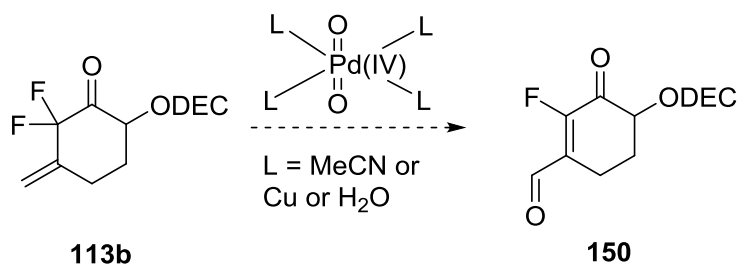
Surprisingly, enal **152** could not be detected. This result suggests that either the formation of enal **150** occurs exclusively for that particular substrate, or its formation is not palladium catalysed. In standard Wacker oxidations, nucleophilic attack by water on the palladium coordinated alkene is a polar addition and selectivity is therefore governed by Markovnikov's rules, with water adding to the more substituted carbon.¹⁶⁰ Along with the fact that the concentration of water in the cyclisation of **112b** would have been very low, it seems unlikely that the classic Wacker mechanism can be used to rationalise the formation of **150**.

If water is not the source of the aldehyde oxygen in **150**, then its incorporation could potentially be due to the presence of molecular oxygen. Most examples of Wacker type oxidations of geminally disubstituted olefins with molecular oxygen often require either high pressure equipment, electrochemical or photochemical techniques and/or unique catalyst systems.^{161,162,163,164} However, Che *et al.* have reported the aldehyde selective ruthenium(IV) catalysed Wacker oxidations of terminal aryl alkenes using oxygen as the terminal oxidant.^{165,166} The authors propose that oxidation occurs *via* an epoxidation/isomerisation process, although they admit that the exact mechanism of action is unclear (**Scheme 53**).



Scheme 53: Reverse Wacker-type oxidation performed by Ru(IV) catalyst.

Like ruthenium, palladium has the ability to exist in the +4 oxidation state and six coordinate palladium (IV) dioxo species are known to exist as reactive intermediates in Pd(II)-catalysed arene oxygenation reactions.¹⁶⁷ If a similar species was formed under the current reaction conditions, then it may be possible for a similar epoxidation/isomerisation mechanism to occur that would lead to the formation of enal **150** (Scheme 54).



Scheme 54: Possible intermediate responsible for formation of enal **150**.

Another possible explanation for the formation of **150** may involve radical chemistry (Scheme 55). The reaction of triplet oxygen with the terminal olefin of **113b** followed by a 1,3 hydrogen atom shift could potentially generate hydroperoxide **154**. Quantum mechanical calculations performed by Zhu *et al.* have predicted that 1,3 hydrogen shifts involving peroxy radicals are inherently slow (41 kcal mol⁻¹), a feature which may account for the low yield of **150**, 8%.¹⁶⁸ Organic hydroperoxides are known to undergo

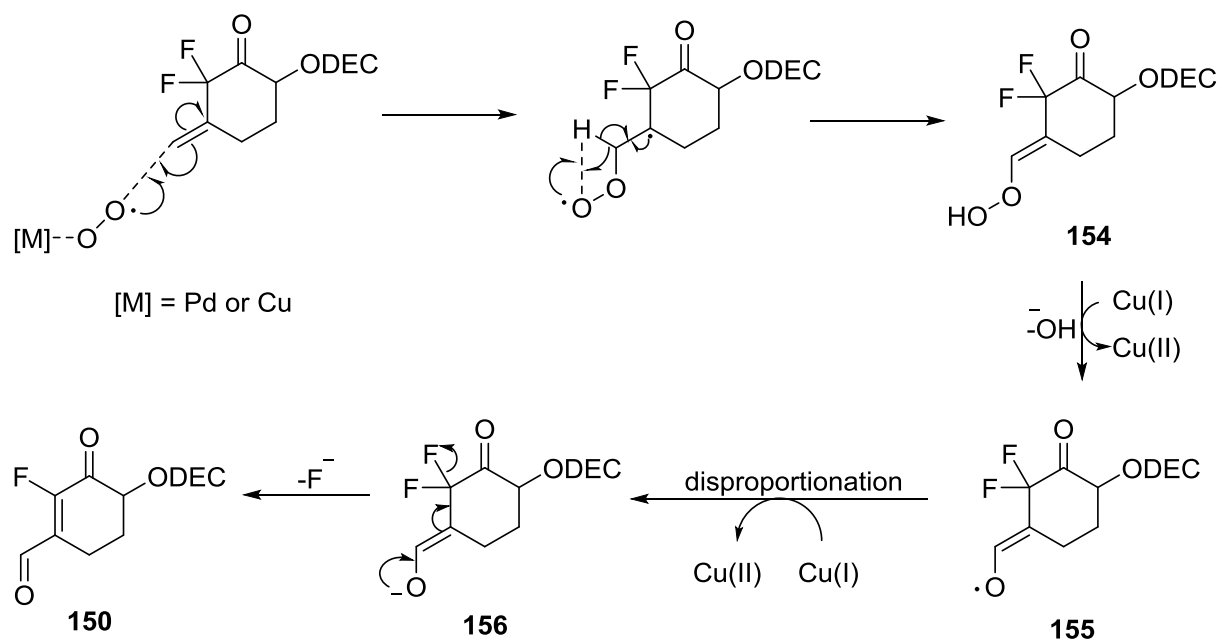
transition metal-ion catalysed decomposition to alkoxy radicals and hydroxide anions (Figure 44).^{169,170}



Figure 44: Transition metal catalysed decomposition of hydroperoxides.

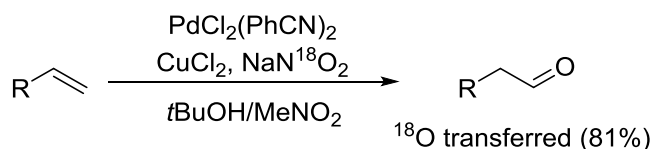
Alkoxide radical **155** could then disproportionate to form the corresponding enolate **156** which could readily eliminate fluoride to afford enal **150**.¹⁷¹

Given the observed regiochemistry of the product a radical based mechanism would make more sense since radical type addition to **113b** would occur selectively at the terminal position. This is due to the increased stability of the tertiary radical intermediate that would be generated.¹⁷² Dioxygen/copper systems are known to exist as well as oxygen coordinated palladium complexes; some feature in a number of oxidative processes *via* radical based chemistry.^{173,174} The existence of such species could also facilitate formation of enal **150** from **113b** if present under the given reaction conditions.



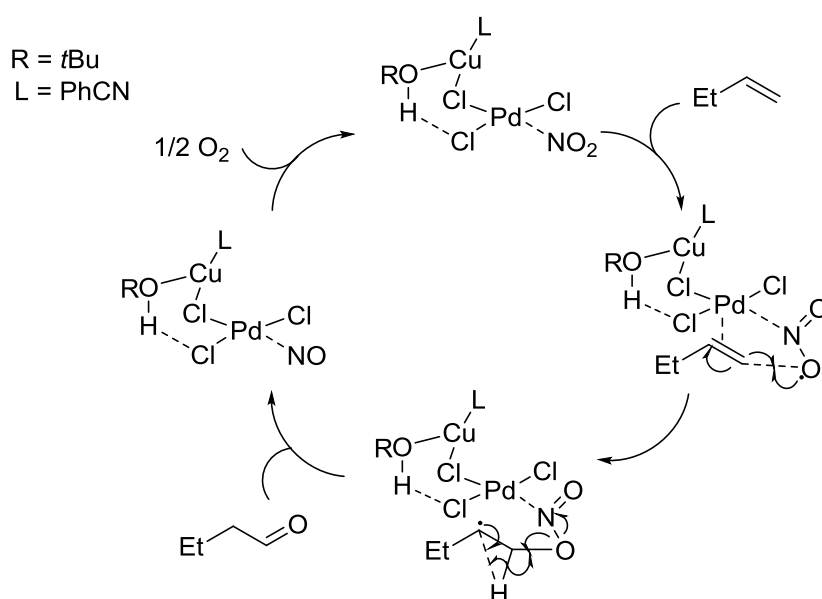
Scheme 55: Proposed radical based mechanism to explain formation of **150**.

Grubbs *et al.* have recently designed a catalyst-controlled Wacker type oxidation and initially proposed a similar radical based mechanism to explain the anti-Markovnikov selectivity observed in their systems (Scheme 56).^{175,176}



Scheme 56: Grubbs' catalyst-controlled Wacker oxidations.

In this case, ^{18}O labelling experiments identified the nitrite salt as the oxidising agent in the reaction. More recently Fu *et al.* performed DFT calculations to validate this radical mechanism and found that a *t*-BuOH-ligated heterobimetallic nitrite Pd-Cu complex was most likely to be the catalytically active species.¹⁷⁷ The observed regioselectivity was attributed to a radical based 1,2-hydride shift (**Scheme 57**).



Scheme 57: Mechanism for aldehyde selective Wacker oxidation.¹⁷⁷

The cyclisation of **112b** was next attempted at 20 mol %, 50 mol % and 100 mol % palladium loading (**Figure 45**).

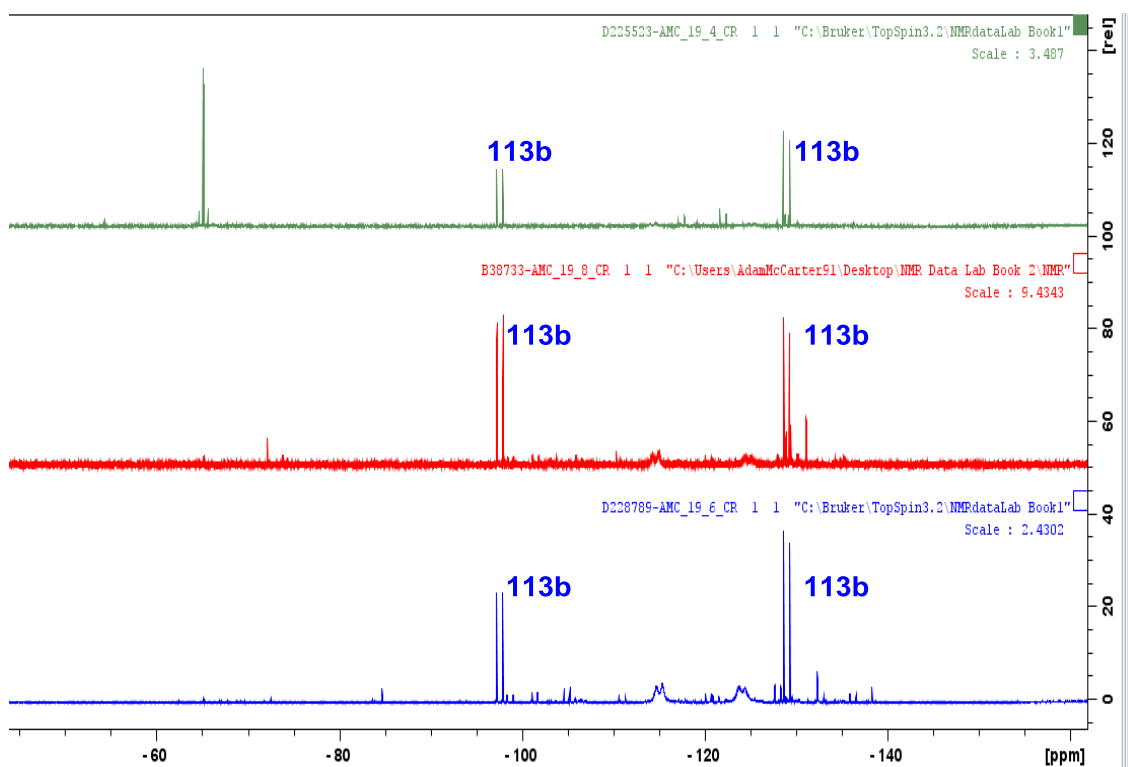


Figure 45: ^{19}F NMR spectra of crude reaction mixture of cyclisation of **112b** to **113b** at A) 20 mol % $\text{Pd}(\text{OAc})_2$, B) 50 mol % $\text{Pd}(\text{OAc})_2$ and C) 100 mol % $\text{Pd}(\text{OAc})_2$.

The result from the reaction with 20 mol % palladium was initially encouraging (spectrum A in **Figure 45**). The two doublets at -97.6 and -129.0 ppm had coupling constants of 252.8 Hz, characteristic of geminal coupling in unsaturated α,α -difluoroketones, therefore these signals were consistent with the formation of the desired product **113b**. Interestingly, enal **150** was not observed in the reaction and it appears that it is formed in reactions with lower catalyst loading which are inherently slower. Although no enal could be detected, a new side product was now present in the reaction. Upon closer inspection of the signals at -65 ppm, it was clear that they were part of an AB system ($(\delta = -65.0, -65.5 \text{ (AB}_q, J_{\text{AB}} = 166.7 \text{ Hz)})$). This AB quartet was also present in the crude reaction mixtures of the 5 mol % and 10 mol % $\text{Pd}(\text{OAc})_2$ experiments though it had not then been identified. The chemical shift at which these signals appeared in the ^{19}F NMR spectra are characteristic of a $-\text{CF}_2\text{X}$ environment and it was expected that this set of signals corresponded to chlorodifluoromethyl ketone (CDFMK) **157** (**Figure 46**). Saegusa *et al.* have successfully chlorinated a range of silyl enol ethers to the corresponding α -chloro ketones by using CuCl_2 as the chlorinating agent.¹⁷⁸ Although the optimised reaction conditions uses CuCl with copper in the +1 oxidation state, initial oxidation of $\text{Cu}(\text{I})$ to $\text{Cu}(\text{II})$ by molecular oxygen is expected generating CuCl_2 *in situ* (a more detailed discussion of the redox cycle will be made in *Section 3.4.4*). Therefore, a

significant build-up of Cu(II) could make difluorinated silyl enol ether **112b** susceptible to chlorination.

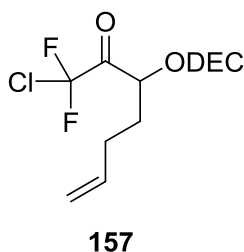
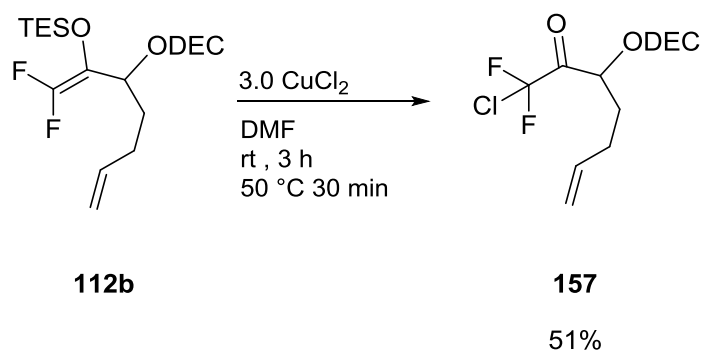


Figure 46: CDFMK suspected to be formed in cyclisation of **112b**.

In an attempt to elucidate the nature of the AB system, CDFMK **157** was synthesised independently using Saegusa's protocol for chlorination (**Scheme 58**).



Scheme 58: Synthesis of CDFMK **154**.

However on comparison of the ¹⁹F NMR of CDFMK **157** with that of the crude reaction mixture at 20 mol % Pd(OAc)₂, it appeared that the two sets of signals were not the same (**Figure 47**).

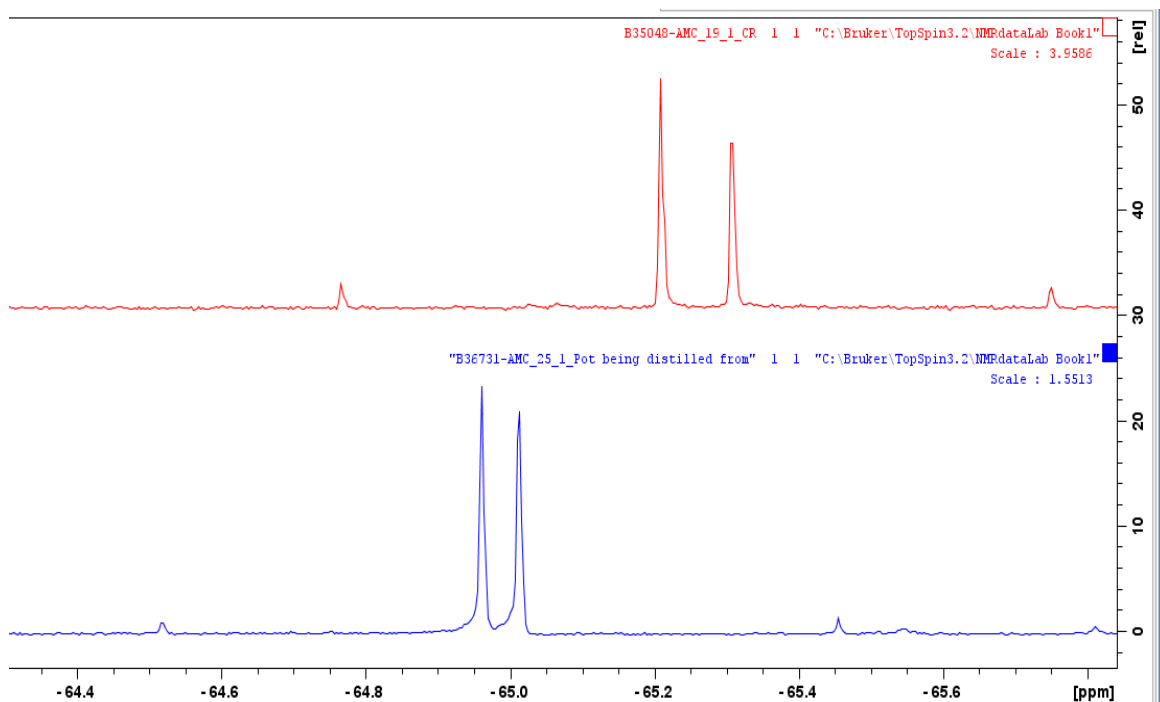
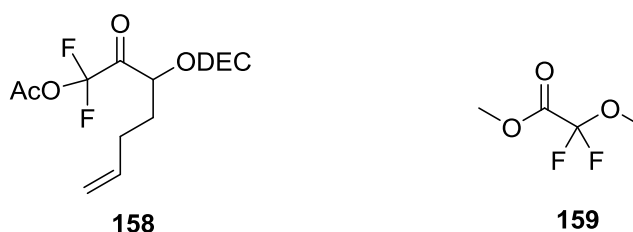


Figure 47: ^{19}F NMR spectra of A) Crude reaction mixture of cyclisation of **112b** to **113b** at 20 mol % Pd and B) independently synthesised CDFMK **157**.

The same spin system clearly exists in both spectra and both have similar coupling constants ($J = 166.8$ Hz); however, the chemical shifts of the two sets of signals differ slightly, $\delta = -65.0, -65.5$ (AB_q , $J_{\text{AB}} = 166.7$ Hz) and $-64.9, -65.1$ (AB_q , $J_{\text{AB}} = 166.8$ Hz) in ^{19}F NMR spectra A and B respectively. The difference in chemical shifts between the two is significant enough to conclude that CDFMK is not present in the crude reaction mixture. The identity of this side product is still unclear; however, another possibility could be that acetate **158** was formed (**Figure 48**).



^{19}F NMR $\delta = -64.9, -65.1$ ppm (AB_q)

^{19}F NMR $\delta = -81.8$ ppm ¹⁷⁴

Figure 48: Potential side product from reaction.

Acetate **158** would still possess a $-\text{CF}_2\text{X}$ chemical environment and presumably adopt a similar AB spin system. Unfortunately there are very few examples in the literature with this particular kind of functionality and the closest related molecule would be methyl ester **159** (**Figure 48**).¹⁷⁹ On comparison of the chemical shift values of **158** and **159**, it

seems unlikely that ketone **158** is responsible for the signals observed experimentally; however, its existence cannot be completely ruled out.

The unidentified side product observed in the 20 mol % experiment was not present when higher catalyst loadings (50 mol % and 100 mol %) were used. However, trace amounts of enal were once again present in the crude reaction mixture (**Figure 49**). At these higher palladium loadings, broad peaks at -115.1 and -124.1 ppm could now also be detected. Similar broad peaks had been observed previously for monomethylated hydrate **117a**, so these signals were attributed to the hydrated form of **113b** (**Figure 49**).

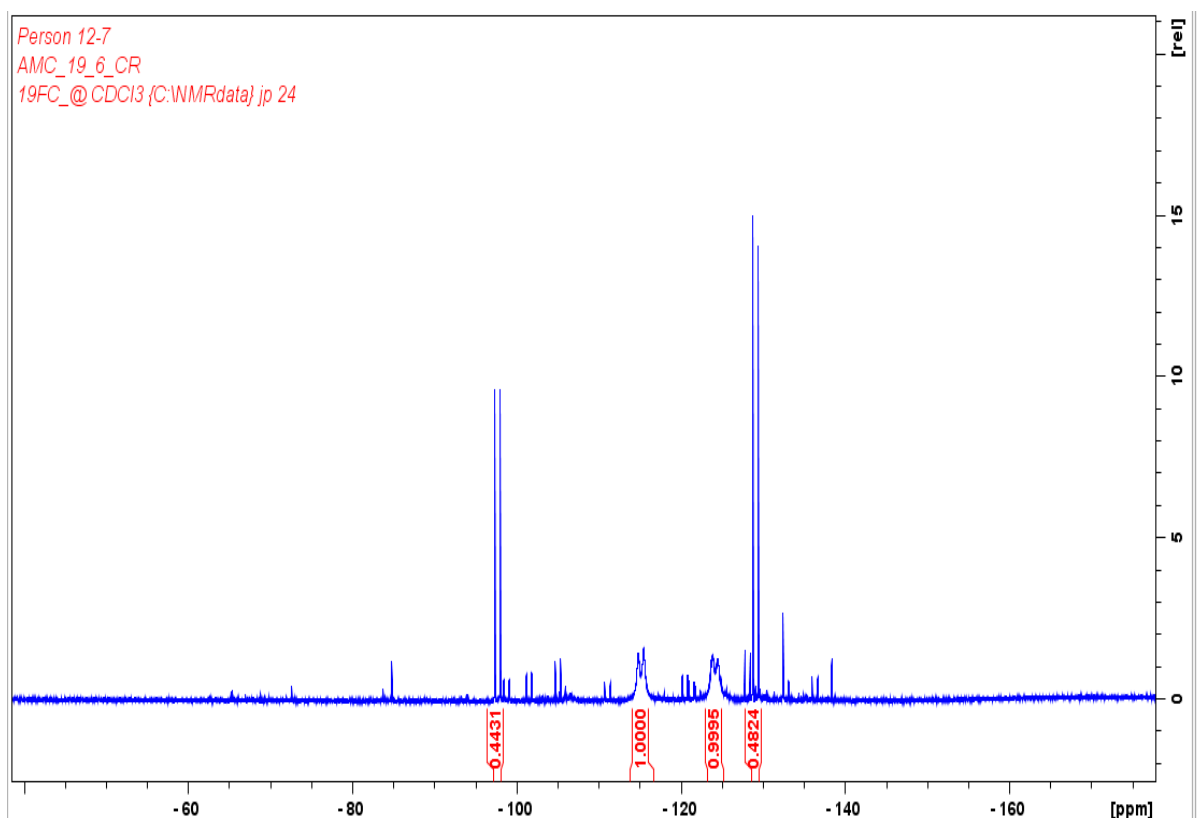


Figure 49: ^{19}F NMR spectrum of the crude reaction mixture with stoichiometric $\text{Pd}(\text{OAc})_2$ containing predominantly ketone **113b** and hydrate **117b**.

Unfortunately isolation of **113b** from both the 50 mol % and 100 mol % reactions proved troublesome. Trituration of the crude reaction mixtures with pentane afforded a gummy solid, even after scavenging (with silica SPM32 or STA3), and attempts to recrystallize the waxy material were unsuccessful. Purification of the crude product by column chromatography initially appeared successful, and following drying, a colourless solid consisting of ketone **113b** and hydrate **117b** was obtained. In an effort to isolate pure ketone **113b**, the mixture was subjected to the standard drying conditions (vacuum oven for 48 hours at 1 mbar and 40 °C). Disappointingly, after this time the mixture had

completely decomposed and no traces of ketone **113b** or hydrate **117b** could be detected. At this stage, when considering the economical and practical limitations of the synthesis no further attempts were made to isolate **113b**.

3.4.3.3 Attempts to synthesise **113i**

Another ketone which could not be isolated successfully was bicyclic heterocycle **113i** (**Figure 50**).

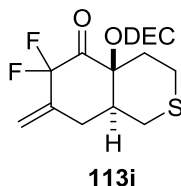


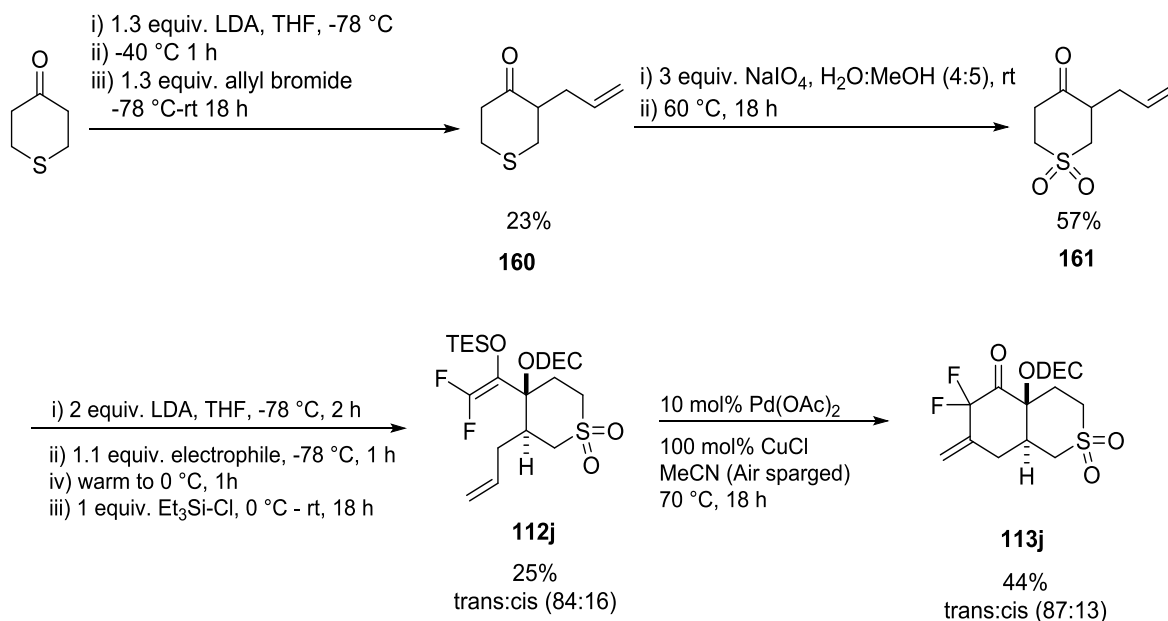
Figure 50: Sulfide heterocycle **113i**.

The inability to cyclise sulfide **113i** was not surprising considering the potential for sulfur to coordinate to palladium. Stahl *et al.* have recently demonstrated that the sulfur atom in DMSO can coordinate strongly to Pd(II) species in solution.¹¹⁴ Owing to the increased Lewis basicity of sulfide **112i** compared to that of sulfur in DMSO, a slow rate of cyclisation was to be expected. Indeed, at 5 mol % Pd(OAc)₂ the reaction was incomplete by TLC after 24 hours. The mixture was left stirring for a further 120 hours until SEE **112i** had been fully consumed; however, after this time an extremely complex mixture was obtained. Peaks at -98.6 and -124.8 ppm were assigned to the desired product but only trace amounts could be detected.

The cyclisation was attempted once more at a loading of Pd(OAc)₂ of 20 mol %. This time the reaction was complete after 96 hours and, as in the cyclisation of **112b**, the higher catalyst loading afforded a cleaner reaction. Unfortunately, product isolation once again proved to be problematic and trituration of the crude material with pentane once again afforded a gummy solid.

Rather than repeat the cyclisation at higher catalyst loadings, it was instead decided to address the issue regarding sulfur coordination to palladium. One way of overcoming this problem would be to oxidise the sulfide precursor to the corresponding sulfone prior to cyclisation. The sulfone analogue would also be an attractive motif from a medicinal chemistry perspective since the sulfone moiety is known to act as a bioisostere for the carbonyl functionality.^{180,181} Oxidation of allylthiopyranone **160** afforded the desired sulfone as a colourless solid in good yield (**Scheme 59**). Unfortunately, as mentioned in

Section 3.4.1, despite vigorous drying attempts of **161** SEE **112j** could only be isolated in 25% yield.



Scheme 59: Overall synthesis of sulfone heterocycle **140j**.

With sulfone **112j** in hand the cyclisation was attempted with 5 mol % Pd(OAc)₂. The cyclisation was successful and SEE was completely consumed after 18 hours. Following standard work up and purification (scavenging and trituration with pentane), NMR analysis of the yellow solid obtained revealed that the material contained trace amounts of what appeared to be aldehyde **162** by the signal at -130.4 ppm in the ¹⁹F NMR spectrum (**Figure 51**).

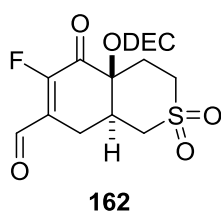


Figure 51: Aldehyde impurity present in crude solid material.

Recrystallisation of the solid with DCM/hexane effectively delivered pure ketone **113j**; however, a result of this extra purification step meant that the yield of **113j** was slightly lower than for other cyclisations (*Section 3.4.3 Table 9*). One final feature to note regarding **113j** is that this was the only α,α -difluoroketone to be obtained as a mixture of *cis*- and *trans*- diastereoisomers. Curiously, in the case of SEE precursors **112f** and **112h**, which were cyclised as a mixture of diastereoisomers, only a single product diastereoisomer (present as a mixture of enantiomers) was observed from the reaction.

3.4.4 Copper/Palladium Screening Experiments

As mentioned previously in *Section 3.1*, the Saegusa-Ito reaction is a palladium(II)-catalysed oxidative carbocyclisation process which, like many palladium(II)-catalysed reactions, requires a co-oxidant to efficiently restore the Pd(0) generated in the reaction to the original +2 oxidation state (**Figure 52**).

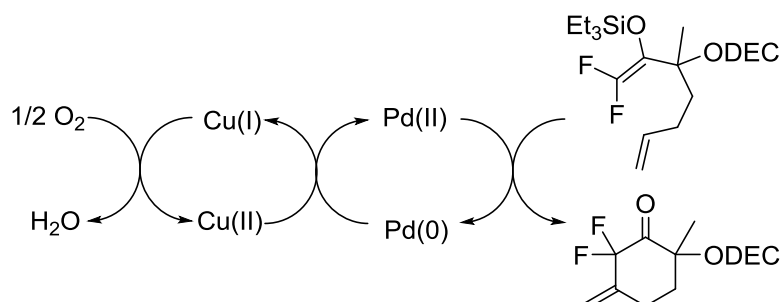
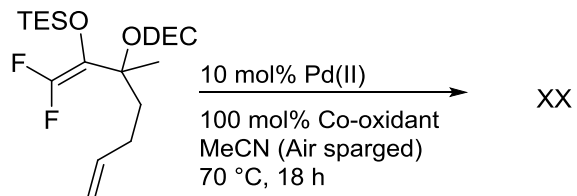


Figure 52: Suspected Pd(II)/Cu(II) redox cycle employed in the cycloalkenylation system.

Following a catalyst and co-oxidant screen conducted during initial optimisation of the reaction, palladium(II) acetate and copper(I) chloride were identified as the most suitable catalyst and co-oxidant for the current system.⁸⁶ However, a second co-oxidant/catalyst screen was conducted in order to attempt to further understand the effects of copper source and catalyst on reaction efficiency. The results of the screening experiments are highlighted in **Table 10**. **SEE 112a** was chosen as the trial substrate and from the various combinations of palladium catalyst and copper salt a number of significant side products were identified.

Table 10: Copper salt and palladium catalyst screening results.



Entry	Pd(II)	Co -oxidant	% Conversion of 139a by ¹⁹ F NMR						Isolated Yield 113a (%)
1	-	CuCl	6	0	0	1	0	3	-
2	Pd(OAc) ₂	-	30	2	65	0	2	1	-
3	PdCl ₂	CuCl	14	78	0	0	0	8	11
4	Pd(OAc) ₂	CuCl	0	97	0	0	3	0	52
5	Pd(OAc) ₂	CuCl ₂	0	0	0	0	0	- ^[a]	-
6	Pd(OAc) ₂	CuOAc	0	87	8	0	5	0	- ^[b]
7	Pd(OAc) ₂	Cu(OAc) ₂	0	19	1	0	0	0	39
8	PdCl ₂	CuOAc	0	66	0	0	34	0	- ^[b]
9	PdCl ₂	Cu(OAc) ₂	0	100	0	0	0	0	40

[a] Only product identified from crude ¹⁹F NMR spectrum [b] Ketone **140a** could not be isolated from the reaction mixture using standard work up/purification procedure.

Entries 1 and 2 in **Table 10** were run as control experiments; however, a significant amount of information regarding reaction mechanism and potential side products could be obtained from these two experiments. As expected in the absence of palladium catalyst (Entry 1 **Table 10**) no cyclised product could be observed and the reaction returned predominantly starting material. However, a new set of signals at -66.9 and -67.6 ppm were now also apparent in the reaction mixture (**Figure 53**).

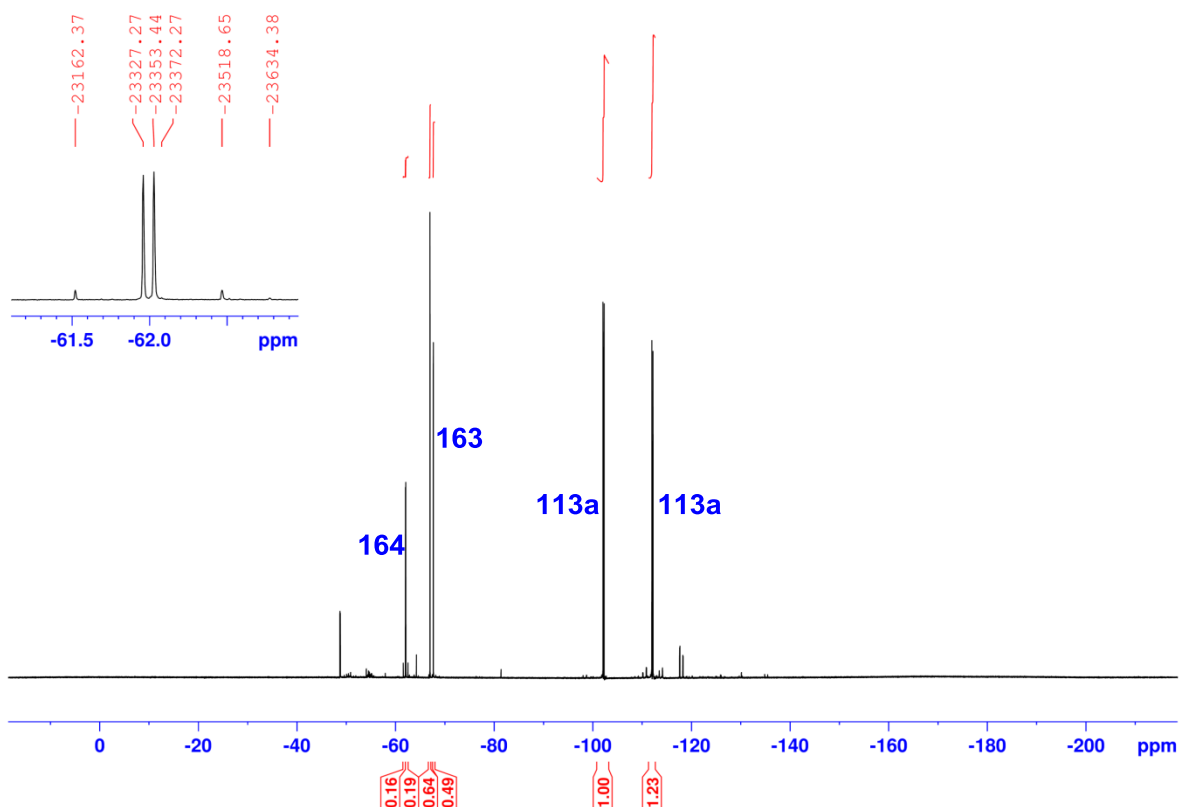


Figure 53: ^{19}F NMR spectrum of crude reaction mixture Entry 1 **Table 10**.

Initially, these were misassigned as a $-\text{CF}_2\text{X}$ type species (where $\text{X} = \text{Cl}$); however, following purification the signals were identified as the *E*- and *Z*-alkenes **163** bearing equivalent fluorine atoms (**Figure 54**).

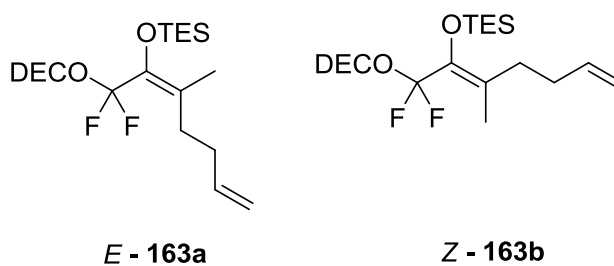
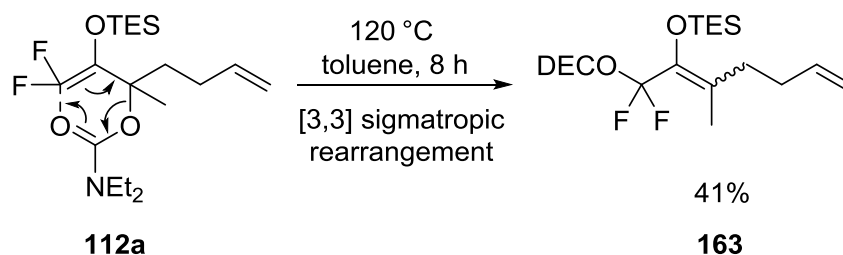


Figure 54: SEE diastereoisomers.

The formation of these species may arise from a [3,3]-sigmatropic rearrangement. Although palladium(II)-catalysed [3,3]-sigmatropic rearrangements are well documented, heating SEE **112a** at 120 °C for 8 hours afforded the rearrangement products **163** so it seems unlikely that the process is palladium mediated in the current system (**Scheme 60**).¹⁸²



Scheme 60: Independent synthesis of **163** by microwave irradiation.

Fortunately, the kinetic barrier for rearrangement is sufficiently high for the cyclisation pathway to be favoured; otherwise, **163** would dominate in the reactions. The formation of **163** is unsurprising as there is a strong driving force for the carbon bearing the fluorine substituents to change hybridisation state from sp^2 to sp^3 . The π system of the alkene in SEE **112a** is destabilized by a repulsive interaction between the fluorine atom lone pairs and the π -orbitals of the sp^2 hybridized carbon atoms (**Figure 55**).¹⁸³

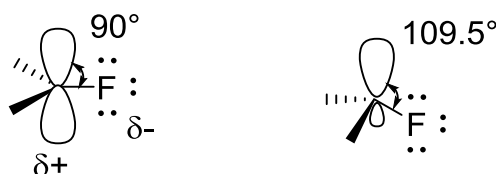
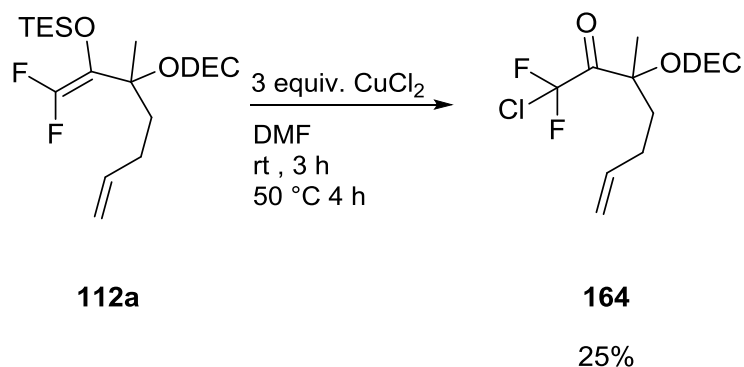


Figure 55: Release of repulsive strain on carbon from $sp^2 \rightarrow sp^3$ hybridization.

Rearrangement of **112a** to **163** induces re-hybridization to the sp^3 state thereby partially relieving this repulsive strain.

An additional set of signals which were characteristic of an AB system were now also visible. The splitting pattern and chemical shift was similar to that observed previously in the attempted cyclisation of SEE **112b** (See *Section 3.4.3.2*). Once again these signals were initially assigned to diastereotopic fluorine atoms present in CDFMK **164** (**Scheme 61**). Initial oxidation of CuCl by molecular oxygen would generate CuCl₂; however, in the absence of a Pd(0) source to reduce CuCl₂ back to CuCl this would inevitably lead to a build-up of CuCl₂. To confirm the presence of CDFMK, **164** was synthesised independently as before using Saegusa's chlorination conditions (**Scheme 61**).



Scheme 61: Synthesis of CDFMK **161**.

Only trace amounts of cyclised product could be detected when SEE **112a** was exposed to Pd(OAc)₂ in the absence of a copper co-catalyst (Entry 2 **Table 10**). It was expected that the reaction would afford a low yield of cyclic product and recovered starting material. However, analysis of the ¹⁹F NMR spectrum of the crude reaction mixture revealed the major product to be DFMK **147a**, characterised by two distinct sets of doublet of doublets at -124.5 and -126.3 ppm (**Figure 56**).

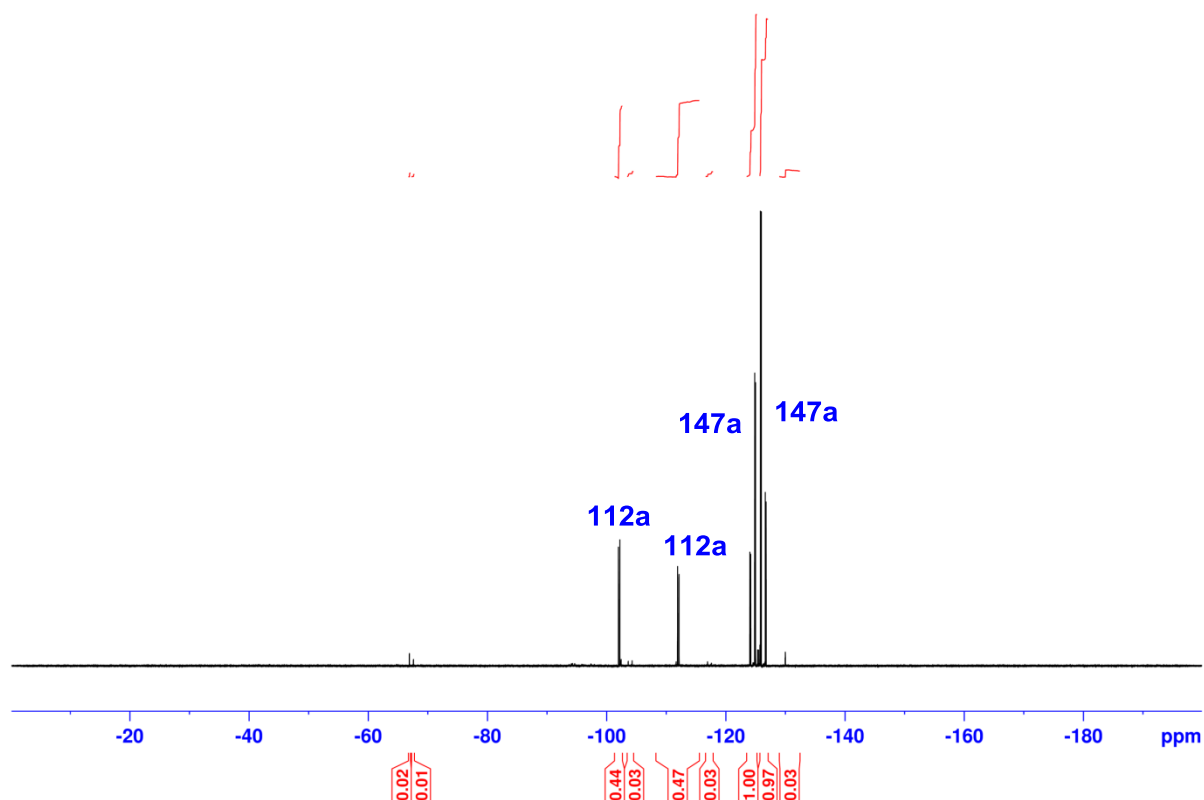
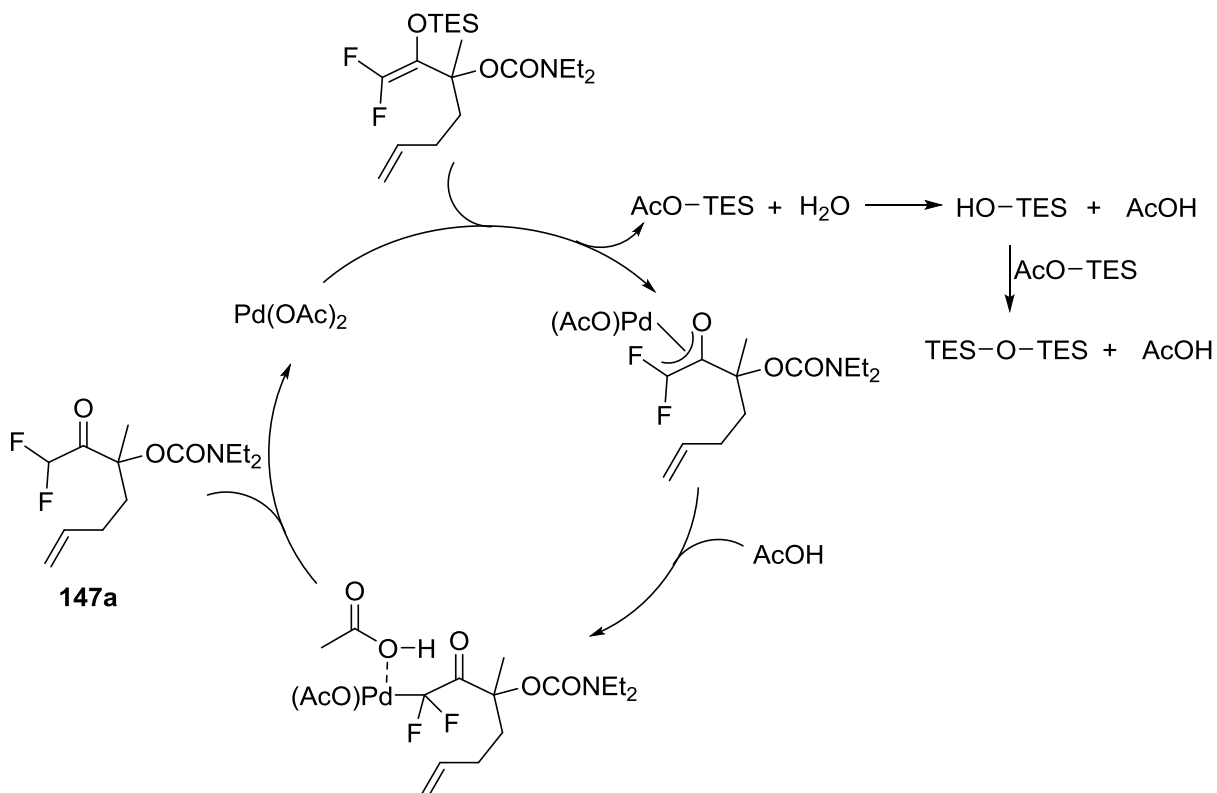


Figure 56: ¹⁹F NMR spectrum of crude reaction mixture of Entry 2 **Table 10**.

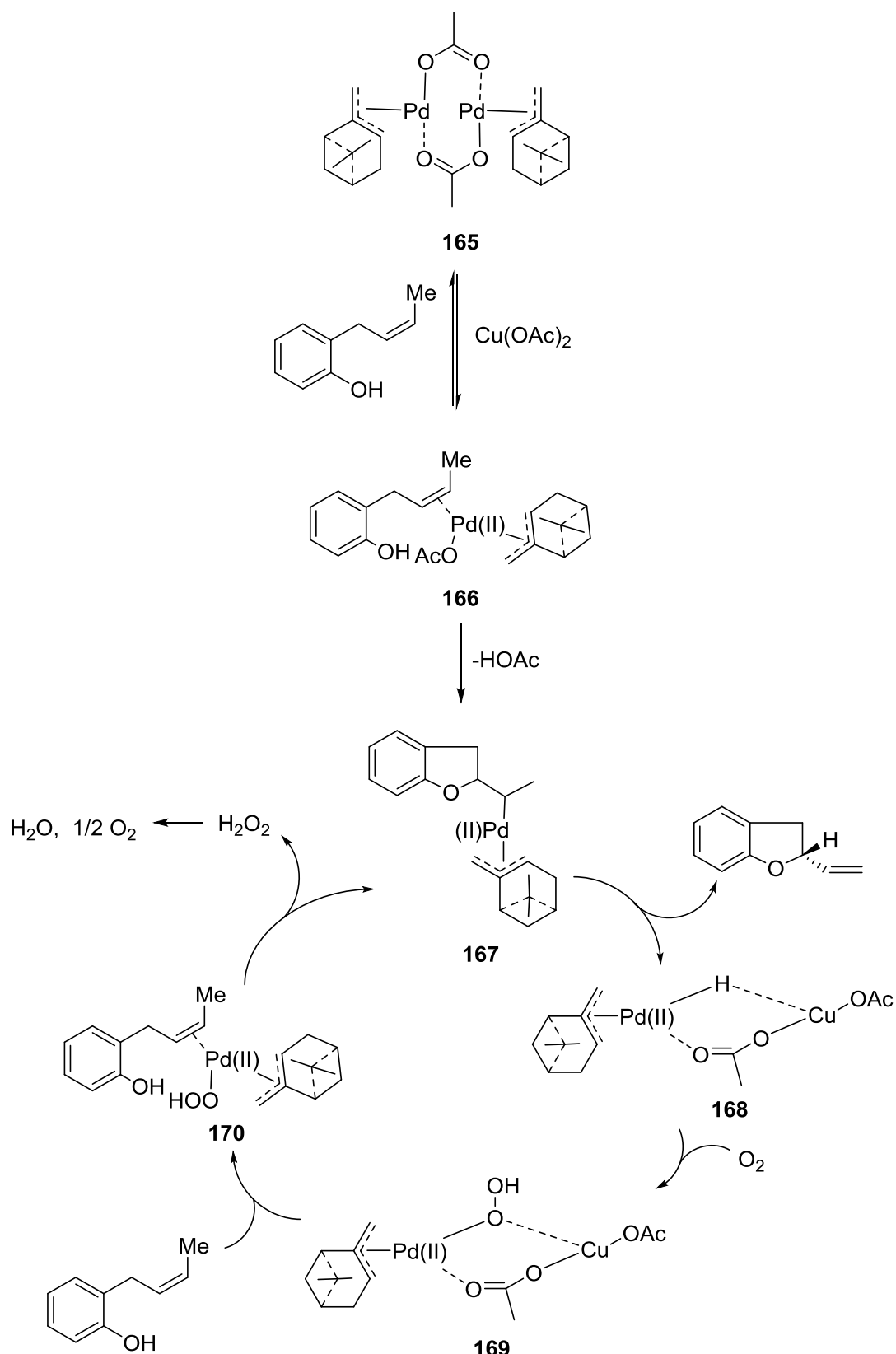
DFMK **147a** is formed as a result of protodesilylation where the silyl group is removed by an acetate ion.⁹² However, only a catalytic quantity of Pd(OAc)₂ was employed in the reaction (10 mol %) which would not account for the levels of DFMK **147a** observed if

palladium was not being turned over. This suggests that a catalytic protodesilylation process is occurring (**Scheme 62**).



Scheme 62: Proposed mechanism of catalytic protodesilylation.

Co-oxidants like copper salts are often thought to act as electron transfer mediators in palladium(II) catalysed oxidative processes by facilitating electron transfer between palladium and oxygen. However, the effective recycling of palladium in the absence of copper chloride suggests that the co-catalyst is in fact playing a fundamental role in generating the catalytically active species for cyclisation. Murahashi *et al.* have provided strong evidence for a Pd-Cu bimetallic complex **169** as the catalytic species in the asymmetric oxidative cyclisation of 2-allylphenols (**Scheme 63**).¹⁸⁴



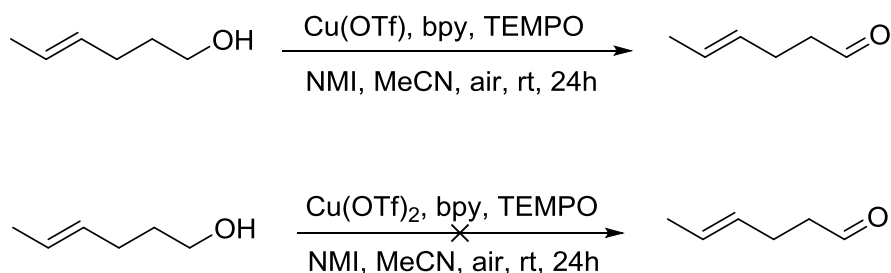
Scheme 63: Murahashi's asymmetric palladium(II)-catalysed oxidative cyclisation.

Palladium dimer **165**, synthesised by the reaction of (-) - β pinene with Pd(OAc)_2 , can coordinate reversibly to the terminal olefin of the substrate to afford monomeric acetate **166**. Subsequent oxypalladation generates intermediate **167** which can then undergo β -

hydride elimination to produce the desired product and bimetallic Pd-H species **168**. Oxidation of this intermediate with molecular oxygen forms hydroperoxo complex **169** which can coordinate to a second substrate molecule to cleave the acetate bridge and reform a monomeric Pd intermediate **170**. Intramolecular nucleophilic attack of the phenoxy group regenerates intermediate **167** and completes the catalytic cycle.

An interesting feature which the authors note is that, unlike conventional palladium(II) oxidative catalysed processes, the formal oxidation state of Pd(II) remains constant throughout this system i.e. an isohypsic process.¹⁸⁵ Based on the results from the Pd(OAc)₂ and CuCl runs (Entries 1 and 2 **Table 10**) it is possible that a similar bimetallic species is operating in the cycloalkenylation mechanism (**Scheme 64**).^{186,187,188,189}

inhibition of the cyclisation (Entry 5 **Table 10**). Despite full consumption of SEE **112a** the reaction afforded a complex mixture in which the only products that could be readily identified were rearrangement products **163a** and **163b**. It appears that the presence of the active reoxidant (assumed to be copper(II)) at the start of the reaction is detrimental whereas it is beneficial for copper to be present initially in the +1 oxidation state, with Cu(II) generated *in situ*. In recent work focussing on alternative oxidation methods for the oxidation of primary alcohols Stahl *et al.* observed similar behaviour where the initial oxidation state of the copper catalyst had a significant impact on reaction efficiency (**Scheme 65**).^{190,191}



Scheme 65: Increased reactivity of copper(I) salts in aerobic oxidations.

Though a copper(II) species is the catalytically active species in the reaction, the rate of oxidation of 4-hexen-1-ol is dramatically decreased when Cu(OTf)₂ is employed (reaction time >24 hours cf. 20 minutes for CuOTf). The origins of this unusual effect are still unclear. Another interesting feature in the CuCl₂ experiment was that no CDFMK **164** could be detected in the reaction mixture. This was highly surprising as the use of CuCl₂ as a chlorinating agent has been clearly demonstrated in the synthesis of **157** and **164** as well as in the control reaction with CuCl (Entry 1 **Table 10**).

Speziali *et al.* have previously stated that the presence of chloride ions in palladium(II) catalysed aerobic oxidations is required to facilitate the recycling of Pd(II).^{192,193} The coordination of chloride ions is thought to bring the redox potentials of the Pd(0)/Pd(II) and Cu(II)/Cu(I) half-cells closer together, resulting in a more thermodynamically favourable electron transfer process. It was therefore expected that the all-acetate reactions would yield little product. Surprisingly, appreciable amounts of cyclised product **113a** were formed when both Cu(OAc) and Cu(OAc)₂ were employed (**Figure 57**).

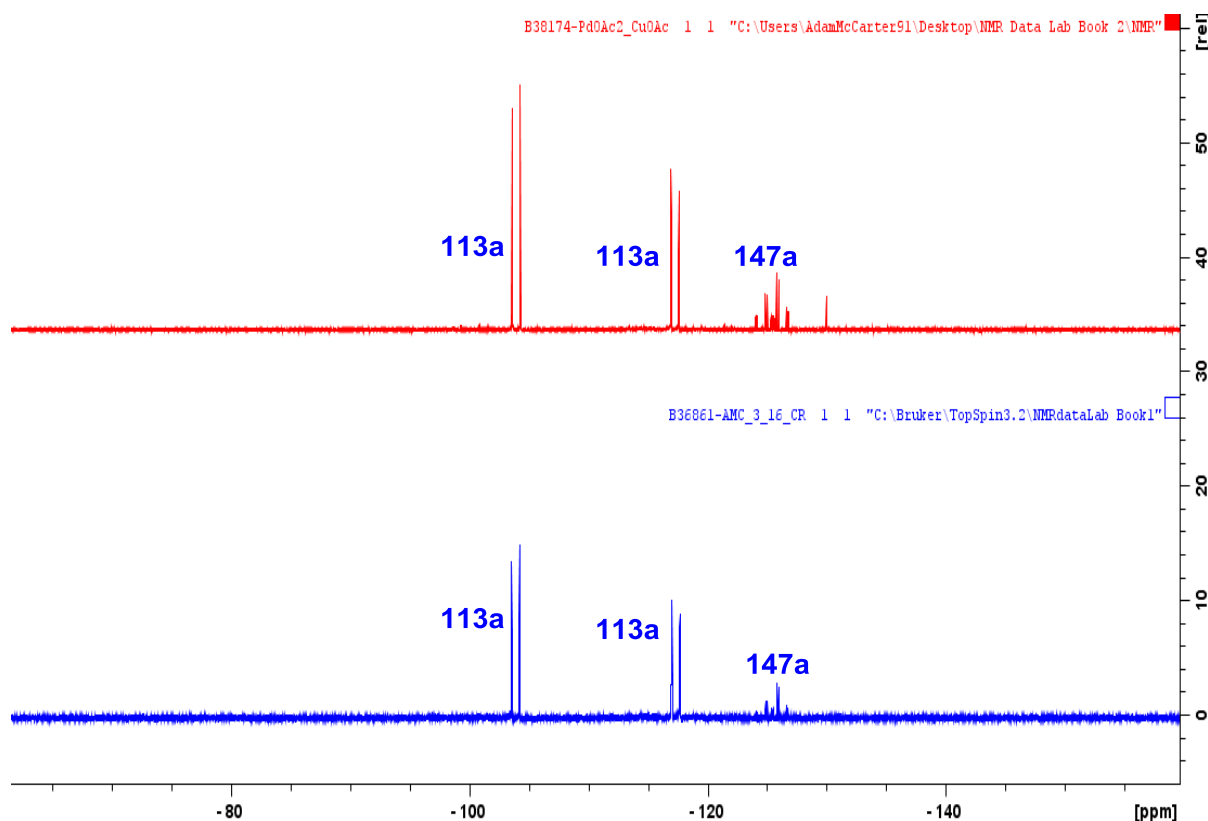


Figure 57: ^{19}F NMR spectra from the crude reaction mixtures of cyclisation of **112a** to **113a** with CuOAc (above) as the co-oxidant and $\text{Cu}(\text{OAc})_2$ (below) as the co-oxidant.

This provides further evidence to suggest that the reoxidation of palladium(0) is performed directly by molecular oxygen and that the co-catalyst is instead required to generate the catalytically active species.

The presence of DFMK **147a** in both reactions is not surprising; acetate ions are responsible for the removal of the silyl group and there is a molar excess present in solution (**Table 10** Entries 6 and 7). However, a new triplet signal at -130 ppm was present in the reaction with CuOAc ($^4J_{\text{H-F}} = 6.7$ Hz). Although the compound was not isolated, the signal was tentatively assigned to that of monomethylated enal **152** on the basis of the chemical shift and coupling constants calculated for **150**, details of which can be found in the accepted manuscript based on this study (**Figure 58**).¹⁹⁴

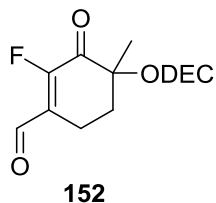


Figure 58: Monomethylated enal **152**.

As in the case of enal **150** the formation of this species may be a result of a slower cyclisation with the oxidation of Cu(I) to Cu(II) required to initiate the redox cycle. Unlike in the CuCl₂ case, the use of Cu(OAc)₂ did not appear to have any effect on reaction efficiency affording a cleaner reaction than when CuOAc was used.

An even slower cyclisation ensued in an all chloride environment (PdCl₂/CuCl), which returned SEE **112a** and [3,3]-rearrangement products (Entry 3 **Table 10**). However, switching the co-oxidant to Cu(OAc)₂ resulted in an extremely clean reaction, comparable to that obtained under the standard conditions (Entry 4 **Table 10**); **140a** was the only product which could be detected in the reaction mixture (Entry 9 **Table 10**). Direct comparison of these three results (Entries 3, 4 and 9 **Table 10**) provides further evidence to suggest that OAc must interact with Pd(II) to form a catalytically-active acetate-bridged bimetallic species. Acetate ions are known to act effectively as bridging ligands between pairs of metal atoms.¹⁹⁵ Again, when CuOAc is used in combination with PdCl₂ it appears that this results in a slower cyclisation and increased levels of enal **152** are now present (Entry 8 **Table 10**).

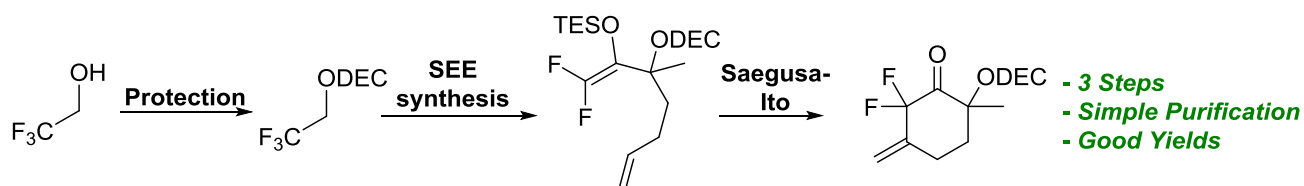
Based on all of the above, a number of conclusions can be drawn from the results of the screening experiments:

- 1- When a chloride-based co-oxidant is employed, it is better for the concentration of Cu(II) to be low at the start of the reaction and for it to be generated slowly *in situ*.
- 2- The redox cycle can operate successfully under chloride-free conditions. The exact role of chloride ions is still unclear but they do not seem to have a significant influence on redox potentials.
- 3- Copper(II) acetate is a more efficient co-oxidant than copper(I) acetate.
- 4- The catalytically active species in an all-acetate environment and in a mixed chloride/acetate environment are very similar if not identical.
- 5- Use of a co-catalyst is required to generate the catalytically active species and to ensure a successful cyclisation.
- 6- The catalytically active species in the reaction is most likely a bimetallic, acetate-bridged Pd/Cu species.

The methodology described in this chapter represents a novel, practical and efficient method for the construction of difluorinated cyclohexenones. It is also the first time that the Saegusa-Ito cyclisation has been used to synthesise selectively fluorinated molecules. The highly active redox system developed affords reaction products which are otherwise difficult to access by other means and further expands the scope of fluorinated building-block based synthesis. Furthermore, the cyclohexenone scaffolds have the potential to serve as valuable intermediates towards the *de novo* synthesis of fluorinated carbasugars.

3.5 Conclusions

The work detailed in this chapter describes the optimisation of a palladium(II) catalysed cycloalkenylation (Saegusa-Ito cyclisation), which may have applications for the synthesis of novel difluorinated sugar analogues. The procedure developed expands upon current building block (*de novo*) synthetic methodology. The desired cyclohexenones could be accessed concisely in three synthetic steps starting from trifluoroethanol (**Scheme 66**).



Scheme 66: Route to difluorinated cyclohexenones.

Following successful cyclisation, difluorinated ketones could be efficiently isolated after treating the crude reaction mixtures with scavenger silica (STA3 and SPM32) and triturating with pentane. The modified work up/purification procedure avoided column chromatography, attenuated hydrate formation and significantly improved ketone yields. In cases where solid mixtures of hydrate and ketone were obtained vacuum oven drying (40 °C, 1 mbar, 2 days) could efficiently deliver pure ketone. The library of difluorinated cyclic ketones has been expanded to include a range of substituted monocycles, bicycles, fused ring heterocycles and spirocycles (**Figure 59**).

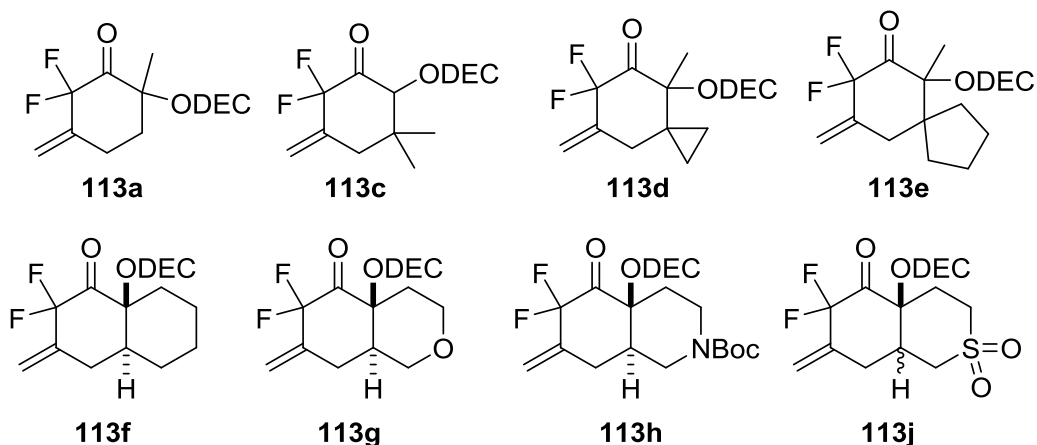


Figure 59: α,α -Difluoroketones synthesised by the new method.

Annulative processes proved to be the most efficient and cyclisations were successful at loadings of 5 mol % Pd(OAc)₂ whereas annulations required slightly higher palladium loadings (10 mol % Pd(OAc)₂). Furthermore, annulations required a degree of substitution along the carbon chain to ensure a clean cyclisation.

Only α,α -difluoroketones **113i** and **113b** could not be successfully isolated (**Figure 60**).

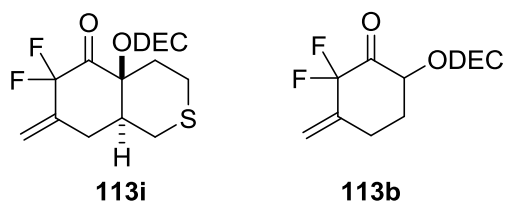
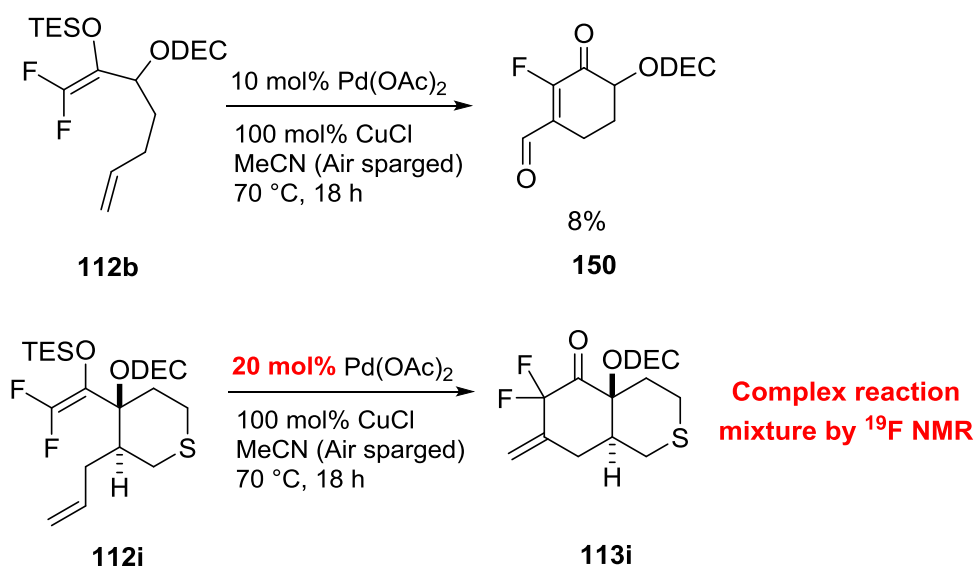


Figure 60: Difluoroketones which could not be successfully isolated.

The cyclisation of sulfide silyl enol ether **139i** was slow due to coordination with Pd(II) whereas the reaction of **139b** afforded a Wacker type product of unusual regiochemistry (**Scheme 67**).



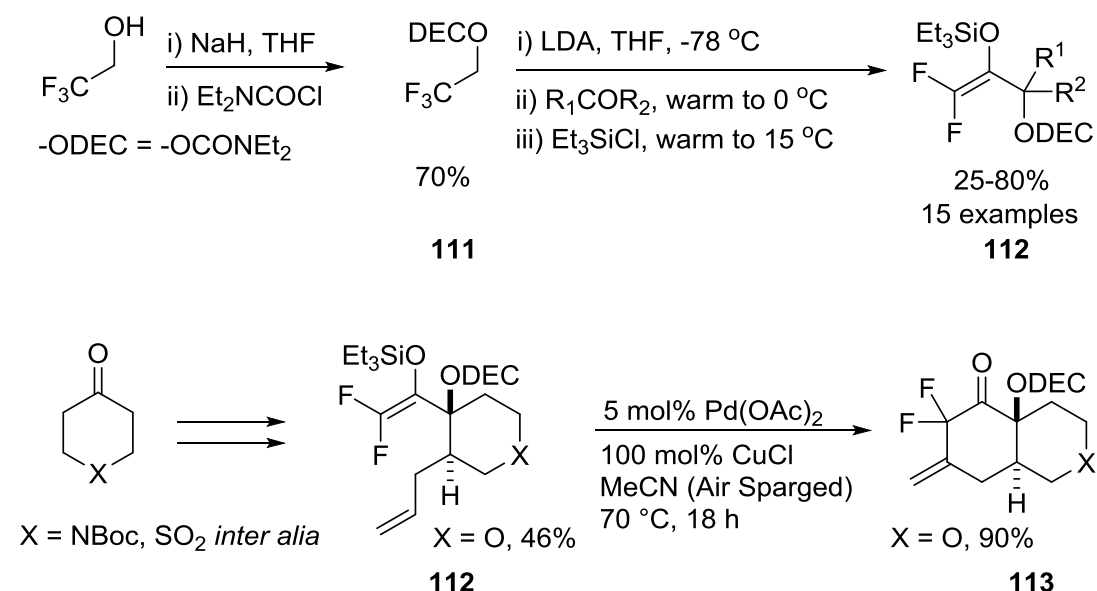
Scheme 67: Unsuccessful cyclisations.

The results of a catalyst and co-oxidant screen revealed that a combination of Pd(OAc)_2 and CuCl provided the most efficient catalytic redox system for the cycloalkenylation. The initial oxidation state of copper played an important role in determining the reaction outcome, with CuCl_2 completely inhibiting the cyclisation. In contrast to previous reports, the presence/absence of chloride ions did not appear to have a major effect on redox effectiveness and cyclisations ensued smoothly in an all-acetate environment.^{192,193} The absence of cyclised product from the control reactions (Pd(OAc)_2 only and CuCl only) highlights the significance of a co-oxidant in maintaining catalytic activity.

4. Chapter 3: Difluorinated Enol Acetals in Difluorinated Carbocycle Synthesis

4.1 Introduction

The previous Chapter illustrates that the Saegusa-Ito cyclisation can provide a concise and efficient protocol for the construction of selectively difluorinated cyclohexenones **113**.¹⁹⁴ The metallated difluoroenol carbamate chemistry allows for the preparation of silyl enol ether precursors **112** in two high yielding steps from trifluoroethanol (**Scheme 68**).¹⁴⁰ These can then be cyclised in moderate to good yields, completing a three step sequence from a widely-available and low cost fluorinated feedstock.



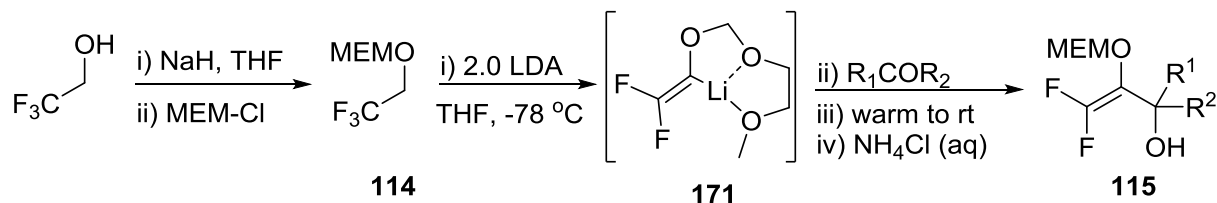
Scheme 68: Synthesis of difluorinated cyclohexenones.

Whilst this method represents a significant expansion of the available repertoire, it is limited by poor atom economy, the use of stoichiometric quantities of copper salt and the short shelf life of the silyl enol ether precursors (1 week below ambient temperature). More atom efficient cyclisations based on difluorinated enol derivatives as carbon nucleophiles would therefore be extremely attractive. The following chapter will describe efforts towards a novel carbocyclisation with improved atom economy.

4.1.1 Difluorinated Enol Acetals

The Percy group has had a long term interest in the chemistry of difluorinated enol acetals **115**, particularly for application in sigmatropic rearrangements.^{196,197,198} Difluorinated enol acetals can be prepared from acetal **114** by treatment with lithium

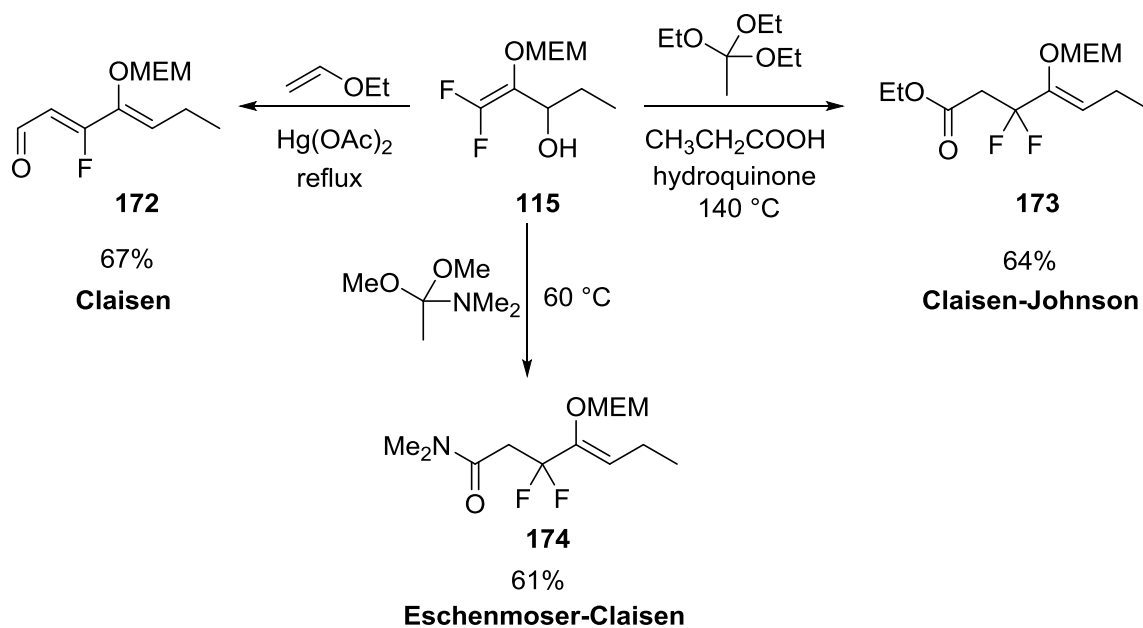
diisopropylamide, followed by trapping with aldehyde or ketone electrophiles to afford difluoroallylic alcohols **115** (Scheme 69).¹³⁹



-OMEM = -OCH₂O(CH₂)₂OCH₃

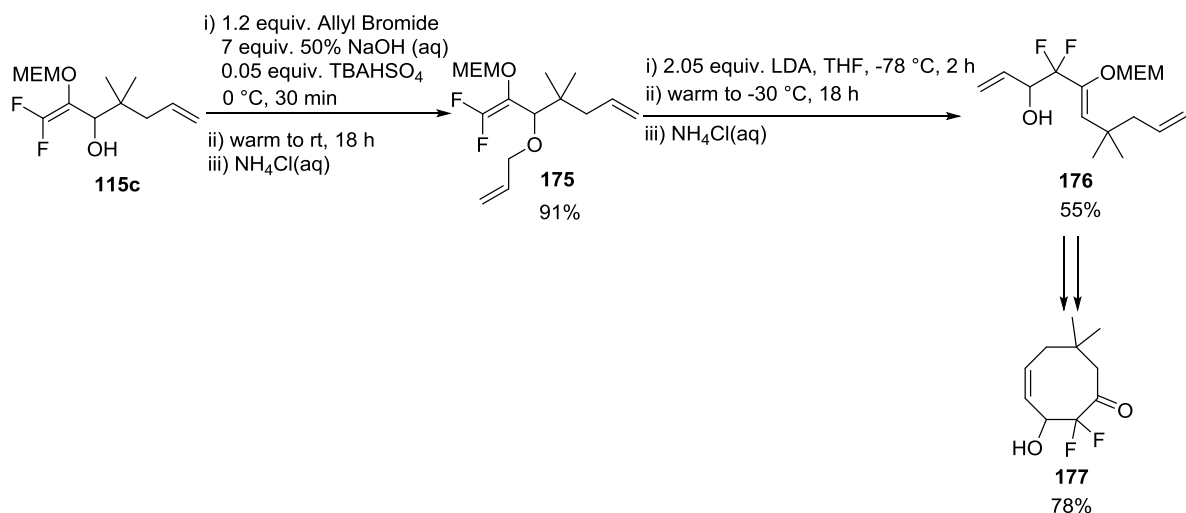
Scheme 69: Synthesis of difluoroallylic alcohols.

Such species have proved effective substrates in [3,3]-rearrangements allowing the CF₂ group to be relocated from a terminal to a mid-chain position β-to a carbonyl group, with the exception of the Claisen rearrangement where rearrangement was followed by subsequent elimination of HF (Scheme 70).¹⁹⁶



Scheme 70 [3,3] rearrangements of difluorinated enol acetals.

Difluorinated enol acetals can also undergo facile [2,3]-Wittig rearrangements to form ring closing metathesis precursors in the synthesis of difluorinated cyclooctenones **177** (Scheme 71).^{197,198}



Scheme 71: [2,3] Wittig rearrangements of difluorinated enol acetals.

Whilst these methoxyethoxymethyl (MEM) enol acetals are relatively stable during purification and storage, they can be cleaved to afford difluoroketones under acidic conditions.¹⁹⁹ However, Percy *et al.* have shown through DFT studies that the energy barrier for enol-keto conversion differs considerably between fluorinated and non-fluorinated enols (**Figure 61**).²⁰⁰

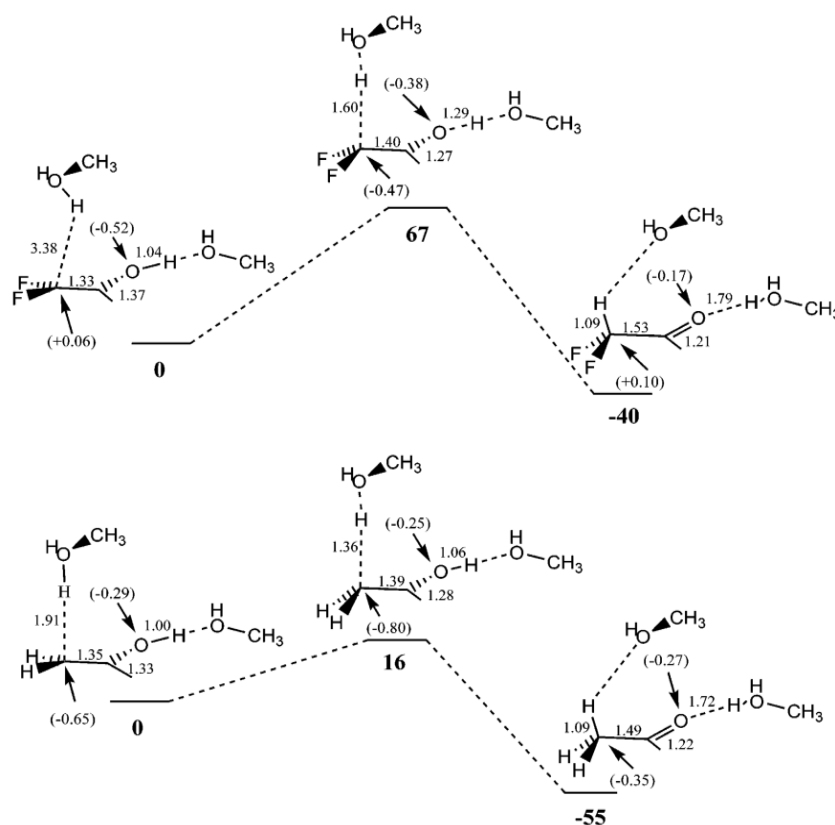
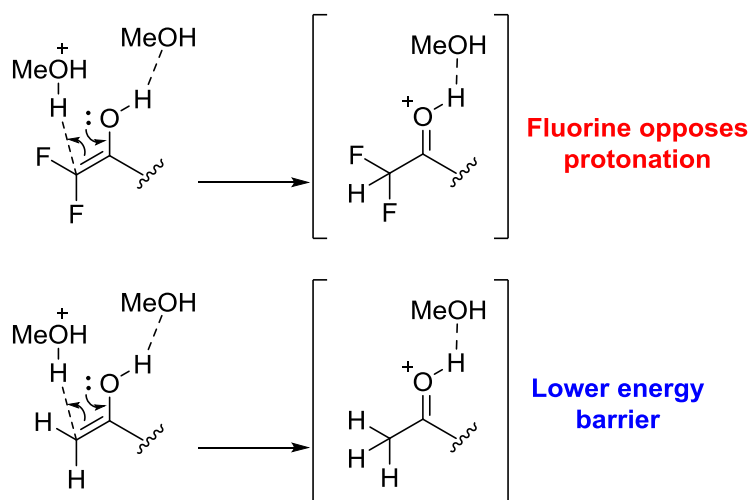


Figure 61: Enol-keto conversion reaction profiles for difluorovinyl alcohol (top) and vinyl alcohol (bottom). Free energies are given in kJ mol⁻¹, bond lengths in Å and atomic charges in parentheses. Calculations were run at the B3LYP/6-311++G** level of theory.

In acidic protic solvent the enol-keto interconversion is expected to proceed via a proton shuttling mechanism involving one protonated solvent molecule, a neutral solvent molecule and the solute. Both enol-keto transformations are favoured energetically; however, a much larger barrier exists for the difluoro species (67 kJ mol^{-1}), compared to vinyl alcohol (16 kJ mol^{-1}). It is expected that the presence of the fluorine atoms opposes tautomerisation due to the formation of the oxacarbenium ion during protonation. This build-up of positive charge would be disfavoured by the strong inductive electron withdrawing effect of the $-\text{CF}_2\text{H}$ group (**Scheme 72**).



Scheme 72: Tautomerisation of difluoroenol (top) and enol (bottom).

A significant kinetic isotope effect (KIE) was also shown to exist for the tautomerisation and at low acid concentrations (0.1 M DCl) the deuterated difluorinated enol intermediate **179** was sufficiently long-lived to be characterised by 2D NMR experiments (**Figure 62**). Enol formation was confirmed by an HMBC experiment which showed cleavage of the formaldehyde acetal which is the basis of the MEM group.

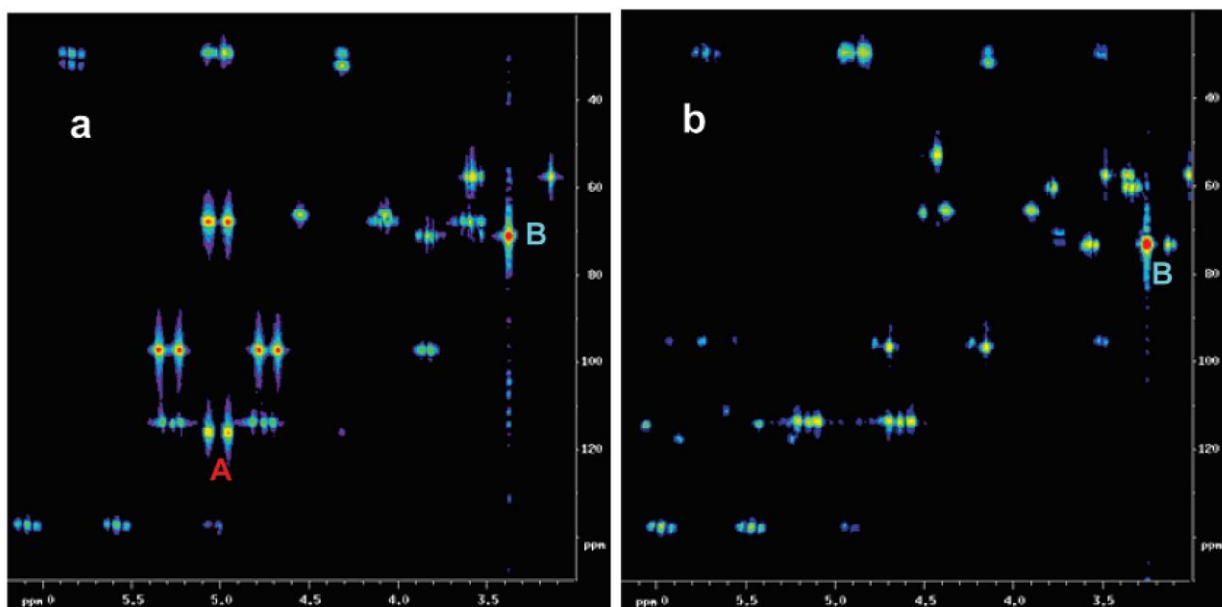
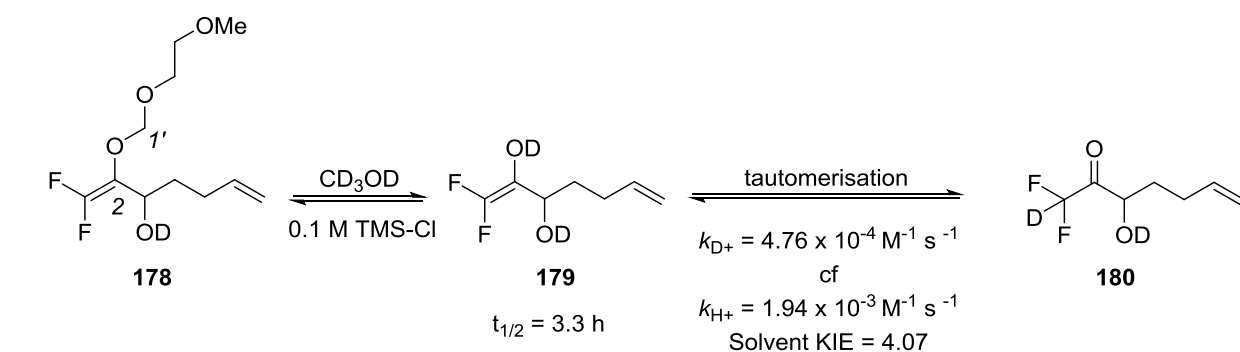
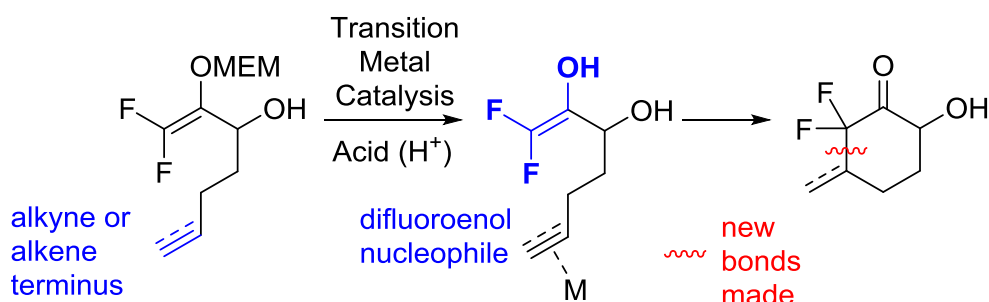


Figure 62: Rate constants and KIE effect of enol/keto interconversion (above) and partial HMBC spectra of **178** (^1H 400 MHz, CD_3OD , 300 K): (a) **178** alone; (b) 100 min after addition of TMS-Cl to 0.01 M. The two spectra were normalised to the same contour level, using peak B.²⁰⁰

The HMBC spectrum of **178** shows a characteristic cross-peak ($^3J_{\text{C-H}}$) linking C2 and the diastereotopic methylene H-1' protons of the MEM group (**Figure 62a**). Following the complete consumption of **178** the ^{13}C NMR of the reaction mixture showed a distinct new C2 carbon and the HMBC connection between this new carbon atom and the H-1' protons was absent (**Figure 62b**). This evidence was consistent with C-O bond cleavage and enol formation.

Whilst the longevity of **179** in protic solution has been demonstrated, the reactivity of difluorinated enols has been neither investigated quantitatively nor exploited in synthesis. The principal hypothesis is that difluorinated enols have significant synthetic potential as carbon nucleophiles which can be realised *via* transition metal-catalysed reactions (**Scheme 73**), particularly those involving cyclisations of alken/ynyl groups catalysed by palladium(II) or gold(I) species.

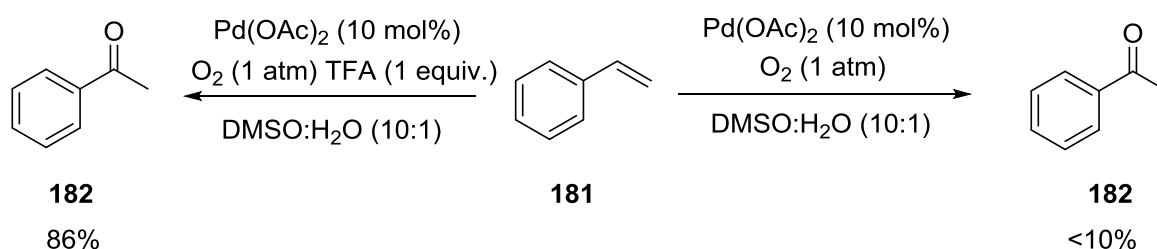


Scheme 73 Synthetic strategy for utilising difluoroenol intermediates in cyclisations.

One major challenge lies in identifying conditions under which both the enol intermediate and catalyst can co-exist. However, there is another possibility; it may be that enol acetals are sufficiently nucleophilic themselves to intercept a metal-complexed alkene or alkyne.^{194,201}

4.1.2 Palladium(II) catalysis

The previously optimised conditions for the palladium-catalysed oxidative cycloalkenylation could provide an interesting starting point for a study of difluorinated enol acetal substrates. There is evidence in the literature to suggest that palladium(II) catalysed oxidations are effectively improved by using either an organic acid solvent or by the addition of a catalytic amount of a strong acid.^{202,203} More recently Wang *et al.* reported an efficient palladium oxidation system for the conversion of terminal olefins **181** to methyl ketones **182**. Though the conditions are described as ligandless, the coordinative abilities of DMSO are widely known.¹¹⁴ In this case molecular oxygen is the sole oxidant and the use of trifluoroacetic acid is necessary to achieve a successful catalytic reaction (**Scheme 74**).²⁰⁴



Scheme 74: Tsuji-Wacker oxidation of styrene under acidic conditions.

These results provide an encouraging precedent and robustly demonstrate the redox systems tolerance of acidic conditions.

4.1.3 Gold(I) catalysis

Gold (in the form of cationic Au(I) complexes in particular) has the ability to match the reactivity of late transition metals such as palladium and platinum by activating C-C π bonds towards nucleophilic attack. Important characteristics of gold include aurophilicity (the tendency of gold complexes to aggregate via formation of favourable Au-Au interactions, *ca.* 3.0 Å, 7-12 kcal/mole)²⁰⁵, high chemical and thermal stability, high electrical conductivity and softness.²⁰⁶ It is the ‘soft’ Lewis acidic character of gold which allows it to bind selectively to ‘soft’ Lewis bases such as π -systems, and activate them. The increase in electrophilicity, which results from coordination of the π -acceptor ligand to the Au centre, triggers nucleophilic attack (which can be intra- or intermolecular) by carbon or heteroatom nucleophiles. The nature of the bonding between gold and π -ligands, including alkenes, allenes and alkynes, can be represented by the Dewar-Chatt-Duncanson (DCD) model.^{207,208} The DCD model describes the bonding between the metal and π -ligand as a synergistic combination of σ -donor, in which electron density is donated from the filled π -orbital of the ligand (alkene) to an empty metal hybrid orbital (Au) of equivalent symmetry, and π -acceptor, in which π -backbonding from one of the filled metal d-orbitals into the π^* -orbital of the ligand occurs (**Figure 63**).²⁰⁹

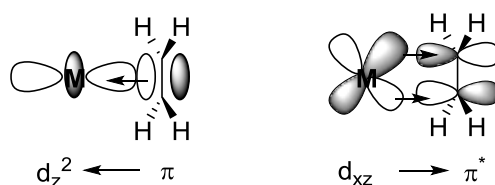


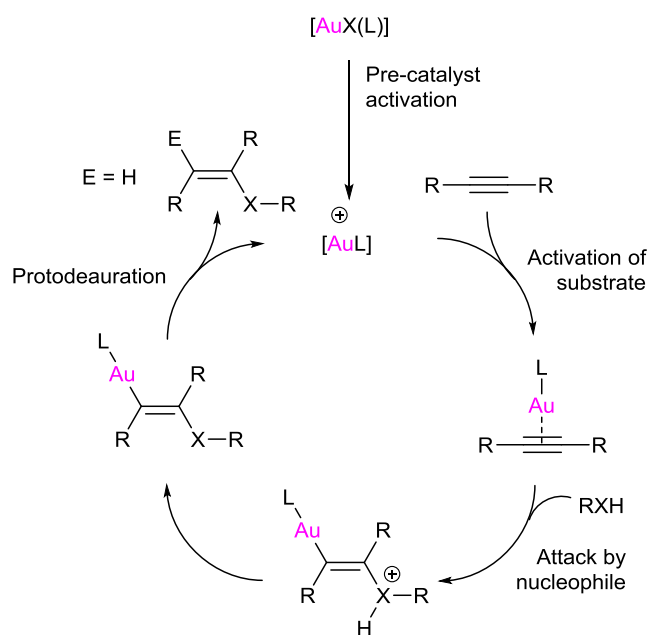
Figure 63: Orbital diagrams depicting σ donation (left) and π -backbonding (right) described by the DCD model for bonding between an alkene and transition metal (Au).

Typically 16-electron π -coordinated gold complexes (e.g. Ph_3PAuCl) are much less catalytically active than their cationic congeners and must be activated by the addition of a silver salt (such as AgSbF_6).²¹⁰ When ethene binds to the cationic gold complex, σ -donation to the metal predominates in the DCD model, making the coordinated ligand strongly electrophilic.

Gold chemistry is also thought to be largely dominated by relativistic effects, attributed to an electron's velocity approaching the speed of light ($c = 3 \times 10^8 \text{ ms}^{-1}$) whilst moving near a heavy nucleus. Thus, the mass of the electrons in gold increase and Bohr radii decrease. This results in an increase in ionisation energy, electrons being attracted closer to the nucleus and an increase in shielding of the d and f orbitals.²¹¹ It is these relativistic

effects which are also invoked to explain the unusually strong bonds to soft Lewis bases such as alkenes.

In several critical respects, the reactivity profiles of gold and palladium are very different. Unlike palladium, gold does not undergo spontaneous oxidative addition.²¹² This can be attributed to the diffuse low-lying 5d-orbitals of gold which are less likely to participate in nucleophilic attack compared to the high-lying 3d-orbitals on palladium.²¹³ Another major mechanistic difference is that gold does not readily undergo β -hydride elimination. This is due to the filled 5d-shell of gold(I) complexes preventing the necessary metal-hydrogen agostic interaction required for the elimination to occur.²¹⁴ Consequently, the redox stability of Au(I) species has allowed the development of alternative modes of reactivity by precluding the oxidative addition/ β -hydride elimination steps common in palladium catalysis. It is generally accepted that most gold catalysed reactions go through four major stages (**Scheme 75**).²¹⁵

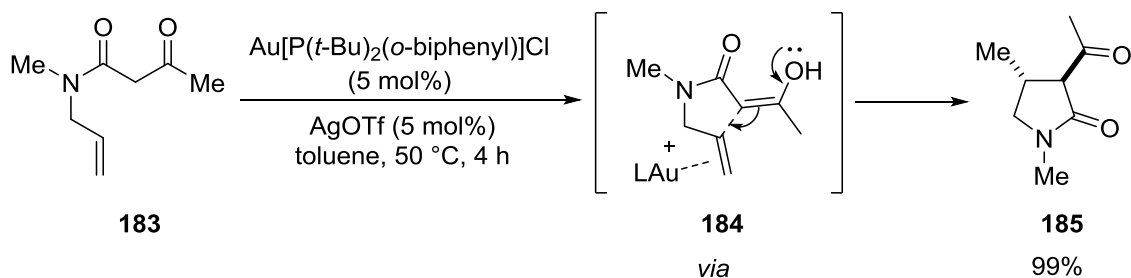


Scheme 75: General catalytic cycle for nucleophilic attack on Au activated π -system.

The first step involves formation of the cationic gold species, commonly generated *in situ* by using a silver salt. The second step involves coordination and activation of the π -ligand. Subsequent nucleophilic attack on this species generates a *trans*-alkenyl gold complex (or alkyl gold complex in the case of alkenes). The final stage involves reaction of this intermediate with an electrophile (E), typically a proton, to afford the final product.

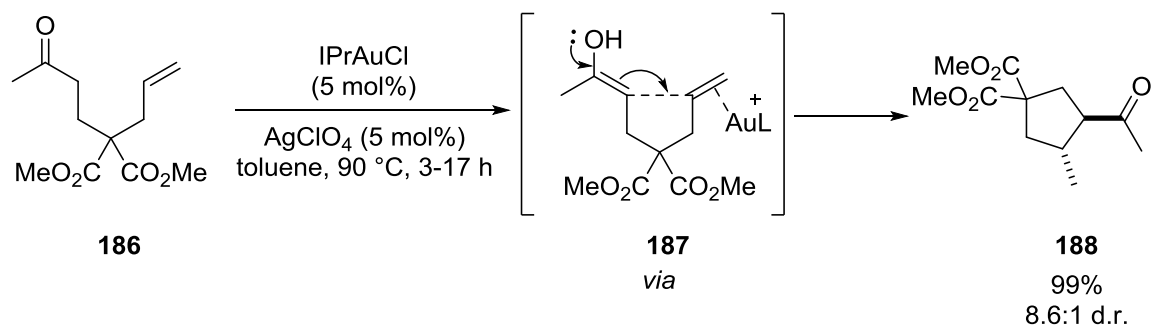
4.1.4 Carbocyclisations of enol species onto gold(I) activated alkenes

A very wide range of gold-catalysed nucleophilic additions of carbon-based nucleophiles to alkynes and allenes have been reported.^{216,217} In comparison, the gold-catalysed addition of carbon-based nucleophiles to activated alkenes has been widely recognized as capricious.²¹⁸ This may be because π -Au-alkyne complexes typically have a lower energy LUMO than π -Au-alkene complexes (by approximately 0.37 eV for the π -Au-ethyne complex compared to the π -Au-ethene complex). Consequently, orbital overlap with the incoming nucleophile is more efficient and π -Au-alkyne complexes are therefore considered to be more electrophilic than π -Au-alkene complexes.²¹⁹ Importantly, the alkyl gold intermediate formed following nucleophilic attack has been shown to be extremely inert to protodeauration, which would result in catalyst sequestration and very slow turnover.^{220,221} However, the direct intramolecular addition of carbon nucleophiles onto unactivated alkenes is an extremely powerful tool for the formation of carbocycles and new stereocentres. In 2007 Che *et al.* reported the gold(I) catalysed intramolecular addition of β -ketoamides to unactivated alkenes to afford a series of highly substituted lactams in good yields and high *trans* selectivity (**Scheme 76**).²²²



Scheme 76: Intramolecular hydroalkylation of β -ketoamides.

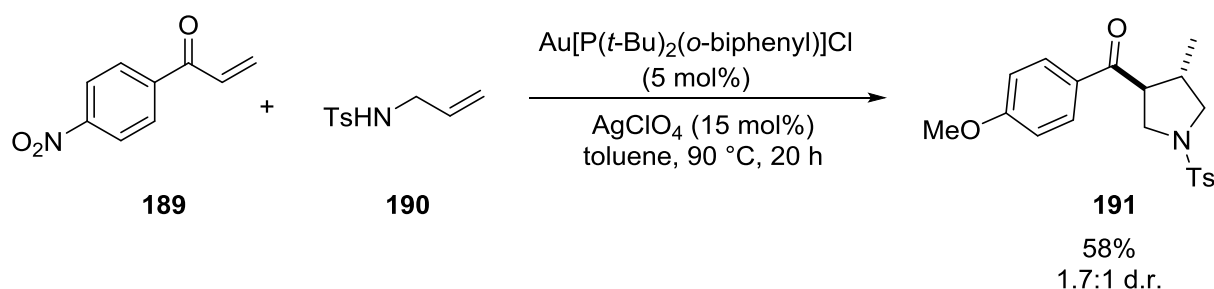
The authors propose that initial gold coordination to the terminal olefin **183** is followed by *exo*-trig addition of the enol form of the β -ketoamide **184**, whilst subsequent protodeauration affords the desired products **185**. However, the methodology is limited to carbon nucleophiles which form their enols easily, a characteristic of active methylene species. More recently the same authors expanded the methodology to include simple ketones as effective carbon nucleophiles (**Scheme 77**).²²³



Scheme 77: Intramolecular hydroalkylation of α -ketones.

The α -alkylation of alkenyl ketones **186** with IPrAuCl/AgClO₄ (5 mol %) effectively afforded a range of cyclohexyl and cyclopentyl derivatives **188** in good yields and good *trans*-diastereoselectivity. Once again the nucleophile is thought to be the enol form of the α -ketone **187**; however, through deuterium labelling experiment the authors believe that the gold catalyst also plays a crucial role in increasing the enol/ketone equilibrium constant ($K_{\text{enol/ketone}}$).

This protocol was further extended to include a gold(I)-catalysed intermolecular N-Michael addition/intramolecular hydroalkylation reaction cascade (**Scheme 78**).²²⁴



Scheme 78: Gold(I) catalysed cascade reaction.

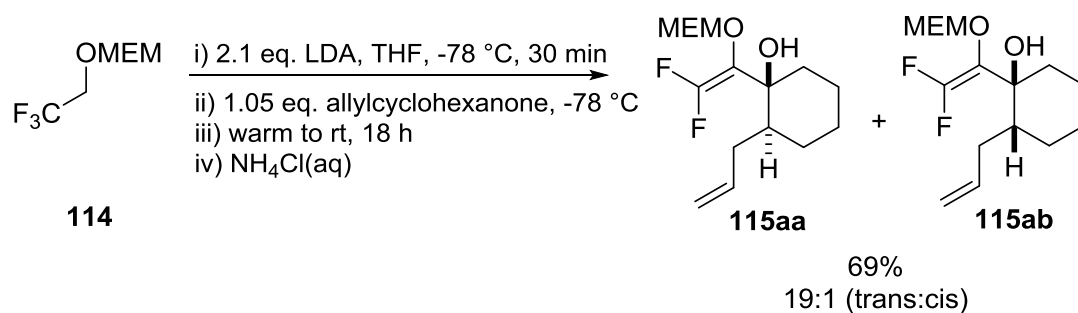
The cascade reaction afforded functionalised pyrrolidines **191** in good yields but with only moderate diastereoselectivity. The findings of Che *et al.* clearly demonstrate the effectiveness of the enol functionality as a carbon nucleophile in gold(I) catalysis and we anticipated that such methodology can be applied to difluoroenol derivatives.

The results detailed in this chapter will focus primarily on the development of a *de novo* synthetic route into difluorinated cyclic α -hydroxy ketones through the application of either palladium(II) or gold(I) catalysis. To achieve this goal, difluorinated enol acetals will be employed as more atom efficient precursors in a novel carbocyclisation reaction.

4.2 Results and Discussion

4.2.1 Palladium Catalysis

The investigation of the Saegusa-Ito cyclisation showed that annulations were generally effective, whereas annulations required a minimum level of substitution on the chain.¹⁹⁴ Difluoroallylic alcohol **115aa/ab** was therefore chosen as a trial substrate to investigate the cyclisation. Allyl alcohol **115aa/ab** was prepared according to the method developed previously in our laboratory and was isolated in good yield as a mixture of *trans*- and *cis*- diastereoisomers (**Scheme 79**).¹³⁹



Scheme 79: Synthesis of trial substrate **115aa/ab**.

With the precursor in hand it was initially decided to follow the methanolysis of **115aa/ab** (in 0.1M MeOH/Me₃SiCl) by ¹⁹F NMR in order to detect the presence of the difluoroenol intermediate **192** generated *in situ* (**Figure 64**).

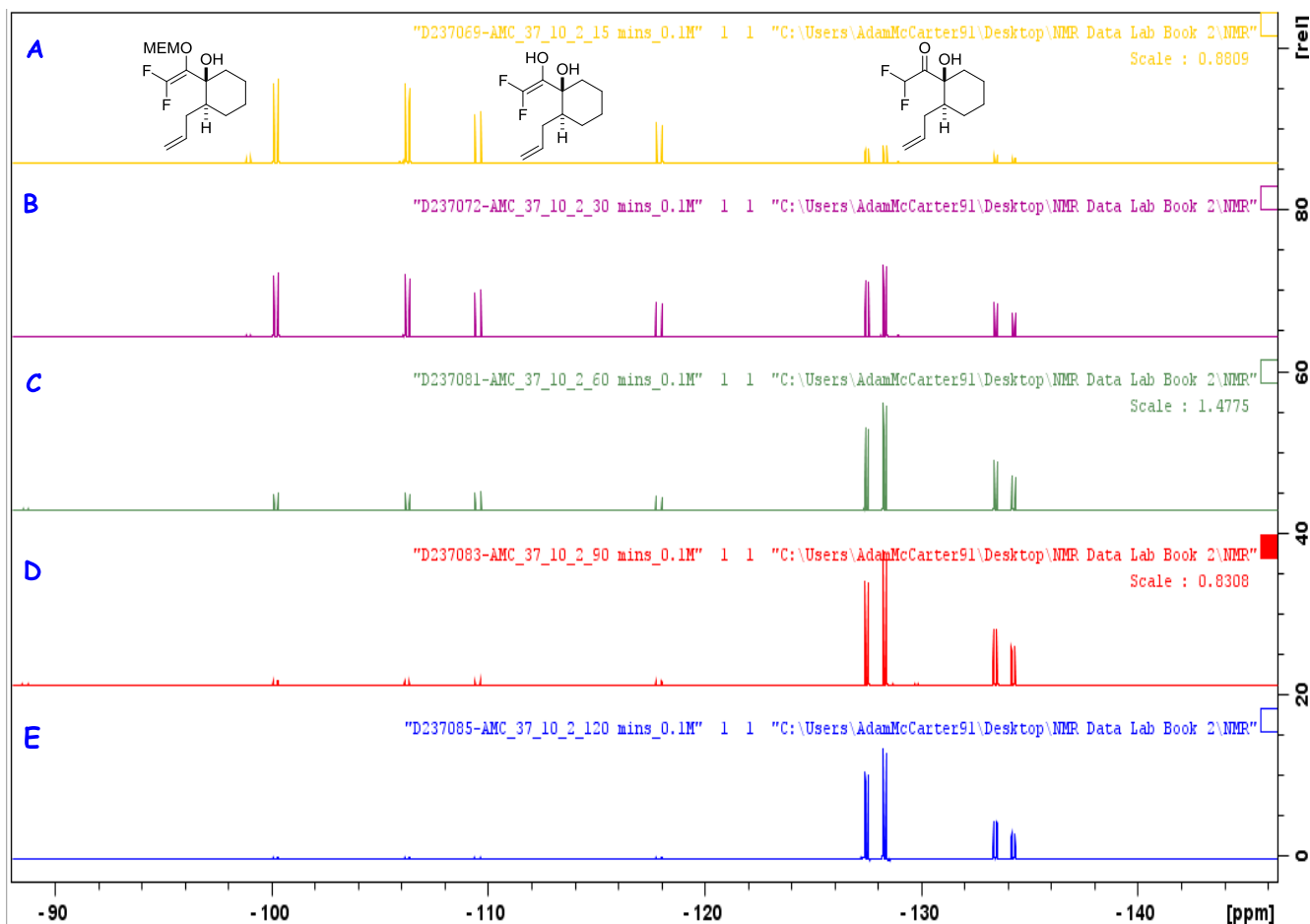
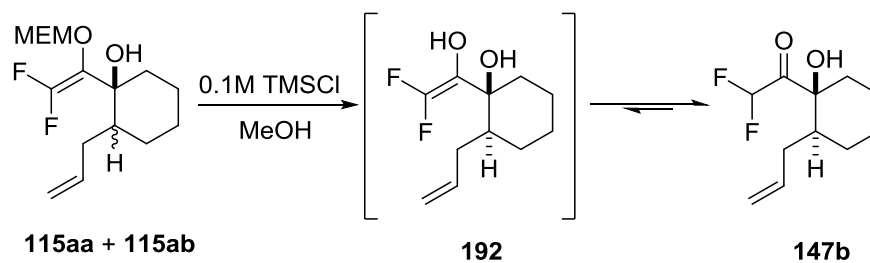
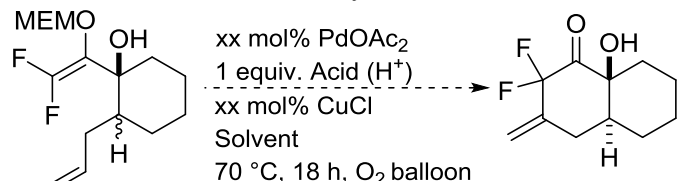


Figure 64: ^{19}F NMR spectra following the methanolysis of **115aa/bab** in 0.1M TMSCl/MeOH after A) 15 minutes, B) 30 minutes, C) 60 minutes, D) 90 minutes and E) 120 minutes.

After fifteen minutes it was clear that two new species had formed in solution. The build-up of the difluoroenol intermediate **192** is characterised by two distinct doublets at -109.5 ($^2J_{\text{F-F}} = 100.7$ Hz) and -117.9 ppm ($^2J_{\text{F-F}} = 100.7$ Hz), consistent with previous reports.²⁰⁰ The doublet of doublets at -127.9 ($^2J_{\text{F-F}} = 315.1$ Hz, $^2J_{\text{F-H}} = 52.2$ Hz) and -133.8 ($^2J_{\text{F-F}} = 315.1$ Hz, $^2J_{\text{F-H}} = 52.2$ Hz) correspond to the difluoromethyl ketone **147b**. Over time, the concentration of allylic alcohol and difluorinated enol begins to decrease until, after two hours, the starting material had been consumed fully. Having confirmed the formation of **192** in solution the potential application was next investigated. Stoichiometric quantities of palladium(II) acetate were employed in the first instance and **115aa/ab** was exposed to the acidic Wacker conditions reported by Wang *et al* (**Entry 1, Table 11**).²⁰⁴

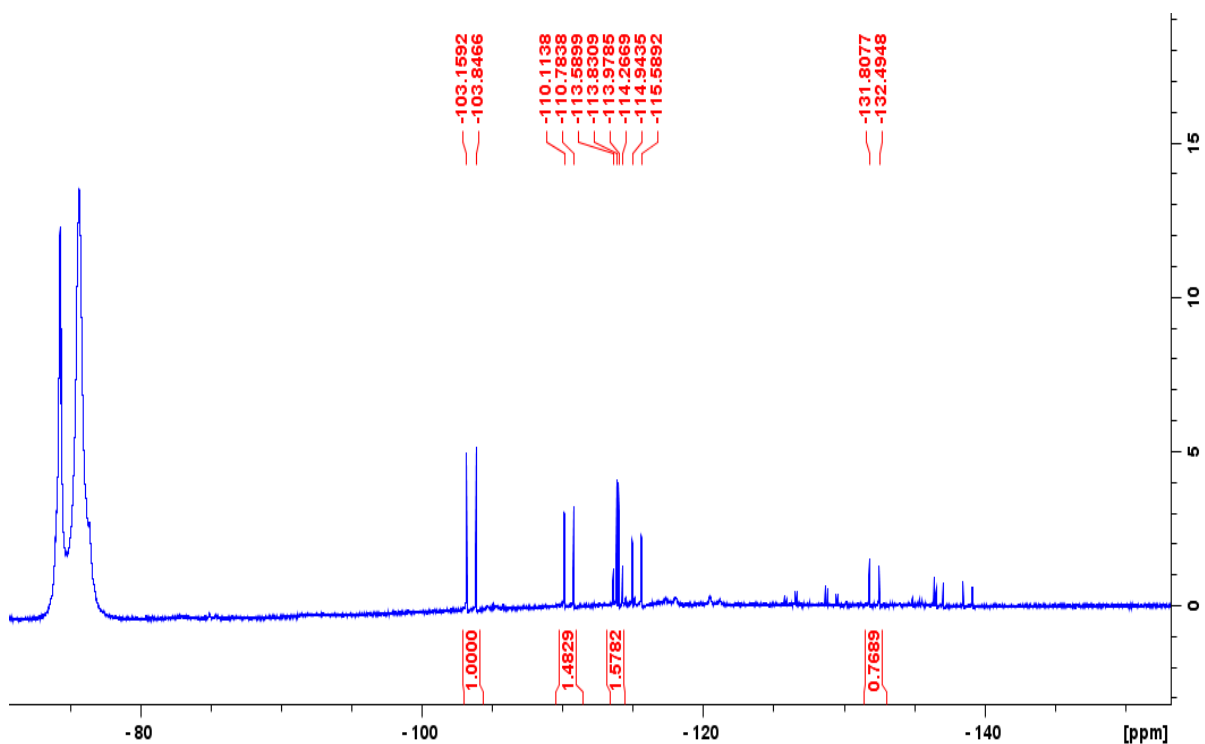
Table 11: Reaction conditions screened for cyclisation of **115aa/ab**.



115aa + 115ab **116**

Entry	Pd(OAc) ₂ (mol %)	CuCl (mol %)	Solvent	Acid	116 Isolated
1	100	0	DMSO:H ₂ O (10:1)	TFA	No
2	100	100	DMSO:H ₂ O (10:1)	TFA	No
3	10	100	DMSO:H ₂ O (10:1)	TFA	No
4	100	100	Acetonitrile:H ₂ O (7:1)	TFA	No
5	20	100	Acetonitrile:H ₂ O (7:1)	TFA	No
6	100	100	Acetonitrile:H ₂ O (7:1)	0.25 M HNO ₃	No
7	100	100	Acetonitrile:H ₂ O (7:1)	0.25 M HBF ₄	No

Analysis of the crude ¹⁹F NMR spectrum revealed some interesting signals (**Figure 65**). The doublet signals at -103.5, -110.4, -113.9 and -132.2 ppm all have large coupling constants ($^2J_{F-F} = 257$ Hz), characteristic of geminal *sp*³ F-F coupling in cyclic compounds.¹⁴⁶

**Figure 65:** ¹⁹F NMR spectrum of crude reaction mixture **Entry 1, Table 11**.

Though high catalyst loadings were required this preliminary result was extremely encouraging. Not only had the starting material been consumed fully but it had also

cyclised. Previously it had been demonstrated that the presence of a copper co-catalyst is essential for the re-oxidation of Pd(0).¹⁹⁴ There is also the possibility that copper salts play an important role in generating catalytically active bimetallic species.^{184,186} In an attempt to ensure a cleaner reaction copper(I) chloride was employed as a co-oxidant (**Entry 2, Table 11**). This resulted in a similar reaction outcome, with the same signals apparent in both crude ¹⁹F NMR spectra and a slightly cleaner reaction. The large quantities of metal salts present in both reactions resulted in particularly challenging purification and, unfortunately, we were unable to isolate any products from the reaction. Attempts to lower the palladium catalyst loading resulted in the formation of an extremely complex mixture by ¹⁹F NMR (**Entry 3, Table 11**). At this stage it was decided to revisit the choice of solvent system. Miller *et al.* had previously described an acidic Wacker oxidation process using an acetonitrile:water (7:1) combination (**Entry 4, Table 11**).²²⁵ This simple solvent switch had a significant impact on the reaction and a new product was now visible in the ¹⁹F NMR spectrum (**Figure 66**).

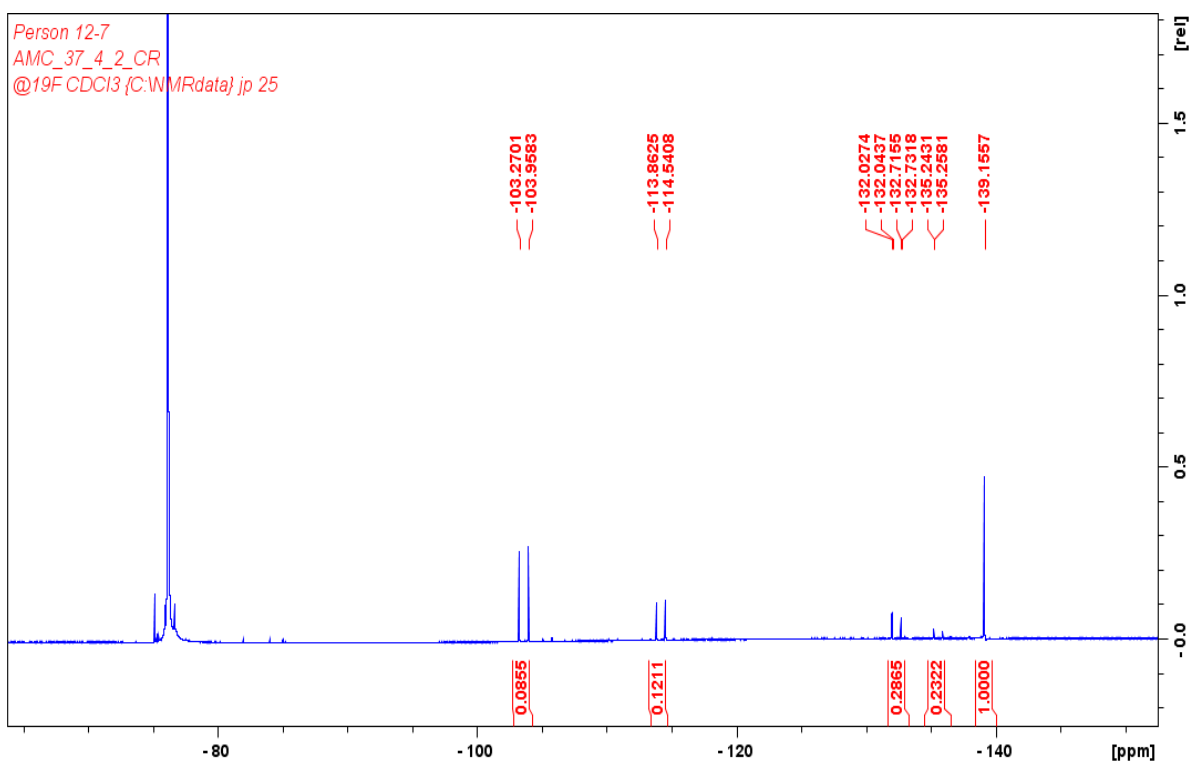


Figure 66: ¹⁹F NMR spectrum of crude reaction mixture **Entry 4, Table 11**.

It was apparent that difluorinated cyclic products had still formed; however, the singlet signal at -139.1 ppm now dominated the reaction mixture. Unfortunately, attempts to lower the catalyst loading once again resulted in a complex reaction mixture (**Entry 5, Table 11**). Miller *et al.* had also demonstrated a significant rate enhancement in Wacker oxidations upon addition of an inorganic acid (0.25 M).²²⁵ To test the applicability of

acids other than TFA in our system standard solutions of 0.25M HBF₄ and HNO₃ were prepared. Unfortunately, changing the acid had no effect and the singlet signal still appeared as the major product (**Entries 6 and 7, Table 11**). Whilst it was not possible to characterise any of the difluorinated products formed from this set of reactions the signal at -139.1 ppm was identified as monofluorinated enone **193**. The crude material was purified by flash column chromatography to isolate **193** in 20% yield and its molecular structure was confirmed by X-ray crystallographic analysis (**Figure 67**).

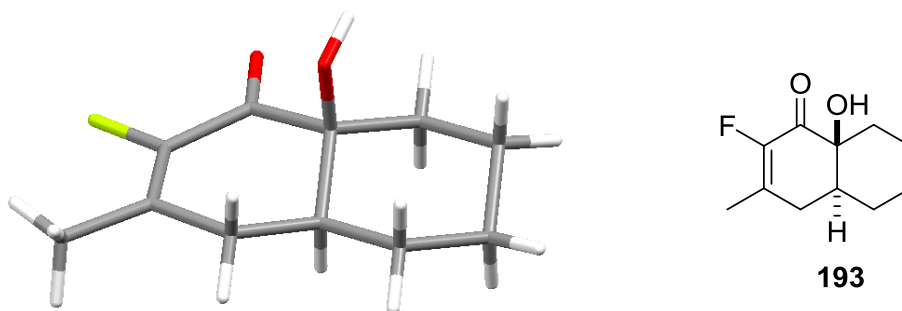
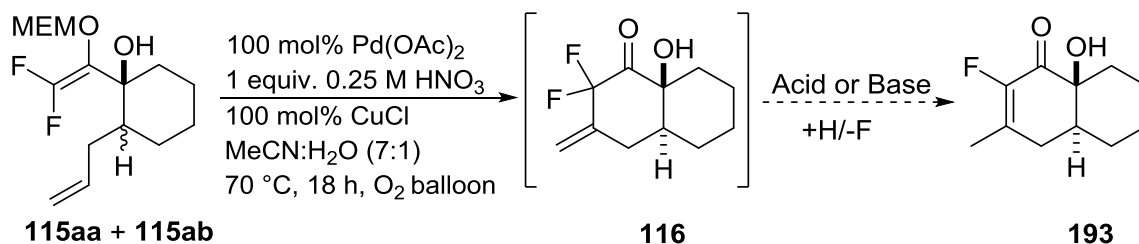


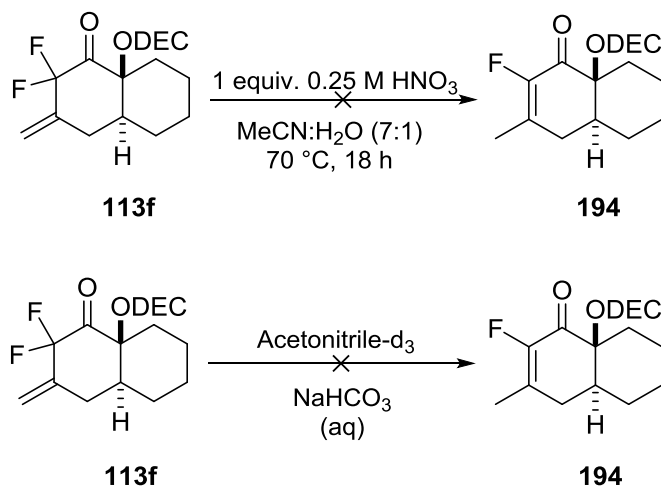
Figure 67: Molecule structure of **193** in the crystal.

The formation of **193** confirms the reactivity of a difluorinated enol acetal derivative in a carbon-carbon bond forming reaction. However, understanding the mechanism for the formation of **193** is not trivial. Initially it was believed that **193** could have originated from the cyclohexenone product which may have been either acid or base sensitive (an NaHCO₃(aq) wash was used during reaction work up (**Scheme 80**)).



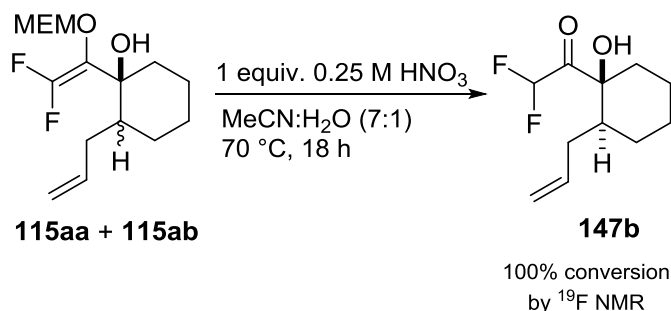
Scheme 80: Proposed formation of **193** from **116**.

Difluoroketone **113f** is structurally very similar to **116** and it is not unreasonable to presume that both species would behave in a similar manner. To test the sensitivity of **113f**, the species was exposed to both acidic and basic conditions (**Scheme 81**).



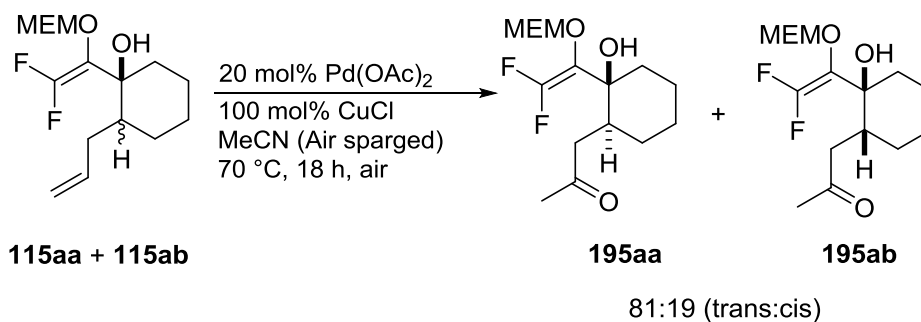
Scheme 81: Attempts to form monofluorinated analogue **194**.

Both sets of reactions returned only starting material **113f**, confirming the stability of the difluoroketone products under the reaction conditions. The necessary control reaction on **115a** and **115b** was then conducted; in the presence of nitric acid and in the absence of metal salts difluoromethyl ketone **147b** was identified as the sole product of the reaction by ^{19}F NMR, indicating that the cyclisation was not solely acid catalysed (**Scheme 82**).



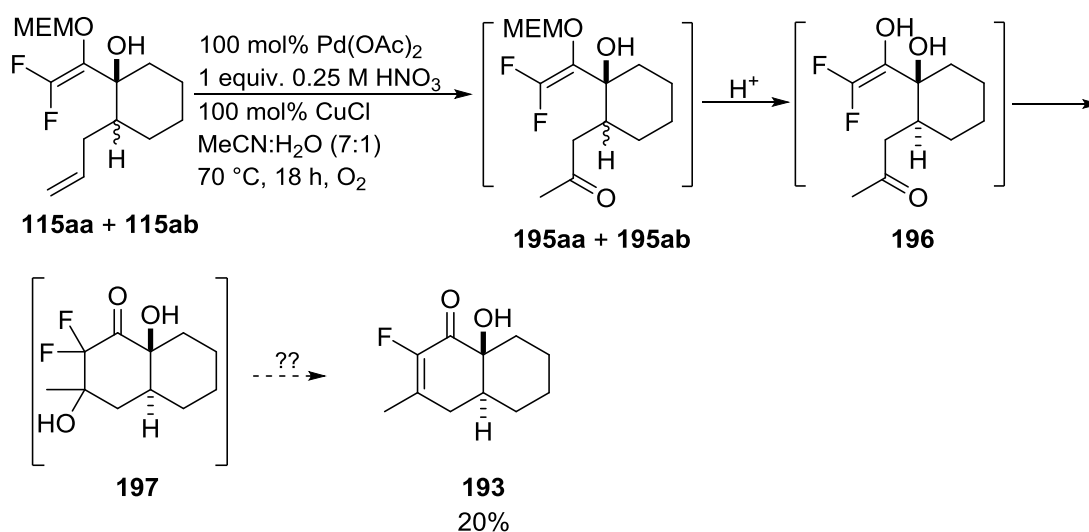
Scheme 82: Treatment of **115aa/ab** under acidic conditions.

Allyl alcohol **115aa/ab** was then subjected to the previously optimised Saegusa-Ito conditions in the absence of any acid (**Scheme 83**).



Scheme 83: Treatment of **115aa/ab** under acid-free conditions.

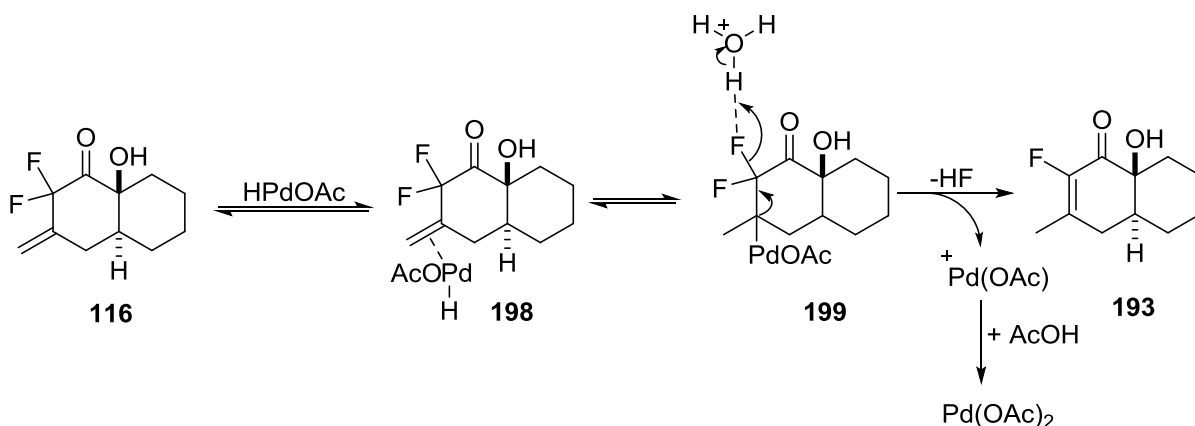
Under these conditions, the formation of methyl ketones **195aa** and **195ab** was noted, formally products of Wacker oxidation. Analysis of the crude ^{19}F NMR spectrum revealed only a slight variation in chemical shift compared to the starting material (± 1 ppm); however, both the ^1H and ^{13}C NMR spectra were unambiguous, with the absence of vinylic proton signals in the ^1H NMR spectrum and a non-fluorinated ketonic $\text{C}=\text{O}$ signal now present in the ^{13}C NMR spectrum. Although **195aa** and **195ab** could not be isolated from the crude reaction mixture, it was possible to synthesise **195aa** and **195ab** independently under the published conditions, albeit not in high purity ($< 90\%$, see section 6.3.5). The reaction conditions employed are very similar to those of prototypical Wacker oxidations, so the formation of **195aa** and **195ab** is unsurprising.⁹⁸ Whilst the silyl enol ether is an effective nucleophile in the Saegusa chemistry, the enol acetal group is clearly not as potent a nucleophile, therefore, the material follows the alternative oxidation pathway.^{226,227} The rate of formation of methyl ketone **195aa** and **195ab** could be enhanced in an acidic system and it was initially believed that an *in situ* Wacker oxidation/cyclisation could account for the formation of monofluorinated enone **193** (**Scheme 84**).^{225,228}



Scheme 84: Proposed route to **193**.

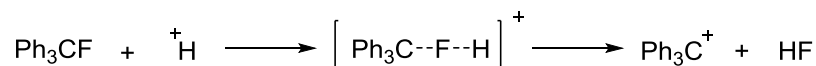
However, it is not possible to form **193** from this tertiary alcohol intermediate **197**.

An alternative hypothesis is that the formation of HPdX species in the reaction system means that there is the possibility for equilibration *via* hydropalladation to form **199** (**Scheme 86**).



Scheme 86: Alternative proposal for formation of **193**.

Kohnstam *et al.* have previously demonstrated that the hydrolysis of trityl fluoride is triggered by the addition of hydrochloric acid and catalysed by hydrofluoric acid molecules formed *in situ* (**Scheme 87**).²²⁹



Scheme 87: Hydrolysis of trityl fluoride.

It is thought that the general acid catalysis arises from the partial covalent bonding between fluorine and an acidic proton, which assists in heterolysis of the C-F linkage.²³⁰ In the current system, hydropalladation followed by acid promoted H-F scission may be responsible for the formation of **193**, whilst the development of conjugation would provide a thermodynamic driving force.

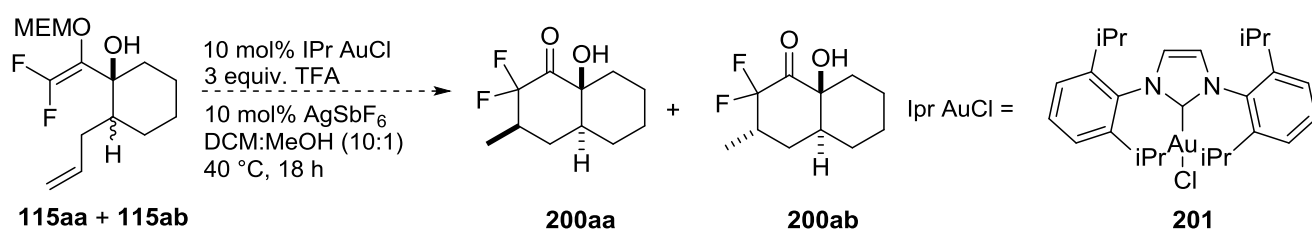
Although the formation of monofluorinated enone **193** is intriguing, it remains an unwanted side product of the reaction and inhibiting its formation appeared challenging. Furthermore, all attempts to reduce the palladium catalyst loading below stoichiometric quantities resulted in the formation of complex reaction mixtures. It was also not possible to isolate any cyclic difluorinated products from the reactions.

At this stage of the study, a reappraisal of the synthetic strategy was conducted. It was believed that gold(I) catalysis offered the unique opportunity to access difluoroketone motifs more efficiently. Firstly, the enol functionality has been shown to serve as an effective nucleophile for gold(I) activated alkenes.²²³ Secondly, it has been demonstrated that the rate of protodeauration is accelerated in the presence of strong organic acids, a prerequisite for difluoroenol formation.^{231,221} Finally, gold catalysts appeared compatible with the conditions required for MEM (methoxyethoxymethyl) cleavage in **115aa/ab**.

Again, allylic alcohol **115aa/ab** was chosen as a model substrate to investigate gold(I) as an alternative cyclisation mediator.

4.2.2 Gold Cyclisation Studies

The investigation commenced using conditions similar to those used by Toste *et al.* for the carbocyclisation of silyl enol ethers onto gold activated alkynes (**Scheme 88**).²³² The NHC-gold(I) complex [(IPr)AuCl] (IPr = 1,3-*bis*(2,6-*diisopropylphenyl*)imidazole-2-ylidene, see **Scheme 88**) was available in our laboratory and was selected as the catalyst in conjunction with the chloride abstractor AgSbF₆. Excess trifluoroacetic acid was utilised in the first instance in order to promote protodeauration.^{231,220}



Scheme 88: Initial trial reaction.

After 18 hours the starting material had been consumed fully and analysis of the crude ¹⁹F NMR spectrum revealed a number of encouraging signals (**Figure 68**).

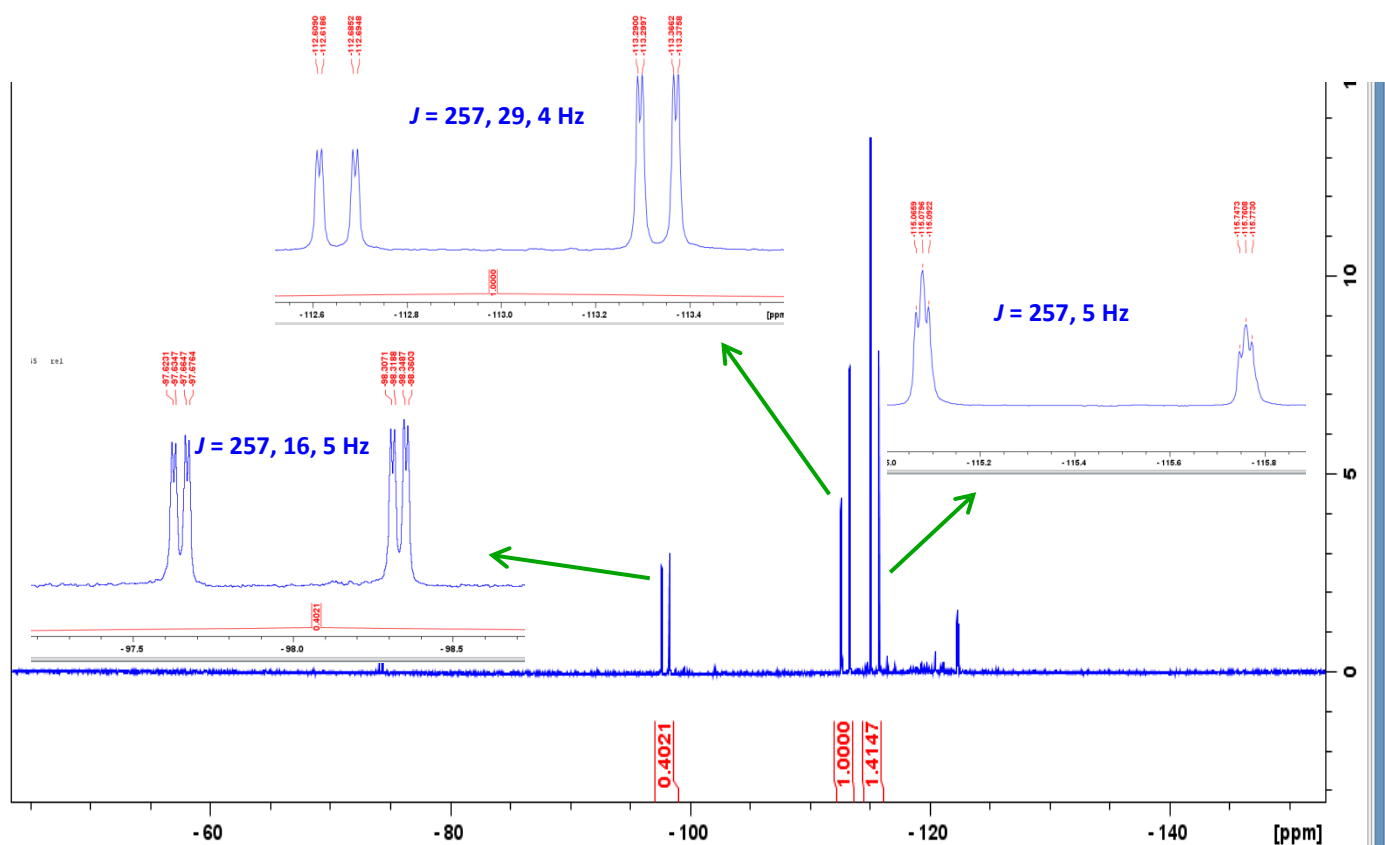


Figure 68: ^{19}F NMR spectrum of the crude reaction mixture of the cyclisation of **115aa/115b** under gold(I) catalysed conditions.

Two chemically distinct products dominated the reaction mixture. The integration shows that the corresponding fluorine for the signal at -98 ppm overlaps that with the signal at -115.4 ppm. Again, large $^2J_{\text{F-F}}$ couplings are observed along with further splitting in each resonance resulting in well resolved splitting patterns. The crude material was purified by flash column chromatography to afford a colourless solid.

The solid material was recrystallized by vapour diffusion ($\text{CHCl}_3/\text{pentane}$) and the molecular structure and relative stereochemistry revealed by X-ray crystallographic analysis (**Figure 69**).

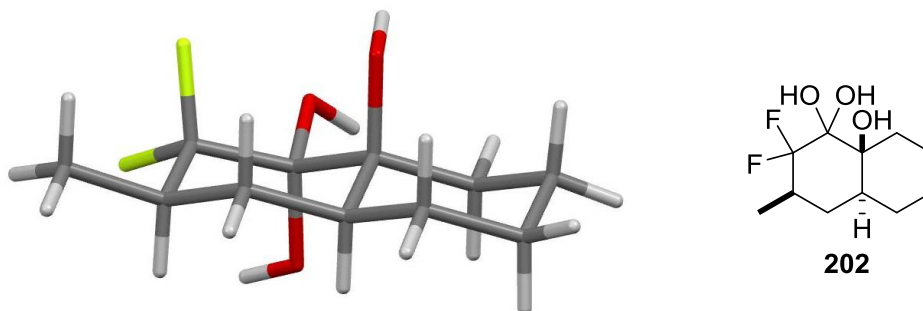


Figure 69: Molecular structure of **202** in the crystal.

The crystal contained four crystallographically independent molecules per asymmetric unit. Three of the molecules were well ordered, corresponding to the hydrated form **202** of the difluoroketone. From previous experience with the α,α -difluoroketones synthesised from the Saegusa series the presence of this material was not surprising.¹⁹⁴ The fourth site contained a large degree of disorder with three separate molecular orientations; however, the largest proportion of the molecules at this site was the desired ketone **200aa**. It was clear from the ^{19}F NMR spectrum of the crystal that two species were present (**Figure 70**).

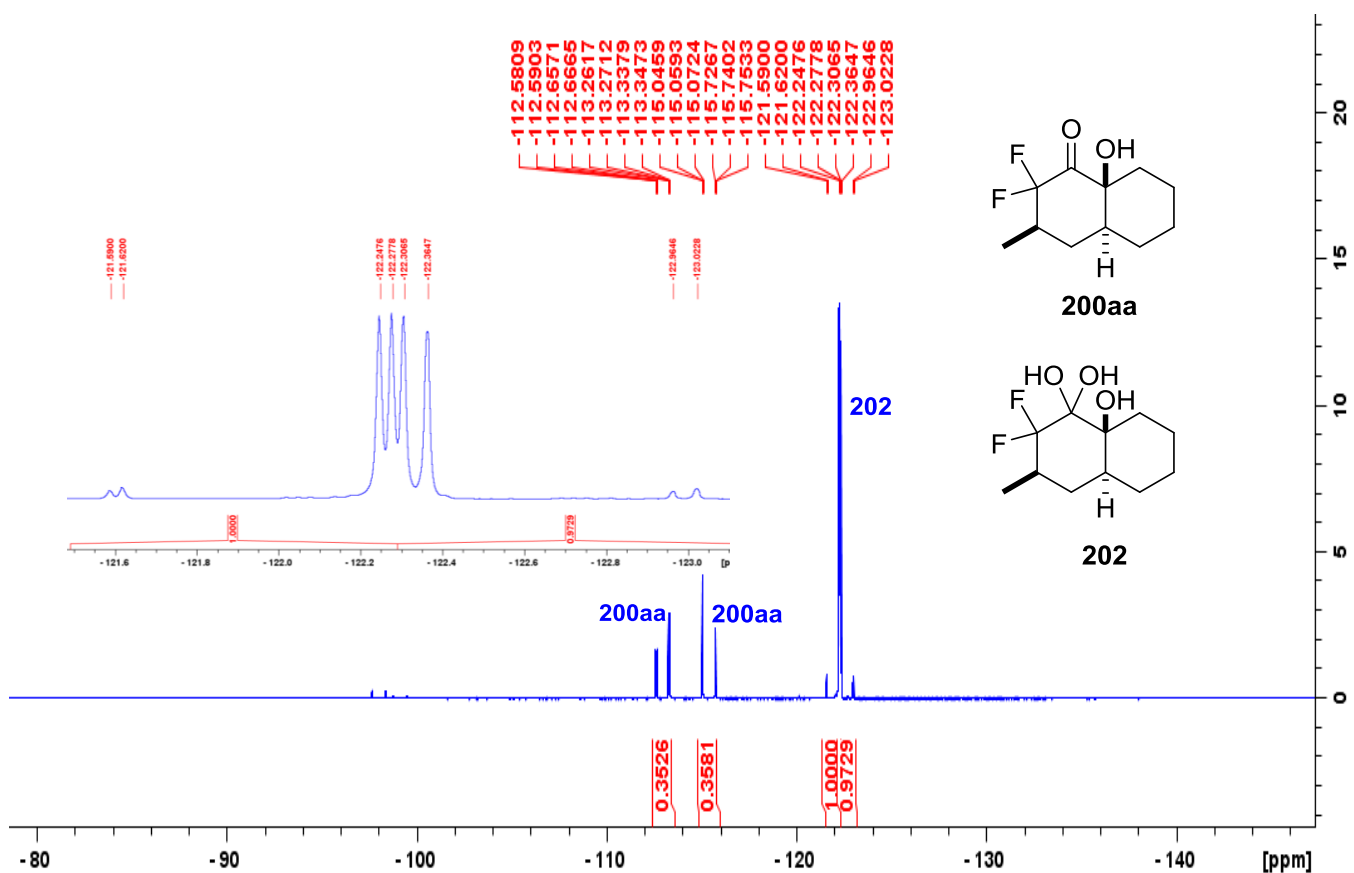


Figure 70: ^{19}F NMR spectrum of the crystal consisting of **200aa** and **202**.

The resonance at -112.9 ppm represents the axial fluorine of the ketone with well resolved $^3J_{\text{HF}}(\text{trans-diaxial})$ couplings ($^3J_{\text{F-H}} = 28.9$ Hz) whilst the signal at -115.4 ppm represents the equatorial fluorine of the ketone which is poorly resolved due to the smaller $^3J_{\text{HF}}(\text{gauche})$ couplings ($^3J_{\text{F-H}} = 5.1$ Hz).²³³ As expected the hydrate signal dominates and is represented by a complex dABq splitting (**Figure 70**). It was not possible to isolate the material corresponding to the signal at -98 ppm in the crude ^{19}F NMR spectrum; however, this was anticipated to correspond to the alternative diastereoisomer (**Figure 71**).

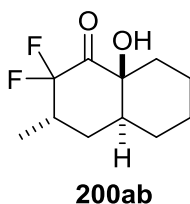


Figure 71: Alternative diastereoisomer **200ab** potentially formed from cyclisation.

This result was especially pleasing as it demonstrated that cyclisation of a difluorinated enol acetal derivative at ambient temperature was feasible. Attention then turned to probing the reaction further and examined the effects of changing the reaction solvent. Toste *et al.* had also previously employed a DCM:H₂O solvent system to conduct their silyl enol ether carbocyclisations.²³² It was surprising to find that this simple solvent switch had a significant impact on the current reaction system (**Figure 72**).



Figure 73: Molecular structure of **203** in the crystal within the ordered site.

Curiously, the ^{19}F NMR spectrum of the crystal showed that at least two distinct chemical species were present in solution. Two molecular sites were present in each asymmetric unit of the crystal and whilst one of these sites was ordered (allowing identification of the acetal) the other site was disordered (**Figure 74**).

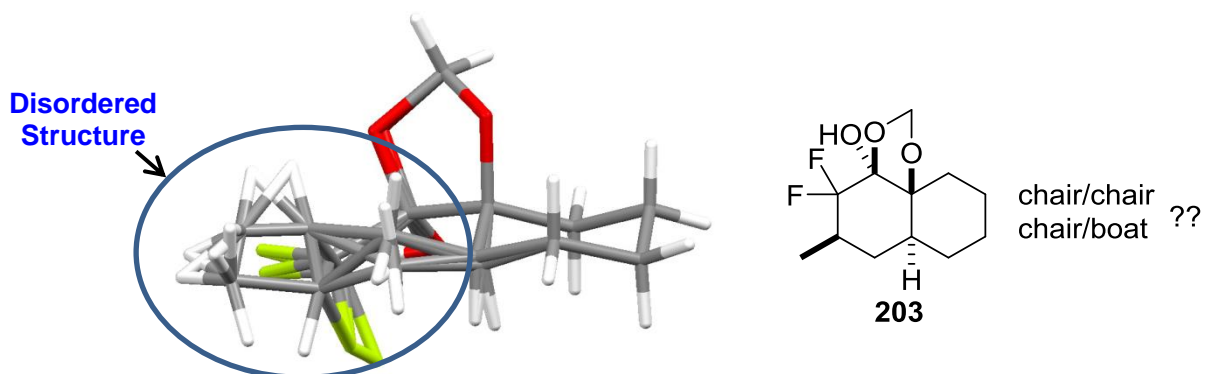


Figure 74: Disordered site in the crystal.

The nature of the second species was ambiguous. It appears as though the disordered site involves a change in stereochemistry at the methine carbon which bears the methyl group. This would be consistent with the presence of two different conformers, the chair/chair and chair/boat decalin structures. There is also the potential to have diastereoisomers for each of these species allowing the possibility of up to four different structures (**Figure 75**).

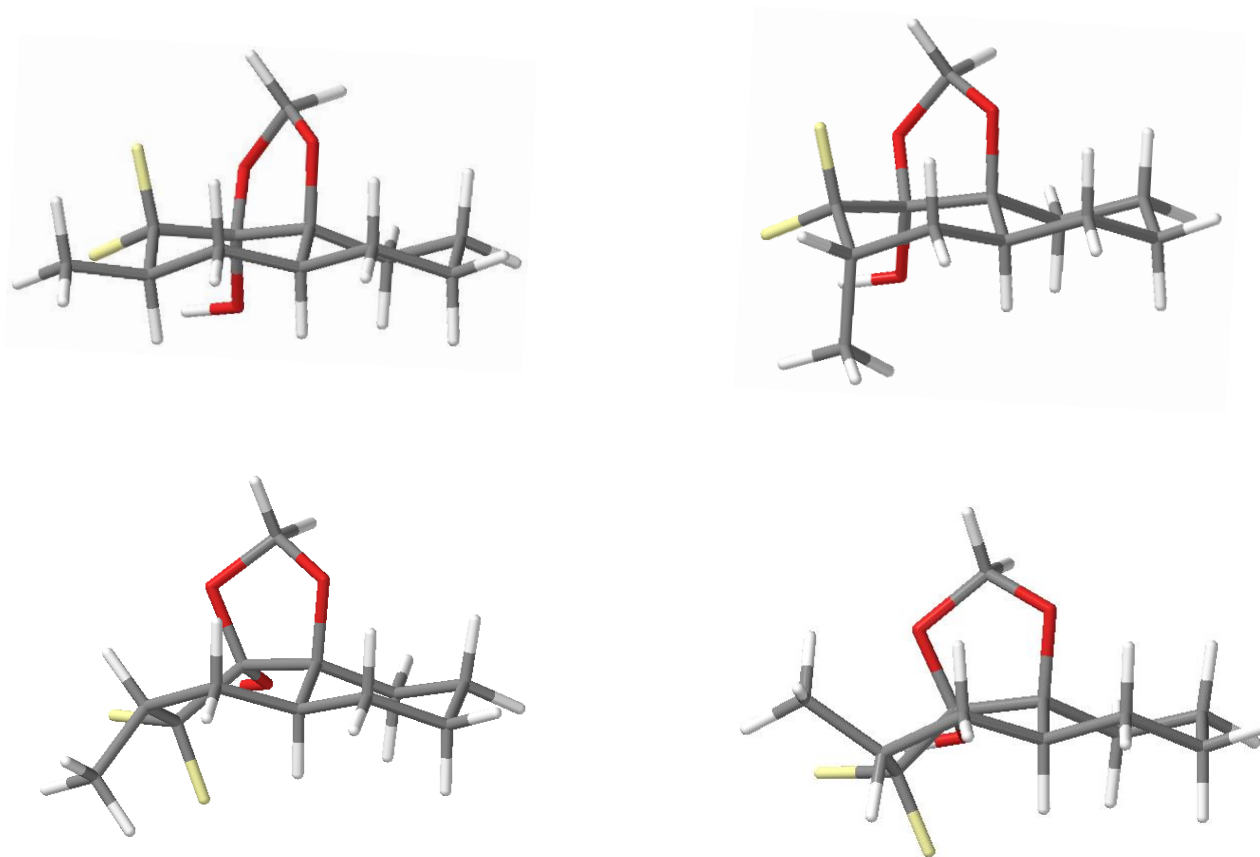


Figure 75: Calculated structures for potential conformers/diastereoisomer combinations for acetal **203**; from top left going clockwise: chair/chair (methyl up), chair/chair (methyl down), chair/boat (methyl up), chair/boat (methyl down). Calculations were run at the B3LYP/6-31G*, M06/6-31G* and ω B97XD/6-31G* levels of theory.

Variable temperature (VT) ^{19}F NMR experiments were carried out (**Figure 76**) to attempt to observe conformational interconversion in solution.

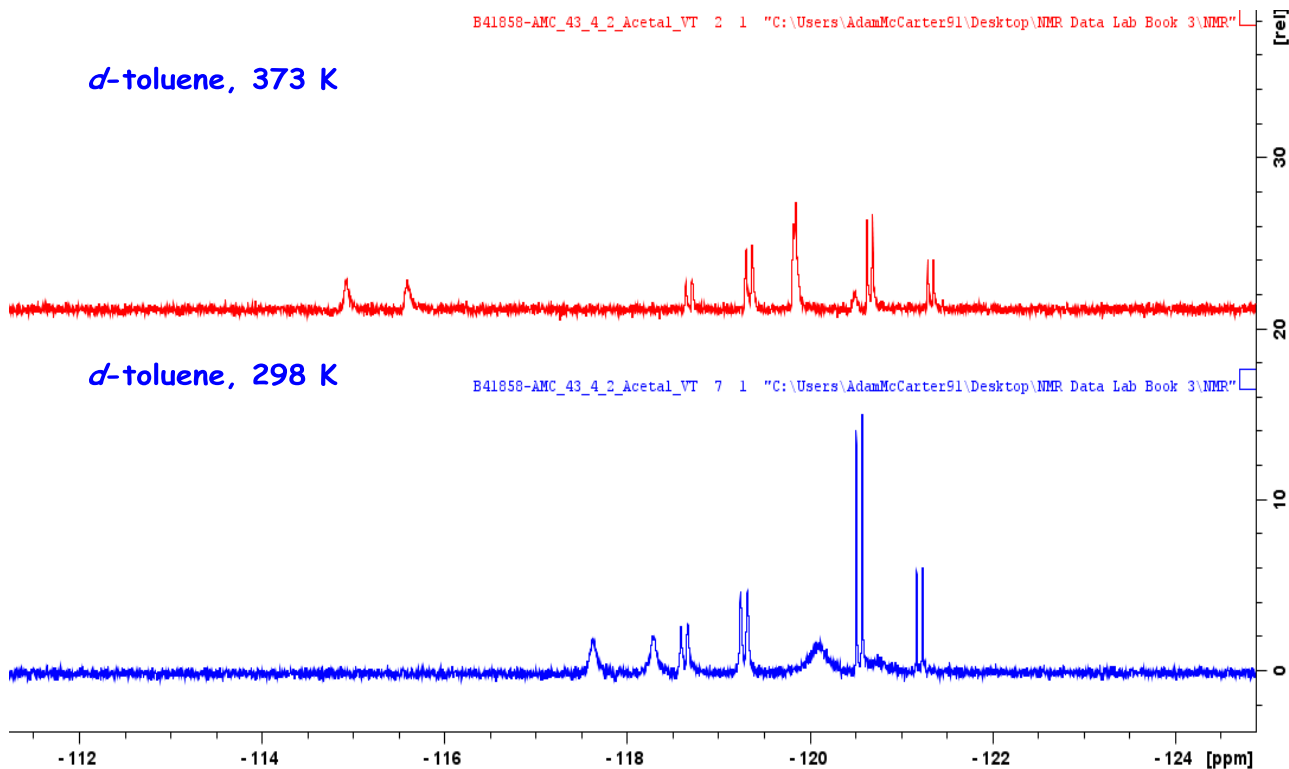


Figure 76: Heated VT-NMR experiment on acetal **203**.

The appearance of the signals changed significantly upon heating. The broad doublet signal at -120 ppm had sharpened and a large change in chemical shift of the broad doublet at -117 ppm to -115 ppm had occurred. The two doublet of doublet signals remained largely unaffected strongly suggesting conformational interconversion of one species. Cooling the sample also had a considerable impact on the appearance of the ^{19}F NMR spectrum (**Figure 77**).

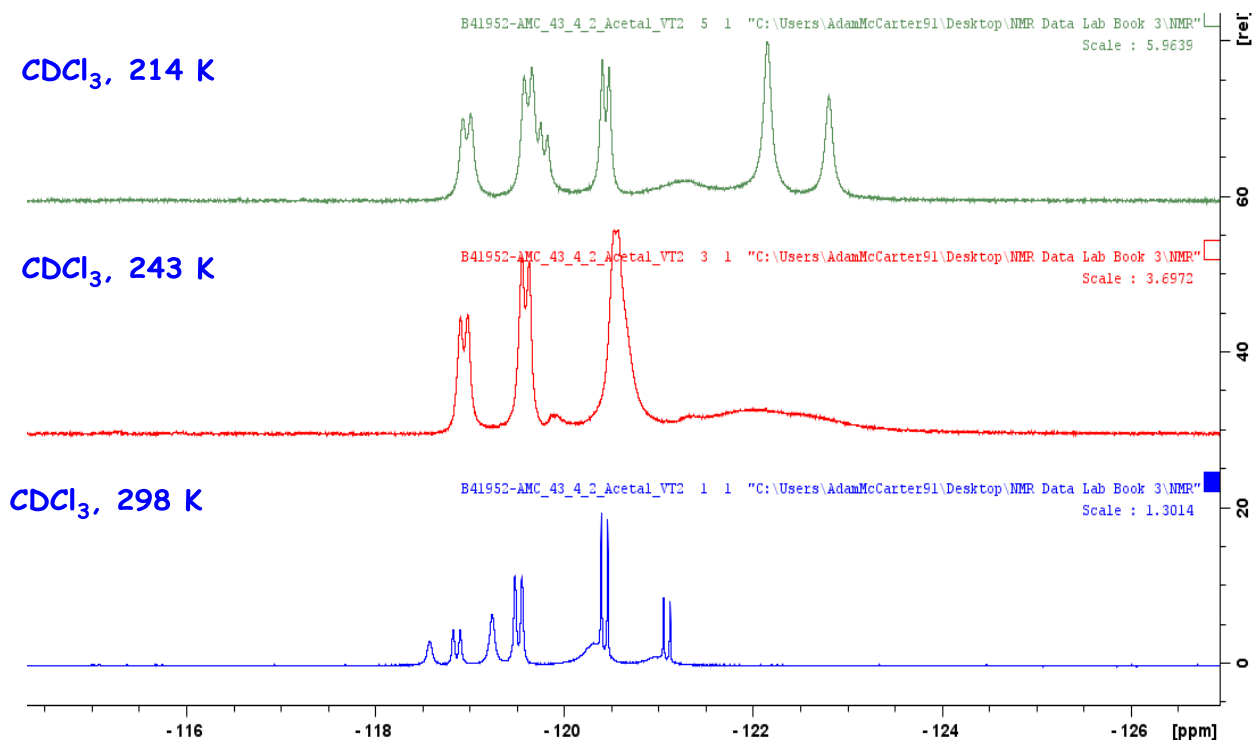
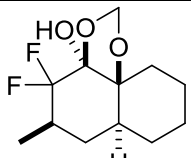
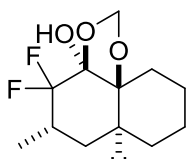
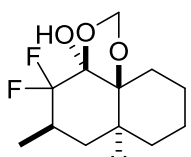
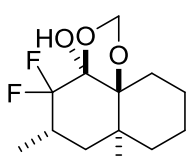


Figure 77: Sub-ambient VT-NMR experiment on acetal **203**.

Peak resolution was observed at 214 K; however, it was not possible to achieve temperatures lower than this with the current NMR instrument. Unfortunately, complete resolution of individual conformer signals could not be observed by VT-NMR. The potential for conformers and diastereoisomers has made the characterisation of acetal **203** particularly challenging. Based on this, DFT calculations to confirm whether or not multiple chair/boat/diastereoisomer conformations are energetically feasible were carried out (Table 12).

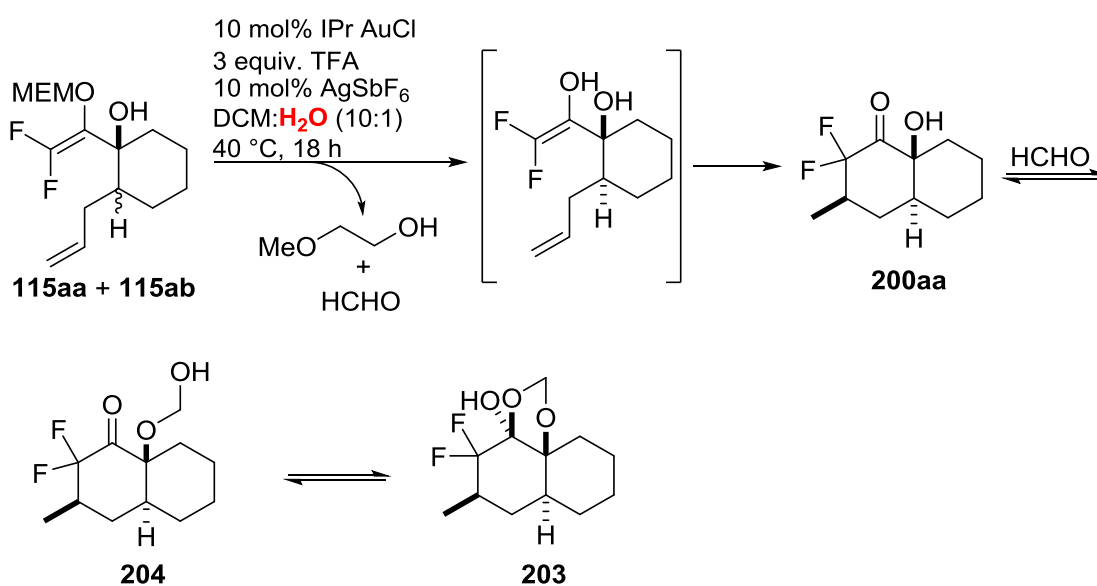
Table 12: DFT calculations on acetal **203** (Spartan 10, 6-31G* basis, gas phase).

Conformation	ΔG° (kcal mol ⁻¹)		
	B3LYP/6-31G*	M06/6-31G*	ω B97X-D/6-31G*
 <p>203a chair/chair</p>	0	0	0
 <p>203b chair/chair</p>	+ 2.00	+ 1.30	+ 1.03
 <p>203c chair/boat</p>	+ 1.20	+ 1.60	+ 0.95
 <p>203d chair/boat</p>	+ 1.00	+ 0.80	+ 0.98

Geometry optimisations were run at three different levels of theory using the Spartan'10 program.²³⁴ The results of these calculations showed very small differences in energies between the various possible conformations. In most cases the difference between conformational energies was within computational margin of error (± 0.5 kcal/mole). Virtually no difference in energies was observed with the ω B97X-D method, whilst at

the highest level of theory available (M06/6-31G*) the difference in energy between the two lowest energy conformations was <1 kcal/mole. The ω B97X-D and M06 methods offer an advantage over B3LYP as they are able to handle dispersive interactions. Together with the results from the VT-NMR experiments these electronic structure calculations provide further evidence for conformational isomers existing in a dynamic equilibrium.²³⁵

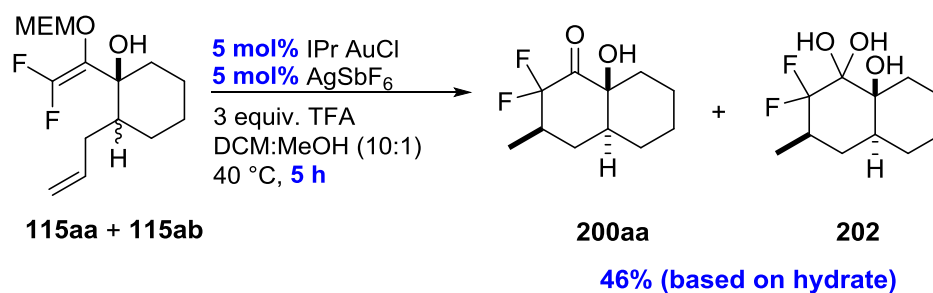
The formation of **203** can be explained by cleavage of the MEM group generating formaldehyde and methoxyethanol. This can then react with α -hydroxy ketone **200aa** to afford **203**. Subsequent cyclisation delivers the observed acetal **203** (Scheme 89).



Scheme 89: Formation of acetal **203**.

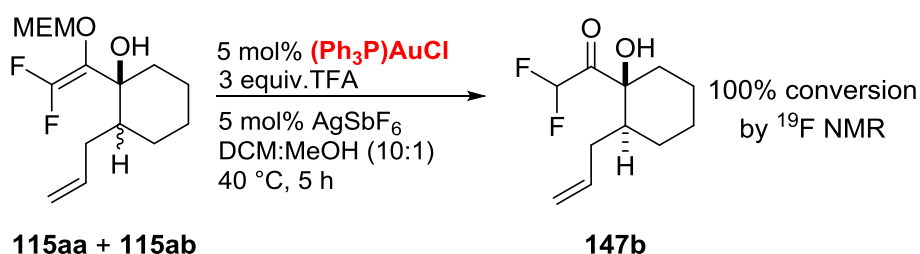
The formation of **203** under the given reaction conditions might appear counterintuitive as cleavage of the methylenedioxy group is often achieved under aqueous acidic conditions.²³⁶ However, Hurwitz *et al.* have previously reported the phosphoric acid catalysed reaction of formaldehyde with *trans*-1,2-cyclohexanediol to form similar dioxole structures.²³⁷ Fortunately, the formation of the tricyclic acetal could be inhibited using the initial DCM:MeOH (10:1) solvent conditions.

It was established that the catalyst loading could be reduced to 5 mol % whilst the cyclisation appeared to be complete after 5 hours, arriving at the reaction conditions in **Scheme 90**.



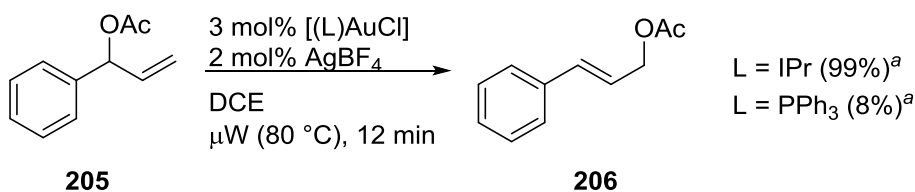
Scheme 90: Reaction optimisation for cyclisation of **115aa/ab**.

No cyclisation occurred when we employed the commonly used chloro(triphenylphosphino)gold(I) [(Ph₃P)AuCl] and only difluoromethyl ketone **147b** could be detected by ¹⁹F NMR (**Scheme 91**).



Scheme 91: Reaction of **115aa/ab** with phosphine ligated Au(I) catalyst.

The bulkier NHC ligand therefore appears to be critical for reactivity within the current system. *N*-heterocyclic carbene ligands combine strong σ -donating properties with a steric profile which imparts greater stability and enhanced reactivity to transition metal complexes.^{238,239,240,241} Nolan *et al.* have also observed a similar reduction in reactivity when a phosphine ligand was used in the gold(I) catalysed rearrangement of allylic acetates **205** (**Scheme 92**).²⁴²



Scheme 92: Ligand effects on Au(I) catalysed isomerisations ^a ¹H NMR conversions.

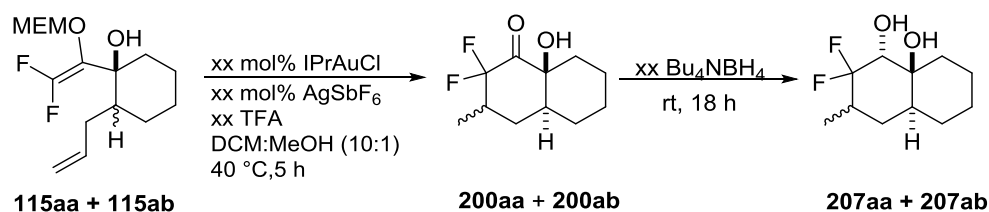
In this case the authors argue that the steric properties of the ligand had the greatest influence on catalytic activity. The greater steric hindrance of the IPr ligand is thought to better protect the gold centre and prevent cluster formation from, or precipitation of Au(0), factors which would inhibit activity.

At this point in the study, reproducibility problems were noted and it was decided to address this issue before embarking upon further reaction optimisation (catalyst loading,

stoichiometry of TFA). Although the DCM:MeOH solvent system inhibited the formation of the unwanted tricyclic acetal **203** it did not solve the problem completely. Following aqueous work up of the crude reaction mixtures increased levels of acetal **203** were observed by ^{19}F NMR. The α -hydroxy ketone could potentially react further during the work up process with any traces of paraformaldehyde still present from the reaction. Attempts to perform alternative ‘dry’ work ups by simply filtering the crude reaction mixture through celite or by removing the reaction solvent under reduced pressure failed, and acetal **203** could consistently be detected. It was therefore decided to avoid isolating **200aa** and, instead, intercept and transform the ketone functionality *in situ*. Jackson *et al.* have reported that cyclic α -hydroxy ketones can be reduced stereoselectively in chlorinated hydrocarbon solvents using tetrabutylammonium borohydride (*n*-Bu₄NBH₄).^{243,244} Furthermore, the 1,2-diol unit is a motif commonly found in natural products such as carbohydrates, polyketides and alkaloids.

4.2.3 Developing a one-pot process

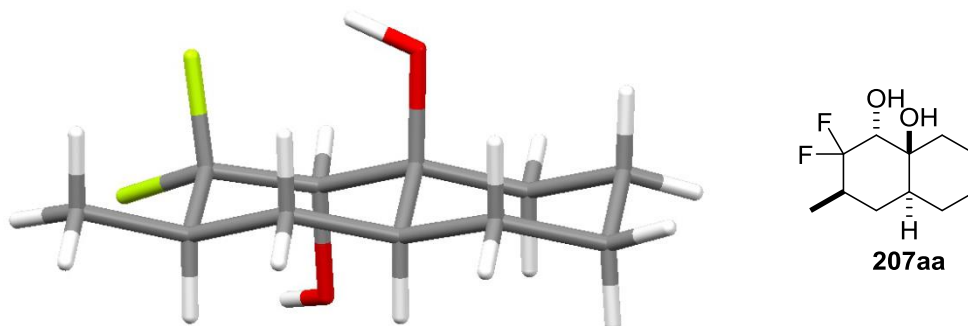
The one pot cyclisation/reduction was investigated with excess reducing agent in the first instance (**Table 13**, Entry 1).

Table 13: Reaction conditions screening for one pot cyclisation/reduction of **115aa/ab**.

Entry	Au (mol %)	Ag (mol %)	TFA equiv.	Bu ₄ NBH ₄ equiv.	Yield (%) ^{a,b}
1	5	5	3	5	14
2	5	5	3	4	58
3	5	5	3	3	60
4	5	5	3	2	29
5	5	5	2	2	54
6	5	5	1	1	28
7	5	5	1	2	57

^a Isolated yield ^b Isolated as a mixture of diastereoisomers

The reduction was successful and difluorinated *trans*-1,2-diol **207aa** was isolated. Indeed, analysis of the ¹⁹F NMR spectrum of the crude reaction mixture revealed that diol **207aa** was the major product of the reaction. Although the yield was low in the first instance, it was reasoned that this could be improved following further optimisation. The diol functionality proved much easier to handle than the previous difluoroketone motifs since the potential for acetal formation had been removed. The diol product readily solidified following chromatography of the crude reaction mixture to form a colourless solid. From this material it was possible to isolate a single crystal for XRD analysis, confirming the *trans*-selectivity of the reduction process (**Figure 78**).

**Figure 78:** Molecular structure of **207aa** in the crystal.

However, the ¹⁹F NMR spectrum of the crystalline material revealed that two chemically distinct species were present in a ratio of 44:6 (**Figure 79**).

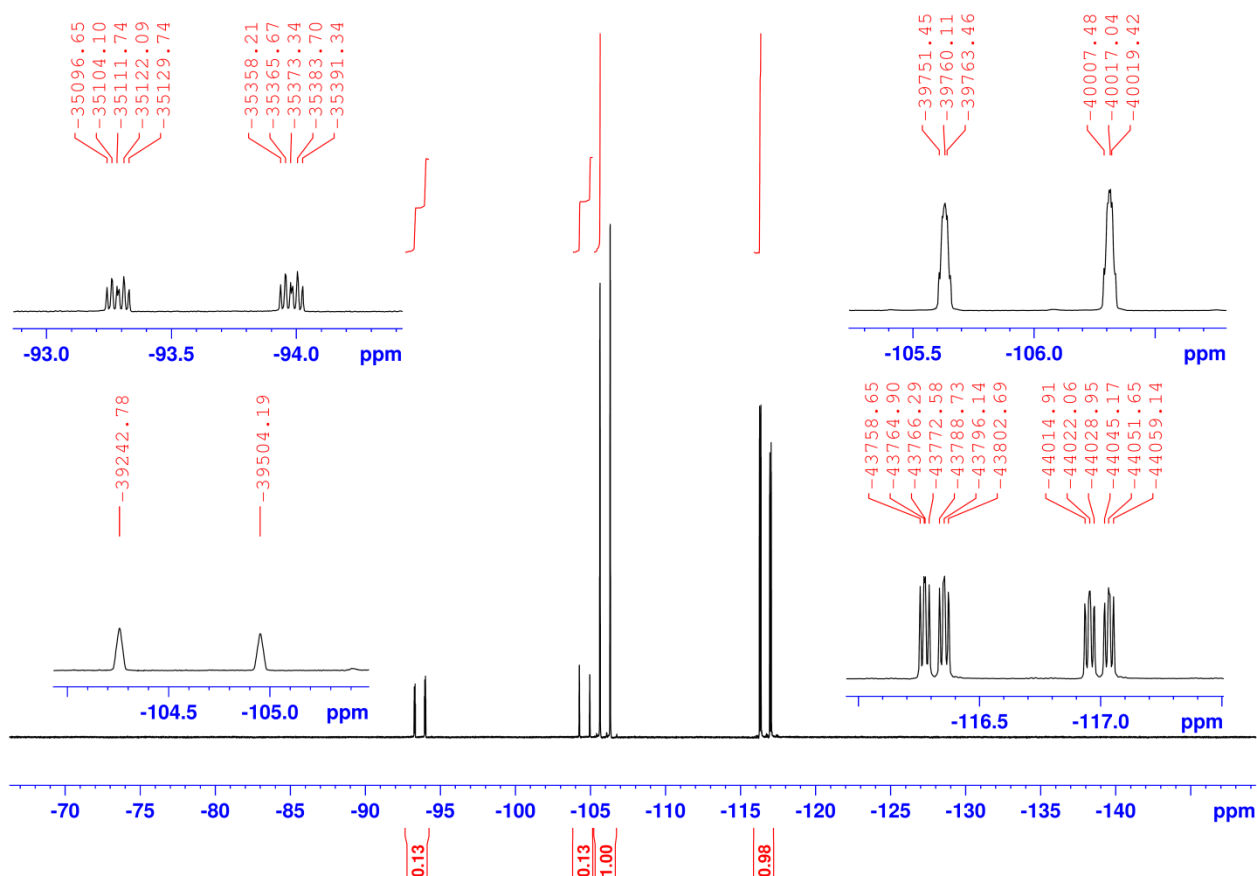


Figure 79: ^{19}F NMR spectrum of the crystal **207aa**.

Furthermore, the ^{19}F NMR spectrum of the remaining bulk solid had a similar appearance, but more of the minor species was now present (18:7). It was believed that this second species was the alternative diastereoisomer **207ab** with the methyl group adopting the axial position (**Figure 80**).

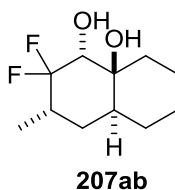


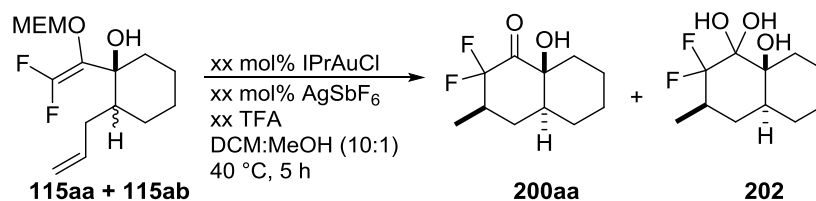
Figure 80: Alternative diastereoisomer observed.

Evidence for this can be inferred from the ^{19}F NMR spectrum by comparing the resonances at -93.6 ppm and at -116.7 ppm. These two signals represent the axial fluorine of each diastereoisomer; however, only the signal at -116.7 ppm has a well resolved $^3J_{\text{HF}}(\text{trans})$ coupling ($^3J_{\text{HF}} = 30$ Hz). This $^3J_{\text{H-F}}$ diaxial splitting is absent for the other diastereoisomer which is represented by a smaller $^3J_{\text{HF}}(\text{gauche})$ coupling at -93.6 ppm ($^3J_{\text{HF}} = 17$ Hz). It is expected that this diastereoisomer would be the minor species as

there is an energetic penalty for positioning the methyl group in the axial position. Unfortunately, it was not possible to separate the diastereomeric mixture by chromatography; however, three successive recrystallizations by vapour diffusion enabled the successful isolation of the diastereomerically pure *trans,trans*-diol **207aa**.

The stoichiometry of reducing agent could be reduced to three without any detrimental effect on reaction yield; however, a reduction in yield was observed when two equivalents of reagent were used (**Table 13, Entry 3 and 4**). At this point the nature of the reducing agent was considered. The use of excess acid in the reaction implies that it could readily react with the reducing agent when added, yet successful reductions were still observed when equimolar amounts of TFA and *n*-Bu₄NBH₄ were used (**Table 13, Entry 3**). Tetrabutylammonium borohydride is known to readily form tetrabutylammonium acyloxyborohydrides in organic acid media.²⁴⁵ Itoh *et al.* have also reported that a combination of sodium borohydride (NaBH₄) and TFA forms sodium trifluoroacetoxyborohydride [NaBH₃(O₂CCF₃)] which readily reduces aromatic and aliphatic nitriles to the corresponding amines under mild conditions.²⁴⁶ It is possible that trifluoroacetoxyborohydride acts as the hydride source in this system. Further optimisation enabled a reduction in the stoichiometry of TFA to one equivalent and of reducing agent to two equivalents, without observing any decrease in the rate of cyclisation (**Table 13, Entry 7**). At this point in the study it was deemed necessary to perform the appropriate control reactions before investigating the substrate scope (**Table 14**).

Table 14: Control reactions.



Entry	Au (mol %)	Ag (mol %)	TFA equiv.	Conversion (%) ^a
1	5	5	-	100
2	5	-	-	0 ^b
3	-	5	-	0 ^b
4	-	-	1	0 ^b
5	5	-	1	0 ^b
6	-	5	1	0 ^b

^a Determined by ¹⁹F NMR ^b Only starting material could be detected

It was surprising to discover that, in the absence of TFA, allylic alcohol **115aa/ab** had been fully consumed and the crude ^{19}F NMR spectrum showed a mixture of ketone and hydrate after 5 hours (**Table 4, Entry 1**). It was initially thought that the reaction proceeded through a difluorinated enol intermediate; however, this result strongly suggests that the difluorinated enol acetal is the nucleophile in the reaction (**Figure 81**).

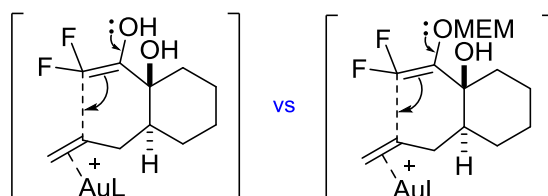


Figure 81: Initially proposed difluorinated enol nucleophile (left) and difluorinated enol acetal nucleophile (right).

Echavarren *et al.* have previously demonstrated the effectiveness of enol ether nucleophiles for cyclisation onto Au(III) activated alkynes; however, the reactivity of enol ethers towards cationic gold activated alkenes has not yet been reported.²⁰¹ As expected, no product could be detected in the Au(I) and Ag(I) only experiments (**Table 14, Entries 2 and 3**, respectively).²⁰⁰ Interesting results were also observed when allylic alcohol **115aa/ab** was exposed to TFA in the absence and presence of both gold and silver salts (**Table 14, Entries 4, 5 and 6**). Acetal protecting groups are known to be readily cleaved in the presence of TFA and a build-up of DFMK **147b** in each reaction was expected (**Figure 82**).²⁴⁷

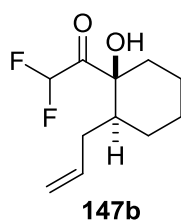
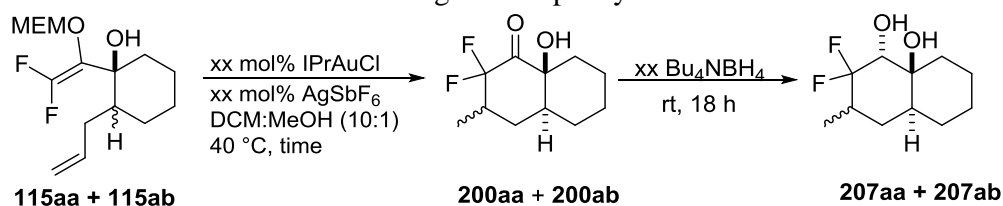


Figure 82: Expected product from TFA control experiments.

Surprisingly, no DFMK could be detected after five hours and only starting material remained in each reaction mixture. These results provide further evidence that a difluorinated enol acetal is the active nucleophile. The inclusion of TFA appears to have no effect on the rate of cyclisation or removal of the MEM protecting group. The complete removal of this highly corrosive reagent from the reaction mixture undoubtedly offers a significant practical advantage. Subsequently, optimisation of the one pot cyclisation/reduction process was revisited (**Table 15**). The exclusion of TFA allowed

reduction of the stoichiometry of reducing agent to one whilst improving the reaction yields previously obtained (**Table 15, Entry 1**).

Table 15: Reaction conditions screening for one pot cyclisation/reduction of **115aa/ab**.



Entry	Au (mol %)	AgSbF ₆ (mol %)	Time (h)	Reducing agent	Yield (%) ^a
1	5	5	5	Bu ₄ NBH ₄	70 ^b
2	2.5	2.5	5	Bu ₄ NBH ₄	68 ^b
3	1	1	22	Bu ₄ NBH ₄	51 ^b
4	5	5	5	NaBH ₄	42 ^b

^a Isolated yield ^b Product was isolated as a mixture of *trans, trans* and *trans, cis* diastereoisomers, major isomer shown (2.6:1).

The catalyst loading could be lowered to 2.5 mol % without any effect on the rate of cyclisation, though a slight decrease in product yield was observed (**Table 15, Entry 2**). However, lower catalyst loadings had a significant impact on reaction yield (**Table 15, Entries 4 and 3**). Although starting material **115aa/ab** was consumed fully purification proved to be particularly troublesome as an unknown impurity co-eluted with the product during chromatography. Multiple purifications were required to achieve a modest yield of **207aa** and **207ab**; however, 5 mol % catalyst loading appeared to be optimal. Replacing the reducing agent to an alternative borohydride salt (NaBH₄) also resulted in lower yields (**Table 5, Entry 4**). It was reasoned that the improved solubility of Bu₄NBH₄ over sodium borohydride in the reaction media accounted for the higher yield of **207aa** and **207ab**.

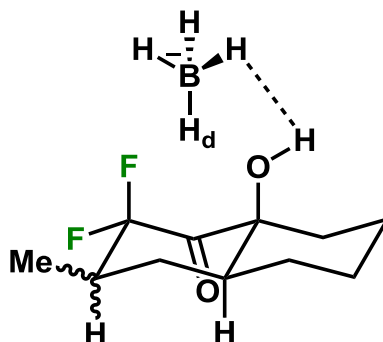


Figure 83: Potential reductive stereocontrol *via* dihydrogen bonding.

Finally, as previously reported by Jackson *et al.*, it is possible that the α -hydroxy functionality is providing some stereocontrol during the reduction as no *cis*-diol was

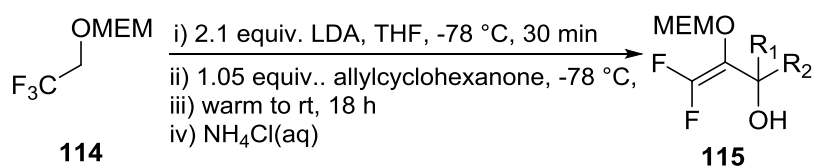
observed in any of the crude reaction mixtures during the optimisation process.²⁴³ The potential for dihydrogen bonding between the ring junction hydroxyl group and the hydrogen atom bonded to boron may account for the *trans*-diol selectivity observed (**Figure 83**).

With the optimisation for the cyclisation of allylic alcohol **115aa/ab** complete, the generality of the methodology was tested by synthesising further difluorinated diol motifs.

4.2.4 Substrate Scope – Allylic Alcohols

A range of difluoroallylic alcohols were prepared in moderate to good yield in order to probe the cyclisation (**Table 16**).

Table 16: Difluorinated allylic alcohols **115** prepared from **114**.^[a]



Electrophile	Product	Yield	dr ^b
		69% ^c	19:1 <i>trans:cis</i>
		32% ^{c, d}	32:1 <i>trans:cis</i>
		56% ^c	3.5:1 <i>trans:cis</i>
		42% ^{c, e}	4.9:1 <i>trans:cis</i>
		73%	-
		64%	-
		61% ^f	-
		31% ^g	-
		30% ^f	-
		37% ^h	4.6:1 <i>E:Z</i>
		19% ^{c, e}	32:1 <i>trans:cis</i>

^a All reactions were carried out with 12 mmol of **114** unless otherwise stated ^b dr determined by ¹⁹F NMR spectroscopy ^c Isolated as a mixture of *cis*- and *trans*- diastereoisomers, major isomer shown ^d At 9.5 mmol scale ^e At 5 mmol scale ^f At 10 mmol scale. ^g At 8 mmol scale. ^h Isolated as a mixture of (*E*)- and (*Z*)- diastereoisomers.

The annulative precursors prepared included the 7-membered ring carbocycle **115ba/115bb** as well as the oxygen and nitrogen containing heterocycles **115ca/115cb** and **115da/115db**. Annulative processes benefit from lower reaction entropies; therefore, it was interesting to determine whether the methodology also tolerated more challenging annulative cyclisations. In this regard, a further 6 annulative precursors were synthesised **115e-j**. Unfortunately both the cyclopropyl and cyclopentane analogues were isolated in slightly diminished yields. Analysis of the crude ^{19}F NMR spectra for both of these reactions found significant quantities of enol acetal **208** present within the reaction mixture (**Figure 84**). The presence of this material indicates that ‘wet’ electrophile had been added to the reaction. However, after repeating each of the reactions under stringently dry conditions acetal **208** was continuously detected. It is, therefore, thought that the pre-existing carbocyclic rings in these ketones might provide significant steric bulk and impede approach of the *in situ* generated vinyl lithium nucleophile.

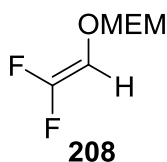


Figure 84: Enol acetal product observed in preparation of allylic alcohols **115h** and **115i**.

A lower yield was also noted for internal alkene **115j**. In this case the yield can be attributed to the more protracted purification required. Following Kugelrohr distillation (63% initial yield) the product had to be purified further by column chromatography to achieve a final yield of 37%. Finally, it was also of interest to test the cyclisation with alkyne containing substrates.

Successful cyclisation of these species would provide ring systems bearing an exocyclic alkene group which would potentially be useful for further functionalisation. A poor yield was observed for alkyne-containing allylic alcohol **115k** and, again, large quantities of **208** were detected in the crude reaction mixture by ^{19}F NMR. We initially attributed the lower yield of alkyne **115k** with competing deprotonation of the alkynyl hydrogen of the electrophile. However, diethyl ketone is more acidic than phenylacetylene in DMSO, (**Figure 85**).²⁴⁸

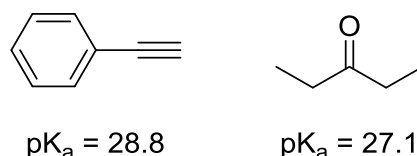


Figure 85: pK_a 's of alkyne protons versus C-H bonds adjacent to carbonyl groups in DMSO.

Therefore, it is reasoned that the ketone electrophile must have been 'wet' prior to addition to the reaction mixture.

It should be noted that a significant effort was invested to resolve issues which arose with regards to allylic alcohol isolation. Initially, crude reaction mixtures were simple to purify using standard silica gel chromatography following aqueous work up. However, during the course of the investigation, the reaction mixtures began to turn black in appearance. The ^{19}F NMR spectra of the crude reactions showed only the desired products; however, attempts to purify these dark mixtures by column chromatography resulted in isolation of the products as dark orange oils which, although clean by NMR, were not compatible with the subsequent cyclisation. After attempting various work up procedures, temperatures, reaction times and reagent addition times it was discovered that filtering the crude reaction mixtures through a large plug of silica followed by Kugelrohr distillation allowed the isolation of the products as pale yellow/colourless oils. With the exceptions of **115da/115db**, **115g** and **115k** all of the allylic alcohols were isolated in this manner.

4.2.5 Substrate Scope – Difluorinated Diols

Annelations enabled the synthesis of 4 novel fused bicyclic difluorinated diol systems. The 6,7-ring system was isolated as a mixture of *trans, trans*-**207ba** and *trans, cis*-**207bb** diastereoisomers (**Table 17, Entry 2**). It was possible to isolate the single *trans, trans*-**207ba** diastereoisomer following repeated recrystallizations of the mixture by vapour diffusion using chloroform/pentane (7%). Unfortunately, heterocycles **207c** and **207d** were isolated in slightly lower yields and diastereoselectivities. The *trans, trans* diastereoisomer was still the major species for both systems; however, the *cis, cis*-diastereoisomer was now present and could not be separated by chromatography or recrystallization. The *cis, cis* stereochemistry was elucidated by careful examination of both the ^{19}F and ^1H NMR spectra (**Figure 86**).

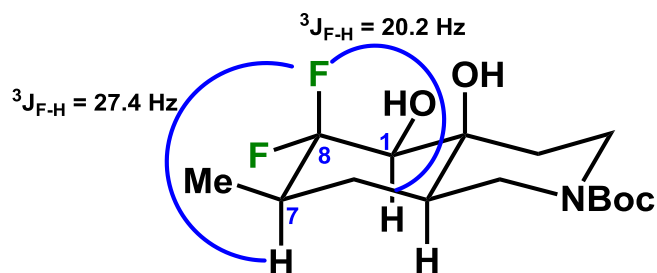
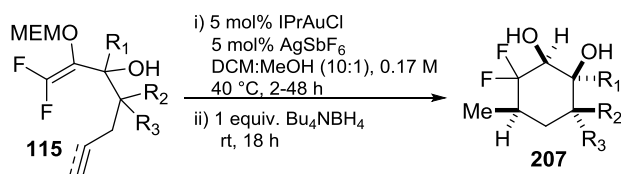


Figure 86: Stereochemical Configuration of *cis, cis*-**207d**.

Taking nitrogen containing heterocycle **207d** as a representative example, the axial fluorine atom appears as a distinct ddd signal at -116.1 ppm in the ^{19}F NMR spectrum ($^2J_{\text{F-F}} = 243.7$, $^3J_{\text{F-H}} = 27.4$, 20.2 Hz). The retention of two large $^3J_{\text{F-H}}$ diaxial couplings confirms the *cis, cis* stereochemistry. Furthermore, the smaller $^3J_{\text{F-H}}$ coupling can be associated through coupling with the hydrogen at the C1 position as the reciprocal 20.2 Hz $^3J_{\text{H-F}}$ coupling can be observed in the ^1H NMR spectrum.

Table 17: Scope of one pot cyclisation/reduction method.

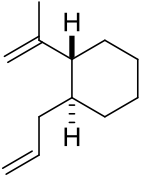
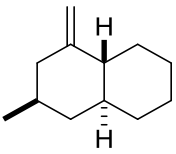
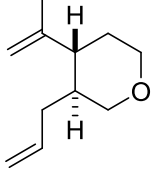
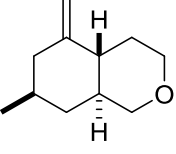
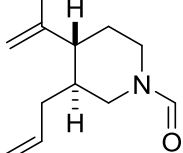
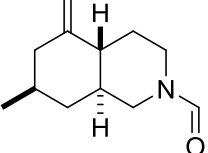


Entry	Allylic Alcohol	Product	Yield(%) ^a	dr ^b
1	115aa/115ab	207a	70	2.6:1 <i>trans,trans:trans,cis</i>
2	115ba/115bb	207b	69	4.9:1 <i>trans,trans:trans,cis</i>
3	115ca/115cb	207c	48	6.7:1.4:1 <i>trans,trans:trans,cis:cis,cis</i>
4	115da/115db	207d	50 ^c	3.4:0.9:1 <i>trans,trans:trans,cis:cis,cis</i>
5	115e	207ea	25 ^d	>20:1
	115e	207eb	16 ^d	>20:1
6	115f	207f	11	>20:1
7	115g	207g	63	>20:1
8	115h	207h	29 ^d	1.3:1:0.1 <i>trans,cis:trans,trans:cis,cis</i>
9	115i	207i	44	3.8:1 <i>trans,trans:cis,trans</i>
10	115j	207j	0	-

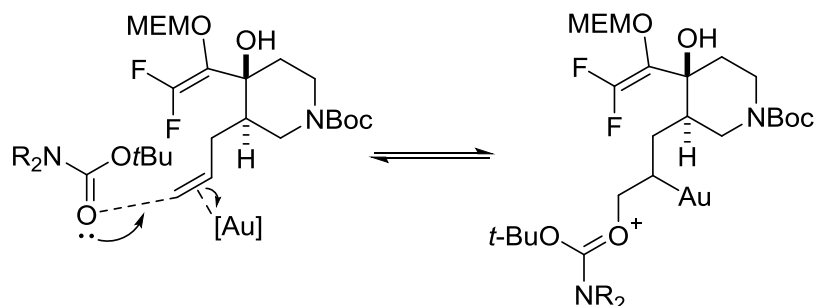
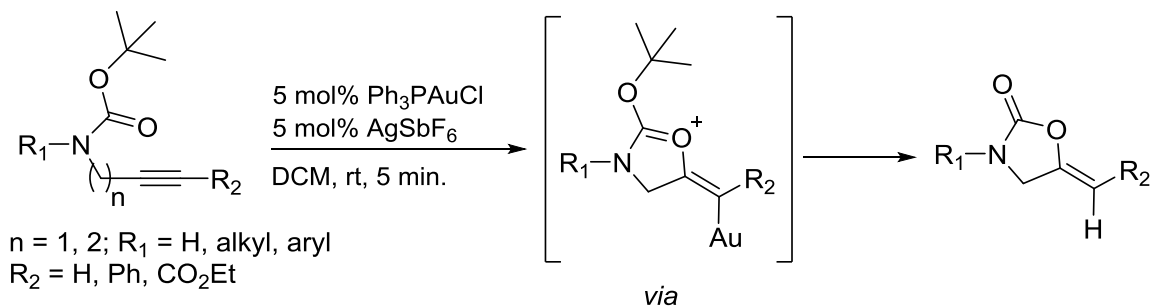
^aIsolated yield. ^bDiastereoisomeric ratio determined by ¹⁹F NMR spectroscopy; for mixtures the major isomer is shown. ^c10 days reaction time. ^dDiastereoisomers could be separated by normal phase chromatography. ^e15 minutes reaction time and TBAB not added.

Intriguingly, the cyclisation of **115da/115db** required 10 days reaction time, longer than any other cyclisation (typically 5-21 hours). In an attempt to rationalise this marked decrease in reactivity DFT calculations were performed to ascertain if there was a significant difference in energy barrier to product formation between different substrates. Calculations on 6 model substrates were conducted using the Spartan'10 program (**Table 18**).²³⁴ The models were selected for computational simplicity. Simple geometry optimisations were performed using a restricted Hartree-Fock method (RHF/6-31G*) followed by single point energy calculations using the T1 thermochemical recipe to calculate heats of formation using dual basis set RI-MP2 techniques (RRIMP2(FC)/6-311++G(2df,2p)[6-311G*]).²⁴⁹

Table 18: DFT calculations on model annulations (Spartan 10., gas phase).

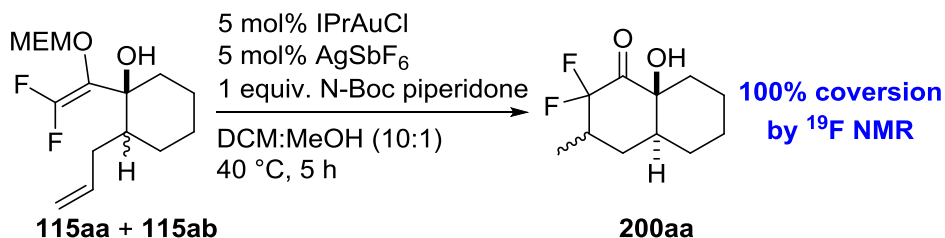
Model starting material	H _f ^o (kJ mol ⁻¹)	Model product	H _f ^o (kJ mol ⁻¹)	ΔH _{reaction} ^o (kJ mol ⁻¹)
	-29.39		-119.70	-90.31
	-129.56		-219.21	-89.65
	-130.23		-219.31	-89.16

The results of these calculations showed no difference in energy between the various transformations, all within computational margin of error (± 0.5 kcal/mole), indicating that the observed reactivity difference was not based on the relative thermodynamics of the product. Although there are no reports in the literature of carbamate groups inhibiting gold catalysis there are examples whereby carbamate group participation is observed. Carretero *et al.* have shown that *N*-Boc protected alkynylamines can react intramolecularly to form oxazolidinone derivatives. The reaction proceeds through the Boc group with the carbonyl oxygen acting as a nucleophile attacking the gold(I) activated alkyne (**Scheme 93**).²⁵⁰



Scheme 93: Carbamate group participation in reaction with alkynes (top) and potential intermolecular interaction in our current system (below).

If such Boc group participation was occurring then this would potentially result in reaction inhibition. To test this hypothesis a spiking experiment was performed whereby one equivalent of *N*-Boc piperidone was used as an additive in one of the known faster cyclisations (**Scheme 94**).²⁵¹



Scheme 94. Spiking experiment performed to test *N*-Boc participation.

After five hours reaction time an aliquot of the reaction mixture was taken up and a ¹⁹F NMR spectrum obtained. The NMR showed complete conversion to the cyclic ketone product and effectively rules out carbamate participation/inhibition. Consequently, it was not possible to rationalise the relative reaction rate for allylic alcohol **115da/115db**.

Monomethylated analogue **207e** was isolated in good overall yield (56%); however, characterisation proved complex as the reaction produced 3 different diastereoisomers. A mixture of *trans*, *trans*-**207ea** and *cis*, *cis*-**207ec** was isolated in 15% yield (1:1.2 respectively). The stereochemistry of the individual species was elucidated by examination of both the ¹⁹F and ¹H NMR spectra as well as a crucial [¹H, ¹⁹F] HOESY experiment (**Figures 87, 88 and 89**).

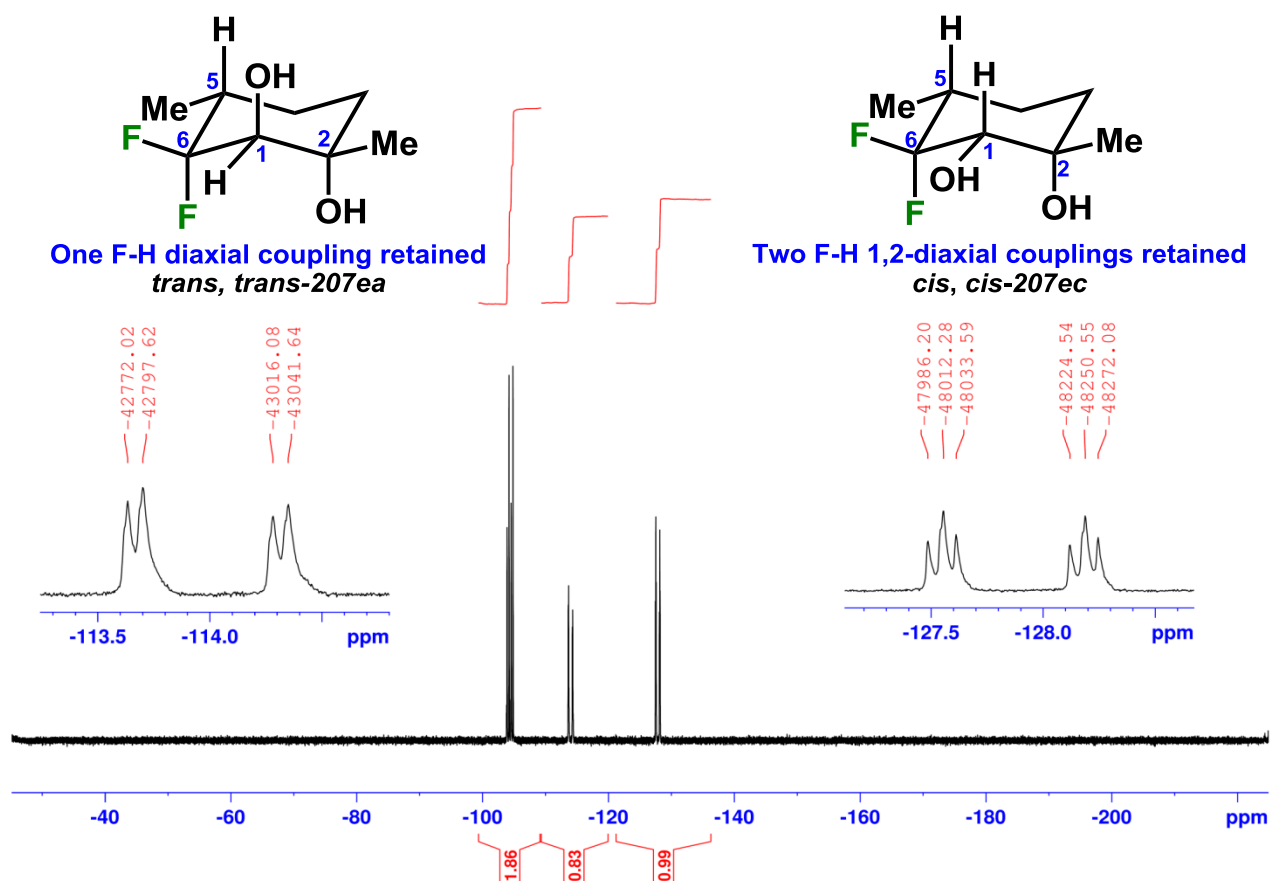


Figure 87: ^{19}F NMR spectrum in $\text{DMSO-}d_6$ at 373 K of *trans,trans*-207ea and *cis,cis*-207ec.

From the ^{19}F NMR spectrum of the mixture a doublet of triplet signal is observed for the *cis,cis* axial fluorine at -127.9 ppm ($^2J_{\text{F-F}} = 238.7$, $^3J_{\text{F-H}} = 20.3$ Hz). This larger $^3J_{\text{F-H}}$ coupling and splitting pattern tells us that the axial fluorine is adjacent to two axial hydrogens at the C1 and C5 positions, thereby setting the stereochemistry at these two chiral centres. A doublet of doublet signal is observed for the *trans,trans* axial fluorine at -114.0 ppm ($^2J_{\text{F-F}} = 243.2$, $^3J_{\text{F-H}} = 25.8$ Hz). This indicates that there is only one axial hydrogen adjacent to the fluorine; however, it is unclear whether this is at the C1 or C5 position. To elucidate this analysis of the ^1H NMR spectrum is required (**Figure 88**).

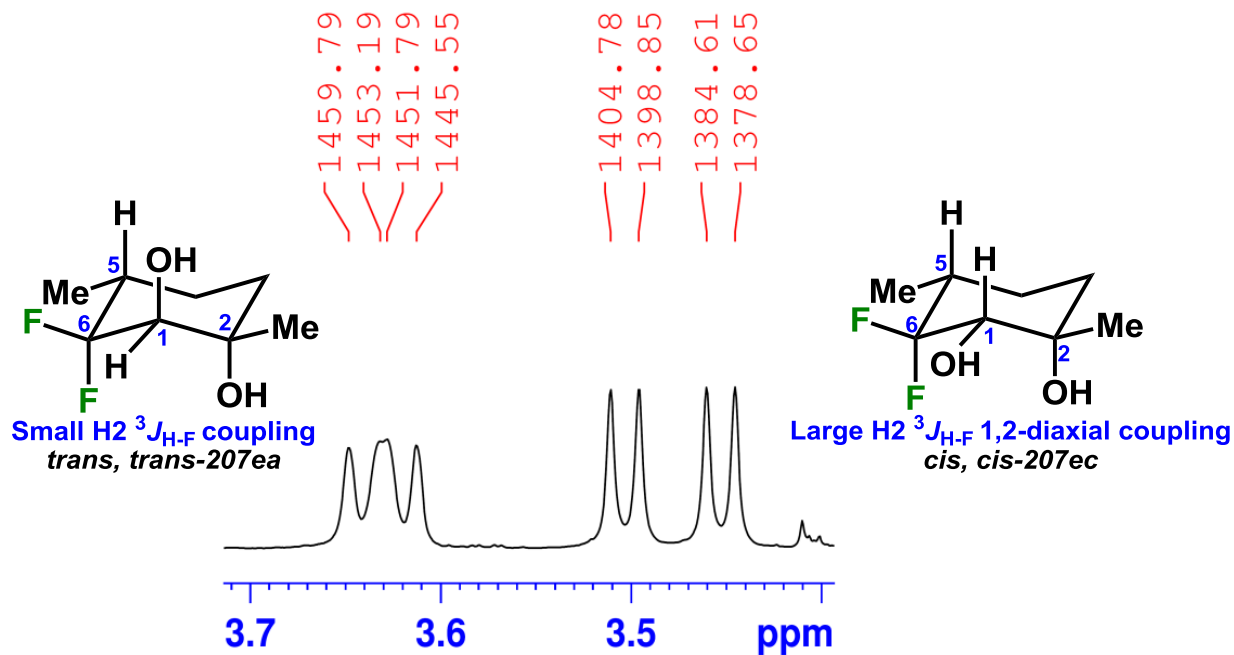


Figure 88: Partial ^1H NMR spectrum of *trans, trans*-207ea and *cis, cis*-207ec.

It should be noted from the ^1H NMR spectrum that a large doublet of doublet signal at 3.48 ppm exists for the C1 hydrogen of the *cis, cis* isomer. This is formed as a result of a large $^3J_{\text{H-F}}$ 1,2-diaxial coupling (20.3 Hz) followed by a smaller $^3J_{\text{H-F}}$ (*gauche*) coupling (6.0 Hz). In comparison, this 1,2-diaxial coupling is absent for the C1 hydrogen in the *trans, trans* species and a smaller doublet of doublet signal is present at 3.63 ppm ($^3J_{\text{H-F}} = 8.1, 6.7$ Hz). This implies that the hydrogen atom must adopt the equatorial position and sets the stereochemistry at the C1 position of the *trans, trans* diastereoisomer. With the stereochemistry at the C1 and C5 positions elucidated for both species the final C2 stereocentre remains. If the C2 methyl group adopts the axial position a strong HOE contact would be present between the axial fluorine of each stereoisomer and the CH_3 group. A [^1H , ^{19}F] HOESY experiment was performed, and revealed that no HOE contact was observed for either stereoisomer (Figure 89).

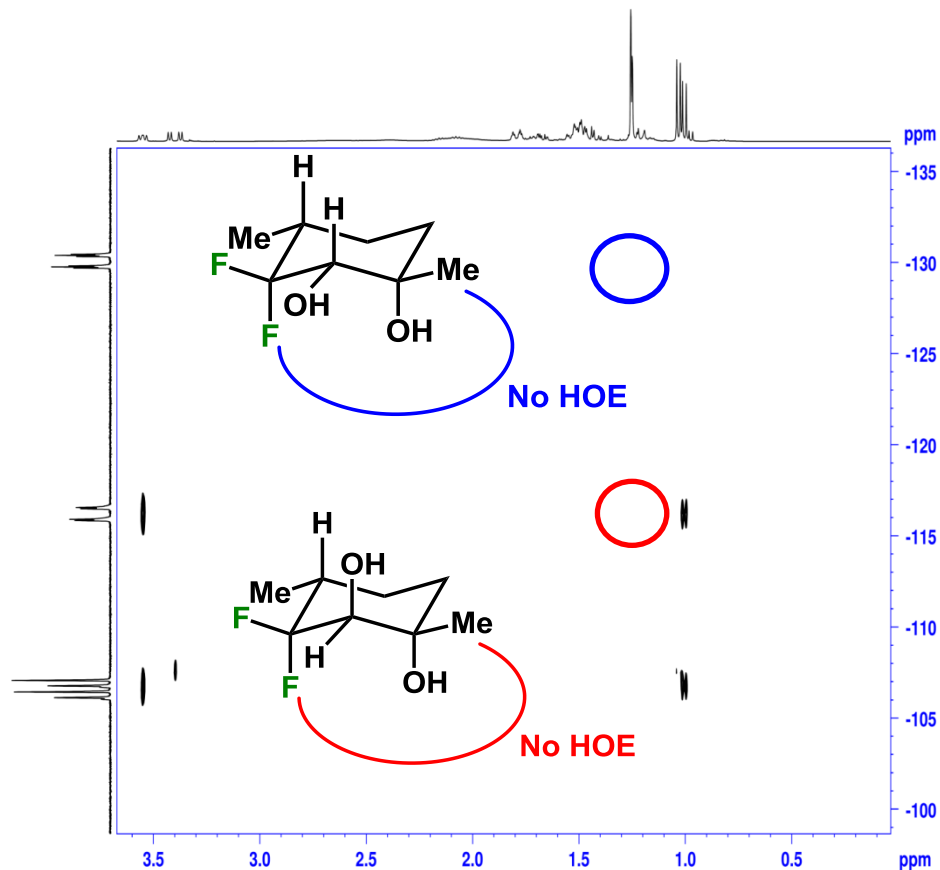


Figure 89: [^1H , ^{19}F] HOESY experiment of *trans,trans*-**207ea** and *cis,cis*-**207ec**.

The result of this experiment shows that the methyl group adopts the equatorial position for both isomers. The formation of *trans* diol species **207ea** can be rationalised through dihydrogen bonding; however, this effect must be weak since formation of the *cis* diol **207ec** occurs. It was possible to isolate both *trans,trans*-**207ea** and *trans,cis*-**207eb** in diastereoisomerically pure forms. Characterisation of *trans,cis*-**207eb** proved less troublesome and its stereochemistry was confirmed by single crystal X-ray diffraction (**Figure 90**).

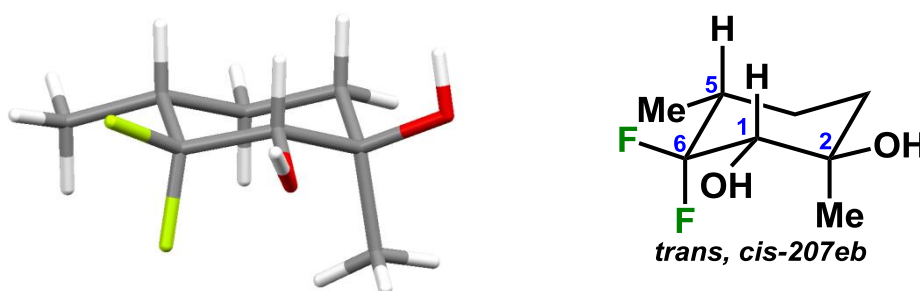


Figure 90: *Trans,cis*-**207eb** in the crystal.

A [^1H , ^{19}F] HOESY was also performed on this substrate to test the robustness of the experiment and a clear HOE cross peak was visible correlating the axial fluorine with the C2 methyl group (**Figure 91**).

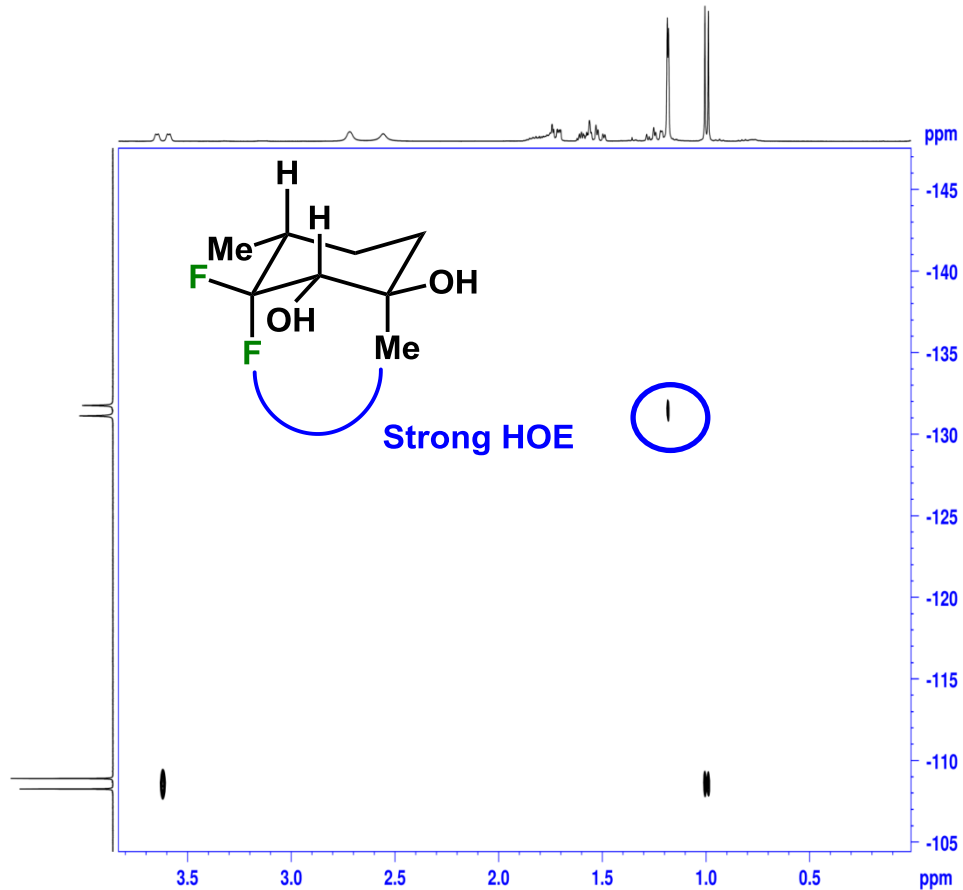


Figure 91: [^1H , ^{19}F] HOESY experiment of *trans, cis*-**207ec**.

The formation of this diastereoisomer containing an axial methyl group is unusual. The cyclohexane A-value for a $-\text{CH}_3$ group is 7.28 kJ/mol, whereas for an $-\text{OH}$ substituent it is 3.64 kJ/mol.²⁵² The formation of this species is therefore thought to be disfavoured; however, it was isolated in an overall yield of 16%.

Annulations required a minimum level of substitution on the chain and a low yield (11%) was obtained for the least substituted system *cis, trans*-**207f**. Surprisingly, it was the *cis*-diol that was isolated in this instance.

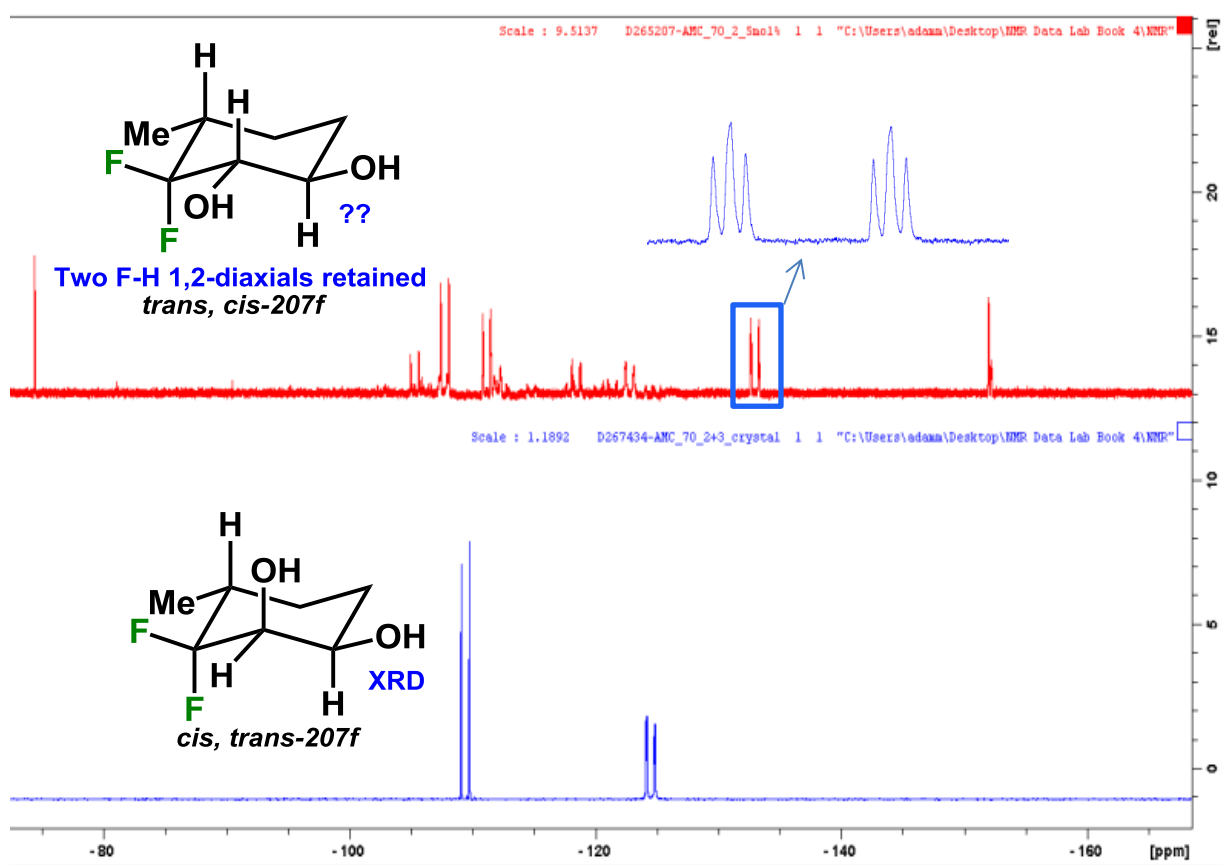


Figure 92: ^{19}F NMR spectrum of crude reaction mixture (above) and pure *cis, trans*-**207f** (below).

Comparison of the ^{19}F NMR spectrum of the crude reaction mixture and purified *cis, trans*-**207f** may offer some explanation with regards to the lower yield and stereoselectivity observed. The crude ^{19}F NMR spectrum is complex with a number of peaks containing large $^2J_{\text{F-F}}$ coupling constants. This arises from the presence of multiple difluorinated cyclic molecules (**Figure 92**). It appears as though the minor diastereoisomer has in fact been isolated, the signals of which are barely detectable in the crude NMR spectrum. Furthermore, one of the major peaks in the crude reaction is a doublet of triplet signal at -132.8 ppm ($^2J_{\text{F-F}} = 239.6$, $^3J_{\text{F-H}} = 25.8$ Hz). With the retention of two $^3J_{\text{F-H}}$ diaxial couplings it is likely that this signal represents the axial fluorine of the *trans, cis* diastereoisomer, the isomer that would be expected from the reaction. Despite the low yield of *cis, trans*-**207f** it was not possible to isolate equivalent unsubstituted cyclic analogues using the Saegusa-Ito methodology so it would appear that the gold-catalysed cyclisation is more efficient.

Diastereoisomerically pure *cis,trans*-**207g** was isolated from the reaction in good yield. Out of all the cyclisations performed this particular substrate proceeded with the greatest overall diastereoselectivity. The stereochemical outcome of this reaction requires some comment. Firstly, the stereochemistry of the methyl group could be attributed to the larger overall strain energy (1,3-diaxial interaction) that would arise from having two axial methyl substituents (each axial methyl group contributing 1.7 kcal/mol strain energy).²⁵³ Secondly, none of the *trans*-diol species was observed from this reaction. This was a surprising result as, it was reasoned that the α -hydroxyl functionality plays a role in the facial selectivity of hydride addition through dihydrogen bonding.^{243,244} However, the observed selectivity for the reduction can be rationalised by application of the Felkin-Ahn model in the reduction of cyclic ketones.²⁵⁴ The stereoselectivity of the reduction is attenuated dramatically upon addition of an axial methyl group at the C-3 position. Wigfield *et al.* have previously demonstrated that the stereochemical effect of an equatorial methyl group is minor in comparison to the introduction of axial substituents at the C-3 and C-5 positions on the cyclohexane ring.²⁵⁵ The bulky tetrabutylammonium borohydride reagent is expected to preferentially attack the equatorial face of the ketone, avoiding the steric interaction between the borohydride molecule and the axial methyl group at C-3 arising from axial face attack (**Figure 93**).²⁵⁶

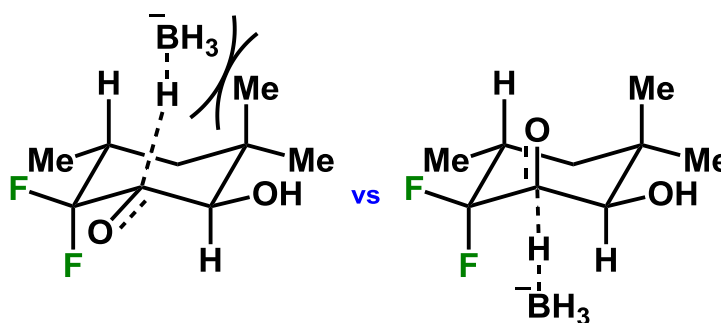


Figure 93: Rationale for observed reduction selectivity with steric interactions upon axial attack (left) and minimal steric interactions upon equatorial attack (right).

Spiro-cyclopropyl analogue **207h** was primarily isolated as a mixture of three diastereoisomers (29%); however, it was also possible to isolate small quantities of both *trans, cis*-**207ha** (6%) and *trans, trans*-**207hb** (5%) as single diastereoisomers (representing an overall yield of 40%, **Figure 94**). Once again analysis of this species proved to be complicated and, due to conformational interconversion, variable temperature (VT) NMR experiments was necessary.²⁵⁷ Along with 2D NMR HOESY experiments and single crystal X-ray diffraction the stereochemistry of each individual species could be confidently assigned.

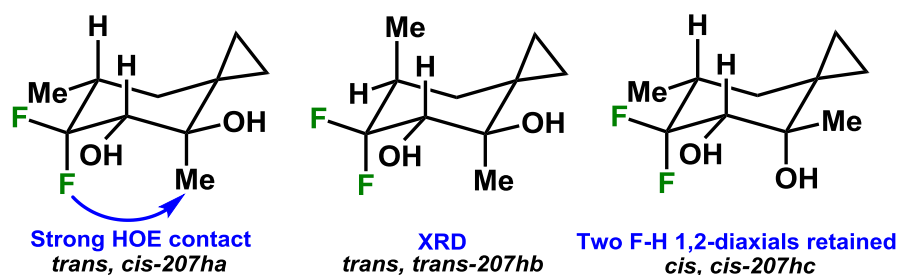


Figure 94: Spiro-cyclopropyl diastereoisomers obtained.

The final diol species formed was spiro-cyclopentyl **207i**. This was isolated as a mixture of both the *trans, trans* and *cis, trans* diastereoisomers (3.8:1, respectively). The stereochemistry of the exocyclic methyl group adjacent to the CF₂ unit and the stereochemical outcome of the reduction can be explained by the presence of the axial CH₂ substituent at the C-3 position on the ring.

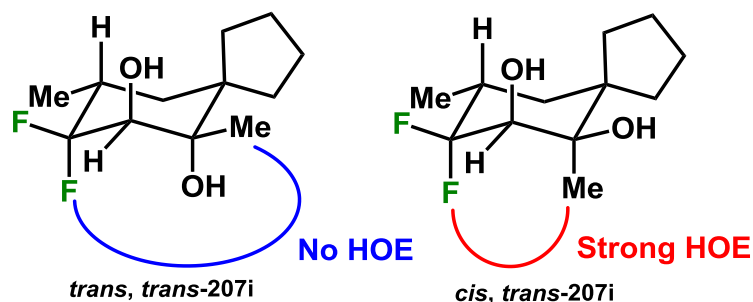


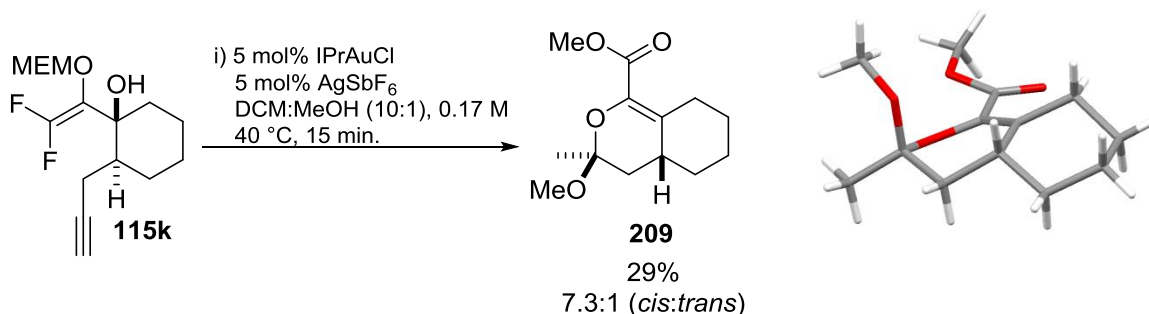
Figure 95: Spiro-cyclopentyl diastereoisomers obtained.

However, the methyl group at the C2 position is found to adopt both the equatorial and axial position. This was confirmed by a [¹H, ¹⁹F] HOESY experiment where an HOE correlation was absent for the *trans, trans* species and present for the *cis, trans* (**Figure 95**).

Unfortunately, the reaction did not tolerate internal alkenes and a complex mixture was returned for the attempted cyclisation of allyl alcohol **115j**. This may be attributed partly to steric effects with the addition of an extra methyl group rendering the olefin too bulky to act as an effective ligand and, therefore, inhibiting catalysis.

The attempted cyclisation of terminal alkyne **115k** initially provided a confusing result. The starting material was fully consumed after fifteen minutes and the ¹⁹F NMR spectrum of the crude reaction mixture revealed no fluorine containing signals. TLC analysis of the crude reaction mixture revealed a number of spots; however, the major spot was significantly less polar than the starting material. This non-polar species was isolated following purification by flash column chromatography. Unfortunately, despite obtaining good quality NMR data and accurate mass analysis, it was not possible to

determine the structure of this unknown species. Fortunately, upon leaving the mixture at 0 °C for one year the material solidified and a crystal was grown by slow evaporation from chloroform/pentane under reduced pressure. X-ray crystallography revealed the structure to be the bicyclic ester derivative **209** (Scheme 95).



Scheme 95: Cyclisation of **115k**.

After re-examining the NMR data, it was clear that the species existed as a mixture of diastereoisomers, a doubling up of signals present in the ¹³C NMR spectrum. The second diastereoisomer in the mixture was *trans*-**209** (Figure 96). The stereochemistry of this was deduced from the ¹H NMR spectrum with the exocyclic methoxy group having a significantly different chemical shift for each individual diastereoisomer.

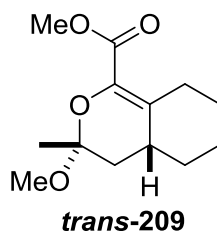
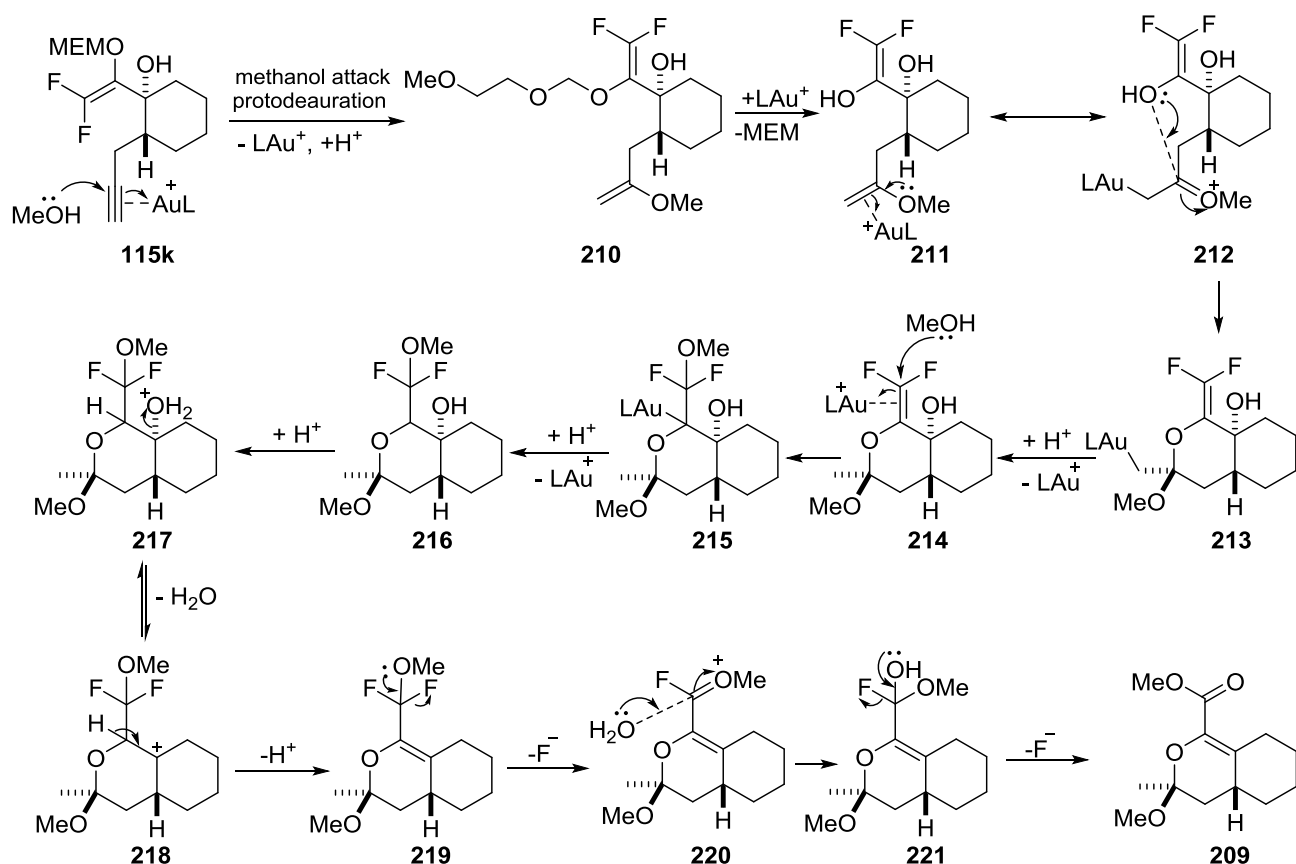


Figure 96: Second diastereoisomer present.

The presence of this exocyclic methoxy group indicates that the alkyne has initially reacted with methanol present in the reaction media. Unlike alkenes, alkynes are known to readily react with methanol under gold(I) catalysis.^{258,259} However, following this initial attack a number of steps must follow to afford the final product and a mechanism is proposed in **Scheme 96**.

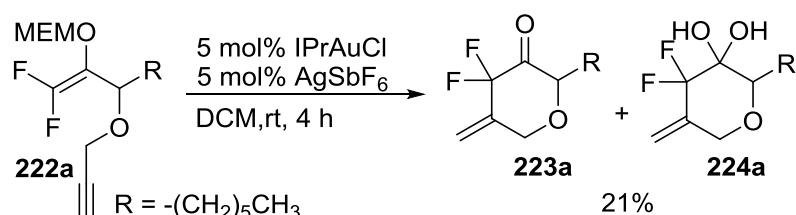


Scheme 96: Proposed mechanism for formation of **209**.

Initial coordination of cationic gold to the terminal alkyne followed by nucleophilic attack of methanol and protodeauration generates enol ether **210**. Loss of the MEM group would afford difluoroenol intermediate **211** which could then re-coordinate with cationic gold. A resonance contributor for this species could be a β -aurylated oxocarbenium ion **212** which may be sufficiently long lived to serve as an electrophile for the subsequent cyclisation. Nucleophilic attack *via* the oxygen of the enol would afford pyran **213**, which could undergo protodeauration to regenerate cationic gold and deliver **214**. Difluorinated olefin **214** could then be activated and undergo nucleophilic attack by a second molecule of methanol followed by protodeauration to afford **216**. Protonation of this species followed by loss of water would generate stabilised tertiary carbocation **218**. This species could then lose a proton to afford dihydropyran **219**. The final mechanistic steps involve the elimination of the two fluorine atoms. The first fluorine is eliminated during the formation of oxocarbenium **220**, the development of conjugation being a driving force for this transformation. This species could then be attacked by water to afford monofluorinated product **221** which undergoes a second fluorine elimination to afford the final non-fluorinated product **209**.

Although the formation of this particular product is surprising, the result itself was encouraging as it shows that the gold coordinated alkyne is sufficiently electrophilic to

methanol, the previously established cyclisation conditions were employed in the absence of this solvent (**Scheme 99**).

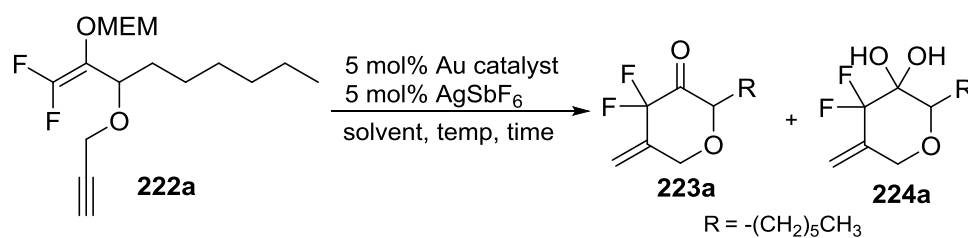


Scheme 99: Initial alkyne cyclisation attempt.

The alkyne was added as a solution in dichloromethane (DCM) to a stirring solution of the gold and silver catalyst in dichloromethane; however, following addition, the mixture darkened instantaneously.

In spite of this, it was possible to isolate the cyclised product as a mixture of both the ketone and corresponding hydrate in an overall yield of 21% (yield based on hydrate component of the mixture). The yield was low in the first instance; however, this was an extremely encouraging preliminary result (the reaction could also be performed at room temperature, an attractive feature from a synthetic perspective). As with the cyclic α , α -difluoroketones synthesised from the Saegusa-Ito series these cyclic pyrans were also susceptible to ketone hydration. Unfortunately, it was not possible to isolate a single molecular species. Attempts to isolate pure ketones by implementing the oven drying procedure resulted in product decomposition and azeotropic mixtures with toluene were also unsuccessful. Therefore, it was only possible to isolate mixtures of ketone and hydrate, and added an extra degree of complexity to the characterisation data collected. However, it was often possible to recrystallise pure hydrate samples. In most instances comparison of the NMR spectra obtained for pure hydrates together with the NMR spectra of mixtures allowed for proton signals to be confidently assigned.

Further optimisation of the reaction primarily focussed on screening solvents for the reaction (**Table 19**).

Table 19: Optimisation of alkyne cyclisation.

Entry	Au catalyst	Temp (°C)	Solvent	Time (h)	Isolated Yield (%) ^a
1	IPrAuCl	rt	DCM	4	21
2	IPrAuCl	rt	Toluene	5	61
3	IPrAuCl	rt	THF	3	0 ^b
4	IPrAuCl	rt	2-MeTHF	21	65
5	IPrAuCl	rt	CPME	5	61
6	IPrAuCl	40	2-MeTHF	2	49
7	Ph ₃ PAuCl	rt	2-MeTHF	24	54

^a Yield calculated based on hydrate. ^b Polymerisation observed.

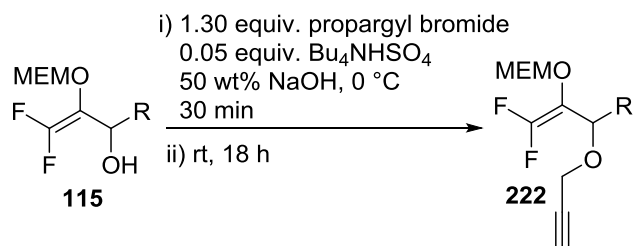
Upon switching to toluene the reaction was complete after 5 hours, and a significant increase in yield was observed (**Table 19, Entry 2**). Once again, the reaction mixture darkened following the addition of the alkyne solution; however, the colour change was not instantaneous and occurred over the course of 2 hours. Whilst toluene appeared suitable for this particular substrate we found it to be incompatible with others and instead formed complex mixtures. As the objective was to identify a generic solvent which was not just substrate specific we decided to continue with further solvent screening. Initially, the reaction performed in tetrahydrofuran (THF) appeared promising. Darkening of the reaction mixture was not observed; however, after 3 hours the mixture had completely polymerised. THF is known to undergo polymerisation in the presence of catalytic quantities of metal halide salts, therefore the AgSbF₆ used in the reaction is likely to be the trigger for this process.²⁶¹ This unwanted polymerisation could be avoided by switching to 2-methyltetrahydrofuran (2-MeTHF). After stirring at room temperature for 21 hours the product was isolated in slightly increased yield (**Table 19, Entry 4**).

Unlike the reactions in DCM and toluene the reaction mixture turned silver over the course of 8 hours. However, after 21 hours the reaction turned dark brown. It appears as though this colour change is harbinger of reaction completion. Pleasingly, this solvent was not substrate specific and was compatible with other cyclisations. The ability to conduct the reaction in this inexpensive, sustainable solvent is an attractive feature of the methodology.²⁶² Using cyclopentyl methyl ether (CPME) as an alternative ethereal

solvent gave similar results to those obtained in toluene (**Table 19, Entry 5**) and also proved ineffective with other substrates screened. Following this screen we decided to use 2-MeTHF as the solvent of choice for moving forward with the investigation. Increasing the reaction temperature significantly decreased the reaction time; however, this was accompanied by a lower product yield. Ph_3PAuCl could also be used as a catalyst for the reaction; however, the best results were achieved by using IPrAuCl . Taking into consideration the complexity of the products and the mild reaction conditions employed, the maximum yield of 65% was considered acceptable and these conditions were used to explore the scope of the reaction

4.2.7 Difluorinated Pyran Substrate Scope

A small palette of allylic alcohols and alkyne substrates were synthesised using the dehydrofluorination/lithiation and propargylation procedures, respectively, described above (**Table 20**).

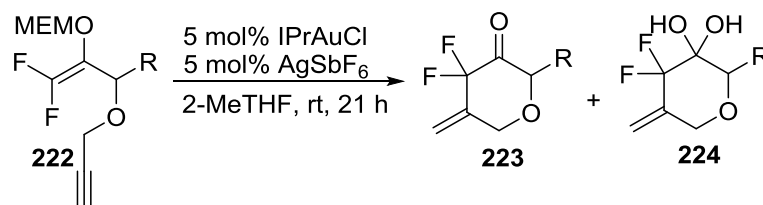
Table 20 – Alkynes Synthesised to Probe the Cyclisation.

Allyl Alcohol	Alkyne	Isolated Yield (%)
 115l	 222a	71
 115m	 222b	68
 115n	 222c	88
 115o	 222d	79
 115p	 222e	74
 115q	 222f	88

Overall the alkynes were isolated in good to excellent yields and included carbocyclic and heterocyclic analogues **222b** and **222c** respectively. Electron neutral **222d**, electron withdrawing **222e** and electron donating **222f** aromatic substrates were also produced. These analogues were especially interesting because between both the Saegusa-Ito and

gold(I) diol methodology, it had not yet been possible to prepare any compounds which contained aromatic systems. The alkynes were then exposed to the cyclisation conditions previously established (**Table 21**).

Table 21 – Scope of Alkyne Cyclisation.



Entry	Alkyne	Product	Isolated Yield ^a	Ketone:Hydrate ^b
1	222a	 224a	65 ^c	1:1
2	222b	 223b	63	7.3:1
3	222c	 224c	62	0:1
4	222d	 224d	52	1:3.8
5	222e	 224e	52	1:6.1
6	222f	 224f	0	-

^a Yield is based upon major component. ^bRatio determined by ¹⁹F NMR spectroscopy; for mixtures the major component is shown. ^cYield based on hydrate.

Carbocyclic analogue **223b** was isolated in comparable yield to the model substrate and, in this case, the ketone existed as the major component in the mixture. In contrast heterocycle **224c** was isolated exclusively as the hydrate. This material was recrystallized by vapour diffusion using tetrahydrofuran/pentane and its structure confirmed by single crystal X-ray diffraction (**Figure 97**).

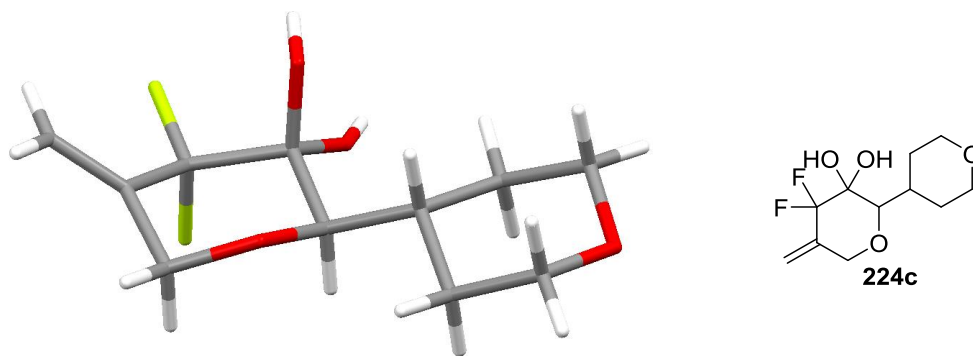


Figure 97: Structure of **224c** in the crystal.

There are a number of characteristics associated with this entity which make it an attractive fragment for drug design. Firstly, the compound is rich in sp^3 character. Lovering *et al.* have found that there is a direct correlation between fraction sp^3 (F_{sp^3}) character in a molecule and clinical success.²⁶³ Their studies showed that those species which contained a higher degree of saturation were more likely to survive the drug discovery process and less likely to fail during clinical trials. The three dimensional nature of compounds containing significant F_{sp^3} character is also thought to improve overall selectivity. Secondly, the molecule contains a variety of hydrogen bond donors and acceptors. The four oxygen atoms exist as strong hydrogen bond acceptors and, although weaker, the two fluorine atoms may also provide some degree of hydrogen bond accepting ability. The two hydroxyl groups will also act as hydrogen bond donors. Importantly, the total number of hydrogen bond donors and acceptors are acceptable and fall within the limits set by Lipinski's rules.⁴⁹ Finally, the alkene functionality also provides a useful site for further functionalisation.

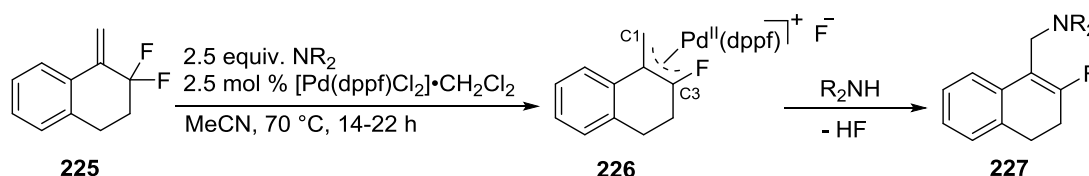
It was also pleasing to note that the reaction tolerated aromatic substituents. Phenyl analogue **224d** and electron withdrawing (trifluoromethyl) phenyl **224e** were isolated in good yield. These were the first examples of a difluorinated cyclic molecule bearing an aromatic substituent that we had managed to synthesise. Unfortunately, it was not possible to isolate electron donating analogue **224f**. The starting material had been consumed fully during the reaction; however, the ^{19}F NMR spectrum of the crude reaction mixture was complex. The desired product could be detected; however, purification proved to be challenging and although a small quantity of **224f** was isolated, it was not of acceptable purity. Overall, this phase of the study showed that the compounds could be synthesised effectively, and demonstrated the good overall scope generating a library of complex fluorinated compounds.

The ability to access further novel compounds would of course be an extremely attractive synthetic feature. The presence of the exocyclic alkene motif within the pyran

scaffold offers a potential vector for further functionalisation. S_N2' allylic aminations have previously been performed on allylic difluoride substrates and it was hypothesised that the pyran templates offered a unique opportunity to achieve such a transformation.

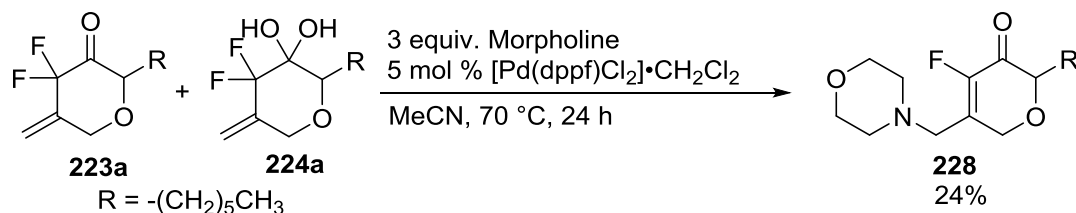
4.2.8 Allylic Amination

The presence of the allylic difluoride group in the system may present the opportunity for functionalisation through C-F activation. The C-F bond is one of the strongest bonds in organic chemistry; however, it has been shown that allylic fluorides can undergo oxidative addition with palladium(0) to form η^3 -allylpalladium(II) compounds.²⁶⁴ This feature has since been utilised by Gouverneur *et al.* in the palladium catalysed nucleophilic substitution of allylic monofluorides.²⁶⁵ When two fluorine atoms are present on the same carbon atom the strength of the C-F bond increases by 10-15 kcal/mol, making oxidative addition more difficult. However, Paquin *et al.* have shown that 3,3-difluoropropenes **225** can undergo a palladium catalysed S_N2' allylic amination to form β -aminofluoroalkenes **227** (Scheme 100).²⁶⁶



Scheme 100: S_N2' amination of allylic difluorides.

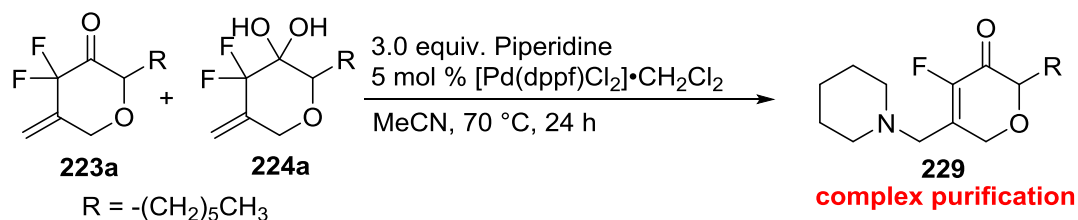
The reaction is thought to proceed *via* oxidative addition to generate the palladium π -allyl complex **226** followed by nucleophilic attack of the amine on C1 to afford amine **227**. Using similar conditions the reaction on difluorinated pyran system **223a/224a** was examined (Scheme 101).



Scheme 101: S_N2' allylic amination of **223a/224a**.

A mixture of hydrate and ketone **223a/224a** was exposed to the reaction conditions using a slightly elevated catalyst loading and increased equivalents of amine. After 24 hours the starting material had been consumed fully. The ^{19}F NMR spectrum was dominated by a singlet at -141.1 ppm, characteristic of an olefinic C-F system.²⁶⁷ Although the crude mixture looked relatively clean by ^{19}F NMR the material had to be purified twice

by flash column chromatography. Pleasingly, it was possible to isolate morpholine derivative **228** albeit in lower yield. The reaction was repeated a number of times; however, multiple purifications were required in each case and consequently 24% was the highest yield which could be obtained. Interestingly, although the reaction was performed using a mixture of ketone and hydrate full conversion of the starting material was observed and amine **228** was isolated as a single species. This suggests that the ketone/hydrate mixture equilibrates in solution to form the ketone which then reacts to deliver the product enone, the development of conjugation being a driving force for the reaction. Monofluoroalkenes have found widespread use in medicinal chemistry so the ability to access such functionality from our difluorinated systems is extremely advantageous.²⁶⁸ The reaction was also attempted with piperidine to synthesise amine derivative **229** (Scheme 102).



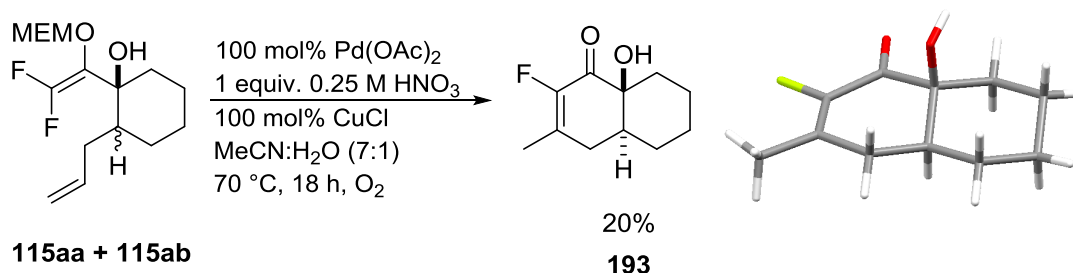
Scheme 102: Attempt to synthesise **229**.

Again, the ¹⁹F NMR spectrum of the crude reaction mixture was dominated by a single peak thought likely to correspond to piperidine adduct **229**. Unfortunately, it was not possible to isolate **229** in sufficient purity even after multiple attempts at column chromatography. Nonetheless, the result from the morpholine experiment demonstrates an important proof of concept in that the pyran systems could potentially serve as useful synthetic building blocks.

In summary, this chapter of the thesis has described two methodologies allowing for the concise synthesis of either difluorinated diol or difluorinated pyran scaffolds (three steps and four steps, respectively from trifluoroethanol, an inexpensive commercial feedstock). Both methods utilise difluorinated enol acetals for the first time as atom efficient carbon nucleophiles. Together with the Saegusa-Ito cyclisation the three methods represent a significant expansion to the field of fluorinated small molecule synthesis.

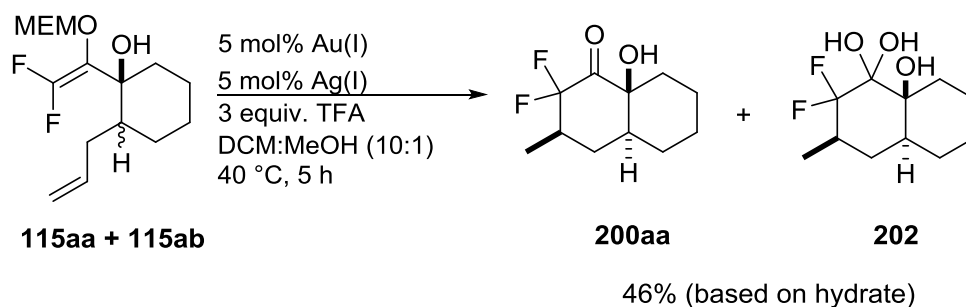
4.3 Conclusions

This chapter has highlighted the progress made in the efforts towards developing more atom efficient cyclisations based on difluorinated enols. Attempts to translate the previously established oxidative palladium(II)-catalysed Saegusa-Ito methodology to enol acetal substrates was unsuccessful and the only product that could be isolated from these reactions was monofluorinated enone **193** (Scheme 103).



Scheme 103: Monofluorinated product formed from palladium(II) chemistry.

Cyclisations could be achieved by utilising a cationic gold(I) cyclisation mediator, generated from NHC-gold(I) complex [(IPr)AuCl] (IPr = 1,3-bis(2,6-diisopropylphenyl)imidazole-2-ylidene) and chloride abstractor AgSbF₆. The annelation of **115aa/ab** proceeded under mild conditions and it was possible to isolate a mixture of ketone **200aa** and the corresponding hydrate **202** (Scheme 104).



Scheme 104: Cyclisation of **115aa/115ab**.

Unfortunately, it proved difficult to isolate a single molecular entity and attempts to dry the material in a vacuum oven (1 mbar, 40 °C) led to product decomposition. Reproducibility issues were also encountered and the presence of tricyclic acetal **203** in crude reaction mixtures was also detected (Figure 98).



Figure 98: Tricyclic acetal **203** formed from cyclisation reactions.

The formation of this product could be suppressed by reducing the ketone *in situ* to afford difluorinated diol **207aa**. Surprisingly, the cyclisation could be performed in the absence of TFA, a result which strongly suggests that the reaction proceeds through an enol acetal nucleophile rather than the difluoroenol (**Figure 99**).

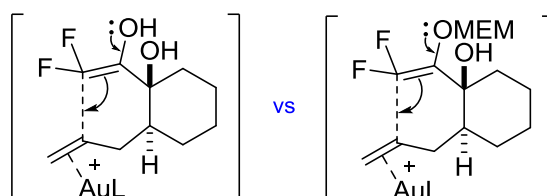


Figure 99: Hypothesised difluoroenol (left) and enol acetal (right) nucleophiles.

The method developed involves a gold(I)-catalysed one pot cyclisation/reduction under mild, acid free, conditions and low catalyst loadings, delivering difluorinated diols in good yields and moderate diastereoselectivities. The cyclisation also boasts a number of significant advantages, such as, improved atom economy, ambient temperatures, and the requirement of fewer protecting groups. The diols synthesised include examples of spirocyclic, heterocyclic and monocyclic compounds (**Figure 100**).

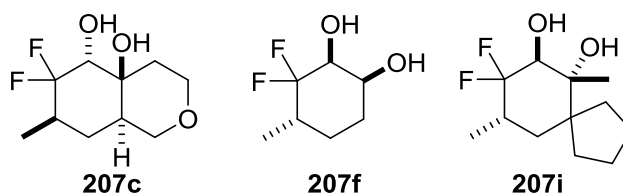


Figure 100: Diols synthesised using one pot cyclisation/reduction method.

The reaction was found not to tolerate internal alkenes and an unusual non-fluorinated pyran was formed when an alkyne was subjected to the reaction conditions (**Figure 101**).

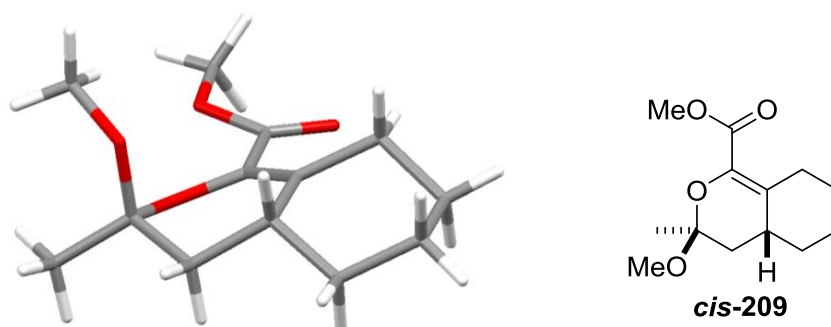


Figure 101: Pyran formed from attempted alkyne cyclisation.

Using similar catalytic conditions alkyne substrates were successfully cyclised to construct difluorinated pyran scaffolds. The alkynes could be cyclised at room temperature in 2-methyltetrahydrofuran to afford products rich in functionality and sp^3 character and are difficult to access by other methods. However, the pyrans were often isolated as mixtures of both ketone and hydrate, and it proved difficult to establish a method whereby a single species could be isolated. The reaction tolerated alicyclic, carbocyclic and heterocyclic substituents, and it was also possible to synthesise compounds containing aromatic substituents (**Figure 102**).

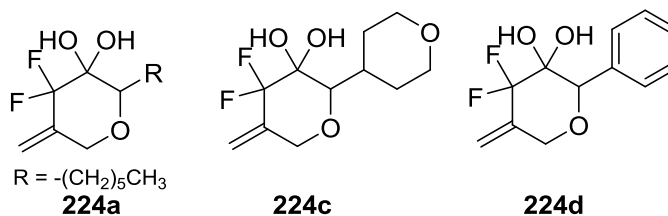
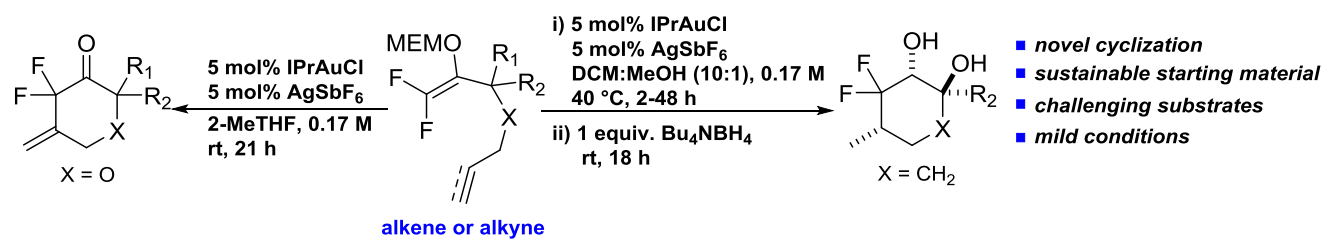


Figure 102: Pyrans synthesised from alkyne cyclisation.

The S_N2' allylic amination was also successful and delivered monofluorinated morpholine derivative **228**. Removal of the α,α -difluoro group also meant that the product could be isolated as a single species, greatly simplifying characterisation. There is also the potential for further derivatisation of this species with the α , β -unsaturated carbonyl functionality providing a potentially useful synthetic handle.

Overall, this chapter has clearly demonstrated the synthetic utility of difluorinated enol acetals and a divergent synthetic strategy has been created which allows for the construction of complex fluorinated fragments (**Scheme 105**).



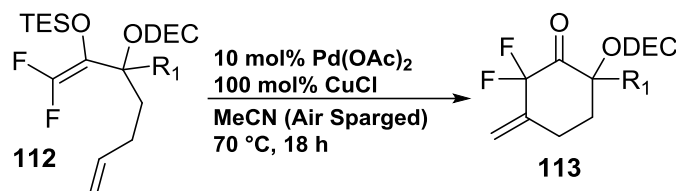
Scheme 105: Divergent synthesis of difluorinated pyrans and diols.

4.4. Overall Conclusions and Future Work

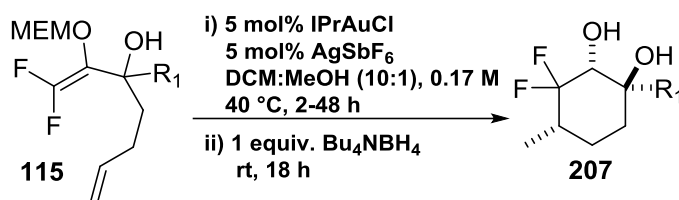
4.4.1 Conclusions

The work described in this thesis has highlighted the development of three methods for the synthesis of selectively difluorinated cyclic molecules which bear close resemblance to fluorinated sugar analogues (**Scheme 106**).

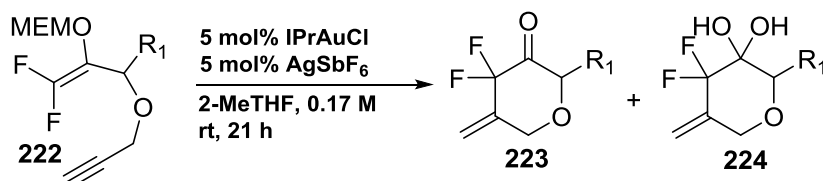
Saegusa Ito:



One-pot alkene cyclisation reduction:



Alkyne cyclisation:



Scheme 106: Cyclisations developed.

The Saegusa-Ito cyclisation allowed for the concise synthesis of difluorinated cyclohexenones **113**. The silyl enol ether precursors **112** were prepared in good yield from trifluoroethanol derivative **111** by utilising a transacylation protocol followed by trapping of the *in situ* generated enolate with chlorotriethylsilane. A combination of palladium(II) acetate and copper(I) chloride proved the most effective redox system for the cyclisation. Both annulations and annelations were performed and lower catalyst loadings (5 mol % Pd(OAc)₂) could be employed for annelative processes. Following effective sequestration of the metal contaminants using scavenger silica (SPM32 or STA3) the cyclic difluoroketones **113** were isolated in good yield by simply triturating crude reaction mixtures with pentane. The ketones often crystallised as the hydrate; however, rigorous oven drying allowed for the isolation of difluoroketones as single species. The least substituted system underwent cyclisation followed by fluorine

elimination and oxidation to afford a Wacker product with reversed regiochemistry **150** (Figure 103).

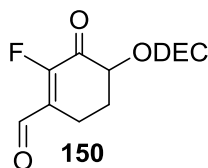


Figure 103: Monofluorinated product isolated from Saegusa-Ito investigation.

The synthesis of sulfide analogue **113i** was unsuccessful, presumably due to the coordinating ability of sulfur with palladium. Instead, preparation of the sulfone analogue prevented catalyst inhibition enabling access to bicyclic sulfone **113j** (Figure 104).

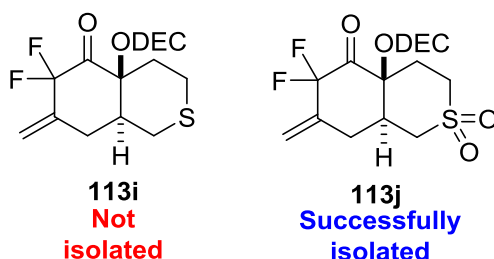


Figure 104: Sulphur based analogues.

In an effort to establish a more atom efficient cyclisation method the cyclisation of difluorinated enol acetals **115** was investigated. Difluoroallylic alcohols **115** were synthesised from trifluoroethanol derivative **114**. Purification of these precursors by Kugelrohr distillation was critical in order for a successful cyclisation to be achieved. The oxidative palladium(II) chemistry developed for the Saegusa-Ito cyclisation could not be translated across to difluorinated enol acetals. A cyclisation was achieved by using stoichiometric quantities of palladium(II) acetate; however, the product isolated was monofluorinated enone **193**. Switching the transition metal catalyst to gold(I) greater led to greater success. A combination of 1,3-*bis*(2,6-diisopropylphenyl-imidazol-2-ylidene)gold(I) chloride (IPrAuCl) and silver hexafluoroantimonate (AgSbF₆) ensured a successful cyclisation and the difluoroketone was isolated as a mixture of ketone **200aa** and hydrate **202** (Figure 105).

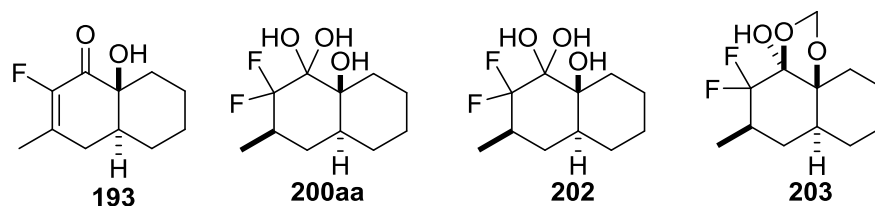


Figure 105: Products isolated from initial enol acetal cyclisation studies.

Oven drying of the mixture resulted in product decomposition and mixtures of diastereoisomers of ketone and hydrate presented complex data sets. Furthermore, tricyclic acetal **203** was a common side product of the reaction and it was not possible to inhibit its formation. To overcome this issue, the ketone functionality was reduced *in situ* to afford difluorinated diols **207** in a one pot cyclisation reduction method. The reaction could be performed under mild acid free conditions providing strong evidence for an enol acetal nucleophile operating within the system. A range of diol fragments were synthesised in moderate to good yields and diastereoselectivities. The stereochemistry of diol structures were revealed through a combination of X-ray crystallography, NMR and 2D [^1H , ^{19}F]-HOESY analysis. The presence of axial substituents on the ring and the α -hydroxy functionality also appear to provide some level of stereocontrol. The cyclisation did not tolerate internal alkenes and cyclisation of a terminal alkyne led to the formation of an unusual non-fluorinated pyran **209** (**Figure 106**).

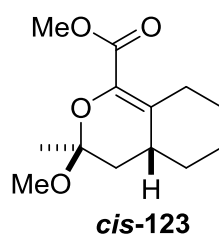


Figure 106: Non-fluorinated pyran isolated from alkyne cyclisation.

Slight modification of the synthetic route enabled access to structurally complex difluorinated pyran templates. Alkyne substrates were cyclised at room temperature in 2-Methyltetrahydrofuran, an inexpensive sustainable solvent. In each case, the pyrans were isolated as mixtures of ketone and hydrate **223/224**. Attempts to oven dry these mixtures led to product decomposition. The reaction tolerated electron withdrawing aromatic substituents; however, electron donating groups led to the formation of complex mixtures.

Finally, the synthetic applicability of difluorinated pyrans was demonstrated. Pyran **223a/224a** was further functionalised by using an $\text{S}_{\text{N}}2'$ allylic amination procedure, allowing for the synthesis of monofluorinated morpholine derivative **228** (**Figure 107**).

Overall, this result demonstrates a valuable proof of concept whereby difluorinated pyran templates could potentially serve as useful synthetic building blocks.

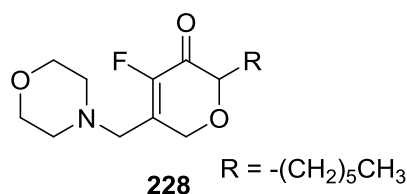


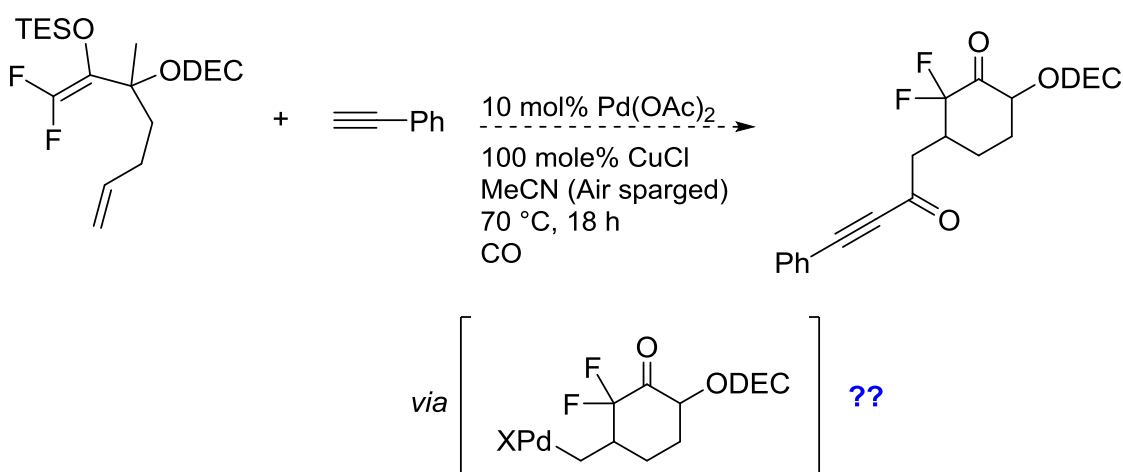
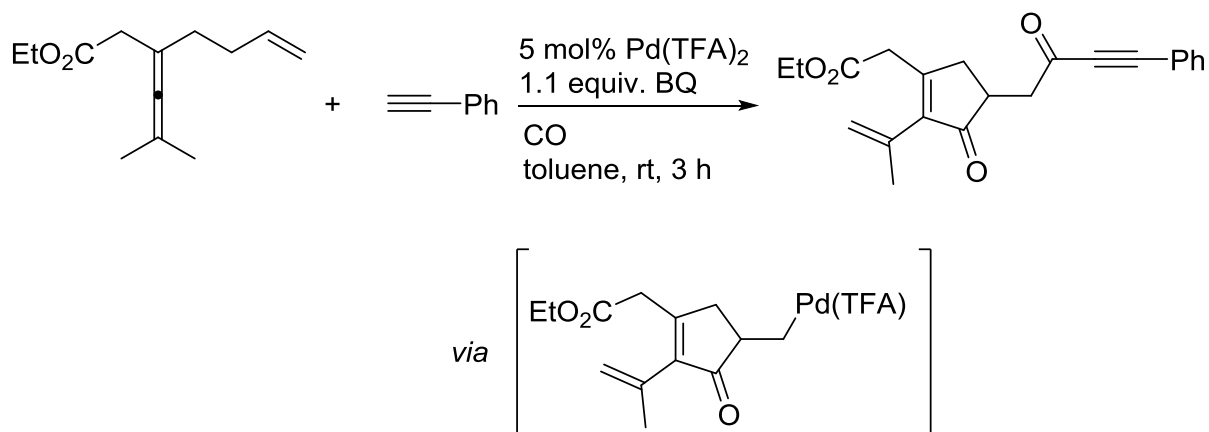
Figure 107: Product of pyran functionalisation isolated.

4.4.2 Future Work

The results of these investigations have opened up a number of different avenues for further work. The nature of the catalytically active species in the Saegusa-Ito cyclisation is currently unknown. The results from the screening experiments suggest that a bimetallic Pd/Cu species could be playing an important role in the redox system. Moreover, there is precedent for Pd/Cu bimetallic species to act as catalysts in the oxidation of alkenes.¹⁸⁸ UV-visible spectroscopic studies could be conducted to gain insight into the nature of the catalytic species present in the reaction. Monitoring the optical absorption of Cu(I) and Cu(II) species over the course of the reaction would enable quantitation of their concentrations. The d^9 configuration of Cu(II) could also be utilised for monitoring the reaction by EPR analysis and could provide a useful tool for further mechanistic studies.¹⁹¹

Explaining the formation of enal **150** from the cyclisations of **113b** is not trivial and it appears that a classic Wacker mechanism is not in operation. Repeating the reaction in the presence of a radical scavenger (TEMPO) could confirm whether or not enal **150** is formed as a result of a radical mechanism.

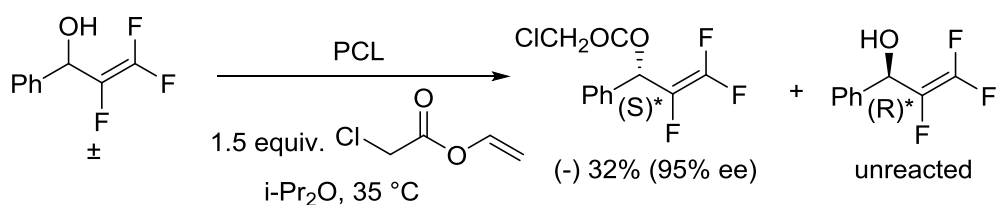
It would also be interesting to determine whether the Saegusa methodology could be further expanded. Recently, Bäckvall *et al.* have reported the *in situ* carbocyclisation/carbonylation of enallenes to form heavily functionalised cyclopentenones (**Scheme 107**).²⁶⁹



Scheme 107: Potential expansion of Saegusa methodology.

If a similar Pd intermediate was also present under the cycloalkenylation reaction conditions then this carbonylation/coupling procedure could potentially provide access to fluorinated molecules with an even greater degree of functionality.

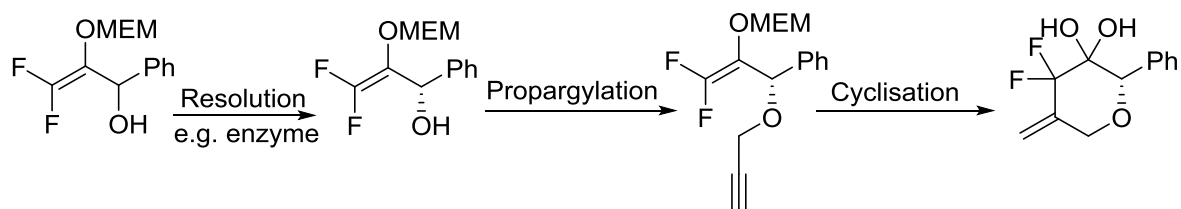
In relation to the gold(I) methodology, it would be interesting to investigate whether an asymmetric synthetic route would be possible. The resolution of difluoroallylic alcohols has previously been demonstrated by Takagi *et al* (**Scheme 108**).²⁷⁰



PCL = Pseudomonas cepacea lipase

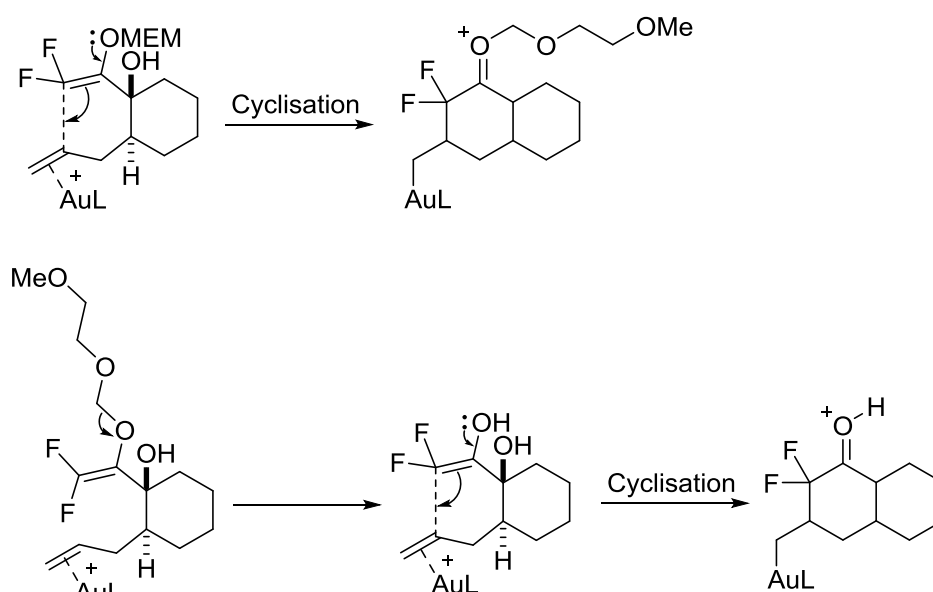
Scheme 108: Chiral resolution of difluoroallylic alcohols.

Allylic alcohols were resolved through a lipase catalysed *trans*-esterification whereby the *S*-enantiomer of the racemic mixture reacted preferentially over the *R*-enantiomer. These species could then be separated and the *S*-allylic alcohol isolated after hydrolysis of the ester with LiOH. It would be best to test this asymmetric route on the alkyne cyclisation since the cyclised product contains only one stereocentre (**Scheme 108**).



Scheme 108: Potential enantioselective route to pyrans.

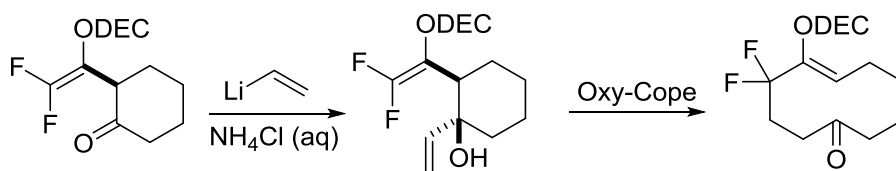
Monitoring of the reaction by NMR might also give further insight into the nature of the nucleophile in the gold(I) catalysed cyclisation. At low acid concentrations we have been able to detect the formation of difluoroenol **192** before tautomerisation to the ketone occurs. The difluoroenol intermediate contains two fluorine atoms attached to a sp^2 hybridised carbon, typically characterised by smaller $^2J_{F-F}$ values. If the reaction is proceeding through a difluoroenol intermediate this would be readily detected by ^{19}F NMR. However, if this species is not being formed then only direct formation of the cyclised product with two fluorine atoms attached to a sp^3 hybridised carbon should be observed, characterised by larger $^2J_{F-F}$ values (**Scheme 109**).



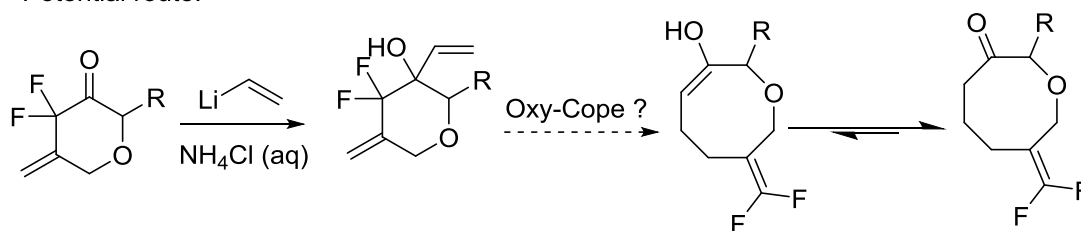
Scheme 109: Possible reaction through enol acetal (top) or enol (bottom).

Further functionalisation of the pyran scaffolds could also be investigated. An interesting reaction to conduct is the addition of vinyl lithium to the the carbonyl group of the pyran. Previous work within the group has successfully added this reagent to cyclic ketones to form oxy-Cope rearrangement precursors. These then successfully rearranged to form fluorinated cyclodecenones (**Scheme 110**).²⁷¹ Addition of vinyl lithium to our pyran scaffolds would afford products possessing a similar oxy-Cope pattern. If these rearranged it would allow access to larger 8 membered ring systems bearing an exocyclic gem difluormethylene group, although formation of this fluorinated sp^2 centre may prove thermodynamically challenging.²⁷²

Previous Work:



Potential route:



Scheme 110: Oxy-Cope reaction performed by Percy group (top) and potential route to larger ring systems (bottom).

6. Chapter 4: Experimental

All characterisation data spectra for all synthesised compounds and Cartesian coordinates are compiled as Supplementary Information and available on request.

6.1 General Experimental

NMR spectra were recorded on Bruker DPX-400, AV-500 and Avance-II+ 600 spectrometers. ^1H , ^{19}F and ^{13}C NMR spectra were recorded using the deuterated solvent as the lock and the residual solvent as the internal reference. The multiplicities of the spectroscopic data are presented in the following manner: s = singlet, d = doublet, dd = double doublet, dt = doublet of triplets, dq = doublet of quartets, dqint = doublet of quintets, ds = doublet of sextets, qd = quartet of doublets, qt = quartet of triplets, ddt = doublet of double triplets, ddd = doublet of doublet of doublets, dddd = doublet of double doublet of doublets, dddt = doublet of double doublet of triplets, dddq = doublet of double doublet of quartets, tdd = triplet of doublet of doublets, td = triplet of doublets, ts = triplet of septets, tt = triplet of triplets t = triplet, q = quartet, m = multiplet and br. = broad. Unless stated otherwise, all couplings refer to 3J homocouplings. IR spectra were recorded on an ATR IR spectrometer, the samples were loaded directly onto a diamond anvil cell either as a neat oil or solid. UV/Vis Spectra were recorded on a Varian Cary[®] 50 UV-Vis Spectrophotometer using Quartz UV cuvettes (1.2 cm diameter) in MeCN. Melting points were recorded on a Griffin melting point apparatus and are uncorrected. GC/MS spectra were obtained on an instrument fitted with a DB5-type column (30 m \times 0.25 μm) running a 40–320 $^\circ\text{C}$ temperature program, ramp rate 20 $^\circ\text{C min}^{-1}$ with helium carrier gas flow at 1 $\text{cm}^3 \text{min}^{-1}$. Chemical ionisation (CI) (methane/ammonia) and Electron Ionisation (EI) mass spectra were recorded on either an Agilent Technologies 5975C mass spectrometer or a FINNIGAN MAT 95 high resolution double focussing (BE) mass spectrometer (EPSRC National Mass Spectrometry Service Centre, Swansea). HRMS measurements were obtained from a Waters GCT Premier MS (CI), Finnigan Mat 95 XP (EI-MS and/or APCI-MS), Thermo Scientific LTQ Orbitrap XL via Advion TriVersa NanoMate infusion (ESI) or Waters Xevo G2-S Atmospheric Solids Analysis Probe (APCI, Positive mode, Xevo) spectrometers (EPSRC National Mass Spectrometry Service Centre, Swansea). Thin layer chromatography was performed on pre-coated aluminium-backed silica gel plates (E. Merck AG, Darmstadt, Germany. Silica gel 60 F254, thickness 0.2 mm). Visualisation was achieved using potassium permanganate dip or UV detection at 254 nm. Column chromatography was performed on silica gel (Zeochem, Zeoprep 60 HYD, 40–63 μm) using a Büchi Sepacore system. Hexane was

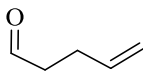
distilled before chromatography. Carbon, Hydrogen and Nitrogen analysis was carried out on a Perkin Elmer 2400 Series II CHNS Analyser (data acquired by Alexander J. Clunie). Metal salts (palladium(II) acetate (reagent grade, 98%), copper(I) chloride (ReagentPlus®, ≥99%), copper(II) chloride (97%), copper(I) acetate (97%), copper(II) acetate (98%), palladium(II) chloride (≥ 99.9%)) were purchased from Sigma Aldrich and used as received. [(IPr)AuCl] (IPr = 1,3-*bis*(2,6-diisopropylphenyl)imidazole-2-ylidene, 95%) and AgSbF₆ (98%) were purchased from Strem Chemicals and used as received. THF was dried using a PureSolv system from Innovative Technology, Inc.. Diisopropylamine was distilled from 4Å molecular sieves (30 °C/140 mbar) and stored under nitrogen over 4Å molecular sieves. All other chemicals were purchased from Sigma Aldrich, Alfa Aesar, or Fluorochem. All compounds were named according to the ChemDraw Professional 15.0 package and checked against Scifinder® chemical database. Metal scavenging silica 3-Mercaptopropyl ethyl sulfide Silica (SPM32; silica size: 60-200 microns; pore size: 60 Å; loading: 0.8 mmol/g) and triamine ethyl sulphide amide silica (STA3 silica size: 60-200 microns; pore size: 60Å; loading: 0.9 mmol/g) was purchased from PhosphonicS Ltd. CuCl₂ was dried by heating to 150 °C for 48 hours. DMF was distilled from CaH₂ (50 °C/18 mbar) and stored under nitrogen over CaH₂. Chlorotrimethylsilane was distilled from CaH₂ (60 °C/430 mbar) and stored under nitrogen over CaH₂ in the refrigerator.

Crystal data measurements were performed with Oxford Diffraction or Rigaku instruments. The datasets for **113h** and **224c** were collected by the NCS, University of Southampton and all other datasets were measured in-house at the University of Strathclyde. Structure solution was by direct methods with the SIR and SHELXS programs and refinement utilised SHELXL-97 (performed by Dr Alan Kennedy).^{273,274} All structures were refined to convergence against F₂ and used all independent reflections. Selected crystallographic and refinement parameters are given below. LDA and *n*-Butyllithium (2.5 M solution in hexanes) was titrated according to the method of Duhamel and Plaquevent.²⁷⁵

6.2 Compounds from Chapter 1

6.2.1 Preparation of electrophiles

Penten-1-al (**S1**)²⁷⁶

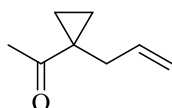


Allyl vinyl ether (5.6 g, 64 mmol) was added to a microwave vial and capped. The vial was placed in a Biotage Microwave and irradiated with stirring for six hours at 150 °C to afford penten-1-al (5.6 g). The material (**S1**) was used directly in the next reaction without further purification.

δ_{H} (400 MHz, CDCl_3): 9.81 (t, $J = 1.9$ Hz, 1H), 5.86 (dt, $J = 16.9, 10.3, 6.6$ Hz, 1H), 5.13-5.01 (m, 2H), 2.63-2.52 (m, 2H), 2.49-2.36 (m, 2H) ppm.

The data was consistent with that reported by Murphy.²⁷⁶

1-(1-Allylcyclopropyl)ethan-1-one (**S2**)²⁷⁷



The synthesis was based on the method described by Schmalz *et al.*²⁷⁷ Trimethylsulfoxonium iodide (15 g, 68 mmol) was taken up in DMSO (220 mL) with stirring and the flask was placed in a water bath at room temperature. Sodium hydride (2.7 g of a 60 % dispersion in mineral oil, 68 mmol) was added in one portion and the mixture was stirred until foaming ceased and all the solid had dissolved (1 hour). 3-methylene-5-hexen-2-one (7.5 g, 60 mmol) was added in a continuous stream and the yellow mixture was stirred overnight. The mixture was poured into water (1250 mL) and extracted with pentane (5 x 100 mL). The combined organic extracts were dried (MgSO_4), filtered and the solution was concentrated carefully at 770 mBar to *ca.* 15 mL (using a rotary evaporator with a DriKold trap). The colourless residue was distilled through a 20 x 1 cm Vigreux column under reduced pressure to afford ketone **S2** (3.19 g, 43 %) as a colourless liquid,

bp 43-45 °C / 6 mmHg.

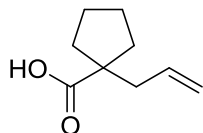
$R_f = 0.36$ (20 % diethyl ether in hexane);

^1H NMR (400 MHz, CDCl_3): δ 5.81 (ddt, $J = 16.3, 11.1, 6.3$ Hz, 1H), 5.09-5.00 (m, 2H), 2.39 (br. d, $J = 6.3$ Hz, 2H), 2.05 (s, 3H), 1.23, 1.22 (ABq, $J_{\text{AB}} = 3.7$ Hz, 2H), 0.81, 0.79 (ABq, $J_{\text{AB}} = 3.7$ Hz, 2H) ppm;

^{13}C NMR (100 MHz, CDCl_3): $\delta = 208.3, 133.5, 116.3, 37.3, 30.9, 25.4, 15.6$ ppm;

$\bar{\nu}$ /(neat) = 3078, 3007, 2909, 1686, 1418, 1362, 1140, 1003, 914 cm^{-1} ;
HRMS (EI-MS): calcd for $\text{C}_8\text{H}_{13}\text{O}$, 125.0961 $[\text{M}+\text{H}]^+$, found: 125.0960;
MS (CI): m/z (%): 125 (9) $[\text{M}+\text{H}]^+$, 83 (100) $[\text{M}-\text{C}_3\text{H}_5]$;
 t_{R} (GC) = 7.49 minutes.

1-(3-Propenyl)cyclopentanecarboxylic acid (**S3**)²⁷⁸



Carboxylic acid **S3** was prepared according to the method of Cameron and co-workers.²⁷⁸ A solution of cyclopentane carboxylic acid (10 g, 88 mmol) in THF (30 mL) was added dropwise over 30 minutes to a stirred solution of LDA (136 mL of a 1.35 M solution in THF/heptane/ethylbenzene, 184 mmol) in THF (228 mL) at 0 °C. After this time, the reaction mixture was heated to 60 °C over 30 minutes and left for a further 30 minutes at this temperature. The reaction was cooled to 0 °C then allyl bromide (7.6 mL, 88 mmol) was added dropwise over 20 minutes. The reaction was allowed to warm to room temperature and stirred for 18 h. Sodium hydroxide (300 mL of a 0.5 M aqueous solution) was added and the aqueous phase separated. The organic phase was extracted with sodium hydroxide (3 x 150 mL of a 0.5 M aqueous solution). The aqueous layer was washed with diethyl ether (150 mL), then acidified to pH 1 (indicator paper) with a minimum volume of concentrated HCl (ca. 75 mL). The product was extracted into dichloromethane (4 x 100 mL) and the organic extracts were combined, dried (MgSO_4) then concentrated under reduced pressure. The crude reaction mixture was purified by distillation to afford the desired product as a light yellow oil. (7.14 g, 53 %, 90 % purity by ^1H NMR and GC).

b.p. = 182 °C / 0.28 mmHg;

R_f = 0.2 (20 % diethyl ether in hexane);

^1H NMR (400 MHz, CDCl_3): δ = 11.76 (br. s, 1H), 5.78 (ddt, J = 16.9, 10.2, 7.0 Hz, 1H), 5.16-4.99 (m, 2H), 2.39 (dt, J = 7.0, 4J = 1.1 Hz, 2H), 2.19-2.02 (m, 2H), 1.72-1.44 (m, 6H) ppm;

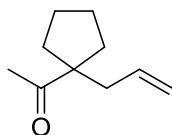
^{13}C NMR (100 MHz, CDCl_3): δ = 184.3, 134.6, 117.7, 53.4, 42.6, 35.6, 25.1 ppm;

$\bar{\nu}$ /(neat) = 3200-2800 (broad, s), 1693, 1405, 1232, 916 cm^{-1} ;

MS (CI): m/z (%): 155 (27) $[\text{M}+\text{H}]^+$, 137 (9) $[\text{M}-\text{OH}]$, 109 (100) $[\text{M}-\text{CO}_2\text{H}]$;

t_{R} (GC) = 10.19 minutes.

1-(1-Allylcyclopentyl)ethan-1-one (**S4**)²⁷⁹



Ketone (**S4**) was prepared according to the method of Kim and co workers.²⁷⁹ Methylolithium (81 mL of a 1.4 M solution in diethyl ether, 114 mmol) was added rapidly to a stirred solution of carboxylic acid **S3** (4.4 g, 28.5 mmol, 90% pure by ¹H NMR and GC) in THF (300 mL) at 0 °C. After 2 hours at 0 °C, freshly distilled chlorotrimethyl silane (122 mL, 0.96 mol) was added rapidly while stirring continued and a precipitate formed. The ice bath was removed and the reaction mixture was allowed to warm to room temperature before being left to stir for one hour further. Hydrochloric acid (200 mL of 1 N aqueous solution) was added and the resulting two phase system stirred at room temperature for thirty minutes. The mixture was transferred into a separating funnel and extracted with diethyl ether (4 x 200 mL). The combined organic extracts were washed with water (150 mL), dried (MgSO₄) and filtered. The bulk solvent was carefully removed under reduced pressure (40 °C, 150 mmHg) and the crude product was purified by distillation to afford **S4** as a colourless oil (3.06 g, 78 %).

b.p. = 44 °C / 2 mmHg;

R_f = 0.4 (10 % diethyl ether in hexane);

¹H NMR (400 MHz, CDCl₃): δ = 5.65 (ddt, *J* = 16.9, 10.2, 7.0 Hz, 1H), 5.11-4.99 (m, 2H), 2.39 (dt, *J* = 7.0, ⁴*J* = 1.3 Hz, 2H), 2.15 (s, 3H), 2.09-1.96 (m, 2H), 1.72-1.44 (m, 6H) ppm;

¹³C NMR (100 MHz, CDCl₃): δ = 211.9, 134.6, 117.4, 59.9, 42.6, 34.1, 25.8, 25.1 ppm;

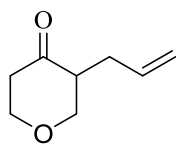
$\bar{\nu}$ /(neat) = 2954, 2872, 1703, 1441, 1357, 1141, 916 cm⁻¹;

HRMS (EI-MS): calcd for C₁₀H₁₆O, [M+H]⁺: 152.1201, found: 152.1205;

MS (CI): *m/z* (%): 181 (5) [M+C₂H₅]⁺, 153 (100) [M+H]⁺, 135 (33), 109 (20) [M-C₂H₃O];

t_R (GC) = 9.47 minutes.

2-Allyltetrahydropyranone (S5)²⁸⁰



Ketone **S5** was prepared according to the method of Bilodeau and co-workers.²⁸⁰ A mixture of allyl alcohol (0.71 g, 12.2 mmol), tetrahydropyran-4-one (3.69 g, 36.7 mmol), DL-proline (0.43 g, 3.67 mmol), Xantphos (0.355 g, 0.61 mmol) and (allylpalladium)chloride dimer (0.112 g, 0.30 mmol) in DMSO (50 mL) was degassed by two freeze-pump-thaw cycles (to 0.15 mmHg). The stirred dark orange mixture was heated to 70 °C overnight. The yellow suspension was cooled to room temperature and poured into water (400 mL). The mixture was extracted with diethyl ether (5 x 50 mL) and the combined organic extracts were washed with a mixture of brine and water (1:1, 100 mL) and dried (Mg₂SO₄). The solvent was removed under reduced pressure to afford the crude pyranone as a yellow oil (2.09 g). The crude product was purified by flash column chromatography (90 g cartridge, 12 % ethyl acetate in hexane) to afford pyranone **S5** as a mobile colourless oil (1.12 g, 22 % based on tetrahydropyranone).

R_f = 0.33 (15 % ethyl acetate in hexane);

¹H NMR (400 MHz, CDCl₃): δ 5.77 (dddd, J = 17.1, 10.4, 8.0, 6.2 Hz, 1H), 5.12-5.03 (m, 2H), 4.24-4.14 (m, 2H), 3.77 (ddd, ² J = 11.4, J = 10.5, 3.7 Hz, 1H), 3.45 (dd, ² J = 11.4, J = 9.1 Hz, 1H), 2.68-2.53 (m, 3H), 2.45 (dt, ² J = 14.7, 3.6 Hz, 1H), 2.10-1.99 (m, 1H) ppm;

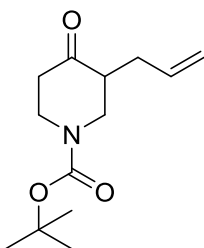
¹³C NMR (100 MHz, CDCl₃): δ = 207.2, 135.1, 116.7, 72.0, 68.4, 50.6, 42.3, 30.0 ppm;

$\bar{\nu}$ /(neat) = 2968, 2916, 2851, 1713, 1641, 1229, 1200, 1157, 1099, 974, 916 cm⁻¹;

MS (CI): m/z (%): 141 (95) [M+H]⁺;

t_R (GC) = 8.49 minutes.

***tert*-Butyl 3-allyl-4-oxopiperidine-1-carboxylate (S6)**



Ketone **S6** was prepared as for (pyranone **S5**) from allyl alcohol (0.226 mL, 3.32 mmol), 1-Boc-4-piperidone (2.00 g, 10.0 mmol), *DL*-proline (0.115 g, 1.00 mmol), Xantphos (0.096 g, 0.166 mmol) and (allylpalladium)chloride dimer (0.031 g, 0.083 mmol) in DMSO (20 mL). The mixture was degassed by two freeze-pump-thaw cycles (to 0.15 mmHg). The stirred dark orange mixture was heated to 70 °C overnight. The yellow suspension was cooled to room temperature and poured into water (100 mL). The mixture was extracted with diethyl ether (5 x 20 mL) and the combined organic extracts were washed with a mixture of brine and water (1:1, 50 mL) and dried (MgSO₄). The solvent was removed under reduced pressure to afford the crude piperidone as a pale orange oil (2.07 g). The crude product was purified by flash column chromatography (90 g cartridge, 20 % ethyl acetate in hexane) to afford **S6** as a clear mobile oil (0.97 g, 40 % based on Boc-piperidone).

R_f = 0.31 (20 % ethyl acetate in hexane);

¹H NMR (400 MHz, CDCl₃): δ = 5.72 (dddd, J = 17.2, 9.9, 7.4, 6.6 Hz, 1H), 5.15-4.89 (m, 2H), 4.42-3.79 (m, 2H), 3.51-3.14 (m, 1H), 3.14-2.69 (m, 1H), 2.63-2.19 (m, 4H), 2.13-1.82 (m, 1H), 1.44 (s, 9H) ppm;

¹³C NMR (100 MHz, CDCl₃): δ = 208.6, 154.4, 134.8, 117.4, 80.3, 49.5, 47.7, 43.6, 40.7, 31.3, 28.3 ppm;

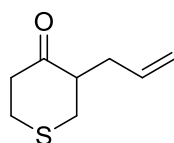
$\bar{\nu}$ /(neat) = 2974, 2930, 1692, 1416, 1366, 1238, 1162 cm⁻¹;

HRMS (NSI-ES): calcd for C₉H₁₄NO₃, 184.0968 [M+H]⁺, found: 184.0963;

MS (CI): m/z (%): 184 (79) [M-C₄H₉+2H]⁺, 140 (80) [M-C₅H₉O₂+2H]⁺, 57 (100) [C₄H₉];

t_R (GC) = 12.53 minutes.

2-Allyl tetrahydrothiopyranone (**S7**)²⁸¹



Ketone **S7** was prepared according to the method of Miftakhov and co-workers.²⁸¹ Tetrahydrothiopyranone (6.00 g, 52 mmol) in THF (20 mL) was added dropwise to a stirring solution of LDA (45.9 mL of a 1.47 M solution in THF/heptane/ethylbenzene) in THF (100 mL) at -78 °C over 15 minutes. The reaction mixture was warmed to -40 °C and stirred at this temperature for 60 minutes. The mixture was cooled to -78 °C before adding allyl bromide (5.7 mL, 67.6 mmol) dropwise over 10 minutes. The stirred pale yellow solution was allowed to warm slowly to ambient temperature (19 °C) overnight. The pale orange solution was quenched with ammonium chloride (200 mL of a saturated aqueous solution) and extracted with ethyl acetate (4 x 150mL). The organic extracts were combined, dried (MgSO₄) and concentrated under reduced pressure to afford the crude product as a dark orange oil (8.74 g). The crude product was purified by flash column chromatography (90 g, 10% diethyl ether in hexane) to afford **S7** as a mobile yellow oil (1.85 g, 23 %).

R_f = 0.35 (40 % diethyl ether in hexane);

¹H NMR (400 MHz, CDCl₃): δ = 5.70 (dddd, J = 17.2, 10.5, 7.8, 6.5 Hz, 1H), 5.14-4.94 (m, 2H), 3.07-2.81 (m, 3H), 2.79-2.46 (m, 5H), 2.19-2.03 (m, 1H) ppm;

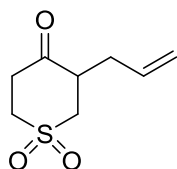
¹³C NMR (100 MHz, CDCl₃): δ = 209.4, 135.1, 117.3, 52.2, 43.9, 35.2, 33.6, 30.8 ppm;
 $\bar{\nu}$ /(neat) = 2904, 1705, 1422, 1273, 914 cm⁻¹;

MS (CI): m/z (%): 185 (17) [M+C₂H₅]⁺, 157 (90) [M+H]⁺;

t_R (GC) = 10.67 minutes.

The data was consistent with that reported by Seto and co-workers.²⁸²

2-Allyl tetrahydrothiopyranone dioxide (**S8**)²⁸³



Ketone **S8** was prepared according to the method of Miyazawa and co workers.²⁸³ A solution of sodium metaperiodate (11.58 g, 54 mmol) in water (72 mL) was added dropwise over 30 minutes to a stirring solution of allyl tetrahydrothiopyranone **157** (2.82 g, 18 mmol) in methanol (90 mL) at room temperature. The mixture was stirred

vigorously as a precipitate formed upon addition of periodate. Following addition the reaction mixture was heated to 60 °C for 18 hours. The reaction was cooled to room temperature and the methanol removed under reduced pressure. Chloroform (100 mL) was added to the residue and the mixture was stirred and filtered to remove sodium iodate. The solids were washed with chloroform (200 mL) and the combined organic extracts were dried (MgSO₄). Removal of the solvent under reduced pressure afforded an orange solid (3.09 g) which was crystallized from dichloromethane/hexane (0.977 g, 29 %) to afford the product as a white granular solid. The mother liquor was concentrated to afford an orange solid which was again crystallized from dichloromethane/hexane (0.339 g, 10 %). The liquor was evaporated to dryness and the remaining residue was purified by flash column chromatography (90 g cartridge, 25 % acetone/hexane) to afford the product as a white granular solid (0.597 g, 18 %). The ketone was dried in a vacuum oven (40 °C, 0.75 mmHg) for 1 week before being used in the next step of the reaction.

m.p. = 92-94 °C (dichloromethane/hexane);

R_f = 0.6 (40 % acetone in hexane);

¹H NMR (400 MHz, CDCl₃): δ = 5.65 (dddd, *J* =, 17.8, 10.8, 8.2, 6.9 Hz, 1H), 5.22-5.02 (m, 2H), 3.51-3.25 (m, 3H), 3.25-3.04 (m, 3H), 2.80 (dt, ²*J* = 15.0, *J* = 4.4 Hz, 1H), 2.67-2.52 (m, 1H), 2.24-2.10 (m, 1H) ppm;

¹³C NMR (100 MHz, CDCl₃): δ = 203.6, 133.3, 119.1, 54.2, 50.3, 46.2, 37.9, 32.6 ppm;

$\bar{\nu}$ /(neat) = 2995, 2943, 1712, 1288, 1122, 912, 852 cm⁻¹;

HRMS (CI): calcd for C₈H₁₆NO₃S, 206.0851 [M+NH₄]⁺, found: 206.0848;

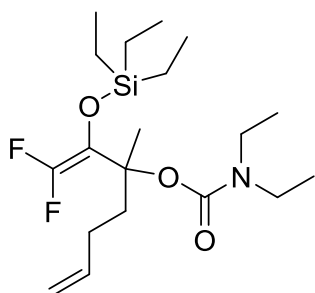
MS (CI): m/z (%): 217 (2) [M+C₂H₅]⁺, 189 (14) [M+H]⁺;

t_R (GC) = 12.62 minutes

elemental analysis calcd (%) for C₈H₁₂O₃S: C, 51.05; H, 6.43; found: C, 49.89; H, 6.20.

6.2.2 General Procedure A – Silyl Enol Ether Preparation

1,1-Difluoro-2-(triethylsilyloxy)-3-(*N,N*-diethylcarbamoyloxy)-3-methyl hepta-1,6-diene (**112a**)



Carbamate **111** (0.88 mL, 5 mmol) was added dropwise over 5-6 minutes at $-78\text{ }^{\circ}\text{C}$ by syringe to a stirred solution of LDA (6.7 mL of a 1.5 M solution in tetrahydrofuran/heptane/ethylbenzene, 10.0 mmol) in THF (11 mL). The clear brown solution was stirred for 2 hours at $-78\text{ }^{\circ}\text{C}$, clearing to a dark orange solution during this time. 5-hexen-2-one (0.54 g, 5.5 mmol) was added neat in a stream over 1 minute. The mixture was stirred at $-78\text{ }^{\circ}\text{C}$ for 1 hour while the brown colour faded to yellow or orange, then brought to $0\text{ }^{\circ}\text{C}$ in an ice bath over 1 hour further. Chlorotriethylsilane (0.84 mL, 5 mmol) was added in one portion. The yellow solution was allowed to warm slowly to room temperature ($15\text{ }^{\circ}\text{C}$) overnight. After 18 hours, the mixture was concentrated under reduced pressure ($40\text{ }^{\circ}\text{C}$, 150-75 mmHg, then 0.1 mmHg) to remove the THF, then treated with hexane (10 mL) to precipitate lithium salts. The suspension was transferred by pipette onto a pad of silica gel (10 g), which had been conditioned with 10 % diethyl ether in hexane, in a sinter funnel (30 mm diameter). The crude product was eluted by washing with 10 % diethyl ether in hexane (200 mL) and the eluent was evaporated under reduced pressure to afford crude silyl enol ether **112a** (1.3 g) as a mobile clear yellow oil. The crude silyl enol ether was purified by flash column chromatography (90 g silica, 10 % diethyl ether in hexane) to afford **112a** as a colourless oil (1.31 g, 67 %)

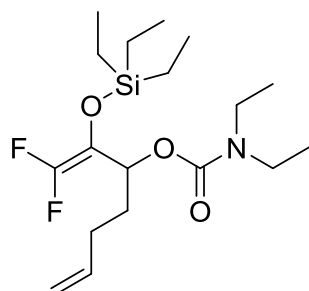
$R_f = 0.25$ (5 % ethyl acetate in hexane);

$^1\text{H NMR}$ (400 MHz, CDCl_3): $\delta = 5.82$ (ddt, $J = 16.7, 10.2, 6.6$ Hz, 1H), 5.07-4.99 (m, 1H), 4.98-4.92 (m, 1H), 3.42-3.07 (m, 4H), 2.16-2.01 (m, 2H), 1.99-1.88 (m, 2H), 1.61 (d, $^5J_{\text{H-F}} = 4.0$ Hz, 3H), 1.10 (t, $J = 7.1$ Hz, 6H), 0.97 (t, $J = 7.9$ Hz, 9H), 0.73-0.64 (m, 6H) ppm;

$^{13}\text{C NMR}$ (125 MHz, CDCl_3): $\delta = 154.0, 153.6$ (dd, $^1J_{\text{C-F}} = 284.1, 279.8$ Hz), 138.2, 115.7 (dd, $^2J_{\text{C-F}} = 32.3, 16.7$ Hz), 114.5, 80.1 (t, $^3J_{\text{C-F}} = 3.5$ Hz), 41.3, 38.1, 28.1, 22.3 (d, $^4J_{\text{C-F}} = 6.9$ Hz), 13.9, 13.4, 6.6, 5.1 ppm;

^{19}F NMR (376 MHz, CDCl_3): $\delta = -102.1$ (d, $^2J = 86.9$ Hz, 1F), -112.0 (dq, $^2J = 86.9$ Hz, $^4J_{\text{F-H}} = 4.0$ Hz, 1F) ppm;
 $\bar{\nu}$ (neat) = 2957, 1703, 1418, 1258, 1169 cm^{-1} ;
HRMS (NSI-ES): calcd for $\text{C}_{19}\text{H}_{36}\text{F}_2\text{NO}_3\text{Si}$, 392.2427 $[\text{M}+\text{H}]^+$, found: 392.2427;
MS (CI): m/z (%): 392 (22) $[\text{M}+\text{H}]^+$, 362 (9) $[\text{M}-\text{C}_2\text{H}_5]$, 350 (19) $[\text{M}-\text{C}_3\text{H}_5]$, 100 (100) $[\text{CONEt}_2]$.

1,1-Difluoro-2-((triethylsilyloxy)-3-(*N,N*-diethylcarbamoyloxy)-hepta-1,6-diene (112b)



Prepared as for **112a** from carbamate (1.76 mL), LDA (13.8 mL of a 1.45 M solution in THF/heptane/ethylbenzene, aldehyde **S1** (1.18 mL, 12 mmol) and TES-Cl (1.68 mL, 10 mmol) in THF (22 mL). Crude product (3.90 g) was purified by flash column chromatography (90 g cartridge, 8 % diethyl ether in hexane) to afford **112b** (2.36 g, 63 %) as a colourless oil.

$R_f = 0.23$ (10 % diethyl ether in hexane);

^1H NMR (400 MHz, CDCl_3): $\delta = 5.79$ (ddt, $J = 16.9, 10.0, 7.0$, 1H), 5.27 (tdd, $J = 7.5, ^4J_{\text{H-F}} = 3.4, 2.5$ Hz, 1H), $5.05-4.98$ (m, 1H), $4.98-4.94$ (m, 1H), $3.48-3.29$ (m, 2H), $3.28-3.08$ (m, 2H), $2.13-1.99$ (m, 2H), $1.94-1.74$ (m, 2H), 1.10 (t, $J = 7.25$ Hz, 6H), 0.96 (t, $J = 7.92$ Hz, 9H), $0.75-0.60$ (m, 6H) ppm;

^{13}C NMR (100 MHz, CDCl_3): $\delta = 154.9, 153.6$ (t, $^1J_{\text{C-F}} = 284.6$ Hz), $137.3, 115.1, 112.3$ (dd, $^2J_{\text{C-F}} = 37.8, 15.2$ Hz), 70.2 (t, $^3J_{\text{C-F}} = 3.8$ Hz), $41.6, 40.9, 30.2, 29.4, 13.9, 13.3, 6.4, 4.9$ ppm;

^{19}F NMR (376 MHz, CDCl_3): $\delta = -103.2$ (d, $^2J = 74.8$ Hz, 1F), -115.0 (dd, $^2J = 74.9$ Hz, $^4J_{\text{F-H}} = 3.4$ Hz, 1F) ppm; the 2.5 Hz $^4J_{\text{H-F}}$ = splitting could not be resolved in the 376 MHz ^{19}F NMR spectrum;

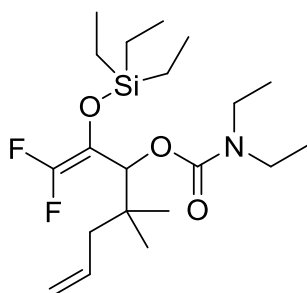
$\bar{\nu}$ (neat) = 2956, 2878, 1759, 1703, 1424, 1266, 1167 cm^{-1} ;

HRMS (APCI-MS): calcd for $\text{C}_{18}\text{H}_{33}\text{F}_2\text{NO}_3\text{Si}$, 378.2271 $[\text{M}+\text{H}]^+$, found: 378.2264;

MS (CI): m/z (%): 378 (23) $[\text{M}+\text{H}]^+$, 336 (10) $[\text{M}-\text{C}_3\text{H}_5]$, 100 (100) $[\text{CONEt}_2]$.

1,1-Difluoro-2-((triethylsilyl)oxy)-3-(*N,N*-diethylcarbamoyloxy)-4,4-dimethyl-hepta-1,6-diene

(112c)



Prepared as for **112a** from carbamate (0.88 mL), LDA (12.2 mL of a 0.82 M solution in THF/Hexanes, 10 mmol), 2,2-dimethyl-4-pentenal (0.56 g, 5.0 mmol) and TES-Cl (0.84 mL, 5 mmol) in THF (11 mL). Crude product (1.75 g) was purified by flash column chromatography (90 g cartridge, 7 % diethyl ether in hexane) to afford **112c** (1.35 g, 67 %) as a pale yellow oil.

R_f = 0.3 (5 % diethyl ether in petroleum ether);

^1H NMR (400 MHz, CDCl_3): δ = 5.82 (ddt, J = 17.5, 10.0, 7.3 Hz, 1H), 5.11-5.07 (m, 1H), 5.07-5.03 (m, 1H), 5.02-4.97 (m, 1H), 3.63-3.33 (m, 2H), 3.28-3.09 (m, 2H), 2.15, 2.09 (dABq, J_{AB} = 13.6, J = 7.4 Hz, 2H), 1.23-1.09 (m, 6H), 1.04-0.94 (m, 15H), 0.78-0.61 (m, 6H) ppm;

^{13}C NMR (100 MHz, CDCl_3): δ = 154.2, 153.5 (t, $^1J_{\text{C-F}}$ = 284.2 Hz), 133.9, 117.0, 111.5 (dd, $^2J_{\text{C-F}}$ = 35.2, 14.7 Hz), 75.1 (t, $^3J_{\text{C-F}}$ = 3.5 Hz), 43.3, 41.0, 40.3, 37.7, 23.2, 22.7, 13.5, 12.7, 5.9, 4.4 ppm;

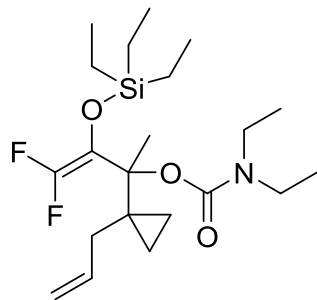
^{19}F NMR (376 MHz, CDCl_3): δ = -103.7 (d, 2J = 77.7 Hz, 1F), -114.6 (dd, 2J = 77.7 Hz, $^4J_{\text{F-H}}$ = 2.9 Hz, 1F) ppm; the 2.9 Hz $^4J_{\text{H-F}}$ = splitting could not be resolved in the 376 MHz ^{19}F NMR spectrum;

$\bar{\nu}$ /(neat) = 2967, 1701, 1425, 1263, 1167, 1063, 1003, 914, 731 cm^{-1} ;

HRMS (NSI-ES): calcd for $\text{C}_{20}\text{H}_{38}\text{F}_2\text{NO}_3\text{Si}$, 406.2584 $[\text{M}+\text{H}]^+$, found: 406.2578;

MS (CI): m/z (%): 406 (34) $[\text{M}+\text{H}]^+$, 376 (19) $[\text{M}-\text{C}_2\text{H}_5]$, 364 (26) $[\text{M}-\text{C}_3\text{H}_5]$, 100 (100) $[\text{CONEt}_2]$.

1,1-Difluoro-2-(triethylsilyloxy)-3-(*N,N*-diethylcarbamoyloxy)-3-methyl-4-(cyclopropyl) hepta-1,6-diene (112d)



Prepared as for **112a** from carbamate (0.88 mL), LDA (6.9 mL of a 1.45 M solution in THF/heptane/ethylbenzene, 10 mmol), ketone **S2** (0.68 g, 5.5 mmol) and TES-Cl (0.84 mL, 5 mmol) in THF (11 mL). Crude product (2.13 g) was purified by flash column chromatography (90 g cartridge, 9 % diethyl ether in hexane) to afford **112d** (1.28 g, 61 %) as a colourless oil.

$R_f = 0.37$ (10 % diethyl ether in hexane);

$^1\text{H NMR}$ (400 MHz, CDCl_3): $\delta = 5.65$ (dddd, $J = 14.6, 12.0, 7.4, 5.2$ Hz, 1H), 5.01-4.97 (m, 1H), 4.96-4.91 (m, 1H), 3.44-2.93 (m, 4H), 2.25 (d, $J = 7.4$ Hz, 2H), 1.69 (d, $^5J_{\text{H-F}} = 5.5$ Hz, 3H), 1.09 (t, $J = 7.1$ Hz, 6H), 0.97 (t, $J = 7.9$ Hz, 10H), 0.75-0.64 (m, 6H), 0.61-0.52 (m, 1H), 0.46-0.37 (m, 1H), 0.36-0.27 (m, 1H) ppm;

$^{13}\text{C NMR}$ (100 MHz, CDCl_3): $\delta = 153.9$ (dd, $^1J_{\text{C-F}} = 283.7, 278.6$ Hz), 153.5, 135.6, 116.7, 115.2 (dd, $^2J_{\text{C-F}} = 33.0, 17.5$ Hz), 80.7 (t, $^3J_{\text{C-F}} = 4.7$ Hz), 41.4, 41.1, 36.7, 26.7, 20.8 (d, $^4J_{\text{C-F}} = 8.3$ Hz), 14.2, 13.4, 8.0, 6.6, 5.5, 5.1 ppm;

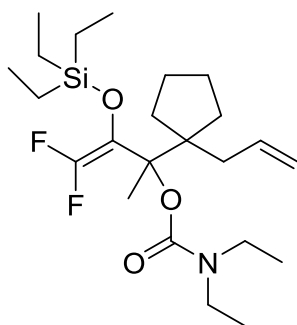
$^{19}\text{F NMR}$ (376 MHz, CDCl_3): $\delta = -102.4$ (d, $^2J = 88.9$ Hz, 1F), -112.1 (dq, $^2J = 88.9$ Hz, $^5J_{\text{F-H}} = 5.5$ Hz, 1F) ppm;

$\bar{\nu}$ /(neat) = 2957, 2359, 1701, 1418, 1258, 1171, 1022 cm^{-1} ;

HRMS (NSI-ES): calcd for $\text{C}_{21}\text{H}_{38}\text{F}_2\text{NO}_3\text{Si}$, 418.2584 $[\text{M}+\text{H}]^+$, found: 418.2583;

MS (CI): m/z (%): 418 (4) $[\text{M}+\text{H}]^+$, 388 (5) $[\text{M}-\text{C}_2\text{H}_5]$, 376 (2) $[\text{M}-\text{C}_3\text{H}_5]$, 301 (5) $[\text{M}-\text{C}_5\text{H}_{10}\text{NO}_2]$, 100 (100) $[\text{CONEt}_2]$.

1,1-Difluoro-2-(triethylsilyloxy)-3-(*N,N*-diethylcarbamoyloxy)-3-methyl-4-(cyclopentyl) hepta-1,6-diene (112e)



Prepared as for **112a** from carbamate (0.88 mL), LDA (6.7 mL of a 1.5 M solution in THF/heptane/ethylbenzene, 10 mmol), ketone **S4** (0.85 g, 5.5 mmol) and TES-Cl (0.84 mL, 5.5 mmol) in THF (11 mL). Crude product (2.06 g) was purified by flash column chromatography (90 g cartridge, 8 % diethyl ether in hexane) to afford **112e** (0.85 g, 38 %) as a mobile yellow oil

$R_f = 0.67$ (20 % diethyl ether in hexane);

$^1\text{H NMR}$ (400 MHz, CDCl_3): $\delta = 5.88$ (dddd, $J = 14.5, 11.2, 9.2, 6.8$ Hz, 1H), 5.13-4.96 (m, 2H), 3.43-3.03 (m, 4H), 2.24 (d, $J = 6.9$ Hz, 2H), 2.11-1.96 (m, 1H), 1.96-1.81 (m, 1H), 1.67 (d, $^5J_{\text{H-F}} = 3.6$ Hz, 3H), 1.61-1.37 (m, 6H), 1.12 (t, $J = 7.2$ Hz, 6H), 0.98 (t, $J = 7.9$ Hz, 9H), 0.79-0.66 (m, 6H) ppm;

$^{13}\text{C NMR}$ (100 MHz, CDCl_3): $\delta = 154.0, 153.7$ (dd, $^1J_{\text{C-F}} = 283.3, 276.9$ Hz), 136.5, 116.8, 115.9 (dd, $^2J_{\text{C-F}} = 30.7, 16.7$ Hz), 84.3 (d, $^3J_{\text{C-F}} = 4.8$ Hz), 54.9, 41.7, 41.4, 41.1, 32.5, 32.3, 26.4, 26.3, 20.0 (d, $^4J_{\text{C-F}} = 5.8$ Hz), 14.1, 13.4, 6.7, 5.3 ppm;

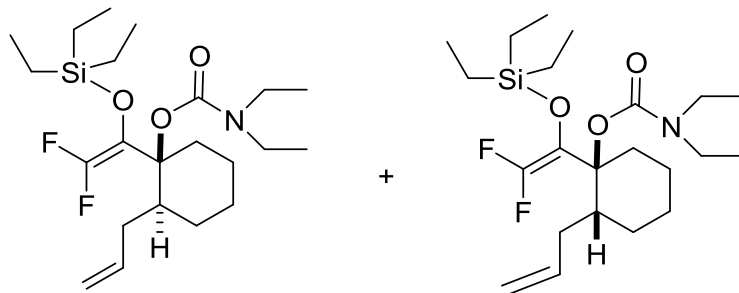
$^{19}\text{F NMR}$ (376 MHz, CDCl_3): $\delta = -103.7$ (d, $^2J = 93.1$ Hz, 1F), -112.5 (dd, $^2J = 93.1, ^5J_{\text{H-F}} = 3.6$ Hz) ppm;

$\bar{\nu}$ (neat) = 2958, 2880, 1746, 1705, 1420, 1256, 735 cm^{-1} ;

HRMS (NSI-ES): calcd for $\text{C}_{23}\text{H}_{42}\text{F}_2\text{NO}_3\text{Si}$, 446.2897 $[\text{M}+\text{H}]^+$, found: 446.2890;

MS (CI): m/z (%): 446 (5) $[\text{M}+\text{H}]^+$, 416 (2) $[\text{M}-\text{C}_2\text{H}_5]$, 404 (18) $[\text{M}-\text{C}_3\text{H}_5]$, 100 (100) $[\text{CONEt}_2]$.

***Trans*-2-allyl-1-(2',2'-difluoro-1'-((triethylsilyl)oxy)ethenyl)-1-(*N,N*-diethylcarbamoyloxy)cyclohexane (*trans*-112f) and *cis*-2-allyl-1-(2',2'-difluoro-1'-((triethylsilyl)oxy)ethenyl)-1-(*N,N*-diethylcarbamoyloxy)cyclohexane (*cis*-112f)**



Prepared as for **112a** from carbamate (0.88 mL), LDA (6.8 mL of a 1.47 M solution in THF/heptane/ethylbenzene, 10 mmol), 2-allylcyclohexanone (0.76 g, 5.5 mmol) and TES-Cl (0.84 mL, 5 mmol) in THF (11 mL). Crude product (2.20 g) was purified by flash column chromatography (90 g cartridge, 9 % diethyl ether in hexane) to afford an inseparable mixture of ***trans*-112f** and ***cis*-112f** (1.54 g, 71 %, 19 : 1) as a pale yellow oil.

$R_f = 0.27$ (5 % diethyl ether in petroleum ether);

$^1\text{H NMR}$ (400 MHz, CDCl_3): $\delta = 5.75$ (dddd, $J = 16.5, 10.7, 8.4, 5.9$ Hz, 1H), 5.08-5.00 (m, 1H), 5.00-4.96 (m, 1H), 3.45-3.14 (m, 4H), 2.89 (br. d, $J = 14.4$ Hz, 1H), 2.46-2.32 (m, 1H), 1.97-1.83 (m, 1H), 1.82-1.63 (m, 4H), 1.62-1.49 (m, 1H), 1.45-1.22 (m, 3H), 1.21-1.08 (m, 6H), 1.00 (t, $J = 8.1$ Hz, 9H), 0.80-0.63 (m, 6H) ppm;

Major *trans*-diastereoisomer **112f** (assigned on the basis of δ and intensity) $^{13}\text{C NMR}$ (100 MHz, CDCl_3): $\delta = 153.7, 153.5$ (dd, $^1J_{\text{C-F}} = 282.8, 277.7$ Hz), 137.6, 115.6, 114.5 (dd, $^2J_{\text{C-F}} = 30.7, 16.7$ Hz), 81.8 (d, $^3J_{\text{C-F}} = 4.2$ Hz), 42.9, 41.5, 41.3, 34.7, 30.3, 26.9, 25.0, 21.0, 14.1, 14.0, 13.3, 6.6, 5.1 ppm;

$^{19}\text{F NMR}$ (376 MHz, CDCl_3): $\delta = -102.6$ (d, $^2J = 92.3$ Hz, 1F), -114.4 (br. d, $^2J = 92.3$ Hz, 1F) ppm;

Minor *cis*-diastereoisomer **112f** (assigned on the basis of δ and intensity)

$^{13}\text{C NMR}$ (100 MHz, CDCl_3): 154.5 (dd, $^1J_{\text{C-F}} = 286.0, 279.7$ Hz), 137.5, 115.7, 82.9 (t, $^3J_{\text{C-F}} = 5.2$ Hz), 41.1, 39.5, 31.9, 25.7, 25.6, 22.9, 19.1 ppm;

$^{19}\text{F NMR}$ (376 MHz, CDCl_3): $\delta = -100.4$ (d, $^2J = 81.7$ Hz, 1F), 110.5 (d, $^2J = 81.7$ Hz, 1F) ppm;

$\bar{\nu}$ (neat) = 2936, 1703, 1416, 1248, 1169 cm^{-1} ;

HRMS (NSI-ES): calcd for $\text{C}_{22}\text{H}_{40}\text{F}_2\text{NO}_3\text{Si}$, 432.2740 $[\text{M}+\text{H}]^+$, found: 432.2738;

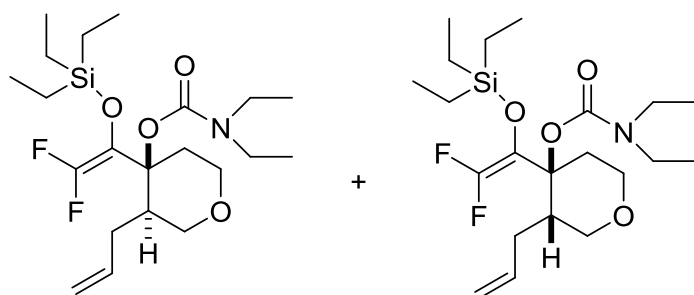
Major *trans*-diastereoisomer **112f**

MS (CI): m/z (%): 432 (14) [M+H]⁺, 402 (4) [M-C₂H₅], 390 (48) [M-C₃H₅], 315 (11) [M-C₅H₁₀NO₂], 100 (100) [CONEt₂];

Minor *cis*-diastereoisomer **112f**

MS (CI): m/z (%): 432 (1) [M+H]⁺, 402 (11) [M-C₂H₅], 390 (4) [M-C₃H₅], 315 (16) [M-C₅H₁₀NO₂], 100 (38) [CONEt₂]

Trans-2-allyl-1-(2',2'-difluoro-1'-((triethylsilyloxy)ethenyl)-1-(N,N-diethylcarbamoyloxy) tetrahydropyran (trans-112g) and cis-2-allyl-1-(2',2'-difluoro-1'-((triethylsilyloxy)ethenyl)-1-(N,N-diethylcarbamoyloxy) tetrahydropyran (cis-112g)



Prepared as for **112a** from carbamate (1.14 mL), LDA (10.5 mL of a 1.24 M solution in THF/heptane/ethylbenzene, 13 mmol), ketone **S5** (1.02 g, 7.2 mmol) and TES-Cl (1.09 mL, 6.5 mmol) in THF (14 mL). Crude product (2.58 g) was purified twice by flash column chromatography (90 g cartridge, 20 % diethyl ether in hexane) to afford **trans-112g** (1.34 g, 43 %) and **cis-112g** (0.087 g, 3 %) as clear mobile oils.

Major *trans*-diastereoisomer **112g**

R_f = 0.55 (40 % diethyl ether in hexane);

¹H NMR (400 MHz, CDCl₃): δ = 5.73 (dddd, *J* = 16.2, 10.9, 7.5, 6.0 Hz, 1H), 5.12-4.97 (m, 2H), 3.86-3.69 (m, 2H), 3.67-3.44 (m, 2H), 3.40-3.16 (m, 4H), 2.87-2.58 (m, 1H), 2.41-2.26 (m, 1H), 2.27-2.06 (m, 2H), 2.02-1.84 (m, 1H), 1.19 (t, *J* = 7.2 Hz, 3H), 1.13 (t, *J* = 7.2 Hz, 3H), 1.00 (t, *J* = 7.9 Hz, 9H), 0.78-0.68 (m, 6H) ppm;

¹³C NMR (100 MHz, CDCl₃): δ = 153.2 (dd, ¹*J*_{C-F} = 283.7, 279.4 Hz), 152.9, 135.9, 115.9, 113.0 (dd, ²*J*_{C-F} = 30.4, 17.1 Hz), 78.9 (d, ³*J*_{C-F} = 4.5 Hz), 66.6, 62.9, 41.3, 41.1, 40.9, 30.0, 29.7, 13.7, 12.8, 6.1, 4.7 ppm;

¹⁹F NMR (376 MHz, CDCl₃): δ = -101.2 (d, ²*J* = 91.4 Hz, 1F), -112.9 (br. d, ²*J* = 91.4 Hz, 1F) ppm;

$\bar{\nu}$ (neat) = 2958, 2876, 1705, 1418, 1257, 1171 cm⁻¹;

HRMS (APCI-MS): calcd for C₂₁H₃₈F₂NO₄Si, 434.2533 [M+H]⁺, found: 434.2523;

MS (CI): m/z (%): 434 (1) [M+H]⁺, 404 (1) [M-C₂H₅], 392 (3) [M-C₃H₅], 100 (39) [CONEt₂];

Minor *cis*-diastereoisomer **112g**

R_f = 0.51 (40 % diethyl ether in hexane);

¹H NMR (400 MHz, CDCl₃): δ = 5.73 (dddd, *J* = 17.9, 9.9, 7.2, 6.0 Hz, 1H), 5.20-4.98 (m, 2H), 3.92-3.71 (m, 3H), 3.64-3.51 (m, 1H), 3.51-3.05 (m, 4H), 2.75-2.61 (m, 1H), 2.44-2.26 (m, 1H), 2.15-2.03 (m, 1H), 2.02-1.84 (m, 2H), 1.21 (t, *J* = 7.4 Hz, 3H), 1.13 (t, *J* = 7.2 Hz, 3H), 0.98 (t, *J* = 7.9 Hz, 9H), 0.79-0.57 (m, 6H) ppm;

¹³C NMR (150 MHz, CDCl₃): δ = 153.6 (dd, ¹J_{C-F} = 286.8, 281.7 Hz), 152.5, 135.7, 115.8, 112.8 (dd, ²J_{C-F} = 32.3, 17.5 Hz), 79.6 (t, ³J_{C-F} = 4.9 Hz), 63.6, 62.1, 40.3, 40.2, 40.0, 30.2, 26.4 (d, ⁴J_{C-F} = 10.4 Hz), 13.3, 12.3, 5.6, 4.1 ppm;

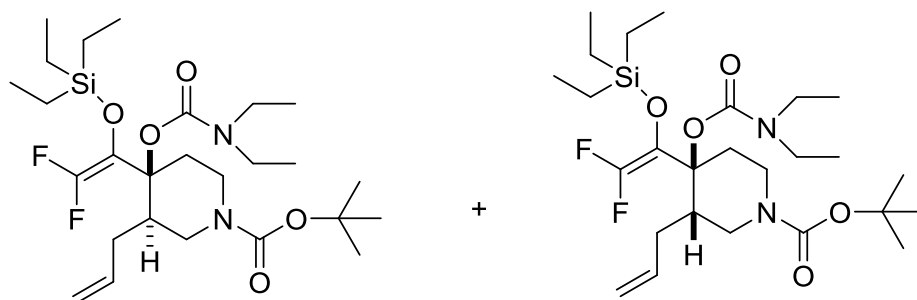
¹⁹F NMR (376 MHz, CDCl₃): δ = -99.3 (d, ²J = 79.2 Hz, 1F), -109.6 (d, ²J = 79.2 Hz, 1F) ppm;

$\bar{\nu}$ (neat) = 2958, 2876, 1699, 1418, 1258, 1158 cm⁻¹;

HRMS (APCI-MS): calcd for C₂₁H₃₈F₂NO₄Si, 434.2533 [M+H]⁺, found: 434.2521;

MS (CI): m/z (%): 434 (1) [M+H]⁺, 404 (1) [M-C₂H₅], 392 (2) [M-C₃H₅], 100 (57) [CONEt₂].

***trans*-tert-Butyl -2-allyl-1-(2',2'-difluoro-1'-((triethylsilyl)oxy)ethenyl)-1 -(N,N-diethylcarbamoyloxy) piperidine-1-carboxylate (*trans*-112h) and *cis*- tert-Butyl -2-allyl-1-(2',2'-difluoro-1'-((triethylsilyl)oxy)ethenyl)-1 -(N,N-diethylcarbamoyloxy) piperidine-1-carboxylate (*cis*-139h).**



Prepared as for **112a** from carbamate (0.88 mL), LDA (6.9 mL of a 1.45 M solution in THF/heptane/ethylbenzene, 10 mmol), ketone **S6** (1.38 g, 5.8 mmol) and TES-Cl (0.84 mL, 5 mmol) in THF (11 mL). Crude product (2.46 g) was purified by flash column chromatography (90 g cartridge, 10 % ethyl acetate in hexane) to afford an inseparable mixture of ***trans*-112h** and ***cis*-112h** (1.52 g, 57 %, 87 : 13) as a viscous yellow oil;

R_f = 0.45 (20 % ethyl acetate in hexane);

^1H NMR (400 MHz, $\text{C}_6\text{D}_4\text{Cl}_2$, 373 K): δ = 5.75 (ddt, J = 16.7, 10.2, 6.5 Hz, 1H), 5.03 (br. d, J = 16.7 Hz, 1H), 4.96 (br. d, J = 10.2 Hz, 1H), 3.82 (app. dd, J = 13.5, 3.9 Hz, 1H), 3.68 (app. dt, J = 13.7, 4.6 Hz, 1H), 3.35-2.99 (m, 6H), 2.83-2.58 (m, 1H), 2.47-2.27 (m, 1H), 2.22-1.85 (m, 3H), 1.42 (s, 9H), 1.02 (t, J = 7.0 Hz, 6H), 0.92 (t, J = 7.6 Hz, 9H), 0.66 (q, J = 7.6 Hz, 6H) ppm;

Major *trans*-diastereoisomer **112h** (assigned on the basis of δ and intensity) ^{13}C NMR (100 MHz, $\text{C}_6\text{D}_4\text{Cl}_2$, 373 K): δ = 154.4, 154.0 (dd, $^1J_{\text{C-F}}$ = 284.3, 280.8 Hz), 153.1, 136.3, 116.0, 114.5 (dd, $^2J_{\text{C-F}}$ = 30.8, 17.3 Hz), 78.9, 44.0, 42.1, 41.6, 39.9, 31.4, 30.0, 28.2, 13.5, 6.3, 5.4 ppm;

^{19}F NMR (376 MHz, $\text{C}_6\text{D}_4\text{Cl}_2$, 373 K): δ = -101.2 (d, 2J = 88.3 Hz, 1F), -111.8 (d, 2J = 88.7 Hz, 1F) ppm;

Minor *cis*-diastereoisomer **112h** (assigned on the basis of δ and intensity) ^{13}C NMR (100 MHz, $\text{C}_6\text{D}_4\text{Cl}_2$, 373 K): δ = 136.5, 116.4, 80.4 (d, $^3J_{\text{C-F}}$ = 4.9 Hz), 41.3, 31.3 ppm;

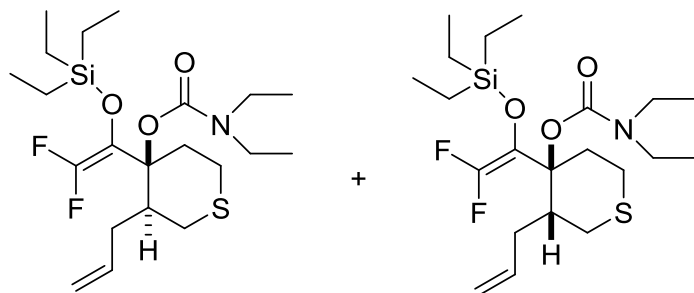
^{19}F NMR (376 MHz, $\text{C}_6\text{D}_4\text{Cl}_2$, 373 K): δ = -100.2 (d, 2J = 82.7 Hz, 1F), -110.1 (d, 2J = 82.3 Hz, 1F) ppm;

$\bar{\nu}$ (neat) = 2956, 2876, 1697, 1416, 1249, 1171 cm^{-1} ;

HRMS (NSI-ES): calcd for $\text{C}_{26}\text{H}_{46}\text{F}_2\text{N}_2\text{O}_5\text{Si}$, 533.3217 $[\text{M}+\text{H}]^+$, found: 533.3208;

MS (NSI-ES): m/z (%): 533 (100) $[\text{M}+\text{H}]^+$.

***Trans*-2-allyl-1-(2',2'-difluoro-1'-((triethylsilyloxy)ethenyl)-1-(*N,N*-diethylcarbamoyloxy) tetrahydrothiopyran (*trans*-112i) and *cis*-2-allyl-1-(2',2'-difluoro-1'-((triethylsilyloxy)ethenyl)-1-(*N,N*-diethylcarbamoyloxy) tetrahydrothiopyran (*cis*-112i)**



Prepared as for **112a** from carbamate (0.88 mL), LDA (6.7 mL of a 1.5 M solution in THF/heptane/ethylbenzene, 10 mmol), ketone **S7** (0.86 g, 5.5 mmol) and TES-Cl (0.84 mL, 5 mmol) in THF (11 mL). Crude product (2.56 g) was purified by flash column chromatography (90 g cartridge, 10 % diethyl ether in hexane) to afford an inseparable mixture of *trans*-**112i** and *cis*-**112i** (1.55 g, 69 %, 92 : 8) as a viscous yellow oil

R_f = 0.43 (20 % diethyl ether in hexane);

^1H NMR (400 MHz, CDCl_3): δ = 5.73 (dddd, J = 14.2, 11.9, 8.8, 5.6 Hz, 1H), 5.16-5.00 (m, 2H), 3.51-3.06 (m, 5H), 2.87-2.57 (m, 3H), 2.54-2.40 (m, 2H), 2.33-2.14 (m, 2H), 2.11-1.87 (m, 1H), 1.19 (t, J = 7.2 Hz, 3H), 1.13 (t, J = 7.2 Hz, 3H), 1.00 (t, J = 7.9 Hz, 9H), 0.80-0.66 (m, 6H) ppm;

Major *trans*-diastereoisomer **112i** (assigned on the basis of δ and intensity) ^{13}C NMR (100 MHz, CDCl_3): δ = 153.4 (dd, $^1J_{\text{C-F}}$ = 284.4, 279.6 Hz), 153.2, 136.4, 116.8, 114.1 (dd, $^2J_{\text{C-F}}$ = 30.4, 17.0 Hz), 80.8 (d, $^3J_{\text{C-F}}$ = 4.8 Hz), 43.2, 41.6, 41.4, 34.1, 32.4, 27.9, 23.3, 14.1, 13.2, 6.6, 5.1 ppm;

^{19}F NMR (376 MHz, CDCl_3): δ = -102.6 (d, 2J = 92.1 Hz, 1F), -114.4 (br. d, 2J = 92.1 Hz, 1F) ppm;

Minor *cis*-diastereoisomer **112i** (assigned on the basis of δ and intensity) ^{13}C NMR (100 MHz, CDCl_3): δ = 154.3 (dd, $^1J_{\text{C-F}}$ = 286.8, 281.2 Hz), 136.5, 114.7 (dd, $^2J_{\text{C-F}}$ = 32.1, 17.7 Hz), 81.2 (t, $^3J_{\text{C-F}}$ = 4.8 Hz), 41.3, 38.9, 30.7, 26.7, 26.6, 26.4, 22.9, 14.2, 13.2, 6.6, 5.1 ppm;

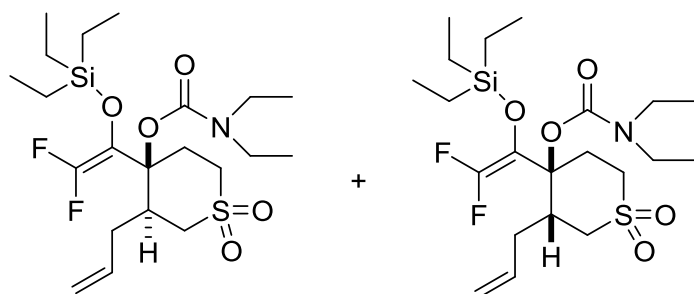
^{19}F NMR (376 MHz, CDCl_3): δ = -100.4 (d, 2J = 82.8 Hz, 1F), -110.5 (d, 2J = 82.8 Hz, 1F) ppm;

$\bar{\nu}$ (neat) = 2954, 2874, 1703, 1416, 1255, 1167, 734 cm^{-1} ;

HRMS (APCI-MS): calcd for $\text{C}_{21}\text{H}_{38}\text{F}_2\text{NO}_3\text{Si}$, 450.2299 $[\text{M}+\text{H}]^+$, found: 450.2304;

MS (CI): m/z (%): 478 (12) $[\text{M}+\text{C}_2\text{H}_5]^+$, 450 (20) $[\text{M}+\text{H}]^+$, 420 (6) $[\text{M}-\text{C}_2\text{H}_5]$, 408 (20) $[\text{M}-\text{C}_3\text{H}_5]$, 100 (100) $[\text{CONEt}_2]$.

***Trans*-2-allyl-1-(2',2'-difluoro-1'-((triethylsilyloxy)ethenyl)-1-(*N,N*-diethylcarbamoyloxy) dioxidotetrahydrothiopyran (*trans*-112j) and *cis*-2-allyl-1-(2',2'-difluoro-1'-((triethylsilyloxy)ethenyl)-1-(*N,N*-diethylcarbamoyloxy) dioxidotetrahydrothiopyran (*cis*-112j).**



Prepared as for **112a** from carbamate (0.84 mL), LDA (8.7 mL of a 1.1 M solution in THF/heptane/ethylbenzene, 9.6 mmol), ketone **S8** (1.01 g, 5.3 mmol) and TES-Cl (0.81 mL, 4.8 mmol) in THF (10.6 mL). Crude product (2.11 g) was purified by flash column

chromatography (90 g cartridge, 30 % diethyl ether in hexane) to afford an inseparable mixture of **trans-112j** and **cis-112j** (0.58 g, 25 %, 84 : 16) as a viscous yellow oil

$R_f = 0.3$ (50 % diethyl ether in hexane);

$^1\text{H NMR}$ (400 MHz, CDCl_3): $\delta = 5.68$ (dddd, $J = 17.2, 10.1, 9.3, 5.7$ Hz, 1H), 5.22 (br. d, $J = 17.2$ Hz, 1H), 5.17 (br. d, $J = 10.1$ Hz, 1H), 3.56-3.23 (m, 4H), 3.23-3.00 (m, 4H), 2.99-2.87 (m, 1H), 2.81-2.65 (m, 1H), 2.64-2.53 (m, 1H), 2.52-2.35 (m, 1H), 2.22-2.05 (m, 1H), 1.16 (t, $J = 7.3$ Hz, 3H), 1.11 (t, $J = 7.3$ Hz, 3H), 0.94 (t, $J = 8.0$ Hz, 9H), 0.76-0.60 (m, 6H) ppm;

Major *trans*-diastereoisomer **112j** (assigned on the basis of δ and intensity) $^{13}\text{C NMR}$ (100 MHz, CDCl_3): $\delta = 154.1$ (dd, $^1J_{\text{C-F}} = 286.5, 281.8$ Hz), 152.8, 134.8, 119.3, 113.6 (dd, $^2J_{\text{C-F}} = 32.7, 19.6$ Hz), 79.7 (t, $^3J_{\text{C-F}} = 4.8$ Hz), 48.0, 47.4, 42.4, 41.7, 41.6, 30.5, 25.0 (d, $^4J_{\text{C-F}} = 10.6$ Hz), 14.2, 13.3, 6.5, 5.1 ppm;

$^{19}\text{F NMR}$ (376 MHz, toluene- d_8 , 363K): $\delta = -100.4$ (d, $^2J = 84.5$ Hz, 1F), -110.6 (d, $^2J = 84.5$ Hz) ppm;

Minor *cis*-diastereoisomer **112j** (assigned on the basis of δ and intensity) $^{13}\text{C NMR}$ (100 MHz, CDCl_3): $\delta = 153.3$ (dd, $^1J_{\text{C-F}} = 283.9, 280.1$ Hz), 152.9, 134.2, 118.7, 112.9 (dd, $^2J_{\text{C-F}} = 30.7, 18.6$ Hz), 78.9 (d, $^3J_{\text{C-F}} = 4.9$ Hz), 51.2, 46.9, 42.0, 34.0, 28.9, 14.1, 13.2 ppm;

$^{19}\text{F NMR}$ (376 MHz, toluene- d_8 , 363 K): $\delta = -101.6$ (d, $^2J = 91.6$ Hz, 1F), -112.5 (d, $^2J = 91.6$ Hz) ppm;

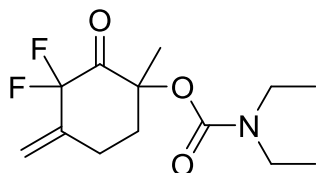
$\bar{\nu}$ (neat) = 2956, 2876, 1749, 1703, 1422, 1258, 1134, 736 cm^{-1} ;

HRMS (NSI-ES): calcd for $\text{C}_{21}\text{H}_{38}\text{F}_2\text{NO}_5\text{Si}$, 482.2203 $[\text{M}+\text{H}]^+$, found: 482.2193;

MS (NSI-ES): m/z (%): 482 (100) $[\text{M}+\text{H}]^+$.

6.2.3 General procedure B: Preparation of α,α -difluoroketones

3,3-Difluoro-1-methyl-4-methylene-2-oxocyclohexyl diethylcarbamate (113a).



Palladium(II) acetate (10 mol %, 22.4 mg) and copper(I) chloride (100 mol %, 99 mg) were suspended in dry acetonitrile (4 mL) that had been sparged with air for 30 minutes through a drawn out pipette. The suspension was warmed to 70 °C then a solution of silyl enol ether **112a** (1.00 mmol, 0.391 g) in dry acetonitrile (1.6 mL) added via syringe in a constant stream. The mixture was then stirred at 70 °C for 18 hours under an air

condenser and open to the atmosphere. The reaction mixture was concentrated and transferred by pipette onto a plug of celite. The product was eluted from the celite with diethyl ether (50 mL). The crude product was taken up in diethyl ether (10 mL) and PhosphonicS STA3 scavenger silica was added. The mixture was stirred for 30 minutes, then the mixture filtered through a 20 μm polyethylene frit and washed with diethyl ether (50 mL). The solvent was removed under reduced pressure to afford crude product as an oil. Trituration in pentane afforded a granular colourless amorphous solid which was dried in a vacuum oven (40 $^{\circ}\text{C}$, 0.75 mmHg, 48 hours) to afford ketone **113a** (0.141 g, 52 %).

$R_f = 0.25$ (40 % diethyl ether in hexane);

^1H NMR (400 MHz, CDCl_3): $\delta = 5.53$ (app. d, $^4J_{\text{H-F}} = 4.00$ Hz, 1H), 5.25 (br. s, 1H), 3.44-3.11 (m, 4H), 2.90-2.66 (m, 1H), 2.54-2.26 (m, 2H), 1.74-1.58 (m, 1H), 1.54 (s, 3H), 1.15 (t, $J = 7.4$ Hz, 3H), 1.09 (t, $J = 7.5$ Hz, 3H) ppm;

^{13}C NMR (100 MHz, CDCl_3): $\delta = 194.2$ (dd, $^2J_{\text{C-F}} = 26.0, 23.2$ Hz), 154.7, 141.1 (t, $^2J_{\text{C-F}} = 20.5$ Hz), 115.5 (t, $^3J_{\text{C-F}} = 7.8$ Hz), 114.2 (dd, $^1J_{\text{C-F}} = 257.0, 253.5$ Hz), 82.1, 42.0, 41.5, 38.2, 26.5 (d, $^3J_{\text{C-F}} = 7.8$ Hz), 21.5, 14.0, 13.2 ppm;

^{19}F NMR (376 MHz, CDCl_3): $\delta = -103.7$ (d, $^2J = 250.4$ Hz, 1F), -117.6 (d, $^2J = 250.4$ Hz, 1F) ppm;

$\bar{\nu}$ (neat) = 2984, 2939, 1749, 1686, 1429, 1281, 1117 cm^{-1} ;

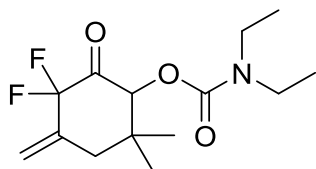
HRMS (EI-MS): calcd for $\text{C}_{13}\text{H}_{20}\text{F}_2\text{NO}_3$, 276.1406 $[\text{M}+\text{H}]^+$, found: 276.1402;

MS (CI): m/z (%): 304 (11) $[\text{M}+\text{C}_2\text{H}_5]^+$, 276 (100) $[\text{M}+\text{H}]^+$, 100 (94) $[\text{CONEt}_2]$;

t_R (GC) = 12.64 minutes;

elemental analysis calcd (%) for $\text{C}_{13}\text{H}_{19}\text{F}_2\text{NO}_3$: C, 56.72; H, 6.96; N, 5.09; found: C, 56.62; H, 6.72; N, 5.10. This analysis was obtained for the amorphous solid obtained following chromatography so no melting point was recorded.

5,5-Difluoro-2,2-dimethyl-4-methylene-6-oxocyclohexyl diethylcarbamate (**113c**)



Ketone (**113c**) was prepared by general procedure B from **112c** (0.5 g, 1.23 mmol) with palladium(II) acetate (5 mol %, 0.0138 g) and copper(I) chloride (100 mol %, 0.122 g) in acetonitrile (6.6 mL) that had been sparged with air for thirty minutes through a drawn out pipette. The usual work-up, according to **113a**, afforded a pale yellow oil which was

triturerated with pentane and dried in a vacuum oven (40 °C, 0.75 mmHg, 48 hours) to afford **113c** as a pale yellow crystalline solid (0.255 g, 72 %).

m.p. = 79-80 °C (recrystallised from hot pentane as a colourless plate);

R_f = 0.25 (40 % diethyl ether in petroleum ether);

^1H NMR (400 MHz, CDCl_3): δ = 5.53 (br. d, $^4J_{\text{H-F}}$ = 5.4 Hz, 1H), 5.51 (d, $^4J_{\text{H-F}}$ = 5.6 Hz, 1H), 5.34 (q, $^4J_{\text{H-F}}$ = 2.8, 4J = 2.80 Hz, 1H), 3.45-3.21 (m, 4H), 2.70 (br. d, 2J = 14.7 Hz, 1H), 2.29 (dd, 2J = 14.7, $^4J_{\text{H-F}}$ = 4.8 Hz, 1H), 1.32-1.08 (m, including 1.20 (s, 3H), 6H), 0.82 (s, 3H) ppm;

^{13}C NMR (400 MHz, CDCl_3): δ = 192.6 (dd, $^2J_{\text{C-F}}$ = 30.7, 23.3 Hz), 153.8, 136.9 (t, $^2J_{\text{C-F}}$ = 20.2 Hz), 117.9 (t, $^3J_{\text{C-F}}$ = 7.4 Hz), 114.2 (dd, $^1J_{\text{C-F}}$ = 264.4, 241.5 Hz), 80.6 (t, $^3J_{\text{C-F}}$ = 3.1 Hz), 41.9 (d, $^3J_{\text{C-F}}$ = 4.1 Hz), 41.2, 38.2, 26.5, 19.3, 13.5, 12.9 ppm (the signal at 41.2 appears for both CH_2 carbons of the DEC group);

^{19}F NMR (376 MHz, CDCl_3): δ = -97.8 (dddq, 2J = 252.8 Hz, $^4J_{\text{F-H}}$ = 5.6, 5.4, 2.8 Hz, 1F), -129.9 (d, 2J = 252.8 Hz, 1F) ppm;

$\bar{\nu}$ (neat) = 2974, 2935, 1766, 1699, 1433, 1178, 1054, 970, 843 cm^{-1} ;

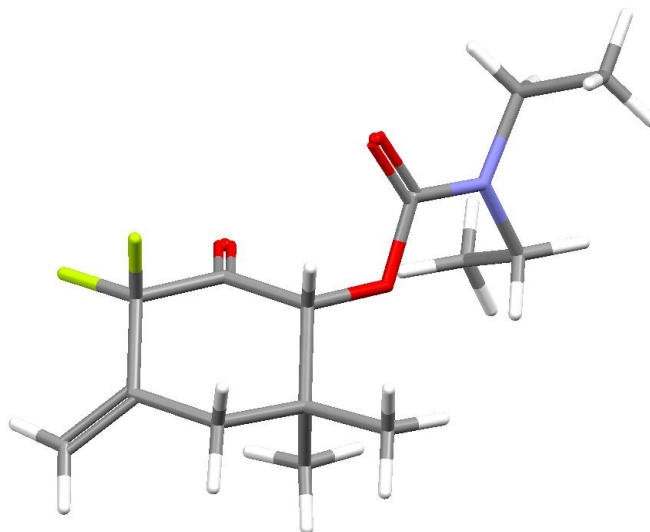
HRMS (EI-MS): calcd for $\text{C}_{14}\text{H}_{22}\text{F}_2\text{NO}_3$, 290.1562 $[\text{M}+\text{H}]^+$, found: 290.1563;

MS (CI): m/z (%): 318 (3) $[\text{M}+\text{C}_2\text{H}_5]^+$, 290 (28) $[\text{M}+\text{H}]^+$, 100 (100) $[\text{CONEt}_2]$;

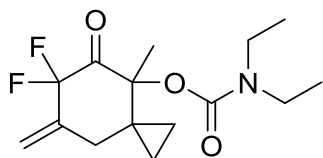
t_R (GC) = 12.80 minutes;

elemental analysis calcd (%) for $\text{C}_{14}\text{H}_{21}\text{F}_2\text{NO}_3$: C, 58.12; H, 7.32; N, 4.84; found: C, 57.47; H, 7.30; N, 4.87.

The identity of this ketone (**113c**) was confirmed by XRD analysis (m.p. = 79-80 °C (pentane)); Crystal data for **113c**: $\text{C}_{14}\text{H}_{21}\text{F}_2\text{NO}_3$, crystal size 0.45 x 0.40 x 0.35 mm^3 , M = 289.32, monoclinic, space group $\text{P}2_1/\text{c}$, unit cell dimensions a = 10.1058(3), b = 13.9164(3), c = 11.7612(4) Å, α = 90°, β = 110.367(3)°, γ = 90°, V = 1550.64(8) Å³, Z = 4, D_{calc} = 1.239 Mg m^{-3} , $F(000)$ = 616, $\mu(\text{Mo-K}\alpha)$ = 0.102 mm^{-1} , T = 123(2) K, 12336 total reflections measured, 4041 independent, (R_{int} = 0.0167). Final R indices (for reflections with $I > 2\sigma(I)$) were $R1$ = 0.0341, $\omega R2$ = 0.0933; R indices (all data) $R1$ = 0.0464, $\omega R2$ = 0.0964.



6,6-Difluoro-4-methyl-7-methylene-5-oxospiro[2.5]octan-4-yl diethylcarbamate (113d)



Ketone (**113d**) was prepared by general procedure B from **112d** (0.513 g, 1.23 mmol) with palladium(II) acetate (10 mol %, 0.0276 g) and copper(I) chloride (100 mol %, 0.122 g) in acetonitrile (6.6 mL) that had been sparged with air for thirty minutes through a drawn out pipette. The usual work-up, according to **113a**, afforded a pale yellow oil which was triturated with pentane and dried in a vacuum oven (40 °C, 0.75 mmHg, 48 hours) to afford **113d** as a light tan-coloured granular amorphous solid (0.247 g, 67 %).

$R_f = 0.30$ (20 % ethyl acetate in hexane);

$^1\text{H NMR}$ (400 MHz, CDCl_3): $\delta = 5.56$ (br. d, $^4J_{\text{H-F}} = 5.2$ Hz, 1H), 5.15 (app. q, $^4J_{\text{H-F}} = 2.2$, $^4J = 2.2$ Hz, 1H), 3.48-3.10 (m, 5H), 1.56 (dd, $^2J = 14.4$, $^4J_{\text{H-F}} = 3.7$ Hz, 1H), 1.29 (s, 3H), 1.19 (t, $J = 7.2$ Hz, 3H), 1.14 (t, $J = 7.2$ Hz, 3H), 1.00-0.92 (m, 1H), 0.67-0.59 (m, 1H), 0.59-0.52 (m, 1H), 0.34-0.25 (m, 1H) ppm;

$^{13}\text{C NMR}$ (100 MHz, CDCl_3): $\delta = 193.1$ (dd, $^2J_{\text{C-F}} = 27.1, 23.2$ Hz), 154.8, 140.1 (t, $^2J_{\text{C-F}} = 20.7$ Hz), 115.1 (t, $^3J_{\text{C-F}} = 7.9$ Hz), 114.1 (dd, $^1J_{\text{C-F}} = 258.9, 250.9$ Hz), 84.6, 42.1, 41.5, 37.2 (d, $^3J_{\text{C-F}} = 3.6$ Hz), 26.4, 15.1, 14.1, 13.2, 9.9, 9.4 ppm;

$^{19}\text{F NMR}$ (376 MHz, CDCl_3): $\delta = -99.4$ (d, $^2J = 247.4$ Hz, 1F), -121.4 (d, $^2J = 247.7$ Hz, 1F) ppm (the ^{19}F - ^1H splittings are not resolved in the 376 MHz $^{19}\text{F NMR}$ spectrum);

$\bar{\nu}$ (neat) = 2978, 2937, 1745, 1692, 1428, 1284, 1115, 768 cm^{-1} ;

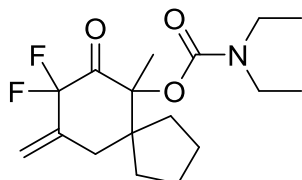
HRMS (NSI-ES): calcd for $\text{C}_{15}\text{H}_{22}\text{F}_2\text{NO}_3$, 302.1562 $[\text{M}+\text{H}]^+$, found: 302.1565;

MS (CI): m/z (%): 330 (2) $[\text{M}+\text{C}_2\text{H}_5]^+$, 302 (20) $[\text{M}+\text{H}]^+$, 100 (100) $[\text{CONEt}_2]^+$;

t_R (GC) = 13.59 minutes;

elemental analysis calcd (%) for $C_{15}H_{21}F_2NO_3$: C, 59.79; H, 7.02; N, 4.65; found: C, 59.14; H, 6.99; N, 4.24. This analysis was obtained for the amorphous solid obtained following chromatography so no melting point was recorded.

8,8-Difluoro-6-methyl-9-methylene-7-oxospiro[4.5]decan-6-yl diethylcarbamate (113e)



Ketone (**113e**) was prepared by general procedure B from **112e** (0.416 g, 0.91 mmol) with palladium(II) acetate (10 mol %, 0.0204 g) and copper (I) chloride (100 mol %, 0.091 g) in acetonitrile (4.9 mL) that had been sparged with air for thirty minutes through a drawn out pipette. The usual work-up, according to **113a**, afforded a colourless oil which was triturated with pentane and dried in a vacuum oven (40 °C, 0.75 mmHg, 48 hours) to afford **113e** as a colourless granular amorphous solid (0.216 g, 72 %).

R_f = 0.50 (40 % diethyl ether in hexane);

1H NMR (400 MHz, $CDCl_3$): δ = 5.58 (br. d, $^4J_{H-F}$ = 5.3 Hz, 1H), 5.19 (app. q, $^4J_{H-F}$ = 2.5, 4J = 2.5 Hz, 1H), 3.42-3.12 (m, 4H), 2.97 (br. d, 2J = 13.70 Hz, 1H), 2.11 (dd, 2J = 13.7, $^4J_{H-F}$ = 4.4 Hz, 1H), 2.08-1.97 (m, 1H), 1.78-1.44 (m, including 1.52 (s, 3H), 5H), 1.36-1.24 (m, 1H), 1.24-1.14 (m, including 1.17 (t, J = 7.0 Hz, 3H), 1H), 1.11 (t, J = 7.0 Hz, 3H) ppm;

^{13}C NMR (100 MHz, $CDCl_3$): δ = 194.4 (dd, $^2J_{C-F}$ = 26.1, 22.9 Hz), 154.7, 139.3 (t, $^2J_{C-F}$ = 20.2 Hz), 116.8 (t, $^3J_{C-F}$ = 7.9 Hz), 114.4 (dd, $^1J_{C-F}$ = 260.6, 250.8 Hz), 87.3, 52.5, 42.2, 41.6, 39.9 (d, $^3J_{C-F}$ = 4.1 Hz), 35.5, 30.9, 26.1, 25.8, 15.5, 14.2, 13.2 ppm;

^{19}F NMR (376 MHz, *d*-toluene, 363K): δ = -97.3 (d, 2J = 247.9 Hz, 1F), -123.1 (d, 2J = 247.9 Hz, 1F) ppm (the ^{19}F - 1H splitting was not resolved in the ^{19}F NMR spectrum).

$\bar{\nu}$ (neat) = 2956, 2872, 1740, 1697, 1422, 1125, 1076, 946 cm^{-1} ;

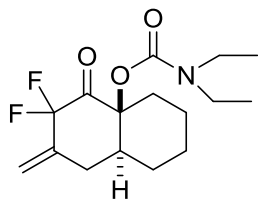
HRMS (NSI-ES): calcd for $C_{17}H_{26}F_2NO_3$, 330.1873 $[M+H]^+$, found: 330.1875;

MS (CI): m/z (%): 358 (3) $[M+C_2H_5]^+$, 330 (49) $[M+H]^+$, 100 (60) $[CONEt_2]$;

t_R (GC) = 15.03 minutes;

elemental analysis calcd (%) for $C_{17}H_{25}F_2NO_3$: C, 61.99; H, 7.65; N, 4.25; found: C, 61.94; H, 7.89; N, 4.20. This analysis was obtained for the amorphous solid obtained following chromatography so no melting point was recorded.

(4aS*,8aS*)-3,3-Difluoro-2-methylene-4-oxooctahydronaphthalen-4a(2H)-yl diethylcarbamate (113f)



Ketone (**113f**) was prepared by general procedure B from *cis/trans*-**112f** (0.524g, 1.22 mmol) with palladium(II) acetate (5 mol %, 0.0137 g) and copper(I) chloride (100 mol %, 0.121 g) in acetonitrile (6.6 mL) that had been sparged with air for thirty minutes through a drawn out pipette. The usual work-up, according to **113a**, afforded a pale yellow oil which was triturated with pentane and dried in a vacuum oven (40 °C, 0.75 mmHg, 48 hours) to afford **113f** as a colourless crystalline solid (0.272 g, 71 %).

NB When the reaction was run in acetonitrile (6.6 mL) that had been sparged with air for thirty minutes through a drawn out pipette under balloon pressure of oxygen the reaction was complete in 5.5 hours. The usual work up afforded a pale yellow oil which was triturated with pentane and dried in a vacuum oven (40 °C, 0.75 mmHg, 48 hours) to afford **113f** as a colourless crystalline solid (0.212 g, 55 %).

m.p. = 56-58 °C (recrystallised from pentane as a colourless plate);

R_f = 0.48 (40 % diethyl ether in hexane);

^1H NMR (400 MHz, CDCl_3): δ = 5.53 (br. d, $^4J_{\text{H-F}} = 5.50$ Hz, 1H), 5.23 (app. q, $^4J = 2.5$, $^4J_{\text{H-F}} = 2.50$ Hz, 1H), 3.52-3.15 (m, 4H), 2.67 (br. t, $J = 13.3$, $^2J = 13.3$ Hz, 1H), 2.48-2.35 (m, 1H), 2.20 (1H, dt, $^2J = 13.3$, $^4J_{\text{H-F}} = 4.0$, $J = 4.0$ Hz, 1H), 1.84-1.25 (m, 8H), 1.22 (t, $J = 7.3$ Hz, 3H), 1.12 (t, $J = 7.3$ Hz, 3H) ppm;

^{13}C NMR (100 MHz, CDCl_3): δ = 194.2 (dd, $^2J_{\text{C-F}} = 25.9$, 22.6 Hz), 153.9, 140.3 (dd, $^2J_{\text{C-F}} = 21.8$, 19.2 Hz), 114.8 (dd, $^3J_{\text{C-F}} = 9.2$, 6.7 Hz), 114.1 (dd, $^1J_{\text{C-F}} = 261.5$, 250.8 Hz), 82.4, 45.9, 41.7, 41.1 33.2 (d, $^3J_{\text{C-F}} = 3.9$ Hz), 27.8, 27.7, 24.4, 19.7, 13.7, 12.7 ppm;

^{19}F NMR (376 MHz, CDCl_3): δ = -97.7 (dddd, $^2J = 244.1$ Hz, $^4J_{\text{F-H}} = 5.5$, 4.0, 2.5 Hz, 1F), -124.8 (dt, $^2J = 244.1$, $^4J_{\text{F-H}} = 3.4$ Hz, 1F) ppm;

$\bar{\nu}$ (neat) = 2934, 1745, 1693, 1429, 1284, 1169, 1071 cm^{-1} ;

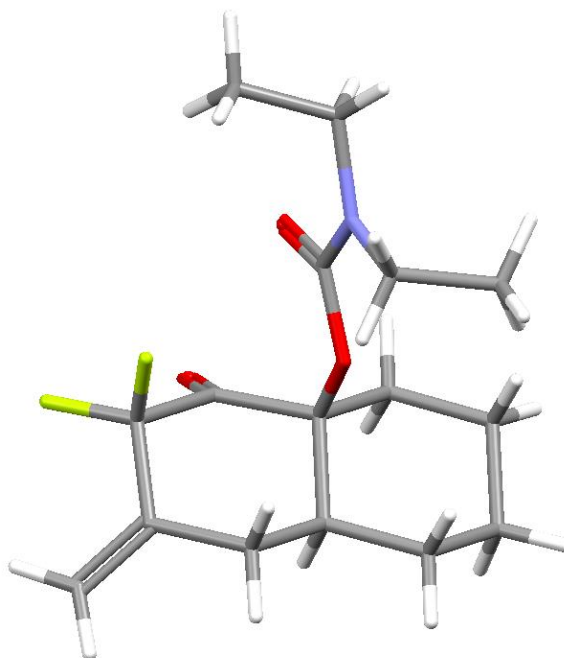
HRMS (EI-MS): calcd for $\text{C}_{16}\text{H}_{24}\text{F}_2\text{NO}_3$, 316.1719 $[\text{M}+\text{H}]^+$, found: 316.1712;

MS (CI): m/z (%): 344 (6) $[\text{M}+\text{C}_2\text{H}_5]^+$, 316 (74) $[\text{M}+\text{H}]^+$, 100 (64) $[\text{CONEt}_2]$;

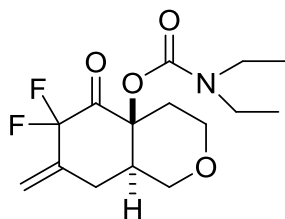
t_R (GC) = 14.80 minutes;

elemental analysis calcd (%) for C₁₆H₂₃F₂NO₃: C, 60.94; H, 7.35; N, 4.44; found: C, 60.58; H, 7.17; N, 4.26. This analysis was obtained for the amorphous solid obtained following chromatography so no melting point was recorded.

The identity of this ketone (**113f**) was confirmed by XRD analysis (m.p. = 100-102 °C (pentane)); Crystal data for **113f**: C₁₆H₂₃F₂NO₃, crystal size 0.25 x 0.10 x 0.03 mm³, *M* = 315.35, monoclinic, space group P2₁/c, unit cell dimensions *a* = 14.1022(6), *b* = 10.8667(4), *c* = 11.1450(5) Å, α = 90°, β = 106.851(4)°, γ = 90°, *V* = 1634.57(11) Å³, *Z* = 4, *D*_{calc} = 1.281 Mg m⁻³, *F*(000) = 672, μ(Mo-Kα) = 0.865 mm⁻¹, *T* = 123(2) K, 6606 total reflections measured, 3202 independent, (*R*_{int} = 0.0199). Final *R* indices (for reflections with *I* > 2σ(*I*)) were *R*1 = 0.0486, ω*R*2 = 0.1319; *R* indices (all data) *R*1 = 0.0534, ω*R*2 = 0.1377.



(4a*S,8a*R**)-6,6-Difluoro-7-methylene-5-oxooctahydro-4a*H*-isochromen-4a-yl diethylcarbamate (**113g**)**



Ketone (**113g**) was prepared by general procedure B from *trans*-**112g** (0.432 g, 1.00 mmol) with palladium(II) acetate (5 mol %, 0.0112 g) and copper(I) chloride (100 mol %, 0.099 g) in acetonitrile (5.5 mL) that had been sparged with air for thirty minutes through a drawn out pipette. The usual work-up, according to **113a**, afforded a pale yellow oil which was triturated with pentane and dried in a vacuum oven (40 °C, 0.75 mmHg, 48 hours) to afford **113g** as a light-tan coloured granular solid (0.285 g, 90 %). m.p. = 96-98 °C (recrystallised from pentane as a tanned plate);

R_f = 0.17 (20 % ethyl acetate in hexane);

^1H NMR (400 MHz, CDCl_3): δ = 5.61 (br. d, $^4J_{\text{H-F}} = 5.0$ Hz, 1H), 5.31 (q, $^4J = 2.5$, $^4J_{\text{H-F}} = 2.5$ Hz, 1H), 4.00-2.90 (m, 1H), 3.83 (dd, $^2J = 11.3$, $J = 4.7$ Hz, 1H), 3.72-3.55 (m, 2H), 3.46-3.15 (m, 4H), 2.59 (br. t, $J = 13.6$, $^2J = 13.6$ Hz, 1H), 2.33-2.14 (m, 3H), 1.26 (t, $J = 7.6$ Hz, 3H), 1.15 (t, $J = 7.6$ Hz, 3H) ppm;

^{13}C NMR (100 MHz, CDCl_3): δ = 192.2 (dd, $^2J_{\text{C-F}} = 26.6$, 23.6 Hz), 153.6, 139.4 (t, $^2J_{\text{C-F}} = 20.6$ Hz), 116.0 (dd, $^3J_{\text{C-F}} = 9.2$, 6.4 Hz), 113.8 (dd, $^1J_{\text{C-F}} = 262.2$, 251.3 Hz), 79.9, 66.1, 62.3, 45.0, 41.9, 41.2, 28.4, 28.1 (d, $^3J_{\text{C-F}} = 3.9$ Hz), 13.8, 12.6 ppm;

^{19}F NMR (376 MHz, CDCl_3): δ = -97.1 (dddd, $^2J = 246.6$ Hz, $^4J_{\text{F-H}} = 5.0$, 4.2, 2.5 Hz, 1F), -124.1 (dt, $^2J = 246.6$, $^4J_{\text{F-H}} = 3.0$ Hz, 1F) ppm;

$\bar{\nu}$ (neat) = 2961, 2878, 1751, 1693, 1433, 1076, 760 cm^{-1} ;

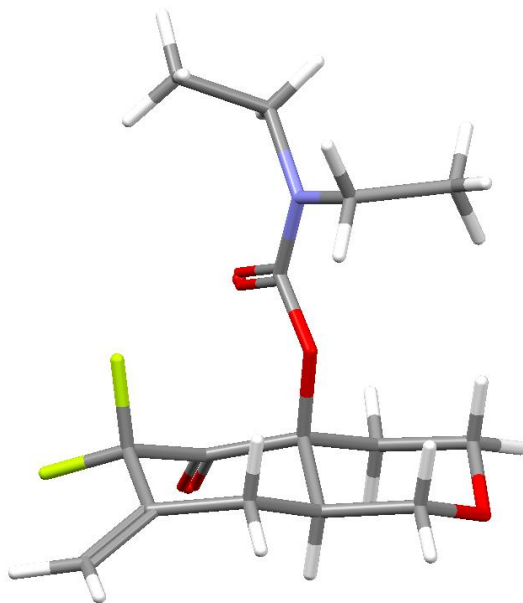
HRMS (NSI-ES): calcd for $\text{C}_{15}\text{H}_{22}\text{F}_2\text{NO}_4$, 318.1511 $[\text{M}+\text{H}]^+$, found: 318.1512;

MS (CI): m/z (%): 346 (12) $[\text{M}+\text{C}_2\text{H}_5]^+$, 318 (100) $[\text{M}+\text{H}]^+$, 100 (58) $[\text{CONEt}_2]$;

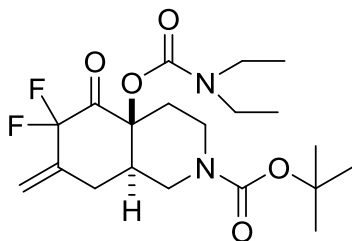
t_R (GC) = 14.81 minutes;

elemental analysis calcd (%) for $\text{C}_{15}\text{H}_{21}\text{F}_2\text{NO}_4$: C, 56.77; H, 6.67; N, 4.41; found: C, 56.60; H, 6.58; N, 4.29.

The identity of this ketone (**113g**) was confirmed by XRD analysis (m.p. = 100-102 °C (diethyl ether)). Crystal Data for **113g**: C₁₅H₂₁F₂NO₄, crystal size 0.40 x 0.20 x 0.15mm³, *M* = 317.33, monoclinic, space group P2₁/n, unit cell dimensions *a* = 6.9457(7)Å, *b* = 9.2125(10)Å, *c* = 24.170(3)Å, $\alpha = 90^\circ$, $\beta = 94.349(11)^\circ$, $\gamma = 90^\circ$, *V* = 1542.1(3)Å³, *Z* = 4, $\rho_{\text{calc}} = 1.367 \text{Mg m}^{-3}$, *F*(000) = 672, $\mu(\text{Mo-K}\alpha) = 0.114 \text{mm}^{-1}$, *T* = 123(2)K, 7683 reflections measured, 3609 independent, (*R*_{int} = 0.0331]. Final *R* indices [*I* > 2σ(*I*)] *R*1 = 0.0467, ω*R*2 = 0.1032; *R* indices (all data) *R*1 = 0.0652, ω*R*2 = 0.1180.



tert-Butyl (4*aS**,8*aR**)-4a-((diethylcarbamoyl)oxy)-6,6-difluoro-7-methylene-5-oxooctahydroisoquinoline-2(1*H*)-carboxylate (**113h**)



Ketone (**113h**) was prepared by general procedure B from *cis/trans*-**112h** (0.534g, 1.0 mmol) with palladium(II) acetate (5 mol %, 0.0112 g) and copper(I) chloride (100 mol %, 0.099 g) in acetonitrile (5.5 mL) that had been sparged with air for thirty minutes through a drawn out pipette. The usual work-up, according to **113a**, afforded a colourless oil which was triturated with pentane and dried in a vacuum oven (40 °C, 0.75 mmHg, 48 hours) to afford **113h** as a colourless granular amorphous solid (0.302 g, 73 %).

m.p. = 112-114 °C (recrystallised from diethyl ether as colourless needles);

R_f = 0.28 (20 % ethyl acetate in hexane);

¹H NMR (400 MHz, CDCl₃, 323K): δ = 5.57 (br. d, ⁴J_{H-F} = 5.3 Hz, 1H), 5.27 (app. q, ⁴J = 2.4, ⁴J_{H-F} = 2.4 Hz, 1H), 4.35-3.88 (m, 2H), 3.54-3.07 (m, 4H), 2.89 (br. t, ²J = 13.0, J = 13.0 Hz, 2H), 2.63 (br. t, ²J = 13.0, J = 13.0 Hz, 1H), 2.35 (dt, ²J = 14.6, ⁵J_{H-F} = 2.3 Hz, 1H), 2.26 (dt, ²J = 14.0, J = 4.0, ⁴J_{H-F} = 4.0 Hz, 1H), 1.98 (app. td, ²J = 14.1, J = 14.1, J = 5.3 Hz, 1H), 1.72 (app. tt, J = 13.0, J = 4.1 Hz, 1H), 1.46 (s, 9H), 1.22 (t, J = 7.2 Hz, 3H), 1.13 (t, J = 7.2 Hz, 3H) ppm;

¹³C NMR (100 MHz, CDCl₃, 323K): δ = 192.6 (dd, ²J_{C-F} = 26.5, 23.6 Hz), 154.5, 154.0, 139.8 (t, ²J_{C-F} = 21.2 Hz), 116.3 (dd, ³J_{C-F} = 9.3, 6.8 Hz), 114.3 (dd, ¹J_{C-F} = 261.5, 250.9 Hz), 81.2, 80.2, 45.1, 43.7, 42.4, 41.6, 38.7, 30.3 (d, ³J_{C-F} = 4.0 Hz), 28.3, 14.1, 13.0 ppm;

¹⁹F NMR (376 MHz, CDCl₃): δ = -97.6 (d, ²J = 245.2 Hz, 1F), -124.6 (d, ²J = 245.5 Hz, 1F) ppm (the ¹⁹F-¹H splitting was not resolved in the ¹⁹F NMR spectrum); the ¹⁹F NMR gave a clear well resolved spectrum at RT and did not require heating. ¹H and ¹³C NMR resolved slightly better when heated to 323K;

$\bar{\nu}$ /(neat) = 2978, 2861, 1755, 1418, 1171, 1067 cm⁻¹;

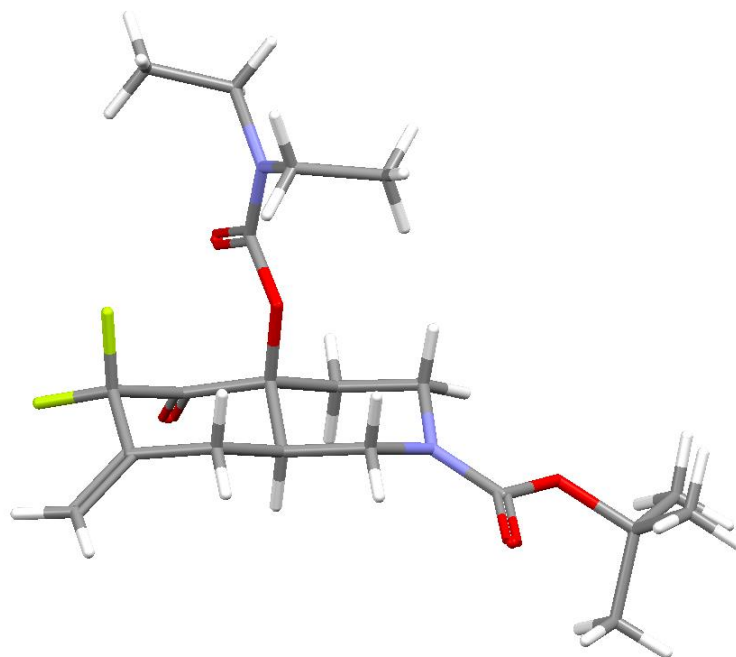
HRMS (NSI-ES): calcd for C₂₀H₃₁F₂N₂O₅, 417.2196 [M+H]⁺, found: 417.2185;

MS (NSI-ES): m/z (%): 417 (100) [M+H]⁺;

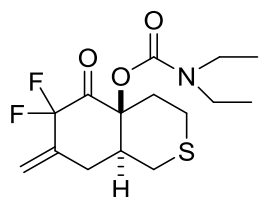
t_R (GC) = 11.31 minutes;

elemental analysis calcd (%) for C₂₀H₃₀F₂N₂O₅: C, 57.68; H, 7.26; N, 6.73; found: C, 57.38; H, 7.25; N, 6.37.

The identity of this ketone (**113h**) was confirmed by XRD analysis (m.p. = 112-114 °C (diethyl ether)). Crystal Data for **113h**: C₂₀H₃₀F₂N₂O₅ crystal size size 0.42 x 0.11 x 0.01mm³, M = 416.46, monoclinic, space group P21/c, unit cell dimensions a = 18.5262(8)Å, b = 9.2405(3)Å, c = 12.7026(5)Å, α = 90°, β = 102.088(4)°, γ = 90°, V = 2126.36(14)Å³, Z = 4, ρ_{calc} = 1.301Mg m⁻³, F(000) = 888, μ(Mo-Kα) = 0.104mm⁻¹, T = 100(2)K. Crystal was twinned by a 180 ° rotation about 1 0 0 . The measured data was thus processed to give a hklf 5 formatted file containing 6337 reflections. The BASF refined to 0.2522(14). Final R indices [I > 2σ(I)] R1 = 0.0946, ωR2 = 0.1864; R indices (all data) R1 = 0.1076, ωR2 = 0.1916. The resulting structure is of relatively low quality but is adequate for the assignment of the trans ring junction stereochemistry.



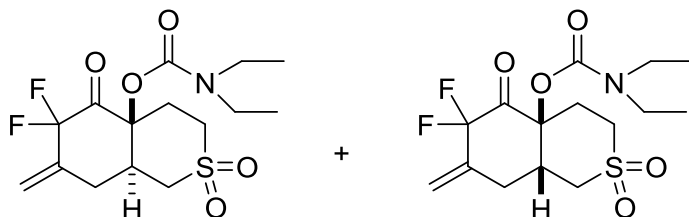
Attempted preparation of (4a*S,8a*S**)-6,6-Difluoro-7-methylene-5-oxooctahydro-4a*H*-isothiochromen-4a-yl diethylcarbamate (**113i**)**



Palladium(II) acetate (5 mol %, 0.0138 g) and copper(I) chloride (100 mol %, 0.122 g) were suspended in dry acetonitrile (4 mL) that had been sparged with air for 30 minutes through a drawn out pipette. The suspension was warmed to 70 °C then a solution of silyl enol ether **112i** (1.23 mmol, 0.553 g) in dry acetonitrile (2.6 mL) added via syringe in a constant stream. The mixture was then stirred at 70 °C for 144 hours under an air condenser and open to the atmosphere. The reaction mixture was concentrated and transferred by pipette onto a plug of celite. The crude material was eluted from the celite with diethyl ether (50 mL). The crude material was taken up in diethyl ether (10 mL) and PhosphonicS STA3 scavenger silica was added. The mixture was stirred for 30 minutes, then the mixture filtered through a 20µm polyethylene frit and washed with diethyl ether (50 mL). The solvent was removed under reduced pressure to afford a complex mixture by ¹⁹F NMR in which **112i** had been fully consumed but only trace amounts of **113i** could be detected with characteristic signals at -98.6 (d, ²J = 245.8 Hz, 1F), -124.8 (d, ²J = 245.8 Hz, 1F) ppm.

(4a*S,8a*S**)-6,6-Difluoro-7-methylene-2,2-dioxido-5-oxooctahydro-4a*H*-isothiochromen-4a-yl diethylcarbamate (*trans*-**113j**) and (4a*S**,8a*R**)-6,6-difluoro-**

**7-methylene-2,2-dioxido-5-oxooctahydro-4aH-isothiochromen-4a-yl
diethylcarbamate (*cis*-113j)**



Ketone (as a mixture of *trans*-113j and *cis*-113j) was prepared by general procedure B from *cis/trans*-112j (0.508 g, 1.05 mmol) with palladium(II) acetate (5 mol %, 0.0118 g) and copper(I) chloride (100 mol %, 0.104g) in acetonitrile (5.6 mL) that had been sparged with air for thirty minutes through a drawn out pipette. The usual work-up, according to 113a, afforded a pale yellow solid which was recrystallized with dichloromethane/hexane and dried in a vacuum oven (40 °C, 0.75 mmHg, 48 hours) to afford an inseparable mixture of *trans*-113j and *cis*-113j (0.17 g, 44 %, 87:13) as pale yellow crystalline needles.

m.p. = 180-182 °C (dichloromethane/hexane);

R_f = 0.29 (40 % ethyl acetate in hexane);

The following signals were attributed to both the minor *cis*-diastereoisomer 113j and major *trans*-diastereoisomer 113j ¹H NMR (400 MHz, CDCl₃): δ = 3.45-2.27 (env, 24H), 1.28-1.07 (m, 12H);

The following signals were attributed to the major *trans*-diastereoisomer 113j (assigned on the basis of δ and intensity) ¹H NMR (400 MHz, CDCl₃): δ = 5.72 (app. d, ⁴J_{H-F} = 3.30 Hz, 1H), 5.37 (br. s, 1H), 3.65-3.48 (m, 1H), 2.24-2.08 (m, 1H) ppm;

¹³C NMR (100 MHz, CDCl₃): δ = 192.0 (t, ²J_{C-F} = 25.7 Hz), 153.4, 136.6 (t, ²J_{C-F} = 20.5 Hz), 118.8 (t, ³J_{C-F} = 7.2 Hz), 113.1 (t, ¹J_{C-F} = 257.0Hz), 79.9, 49.8, 47.5, 42.0, 41.3, 40.5, 31.5, 29.2, 13.6, 12.6 ppm;

¹⁹F NMR (376 MHz, (CD₃)₂SO, 373 K): δ = -105.6 (br. d, ²J = 249.3 Hz, 1F), -110.3 (br. d, ²J = 249.3 Hz, 1F) ppm (the ¹⁹F-¹H splittings are not resolved in the 376 MHz ¹⁹F NMR spectrum);

The following signals were attributed to the minor *cis*-diastereoisomer 113j (assigned on the basis of δ and intensity) ¹H NMR (400 MHz, CDCl₃): δ = 5.65 (br. d, ⁴J_{H-F} = 5.00 Hz, 1H), 5.30 (s, 1H);

¹³C NMR (100 MHz, CDCl₃): δ = 152.9, 137.2 (t, ²J_{C-F} = 21.1 Hz), 117.6 (t, ³J_{C-F} = 7.1 Hz), 79.0, 51.1, 45.8, 43.3, 42.2, 41.4, 32.0 (d, ³J_{C-F} = 4.4 Hz), 27.0, 13.8, 12.5 ppm;

^{19}F NMR (376 MHz, $(\text{CD}_3)_2\text{SO}$, 373 K): $\delta = -97.3$ (dddd, $^2J = 242.9$, $^4J_{\text{F-H}} = 5.0, 3.3, 2.5$ Hz, 1F), -123.0 (d, $^2J = 242.9$ Hz, 1F) ppm;

$\bar{\nu}$ (neat) = 2978, 2941, 1740, 1698, 1433, 1318, 1288, 1133, 1098 cm^{-1} ;

HRMS (NSI-ES): calcd for $\text{C}_{15}\text{H}_{22}\text{F}_2\text{NO}_5\text{S}$, 366.1181 $[\text{M}+\text{H}]^+$, found: 366.1183;

Major *trans*- diastereoisomer **113j**

MS (CI): m/z (%): 394 (14) $[\text{M}+\text{C}_2\text{H}_5]^+$, 366 (100) $[\text{M}+\text{H}]^+$, 100 (100) $[\text{CONEt}_2]$;

t_{R} (GC) = 16.66 minutes;

Minor *cis*- diastereoisomer **113j**

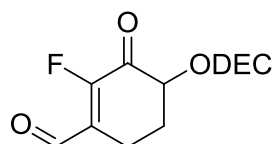
MS (CI): m/z (%): 394 (15) $[\text{M}+\text{C}_2\text{H}_5]^+$, 366 (100) $[\text{M}+\text{H}]^+$, 100 (100) $[\text{CONEt}_2]$;

t_{R} (GC) = 16.84 minutes;

satisfactory elemental analysis could not be obtained for this compound; calcd (%) for $\text{C}_{15}\text{H}_{21}\text{F}_2\text{NO}_5\text{S}$: C, 49.31; H, 5.79; N, 3.83; found: C, 48.84; H, 5.49; N, 3.74.

6.2.4 Synthesis of reverse Wacker oxidation product.

3-Fluoro-4-formyl-2-oxocyclohex-3-en-1-yl diethylcarbamate (**150**)



Palladium(II) acetate (10 mol %, 0.0224 g) and copper(I) chloride (100 mol % 0.099 g) were suspended in dry acetonitrile (4 mL) that had been sparged with oxygen through a drawn out pipette. The resulting mixture was stirred at 70 °C for 5 minutes then a solution of difluorinated silyl enol ether **112b** (0.377 g, 1 mmol) in acetonitrile (1.4 mL) was added in a stream *via* syringe. The suspension was stirred at this temperature for 48 hours under an air condenser and open to the atmosphere. The reaction mixture was then concentrated under reduced pressure and diethyl ether (20 mL) was added. The resulting suspension was transferred by pipette onto a plug of celite (3.4 g) and the crude product eluted by washing with diethyl ether (60 mL). The mixture was placed over 3-mercaptopropyl ethyl sulfide silica (SPM32, 0.79 g) and the mixture was stirred for 30 minutes before being filtered through a 20 μm polyethylene frit and the silica washed with diethyl ether (50 mL). The ether phases were combined and evaporated to dryness under reduced pressure to afford a viscous orange oil. The crude product was purified by flash column chromatography (8g cartridge, 20 % acetone in hexane) to afford **150** as a pale orange oil (0.0214 g, 8 %).

$R_f = 0.37$ (30 % acetone in hexane);

^1H NMR (400 MHz, CDCl_3): δ = 10.36 (s, 1H), 5.43 (dd, J = 13.4, 5.2 Hz, 1H), 3.55-3.15 (m, 4H), 2.90-2.73 (m, 1H), 2.57-2.46 (m, 1H), 2.45-2.36 (m, 1H), 2.24-2.06 (m, 1H), 1.18 (t, J = 6.84 Hz, 6H) ppm;

^{13}C NMR (100 MHz, CDCl_3): δ = 189.8 (d, $^2J_{\text{C-F}}$ = 20.2 Hz), 188.8 (d, $^3J_{\text{C-F}}$ = 10.1 Hz), 157.2 (d, $^1J_{\text{C-F}}$ = 288.3 Hz), 154.3, 129.7, 74.3 (d, $^3J_{\text{C-F}}$ = 5.3 Hz), 42.3, 41.5, 27.8, 17.9, 13.9, 13.3 ppm;

^{19}F NMR (373 MHz, CDCl_3): δ = -131.1 (t, $^4J_{\text{F-H}}$ = 6.8 Hz) ppm;

$\bar{\nu}$ /(neat) = 2974, 2876, 1682, 1428, 1271, 1169, 1065 cm^{-1} ;

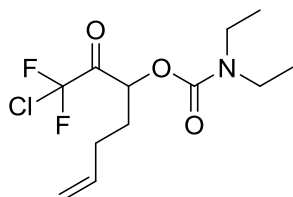
HRMS (NSI): calcd for $\text{C}_{18}\text{H}_{33}\text{F}_2\text{NO}_3\text{Si}$, 258.1136 $[\text{M}+\text{H}]^+$, found: 258.1138;

MS (CI): m/z (%): 286 (3) $[\text{M}+\text{C}_2\text{H}_5]^+$, 258 (10) $[\text{M}+\text{H}]^+$, 100 (100) $[\text{CONEt}_2]$;

t_{R} (GC) = 13.64 minutes;

UV/Vis (MeCN): λ^{max} (ϵ) = 257 nm (53 170).

6.2.5 Synthesis of 1-chloro-1,1-difluoro-2-oxo-3-(*N,N*-diethylcarbamoyloxy)-hepta-1,6-diene (**157**)



Chlorodifluoromethylketone **157** was prepared according to the method of Ito and co-workers.¹⁷⁸ CuCl_2 was dried by heating to 150 °C for 48 hours. Silyl enol ether **112b** was added to a solution of CuCl_2 (0.403 g, 3 mmol) in freshly distilled DMF (4 mL) (0.377 g, 1 mmol) dropwise at room temperature. The mixture was stirred at room temperature for 3 hours and at 50 °C for 0.5 hours and then quenched with ice-cold water (15 mL). The mixture was extracted with diethyl ether (4 x 20 mL) and washed with 5% Aqueous HCl (15 mL) and brine (15 mL). The organic extracts were dried with MgSO_4 and concentrated under reduced pressure to afford the crude product as a dark red oil (0.262 g). The residue was purified by Kugelrohr distillation. Impurities were distilled off (7 mbar, 134 °C) to afford **157** as a dark red oil (0.151 g, 51 %)

R_f = 0.29 (40 % diethyl ether in hexane);

^1H NMR (400 MHz, CDCl_3): δ = 5.81 (ddt, J = 17.9, 12.5, 5.5 Hz, 1H), 5.40 (dd, J = 8.5, $^4J_{\text{H-F}}$ = 3.8 Hz, 1H), 5.16-4.98 (m, 2H), 3.52-3.14 (m, 4H), 2.34-2.14 (m, 2H), 2.13-1.87 (m, 2H), 1.29-1.03 (m, 6H) ppm;

^{13}C NMR (100 MHz, CDCl_3): δ = 189.7 (t, $^2J_{\text{C-F}}$ = 29.5 Hz), 154.4, 136.1, 119.6 (t, $^1J_{\text{C-F}}$ = 307.3 Hz), 116.3, 73.3, 42.2, 41.5, 30.1, 29.3, 13.9, 13.3 ppm;

^{19}F NMR (373 MHz, CDCl_3): $\delta = -64.9, -65.1$ (AB_q , $J_{\text{AB}} = 166.8$ Hz, 2F) ppm (The ^{19}F - ^1H splitting was not resolved in the ^{19}F NMR)

$\bar{\nu}$ (neat) = 2980, 2937, 1668, 1431, 1273, 1169, 1130, 916, 767 cm^{-1} ;

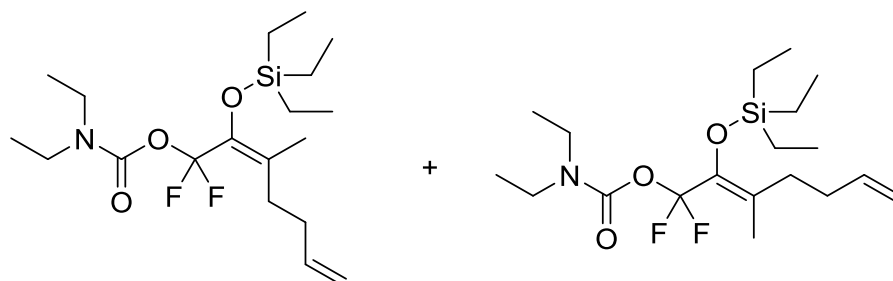
HRMS [NSI (M+H) found: 298.1019, Calc. for $\text{C}_{12}\text{H}_{19}^{35}\text{ClF}_2\text{NO}_3$: 298.1016];

MS (CI): m/z (%): 326 (22) [$\text{M}+\text{C}_2\text{H}_5$] $^+$, 298 (88) [$\text{M}+\text{H}$] $^+$, 262 (19) [$\text{M}-\text{Cl}$], 100 (100) [CONEt_2];

t_{R} (GC) = 11.65 minutes;

6.2.6 Synthesis of rearrangements products

1,1-Difluoro-2-(triethylsilyloxy)-1-(*N,N*-diethylcarbamoyloxy)-3-methyl hepta-2*E*,6-diene (163a) and **1,1-difluoro-2-(triethylsilyloxy)-1-(*N,N*-diethylcarbamoyloxy)-3-methyl hepta-2*Z*,6-diene (163b)**.



A solution of **112a** (0.391 g, 1 mmol) in toluene (2.5 mL) was irradiated at 120 °C for 8 hours in a sealed microwave vial. The tube was cooled to room temperature and the vial cap was pierced with a syringe containing a dry scrub (KF). Cold sodium hydrogen carbonate (5 mL of a saturated aqueous solution) was then added to the vial via syringe. The quenched reaction mixture was stirred for 5 minutes then the vial was opened and the solution was extracted with toluene (3 x 3 mL). The combined organic extracts were dried (MgSO_4), filtered and concentrated under reduced pressure to afford a pale orange oil (0.258 g). The crude product was purified by flash column chromatography (40 g cartridge, 7 % diethyl ether in hexane) to afford an inseparable mixture of **163a** and **163b** as a colourless oil (0.159 g, 41 %, 77:23).

$R_f = 0.45$ (20 % diethyl ether in hexane);

^1H NMR (400 MHz, CDCl_3): $\delta = 5.73$ (dddd, $J = 17.0, 10.1, 7.0, 6.0$ Hz, 1H), 5.16-4.88 (m, 2H), 3.46-3.20 (m, 4H), 2.38-2.24 (m, 2H), 2.23-2.11 (m, 2H), 1.79 (t, $^5J_{\text{H-F}} = 2.6$ Hz, 3H, minor *Z*-diastereoisomer), 1.73 (t, $^5J_{\text{H-F}} = 2.3$ Hz, 3H, major *E*-diastereoisomer), 1.16 (t, $J = 7.2$ Hz, 6H), 0.99 (t, $J = 7.9$ Hz, 9H), 0.73 (q, $J = 7.9$ Hz, 6H) ppm;

Major *E*-diastereoisomer **163a** (assigned on the basis of δ and intensity) ^{13}C NMR (100 MHz, CDCl_3): $\delta = 149.1, 137.7, 136.3$ (t, $^2J_{\text{C-F}} = 32.9$ Hz), 121.3 (t, $^3J_{\text{C-F}} = 3.1$ Hz),

119.2 (t, $^1J_{C-F} = 265.4$ Hz), 114.1, 41.2, 31.9, 30.5 (t $^4J_{C-F} = 3.1$ Hz), 16.8, *13.4, *12.5, 6.1, 4.7 ppm;

^{19}F NMR (373 MHz, CDCl_3): $\delta = -66.9$ (s) ppm (the ^{19}F - ^1H splitting was not resolved in the ^{19}F NMR spectrum);

Minor *Z*-diastereoisomer **163b** (assigned on the basis of δ and intensity) ^{13}C NMR (100 MHz, CDCl_3): $\delta = 148.9, 137.6, 136.0$ (t, $^2J_{C-F} = 32.0$ Hz), 120.6 (t, $^3J_{C-F} = 3.1$ Hz), 119.1 (t, $^1J_{C-F} = 265.4$ Hz), 114.0, 41.3, 31.7, 30.6, 15.1 (t, $^4J_{C-F} = 3.00$ Hz), *13.4, *12.5, 6.2, 4.7 ppm;

^{19}F NMR (373 MHz, CDCl_3): $\delta = -67.6$ (s) ppm (the ^{19}F - ^1H splitting was not resolved in the ^{19}F NMR spectrum);

$\bar{\nu}$ /(neat) = 2958, 2880, 1740, 1072, 733 cm^{-1} ;

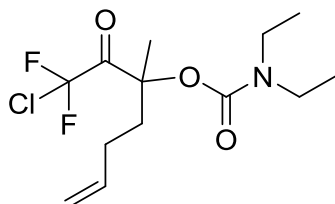
HRMS (NSI): calcd for $\text{C}_{19}\text{H}_{36}\text{F}_2\text{NO}_3\text{Si}$, 392.2427 $[\text{M}+\text{H}]^+$, found: 392.2421;

MS (CI): m/z (%): 392 (14) $[\text{M}+\text{H}]^+$, 350 (28) $[\text{M}-\text{C}_3\text{H}_5]$, 100 (100) $[\text{CONEt}_2]$;

t_R (GC) = 14.63 minutes;

*the signals at 13.4 and 12.5 are associated with the two CH_3 carbons of the DEC group in both diastereoisomers.

6.2.7 Synthesis of 1-Chloro-1,1-difluoro -3-(*N,N*-diethylcarbamoyloxy)-3-methylhepta-1,6-dien-2-one (**164**)



Chlorodifluoromethylketone **164** was prepared according to the method of Ito and co-workers.¹⁷⁸ Silyl enol ether **112a** (0.626 g, 1.6 mmol) was added dropwise to a solution of copper(II) chloride (1.000 g, 7.4 mmol) in freshly distilled DMF (6.4 mL) at room temperature. The mixture was stirred at room temperature for 3 hours then at 50 °C for 4 hours, then quenched with ice-water (50 mL). The mixture was extracted with diethyl ether (5 x 10 mL), then the extracts were combined and washed with hydrochloric acid (30 mL of a 5 % aqueous solution) followed by brine (30 mL). The combined organic extracts were dried (MgSO_4) and concentrated under reduced pressure to afford the crude product as a dark red oil (0.467 g). The residue was purified by flash column chromatography (40 g cartridge, 5-8 % diethyl ether in hexane) to afford **164** as a colourless oil (0.126 g, 25 %)

$R_f = 0.44$ (20 % diethyl ether in hexane);

this time. The mixture was quenched with saturated aqueous ammonium chloride (30 mL) and extracted with ethyl acetate (4 x 60mL). The combined organic extracts were dried (MgSO₄), filtered and concentrated to afford crude allylic alcohols **115aa** and **115ab** (3.23 g) as a dark brown oil. The material was taken up in dichloromethane and transferred by pipette to a glass sinter funnel (diameter 7.5 cm) containing a pad of silica (54 g). The product was then eluted from the plug with 70 % diethyl ether/hexane (600 mL). The solvent was evaporated under reduced pressure to afford the product as a pale orange oil (2.93 g). The crude allylic alcohol was purified by Kugelrohr distillation to afford an inseparable mixture of *trans*-**115aa** and *cis*-**115ab** as a pale yellow oil (2.53 g, 69 %, 95:5).

b.p. = 97 °C / 0.04 mmHg;

R_f = 0.27 (40 % diethyl ether in hexane);

¹H NMR (400 MHz, CDCl₃): δ = 5.77 (dddd, *J* = 17.0, 10.1, 8.5, 5.8 Hz, 1H), 5.06-4.95 (m, 2H), 4.93 (app. s, 2H), 3.94-3.81 (m, 2H), 3.62-3.54 (m, 2H), 3.40 (s, 3H), 2.62 (br. s, 1H), 2.29-2.16 (m, 1H), 1.98-1.88 (m, 1H), 1.86-1.08 (envelope, 9H) ppm;

¹³C NMR (100 MHz, CDCl₃): δ = 154.4 (t, ¹J_{C-F} = 287.1 Hz), 137.6, 121.5 (dd, ²J_{C-F} = 33.1, 10.3 Hz), 115.8, 98.7 (t, ⁴J_{C-F} = 4.2 Hz), 73.7 (d, ³J_{C-F} = 5.6 Hz), 71.6, 68.9, 58.9, 41.9 (d, ⁴J_{C-F} = 4.8 Hz), 37.1 (t, ⁴J_{C-F} = 2.9 Hz), 35.2, 26.4, 25.3, 21.2 ppm;

Major *trans*-diastereoisomer **115aa** (assigned on the basis of δ and intensity) ¹⁹F NMR (376 MHz, CDCl₃): δ = -98.8 (d, ²J = 73.4 Hz, 1F), -103.6 (d, ²J = 73.4 Hz, 1F) ppm;*

Minor *cis*-diastereoisomer **115ab** (assigned on the basis of δ and intensity) ¹⁹F NMR (376 MHz, CDCl₃): δ = -97.5 (d, ²J = 68.6 Hz, 1F), 104.4 (d, ²J = 68.6 Hz, 1F) ppm;

$\bar{\nu}$ (neat) = 3450, 2934, 1738, 1450, 1104, 1059 cm⁻¹;

HRMS (NSI): calcd for C₁₅H₂₈F₂O₄N, 324.1981 [M+NH₄]⁺, found: 324.1983;

MS (CI): *m/z* (%): 201 (14) [M-C₄H₉O₃]⁺, 89 (100) [C₄H₉O₂]⁺, 59 (85) [C₃H₇O]⁺**

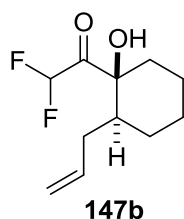
t_R (GC) = 13.17 minutes.

* this is by comparison with compounds from the Saegusa-Ito series (See compound **112f**).¹⁹⁴

** the *cis*- and *trans*-stereoisomers appeared as one peak by GC.

6.3.2 Synthesis of difluoromethylketone **147b**

trans-1-(2-allyl-1-hydroxycyclohexyl)-2,2-difluoroethan-1-one (**147b**)



Difluoromethyl ketone **147b** was prepared according to the procedure of Percy and co-workers.²⁸⁴ A mixture of **115aa** and **115ab** (0.306 g, 1 mmol) was taken up in Methanol (2 mL) and added to a round bottom flask. The mixture was cooled to 0 °C using an ice bath. Chlorotrimethylsilane (0.076 mL, 0.6 mmol) was added in one portion and the resulting pale yellow solution stirred at ambient temperature for 4 hours. After consumption of starting material (by TLC), the reaction was concentrated to afford a pale yellow oil (0.220 g). The crude material was purified by flash column chromatography (40 g cartridge, 20 % diethyl ether in hexane) to afford **147b** as a colourless oil (0.132 g, 61 %).

$R_f = 0.44$ (40 % diethyl ether in hexane);

¹H NMR (400 MHz, CDCl₃): $\delta = 6.23$ (dd, $^2J_{\text{H-F}} = 53.9, 52.4$ Hz, 1H), 5.68 (dddd, $J = 14.2, 10.5, 8.5, 8.3$ Hz, 1H), 5.07-5.02 (m, 1H), 5.02-4.99 (m, 1H), 2.63 (br. s, 1H), 2.14-2.01 (m, 1H), 2.01-1.91 (m, 2H), 1.85-1.51 (envelope, 6H), 1.48-1.24 (m, 1H) ppm;

¹³C NMR (100 MHz, CDCl₃): $\delta = 202.6$ (t, $^2J_{\text{C-F}} = 21.9$ Hz), 136.0, 116.8, 108.1 (dd, $^1J_{\text{C-F}} = 252.0, 250.1$ Hz), 80.8, 41.2, 35.6, 35.1, 26.2, 24.6, 19.7 ppm;

¹⁹F NMR (376 MHz, CDCl₃): $\delta = -125.3$ (dd, $^2J = 317.5, ^2J_{\text{F-H}} = 52.7$ Hz, 1F), -129.3 (dd, $^2J = 317.5, ^4J_{\text{F-H}} = 53.5$ Hz, 1F) ppm;

$\bar{\nu}$ (neat) = 3650-3350 (broad), 2939, 1744, 1452, 1063, 994 cm⁻¹;

HRMS (EI): calcd for C₁₁H₁₆F₂O₂, 218.1118 [M], found: 218.1120;

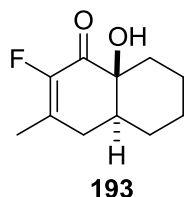
MS (CI): m/z (%): 219 (100) [M+H]⁺, 201 (44) [M-OH]⁺;

t_R (GC) = 10.40, 10.49 minutes.*

*The material, though present as a unique chemical species by ¹⁹F, ¹³C and ¹H NMR, appeared as 2 peaks in the GC-MS with identical fragmentation patterns (ion mass and relative abundance).

6.3.3 Synthesis of monofluorinated enone **193**

(4*aS**,8*aS**)-2-fluoro-8*a*-hydroxy-3-methyl--hexahydronaphthalen-1(4*H*)-one (**193**)



Palladium(II) acetate (100 mol %, 0.448 g) and copper(I) chloride (100 mol %, 0.200 g) were suspended in a mixture of acetonitrile and water (7 mL, 6:1). An oxygen balloon was attached and the suspension was warmed to 70 °C. A solution of allyl alcohol **115aa** and **115ab** (0.612 g, 2 mmol) in acetonitrile (1 mL) was added via syringe in a constant stream and the mixture was stirred at 70 °C for 18 hours under balloon pressure of oxygen. The reaction was allowed to cool to room temperature then taken up in ethyl acetate (40 mL) and transferred to a separating funnel containing distilled water (150 mL). The organic layer was separated and the aqueous layer extracted with ethyl acetate (4 x 40 mL). The original organic layer and the extracts were combined and washed with saturated aqueous sodium bicarbonate (40 mL), dried (MgSO₄), filtered and concentrated under reduced pressure to afford the crude product as a dark orange oil (0.217 g). The crude material was purified by flash column chromatography (40 g silica, 5-15 % acetone in hexane) to afford **193** as a colourless solid (0.100 g, 25 %). The solid was purified further by vapour diffusion (CHCl₃/Pentane) to afford **193** as colourless plates (0.080 g, 20 %).

m.p. = 98-100 °C (chloroform/pentane vapour diffusion);

R_f = 0.67 (40 % acetone in hexane);

¹H NMR (400 MHz, CDCl₃): δ = 2.62-2.45 (m, 1H), 2.21-2.00 (m, 2H), 1.94 (d, ⁴J_{H-F} = 2.1 Hz, 3H), 1.92-1.82 (m, 1H), 1.82-1.48 (envelope, 6H), 1.44-1.18 (m, 2H) ppm;

¹³C NMR (100 MHz, CDCl₃): δ = 190.0 (d, ²J_{C-F} = 16.8 Hz), 148.5 (d, ¹J_{C-F} = 254.1 Hz), 136.8 (d, ²J_{C-F} = 10.2 Hz), 72.2 (d, ³J_{C-F} = 4.0 Hz), 40.7, 33.2 (d, ³J_{C-F} = 3.3 Hz), 31.1, 26.4, 24.7, 19.9, 15.4 (d, ³J_{C-F} = 5.7 Hz) ppm;

¹⁹F NMR (376 MHz, CDCl₃): δ = -138.9 (s) ppm;

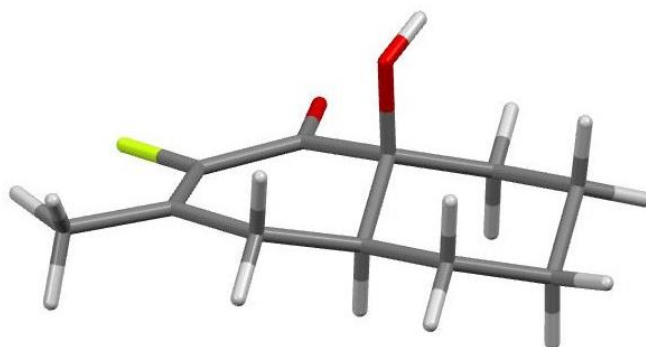
$\bar{\nu}$ (neat) = 3600-3200 (broad), 2941, 1751, 1677, 1647, 1167, 899, 826 cm⁻¹;

HRMS (NSI): calcd for C₁₁H₁₆FO₂, 199.1129 [M+H]⁺, found: 199.1129;

MS (CI): *m/z* (%): 227 (1) [M+C₂H₅]⁺, 199 (14) [M+H]⁺, 181 (100) [M-OH]⁺;

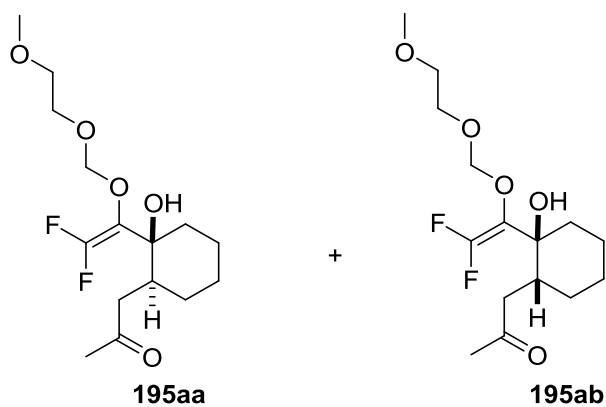
t_R (GC) = 12.69 minutes;

elemental analysis calcd (%) for C₁₁H₁₅FO₂: C, 66.65; H, 7.63; found: C, 66.46; H, 7.65. The identity of this enone (**193**) was confirmed by XRD analysis (m.p. = 98-100 °C (chloroform/pentane)). Crystal Data for **193**: C₁₁H₁₅FO₂, crystal size 0.25 x 0.18 x 0.03 mm³, *M* = 198.23, triclinic, space group P-1, unit cell dimensions *a* = 9.3298(5) Å, *b* = 10.0084(13) Å, *c* = 11.3166(7) Å, α = 85.740(9)°, β = 74.091(5)°, γ = 86.732(7)°, *V* = 1012.68(16) Å³, *Z* = 4, ρ_{calc} = 1.300 Mg m⁻³, *F*(000) = 424, μ (Mo-K α) = 0.100 mm⁻¹, *T* = 123(2)K, 6571 reflections measured, 6571 independent, (*R*_{int} = 0.0000). Final *R* indices [*I* > 2 σ (*I*)] *R*1 = 0.0481, ωR 2 = 0.1040; *R* indices (all data) *R*1 = 0.1050, ωR 2 = 0.1234.



6.3.4 Synthesis of Wacker oxidation product **195aa** and **195ab**

trans-1-((1*S**,2*S**)-2-(2,2-difluoro-1-((2-methoxyethoxy)methoxy)vinyl)-2-hydroxycyclohexyl)propan-2-one (*trans*-**195aa**) and *cis*-1-((1*R**,2*S**)-2-(2,2-difluoro-1-((2-methoxyethoxy)methoxy)vinyl)-2-hydroxycyclohexyl)propan-2-one (*cis*-**195ab**)



Trans- and *cis*- methyl ketone **195aa** and **195ab** were prepared according to a method similar to that reported by Ito and co-workers.²⁸⁵ Palladium(II) chloride (37 mol %,

0.066 g) and copper(II) acetate hydrate (200 mol %, 0.363 g) were suspended in a mixture of *N,N*-dimethylacetamide and water (3.4 mL, 7.5:1 v/v). A solution of allyl alcohol **115aa** and **115ab** (0.306 g, 1 mmol) in *N,N*-dimethylacetamide (1 mL) was added dropwise *via* syringe and the resulting solution stirred at room temperature under balloon pressure of oxygen for 48 hours. The reaction mixture was filtered through a plug of Celite and the filtrate was diluted with ethyl acetate (50 mL). The organic layer was washed thoroughly with water (4 x 50 mL) before being separated, dried (MgSO₄) and concentrated to afford a dark red oil (0.207 g). The crude material was purified by flash column chromatography (40 g silica, 35 % diethyl ether in hexane) to afford an inseparable mixture of *trans*-**195aa** and *cis*-**195ab** (<95 % purity) as a yellow oil (0.104 g, 32 %, 81:19).

R_f = 0.40 (40 % diethyl ether in hexane);

¹H NMR (400 MHz, CDCl₃): δ = 5.09-4.83 (m, 2H), 3.97-3.79 (m, 2H), 3.61-3.51 (m, 2H), 3.40 (s, 3H), 3.11 (br. s, 1H), 2.58 (dd, ²J = 17.5, J = 3.0 Hz, 1H), 2.42 (dd, ²J = 17.5, J = 8.8 Hz, 1H), 2.13 (s, 2H), 1.89-1.13 (envelope, 10H) ppm;

¹³C NMR (100 MHz, CDCl₃): δ = 207.8, 153.6 (t, ¹J_{C-F} = 288.5 Hz), 120.7 (dd, ²J_{C-F} = 32.2, 10.2 Hz), 97.8 (t, ⁴J_{C-F} = 3.5 Hz), 72.1 (d, ³J_{C-F} = 5.5 Hz), 70.6, 68.0, 57.9, 44.3, 37.0 (d, ⁴J_{C-F} = 4.5 Hz), 35.7, 29.6, 26.5, 24.1, 20.1 ppm;

Major *trans*-diastereoisomer **195aa** (assigned on the basis of intensity) ¹⁹F NMR (376 MHz, CDCl₃): δ = -98.1 (d, ²J = 71.9 Hz, 1F), -102.9 (d, ²J = 71.9 Hz, 1F) ppm;

Minor *cis*-diastereoisomer **195ab** (assigned on the basis of intensity) ¹⁹F NMR (376 MHz, CDCl₃): δ = -94.7 (d, ²J = 64.3 Hz, 1F), 102.5 (d, ²J = 64.3 Hz, 1F) ppm;

$\bar{\nu}$ (neat) = 3650-3200 (broad), 2926, 1734, 1712, 1102, 1059, 948, 849 cm⁻¹;

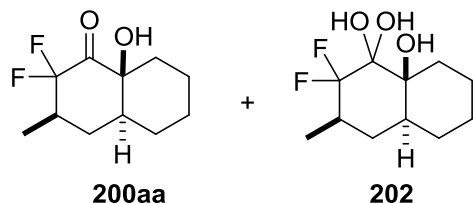
MS (CI): *m/z* (%): 265 (1) [M-C₃H₅O]⁺, 229 (2) [M-C₃H₆O₂F]⁺, 89 (100) [C₄H₉O₂]⁺, 59 (86) [C₃H₇O]⁺;

t_R (GC) = 13.02 minutes.

HRMS could not be obtained for this compound. The sample was taken up in DCM and analysed by ammonia CI on a Thermo MAT 95 and by positive ion APCI (ASAP) on a Waters Xevo G2-S. Although the intact molecular species was not observed, intense ions were yielded that could not be readily assigned.

6.3.5 Synthesis of α -hydroxy ketone **200aa** and hydrate **202**

Preparation of (3*R**,4*aS**,8*aS**)-2,2-difluoro-8*a*-hydroxy-3-methyloctahydronaphthalen-1(2*H*)-one (**200aa**) and (3*R**,4*aS**,8*aS**)-2,2-difluoro-3-methyloctahydronaphthalene-1,1,8*a*-triol (**202**)



1,3-Bis(2,6-diisopropylphenyl-imidazol-2-ylidene)gold(I) chloride (5 mol %, 0.031 g) was taken up in dichloromethane (1 mL) and added *via* syringe to dichloromethane (3.4 mL). The solution was stirred at room temperature then a solution of silver hexafluoroantimonate(V) (5 mol %, 0.017 g) in methanol (0.6 mL) was added as a stream *via* syringe. An off-white precipitate formed after the addition was complete. An air condenser (open to the atmosphere) was fitted, and the suspension was heated to 40 °C. A solution of allyl alcohol **115aa** and **115ab** (0.306 g, 1 mmol) in dichloromethane (1 mL) was added in a stream *via* syringe. The solution was stirred at this temperature for 30 minutes, then trifluoroacetic acid (0.23 mL, 3 mmol) was added dropwise. The mixture was stirred at 40 °C for 18 hours, then transferred by pipette to a glass sinter funnel (diameter 4.2 cm) containing a pad of celite (7 g). The celite plug was washed with diethyl ether (150 mL). The filtrate was concentrated to afford a pale yellow oil (0.285 g). This oil was taken up diethyl ether (50 mL) and the solution was washed with sodium bicarbonate (20 mL of a saturated aqueous solution). The organic layer was separated, dried (MgSO₄) and concentrated to afford the crude product as a dark red solid (0.292 g). The material was taken up in dichloromethane and transferred by pipette to a glass sinter funnel (diameter 2.3 cm) containing a pad of silica (5 g). Catalyst residues were removed by eluting with dichloromethane (20 mL). The product was then eluted from the plug with 3 % methanol in dichloromethane (50 mL). The solvent was evaporated under reduced pressure to afford the product as a pale yellow solid below a yellow oil. The material was filtered and washed with pentane at the pump to afford a mixture of **200aa** and **202** as a colourless solid ((0.109 g, 46 %) based on **hydrate 202**). m.p. = 76-78 °C (recrystallised from chloroform/pentane vapour diffusion as a colourless prism);

R_f = 0.31 (30 % ethyl acetate in hexane);

The following signals were attributed to both the minor ketone **200aa** and major hydrate **202** ^1H NMR (400 MHz, CDCl_3): $\delta = 2.34\text{--}1.86$ (m, 2H), 1.86–1.22 (envelope, 16H);

The following signals were attributed to the major product hydrate **202** (assigned on the basis of δ and intensity)

^1H NMR (400 MHz, CDCl_3): $\delta = 3.42$ (s, 1H), 2.93 (s, 1H), 1.08 (d, $J = 6.9$ Hz, 3H) ppm;

^{13}C NMR (100 MHz, CDCl_3): $\delta = 122.3$ (t, $^1J_{\text{C-F}} = 253.5$ Hz), 93.3 (t, $^2J_{\text{C-F}} = 22.8$ Hz), 74.8, 38.1, 34.3 (t, $^2J_{\text{C-F}} = 22.8$ Hz), 31.3 (d, $^3J_{\text{C-F}} = 7.6$ Hz), 30.9, 27.0, 24.9, 19.8, 11.5 (t, $^3J_{\text{C-F}} = 4.4$ Hz) ppm;

^{19}F NMR (376 MHz, CDCl_3): $\delta = -122.0$ (one half of a double ABq, $J_{\text{AB}} = 247.5$, $^3J_{\text{F-H}} = 10.3$ Hz, 1F), -122.4 (one half of a double ABq, $J_{\text{AB}} = 247.5$, $^3J_{\text{F-H}} = 23.2$ Hz, 1F) ppm;

The following signals were attributed to the minor product ketone **200aa** (assigned on the basis of δ and intensity)

^1H NMR (400 MHz, CDCl_3): $\delta = 1.20$ (d, $J = 6.8$ Hz, 3H) ppm;

^{13}C NMR (100 MHz, CDCl_3): $\delta = 197.2$ (t, $^2J_{\text{C-F}} = 22.0$ Hz), 117.0 (dd, $^1J_{\text{C-F}} = 259.6$, 253.5 Hz), 75.9, 44.1, 40.0 (dd, $^2J_{\text{C-F}} = 23.2$, 19.8 Hz), 32.1 (d, $^3J_{\text{C-F}} = 6.4$ Hz), 28.6, 26.2, 24.7, 19.4, 11.3 (d, $^3J_{\text{C-F}} = 7.4$ Hz) ppm;

^{19}F NMR (376 MHz, CDCl_3): $\delta = -112.9$ (dd, $^2J = 256.9$, $^3J_{\text{F-H}} = 28.9$ Hz, 1F), -115.4 (dt, $^2J = 256.9$, $^3J_{\text{F-H}} = ^4J_{\text{F-H}} = 5.1$ Hz, 1F) ppm;

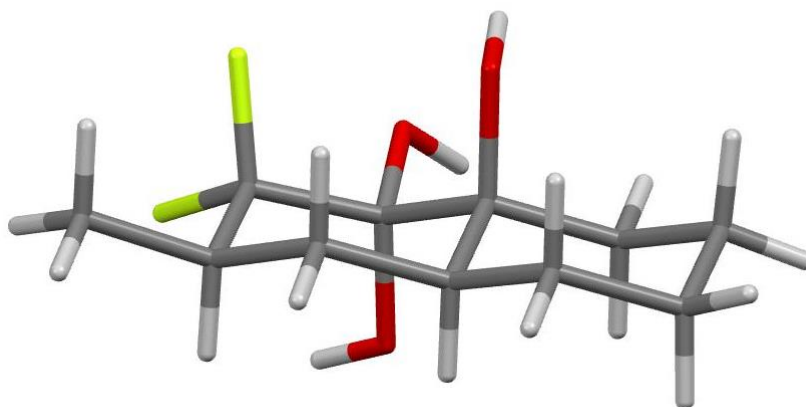
$\bar{\nu}$ (neat) = 3650–3100 (broad), 2934, 1742, 1459, 1074, 996, 976 cm^{-1} ;

HRMS (ASAP): calcd for $\text{C}_{11}\text{H}_{15}\text{F}_2\text{O}$, 201.1091 [M+H-H₂O], found: 201.1096;

MS (EI): m/z (%): 218 (4) [M]⁺;

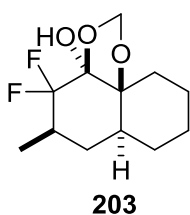
t_{R} (GC) = 11.26 minutes;

The identity of the mixture (**200aa** and **202**) was confirmed by XRD analysis (m.p. = 76–78 °C (chloroform/pentane)). Crystal Data for **200aa** and **202**: $\text{C}_{11}\text{H}_{17.46}\text{F}_2\text{O}_{2.85}$, crystal size 0.3 x 0.2 x 0.03 mm^3 , $M = 233.28$, triclinic, space group P-1, unit cell dimensions $a = 11.3756(5)$ Å, $b = 11.9233(5)$ Å, $c = 18.6426(8)$ Å, $\alpha = 73.326(4)^\circ$, $\beta = 78.588(4)^\circ$, $\gamma = 70.646(4)^\circ$, $V = 2270.56(19)$ Å³, $Z = 8$, $\rho_{\text{calc}} = 1.365$ Mg m⁻³, $F(000) = 994$, $\mu(\text{Mo-K}\alpha) = 0.117$ mm⁻¹, $T = 123(2)$ K, 19665 reflections measured, 9971 independent, ($R_{\text{int}} = 0.0317$). Final R indices [$I > 2\sigma(I)$] $R1 = 0.0642$, $\omega R2 = 0.1707$; R indices (all data) $R1 = 0.0889$, $\omega R2 = 0.1944$. The resulting structure was of relatively low quality but was adequate for the assignment of the *trans* ring junction stereochemistry.



6.3.6 Synthesis of tricyclic acetal 203

Preparation of (3a*S**,5*R**,6a*S**,10a*S**)-4,4-difluoro-5-methyloctahydro-3a*H*-naphtho[1,8a-d][1,3]dioxol-3a-ol (203)



1,3-*Bis*(2,6-diisopropylphenyl-imidazol-2-ylidene)gold(I) chloride (5 mol %, 0.031 g) was taken up in dichloromethane (1 mL) and added *via* syringe to dichloromethane (3.4 mL). The solution was stirred at room temperature then a solution of silver hexafluoroantimonate(V) (5 mol %, 0.017 g) in methanol (0.6 mL) was added as a stream *via* syringe. An off-white precipitate formed after the addition was complete. An air condenser (open to the atmosphere) was fitted, and the suspension was heated to 40 °C. A solution of allyl alcohol **115aa** and **115ab** (0.306 g, 1 mmol) in dichloromethane (1 mL) was added in a stream *via* syringe. The solution was stirred at this temperature for 30 minutes before adding trifluoroacetic acid (0.23 mL, 3 mmol) dropwise. The mixture was stirred at 40 °C for 18 hours. After this time the reaction mixture was transferred by pipette to a glass sinter filled with celite (7 g) and the celite plug washed with diethyl ether (150 mL). The filtrate was concentrated to afford a dark orange oil (0.292 g). This oil was taken up diethyl ether (50 mL) and washed with an aqueous saturated solution of sodium bicarbonate (20 mL). The organic phase was separated, dried over magnesium sulphate and concentrated to afford the crude product as a pale yellow oil (0.292 g). The crude material was purified by flash column chromatography

(40 g silica, 25 % ethyl acetate in hexane) to afford **203** as a colourless oil which solidified upon freezing to afford **203** as colourless needles (0.046 g, 19 %).

m.p. = 52-54 °C (colourless plated crystals were grown by slow evaporation from 25 % ethyl acetate in hexane under reduced pressure);

$R_f = 0.29$ (100 % dichloromethane);

The following signals were attributed to both conformers: ^1H NMR (400 MHz, CDCl_3): $\delta = 5.21$ (d, $^2J = 7.4$ Hz, 1H), 5.12 (d, $^2J = 7.4$ Hz, 1H), 3.31 (br. d, $^4J_{\text{H-F}} = 5.3$ Hz, 1H), 2.98 (br. s, 1H), 2.57-2.31 (m, 1H), 2.16-1.20 (envelope, 11H), 1.10 (d, $J = 7.4$ Hz, 3H) ppm;

The following signals were attributed to one conformer solution

^{13}C NMR (100 MHz, CDCl_3): $\delta = 122.2$ (t, $^1J_{\text{C-F}} = 251.4$ Hz), 99.5 (t, $^2J_{\text{C-F}} = 23.5$ Hz), 92.2, 85.0, 36.4, 31.1 (d, $^3J_{\text{C-F}} = 6.8$ Hz), 29.9 (t, $^2J_{\text{C-F}} = 21.3$ Hz), 28.9, 27.6, 25.2, 21.9, 13.5 (t, $^3J_{\text{C-F}} = 4.8$ Hz) ppm;

^{19}F NMR (376 MHz, CDCl_3): $\delta = -119.0$, (app. d, $^2J = 250.5$ Hz, 1F), -120.7 , (app. d, $^2J = 250.5$ Hz, 1F) ppm ;

The following signals were attributed to the second conformer in solution

^{13}C NMR (150 MHz, CDCl_3): $\delta = 122.1$ (dd, $^1J_{\text{C-F}} = 255.5, 249.7$ Hz), 100.0 (t, $^2J_{\text{C-F}} = 25.3$ Hz), 93.5 (d, $^4J_{\text{C-F}} = 2.9$ Hz) , 82.1, 39.7, 36.0 (t, $^2J_{\text{C-F}} = 22.3$ Hz) , 32.0 (d, $^3J_{\text{C-F}} = 7.1$ Hz), 28.3, 27.2, 25.5, 20.7, 12.3 (t, $^3J_{\text{C-F}} = 4.6$ Hz) ppm;

^{19}F NMR (376 MHz, CDCl_3): $\delta = -119.3$, (dd, $^2J = 247.3, ^3J_{\text{F-H}} = 29.3$ Hz, 1F), -120.8 , (dd, $^2J = 247.3, ^3J_{\text{F-H}} = 25.6$ Hz, 1F) ppm;

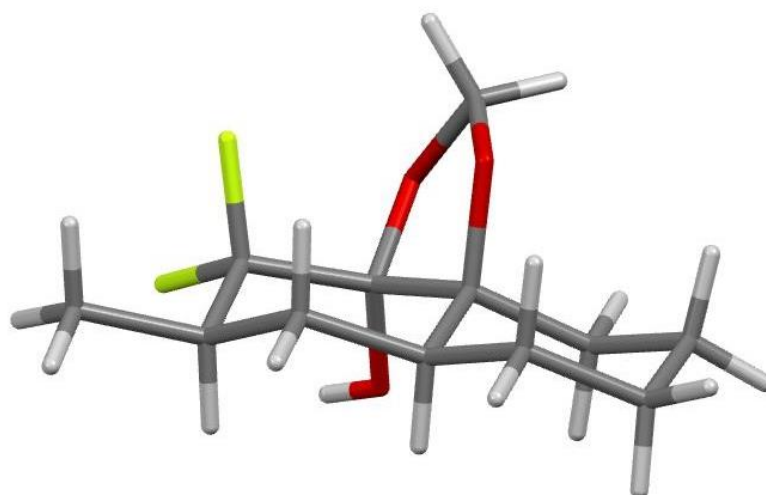
$\bar{\nu}$ /(neat) = 3600-3200 (broad), 2926, 1742, 1448, 1087, 981 cm^{-1} ;

HRMS (ASAP): calcd for $\text{C}_{12}\text{H}_{18}\text{F}_2\text{O}_3$, 248.1224 [M], found: 248.1228;

MS (EI): m/z (%): 202 (4) $[\text{M}-\text{CH}_2\text{O}_2]^+$, 181 (100) $[\text{M}-\text{CH}_4\text{O}_2\text{F}]^+$, 151 (21) $[\text{M}-\text{C}_2\text{H}_6\text{O}_3\text{F}]^+$;

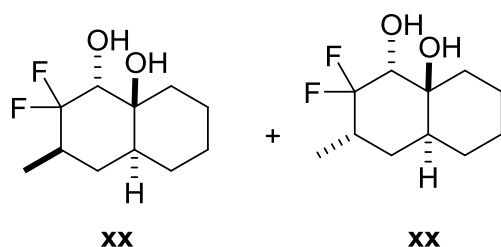
t_R (GC) = 11.41 minutes;

The identity of acetal (**203**) was confirmed by XRD analysis. Crystal Data for **203**: $\text{C}_{12}\text{H}_{18}\text{F}_2\text{O}_3$, crystal size 0.24 x 0.10 x 0.06 mm^3 , $M = 248.26$, monoclinic, space group $\text{P}2_{1/c}$, unit cell dimensions $a = 6.1120(4)$ Å, $b = 11.9285(4)$ Å, $c = 32.307(2)$ Å, $\alpha = 90^\circ$, $\beta = 93.037(5)^\circ$, $\gamma = 90^\circ$, $V = 2352.1(3)$ Å³, $Z = 8$, $\rho_{\text{calc}} = 1.402$ Mg m^{-3} , $F(000) = 1056$, $\mu(\text{Mo-K}\alpha) = 0.119$ mm^{-1} , $T = 123(2)\text{K}$, 21617 reflections measured, 5081 independent, ($R_{\text{int}} = 0.0627$). Final R indices [$I > 2\sigma(I)$] $R1 = 0.0745$, $\omega R2 = 0.1808$; R indices (all data) $R1 = 0.1266$, $\omega R2 = 0.2160$. The resulting structure is of relatively low quality but is adequate for the assignment of the *trans* ring junction stereochemistry.



6.3.7 General Procedure D – Difluorinated Diol Preparation

Preparation of (1*R**,3*R**,4*aS**,8*aS**)-2,2-difluoro-3-methyloctahydronaphthalene-1,8*a*(1*H*)-diol (207aa) and (1*R**,3*S**,4*aS**,8*aS**)-2,2-difluoro-3-methyloctahydronaphthalene-1,8*a*(1*H*)-diol (207ab)



1,3-*Bis*(2,6-*diisopropylphenyl-imidazol-2-ylidene*)gold(I) chloride (5 mol %, 0.031 g) was taken up in dichloromethane (1 mL) and added *via* syringe to dichloromethane (3.4 mL). The solution was stirred at room temperature then a solution of silver hexafluoroantimonate(V) (5 mol %, 0.017 g) in methanol (0.6 mL) was added as a stream *via* syringe. An off-white precipitate formed after the addition was complete. The flask was fitted with an air condenser (open to the atmosphere), and the suspension was heated to 40 °C. A solution of allyl alcohol **115aa** and **115ab** (0.306 g, 1 mmol) in dichloromethane (1 mL) was added in a stream *via* syringe. After stirring for 5 hours at 40 °C the reaction was allowed to cool to room temperature. Solid tetrabutylammonium borohydride (0.258 g, 1 mmol) was added to the flask in small portions. A slight effervescence was observed as the reducing agent was added and the reaction mixture darkened from colourless to dark brown. The reaction mixture was then allowed to stir at room temperature for 18 hours, then was quenched with hydrogen peroxide (10 mL of a 3 wt % aqueous solution), followed by sodium hydroxide (5 mL of a 10 wt % aqueous

solution). The mixture was transferred to a separating funnel and the organic layer was removed. The aqueous layer was extracted with dichloromethane (4 x 40 mL). The combined organic extracts were then washed with sodium sulfite (10 mL of a saturated aqueous solution). The organic layer was separated, dried (MgSO₄) and concentrated under reduced pressure to afford the crude product as a viscous pale yellow oil (0.280 g). The crude material was purified by flash column chromatography (40 g silica, 2 % acetone in dichloromethane) to afford an inseparable mixture of *trans,trans*-**207aa** and *trans,cis*-**207ab** as a colourless solid (0.154 g, 70 %, 2.6:1).

R_f = 0.47 (5 % acetone in dichloromethane);

The following signals were attributed to both the minor *trans,cis*-diastereoisomer **207aa** and major *trans,trans*-diastereoisomer **207ab** ¹H NMR (400 MHz, CDCl₃): δ = 3.60-3.47 (m, 1H), 2.42-2.17 (m, 1H), 1.97-1.27 (envelope, 17H) ppm;

The following signals were attributed to the major *trans,trans*-diastereoisomer **207aa** (assigned on the basis of δ and intensity)

¹H NMR (400 MHz, CDCl₃): δ = 2.14 (t, *J* = 2.8 Hz, 1H), 1.06 (d, *J* = 6.9 Hz, 3H) ppm;

¹³C NMR (100 MHz, CDCl₃): δ = 124.0 (t, ¹J_{C-F} = 248.2 Hz), 74.2 (dd, ²J_{C-F} = 27.7, 21.4 Hz), 72.7 (d, ³J_{C-F} = 5.2 Hz), 36.6, 33.7, 32.8 (t, ²J_{C-F} = 21.4 Hz), 32.6 (d, ³J_{C-F} = 8.5 Hz), 26.6, 25.1, 19.8, 11.2 (d, ³J_{C-F} = 5.6 Hz) ppm;

¹⁹F NMR (376 MHz, CDCl₃): δ = -105.9 (dq, ²J = 256.5, ³J_{F-H} = ⁴J_{F-H} = 4.8 Hz, 1F), -116.6 (ddt, ²J = 256.5, ³J_{F-H} = 30.3, ³J_{F-H} = ⁴J_{F-H} = 7.6 Hz, 1F) ppm;

The following signals were attributed to the minor *trans,cis*-diastereoisomer **207ab** (assigned on the basis of δ and intensity)

¹H NMR (400 MHz, CDCl₃): δ = 2.11 (t, *J* = 2.7 Hz, 1H) ppm;

¹³C NMR (100 MHz, CDCl₃): δ = 123.4 (dd, ¹J_{C-F} = 253.8, 242.5 Hz), 75.3 (dd, ²J_{C-F} = 28.9, 21.7 Hz), 72.3 (d, ³J_{C-F} = 5.8 Hz), 35.1 (dd, ²J_{C-F} = 23.4, 21.0 Hz), 31.1, 30.8 (d, ³J_{C-F} = 7.3 Hz), 26.8, 25.3, 19.9, 14.2 (dd, ³J_{C-F} = 9.4, 3.7 Hz) ppm;

¹⁹F NMR (376 MHz, CDCl₃): δ = -93.6 (ddt, ²J = 261.3, ³J_{F-H} = 17.6, ³J_{F-H} = ⁴J_{F-H} = 8.0 Hz), -104.5 (d, ²J = 261.3 Hz) ppm;

$\bar{\nu}$ (neat) = 3608, 3450, 2919, 1446, 1069, 985 cm⁻¹;

HRMS (ASAP): calcd for C₁₁H₁₇F₂O₂, 219.1197 [M-H]⁺, found: 219.1194;

MS (EI): *m/z* (%): 220 (3) [M]⁺, 182 (13) [M-2F]⁺;

t_R (GC) = 11.27 minutes;*

elemental analysis calcd (%) for C₁₁H₁₈F₂O₂: C, 59.98; H, 8.24; found: C, 59.75; H, 8.17. This analysis was obtained for the amorphous solid obtained following chromatography so no melting point was recorded.

* the individual diastereoisomers appeared as one peak by GC

Diastereomerically pure *trans,trans* **207aa** could be obtained by performing three vapour diffusion recrystallisations (chloroform/pentane) of the mixed solid diol (0.024g, 11%).

m.p. = 84-86 °C (recrystallised from chloroform/pentane vapour diffusion as a colourless plate);

$R_f = 0.47$ (5 % acetone in dichloromethane);

$^1\text{H NMR}$ (400 MHz, CDCl_3): $\delta = 3.54$ (td, $J_{\text{H-F}} = 6.0$, $J = 3.2$ Hz, 1H), 2.38-2.16 (m, 1H), 2.14 (td, $J = {}^4J_{\text{H-F}} = 3.0$, ${}^4J_{\text{H-F}} = 1.0$ Hz, 1H), 1.85 (tdd, ${}^2J = J = 13.3$, $J = 4.9$, ${}^4J = 1.2$ Hz, 1H), 1.80-1.19 (envelope, 11H), 1.08 (d, $J = 6.9$ Hz, 3H) ppm;

$^{13}\text{C NMR}$ (100 MHz, CDCl_3): $\delta = 124.0$ (t, ${}^1J_{\text{C-F}} = 248.2$ Hz), 74.2 (dd, ${}^2J_{\text{C-F}} = 27.7$, 21.4 Hz), 72.7 (d, ${}^3J_{\text{C-F}} = 5.2$ Hz), 36.6, 33.7, 32.8 (t, ${}^2J_{\text{C-F}} = 21.4$ Hz), 32.6 (d, ${}^3J_{\text{C-F}} = 8.5$ Hz), 26.6, 25.1, 19.8, 11.2 (d, ${}^3J_{\text{C-F}} = 5.6$ Hz) ppm;

$^{19}\text{F NMR}$ (376 MHz, CDCl_3): $\delta = -105.9$ (dq, ${}^2J = 256.5$, ${}^3J_{\text{F-H}} = {}^4J_{\text{F-H}} = 4.8$ Hz), -116.6 (ddt, ${}^2J = 256.5$, ${}^3J_{\text{F-H}} = 30.3$, ${}^3J_{\text{F-H}} = {}^4J_{\text{F-H}} = 7.6$ Hz) ppm;

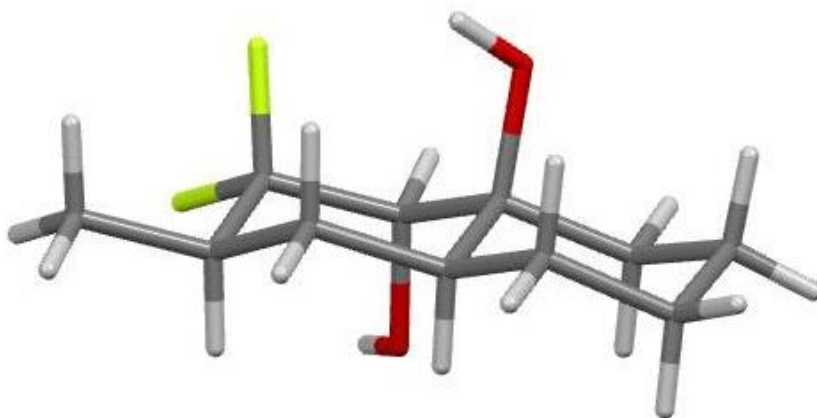
$\bar{\nu}$ /(neat) = 3617, 3450, 2922, 1446, 1068, 985, 957 cm^{-1} ;

MS (EI): m/z (%): 220 (2) $[\text{M}]^+$, 182 (19) $[\text{M}-2\text{F}]^+$;

t_R (GC) = 11.27 minutes;

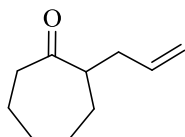
elemental analysis calcd (%) for $\text{C}_{11}\text{H}_{18}\text{F}_2\text{O}_2$: C, 59.98; H, 8.24; found: C, 60.12; H, 8.48.

The identity of diol (**207aa**) was confirmed by XRD analysis (m.p. = 84-86 °C (chloroform/pentane)). Crystal Data for **207aa**: $\text{C}_{11}\text{H}_{18}\text{F}_2\text{O}_2$, crystal size 0.35 x 0.25 x 0.05 mm^3 , $M = 220.25$, monoclinic, space group $\text{P2}_1/\text{c}$, unit cell dimensions $a = 9.5614(9)$ Å, $b = 23.1922(14)$ Å, $c = 10.6309(9)$ Å, $\alpha = 90^\circ$, $\beta = 114.258(11)^\circ$, $\gamma = 90^\circ$, $V = 2149.3(3)$ Å³, $Z = 8$, $\rho_{\text{calc}} = 1.361$ Mg m^{-3} , $F(000) = 944$, $\mu(\text{Mo-K}\alpha) = 0.114$ mm^{-1} , $T = 123(2)\text{K}$, 5176 reflections measured, 5176 independent, ($R_{\text{int}} = 0.0000$). Final R indices [$I > 2\sigma(I)$] $R1 = 0.0623$, $\omega R2 = 0.1565$; R indices (all data) $R1 = 0.1011$, $\omega R2 = 0.1688$.



6.3.8 Preparation of electrophiles

2-Allylcycloheptanone (**S9**)²⁸⁷



2-Allylcycloheptanone (**S9**) was prepared according to the method of Fleming *et al.*²⁸⁶ A solution of cycloheptanone (16.8 g, 150 mmol), allyl alcohol (20.3 g, 350 mmol), 2,2-dimethoxypropane (16.7 g, 160 mmol), *p*-toluenesulfonic acid (0.01 g, 0.05 mmol) and toluene (130 mL) was heated in a flask fitted with a Vigreux column and a distillation head. The mixture was distilled at atmospheric pressure with the still head temperature maintained at 62 °C. The temperature was increased until the head temperature reached 100 °C. The reaction mixture was cooled, stirred with anhydrous potassium carbonate and filtered. Further distillation of the crude material at reduced pressure removed remaining toluene and cycloheptanone and afforded 2-allylcycloheptanone (7.30 g, 32 %) as a colourless oil;

b.p. 86 °C / 5 mm Hg;

¹H NMR (400 MHz, CDCl₃): δ = 5.76 (ddt, *J* = 17.2, 10.1, 7.2 Hz, 1H), 5.09-4.94 (m, 2H), 2.68-2.36 (m, 4H), 2.18-2.01 (m, 1H), 1.99-1.76 (4H, m), 1.78-1.53 (m, 1H), 1.53-1.23 (m, 3H) ppm;

¹³C NMR (100 MHz, CDCl₃): δ = 214.9, 135.7, 115.9, 51.1, 42.6, 35.7, 30.0, 29.0, 28.2, 23.8 ppm;

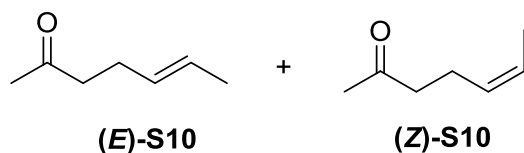
$\bar{\nu}$ (neat) = 1698, 1629 cm⁻¹;

MS (CI): *m/z* (%): 153 (100) [M+H]⁺, 125 (1) [M-C₂H₃], 111 (4) [M-C₃H₅];

t_R (GC) = 8.75 minutes.

The data was consistent with that reported previously.²⁸⁶

(E)-5-hepten-2-one (S10) and (Z)-5-hepten-2-one (S10)²⁸⁷



Ketones (*E*)-**S10** and (*Z*)-**S10** were prepared according to the procedure of Bäckvall and co-workers.²⁸⁷ A mixture of crotyl bromide (8.0 mL, 78 mmol), pentane-2,4-dione (8.8 mL, 86 mmol) and anhydrous sodium carbonate (9.25 g, 87 mmol) was refluxed in 99 % ethanol (100 mL) for 24 hours. The solvent was removed under reduced pressure and the remaining solid partitioned between diethyl ether (100 mL) and water (50 mL). The aqueous phase was extracted with diethyl ether (4 x 50 mL) and the combined organic extracts washed with brine (100 mL), dried (MgSO₄), filtered and concentrated to afford the crude product as a pale yellow oil (6.08 g). The crude material was purified by flash column chromatography (90 g cartridge, 25 % ethyl acetate in hexane) followed by Kugelrohr distillation to afford an inseparable mixture of (*E*)-**S10** and (*Z*)-**S10** as a colourless oil (4.01 g, 46 %, 82:18).

b.p = 74 °C / 9 mmHg;

R_f = 0.37 (20 % diethyl ether in hexane);

The following signals were attributed to both the minor (*E*)-**S10** and major (*Z*)-**S10** alkene ¹H NMR (400 MHz, CDCl₃): δ = 5.57-5.25 (m, 2H), 2.48 (t, *J* = 7.4 Hz, 2H), 2.32 (q, *J* = 7.4 Hz, 2H, minor *Z*-diastereoisomer), 2.25 (q, *J* = 7.4 Hz, 2H, major *E*-diastereoisomer), 2.14 (s, 3H, minor *Z*-diastereoisomer), 2.13 (s, 3H, major *E*-diastereoisomer), 1.64 (d, *J* = 6.2 Hz, 3H);

Major *E*-diastereoisomer **S10** (assigned on the basis of δ and intensity) ¹³C (100 MHz, CDCl₃): δ = 208.0, 128.9, 125.4, 43.0, 29.4, 26.3, 17.3;

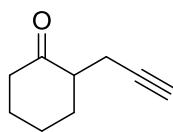
Minor *Z*-diastereoisomer **S10** (assigned on the basis of δ and intensity) ¹³C (100 MHz, CDCl₃): δ = 128.1, 124.6, 42.9, 20.8, 12.2;

$\bar{\nu}$ (neat) = 2919, 1714, 1361, 1164, 968 cm⁻¹;

MS (EI): *m/z* (%): 112 (62) [M], 97 (88) [M-CH₃]⁺, 55 (100) [M-C₃H₅O]⁺;

t_R (GC) = 6.21 minutes.

Preparation of 2-(prop-2-ynyl)cyclohexanone (**S11**)²⁸⁸



S11

Ketone **S11** was prepared according to the procedure of Dake and co-workers.²⁸⁸ *n*-Butyllithium (64.1 mL of a 1.90 M solution in hexanes, 122 mmol) was added dropwise to a solution of diisopropylamine (18 mL, 128 mmol) in THF (150 mL) at -78 °C. The solution was stirred for 15 minutes then cyclohexanone (12 mL, 116 mmol) was added dropwise and the cold solution stirred for an additional 30 minutes. The cold enolate solution was then transferred *via* cannula to a solution of propargyl bromide (16.2 mL of a 80% wt/wt solution in toluene, 145 mmol) in THF (150 mL) at -78 °C. The reaction was stirred at this temperature for 1.5 hours then allowed to warm to room temperature and stirred for an additional 5 hours. The orange reaction mixture was diluted with diethyl ether (200 mL) and washed sequentially with water (200 mL) and brine (200 mL). The combined aqueous phases were extracted with a further portion of diethyl ether (200 mL) and the original organic phase and the new extract were combined, dried (MgSO₄), filtered and carefully concentrated under reduced pressure (200 mbar, 40 °C) to afford the crude product as an orange oil (35 g). The material was transferred by pipette to a glass sinter funnel (diameter 7.5 cm) containing a pad of silica (35 g). The product was then eluted from the plug with 10% diethyl ether/pentane (1 L). The solvent was evaporated under reduced pressure to afford the crude product as a pale yellow oil (12.6 g). The ketone was purified further by distillation to afford **S11** as a colourless oil (2.86 g, 18 %).

b.p = 51 °C / 0.08 mmHg;

R_f = 0.44 (10 % diethyl ether in pentane);

¹H NMR (400 MHz, CDCl₃): δ = 2.62 (ddd, ²J = 17.1, J = 4.6, 2.8 Hz, 1H), 2.56-2.37 (m, 3H), 2.37-2.25 (m, 1H), 2.20 (ddd, ²J = 17.1, J = 8.3, 2.8 Hz, 1H), 2.14-2.05 (m, 1H), 1.96 (t, ⁴J = 2.8 Hz, 1H), 1.95-1.87 (m, 1H), 1.77-1.59 (m, 2H), 1.42 (ddd, ²J = 25.4, J = 12.8, 3.8 Hz, 1H) ppm;

¹³C (100 MHz, CDCl₃): δ = 210.8, 82.6, 69.4, 49.5, 41.9, 33.2, 27.8, 25.1, 18.8 ppm;

$\bar{\nu}$ (neat) = 3283, 2932, 1706, 1450, 1130 cm⁻¹;

MS (EI): *m/z* (%): 136 (16) [M], 135 (55) [M-H]⁺;

t_R (GC) = 8.99 minutes.

^{13}C NMR (100 MHz, CDCl_3): δ = 155.0 (t, $^1J_{\text{C-F}}$ = 290.7 Hz), 136.4, 121.4 (dd, $^2J_{\text{C-F}}$ = 31.2, 12.0 Hz), 116.0, 70.9, 68.2, 63.6, 62.5 (d, $^3J_{\text{C-F}}$ = 4.8 Hz), 41.7, 40.0, 31.7 ppm;

^{19}F NMR (376 MHz, CDCl_3): δ = -96.7 (d, 2J = 66.4 Hz, 1F), 104.5 (dt, 2J = 68.6, $^5J_{\text{F-H}}$ = 4.9 Hz, 1F) ppm;

$\bar{\nu}$ /(neat) = 3443, 2928, 1736, 1100, 1056 cm^{-1} ;

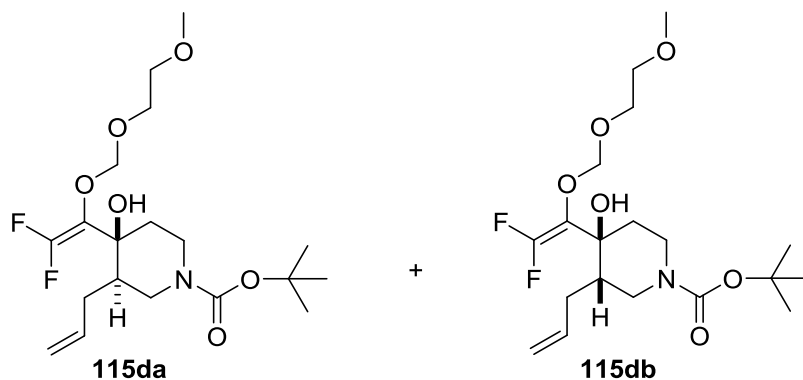
HRMS (APCI): calcd for $\text{C}_{14}\text{H}_{26}\text{F}_2\text{O}_5\text{N}$, 326.1774 $[\text{M}+\text{NH}_4]^+$, found: 326.1772;

MS (CI): m/z (%): 326 (100) $[\text{M}+\text{NH}_4]^+$;

t_{R} (GC) = 13.73 minutes (major *trans*-diastereoisomer), 13.66 minutes (minor *cis*-diastereoisomer)

* this is by comparison with compounds from the Saegusa-Ito series (See compound **112f**).¹⁹⁴

***trans*-tert-butyl -3-allyl-4-(2,2-difluoro-1-((2-methoxyethoxy)methoxy)vinyl)-4-hydroxypiperidine-1-carboxylate (*trans*-115da) and *cis*-tert-butyl -3-allyl-4-(2,2-difluoro-1-((2-methoxyethoxy)methoxy)vinyl)-4-hydroxypiperidine-1-carboxylate (*cis*-115db)**



Prepared as for **115aa** and **115ab** from acetal (0.79 mL, 5 mmol), commercial LDA (5.9 mL of a 1.70 M solution in THF/heptane/ethylbenzene, 24 mmol) and *tert*-butyl 3-allyl-4-oxopiperidine-1-carboxylate (1.19 g, 5 mmol) in THF (5 mL). The mixture was quenched with saturated aqueous ammonium chloride (20 mL) and extracted with ethyl acetate (4 x 60 mL). The combined organic extracts were dried (MgSO_4), filtered and concentrated to afford crude allylic alcohols *trans*-**115da** and *cis*-**115db** (2.01 g) as a viscous orange oil. The crude allylic alcohol was purified by flash column chromatography (90 g cartridge, 45% ethyl acetate in hexane) to afford an inseparable mixture of *trans*-**115da** and *cis*-**115db** as a pale orange oil (0.86 g, 42 %, 83:17).

R_{f} = 0.59 (50 % ethyl acetate in hexane);

^1H NMR (400 MHz, CDCl_3): δ = 5.79 (dddd, J = 17.3, 10.1, 8.5, 5.7 Hz, 1H), 5.14-4.99 (m, 2H), 4.94 (s, 2H), 4.17-3.71 (m, 4H), 3.70-3.51 (m, 2H), 3.41 (s, 3H), 3.31-3.04 (m, 2H), 2.87 (br. s, 1H), 2.34-2.18 (m, 1H), 2.06-1.73 (m, 4H), 1.47 (s, 9H) ppm (the ^1H NMR gave a clear well resolved spectrum at RT and did not require heating).

Major *trans*-diastereoisomer **115da** (assigned on the basis of δ and intensity) ^{13}C NMR (150 MHz, toluene- d_8 , 373 K): δ = 154.7 (t, $^1J_{\text{C-F}}$ = 288.1 Hz), 154.2, 137.0, 121.2 (dd, $^2J_{\text{C-F}}$ = 32.4, 10.7 Hz), 115.5, 98.8 (dd, $^4J_{\text{C-F}}$ = 5.8, 3.4 Hz), 78.4, 72.1 (d, $^3J_{\text{C-F}}$ = 5.2 Hz), 71.5, 69.0, 58.0, 44.0, 41.3 (d, $^4J_{\text{C-F}}$ = 4.2 Hz), 39.6, 36.5 (t, $^4J_{\text{C-F}}$ = 3.2 Hz), 31.9, 28.1 ppm;

^{19}F (376 MHz, toluene- d_8 , 373 K): δ = -98.6 (d, 2J = 74.3 Hz, 1F), -104.6 (d, 2J = 74.3 Hz, 1F) ppm;*

Minor *cis*-diastereoisomer **115db** (assigned on the basis of δ and intensity) ^{13}C NMR (150 MHz, toluene- d_8 , 373 K): δ = 155.7 (t, $^1J_{\text{C-F}}$ = 289.3 Hz), 154.6, 136.4, 115.8, 78.3, 72.4 (dd, $^3J_{\text{C-F}}$ = 4.6, 2.3 Hz), 71.4, 68.8, 50.1, 42.9, 40.9, 39.7, 32.1, 28.1 ppm;

^{19}F (376 MHz, toluene- d_8 , 373 K): δ = -97.5 (d, 2J = 69.1 Hz, 1F), -104.8 (d, 2J = 69.1 Hz, 1F) ppm;

$\bar{\nu}$ (neat) = 3430, 2926, 1736, 1666, 1426, 1158, 1056, 989 cm^{-1} ;

HRMS (NSI-ES): calcd for $\text{C}_{19}\text{H}_{32}\text{F}_2\text{NO}_6$, 408.2192 $[\text{M}+\text{H}]^+$, found: 408.2189;

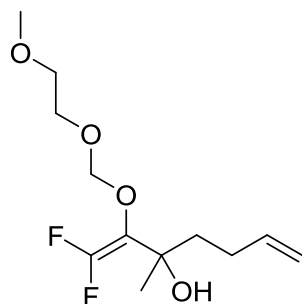
MS (CI): m/z (%): 408 (100) $[\text{M}+\text{H}]^+$;

t_{R} (GC) = 14.91 minutes.**

* this is by comparison with compounds from the Saegusa-Ito series (See compound **112f**).¹⁹⁴

** the *cis*- and *trans*-stereoisomers appeared as one peak by GC.

1,1-difluoro-2-((2-methoxyethoxy)methoxy)-3-methylhepta-1,6-dien-3-ol (**115e**)



115e

Prepared as for **115aa** and **115ab** from acetal (1.90 mL, 12 mmol), *n*-butyllithium (12.9 mL of a 1.94 M solution in hexanes, 25 mmol), diisopropylamine (3.70 mL, 26 mmol)

and 5-hexen-2-one (1.39 mL, 12 mmol) in THF (12 mL). The crude product (2.54 g) was purified by Kugelrohr distillation to afford **115e** (2.33 g, 73 %) as a pale yellow oil.

b.p. = 78 °C / 0.04 mmHg;

R_f = 0.27 (50 % diethyl ether in hexane);

¹H NMR (400 MHz, CDCl₃): δ = 5.85 (ddt, *J* = 16.9, 10.1, 6.5 Hz, 1H), 5.06 (dq, *J* = 16.9, ⁴*J* = ²*J* = 1.9 Hz, 1H), 5.00 (d, ²*J* = 6.4 Hz, 1H), 4.97 (dq, *J* = 10.1, ⁴*J* = ²*J* = 1.9 Hz, 1H), 4.93 (d, ²*J* = 6.4 Hz, 1H), 3.98-3.81 (m, 2H), 3.59 (br. t, *J* = 4.8 Hz, 2H), 3.41 (s, 3H), 3.39 (br. s, 1H), 2.10 (app. qt, *J* = 7.6, ⁴*J* = 1.9 Hz, 2H), 1.87-1.68 (m, 2H), 1.42 (d, ⁵*J*_{H-F} = 4.8 Hz, 3H) ppm;

¹³C (100 MHz, CDCl₃): δ = 154.2 (t, ¹*J*_{C-F} = 288.6 Hz), 137.8, 121.0 (dd, ²*J*_{C-F} = 32.7, 10.5 Hz), 114.0, 98.5 (t, ⁴*J*_{C-F} = 4.1 Hz), 71.1 (d, ³*J*_{C-F} = 3.7 Hz), 71.0, 68.5, 58.5, 39.3, 28.1, 24.5 (d, ⁴*J*_{C-F} = 7.1 Hz) ppm;

¹⁹F (376 MHz, CDCl₃): δ = -98.4 (d, ²*J* = 70.9 Hz, 1F), -103.9 (app. dq, ²*J* = 70.9 Hz, ⁵*J*_{F-H} = 4.8 Hz, 1F) ppm;

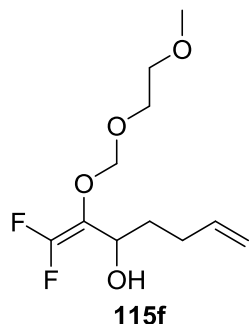
$\bar{\nu}$ /(neat) = 3447, 2928, 1736, 1102, 1024 cm⁻¹;

HRMS (NSI-ES): calcd for C₁₂H₂₀F₂O₄Na, 289.1222 [M+Na]⁺, found: 289.1221;

MS (CI): *m/z* (%): 161 (4) [M-C₄H₉O₃]⁺, 89 (73) [C₄H₉O₂]⁺, 59 (100) [C₃H₇O]⁺;

t_R (GC) = 11.38 minutes.

1,1-difluoro-2-((2-methoxyethoxy)methoxy)hepta-1,6-dien-3-ol (**115f**)



Prepared as for **115aa** and **115ab** from acetal (1.90 mL, 12 mmol), *n*-butyllithium (12.9 mL of a 1.94 M solution in hexanes, 25 mmol), diisopropylamine (3.70 mL, 26 mmol) and pentenal (1.37 g, 12 mmol) in THF (12 mL). The crude allylic alcohol (2.69 g) was purified by Kugelrohr distillation to afford **115f** as a pale yellow oil (1.93 g, 64 %).

b.p. = 78 °C / 0.05 mmHg;

R_f = 0.32 (20 % ethyl acetate in hexane);

¹H NMR (400 MHz, CDCl₃): δ = 5.81 (ddt, *J* = 16.7, 10.2, 6.7 Hz, 1H), 5.10- 4.93 (m, including 5.00 (d, ²*J* = 6.4 Hz, 1H), 2H), 4.88 (br. d, ²*J* = 6.4 Hz, 1H), 4.33-4.20 (m, 1H),

3.96 (ddd, $^2J = 10.8$, $J = 6.8$, 3.5 Hz, 1H), 3.77 (ddd, $^2J = 10.8$, $J = 4.8$, 2.7 Hz, 1H), 3.62-3.53 (m, 2H), 3.36 (s, 3H), 3.31 (br. d, $J = 8.2$ Hz, 1H), 2.22-2.02 (m, 2H), 1.89-1.65 (m, 2H) ppm;

^{13}C NMR (100 MHz, CDCl_3): $\delta = 154.2$ (dd, $^1J_{\text{C-F}} = 292.8$, 285.1 Hz), 137.2, 117.7 (dd, $^2J_{\text{C-F}} = 37.1$, 10.1 Hz), 114.6, 97.5 (t, $^4J_{\text{C-F}} = 3.7$ Hz), 70.9, 68.0, 66.0, 58.5, 32.6, 29.2 ppm;

^{19}F NMR (376 MHz, CDCl_3): $\delta = -100.2$ (d, $^2J = 64.2$ Hz, 1F), -109.7 (d, $^2J = 64.2$ Hz, 1F) ppm;

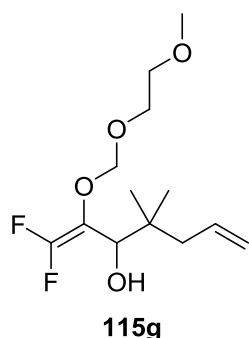
$\bar{\nu}$ (neat) = 3350, 2932, 1751, 1055, 1020, 955 cm^{-1} ;

MS (EI): m/z (%): 252 (3) $[\text{M}]^+$, 235 (1) $[\text{M-OH}]^+$, 89 (80) $[\text{C}_4\text{H}_9\text{O}_2]^+$, 59 (100) $[\text{C}_3\text{H}_7\text{O}]^+$;

t_{R} (GC) = 10.78 minutes.

The data was consistent with that previously reported.²⁰⁰

1,1-Difluoro-2-(2-methoxyethoxymethoxy)-4,4-dimethylhepta-1,6-dien-3-ol (115g)



Prepared as for **115aa** and **115ab** from acetal (1.58 mL, 10 mmol), *n*-butyllithium (15.7 mL of a 1.27 M solution in hexanes, 20 mmol), diisopropylamine (3.38 mL, 24 mmol) and 2,2-dimethylpenten-4-al (1.12 g, 10 mmol) in THF (11 mL). The mixture was quenched with saturated aqueous ammonium chloride (20 mL) and extracted with ethyl acetate (4 x 60 mL). The combined organic extracts were dried (MgSO_4), filtered and concentrated to afford crude allylic alcohol **115g** (3.05 g) as a dark yellow oil. The crude allylic alcohol was purified by flash column chromatography (90 g cartridge, 15 % ethyl acetate in hexane) to afford **115g** as a pale yellow oil (1.71 g, 61 %).

$R_f = 0.20$ (20 % ethyl acetate in hexane);

^1H NMR (400 MHz, CDCl_3): $\delta = 5.96$ -5.75 (m, 1H), 5.12-5.02 (m, including 5.05 (d, $^2J = 6.5$ Hz, 1H), 2H), 4.86 (br. d, $^2J = 6.5$ Hz, 1H), 4.04-3.98 (m, 1H), 3.97-3.92 (m, 1H) 3.83-3.74 (m, 1H), 3.62-3.55 (m, 2H), 3.41 (s, 3H), 3.15 (d, $J = 7.5$ Hz, 1H), 2.18 (one

half of a double ABq, $J_{AB} = 13.6$, $J = 7.5$ Hz, 1H), 2.04 (one half of a double ABq, $J_{AB} = 13.6$, $J = 7.5$ Hz, 1H), 0.97 (s, 3H), 0.92 (s, 3H) ppm;

^{13}C NMR (100 MHz, CDCl_3): $\delta = 154.5$ (dd, $^1J_{\text{C-F}} = 292.4$, 285.6 Hz), 134.5, 117.0, 117.0 (dd, $^2J_{\text{C-F}} = 35.4$, 10.1 Hz), 98.0 (t, $^4J_{\text{C-F}} = 3.8$ Hz), 72.2, 71.0, 68.5, 58.6, 43.1, 38.5, 22.6, 22.5 ppm;

^{19}F NMR (376 MHz, CDCl_3): $\delta = -100.4$ (d, $^2J = 65.5$ Hz, 1F), -109.7 (dd, $^2J = 65.5$, $^4J_{\text{F-H}} = 4.3$ Hz, 1F) ppm;

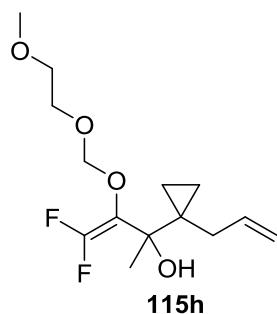
$\bar{\nu}$ (neat) = 3450, 2893, 1745, 1470, 1232, 1026, 956 cm^{-1} ;

MS (CI): m/z (%): 263 (1) $[\text{M-OH}]^+$, 207 (19) $[\text{M-C}_4\text{H}_9\text{O}]^+$, 89 (100) $[\text{C}_4\text{H}_9\text{O}_2]^+$, 59 (63) $[\text{C}_3\text{H}_7\text{O}]^+$;

t_R (GC) = 11.76 minutes.

The data was consistent with that previously reported.¹⁹⁸

1,1-Difluoro-2-((methoxyethoxy)methoxy)-3-methyl-4-cyclopropyl-hepta-1,6-dien-3-ol (115h)



Prepared as for **115aa** and **115ab** from acetal (1.26 mL, 8 mmol), *n*-butyllithium (8.3 mL of a 1.98 M solution in hexanes, 16 mmol), diisopropylamine (2.38 mL, 17 mmol) and 1-(1-allylcyclopropyl)ethan-1-one (1.00 g, 8 mmol) in THF (8 mL). The crude product (1.41 g) was purified by Kugelrohr distillation to afford **115h** (0.730 g, 31 %) as a pale yellow oil.

b.p. = 93 °C / 0.06 mmHg;

$R_f = 0.54$ (40 % ethyl acetate in hexane);

^1H NMR (400 MHz, CDCl_3): $\delta = 5.70$ (ddt, $J = 17.3$, 10.2 , 7.3 Hz, 1H), 5.11-4.96 (m, including 5.05 (d, $^2J = 6.4$ Hz, 1H), 2H), 4.91 (d, $^2J = 6.4$ Hz, 1H), 4.00-3.80 (m, 2H), 3.59 (t, $J = 4.8$ Hz, 2H), 3.41 (s, 3H), 3.12 (br. s, 1H), 2.34-2.13 (m, 2H), 1.42 (d, $^5J_{\text{H-F}} = 5.8$ Hz, 3H), 0.84-0.75 (m, 1H), 0.63 (ddd, $^2J = 9.9$, $J = 5.8$, 4.3 Hz, 1H) 0.45-0.35 (m, 1H), 0.29 (ddd, $^2J = 9.9$, $J = 5.5$, 4.3 Hz, 1H) ppm;

^{13}C (100 MHz, CDCl_3): $\delta = 154.6$ (t, $^1J_{\text{C-F}} = 288.8$ Hz), 135.6, 120.3 (dd, $^2J_{\text{C-F}} = 32.6$, 11.5 Hz), 116.0, 98.4 (t, $^4J_{\text{C-F}} = 4.2$ Hz), 72.1 (d, $^3J_{\text{C-F}} = 6.3$ Hz), 71.1, 68.6, 58.5, 37.1, 25.6, 22.9 (d, $^4J_{\text{C-F}} = 8.5$ Hz), 7.0, 5.1 ppm;

^{19}F (376 MHz, CDCl_3): $\delta = -97.7$ (d, $^2J = 68.4$ Hz, 1F), -102.7 (dq, $^2J = 68.4$ Hz, $^5J_{\text{F-H}} = 5.8$ Hz, 1F) ppm;

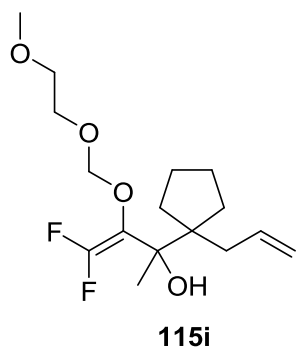
$\bar{\nu}$ (neat) = 3465, 2887, 1736, 1022, 937 cm^{-1} ;

HRMS (ESI): calcd for $\text{C}_{14}\text{H}_{26}\text{F}_2\text{O}_4\text{N}$, 310.1824 $[\text{M}+\text{NH}_4]^+$, found: 310.1826;

MS (EI): m/z (%): 161 (2) $[\text{M}-\text{C}_6\text{H}_9\text{F}_2\text{O}_3]^+$, 89 (69) $[\text{C}_4\text{H}_9\text{O}_2]^+$, 59 (100) $[\text{C}_3\text{H}_7\text{O}]^+$;

t_{R} (GC) = 12.75 minutes.

1,1-Difluoro-2-((methoxyethoxy)methoxy)-3-methyl-4-cyclopentyl-hepta-1,6-dien-3-ol (115i)



Prepared as for **115aa** and **115ab** from acetal (1.58 mL, 10 mmol), *n*-butyllithium (9.8 mL of a 2.04 M solution in hexanes, 20 mmol), diisopropylamine (3.38 mL, 24 mmol) and 1-(1-allylcyclopentyl)ethan-1-one (1.52 g, 10 mmol) in THF (11 mL). The crude product (2.13 g) was purified by Kugelrohr distillation to afford **115i** (0.965 g, 30%) as a pale yellow oil.

b.p. = 100 °C / 0.04 mmHg;

$R_f = 0.30$ (40 % diethyl ether in hexane);

^1H NMR (400 MHz, CDCl_3): $\delta = 5.70$ (ddt, $J = 17.3, 10.1, 7.3$ Hz, 1H), 5.11-4.99 (m, including 5.04 (d, $^2J = 6.3$ Hz, 1H), 2H), 4.88 (dt, $^2J = 6.4, ^5J_{\text{H-F}} = 1$ Hz, 1H), 3.94-3.80 (m, 2H), 3.58 (t, $J = 4.8$ Hz, 2H), 3.40 (s, 3H), 3.12 (br. s, 1H), 2.19 (d, $J = 7.3$ Hz, 2H), 1.88-1.74 (m, 2H), 1.68-1.35 (m, including 1.41 (d, $^5J_{\text{H-F}} = 5.4$ Hz, 3H), 6H) ppm;

^{13}C (100 MHz, CDCl_3): $\delta = 155.0$ (t, $^1J_{\text{C-F}} = 288.3$ Hz), 136.2, 120.3 (dd, $^2J_{\text{C-F}} = 32.1$, 11.3 Hz), 116.3, 99.0 (t, $^4J_{\text{C-F}} = 4.7$ Hz), 75.9 (d, $^3J_{\text{C-F}} = 4.8$ Hz), 71.1, 68.9, 58.5, 54.1, 41.1, 32.1, 31.6, 25.9, 25.2, 22.3 (d, $^4J_{\text{C-F}} = 8.6$ Hz) ppm;

Hz), 98.9 (t, $^4J_{C-F} = 3.9$ Hz), 71.7 (d, $^3J_{C-F} = 4.2$ Hz), 71.5, 68.9, 59.0, 40.4 (t $^4J_{C-F} = 2.7$ Hz), 27.4, 25.0 (d, $^4J_{C-F} = 7.4$ Hz) 17.9 ppm;

^{19}F (376 MHz, CDCl_3): $\delta = -98.4$ (d, $^2J = 70.5$ Hz, 1F), -103.9 ppm (d, $^2J = 70.5$ Hz, 1F); the ^{19}F - ^1H splitting was not resolved in the ^{19}F NMR spectrum;

Minor *Z*-diastereoisomer **115jb** (assigned on the basis of δ and intensity) ^{13}C NMR (100 MHz, CDCl_3): $\delta = 154.8$ (t, $^1J_{C-F} = 288.9$ Hz), 129.9, 124.3, 121.4 (dd, $^2J_{C-F} = 33.0$. 11.2 Hz), 52.3, 41.8, 40.3 (t $^4J_{C-F} = 2.9$ Hz), 27.1, 26.7, 21.9, 12.6 ppm;

^{19}F (376 MHz, CDCl_3): $\delta = -98.3$ (d, $^2J = 69.7$ Hz, 1F), -103.8 ppm (d, $^2J = 69.7$ Hz, 1F); the ^{19}F - ^1H splitting was not resolved in the ^{19}F NMR spectrum;

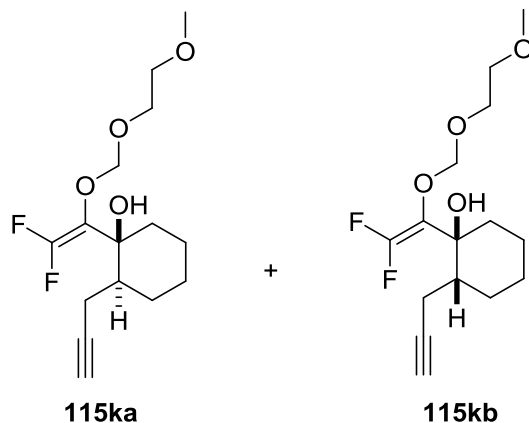
$\bar{\nu}$ (neat) = 3460, 2924, 1738, 1104, 1027, 964 cm^{-1} ;

HRMS (NSI-ES): calcd for $\text{C}_{13}\text{H}_{26}\text{F}_2\text{O}_4\text{Na}$, 298.1824 $[\text{M}+\text{NH}_4]^+$, found: 298.1828;

MS (CI): m/z (%): 263 (26) $[\text{M}-\text{OH}]^+$, 262 (100) $[\text{M}-\text{H}_2\text{O}]^+$;

t_R (GC) = 11.51 minutes.

***Trans*-1-(2,2-difluoro-1-((2-methoxyethoxy)methoxy)vinyl)-2-(prop-2-yn-1-yl)cyclohexan-1-ol** (*trans*-**115ka**) and ***cis*-1-(2,2-difluoro-1-((2-methoxyethoxy)methoxy)vinyl)-2-(prop-2-yn-1-yl)cyclohexan-1-ol** (*cis*-**115kb**)



Prepared as for **115aa** and **115ab** from acetal (0.79 mL, 5 mmol), *n*-butyllithium (5.4 mL of a 1.84 M solution in hexanes, 10 mmol), diisopropylamine (1.69 mL, 12 mmol) and 2-(prop-2-ynyl)cyclohexanone **S11** (0.68 g, 5 mmol) in THF (5 mL). The mixture was quenched with saturated aqueous ammonium chloride (20 mL) and extracted with ethyl acetate (4 x 60 mL). The combined organic extracts were dried (MgSO_4), filtered and concentrated to afford crude allylic alcohols *trans*-**115ka** and *cis*-**115kb** (1.30 g) as an orange oil. The crude allylic alcohol was purified by flash column chromatography using a Thompson Single Step cartridge (90 g cartridge, 20 % ethyl acetate in hexane) to

afford an inseparable mixture of *trans*-**115ka** and *cis*-**115kb** as a pale orange oil (0.291 g, 19 %, 97:3).

$R_f = 0.82$ (50 % ethyl acetate in hexane);

$^1\text{H NMR}$ (400 MHz, CDCl_3): $\delta = 4.94$ (app. s, 2H), 3.94-3.81 (m, 2H), 3.59 (app. t, $J = 4.8$ Hz, 2H), 3.41 (s, 3H), 2.93 (s, 1H), 2.34 (dt, $^2J = 16.9$, $J = ^4J = 2.8$ Hz, 1H), 2.20 (ddd, $^2J = 16.9$, $J = 8.9$, $^4J = 2.8$ Hz, 1H), 1.99 (t, $^4J = 2.8$ Hz, 1H), 1.94-1.47 (envelope, 8H), 1.36-1.21 (m, 1H) ppm;

$^{13}\text{C NMR}$ (100 MHz, CDCl_3): $\delta = 154.0$ (t, $^1J_{\text{C-F}} = 289.2$ Hz), 120.8 (dd, $^2J_{\text{C-F}} = 32.9$, 10.0 Hz), 98.3 (t, $^4J_{\text{C-F}} = 4.5$ Hz), 83.3, 72.6 (d, $^3J_{\text{C-F}} = 5.6$ Hz), 71.1, 68.8, 68.5, 58.5, 41.1 (d, $^4J_{\text{C-F}} = 4.7$ Hz), 36.4 (t, $^4J_{\text{C-F}} = 3.1$ Hz), 26.1, 24.7, 20.6, 19.7 ppm;

Major *trans*-diastereoisomer **115ka** (assigned on the basis of δ and intensity) ^{19}F (376 MHz, CDCl_3): $\delta = -98.0$ (d, $^2J = 72.3$ Hz, 1F), -103.1 (d, $^2J = 72.3$ Hz, 1F) ppm;*

Minor *cis*-diastereoisomer **115kb** (assigned on the basis of δ and intensity) ^{19}F (376 MHz, CDCl_3): $\delta = -96.7$ (d, $^2J = 67.2$ Hz, 1F), -103.7 (d, $^2J = 67.2$ Hz, 1F) ppm;

$\bar{\nu}(\text{neat}) = 3452, 3302, 2928, 1734, 1216, 1056 \text{ cm}^{-1}$;

HRMS (ESI): calcd for $\text{C}_{15}\text{H}_{23}\text{F}_2\text{O}_4$, 305.1564 $[\text{M}+\text{H}]^+$, found: 305.1557;

MS (CI): m/z (%): 305 (10) $[\text{M}+\text{H}]^+$, 322 (15) $[\text{M}+\text{NH}_4]^+$;

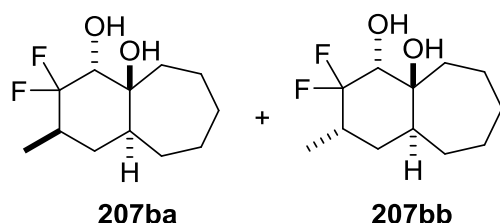
t_R (GC) = 12.90 minutes.**

*this is by comparison with compounds from the Saegusa-Ito series (See compound **112f**).¹⁹⁴

**the *cis*- and *trans*-stereoisomers appeared as one peak by GC.

6.3.10 Scope of cyclisation/reduction methodology

(**2R***,**4R***,**4aS***,**9aS***)-3,3-Difluoro-2-methyldecahydro-4a*H*-benzo[7]annulene-4,4a-diol (**207ba**) and (**2S***,**4R***,**4aS***,**9aS***)-3,3-difluoro-2-methyldecahydro-4a*H*-benzo[7]annulene-4,4a-diol (**207bb**)



Diols **207ba** and **207bb** were prepared according to general procedure D for **207aa/207ab** from **115ba/115bb** (0.320 g, 1.00 mmol) with 1,3-*bis*(2,6-diisopropylphenyl)imidazol-2-ylidene)gold(I) chloride (5 mol %, 0.031 g) and silver hexafluoroantimonate(V) (5 mol %, 0.017 g) in dichloromethane (5.4 mL) and methanol

(0.6 mL). After stirring for 5 hours at 40 °C the reaction was allowed to cool to room temperature. Solid tetrabutylammonium borohydride (0.258 g, 1 mmol) was added to the flask in small portions. The reaction mixture was then allowed to stir at room temperature for 18 hours. The usual work up, according to **207aa/207ab**, afforded a viscous pale yellow oil (0.323 g). The crude material was purified by flash column chromatography (40 g silica, 1 % acetone in dichloromethane) to afford an inseparable mixture of *trans,trans*-**207ba** and *trans,cis*-**207bb** as a colourless solid (0.162 g, 69 %, 4.9:1).

$R_f = 0.34$ (1 % acetone in dichloromethane);

The following signals were attributed to both the minor *trans,cis*-diastereoisomer **207bb** and major *trans,trans*-diastereoisomer **207ba** ^1H NMR (400 MHz, CDCl_3): $\delta = 3.52$ (td, $J_{\text{H-F}} = 5.9$, $J = 3.2$ Hz, 1H), 1.99-1.17 (envelope, 15H) ppm;

The following signals were attributed to the major *trans,trans*-diastereoisomer **207ba** (assigned on the basis of δ and intensity)

^1H NMR (400 MHz, CDCl_3): $\delta = 2.35$ -2.14 (m, including 2.29 (t, $J = ^4J_{\text{H-F}} = 3.2$ Hz, 1H), 1H), 2.09-1.99 (m, 1H), 1.04 (d, $J = 6.8$ Hz, 3H) ppm;

^{13}C NMR (100 MHz, MeOD): $\delta = 123.1$ (t, $^1J_{\text{C-F}} = 248.3$ Hz), 75.5 (dd, $^2J_{\text{C-F}} = 27.6$, 20.5 Hz), 74.6 (d, $^3J_{\text{C-F}} = 5.5$ Hz), 40.2, 39.2, 34.3 (d, $^3J_{\text{C-F}} = 8.5$ Hz), 32.6 (t, $^2J_{\text{C-F}} = 22.0$ Hz), 28.0, 27.0, 26.1, 19.8, 10.2 (d, $^3J_{\text{C-F}} = 5.7$ Hz) ppm;

^{19}F NMR (376 MHz, CDCl_3): $\delta = -107.6$ (app. ds, $^2J = 256.3$, $^3J_{\text{F-H}} = ^4J_{\text{F-H}} = 3.2$ Hz, 1F), -117.1 (dddd, $^2J = 256.3$, $^3J_{\text{F-H}} = 30.2$, $^3J_{\text{F-H}} = 8.9$, $^4J_{\text{F-H}} = 6.0$ Hz, 1F) ppm;

The following signals were attributed to the minor *trans,cis* -diastereoisomer **207bb** (assigned on the basis of δ and intensity)

^{13}C NMR (100 MHz, MeOD): $\delta = 122.7$ (dd, $^1J_{\text{C-F}} = 251.0$, 243.2 Hz), 76.6 (dd, $^2J_{\text{C-F}} = 28.7$, 20.5 Hz), 74.3 (d, $^3J_{\text{C-F}} = 5.4$ Hz), 39.0, 35.0, 34.9 (dd, $^2J_{\text{C-F}} = 23.8$, 21.1 Hz), 32.6 (d, $^3J_{\text{C-F}} = 6.4$ Hz), 28.2, 27.1, 26.3, 13.4 (dd, $^3J_{\text{C-F}} = 9.7$, 4.0 Hz) ppm;

^{19}F NMR (376 MHz, CDCl_3): $\delta = -93.7$ (ddt, $^2J = 261.3$, $^3J_{\text{F-H}} = 18.3$, $^3J_{\text{F-H}} = ^4J_{\text{F-H}} = 8.1$ Hz), -106.5 (d, $^2J = 261.3$ Hz) ppm;

$\bar{\nu}$ (neat) = 3601, 3333, 2908, 1463, 1084, 979 cm^{-1} ;

HRMS (APCI): calcd for $\text{C}_{12}\text{H}_{20}\text{F}_2\text{O}_2$, 234.1431 $[\text{M}]^+$, found: 234.1432;

MS (EI): m/z (%): 234 (1) $[\text{M}]^+$, 196 (9) $[\text{M}-2\text{F}]^+,*$

t_R (GC) = 12.80 minutes.*

elemental analysis calcd (%) for $\text{C}_{12}\text{H}_{20}\text{F}_2\text{O}_2$: C, 61.52; H, 8.60; found: C, 61.40; H, 8.38. This analysis was obtained for the amorphous solid obtained following chromatography so no melting point was recorded.

* the individual diastereoisomers appeared as one peak by GC.

Diastereomerically pure *trans*, *trans*-**207ba** could be obtained by performing three vapour diffusion recrystallisations (chloroform/pentane) of the mixed solid diol (0.018g, 7%).

m.p. = 96-98 °C (recrystallised from chloroform/pentane vapour diffusion as a colourless plate);

R_f = 0.34 (1 % acetone in dichloromethane);

¹H NMR (400 MHz, CDCl₃): δ = 3.54 (td, J_{H-F} = 5.9, J = 3.2 Hz, 1H), 2.36-2.15 (m, 2H), 2.12-1.99 (m, 1H), 1.90-1.23 (envelope, 13H), 1.06 (d, J = 6.8 Hz, 3H) ppm;

¹³C NMR (100 MHz, CDCl₃): δ = 124.0 (t, ¹J_{C-F} = 247.8 Hz), 76.1 (dd, ²J_{C-F} = 27.4, 20.8 Hz), 74.8 (d, ³J_{C-F} = 5.1 Hz), 40.2, 39.2, 34.3 (d, ³J_{C-F} = 8.6 Hz), 32.5 (t, ²J_{C-F} = 21.7 Hz), 28.1, 27.2, 26.3, 20.0, 11.0 (d, ³J_{C-F} = 5.2 Hz) ppm;

¹⁹F NMR (376 MHz, CDCl₃): δ = -107.6 (app. ds, ²J = 256.3, ³J_{F-H} = ⁴J_{F-H} = 3.2 Hz, 1F), -117.1 (dddd, ²J = 256.3, ³J_{F-H} = 30.2, ³J_{F-H} = 8.9, ⁴J_{F-H} = 6.0 Hz, 1F) ppm;

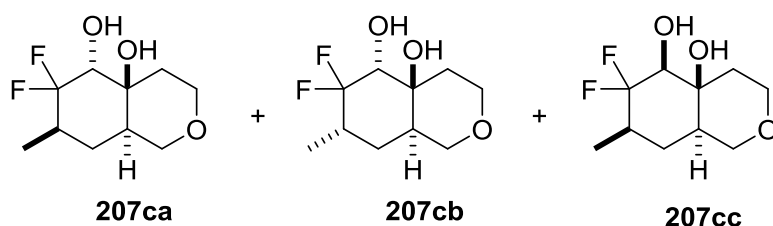
$\bar{\nu}$ /(neat) = 3601, 3333, 2908, 1463, 1084, 979 cm⁻¹;

MS (EI): *m/z* (%): 234 (1) [M]⁺, 196 (9) [M-2F]⁺;

t_R (GC) = 12.80 minutes.

elemental analysis calcd (%) for C₁₂H₂₀F₂O₂: C, 61.52; H, 8.60; found: C, 61.37; H, 8.50.

(4aS*,5R*,7R*,8aR*)-6,6-Difluoro-7-methyloctahydro-4aH-isochromene-4a,5-diol (207ca), **(4aS*,5R*,7S*,8aR*)-6,6-difluoro-7-methyloctahydro-4aH-isochromene-4a,5-diol (207cb)** and **(4aS*,5S*,7R*,8aR*)-6,6-difluoro-7-methyloctahydro-4aH-isochromene-4a,5-diol (207cc)**



Diols **207ca**, **207cb** and **207cc** were prepared according to general procedure D for **207aa/207ab** from **115ca/115cb** (0.308 g, 1.00 mmol) with 1,3-bis(2,6-diisopropylphenyl-imidazol-2-ylidene)gold(I) chloride (5 mol %, 0.031 g) and silver hexafluoroantimonate(V) (5 mol %, 0.017 g) in dichloromethane (5.4 mL) and methanol (0.6 mL). After stirring for 6.5 hours at 40 °C the reaction was allowed to cool to room temperature. Solid tetrabutylammonium borohydride (0.258 g, 1 mmol) was added to the

flask in small portions. The reaction mixture was then allowed to stir at room temperature for 18 hours. The usual work up, according to **207aa/207ab**, afforded a viscous pale yellow oil (0.300 g). The crude material was purified by flash column chromatography (40 g silica, 10 % acetone in dichloromethane) to afford an inseparable mixture of *trans,trans*-**207ca**, *trans,cis*-**207cb** and *cis,cis*-**207cc** as a colourless solid (0.107 g, 48 %, 6.7:1.4:1).

$R_f = 0.39$ (20 % acetone in dichloromethane);

The following signals were attributed to the minor *trans,cis* **207cb** and *cis,cis* diastereoisomers **207cc** and the major *trans,trans*-diastereoisomer **207ca** ^1H NMR (400 MHz, CDCl_3): $\delta = 3.93\text{-}3.78$ (m, 3H), 3.65-3.46 (m, 4H), 2.47-1.47 (envelope, 6H), 1.43-1.15 (envelope, 4H) ppm;

The following signals were attributed to the major *trans,trans*-diastereoisomer **207ca** (assigned on the basis of δ and intensity)

^1H NMR (400 MHz, CDCl_3): $\delta = 2.70$ (t, $J = {}^4J_{\text{H-F}} = 3.0$ Hz, 1H), 1.09 (d, $J = 6.9$ Hz, 3H) ppm;

^{13}C NMR (100 MHz, CDCl_3): $\delta = 123.7$ (dd, ${}^1J_{\text{C-F}} = 250.5, 246.7$ Hz), 73.2 (dd, ${}^2J_{\text{C-F}} = 27.7, 21.6$ Hz), 70.6 (d, ${}^3J_{\text{C-F}} = 5.7$ Hz), 66.1, 62.1, 36.5, 33.6, 32.7 (t, ${}^2J_{\text{C-F}} = 22.1$ Hz), 27.1 (d, ${}^3J_{\text{C-F}} = 8.3$ Hz), 11.2 (dd, ${}^3J_{\text{C-F}} = 6.2, 2.8$ Hz) ppm;

^{19}F NMR (376 MHz, CDCl_3): $\delta = -105.8$ (dq, ${}^2J = 258.4, {}^3J_{\text{F-H}} = {}^4J_{\text{F-H}} = 4.2$ Hz, 1F), -117.1 (dddd, ${}^2J = 258.4, {}^3J_{\text{F-H}} = 30.5, {}^3J_{\text{F-H}} = 10.7, {}^4J_{\text{F-H}} = 5.9$ Hz, 1F) ppm;

The following signals were attributed to the *trans,cis*-diastereoisomer **207cb** (assigned on the basis of δ and intensity)

^1H NMR (400 MHz, CDCl_3): $\delta = 2.65$ (t, $J = {}^4J_{\text{H-F}} = 2.9$ Hz, 1H), 1.12 (d, $J = 6.9$ Hz, 3H) ppm;

^{13}C NMR (100 MHz, CDCl_3): $\delta = 123.1$ (dd, ${}^1J_{\text{C-F}} = 254.8, 241.6$ Hz), 74.3 (dd, ${}^2J_{\text{C-F}} = 29.0, 21.9$ Hz), 70.4 (d, ${}^3J_{\text{C-F}} = 7.7$ Hz), 66.5, 62.2, 41.1, 34.8 (t, ${}^2J_{\text{C-F}} = 22.5$ Hz), 31.3, 27.0 (d, ${}^3J_{\text{C-F}} = 8.3$ Hz), 14.1 (dd, ${}^3J_{\text{C-F}} = 9.9, 4.0$ Hz) ppm;

^{19}F NMR (376 MHz, CDCl_3): $\delta = -93.7$ (dddd, ${}^2J = 263.9, {}^3J_{\text{F-H}} = 18.0, 10.4, {}^4J_{\text{F-H}} = 6.7$ Hz, 1F), -104.3 (d, ${}^2J = 263.9$ Hz, 1F) ppm;

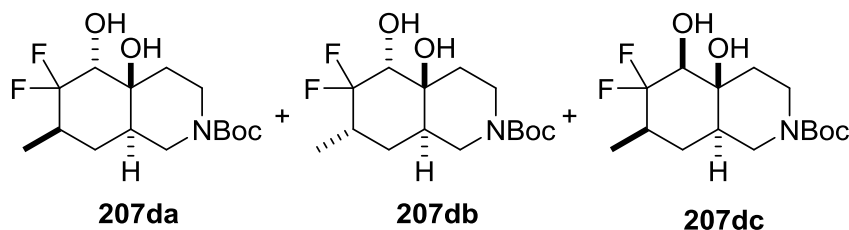
The following signals were attributed to the *cis,cis*-diastereoisomer **207cc** (assigned on the basis of δ and intensity)

^1H NMR (400 MHz, CDCl_3): $\delta = 2.84$ (d, $J = 6.5$ Hz, 1H) ppm;

^{13}C NMR (100 MHz, CDCl_3): $\delta = 75.0$ (t, ${}^2J_{\text{C-F}} = 19.3$ Hz), 70.2 (d, ${}^3J_{\text{C-F}} = 5.4$ Hz), 65.6, 62.7, 36.8 (dd, ${}^2J_{\text{C-F}} = 23.3, 21.2$ Hz), 34.9, 29.2, 25.3 (d, ${}^3J_{\text{C-F}} = 7.0$ Hz), 11.3 (dd, ${}^3J_{\text{C-F}} = 6.2, 2.9$ Hz) ppm;

^{19}F NMR (376 MHz, CDCl_3): $\delta = (-106.7) - (-107.6)$ (m, including -107.1 (app. d, $^2J = 243.7$ Hz, 1F)), -104.4 (dddd, $^2J = 243.7$, $^3J_{\text{F-H}} = 28.2$, 20.1 , $^4J_{\text{F-H}} = 4.6$ Hz, 1F) ppm;
 $\bar{\nu}$ (neat) = 3331, 2878, 2908, 1472, 1091, 966 cm^{-1} ;
 HRMS (APCI): calcd for $\text{C}_{10}\text{H}_{17}\text{F}_2\text{O}_3$, 223.1146 $[\text{M}+\text{H}]^+$, found: 223.1142;
 MS (EI): m/z (%): 222 (1) $[\text{M}]^+$ (major *trans, trans* diastereoisomer, minor *trans, cis* diastereoisomer and minor *cis, cis* diastereoisomer);
 t_{R} (GC) = 12.27 minutes (major *trans, trans* diastereoisomer), 12.34 minutes (minor *trans, cis* diastereoisomer), 12.69 (minor *cis, cis* diastereoisomer);
 elemental analysis calcd (%) for $\text{C}_{10}\text{H}_{16}\text{F}_2\text{O}_3$: C, 54.05; H, 7.26; found: C, 54.05; H, 6.93. This analysis was obtained for the amorphous solid obtained following chromatography so no melting point was recorded.

***tert*-Butyl (4a*S**,5*R**,7*R**,8a*R**)-6,6-difluoro-4a,5-dihydroxy-7-methyloctahydroisoquinoline-2(1*H*)-carboxylate (207da), *tert*-butyl (4a*S**,5*R**,7*S**,8a*R**)-6,6-difluoro-4a,5-dihydroxy-7-methyloctahydroisoquinoline-2(1*H*)-carboxylate (207db) and *tert*-butyl (4a*S**,5*S**,7*R**,8a*R**)-6,6-difluoro-4a,5-dihydroxy-7-methyloctahydroisoquinoline-2(1*H*)-carboxylate (207dc)**



Diols **207da**, **207db** and **207dc** were prepared according to general procedure D for **207aa/207ab** from **115da/115db** (0.407 g, 1.00 mmol) with 1,3-*bis*(2,6-diisopropylphenyl-imidazol-2-ylidene)gold(I) chloride (5 mol %, 0.031 g) and silver hexafluoroantimonate(V) (5 mol %, 0.017 g) in dichloromethane (5.4 mL) and methanol (0.6 mL). After stirring for 240 hours at 40 °C the reaction was allowed to cool to room temperature. Solid tetrabutylammonium borohydride (0.258 g, 1 mmol) was added to the flask in small portions. The reaction mixture was then allowed to stir at room temperature for 18 hours. The usual work up, according to **207aa/207ab**, afforded a viscous pale yellow oil (0.434 g). The crude material was purified by flash column chromatography (40 g silica, 5-8 % acetone in dichloromethane) to afford an inseparable mixture of *trans,trans*-**207da**, *trans,cis*-**207db** and *cis,cis*-**207dc** as a colourless solid (0.160 g, 50 %, 3.4:0.9:1).

$R_f = 0.31$ (10 % acetone in dichloromethane);

The following signals were attributed to the minor *trans,cis*-**207db** and *cis,cis*-**207dc** diastereoisomers and the major *trans,trans*-diastereoisomer **207da** ^1H NMR (600 MHz, pyridine- d_5 , 373 K): $\delta = 4.35$ - 4.21 (m, 1H), 4.20 - 4.05 (m, 1H), 3.69 - 3.27 (m, 2H), 3.28 - 3.06 (m, 1H), 2.63 - 2.35 (m, 2H), 2.33 - 2.14 (m, 1H), 2.14 - 1.77 (m, 1H), 1.77 - 1.51 (m, including 1.60 (s, 9H), 15H), 1.39 - 1.22 (m, 2H) ppm;

The following signals were attributed to the major *trans,trans*-diastereoisomer **207da** (assigned on the basis of δ and intensity)

^1H NMR (600 MHz, pyridine- d_5 , 373 K): $\delta = 6.97$ (br. s, 1H), 4.59 (br. s, 1H), 3.95 (t, $J = {}^4J_{\text{H-F}} = 6.2$ Hz, 1H), 1.17 (d, $J = 7.0$ Hz, 3H) ppm;

^{13}C NMR (100 MHz, CDCl_3): $\delta = 154.3$, 123.8 (dd, ${}^1J_{\text{C-F}} = 251.5$, 246.5 Hz), 79.1 , 73.3 (dd, ${}^2J_{\text{C-F}} = 27.8$, 21.9 Hz), 71.2 (d, ${}^3J_{\text{C-F}} = 5.7$ Hz), 11.1 (d, ${}^3J_{\text{C-F}} = 5.1$ Hz) ppm;

The ^{13}C NMR spectral region ranging from 46 - 26 ppm was poorly resolved at 298 K. The ^{13}C NMR spectrum was recorded in pyridine- d_5 at 373 K to resolve this region.

^{13}C NMR (150 MHz, pyridine- d_5 , 373 K): $\delta = 44.2$, 39.3 , 37.4 , 34.8 , 33.6 (t, ${}^2J_{\text{C-F}} = 22.5$ Hz), 30.0 (d, ${}^3J_{\text{C-F}} = 8.4$ Hz), 28.4 ppm;

^{19}F NMR (376 MHz, CDCl_3): $\delta = -106.2$ (dq, ${}^2J = 258.2$, ${}^3J_{\text{F-H}} = {}^4J_{\text{F-H}} = 4.7$ Hz, 1F), -117.1 (br. ddt, ${}^2J = 258.2$, ${}^3J_{\text{F-H}} = 30.0$, ${}^3J_{\text{F-H}} = {}^4J_{\text{F-H}} = 6.5$ Hz, 1F) ppm (the ^{19}F NMR spectrum was well resolved at 273 K and did not require heating. ^1H and ^{13}C NMR resolved slightly better when heated to 373 K).

The following signals were attributed to the *trans,cis*-diastereoisomer **207db** (assigned on the basis of δ and intensity)

^1H NMR (600 MHz, pyridine- d_5 , 373 K): $\delta = 1.41$ (d, $J = 7.4$ Hz, 1H) ppm;

^{13}C NMR (100 MHz, CDCl_3): $\delta = 79.2$, 74.4 (dd, ${}^2J_{\text{C-F}} = 28.9$, 21.7 Hz), 71.1 (d, ${}^3J_{\text{C-F}} = 7.9$ Hz), 14.2 (dd, ${}^3J_{\text{C-F}} = 9.9$, 3.4 Hz) ppm;

The ^{13}C NMR spectral region ranging from 46 - 26 ppm was poorly resolved at 298 K. The ^{13}C NMR spectrum was recorded in pyridine- d_5 at 373 K to resolve this region.

^{13}C NMR (150 MHz, pyridine- d_5 , 373 K): $\delta = 44.7$, 39.7 , 37.7 (t, ${}^2J_{\text{C-F}} = 22.1$ Hz), 35.5 , 29.8 (d, ${}^3J_{\text{C-F}} = 7.8$ Hz) ppm;

^{19}F NMR (376 MHz, CDCl_3): $\delta = -93.1$ (dddd, ${}^2J = 263.9$, ${}^3J_{\text{F-H}} = 18.0$, 10.4 , ${}^4J_{\text{F-H}} = 6.8$ Hz, 1F), -104.7 (d, ${}^2J = 263.9$ Hz, 1F) ppm;

The following signals were attributed to the *cis,cis*-diastereoisomer **207dc** (assigned on the basis of δ and intensity)

^1H NMR (600 MHz, pyridine- d_5 , 373 K): $\delta = 4.63$ (br. s, 1H), 3.99 (t, $J = {}^4J_{\text{H-F}} = 6.3$ Hz, 1H), 3.76 (dd, $J_{\text{H-F}} = 20.2$, $J = 6.3$ Hz, 1H), 1.16 (d, $J = 6.8$ Hz, 3H) ppm;

^{13}C NMR (100 MHz, CDCl_3): $\delta = 79.1, 74.9$ (t, $^2J_{\text{C-F}} = 20.4$ Hz), 70.8 (d, $^3J_{\text{C-F}} = 5.8$ Hz), 11.3 (dd, $^3J_{\text{C-F}} = 5.6, 2.9$ Hz) ppm;

The ^{13}C NMR spectral region ranging from 46-26 ppm was poorly resolved at 298 K.

The ^{13}C NMR spectrum was recorded in pyridine- d_5 at 373 K to resolve this region.

^{13}C NMR (150 MHz, pyridine- d_5 , 373 K): $\delta = 43.9, 41.7, 39.3, 36.1$ (t, $^2J_{\text{C-F}} = 23.2$ Hz), $32.3, 28.5$ (d, $^3J_{\text{C-F}} = 7.1$ Hz) ppm;

^{19}F NMR (376 MHz, CDCl_3): $\delta = -107.6$ (d, $^2J = 243.7$ Hz, 1F), -116.1 (ddd, $^2J = 243.7$, $^3J_{\text{F-H}} = 27.4, 20.2$ Hz, 1F) ppm;

$\bar{\nu}$ (neat) = 3274, 2924, 1656, 1158, 870 cm^{-1} ;

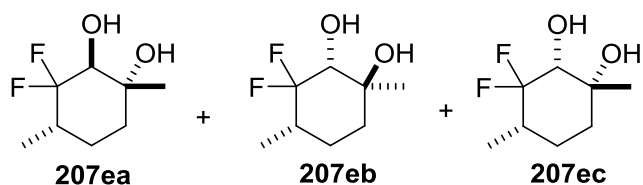
HRMS (APCI): calcd for $\text{C}_{15}\text{H}_{26}\text{F}_2\text{O}_4\text{N}_1$, 322.1830 $[\text{M}+\text{H}]^+$, found: 322.1831;

MS (EI): m/z (%): 321 (3) $[\text{M}]^+$, 247 (23) $[\text{M}-\text{C}_4\text{H}_{10}\text{O}]^+$ (major *trans, trans* diastereoisomer), 321 (1) $[\text{M}]^+$, 247 (24) $[\text{M}-\text{C}_4\text{H}_{10}\text{O}]^+$ (minor *trans, cis* diastereoisomer), 321 (2) $[\text{M}]^+$, 247 (22) $[\text{M}-\text{C}_4\text{H}_{10}\text{O}]$ (minor *cis, cis* diastereoisomer);

t_{R} (GC) = 15.06 minutes (major *trans, trans* diastereoisomer), 15.15 minutes (minor *trans, cis* diastereoisomer), 14.99 (minor *cis, cis* diastereoisomer);

elemental analysis calcd (%) for $\text{C}_{15}\text{H}_{25}\text{F}_2\text{NO}_4$: C, 56.06; H, 7.84; N, 4.36; found: C, 56.37; H, 7.86; N, 4.34. This analysis was obtained for the amorphous solid obtained following chromatography so no melting point was recorded.

(1R*,2S*,4S*)-3,3-Difluoro-1,4-dimethylcyclohexane-1,2-diol (207ea),
(1S*,2R*,4S*)-3,3-difluoro-1,4-dimethylcyclohexane-1,2-diol (207eb) and
(1R*,2R*,4S*)-3,3-difluoro-1,4-dimethylcyclohexane-1,2-diol (207ec)



Diols **207ea**, **207eb** and **207ec** were prepared according to general procedure D for **207aa/207ab** from **115e** (0.327 g, 1.23 mmol) with 1,3-*bis*(2,6-diisopropylphenyl-imidazol-2-ylidene)gold(I) chloride (5 mol %, 0.038 g) and silver hexafluoroantimonate(V) (5 mol %, 0.021 g) in dichloromethane (6.6 mL) and methanol (0.7 mL). After stirring for 18 hours at 40 °C the reaction was allowed to cool to room temperature. Solid tetrabutylammonium borohydride (0.317 g, 1.23 mmol) was added to the flask in small portions. The reaction mixture was then allowed to stir at room

temperature for 18 hours. The usual work up, according to **207aa/207ab**, afforded a viscous pale yellow oil (0.320 g). The crude material was purified by flash column chromatography (40 g silica, 30 % ethyl acetate in hexane) to afford a mixture of *cis,cis*-**207ec** and *trans,trans*-**207ea** as a pale yellow oil (33.7 mg, 15 %, 1.2:1), *trans,trans*-**207ea** as a pale yellow oil (55.5 mg, 25 %) and *trans,cis*-**207eb** as a colourless solid (35.6 mg, 16 %).

R_f *cis,cis*-**207ec** = 0.25 (10 % acetone in dichloromethane);

R_f *trans,trans*-**207ea** = 0.31 (10 % acetone in dichloromethane);

The following signals were attributed to both the major *cis,cis*-diastereoisomer **207ec** and minor *trans,trans*-diastereoisomer **207ea** ^1H NMR (400 MHz, CDCl_3): δ = 2.35-1.97 (m, 3H), 1.95-1.68 (m, 3H), 1.68-1.42 (m, 5H) ppm;

The following signals were attributed to the major *cis,cis*-diastereoisomer **207ec** (assigned on the basis of δ and intensity)

^1H NMR (400 MHz, CDCl_3): δ = 3.48 (dd, $J_{\text{H-F}} = 20.3, 6.0$ Hz, 1H), 1.34 (s, 3H), 1.11 (d, $J = 6.7$ Hz, 3H) ppm;

^{13}C NMR (150 MHz, CDCl_3): δ = 121.9 (t, $^1J_{\text{C-F}} = 246.8$ Hz), 74.3 (t, $^2J_{\text{C-F}} = 20.3$ Hz), 71.9 (d, $^3J_{\text{C-F}} = 6.9$ Hz), 36.7 (dd, $^2J_{\text{C-F}} = 23.3, 20.5$ Hz), 35.3, 25.9, 24.8 (d, $^4J_{\text{C-F}} = 7.8$ Hz), 11.0 (d, $^3J_{\text{C-F}} = 4.3$ Hz) ppm;

^{19}F NMR (376 MHz, $\text{DMSO-}d_6$, 373 K): δ = -104.6 (d, $^2J = 238.7$ Hz, 1F), -127.9 (dt, $^2J = 238.7, ^3J_{\text{F-H}} = 20.3$ Hz, 1F) ppm (the ^1H and ^{13}C NMR gave clear well resolved spectra at RT and did not require heating. ^{19}F NMR resolved better when heated to 373 K).

The following signals were attributed to the minor *trans,trans*-diastereoisomer **207ea** (assigned on the basis of δ and intensity)

^1H NMR (400 MHz, CDCl_3): δ = 3.63 (dd, $J_{\text{H-F}} = 8.1, 6.7$ Hz, 1H), 1.33 (s, 3H), 1.08 (d, $J = 6.9$ Hz, 3H) ppm;

^{13}C NMR (150 MHz, CDCl_3): δ = 123.4 (t, $^1J_{\text{C-F}} = 248.1$ Hz), 73.4 (dd, $^2J_{\text{C-F}} = 26.8, 21.6$ Hz), 72.3 (d, $^3J_{\text{C-F}} = 4.3$ Hz), 31.9 (t, $^2J_{\text{C-F}} = 21.4$ Hz), 31.5, 24.7 (d, $^3J_{\text{C-F}} = 7.4$ Hz), 24.7 (d, $^4J_{\text{C-F}} = 7.4$ Hz), 10.9 (d, $^3J_{\text{C-F}} = 4.5$ Hz) ppm;

^{19}F NMR (376 MHz, $\text{DMSO-}d_6$, 373 K): δ = -104.2 (d, $^2J = 243.2$ Hz, 1F), -114.0 (dd, $^2J = 243.2, ^3J_{\text{F-H}} = 25.8$ Hz, 1F) ppm;

$\bar{\nu}$ /(neat) = 3392, 2941, 1461, 1066, 994 cm^{-1} ;

HRMS (ESI): calcd for $\text{C}_8\text{H}_{18}\text{F}_2\text{O}_2\text{N}_1$, 198.1300 $[\text{M}+\text{NH}_4]^+$, found: 198.1300;

MS (EI): m/z (%): 142 (8) $[\text{M}-2\text{F}]^+$ (major *cis,cis* diastereoisomer), 142 (7) $[\text{M}-2\text{F}]^+$ (minor *trans,trans* diastereoisomer);

t_R (GC) = 8.77 minutes (major *cis,cis* diastereoisomer), 8.54 minutes (minor *trans, trans* diastereoisomer).

Diastereomerically pure *trans, trans*-**207ea**:

R_f = 0.31 (10 % acetone in dichloromethane);

^1H NMR (400 MHz, CDCl_3): δ = 3.62 (dd, $J_{\text{H-F}} = 8.1, 6.7$ Hz, 1H), 2.81 (br. s, 1H), 2.40-1.97 (m, 2H), 1.81-1.69 (m, 1H), 1.67-1.45 (m, 3H), 1.33 (s, 3H), 1.07 (d, $J = 6.9$ Hz, 3H) ppm;

^{13}C NMR (100 MHz, CDCl_3): δ = 123.9 (t, $^1J_{\text{C-F}} = 247.0$ Hz), 73.9 (dd, $^2J_{\text{C-F}} = 26.9, 21.7$ Hz), 72.8 (d, $^3J_{\text{C-F}} = 4.2$ Hz), 32.4 (t, $^2J_{\text{C-F}} = 21.8$ Hz), 32.0, 25.2 (d, $^3J_{\text{C-F}} = 7.3$ Hz), 25.2 (d, $^4J_{\text{C-F}} = 7.3$ Hz), 11.5 (t, $^3J_{\text{C-F}} = 4.1$ Hz) ppm;

^{19}F NMR (376 MHz, $\text{DMSO-}d_6$, 373 K): δ = -104.2 (d, $^2J = 243.2$ Hz, 1F), -114.0 (dd, $^2J = 243.2, ^3J_{\text{F-H}} = 25.8$ Hz, 1F) ppm;

$\bar{\nu}$ (neat) = 3392, 2941, 1461, 1066, 994 cm^{-1} ;

MS (EI): m/z (%): 142 (7) $[\text{M}-2\text{F}]^+$;

t_R (GC) = 8.54 minutes;

Diastereomerically pure *trans, cis*-**207eb**:

m.p. = 58-60 °C (recrystallised from chloroform/pentane vapour diffusion as a colourless plate);

R_f = 0.33 (20 % acetone in dichloromethane);

^1H NMR (400 MHz, CDCl_3): δ = 3.71 (dd, $J_{\text{H-F}} = 22.5, 4.6$ Hz, 1H), 2.81 (br. s, 1H), 2.64 (s, 1H), 1.99-1.76 (m, 2H), 1.74-1.54 (m, 2H), 1.34 (td, $^2J = J = 13.7, J = 4.9$ Hz, 1H), 1.27 (d, $^5J_{\text{H-F}} = 2.3$ Hz, 3H), 1.09 (d, $J = 6.9$ Hz, 3H) ppm;

^{13}C NMR (100 MHz, CDCl_3): δ = 121.9 (dd, $^1J_{\text{C-F}} = 249.0, 245.2$ Hz), 77.9 (t, $^2J_{\text{C-F}} = 20.5$ Hz), 73.4 (d, $^3J_{\text{C-F}} = 7.8$ Hz), 37.1 (t, $^2J_{\text{C-F}} = 21.8$ Hz), 36.2, 26.5 (d, $^3J_{\text{C-F}} = 8.5$ Hz), 19.7 (d, $^4J_{\text{C-F}} = 6.7$ Hz), 11.3 (dd, $^3J_{\text{C-F}} = 5.5, 2.4$ Hz) ppm;

^{19}F NMR (376 MHz, CDCl_3): δ = -108.6 (d, $^2J = 239.9$ Hz, 1F), -131.5 (dt, $^2J = 239.9, ^3J_{\text{F-H}} = 22.5$ Hz, 1F) ppm;

$\bar{\nu}$ (neat) = 3382, 2945, 1455, 1031, 988 cm^{-1} ;

HRMS (ESI): calcd for $\text{C}_8\text{H}_{18}\text{F}_2\text{O}_2\text{N}_1$, 198.1300 $[\text{M}+\text{NH}_4]^+$, found: 198.1300;

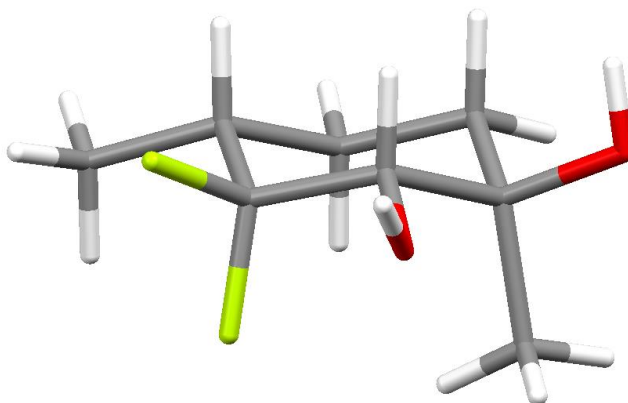
MS (EI): m/z (%): 142 (7) $[\text{M}-2\text{F}]^+$;

t_R (GC) = 8.96 minutes;

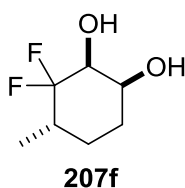
satisfactory elemental analysis could not be obtained for this compound²⁸⁹; calcd (%) for $\text{C}_8\text{H}_{14}\text{F}_2\text{O}_2$: C, 53.32; H, 7.83; found: C, 52.69; H, 7.73.

The identity of *trans, cis* diol **207eb** was confirmed by XRD analysis (m.p. = 58-60 °C (chloroform/pentane)). Crystal Data for **207eb**: $\text{C}_8\text{H}_{14}\text{F}_2\text{O}_2$, crystal size 0.28 x 0.16 x 0.03

mm³, $M = 180.19$, monoclinic, space group $P2_{1/c}$, unit cell dimensions $a = 12.0498(6)$ Å, $b = 19.0558(6)$ Å, $c = 11.4322(4)$ Å, $\alpha = 90^\circ$, $\beta = 100.490(4)^\circ$, $\gamma = 90^\circ$, $V = 2581.17(18)$ Å³, $Z = 12$, $\rho_{\text{calc}} = 1.391$ Mg m⁻³, $F(000) = 1152$, $\mu(\text{Mo-K}\alpha) = 1.084$ mm⁻¹, $T = 123(2)$ K, 9605 reflections measured, 4991 independent, ($R_{\text{int}} = 0.0392$). Final R indices [$I > 2\sigma(I)$] $R1 = 0.0535$, $\omega R2 = 0.1269$; R indices (all data) $R1 = 0.0800$, $\omega R2 = 0.1446$.



(1*S,2*S**,4*S**)-3,3-difluoro-4-methylcyclohexane-1,2-diol (207f)**



Diol **207f** was prepared according to general procedure D for **207aa/207ab** from **115f** (0.252 g, 1.00 mmol) with 1,3-*bis*(2,6-diisopropylphenyl-imidazol-2-ylidene)gold(I) chloride (5 mol %, 0.031 g) and silver hexafluoroantimonate(V) (5 mol %, 0.017 g) in dichloromethane (5.4 mL) and methanol (0.6 mL). After stirring for 21 hours at 40 °C the reaction was allowed to cool to room temperature. Solid tetrabutylammonium borohydride (0.258 g, 1 mmol) was added to the flask in small portions. The reaction mixture was then allowed to stir at room temperature for 18 hours. The usual work up, according to **207aa/207ab**, afforded a viscous pale yellow oil (0.294 g). The crude material was purified by flash column chromatography (40 g silica, 15-25 % acetone in dichloromethane) to afford **207f** as a colourless solid (0.039 g). This material was purified further by recrystallization by vapour diffusion (methanol/pentane) to afford *cis*, *trans*-**207f** as a colourless plate (0.021 g, 11 %).

m.p. = 118-120 °C (recrystallised from methanol/pentane as a colourless plate);

$R_f = 0.42$ (20 % acetone in dichloromethane);

^1H NMR (600 MHz, MeOD): δ = 3.84 (dt, J = 8.3, $J_{\text{H-F}}$ = 3.7 Hz, 1H), 3.71-3.61 (m, 1H), 2.22-2.06 (m, 1H), 1.77-1.68 (m, 1H), 1.68-1.59 (m, 2H), 1.18 (qd, $^2J = J$ = 13.5, J = 3.9 Hz, 1H), 1.01 (d, J = 6.9 Hz, 3H) ppm;

^{13}C NMR (150 MHz, MeOD): δ = 123.5 (dd, $^1J_{\text{C-F}}$ = 252.8, 242.5 Hz), 71.5 (dd, $^2J_{\text{C-F}}$ = 33.8, 21.6 Hz), 69.2 (d, $^3J_{\text{C-F}}$ = 7.6 Hz), 31.8 (t, $^2J_{\text{C-F}}$ = 22.0 Hz), 26.7 (d, $^3J_{\text{C-F}}$ = 8.4 Hz), 26.5, 10.4 (t, $^3J_{\text{C-F}}$ = 3.9 Hz) ppm;

^{19}F NMR (376 MHz, MeOD): δ = (-108.9) – (-109.9) (m, including -109.3 (app. d, 2J = 250.3 Hz, 1F)), -124.5 (dd, 2J = 250.3, $^3J_{\text{F-H}}$ = 29.6 Hz, 1F) ppm;

$\bar{\nu}$ (neat) = 3400 (broad), 2963, 1457, 1046, 957 cm^{-1} ;

HRMS (APCI): calcd for $\text{C}_7\text{H}_{16}\text{F}_2\text{O}_2\text{N}$, 184.1144 $[\text{M}+\text{NH}_4]^+$, found: 184.1141;

MS (CI): m/z (%): 184 (100) $[\text{M}+\text{NH}_4]^+$;

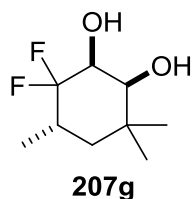
t_{R} (GC) = 9.44 minutes;

elemental analysis calcd (%) for $\text{C}_7\text{H}_{12}\text{F}_2\text{O}_2$: C, 50.60; H, 7.28; found: C, 50.09; H, 7.06.

The identity of diol (**207f**) was confirmed by XRD analysis (m.p. = 118-120 °C (methanol/pentane)). Crystal Data for **207f**: $\text{C}_7\text{H}_{12}\text{F}_2\text{O}_2$, crystal size 0.30 x 0.15 x 0.08 mm^3 , M = 166.17, orthorhombic, space group P_{bca} , unit cell dimensions a = 8.1651(4) Å, b = 8.2944(4) Å, c = 22.5849(10) Å, α = 90°, β = 90°, γ = 90°, V = 1529.55(13) Å³, Z = 8, ρ_{calc} = 1.443 Mg m^{-3} , $F(000)$ = 704, $\mu(\text{Mo-K}\alpha)$ = 0.134 mm^{-1} , T = 150(2)K, 10117 reflections measured, 1992 independent, (R_{int} = 0.0291). Final R indices [$I > 2\sigma(I)$] $R1$ = 0.0371, $\omega R2$ = 0.0859; R indices (all data) $R1$ = 0.0464, $\omega R2$ = 0.0927.



(1S*,2S*,4S*)-3,3-difluoro-4,6,6-trimethylcyclohexane-1,2-diol (207g)



Diol **207g** was prepared according to general procedure D for **207aa/207ab** from **115g** (0.280 g, 1.00 mmol) with 1,3-bis(2,6-diisopropylphenyl-imidazol-2-ylidene)gold(I) chloride (5 mol %, 0.031 g) and silver hexafluoroantimonate(V) (5 mol %, 0.017 g) in dichloromethane (5.4 mL) and methanol (0.6 mL). After stirring for 48 hours at 40 °C the reaction was allowed to cool to room temperature. Solid tetrabutylammonium borohydride (0.258 g, 1 mmol) was added to the flask in small portions. The reaction mixture was then allowed to stir at room temperature for 18 hours. The usual work up, according to **207aa/207ab**, afforded a viscous pale yellow oil (0.586 g). The crude material was purified by flash column chromatography (40 g silica, 5 % acetone in dichloromethane) to afford *cis,trans*-**207g** as a colourless solid (0.123 g, 63 %).

m.p. = 82-84 °C (recrystallised from diethyl ether/pentane vapour diffusion as a colourless plate);

$R_f = 0.25$ (5 % acetone in dichloromethane);

$^1\text{H NMR}$ (400 MHz, CDCl_3): $\delta = 4.04$ (tt, $J_{\text{H-F}} = 6.6$, $J = 3.5$ Hz, 1H), 3.49-3.38 (m, 1H), 2.46-2.24 (m, (including 2.39 (app. d, $J = 3.5$ Hz, 1H) and 2.29 (d, $J = 9.6$ Hz, 1H)), 1H), 1.43 (ddd, $^2J = 14.1$, $^4J_{\text{H-F}} = 6.2$, $J = 4.2$ Hz, 1H), 1.26 (br. t, $^2J = J = 14.1$ Hz, 1H), 1.07 (s, 3H), 1.06 (d, $J = 6.2$ Hz, 3H), 1.03 (s, 3H) ppm;

$^{13}\text{C NMR}$ (150 MHz, CDCl_3): $\delta = 122.8$ (dd, $^1J_{\text{C-F}} = 251.1$, 243.3 Hz), 74.2 (d, $^3J_{\text{C-F}} = 6.7$ Hz), 71.5 (dd, $^2J_{\text{C-F}} = 36.3$, 22.2 Hz), 41.6 (d, $^3J_{\text{C-F}} = 8.8$ Hz), 34.8, 29.2, 28.8 (t, $^2J_{\text{C-F}} = 21.5$ Hz), 19.9, 10.9 (t, $^3J_{\text{C-F}} = 3.7$ Hz) ppm;

$^{19}\text{F NMR}$ (376 MHz, CDCl_3): $\delta = (-109.0) - (-109.9)$ (m, including -109.4 (app. d, $^2J = 253.0$ Hz, 1F)), -124.5 (dddd, $^2J = 253.0$, $^3J_{\text{F-H}} = 28.9$, 6.2, $^4J_{\text{F-H}} = 4.2$ Hz, 1F) ppm;

$\bar{\nu}$ /(neat) = 3350, 2926, 1465, 1371, 1005 cm^{-1} ;

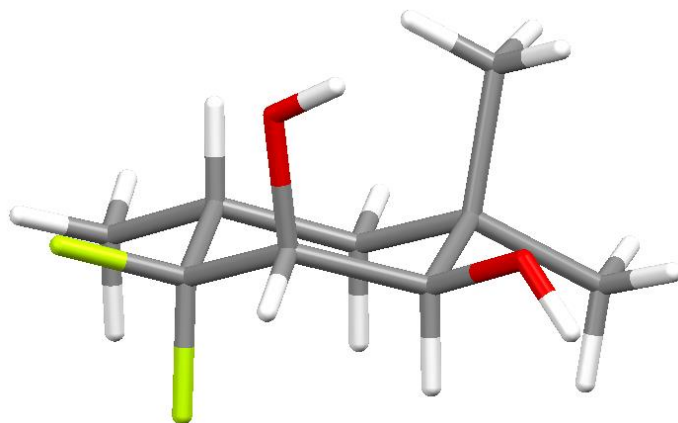
HRMS (NSI-ES): calcd for $\text{C}_9\text{H}_{16}\text{F}_2\text{O}_2\text{Na}$, 217.1011 $[\text{M}+\text{Na}]^+$, found: 217.1012;

MS (EI): m/z (%): 161(3) $[\text{M}-\text{CH}_3\text{F}]^+$, 102 (61) $[\text{M}-\text{C}_4\text{H}_6\text{F}_2]^+$, 72(100) $[\text{M}-\text{C}_6\text{H}_{12}\text{F}_2]^+$;

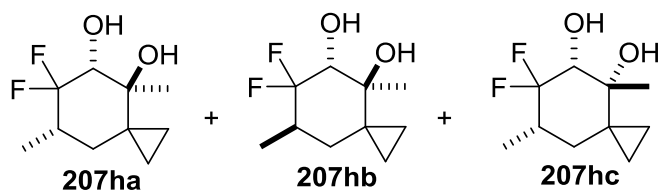
t_R (GC) = 9.64 minutes;

elemental analysis calcd (%) for $\text{C}_9\text{H}_{16}\text{F}_2\text{O}_2$: C, 55.66; H, 8.30; found: C, 55.35; H, 8.23.

The identity of diol (**207g**) was confirmed by XRD analysis (m.p. = 82-84 °C (diethyl ether/pentane)). Crystal Data for **207g**: C₉H₁₆F₂O₂, crystal size 0.35 x 0.30 x 0.03 mm³, *M* = 194.22, monoclinic, space group C_{2/c}, unit cell dimensions *a* = 23.884(3) Å, *b* = 7.4165(11) Å, *c* = 10.9080(15) Å, α = 90°, β = 94.654(13)°, γ = 90°, *V* = 1925.9 (5) Å³, *Z* = 8, ρ_{calc} = 1.340 Mg m⁻³, *F*(000) = 832, μ(Mo-Kα) = 0.117 mm⁻¹, *T* = 130(2)K, 7929 reflections measured, 2148 independent, (*R*_{int} = 0.0414]. Final *R* indices [*I* > 2σ(*I*)] *R*1 = 0.0437, ω*R*2 = 0.1121; *R* indices (all data) *R*1 = 0.0544, ω*R*2 = 0.1223.



(4*S**,5*R**,7*S**)-6,6-Difluoro-4,7-dimethylspiro[2.5]octane-4,5-diol (**207ha**),
 (4*S**,5*R**,7*R**)-6,6-difluoro-4,7-dimethylspiro[2.5]octane-4,5-diol (**207hb**) and
 (4*R**,5*R**,7*S**)-6,6-difluoro-4,7-dimethylspiro[2.5]octane-4,5-diol (**207hc**)



Diols **207ha**, **207hb** and **207hc** were prepared according to general procedure D for **207aa/207ab** from **115h** (0.352 g, 1.21 mmol) with 1,3-*bis*(2,6-diisopropylphenyl-imidazol-2-ylidene)gold(I) chloride (5 mol %, 0.037 g) and silver hexafluoroantimonate(V) (5 mol %, 0.021 g) in dichloromethane (6.5 mL) and methanol (0.7 mL). After stirring for 18 hours at 40 °C the reaction was allowed to cool to room temperature. Solid tetrabutylammonium borohydride (0.311 g, 1.21 mmol) was added to the flask in small portions. The reaction mixture was then allowed to stir at room temperature for 18 hours. The usual work up, according to **207aa/207ab**, afforded a viscous pale yellow oil (0.564 g). The crude material was purified by flash column

chromatography (40 g silica, 6 % acetone in dichloromethane) to afford a mixture *trans,cis-207ha*, *trans,trans-207hb* and *cis,cis-207hc* (0.125 g). The material was further purified by flash column chromatography (40 g silica, 38 % ethyl acetate in hexane) to afford a mixture of *trans,cis-207ha*, *trans,trans-207hb* and *cis,cis-207hc* (73.4 mg, 29 %, 1.3:1:0.1) as a pale yellow oil, *trans,cis-207ha* as a pale yellow oil (13.8 mg, 6 %) and *trans,trans-207hb* as a colourless solid (12.8 mg, 5 %).

R_f *trans,cis-207ha* = 0.52 (10 % acetone in dichloromethane);

R_f *trans,trans-207hb* = 0.61 (10 % acetone in dichloromethane);

cis,cis-207hc co eluted with the *trans,trans* diastereoisomer;

The following signals were attributed to the major *trans,cis*-diastereoisomer **207ha** and minor *trans,trans-207hb* and *cis, cis*-diastereoisomers **207hc** ^1H NMR (600 MHz, DMSO- d_6 , 373 K): δ = 3.63-3.48 (m, 1H), 0.84-0.74 (m, 2H), 0.22-0.06 (m, 3H) ppm;

The following signals were attributed to the major *trans,cis*-diastereoisomer **207ha** (assigned on the basis of δ and intensity)

^1H NMR (600 MHz, DMSO- d_6 , 373 K): δ = 4.81 (br. s, 1H), 3.78 (br. s, 1H), 2.09-1.91 (m, 1H), 1.75 (br. t, $^2J = J = 13.4$ Hz, 1H), 1.16 (d, $^5J_{\text{H-F}} = 2.2$ Hz, 3H), 0.97 (d, $J = 6.8$ Hz, 3H), 0.91-0.84 (m, 1H), 0.59 (ddd, $^2J = 9.3$, $J = 5.7$, 3.8 Hz, 1H) ppm;

^{13}C NMR (150 MHz, DMSO- d_6 , 373 K): δ = 123.8 (t, $^1J_{\text{C-F}} = 247.0$ Hz), 77.5 (t, $^2J_{\text{C-F}} = 19.1$ Hz), 72.2 (d, $^3J_{\text{C-F}} = 8.3$ Hz), 37.8 (d, $^3J_{\text{C-F}} = 8.7$ Hz), 36.7 (t, $^2J_{\text{C-F}} = 22.3$ Hz), 25.6, 20.0 (d, $^4J_{\text{C-F}} = 5.6$ Hz), 11.8, 8.5, 6.6 ppm;

^{19}F NMR (376 MHz, DMSO- d_6 , 373 K): δ = -104.7 (dq, $^2J = 240.6$, $^3J_{\text{F-H}} = ^4J_{\text{F-H}} = 4.9$ Hz, 1F), -127.9 (dt, $^2J = 240.6$, $^3J_{\text{F-H}} = 24.2$ Hz, 1F) ppm;

The following signals were attributed to the minor *trans,trans*-diastereoisomer **207hb** (assigned on the basis of δ and intensity)

^1H NMR (600 MHz, DMSO- d_6 , 373 K): δ 4.90 (br. s, 1H), 3.75 (br. s, 1H), 2.37-2.21 (m, 1H), 1.57 (br. dd, $^2J = 13.9$, $J = 8.0$ Hz, 1H), 1.34-1.25 (m, 1H), 1.04 (d, $J = 7.1$ Hz, 3H), 1.02 (s, 3H), 0.55-0.48 (m, 1H) ppm;

^{13}C NMR (150 MHz, DMSO- d_6 , 373 K): δ = 125.0 (t, $^1J_{\text{C-F}} = 248.1$ Hz), 74.7 (t, $^2J_{\text{C-F}} = 22.5$ Hz), 73.6, 36.8, 35.0 (t, $^2J_{\text{C-F}} = 22.2$ Hz), 22.5, 21.0 (d, $^4J_{\text{C-F}} = 5.6$ Hz), 13.4, 8.5, 7.9 ppm;

^{19}F NMR (376 MHz, DMSO- d_6 , 373 K): δ = -106.7 (br. d, $^2J = 243.4$ Hz, 1F), -110.1 (d, $^2J = 243.4$ Hz, 1F) ppm;

The following signals were attributed to the minor *cis,cis*-diastereoisomer **207hc** (assigned on the basis of δ and intensity)

^1H NMR (600 MHz, DMSO- d_6 , 373 K): δ 0.99 (d, $J = 6.7$ Hz, 3H) ppm;

^{13}C NMR (150 MHz, DMSO- d_6 , 373 K): $\delta = 37.4$ (d, $^3J_{\text{C-F}} = 8.0$ Hz), 29.3, 12.1, 9.9, 8.2 ppm;

^{19}F NMR (376 MHz, DMSO- d_6 , 373 K): $\delta = -103.2$ (d, $^2J = 238.9$ Hz, 1F), -127.0 (dt, $^2J = 238.9$, $^3J_{\text{F-H}} = 26.5$ Hz, 1F) ppm;

$\bar{\nu}$ /(neat) = 3427, 2933, 1465, 1026, 991 cm^{-1} ;

HRMS (APCI): calcd for $\text{C}_{10}\text{H}_{15}\text{F}_2\text{O}_1$, 189.1091 $[\text{M}-\text{H}_2\text{O}+\text{H}]^+$, found: 189.1089;

MS (EI): m/z (%): 168 (12) $[\text{M}-2\text{F}]^+$ (major *trans*, *cis* diastereoisomer), 168 (21) $[\text{M}-2\text{F}]^+$ (minor *trans*, *trans* diastereoisomer), 168 (30) $[\text{M}-2\text{F}]^+$ (minor *cis*, *cis* diastereoisomer);

t_{R} (GC) = 10.71 minutes (major *trans*, *cis* diastereoisomer), 10.84 minutes (minor *trans*, *trans* diastereoisomer), 11.00 (minor *cis*, *cis* diastereoisomer).

Diastereomerically pure *trans*, *cis* **207ha**:

^1H NMR (600 MHz, DMSO- d_6 , 373 K): $\delta = 4.84$ (br. d, $J = 5.5$ Hz, 1H), 3.81 (br. s, 1H), 3.51 (dt, $J_{\text{H-F}} = 24.2$, 5.5, $J = 5.5$ Hz, 1H), 2.09-1.92 (m, 1H), 1.74 (br. t, $^2J = J = 13.6$ Hz, 1H), 1.14 (d, $^5J_{\text{H-F}} = 2.2$ Hz, 3H), 0.96 (d, $J = 6.8$ Hz, 3H), 0.90-0.83 (m, 1H), 0.79 (dt, $^2J = 13.6$, $^4J_{\text{H-F}} = J = 4.6$ Hz, 1H), 0.58 (ddd, $^2J = 9.3$, $J = 5.7$, 3.8 Hz, 1H), 0.21-0.13 (m, 1H), 0.13-0.03 (m, 1H) ppm;

^{13}C NMR (150 MHz, DMSO- d_6 , 373 K): $\delta = 122.7$ (dd, $^1J_{\text{C-F}} = 249.8$, 244.8 Hz), 76.5 (t, $^2J_{\text{C-F}} = 19.4$ Hz), 71.2 (d, $^3J_{\text{C-F}} = 9.0$ Hz), 36.8 (d, $^3J_{\text{C-F}} = 9.0$ Hz), 35.7 (t, $^2J_{\text{C-F}} = 21.9$ Hz), 24.5, 19.0 (d, $^4J_{\text{C-F}} = 6.1$ Hz), 10.8 (dd, $^3J_{\text{C-F}} = 5.8$, 2.5 Hz), 7.4, 5.5 ppm;

^{19}F NMR (376 MHz, DMSO- d_6 , 373 K): $\delta = -104.7$ (app. dq, $^2J = 240.6$, $^3J_{\text{F-H}} = ^4J_{\text{F-H}} = 4.9$ Hz, 1F), -127.9 (dt, $^2J = 240.6$, $^3J_{\text{F-H}} = 24.2$ Hz, 1F) ppm;

$\bar{\nu}$ /(neat) = 3427, 2938, 1376, 1231, 1090, 991 cm^{-1} ;

HRMS (APCI): calcd for $\text{C}_{10}\text{H}_{20}\text{F}_2\text{O}_2\text{N}_1$, 224.1462 $[\text{M}+\text{NH}_4]^+$, found: 224.1458;

MS (EI): m/z (%): 168 (12) $[\text{M}-2\text{F}]^+$;

t_{R} (GC) = 10.71 minutes;

Diastereomerically pure *trans*, *trans* **207hb**:

m.p. = 66-68 $^{\circ}\text{C}$ (recrystallised from chloroform/pentane as a colourless plate);

^1H NMR (600 MHz, DMSO- d_6 , 373 K): δ 4.92 (br. d, $J = 5.8$ Hz, 1H), 3.77 (br. s, 1H), 3.51 (dt, $J_{\text{H-F}} = 15.2$, 5.9, $J = 5.9$ Hz, 1H), 2.34-2.22 (m, 1H), 1.56 (br. dd, $^2J = 13.9$, $J = 8.0$ Hz, 1H), 1.29 (br. d, $^2J = 13.9$ Hz, 1H), 1.04 (d, $J = 7.2$ Hz, 3H), 1.01 (s, 3H), 0.76 (br. dt, $^2J = 9.1$, $J = 4.1$ Hz, 1H), 0.54-0.48 (m, 1H), 0.17 (ddd, $^2J = 9.1$, $J = 5.5$, 4.3 Hz, 1H), 0.13 (ddd, $^2J = 9.2$, $J = 5.2$, 3.6 Hz, 1H) ppm;

^{13}C NMR (150 MHz, DMSO- d_6 , 373 K): $\delta = 124.0$ (t, $^1J_{\text{C-F}} = 248.5$ Hz), 73.6 (t, $^2J_{\text{C-F}} = 22.3$ Hz), 72.5, 35.8 (t, $^3J_{\text{C-F}} = 3.9$ Hz), 33.9 (t, $^2J_{\text{C-F}} = 21.9$ Hz), 21.4, 20.0 (d, $^4J_{\text{C-F}} = 4.0$ Hz), 12.4 (t, $^3J_{\text{C-F}} = 5.1$ Hz), 7.4, 6.9 ppm;

^{19}F NMR (376 MHz, $\text{DMSO-}d_6$, 373 K): $\delta = -106.7$ (br. d, $^2J = 243.4$ Hz, 1F), -110.1 (d, $^2J = 243.4$ Hz, 1F) ppm (the ^{19}F - ^1H splitting was not resolved in the ^{19}F NMR spectrum); $\bar{\nu}(\text{neat}) = 3382, 2931, 1380, 1023, 824$ cm^{-1} ;

HRMS (APCI): calcd for $\text{C}_{10}\text{H}_{15}\text{F}_2\text{O}_1$, 189.1091 $[\text{M}-\text{H}_2\text{O}+\text{H}]^+$, found: 189.1087;

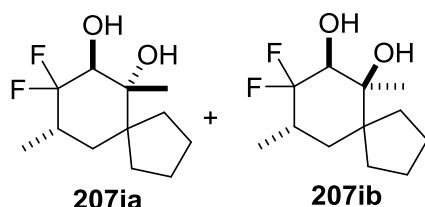
MS (EI): m/z (%): 168 (21) $[\text{M}-2\text{F}]^+$;

t_{R} (GC) = 10.84 minutes;

The identity of *trans, trans* diol **207hb** was confirmed by XRD analysis (m.p. = 66-68 °C (chloroform/pentane)). Crystal Data for **207hb**: $\text{C}_{10}\text{H}_{16}\text{F}_2\text{O}_2$, crystal size 0.30 x 0.18 x 0.02 mm^3 , $M = 206.23$, orthorhombic, space group P_{naa} , unit cell dimensions $a = 9.904(2)$ Å, $b = 22.127(7)$ Å, $c = 9.113(2)$ Å, $\alpha = 90^\circ$, $\beta = 90^\circ$, $\gamma = 90^\circ$, $V = 1997.1(9)$ Å 3 , $Z = 8$, $\rho_{\text{calc}} = 1.372$ Mg m^{-3} , $F(000) = 880$, $\mu(\text{Mo-K}\alpha) = 0.117$ mm^{-1} , $T = 153(2)\text{K}$, 10320 reflections measured, 1747 independent, ($R_{\text{int}} = 0.1439$). Final R indices [$I > 2\sigma(I)$] $R1 = 0.0854$, $\omega R2 = 0.2166$; R indices (all data) $R1 = 0.1202$, $\omega R2 = 0.2508$.



(6R*,7S*,9S*)-8,8-Difluoro-6,9-dimethylspiro[4.5]decane-6,7-diol (207ia) and (6S*,7S*,9S*)-8,8-difluoro-6,9-dimethylspiro[4.5]decane-6,7-diol (207ib)



Diols **207ia** and **207ib** were prepared according to general procedure D for **207aa/207ab** from **115i** (0.339 g, 1.06 mmol) with 1,3-bis(2,6-diisopropylphenyl-imidazol-2-ylidene)gold(I) chloride (5 mol %, 0.033 g) and silver hexafluoroantimonate(V) (5 mol %, 0.018 g) in dichloromethane (5.4 mL) and methanol (0.6 mL). After stirring for 2

hours at 40 °C the reaction was allowed to cool to room temperature. Solid tetrabutylammonium borohydride (0.273 g, 1.06 mmol) was added to the flask in small portions. The reaction mixture was then allowed to stir at room temperature for 18 hours. The usual work up, according to **207aa/207ab**, afforded a viscous pale yellow oil (0.395 g). The crude material was purified by flash column chromatography (40 g silica, 6% acetone in dichloromethane) to afford a mixture of *trans,trans*-**207ia**, and *cis,trans*-**207ib** (0.168 g). The material was further purified by flash column chromatography (40 g silica, 6 % acetone in dichloromethane) to afford an inseparable mixture of *trans,trans*-**207ia**, and *cis,trans*-**207ib** (0.108 g, 44 %, 3.8:1).

$R_f = 0.7$ (8 % acetone in dichloromethane);

The following signals were attributed to both the minor *cis,trans*-diastereoisomer **207ib** and major *trans,trans*-diastereoisomer **207ia** ^1H NMR (400 MHz, CDCl_3): $\delta = 2.48\text{-}2.13$ (m, including 2.23 (br.s, 1H), 1H), 2.04-1.38 (envelope, 13H), 1.37-1.22 (m, including 1.33 (s, 3H), 6H) ppm;

The following signals were attributed to the major *trans,trans*-diastereoisomer **207ia** (assigned on the basis of δ and intensity)

^1H NMR (400 MHz, CDCl_3): $\delta = 3.64$ (t, $J_{\text{H-F}} = 5.8$ Hz, 1H), 2.23 (br. s, 1H), 1.33 (s, 3H), 1.07 (d, $J = 6.9$ Hz, 3H) ppm;

^{13}C NMR (100 MHz, MeOD): $\delta = 127.1$ (t, $^1J_{\text{C-F}} = 247.7$ Hz), 79.8 (d, $^3J_{\text{C-F}} = 5.3$ Hz), 79.2 (dd, $^2J_{\text{C-F}} = 27.8, 20.7$ Hz), 52.0, 43.2 (d, $^3J_{\text{C-F}} = 8.0$ Hz), 38.8, 36.8, 33.5 (t, $^2J_{\text{C-F}} = 21.5$ Hz), 29.7, 27.4, 24.4, 14.3 (d, $^3J_{\text{C-F}} = 4.3$ Hz) ppm;

^{19}F NMR (376 MHz, CDCl_3): $\delta = -107.6$ (d, $^2J = 253.2$ Hz, 1F), -116.2 (dd, $^2J = 253.2, ^3J_{\text{F-H}} = 28.7$ Hz, 1F) ppm (the ^{19}F - ^1H splitting was not resolved in the ^{19}F NMR spectrum).

The following signals were attributed to the minor *cis,trans*-diastereoisomer **207ib** (assigned on the basis of δ and intensity)

^1H NMR (400 MHz, CDCl_3): $\delta = 3.67$ (t, $J_{\text{H-F}} = 6.6$ Hz, 1H), 2.69 (br. s, 1H), 2.65 (br. s, 1H) 1.26 (d, $^5J_{\text{H-F}} = 4.1$ Hz, 3H), 1.05 (d, $J = 6.3$ Hz, 3H) ppm;

^{13}C NMR (100 MHz, MeOD): $\delta = 126.9$ (dd, $^1J_{\text{C-F}} = 248.7, 243.0$ Hz), 80.5 (dd, $^2J_{\text{C-F}} = 32.9, 20.4$ Hz), 76.7 (d, $^3J_{\text{C-F}} = 6.9$ Hz), 52.9, 41.4 (d, $^3J_{\text{C-F}} = 8.7$ Hz), 38.2, 33.6, 33.0 (t, $^2J_{\text{C-F}} = 21.8$ Hz), 28.0, 25.4, 25.3 (d, $^4J_{\text{C-F}} = 8.4$ Hz), 13.9 (d, $^3J_{\text{C-F}} = 5.4$ Hz) ppm;

^{19}F NMR (376 MHz, CDCl_3): $\delta -105.9$ (dq, $^2J = 253.7, ^3J_{\text{F-H}} = ^4J_{\text{F-H}} = 5.4$ Hz, 1F), -117.5 (dd, $^2J = 253.7, ^3J_{\text{F-H}} = 28.9$ Hz, 1F) ppm (the 6.6 Hz ^{19}F - ^1H splitting was not resolved in the ^{19}F NMR spectrum);

$\bar{\nu}(\text{neat}) = 3600, 3331, 2947, 1454, 1383, 1086, 978 \text{ cm}^{-1}$;

HRMS (APCI): calcd for C₁₂H₂₂F₂O₂N₁, 252.1770 [M-H]⁺, found: 252.1769;

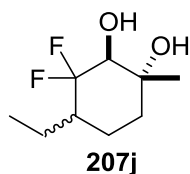
MS (EI): *m/z* (%): 219 (1) [M-CH₃]⁺;

t_R (GC) = 12.17 minutes;*

elemental analysis calcd (%) for C₁₂H₂₀F₂O₂: C, 61.52; H, 8.60; found: C, 61.76; H, 8.64. This analysis was obtained for the amorphous solid obtained following chromatography so no melting point was recorded.

* the individual diastereoisomers appeared as one peak by GC-MS.

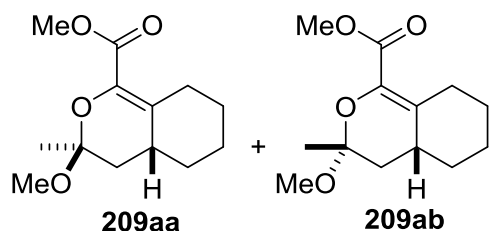
Attempted preparation of (1*R,2*S**)-4-ethyl-3,3-difluoro-1-methylcyclohexane-1,2-diol (207j)**



1,3-*bis*(2,6-diisopropylphenyl-imidazol-2-ylidene)gold(I) chloride (5 mol %, 0.031 g) and silver hexafluoroantimonate(V) (5 mol %, 0.017 g) was suspended in dichloromethane (5.4 mL) and methanol (0.6 mL). The suspension was heated to 40 °C then a solution of **115ja/115jb** (0.280g, 1.00 mmol) in dichloromethane (1mL) was added in a stream *via* syringe. The reaction was stirred at 40 °C for 21 hours. After this time the reaction was allowed to cool to room temperature. The solvent was removed under reduced pressure and the residue taken up in ethyl acetate (20 mL). The organics were washed with saturated aqueous sodium bicarbonate (15 mL). The aqueous layer was further extracted with ethyl acetate (3 x 15 mL) and the organics combined, dried over magnesium sulphate and concentrated under reduced pressure to afford the crude product as a dark orange oil (0.198 g). ¹⁹F NMR analysis of the crude reaction revealed no signs of the desired product and a complex mixture was produced.

6.3.11 Synthesis of non-fluorinated pyran 209

Cis-methyl (3*S**,4*aR**)-3-methoxy-3-methyl-4,4*a*,5,6,7,8-hexahydro-3*H*-isochromene-1-carboxylate (**209aa**) and *trans*-methyl (3*R**,4*aR**)-3-methoxy-3-methyl-4,4*a*,5,6,7,8-hexahydro-3*H*-isochromene-1-carboxylate (**209ab**)



Esters **209aa** and **209ab** were prepared according to the general procedure for **207aa/207ab** from **115ka/115kb** (0.253 g, 0.83 mmol) with 1,3-*bis*(2,6-diisopropylphenyl-imidazol-2-ylidene)gold(I) chloride (5 mol %, 0.026 g) and silver hexafluoroantimonate(V) (5 mol %, 0.014 g) in dichloromethane (4.5 mL) and methanol (0.5 mL). After stirring for 15 minutes at 40 °C the reaction was allowed to cool to room temperature. The solvent was removed under reduced pressure and the residue taken up in ethyl acetate (20 mL). The organics were washed with saturated aqueous sodium bicarbonate (15 mL). The aqueous layer was further extracted with ethyl acetate (3 x 15 mL) and the organics combined, dried over magnesium sulphate and concentrated under reduced pressure to afford the crude product as a dark orange oil (0.204 g). The crude material was purified by flash column chromatography using a Thomson Single Step cartridge (12 g silica, 0-5 % acetone in dichloromethane) to afford an inseparable mixture of *cis*-**209aa**, and *trans*-**209ab** as a pale yellow oil. After storing the material in the freezer at 0 °C for one year the material solidified to afford a pale yellow solid (0.057 g, 29 %, 7.3:1).

m.p. = 40-42 °C (crystals were grown by slow evaporation from chloroform/pentane under reduced pressure as small colourless prisms);

R_f = 0.54 (10 % ethyl acetate in hexane);

The following signals were attributed to both the minor *trans*-diastereoisomer **209ab** and major *cis*-diastereoisomer **209aa** ¹H NMR (400 MHz, CDCl₃): δ = 3.79 (s, 3H), 3.53-3.42 (m, 1H), 1.97-1.61 (envelope, 5H), 1.47 (s, 3H), 1.45-1.22 (m, 4H) ppm;

The following signals were attributed to the major *cis*-diastereoisomer **209aa** (assigned on the basis of δ and intensity)

^1H NMR (400 MHz, CDCl_3): $\delta = 3.25$ (s, 3H), 2.35-2.22 (m, 1H), 2.00 (dd, $^2J = 13.7$, 7.0 Hz, 1H), 1.07 (dq, $^2J = J = 12.5$, $J = 3.6$ Hz, 1H) ppm;

^{13}C NMR (100 MHz, CDCl_3): $\delta = 164.2$, 132.7, 128.7, 97.1, 51.2, 48.6, 40.2, 33.3, 31.7, 27.1, 26.2, 25.1, 22.2 ppm;

The following signals were attributed to the minor *trans*-diastereoisomer **209ab** (assigned on the basis of δ and intensity)

^1H NMR (400 MHz, CDCl_3): $\delta = 3.31$ (s, 3H) ppm;

^{13}C NMR (100 MHz, CDCl_3): $\delta = 164.1$, 132.9, 128.5, 98.3, 51.2, 48.4, 37.6, 34.6, 34.4, 28.1, 27.3, 26.0, 21.8 ppm;

$\bar{\nu}$ (neat) = 2921, 1719, 1435, 1279, 1115, 1045, 881 cm^{-1} ;

HRMS (APCI): calcd for $\text{C}_{13}\text{H}_{24}\text{O}_4\text{N}_1$, 258.1700 $[\text{M}+\text{NH}_4]^+$, found: 258.1701;

MS (EI): m/z (%): 240 (1) $[\text{M}]^+$ (*cis* and *trans* diastereoisomers)

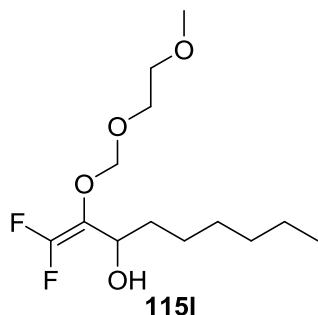
t_R (GC) = 12.19 minutes (major *cis* diastereoisomer), 12.26 minutes (minor *trans* diastereoisomer).

The identity of *cis*, ester (**209aa**) was confirmed by XRD analysis (m.p. = 40-42 °C (chloroform/pentane)). Crystal Data for **209aa**: $\text{C}_{13}\text{H}_{20}\text{O}_4$, crystal size 0.30 x 0.22 x 0.05 mm^3 , $M = 240.29$, monoclinic, space group $\text{P}2_{1/n}$, unit cell dimensions $a = 10.0913(3)$ Å, $b = 8.5428(2)$ Å, $c = 15.3195(4)$ Å, $\alpha = 90^\circ$, $\beta = 105.197(3)^\circ$, $\gamma = 90^\circ$, $V = 1265.39(6)$ Å³, $Z = 4$, $\rho_{\text{calc}} = 1.261$ Mg m^{-3} , $F(000) = 520$, $\mu(\text{Mo-K}\alpha) = 0.758$ mm^{-1} , $T = 123(2)\text{K}$, 4956 reflections measured, 2487 independent, ($R_{\text{int}} = 0.0118$). Final R indices [$I > 2\sigma(I)$] $R1 = 0.0393$, $\omega R2 = 0.1051$; R indices (all data) $R1 = 0.0415$, $\omega R2 = 0.1073$.



6.3.11 Preparation of allylic alcohols to investigate scope of alkyne cyclisation

1,1-difluoro-2-((2-methoxyethoxy)methoxy)non-1-en-3-ol (**115l**)



Prepared as for **115aa** and **115ab** from acetal (1.90 mL, 12 mmol), *n*-butyllithium (12.9 mL of a 1.94 M solution in hexanes, 25 mmol), diisopropylamine (3.70 mL, 26 mmol) and heptanal (1.37 g, 12 mmol) in THF (12 mL). The crude allylic alcohol (2.63 g) was purified by Kugelrohr distillation to afford **115l** as a pale yellow oil (2.20 g, 65 %).

b.p. = 102 °C / 0.05 mmHg;

R_f = 0.21 (50 % diethyl ether in hexane);

¹H NMR (400 MHz, CDCl₃): δ = 5.00 (d, ²J = 6.8 Hz, 1H), 4.88 (d, ²J = 6.8 Hz, 1H), 4.24 (dtdd, J = 9.3, J = 7.4, ⁴J_{H-F} = 3.6, 2.0 Hz, 1H), 3.96 (ddd, ²J = 10.8, J = 6.4, 3.5 Hz, 1H), 3.78 (ddd, ²J = 10.8, J = 5.0, 3.1 Hz, 1H), 3.66-3.53 (m, 2H), 3.40 (s, 3H), 3.20 (d, J = 9.3 Hz, 1H), 1.79-1.52 (m, 2H), 1.41-1.20 (m, 8H), 0.88 (t, J = 6.9 Hz, 3H) ppm;

¹³C NMR (100 MHz, CDCl₃): δ = 154.7 (dd, ¹J_{C-F} = 291.6, 284.7 Hz), 118.2 (dd, ²J_{C-F} = 36.3, 9.8 Hz), 98.0, 71.4, 68.4, 67.1, 58.9, 33.9, 31.7, 29.0, 25.4, 22.5, 13.9 ppm;

¹⁹F (376 MHz, CDCl₃): δ = -100.5 (d, ²J = 63.7 Hz, 1F), -110.1 (d, ²J = 63.7 Hz, 1F) ppm; (the ¹⁹F-¹H splitting was not resolved in the ¹⁹F NMR spectrum);

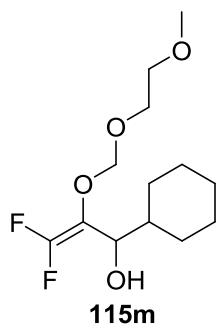
$\bar{\nu}$ (neat) = 3421, 2924, 1749, 1232, 1054, 955 cm⁻¹;

HRMS (ESI): calcd for C₁₃H₂₄F₂O₄Na, 305.1535 [M+Na]⁺, found: 305.1532;

MS (CI): *m/z* (%): 283 (1) [M+H]⁺, 265 (2) [M-OH]⁺, 89 (78) [C₄H₉O₂]⁺, 59 (100) [C₃H₇O]⁺;

t_R (GC) = 12.41 minutes.

1,1 Difluoro-2-((2-methoxyethoxy)methoxy) 3-cyclohexyl prop-2-en-3-ol (115m)



Prepared as for **115aa** and **115ab** from acetal (1.90 mL, 12 mmol), *n*-butyllithium (11.9 mL of a 2.10 M solution in hexanes, 25 mmol), diisopropylamine (3.70 mL, 26 mmol) and cyclohexanecarboxaldehyde (1.34 g, 12 mmol) in THF (12 mL). The crude allylic alcohol (3.12 g) was purified by Kugelrohr distillation to afford **115m** as a pale yellow oil (2.60 g, 77 %).

b.p. = 102 °C / 0.06 mmHg;

R_f = 0.3 (50 % diethyl ether in hexane);

¹H NMR (400 MHz, CDCl₃): δ = 5.01 (d, ²J = 6.8 Hz, 1H), 4.87 (d, ²J = 6.8 Hz, 1H), 3.96 (ddd, ²J = 10.8, J = 6.0, 3.1 Hz, 1H), 3.87 (br. d, J = 8.3 Hz, 1H), 3.78 (ddd, ²J = 10.8, J = 4.8, 3.0 Hz, 1H), 3.65-3.53 (m, 2H), 3.40 (s, 3H), 3.18 (br. s, 1H), 2.10 (br. d, ²J = 13.7 Hz, 1H), 1.86-1.52 (m, 5H), 1.34-1.10 (m, 3H), 1.08-0.94 (m, 1H), 0.94-0.79 (m, 1H) ppm;

¹³C NMR (100 MHz, CDCl₃): δ = 154.6 (dd, ¹J_{C-F} = 292.2, 285.2 Hz), 117.0 (dd, ²J_{C-F} = 37.7, 10.0 Hz), 97.5 (t, ⁴J_{C-F} = 3.6 Hz), 71.2, 70.9, 68.0, 58.4, 40.2, 29.0, 28.3, 25.9, 25.3, 25.2 ppm;

¹⁹F (376 MHz, CDCl₃): δ = -100.6 (d, ²J = 65.5 Hz, 1F), -110.6 (d, ²J = 65.5 Hz, 1F) ppm;

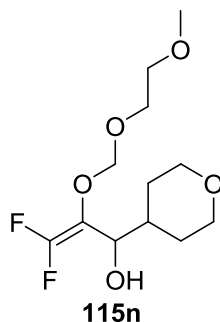
$\bar{\nu}$ (neat) = 3463, 2921, 1749, 1232, 1013, 953 cm⁻¹;

HRMS (APCI): calcd for C₁₃H₂₆F₂O₄N₁, 298.1824 [M+NH₄]⁺, found: 298.1819;

MS (EI): *m/z* (%): 204 (2) [M-C₄H₉F]⁺, 89 (100) [C₄H₉O₂]⁺, 59 (100) [C₃H₇O]⁺;

t_R (GC) = 12.65 minutes.

1,1-difluoro-2-((2-methoxyethoxy)methoxy)-3-(tetrahydro-2H-pyran-4-yl)prop-2-en-3-ol (115n)



Prepared as for **115aa** and **115ab** from acetal (1.90 mL, 12 mmol), *n*-butyllithium (11.9 mL of a 2.10 M solution in hexanes, 25 mmol), diisopropylamine (3.70 mL, 26 mmol) and 4-formyltetrahydropyran (1.37 g, 12 mmol) in THF (12 mL). The crude allylic alcohol (2.71 g) was purified by flash column chromatography (90 g cartridge, 90 % diethyl ether in hexane) to afford **115n** as a pale yellow oil (1.94 g, 57 %).

$R_f = 0.30$ (90 % diethyl ether in hexane);

$^1\text{H NMR}$ (400 MHz, CDCl_3): $\delta = 5.00$ (d, $J = 6.6$ Hz, 1H), 4.88 (d, $J = 6.6$ Hz, 1H), 4.09-3.84 (m, 4H), 3.77 (ddd, $^2J = 10.8$, $J = 4.5$, 3.1 Hz, 1H), 3.65-3.52 (m, 2H), 3.45-3.30 (m, 6H), 2.03-1.92 (m, 1H), 1.91-1.75 (m, 1H), 1.52-1.31 (m, 2H), 1.23 (qd, $J = 11.9$, 4.4 Hz, 1H) ppm;

$^{13}\text{C NMR}$ (100 MHz, CDCl_3): $\delta = 154.7$ (dd, $^1J_{\text{C-F}} = 292.8$, 285.6 Hz), 116.5 (dd, $^2J_{\text{C-F}} = 37.2$, 11.0 Hz), 97.4 (t, $^4J_{\text{C-F}} = 3.8$ Hz), 70.9, 70.8 (t, $^3J_{\text{C-F}} = 3.0$ Hz), 68.0, 67.2, 66.9, 58.5, 37.6, 29.3, 28.2 ppm;

$^{19}\text{F NMR}$ (376 MHz, CDCl_3): $\delta = -99.7$ (d, $^2J = 64.0$ Hz, 1F), -109.9 (d, $^2J = 64.0$ Hz, 1F) ppm;

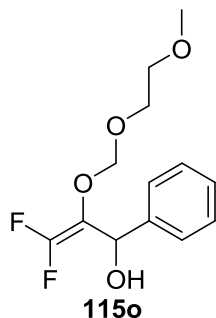
$\bar{\nu}$ (neat) = 3404, 2915, 1749, 1230, 1026, 955 cm^{-1} ;

HRMS (ESI): calcd for $\text{C}_{12}\text{H}_{24}\text{F}_2\text{O}_5\text{N}_1$, 300.1617 $[\text{M}+\text{NH}_4]^+$, found: 300.1620;

MS (EI): m/z (%): 281 (1) $[\text{M}-\text{H}]^+$, 89 (92) $[\text{C}_4\text{H}_9\text{O}_2]^+$, 59 (100) $[\text{C}_3\text{H}_7\text{O}]^+$;

t_R (GC) = 12.88 minutes.

1,1-difluoro-2-((2-methoxyethoxy)methoxy)-3-phenylprop-2-en-3-ol (115o)



Prepared as for **115aa** and **115ab** from acetal (1.90 mL, 12 mmol), *n*-butyllithium (12.9 mL of a 1.94 M solution in hexanes, 25 mmol), diisopropylamine (3.70 mL, 26 mmol) and benzaldehyde (1.27 g, 12 mmol) in THF (12 mL). The crude allylic alcohol (2.69 g) was purified by Kugelrohr distillation to afford **115o** as a pale yellow oil (1.94 g, 59 %).

b.p. = 102 °C / 0.04 mmHg;

R_f = 0.31 (50 % diethyl ether in hexane);

^1H NMR (400 MHz, CDCl_3): δ = 7.48- 7.29 (m, 5H), 5.52 (br. s, 1H), 4.94 (d, 2J = 6.7 Hz, 1H), 4.86 (d, 2J = 6.7 Hz, 1H), 3.91 (br. s, 1H), 3.79-3.70 (m, 1H), 3.67-3.60 (m, 1H), 3.51 (t, J = 4.8 Hz, 2H), 3.38 (s, 3H) ppm;

^{13}C NMR (100 MHz, CDCl_3): δ = 154.5 (dd, $^1J_{\text{C-F}}$ = 293.1, 286.7 Hz), 139.7, 127.8, 127.1, 125.4, 117.6 (dd, $^2J_{\text{C-F}}$ = 36.1, 10.6 Hz), 97.3 (t, $^4J_{\text{C-F}}$ = 3.4 Hz), 70.8, 68.0, 67.9 (d, $^3J_{\text{C-F}}$ = 3.6 Hz), 58.5 ppm;

^{19}F NMR (376 MHz, CDCl_3): δ = -99.3 (d, 2J = 61.7 Hz, 1F), -109.2 (d, 2J = 61.7 Hz, 1F) ppm;

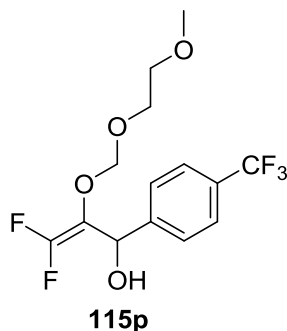
$\bar{\nu}$ /(neat) = 3411, 2926, 1749, 1230, 1020, 955 cm^{-1} ;

MS (EI): m/z (%): 160 (1) $[\text{M}-\text{C}_4\text{H}_9\text{O}_3]^+$, 107 (7) $[\text{C}_7\text{H}_7\text{O}]^+$, 89 (65) $[\text{C}_4\text{H}_9\text{O}_2]^+$, 59 (100) $[\text{C}_3\text{H}_7\text{O}]^+$;

t_R (GC) = 12.83 minutes.

The data was consistent with that previously reported.¹³⁹

1,1-difluoro-2-((2-methoxyethoxy)methoxy)-3-(4-(trifluoromethyl)phenyl)prop-2-en-3-ol (115p)



Prepared as for **115aa** and **115ab** from acetal (1.90 mL, 12 mmol), *n*-butyllithium (11.9 mL of a 2.10 M solution in hexanes, 25 mmol), diisopropylamine (3.70 mL, 26 mmol) and *p*-trifluoromethylbenzaldehyde (2.09 g, 12 mmol) in THF (12 mL). The crude allylic alcohol (4.99 g) was purified by Kugelrohr distillation followed by flash column chromatography (90 g cartridge, 60 % diethyl ether in petroleum ether) to afford **115p** as a colourless oil (0.87 g, 21 %).

b.p. = 113 °C / 0.05 mmHg;

R_f = 0.62 (5 % acetone in dichloromethane);

^1H NMR (400 MHz, CDCl_3): δ = 7.64 (d, J = 8.4 Hz, 2H), 7.57 (d, J = 8.4 Hz, 2H), 5.53 (br. d, J = 8.7 Hz, 1H), 4.93 (d, 2J = 6.7 Hz, 1H), 4.87 (d, 2J = 6.7 Hz, 1H), 3.85 (d, J = 8.7 Hz, 1H), 3.76 (ddd, 2J = 10.8, J = 5.9, 3.8 Hz, 1H), 3.64 (ddd, 2J = 10.8, J = 4.9, 3.1 Hz, 1H), 3.58-3.48 (m, 2H), 3.39 (s, 3H) ppm;

^{13}C NMR (100 MHz, CDCl_3): δ = 154.5 (dd, $^1J_{\text{C-F}}$ = 293.4, 287.4 Hz), 143.9, 129.3 (q, $^2J_{\text{C-F}}$ = 32.3 Hz), 125.8, 124.7 (q, $^3J_{\text{C-F}}$ = 3.5 Hz), 123.6 (q, $^1J_{\text{C-F}}$ = 271.8 Hz), 117.3 (dd, $^2J_{\text{C-F}}$ = 36.0, 11.3 Hz), 97.3 (t, $^4J_{\text{C-F}}$ = 3.9 Hz), 70.7, 68.0, 67.5 (d, $^3J_{\text{C-F}}$ = 3.4 Hz), 58.4 ppm;

^{19}F NMR (376 MHz, CDCl_3): δ = -62.5 (s, 3F), -98.5 (dd, 2J = 60.1, $^4J_{\text{F-H}}$ = 2.0 Hz, 1F), -108.5 (dd, 2J = 60.1, $^4J_{\text{F-H}}$ = 3.2 Hz, 1F) ppm;

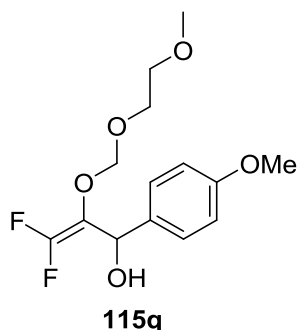
$\bar{\nu}$ (neat) = 3419, 2930, 1751, 1325, 1112, 1067, 1017 cm^{-1} ;

HRMS (APCI): calcd for $\text{C}_{14}\text{H}_{19}\text{F}_5\text{O}_4\text{N}_1$, 360.1229 $[\text{M}+\text{NH}_4]^+$, found: 360.1231;

MS (EI): m/z (%): 323 (1) $[\text{M}-\text{F}]^+$, 175 (9) $[\text{C}_8\text{H}_6\text{F}_3\text{O}]^+$, 89 (63) $[\text{C}_4\text{H}_9\text{O}_2]^+$, 59 (100) $[\text{C}_3\text{H}_7\text{O}]^+$;

t_R (GC) = 12.49 minutes.

**1,1-difluoro-2-((2-methoxyethoxy)methoxy)-3-(4-methoxyphenyl)prop-2-en-3-ol
(115q)**



Prepared as for **115aa** and **115ab** from acetal (1.90 mL, 12 mmol), *n*-Butyllithium (11.9 mL of a 2.10 M solution in hexanes, 25 mmol), diisopropylamine (3.70 mL, 26 mmol) and *p*-methoxybenzaldehyde (1.63 g, 12 mmol) in THF (12 mL). The crude allylic alcohol (3.28 g) was purified by flash column chromatography (90 g cartridge, 70 % diethyl ether in hexane) to afford **115q** as a yellow oil (2.39 g, 65 %).

$R_f = 0.42$ (70 % diethyl ether in hexane);

^1H NMR (400 MHz, CDCl_3): $\delta = 7.34$ (d, $J = 8.6$ Hz, 2H), 6.89 (d, $J = 8.6$ Hz, 2H), 5.51-5.37 (br. dt, $J = 7.7$, $^4J_{\text{H-F}} = 2.7$ Hz, 1H), 4.93 (d, $^2J = 6.6$ Hz, 1H), 4.82 (d, $^2J = 6.6$ Hz, 1H), 3.85 (br. dd, $J = 7.7$, $^5J_{\text{H-F}} = 2.4$ Hz, 1H), 3.80 (s, 3H), 3.77-3.69 (m, 1H), 3.67-3.60 (m, 1H), 3.49 (t, $J = 4.8$ Hz, 2H), 3.38 (s, 3H) ppm;

^{13}C NMR (100 MHz, CDCl_3): $\delta = 158.5$, 154.4 (dd, $^1J_{\text{C-F}} = 292.9$, 286.3 Hz), 131.8, 126.6, 117.5 (dd, $^2J_{\text{C-F}} = 35.5$, 10.1 Hz), 113.2, 97.3 (t, $^4J_{\text{C-F}} = 3.3$ Hz), 70.8, 68.0, 67.6 (d, $^3J_{\text{C-F}} = 3.2$ Hz), 58.4, 54.7 ppm;

^{19}F NMR (376 MHz, CDCl_3): $\delta = -99.6$ (d, $^2J = 62.4$ Hz, 1F), -109.4 (d, $^2J = 62.4$ Hz, 1F) ppm; (the ^{19}F - ^1H splittings are not resolved in the 376 MHz ^{19}F NMR spectrum);

$\bar{\nu}$ (neat) = 3415, 2932, 1749, 1511, 1245, 1026, 957 cm^{-1} ;

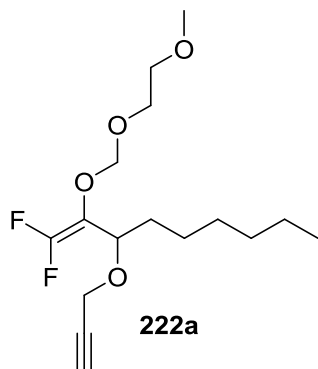
MS (EI): m/z (%): 195 (2) $[\text{M}-\text{C}_4\text{H}_{10}\text{O}_2\text{F}]^+$, 89 (69) $[\text{C}_4\text{H}_9\text{O}_2]^+$, 59 (100) $[\text{C}_3\text{H}_7\text{O}]^+$;

t_R (GC) = 14.39 minutes.

The data was consistent with that previously reported.¹³⁹

6.3.12 General Procedure E – Propargyl Ether Preparation

1,1-Difluoro-2-([methoxyethoxy]- methoxy) 3-(Propargyloxy)hexane (**222a**)



Propargyl ether **222a** was prepared according to the procedure of Percy and co-workers.¹⁹⁷ Propargyl bromide (0.78 mL of an 80 wt % solution in toluene, 7.0 mmol) was added dropwise to a vigorously stirred mixture of allylic alcohol **115I** (1.54g, 5.4 mmol) and tetra(*n*-butyl)ammonium hydrogen sulfate (0.085 g, 0.25 mmol) in aqueous sodium hydroxide (4.5 mL, 50 wt %) at 0 °C. The reaction mixture was allowed to warm to room temperature and stirred for 18 hours. The mixture was quenched with aqueous saturated ammonium chloride (20 mL) and transferred to a separating funnel. Water (10 mL) was added and the product was extracted with diethyl ether (4 x 50 mL). The combined organic extracts were dried (MgSO₄), filtered and concentrated under reduced pressure to afford the crude product as a yellow oil (1.91 g). The crude propargyl ether was purified by flash column chromatography (90 g cartridge, 20 % diethyl ether in hexane) to afford **222a** as a colourless oil (1.23 g, 71 %).

R_f = 0.62 (50 % diethyl ether in hexane);

¹H NMR (400 MHz, CDCl₃): δ = 5.04 (d, ²J = 6.2 Hz, 1H), 4.95 (d, ²J = 6.2 Hz, 1H), 4.28-4.18 (m, including 4.22 (dd, ²J = 15.7, ⁴J = 2.2 Hz, 1H), 1H), 4.09 (dd, ²J = 15.7, ⁴J = 2.2 Hz, 1H), 3.94-3.76 (m, 1H), 3.59 (t, J = 4.9 Hz, 2H), 3.41 (s, OCH₃, 3H), 3.42 (t, ⁴J = 2.2 Hz, 1H), 1.86-1.61 (m, 2H), 1.50-1.20 (m, 8H), 0.90 (t, J = 6.9 Hz, 3H) ppm;

¹³C NMR (100 MHz, CDCl₃): δ = 155.7 (dd, ¹J_{C-F} = 295.0, 285.5 Hz), 111.4 (dd, ²J_{C-F} = 36.3, 10.5 Hz), 96.4 (t, ⁴J_{C-F} = 3.3 Hz), 78.9, 73.7, 73.6 (t, ⁴J_{C-F} = 3.0 Hz), 71.1, 67.8, 58.4, 54.9, 31.1, 28.4, 24.8, 22.0, 13.5 ppm;

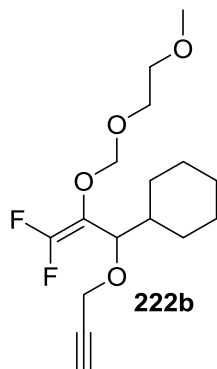
¹⁹F (376 MHz, CDCl₃): δ = -96.9 (d, ²J = 62.3 Hz, 1F), -109.0 (d, ²J = 62.3 Hz, 1F) ppm;

$\bar{\nu}$ (neat) = 3309, 2924, 1747, 1236, 1074, 955 cm⁻¹;

HRMS (ESI): calcd for C₁₆H₃₀F₂O₄N₁, 338.2137 [M+NH₄]⁺, found: 338.2139;

MS (CI): m/z (%): 281 (1) $[M-C_3H_3]^+$, 265 (4) $[M-C_3H_3O]^+$, 245 (6) $[M-C_3H_7O_2]^+$, 153 (4) $[C_{10}H_{17}O]^+$, 89 (78) $[C_4H_9O_2]^+$, 59 (100) $[C_3H_7O]^+$;
 t_R (GC) = 12.76 minutes.

1,1-Difluoro-2-([methoxyethoxy]- methoxy) 3-(Propargyloxy)-cyclohexane (222b)



Prepared as for **222a** from allylic alcohol **115m** (2.24 g, 8.40 mmol), propargyl bromide (1.15 mL of an 80 wt % solution in toluene, 9.9 mmol) and tetra(*n*-butyl)ammonium hydrogen sulfate (0.126 g, 0.34 mmol) in aqueous sodium hydroxide (6.6 mL, 50 wt %) at 0 °C. The crude ether (2.39 g) was purified by flash column chromatography (90 g cartridge, 15 % diethyl ether in hexane) to afford **222b** as a colourless oil (1.72 g, 68 %). R_f = 0.42 (30 % diethyl ether in hexane);

1H NMR (400 MHz, $CDCl_3$): δ = 5.02 (d, 2J = 6.4 Hz, 1H), 4.92 (d, 2J = 6.4 Hz, 1H), 4.20 (dd, 2J = 15.7, 4J = 2.4 Hz, 1H), 4.05 (dd, 2J = 15.7, 4J = 2.4 Hz, 1H), 3.92-3.83 (m, 2H), 3.82-3.73 (m, 1H), 3.57 (t, J = 4.9 Hz, 2H), 3.39 (s, 3H,), 2.39 (t, 4J = 2.4 Hz, 1H), 2.10 (br. d, 2J = 13.7 Hz, 1H), 1.86-1.52 (m, 5H), 1.37-1.09 (m, 3H), 1.07-0.82 (m, 2H) ppm;

^{13}C NMR (100 MHz, $CDCl_3$): δ = 156.2 (dd, $^1J_{C-F}$ = 295.5, 284.9 Hz), 110.5 (dd, $^2J_{C-F}$ = 36.3, 10.0 Hz), 96.4 (t, $^4J_{C-F}$ = 3.2 Hz), 79.1, 78.4 (t, $^3J_{C-F}$ = 3.5 Hz), 73.6, 71.1, 67.8, 58.5, 55.2, 38.2, 29.2, 28.2, 25.9, 25.2, 25.1 ppm;

^{19}F (376 MHz, $CDCl_3$): δ = -96.8 (d, 2J = 63.7 Hz, 1F), -109.6 (d, 2J = 63.7 Hz, 1F) ppm;

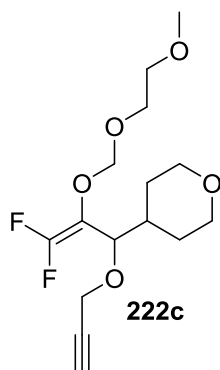
$\bar{\nu}$ (neat) = 3305, 2921, 1745, 1232, 1045, 957 cm^{-1} ;

HRMS (APCI): calcd for $C_{16}H_{28}F_2O_4N_1$, 336.1986 $[M+NH_4]^+$, found: 336.1981;

MS (ED): m/z (%): 243 (3) $[M-C_3H_7O_2]^+$, 187 (25) $[M-C_7H_{15}O_2]^+$, 89 (71) $[C_4H_9O_2]^+$, 59 (100) $[C_3H_7O]^+$;

t_R (GC) = 13.04 minutes.

1,1-Difluoro-2-([methoxyethoxy]- methoxy) 3-(Propargyloxy)- tetrahydro-2H-pyran-4-yl (222c)



Prepared as for **222a** from allylic alcohol **115n** (1.84 g, 6.5 mmol), propargyl bromide (1.00 mL of an 80 wt % solution in toluene, 8.5 mmol) and tetra(*n*-butyl)ammonium hydrogen sulfate (0.107 g, 0.29 mmol) in aqueous sodium hydroxide (5.3 mL, 50 wt %) at 0 °C. The crude ether (2.22 g) was purified by flash column chromatography (90 g cartridge, 50 % diethyl ether in hexane) to afford **222c** as a pale yellow oil (1.82 g, 88 %).

R_f = 0.32 (50 % diethyl ether in hexane);

^1H NMR (400 MHz, CDCl_3): δ = 5.01 (d, 2J = 6.6 Hz, 1H), 4.93 (d, 2J = 6.6 Hz, 1H), 4.26-4.17 (m, 1H), 4.10-4.03 (m, 1H), 4.02-3.82 (m, 4H), 3.82-3.73 (m, 1H), 3.56 (t, J = 5.1 Hz, 2H), 3.42-3.32 (m, 5H), 2.41 (t, 4J = 2.3 Hz, 1H), 2.04-1.90 (m, 2H), 1.55-1.45 (m, 1H), 1.44-1.17 (m, 2H) ppm;

^{13}C NMR (100 MHz, CDCl_3): δ = 156.3 (dd, $^1J_{\text{C-F}}$ = 294.9, 285.3 Hz), 110.0 (dd, $^2J_{\text{C-F}}$ = 36.5, 10.3 Hz), 96.5 (t, $^4J_{\text{C-F}}$ = 3.4 Hz), 78.8, 77.8 (t, $^3J_{\text{C-F}}$ = 3.6 Hz), 73.9, 71.1, 67.8, 67.1, 66.8, 58.5, 55.2, 35.7, 29.5, 28.0 ppm;

^{19}F NMR (376 MHz, CDCl_3): δ = -95.9 (d, 2J = 61.6 Hz, 1F), -108.9 (d, 2J = 61.6 Hz, 1F) ppm;

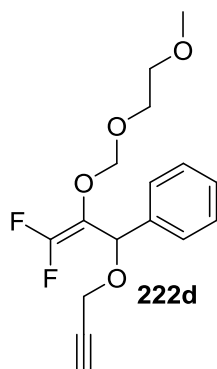
$\bar{\nu}$ (neat) = 3263, 2915, 1745, 1229, 1046, 948 cm^{-1} ;

HRMS (ESI): calcd for $\text{C}_{15}\text{H}_{26}\text{F}_2\text{O}_5\text{N}_1$, 338.1774 $[\text{M}+\text{NH}_4]^+$, found: 338.1775;

MS (EI): m/z (%): 281 (1) $[\text{M}-\text{C}_3\text{H}_3]^+$, 89 (100) $[\text{C}_4\text{H}_9\text{O}_2]^+$, 59 (96) $[\text{C}_3\text{H}_7\text{O}]^+$;

t_R (GC) = 13.36 minutes.

1,1-difluoro-2-([methoxyethoxy]- methoxy) 3-(Propargyloxy)- phenyl (222d)



Prepared as for **222a** from allylic alcohol **115o** (1.90 g, 6.9 mmol), propargyl bromide (1.00 mL of an 80 wt % solution in toluene, 9.0 mmol) and tetra(*n*-butyl)ammonium hydrogen sulfate (0.107 g, 0.31 mmol) in aqueous sodium hydroxide (5.6 mL, 50 wt %) at 0 °C. The crude ether (2.14 g) was purified by flash column chromatography (90 g cartridge, 25 % diethyl ether in hexane) to afford **222d** as a pale yellow oil (1.71 g, 79 %).

$R_f = 0.27$ (20 % diethyl ether in hexane);

$^1\text{H NMR}$ (400 MHz, CDCl_3): $\delta = 7.47\text{--}7.29$ (m, 5H), 5.46 (t, $^4J_{\text{H-F}} = 3.5$ Hz, 1H), 4.96 (d, $^2J = 6.4$ Hz, 1H), 4.86 (d, $^2J = 6.4$ Hz, 1H), 4.28 (t, $^4J = 2.4$ Hz, 2H), 3.79-3.67 (m, 1H), 3.53 (t, $J = 4.6$ Hz, 2H), 3.39 (s, 3H), 2.48 (t, $^4J = 2.4$ Hz, 1H) ppm;

$^{13}\text{C NMR}$ (100 MHz, CDCl_3): $\delta = 155.6$ (dd, $^1J_{\text{C-F}} = 294.3, 287.7$ Hz), 136.7, 127.9, 127.6, 126.2, 112.7 (dd, $^2J_{\text{C-F}} = 35.4, 11.9$ Hz), 96.7 (t, $^4J_{\text{C-F}} = 3.2$ Hz), 78.5, 74.5, 74.4 (app. d, $^3J_{\text{C-F}} = 2.5$ Hz), 71.0, 67.8, 58.5, 55.2 ppm;

$^{19}\text{F NMR}$ (376 MHz, CDCl_3): $\delta = -96.8$ (d, $^2J = 59.8$ Hz, 1F), -107.8 (dd, $^2J = 59.8, ^4J_{\text{F-H}} = 3.5$ Hz, 1F) ppm;

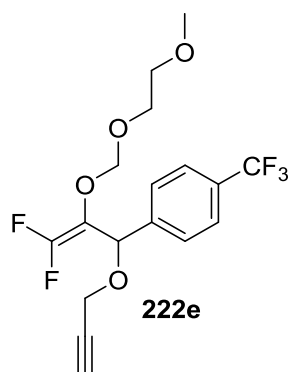
$\bar{\nu}$ (neat) = 3284, 2920, 1746, 1231, 1054, 954 cm^{-1} ;

HRMS (APCI): calcd for $\text{C}_{16}\text{H}_{22}\text{F}_2\text{O}_4\text{N}_1$, 330.1517 $[\text{M}+\text{NH}_4]^+$, found: 330.1520;

MS (EI): m/z (%): 145 (3) $[\text{C}_{10}\text{H}_9\text{O}]^+$, 89 (92) $[\text{C}_4\text{H}_9\text{O}_2]^+$, 59 (100) $[\text{C}_3\text{H}_7\text{O}]^+$;

t_R (GC) = 13.42 minutes.

1,1-Difluoro-2-([methoxyethoxy]- methoxy) 3 - (Propargyloxy)- 4-(trifluoromethyl)phenyl (222e)



Prepared as for **222a** from allylic alcohol **115p** (0.813 g, 2.4 mmol), propargyl bromide (0.35 mL of an 80 wt % solution in toluene, 3.0 mmol) and tetra(*n*-butyl)ammonium hydrogen sulfate (0.037 g, 0.10 mmol) in aqueous sodium hydroxide (3.0 mL, 50 wt %) at 0 °C. The crude ether (0.917 g) was purified by flash column chromatography (90 g cartridge, 20 % diethyl ether in hexane) to afford **222e** as a colourless oil (0.679 g, 74 %).

R_f = 0.49 (5 % acetone in dichloromethane);

¹H NMR (400 MHz, CDCl₃): δ = 7.65 (d, *J* = 8.2 Hz, 2H), 7.56 (d, *J* = 8.4 Hz, 2H), 5.51 (br. t, ⁴*J*_{H-F} = 2.7 Hz, 1H), 4.97 (d, ²*J* = 6.2 Hz, 1H), 4.79 (d, ²*J* = 6.2 Hz, 1H), 4.31 (d, ⁴*J* = 2.5 Hz, 2H), 3.75-3.69 (m, 2H), 3.55-3.49 (m, 2H), 3.39 (s, 3H), 2.49 (t, ⁴*J* = 2.5 Hz, 1H) ppm;

¹³C NMR (100 MHz, CDCl₃): δ = 155.7 (dd, ¹*J*_{C-F} = 294.6, 287.0 Hz), 140.9, 129.8 (q, ²*J*_{C-F} = 32.8 Hz), 126.5, 124.8 (q, ³*J*_{C-F} = 3.5 Hz), 123.7 (q, ¹*J*_{C-F} = 272.7 Hz), 112.0 (dd, ²*J*_{C-F} = 36.0, 11.3 Hz), 96.7 (t, ⁴*J*_{C-F} = 3.3 Hz), 78.0, 74.8, 73.9 (t, ³*J*_{C-F} = 3.2 Hz), 70.9, 67.9, 58.5, 55.4 ppm;

¹⁹F NMR (376 MHz, CDCl₃): δ = -62.6 (s, 3F), -95.8 (d, ²*J* = 58.7 Hz, 1F), -107.3 (dd, ²*J* = 58.7, ⁴*J*_{F-H} = 3.4 Hz, 1F) ppm;

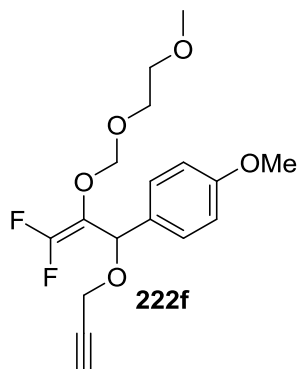
$\bar{\nu}$ (neat) = 3305, 2921, 1747, 1325, 1112, 1067, 1019 cm⁻¹;

HRMS (APCI): calcd for C₁₇H₂₁F₅O₄N₁, 398.1385 [M+NH₄]⁺, found: 398.1383;

MS (ED): *m/z* (%): 361 (1) [M-F]⁺, 213 (4) [M-C₇H₁₀F₃O]⁺, 89 (96) [C₄H₉O₂]⁺, 59 (100) [C₃H₇O]⁺;

t_R (GC) = 13.00 minutes.

1,1-Difluoro-2-([methoxyethoxy]- methoxy) 3-(Propargyloxy)- 4-(methoxy)phenyl (222f)



Prepared as for **222f** from allylic alcohol **115q** (2.22 g, 7.3 mmol), propargyl bromide (1.06 mL of an 80 wt % solution in toluene, 9.0 mmol) and tetra(*n*-butyl)ammonium hydrogen sulfate (0.113 g, 0.31 mmol) in aqueous sodium hydroxide (6.0 mL, 50 wt %) at 0 °C. The crude ether (2.73 g) was purified by flash column chromatography (90 g cartridge, 50 % diethyl ether in hexane) to afford **222f** as a pale yellow oil (2.19 g, 88 %).

$R_f = 0.39$ (50 % diethyl ether in hexane);

$^1\text{H NMR}$ (400 MHz, CDCl_3): $\delta = 7.35$ (d, $J = 8.6$ Hz, 2H), 6.90 (d, $J = 8.6$ Hz, 2H), 5.51-5.37 (t, $^4J_{\text{H-F}} = 3.2$ Hz, 1H), 4.96 (d, $^2J = 6.3$ Hz, 1H), 4.76 (d, $^2J = 6.3$ Hz, 1H), 4.24, 4.21 (dABq, $J_{\text{AB}} = 15.9$, $^4J = 2.4$ Hz, 2H), 3.81 (s, 3H), 3.77-3.72 (m, 2H), 3.53 (t, $J = 4.9$ Hz, 2H), 3.38 (s, 3H), 2.47 (t, $^4J = 2.4$ Hz, 1H) ppm;

$^{13}\text{C NMR}$ (100 MHz, CDCl_3): $\delta = 159.0$, 155.5 (dd, $^1J_{\text{C-F}} = 294.1$, 286.1 Hz), 128.7, 127.5, 113.3, 112.8 (dd, $^2J_{\text{C-F}} = 34.6$, 10.7 Hz), 96.7 (t, $^4J_{\text{C-F}} = 3.5$ Hz), 78.5, 74.4, 74.1 (t, $^3J_{\text{C-F}} = 3.2$ Hz), 71.0, 67.8, 58.5, 55.0, 54.7 ppm;

$^{19}\text{F NMR}$ (376 MHz, CDCl_3): $\delta = -97.2$ (d, $^2J = 60.1$ Hz, 1F), -107.9 (d, $^2J = 60.1$, $^4J_{\text{F-H}} = 3.2$ Hz, 1F) ppm;

$\bar{\nu}$ (neat) = 3283, 2898, 1745, 1513, 1247, 1054, 955 cm^{-1} ;

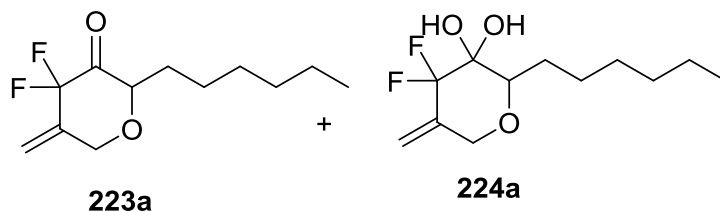
HRMS (ESI): calcd for $\text{C}_{17}\text{H}_{24}\text{F}_2\text{O}_5\text{N}_1$, 360.1617 $[\text{M}+\text{NH}_4]^+$, found: 360.1620;

MS (EI): m/z (%): 198 (19) $[\text{M}-\text{C}_7\text{H}_{12}\text{O}_3]^+$, 89 (76) $[\text{C}_4\text{H}_9\text{O}_2]^+$, 59 (100) $[\text{C}_3\text{H}_7\text{O}]^+$;

t_R (GC) = 14.55 minutes.

6.3.13 General Procedure F – Difluorinated Pyran Preparation

Preparation of 4,4-Difluoro-2-hexyl-5-methylenedihydro-2H-pyran-3(4H)-one (**223a**) and 3,3-dihydroxy-4,4-difluoro-2-hexyl-5-methylenedihydro-2H-pyran (**224a**)



1,3-*bis*(2,6-diisopropylphenyl-imidazol-2-ylidene)gold(I) chloride (5 mol %, 0.031 g) and silver hexafluoroantimonate(V) (5 mol %, 0.017 g) were added to a round bottom flask. 2-methyltetrahydrofuran (5 mL) was added and the solution stirred at room temperature (25 °C). During stirring, an off-white precipitate formed. The solution was stirred at room temperature then a solution of ether **222a** (0.320 g, 1 mmol) in 2-methyltetrahydrofuran (1 mL) was added in a stream *via* syringe. The mixture was stirred for 21 hours at room temperature then concentrated under reduced pressure to afford the crude product as a viscous dark brown oil (0.312 g). The crude material was purified by flash column chromatography (40 g silica, 3 % acetone in dichloromethane) to afford an inseparable mixture of ketone **223a** and hydrate **224a** as a colourless solid (0.163 g, 65 %, 1:1). A small sample of crystalline hydrate **224a** was prepared by recrystallisation of the mixture by vapour diffusion using chloroform/pentane (8 mg, 3 %).

m.p. = 70-72 °C (recrystallised from chloroform/pentane as small colourless needles)

R_f = 0.57 (10 % acetone in dichloromethane);

The following signals were attributed to both ketone **223a** and hydrate **224a** ^1H NMR (400 MHz, CDCl_3): δ = 2.00-1.19 (envelope, 20H), 0.90 (t, J = 7.0 Hz, 6H) ppm;

The following signals were attributed to ketone **223a** (assigned on comparison of the ^1H NMR spectrum of crystalline hydrate **224a** grown from chloroform/pentane with the ^1H NMR spectrum of the mixture and 2D NMR data)

^1H NMR (400 MHz, CDCl_3): δ = 5.79 (br. d, $^4J_{\text{H-F}}$ = 4.0 Hz, 1H), 5.59 (app. q, $^4J_{\text{H-F}}$ = 4J = 1.4 Hz, 1H), 4.54 (br. d, 2J = 13.8 Hz, 1H), 4.42 (br. d, 2J = 13.8 Hz, 1H), 4.17-4.10 (m, 1H) ppm;

^{13}C NMR (100 MHz, CDCl_3): $\delta = 194.7$ (dd, $^2J_{\text{C-F}} = 27.9, 22.9$ Hz), 138.1 (t, $^2J_{\text{C-F}} = 18.9$ Hz), 116.9 (t, $^3J_{\text{C-F}} = 7.5$ Hz), 109.9 (dd, $^1J_{\text{C-F}} = 261.2, 246.0$ Hz), 81.3 (d, $^3J_{\text{C-F}} = 2.9$ Hz), 67.8 (d, $^3J_{\text{C-F}} = 3.3$ Hz), $31.2, 28.7, 25.3, 24.4, 22.1, 13.5$ ppm;

^{19}F NMR (376 MHz, CDCl_3): $\delta = -105.6$ (d, $^2J = 265.6$ Hz, 1F), -120.0 (d, $^2J = 265.6$ Hz, 1F) ppm (the ^{19}F - ^1H splittings are not resolved in the 376 MHz ^{19}F NMR spectrum).

The following signals were attributed to hydrate **224a** (See page 162 of Results and Discussion)

^1H NMR (400 MHz, CDCl_3): $\delta = 5.67$ (d, $^4J_{\text{H-F}} = 4.9$ Hz, 1H), 5.39 (app. q, $^4J_{\text{H-F}} = 4J = 1.8$ Hz, 1H), 4.32 (dd, $^2J = 12.9, ^4J_{\text{H-F}} = 4.2$ Hz, 1H), 4.17 (br. d, $^2J = 12.9$ Hz, 1H), 3.65 - 3.50 (m, 1H), 3.13 (br. s, 1H), 3.02 (br. s, 1H) ppm;

^{13}C NMR (100 MHz, CDCl_3): $\delta = 136.4$ (t, $^2J_{\text{C-F}} = 20.5$ Hz), 115.5 (dd, $^1J_{\text{C-F}} = 261.1, 244.3$ Hz), 115.2 (t, $^3J_{\text{C-F}} = 7.0$ Hz), 92.7 (dd, $^2J_{\text{C-F}} = 27.5, 20.1$ Hz), 79.4 (d, $^3J_{\text{C-F}} = 2.9$ Hz), 68.7 (d, $^3J_{\text{C-F}} = 4.4$ Hz), $31.1, 28.8, 28.5, 26.0, 22.0, 13.5$ ppm;

^{19}F NMR (376 MHz, CDCl_3): $\delta = -107.7$ (d, $^2J = 240.6$ Hz, 1F), -138.7 (d, $^2J = 240.6$ Hz, 1F) ppm; (the ^{19}F - ^1H splittings are not resolved in the 376 MHz ^{19}F NMR spectrum);

$\bar{\nu}$ (neat) = $3387, 2922, 1470, 1242, 1085, 933$ cm^{-1} ;

HRMS (APCI): calcd for $\text{C}_{12}\text{H}_{19}\text{F}_2\text{O}_2$, 233.1353 $[\text{M}+\text{H}]^+$, found: 233.1352 ;

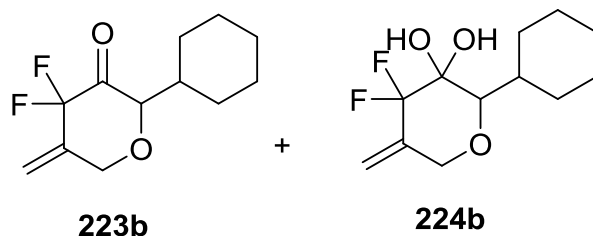
MS (EI): m/z (%): 232 (1) $[\text{M}]^+$, 119 (32) $[\text{M}-\text{C}_7\text{H}_{13}\text{O}]^+$,**

t_{R} (GC) = 11.22 minutes.**

*accurate mass was calculated for the ketone component of the mixture

**the mixture appeared as one peak by GC-MS, masses corresponded to that of the ketone.

2-Cyclohexyl-4,4-difluoro-5-methylenedihydro-2H-pyran-3(4H)-one (**223b**) and 3,3-dihydroxy-2-cyclohexyl-4,4-difluoro-5-methylenedihydro-2H-pyran (**224b**)



Ketone **223b** and hydrate **224b** were prepared according to general procedure F from ether **222b** (0.318 g, 1.00 mmol) with 1,3-bis(2,6-diisopropylphenyl-imidazol-2-ylidene)gold(I) chloride (5 mol %, 0.031 g) and silver hexafluoroantimonate(V) (5 mol %, 0.017 g) in 2-methyltetrahydrofuran (6.0 mL). After stirring for 21 hours at room temperature the reaction mixture was concentrated under reduced pressure to afford the

crude product as a viscous dark brown oil (0.369 g). The crude material was purified by flash column chromatography (40 g silica, 5 % acetone in dichloromethane) to afford an inseparable mixture of ketone **223b** and hydrate **224b** as a colourless solid (0.145 g, 63 %, 7.3:1).

$R_f = 0.46$ (5 % acetone in dichloromethane);

The following signals were attributed to both ketone **223b** and hydrate **224b** ^1H NMR (400 MHz, CDCl_3): $\delta = 2.15\text{-}1.89$ (m, 1H), 1.89-1.55 (m, 5H), 1.47-1.09 (m, 5H) ppm;

The following signals were attributed to ketone **223b** (assigned on the basis of δ and intensity)

^1H NMR (400 MHz, CDCl_3): $\delta = 5.82\text{-}5.74$ (m, 1H), 5.47 (br. s, 1H), 4.60 (app. dt, $^2J = 14.0$, $^4J = 1.4$ Hz, 1H), 4.37 (app. dq, $^2J = 14.0$, $^4J = ^4J_{\text{H-F}} = 1.4$ Hz, 1H), 3.91 (dt, $J = 5.0$, $^4J_{\text{H-F}} = 2.9$ Hz, 1H) ppm;

^{13}C NMR (100 MHz, CDCl_3): $\delta = 195.1$ (t, $^2J_{\text{C-F}} = 25.1$ Hz), 137.9 (t, $^2J_{\text{C-F}} = 18.7$ Hz), 116.8 (t, $^3J_{\text{C-F}} = 7.5$ Hz), 109.6 (dd, $^1J_{\text{C-F}} = 257.0$, 250.5 Hz), 85.7, 67.5, 37.8, 28.7, 26.6, 25.6 ppm;

^{19}F NMR (376 MHz, CDCl_3): $\delta = -111.7$ (dt, $^2J = 265.4$, $^4J_{\text{F-H}} = 2.7$ Hz, 1F), -120.0 (dq, $^2J = 265.4$, $^4J_{\text{F-H}} = 2.9$ Hz, 1F) ppm;

The following signals were attributed to hydrate **224b** (assigned on the basis of δ and intensity)

^1H NMR (400 MHz, CDCl_3): $\delta = 5.65$ (d, $^4J_{\text{H-F}} = 4.9$ Hz, 1H), 5.37 (app. q, $^4J_{\text{H-F}} = ^4J = 1.9$ Hz, 1H), 4.33 (dd, $^2J = 12.9$, $^4J_{\text{H-F}} = 4.2$ Hz, 1H), 4.13 (br. d, $^2J = 12.9$ Hz, 1H), 3.37-3.32 (m, 1H), 3.24 (br. s, 1H), 3.08 (br. s, 1H) ppm;

^{13}C NMR (100 MHz, CDCl_3): $\delta = 136.5$ (t, $^2J_{\text{C-F}} = 20.6$ Hz), 115.6 (dd, $^1J_{\text{C-F}} = 259.9$, 244.8 Hz), 115.1 (t, $^3J_{\text{C-F}} = 7.0$ Hz), 93.9 (dd, $^2J_{\text{C-F}} = 26.6$, 20.1 Hz), 82.5 (d, $^3J_{\text{C-F}} = 1.7$ Hz), 69.0 (d, $^3J_{\text{C-F}} = 4.4$ Hz), 36.2, 30.9, 27.6, 25.4 ppm;

^{19}F NMR (376 MHz, CDCl_3): $\delta = -107.1$ (d, $^2J = 240.6$ Hz, 1F), -139.4 (d, $^2J = 240.6$ Hz, 1F) ppm (the ^{19}F - ^1H splittings are not resolved in the 376 MHz ^{19}F NMR spectrum);

$\bar{\nu}/(\text{neat}) = 3404, 2917, 1452, 1217, 1091, 935 \text{ cm}^{-1}$;

HRMS (APCI): calcd for $\text{C}_{12}\text{H}_{20}\text{F}_2\text{O}_2\text{N}_1$, 248.1457 $[\text{M}+\text{NH}_4]^+$, found: 248.1459;*

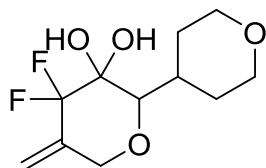
MS (EI): m/z (%): 230 (2) $[\text{M}]^+$, 202 (58) $[\text{M}-\text{C}_2\text{H}_4]^+$,**

t_R (GC) = 11.41 minutes.**

*accurate mass was calculated for the ketone component of the mixture

**the mixture appeared as one peak by GC-MS, masses corresponded to that of the ketone.

3,3-Dihydroxy-4,4-difluoro-5-methylenehexahydro-2H,2'H-[2,4'-bipyran] (224c)



224c

Hydrate **224c** was prepared according to general procedure F from ether **222c** (0.320 g, 1.00 mmol) with 1,3-bis(2,6-diisopropylphenyl-imidazol-2-ylidene)gold(I) chloride (5 mol %, 0.031 g) and silver hexafluoroantimonate(V) (5 mol %, 0.017 g) in 2-Methyltetrahydrofuran (6.0 mL). After stirring for 21 hours at room temperature the reaction mixture was concentrated under reduced pressure to afford the crude product as a viscous dark brown oil (0.393 g). The crude material was purified by flash column chromatography (40 g silica, 15 % acetone in dichloromethane) to afford hydrate **224c** as a colourless solid (0.154 g, 62 %).

m.p. = 102-104 °C (recrystallised from tetrahydrofuran/pentane by vapour diffusion as a colourless needles);

R_f = 0.35 (20 % acetone in dichloromethane);

¹H NMR (400 MHz, DMSO-*d*₆): δ = 6.36 (s, 1H), 6.03 (s, 1H), 5.41 (d, ⁴J_{H-F} = 4.90 Hz, 1H), 5.34 (br. s, 1H), 4.30 (dd, ²J = 12.9, ⁴J_{H-F} = 4.2 Hz, 1H), 3.94 (d, ²J = 12.9 Hz, 1H), 3.81 (dd, ²J = 11.5, J = 4.5 Hz, 2H), 3.29 (dd, ²J = 11.5, J = 2.2 Hz, 1H), 3.23 (dd, ²J = 11.5, J = 2.2 Hz, 1H), 3.11 (t, J = ⁴J_{H-F} = 4.0 Hz, 1H), 2.17-2.03 (m, 1H), 1.85-1.75 (m, 1H), 1.74-1.64 (m, 1H), 1.46 (qd, ²J = J = 12.1, J = 4.5 Hz, 1H), 1.36 (qd, ²J = J = 12.1, J = 4.5 Hz, 1H) ppm;

¹³C NMR (150 MHz, DMSO-*d*₆): δ = 138.6 (t, ²J_{C-F} = 19.9 Hz), 117.0 (dd, ¹J_{C-F} = 262.8, 240.9 Hz), 114.1 (t, ³J_{C-F} = 7.7 Hz), 94.1 (dd, ²J_{C-F} = 26.1, 19.3 Hz), 83.0 (d, ³J_{C-F} = 2.7 Hz), 68.6 (d, ³J_{C-F} = 4.1 Hz), 67.7, 67.6, 34.0, 31.7, 29.0 ppm;

¹⁹F NMR (376 MHz, DMSO-*d*₆): δ = -104.6 (d, ²J = 236.8 Hz, 1F), -136.0 (d, ²J = 236.8 Hz, 1F) ppm; (the ¹⁹F-¹H splittings are not resolved in the 376 MHz ¹⁹F NMR spectrum);

$\bar{\nu}$ /(neat) = 3287, 2846, 1446, 1297, 1052, 914 cm⁻¹;

HRMS (APCI): calcd for C₁₁H₁₈F₂O₃N₁, 250.1249 [M+NH₄]⁺, found: 250.1253;*

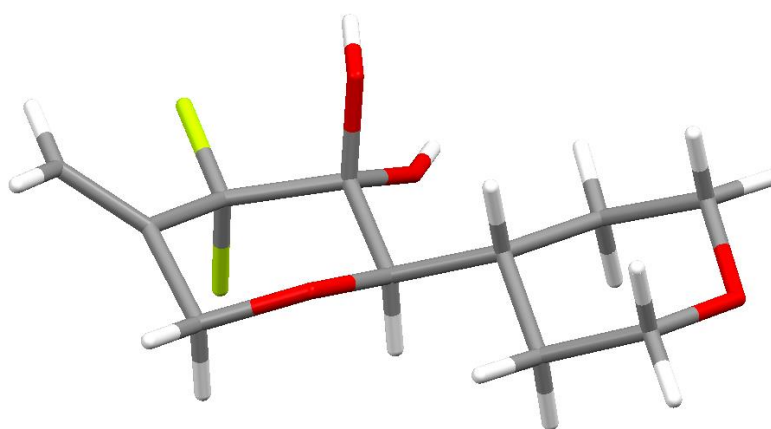
MS (EI): *m/z* (%): 232 (2) [M]⁺, 202 (7) [M-C₂H₄]⁺,**

t_R (GC) = 11.69 minutes.**

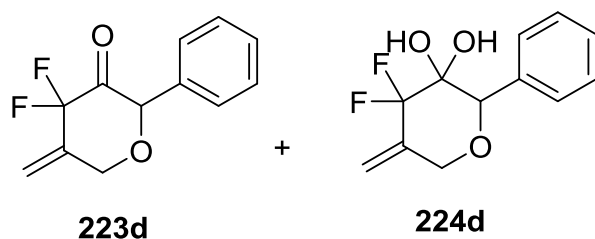
*accurate mass was calculated for the ketone component.

**the mixture appeared as one peak by GC-MS, masses corresponded to that of the ketone.

The identity of hydrate (**224c**) was confirmed by XRD analysis (m.p. = 102-104 °C (tetrahydrofuran/pentane). Crystal Data for **224c**: C₁₁H₁₆F₂O₄, crystal size 0.18 x 0.01 x 0.005 mm³, *M* = 250.24, orthorhombic, space group Pca2₁, unit cell dimensions *a* = 18.0944(13) Å, *b* = 6.5258(5) Å, *c* = 18.8242(14) Å, $\alpha = 90^\circ$, $\beta = 90^\circ$, $\gamma = 90^\circ$, *V* = 2222.8(3) Å³, *Z* = 8, ρ_{calc} = 1.496 Mg m⁻³, *F*(000) = 1056, $\mu(\text{Mo-K}\alpha)$ = 0.133 mm⁻¹, *T* = 100(2)K, 11704 reflections measured, 4342 independent, (*R*_{int} = 0.0986]. Final *R* indices [*I* > 2 σ (*I*)] *R*1 = 0.0709, ωR 2 = 0.1692; *R* indices (all data) *R*1 = 0.0969, ωR 2 = 0.1822.



4,4-Difluoro-5-methylene-2-phenyldihydro-2H-pyran-3(4H)-one (223d) and **3,3-dihydroxy-4,4-difluoro-5-methylene-2-phenyldihydro-2H-pyran (224d)**



Ketone **223d** and hydrate **224d** were prepared according to general procedure F from ether **222d** (0.312 g, 1.00 mmol) with 1,3-bis(2,6-diisopropylphenyl-imidazol-2-ylidene)gold(I) chloride (5 mol %, 0.031 g) and silver hexafluoroantimonate(V) (5 mol %, 0.017 g) in 2-Methyltetrahydrofuran (6.0 mL). After stirring for 21 hours at room temperature the reaction mixture was concentrated under reduced pressure to afford the crude product as a viscous dark brown oil (0.324 g). The crude material was purified by flash column chromatography (40 g silica, 3 % acetone in dichloromethane) to afford an

inseparable mixture of ketone **223d** and hydrate **224d** as a colourless solid (0.126 g, 52 %, 1:3.8).

m.p. = 76-78 °C (recrystallised from ethyl acetate/hexane by vapour diffusion as a colourless plate);

R_f = 0.53 (10 % acetone in dichloromethane);

The following signals were attributed to both ketone **223d** and hydrate **224d** ¹H NMR (400 MHz, CDCl₃): δ = 7.64-7.32 (m, 5H) ppm;

The following signals were attributed to ketone **223d** (assigned on the basis of δ and intensity)

¹H NMR (400 MHz, CDCl₃): δ = 5.91-5.86 (m, 1H), 5.58 (app. q, ⁴J_{H-F} = ⁴J = 1.5 Hz, 1H), 5.24 (t, ⁴J_{H-F} = 3.1 Hz, 1H), 4.71 (app. dq, ²J = 13.8, ⁴J = ⁴J_{H-F} = 1.1 Hz, 1H), 4.61 (br. d, ²J = 13.8 Hz, 1H) ppm;

¹³C NMR (100 MHz, CDCl₃): δ = 193.0 (dd, ²J_{C-F} = 27.3, 23.4 Hz), 137.6 (t, ²J_{C-F} = 19.3 Hz), 132.8, 128.6, 128.1, 127.0, 117.5 (t, ³J_{C-F} = 7.4 Hz), 110.2 (dd, ¹J_{C-F} = 260.4, 248.7 Hz), 83.6, 67.8 (d, ³J_{C-F} = 2.7 Hz) ppm;

¹⁹F NMR (376 MHz, CDCl₃): δ = -107.2 - -108.0 (m, including -107.6 (app. d, ²J = 264.5 Hz, 1F)), -116.3 (d, ²J = 264.5, 1F) ppm; (the ¹⁹F-¹H splittings are not resolved in the 376 MHz ¹⁹F NMR spectrum);

The following signals were attributed to hydrate **224d** (assigned on the basis of δ and intensity)

¹H NMR (400 MHz, CDCl₃): δ = 5.73 (d, ⁴J_{H-F} = 4.9 Hz, 1H), 5.46 (app. q, ⁴J_{H-F} = ⁴J = 1.7 Hz, 1H), 4.77-4.71 (m, 1H), 4.49 (dd, ²J = 13.1, ⁴J_{H-F} = 4.0 Hz, 1H), 4.38 (br. d, ²J = 13.1 Hz, 1H), 2.88 (br. s, 2H) ppm;

¹³C NMR (100 MHz, CDCl₃): δ = 136.1 (t, ²J_{C-F} = 19.9 Hz), 133.0, 128.5, 127.9, 127.6, 115.5 (t, ¹J_{C-F} = 262.8 Hz), 115.2 (t, ³J_{C-F} = 7.1 Hz), 92.2 (dd, ²J_{C-F} = 27.7, 19.7 Hz), 80.5 (d, ³J_{C-F} = 3.2 Hz), 68.7 (d, ³J_{C-F} = 4.5 Hz) ppm;

¹⁹F NMR (376 MHz, CDCl₃): δ = -106.8 (d, ²J = 242.3 Hz, 1F), -137.2 (app. quint, ²J = 242.3, ⁴J_{F-H} = 2.0 Hz, 1F) ppm;

$\bar{\nu}$ /(neat) = 3306, 2905, 1713, 1326, 1203, 1047, 946 cm⁻¹;

HRMS (APCI): calcd for C₁₂H₁₁F₂O₂, 225.0727 [M+H]⁺, found: 225.0723;*

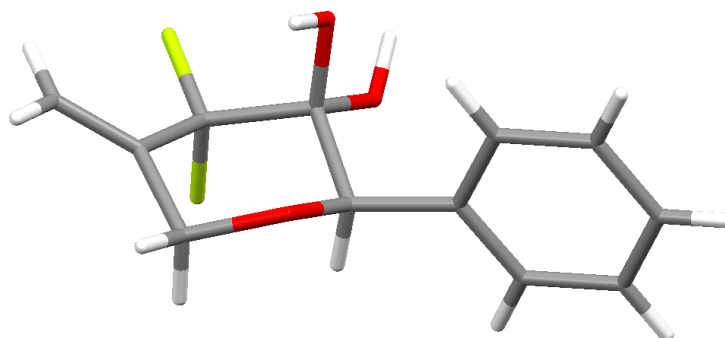
MS (EI): *m/z* (%): 147 (4) [M-C₆H₅]⁺, 90 (100) [M-C₉H₉O]⁺,**

t_R (GC) = 11.82 minutes.**

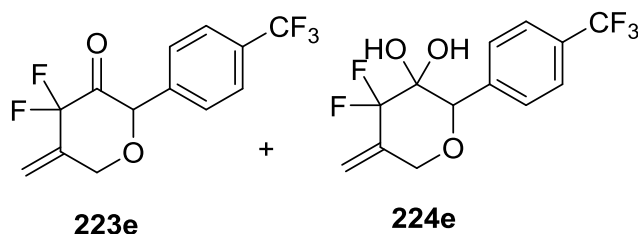
*accurate mass was calculated for the ketone component of the mixture

**the mixture appeared as one peak by GC-MS, masses corresponded to that of the ketone.

The identity of hydrate (**224d**) was confirmed by XRD analysis (m.p. = 76-78 °C (ethyl acetate/hexane). Crystal Data for **224d**: C₁₂H₁₂F₂O₃, crystal size 0.40 x 0.20 x 0.10 mm³, *M* = 242.22, monoclinic, space group P2_{1/c}, unit cell dimensions *a* = 10.4923(3) Å, *b* = 10.7404(3) Å, *c* = 9.7896(14) Å, α = 90°, β = 97.835(3)°, γ = 90°, *V* = 1093.91(6) Å³, *Z* = 4, ρ_{calc} = 1.471 Mg m⁻³, *F*(000) = 504, μ(Mo-Kα) = 1.095 mm⁻¹, *T* = 123(2)K, 3671 reflections measured, 2131 independent, (*R*_{int} = 0.0305]. Final *R* indices [*I* > 2σ(*I*)] *R*1 = 0.0474, ω*R*2 = 0.1291; *R* indices (all data) *R*1 = 0.0495, ω*R*2 = 0.1314.



4,4-Difluoro-5-methylene-2-(4-(trifluoromethyl)phenyl)dihydro-2H-pyran-3(4H)-one (223e) and 3,3-dihydroxy-4,4-difluoro-5-methylene-2-(4-(trifluoromethyl)phenyl)dihydro-2H-pyran (224e)



Ketone **223e** and hydrate **224e** were prepared according to general procedure F from ether **222e** (0.380 g, 1.00 mmol) with 1,3-bis(2,6-diisopropylphenyl-imidazol-2-ylidene)gold(I) chloride (5 mol %, 0.031 g) and silver hexafluoroantimonate(V) (5 mol %, 0.017 g) in 2-Methyltetrahydrofuran (6.0 mL). After stirring for 21 hours at room temperature the reaction mixture was concentrated under reduced pressure to afford the crude product as a viscous dark brown oil (0.376 g). The crude material was purified by flash column chromatography (40 g silica, 2 % acetone in dichloromethane) to afford an inseparable mixture of ketone **223e** and hydrate **224e** as a colourless solid (0.161 g, 52 %, 1:6.1).

*R*_f = 0.45 (5 % acetone in dichloromethane);

The following signals were attributed to both ketone **223e** and hydrate **224e** ^1H NMR (400 MHz, CDCl_3): $\delta = 7.67, 7.65$ (ABq, $J_{\text{AB}} = 8.7$ Hz, 4H) ppm;

The following signals were attributed to ketone **223e** (assigned on the basis of δ and intensity)

^1H NMR (400 MHz, CDCl_3): $\delta = 7.49$ (d, $J = 8.4$ Hz, 2H), 5.92-5.88 (m, 1H), 5.61 (q, $^4J_{\text{H-F}} = ^4J = 1.4$ Hz, 1H), 5.30 (t, $^4J_{\text{H-F}} = 3.2$ Hz, 1H), 4.73 (dq, $^2J = 13.9$, $^4J = ^4J_{\text{H-F}} = 1.2$ Hz, 1H), 4.64 (br. d, $^2J = 13.9$ Hz, 1H) ppm;

^{13}C NMR (100 MHz, CDCl_3): $\delta = 192.2$ (dd, $^2J_{\text{C-F}} = 27.7, 23.4$ Hz), 137.3 (t, $^2J_{\text{C-F}} = 19.1$ Hz), 136.5, 130.7 (q, $^2J_{\text{C-F}} = 32.8$ Hz), 127.2, 125.0 (q, $^3J_{\text{C-F}} = 3.9$ Hz), 117.9 (t, $^3J_{\text{C-F}} = 7.5$ Hz), 110.2 (dd, $^1J_{\text{C-F}} = 260.3, 247.3$ Hz), 82.7, 68.1 (d, $^3J_{\text{C-F}} = 3.3$ Hz) ppm (the large $^1J_{\text{CF}_3}$ quartet could not be observed in the 100 MHz ^{13}C NMR spectrum);

^{19}F NMR (376 MHz, CDCl_3): $\delta = -62.8$ (s, 3F), -107.0 (d, $^2J = 265.4$ Hz, 1F), -117.4 (d, $^2J = 265.4$, 1F) ppm (the ^{19}F - ^1H splittings are not resolved in the 376 MHz ^{19}F NMR spectrum).

The following signals were attributed to hydrate **224e** (assigned on the basis of δ and intensity)

^1H NMR (400 MHz, CDCl_3): $\delta = 5.76$ (d, $^4J_{\text{H-F}} = 4.8$ Hz, 1H), 5.49 (app. q, $^4J_{\text{H-F}} = ^4J = 1.8$ Hz, 1H), 4.82-4.77 (m, 1H), 4.51 (dd, $^2J = 13.1$, $^4J_{\text{H-F}} = 4.1$ Hz, 1H), 4.38 (br. d, $^2J = 13.1$ Hz, 1H), 3.09 (br. s, 1H), 2.81 (br. s, 1H) ppm;

^{13}C NMR (100 MHz, CDCl_3): $\delta = 137.2, 135.7$ (t, $^2J_{\text{C-F}} = 20.2$ Hz), 130.5 (q, $^2J_{\text{C-F}} = 32.6$ Hz), 128.1, 124.5 (q, $^3J_{\text{C-F}} = 3.7$ Hz), 123.8 (q, $^1J_{\text{C-F}} = 272.3$ Hz), 115.6 (t, $^3J_{\text{C-F}} = 7.1$ Hz), 115.3 (dd, $^1J_{\text{C-F}} = 261.8, 242.8$ Hz), 92.3 (dd, $^2J_{\text{C-F}} = 28.6, 20.8$ Hz), 79.9 (d, $^3J_{\text{C-F}} = 2.8$ Hz), 68.7 (d, $^3J_{\text{C-F}} = 4.6$ Hz) ppm;

^{19}F NMR (376 MHz, CDCl_3): $\delta = -62.7$ (s, 3F), -106.9 (d, $^2J = 241.7$ Hz, 1F), -137.2 (app. quint, $^2J = 241.7$, $^4J_{\text{F-H}} = 1.9$ Hz, 1F) ppm;

$\bar{\nu}$ (neat) = 3621, 3259, 2921, 1708, 1323, 1067, 952 cm^{-1} ;

HRMS (APCI): calcd for $\text{C}_{13}\text{H}_{13}\text{F}_5\text{O}_2\text{N}_1$, 310.0861 $[\text{M}+\text{NH}_4]^+$, found: 310.0857;*

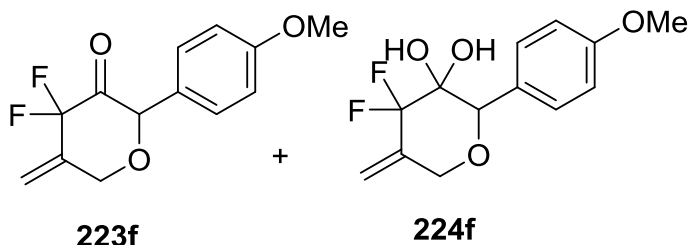
MS (EI): m/z (%): 292 (1) $[\text{M}]^+$, 145 (63) $[\text{C}_7\text{H}_4\text{F}_3]^+$, 90 (100) $[\text{M}-\text{C}_{10}\text{H}_8\text{F}_3\text{O}]^+$,**

t_{R} (GC) = 11.57 minutes.**

*accurate mass was calculated for the ketone component of the mixture

**the mixture appeared as one peak by GC-MS, masses corresponded to that of the ketone

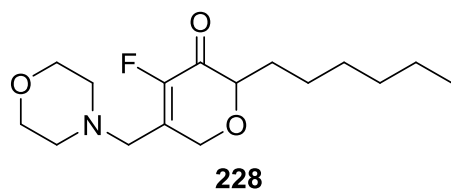
Attempted preparation of 4,4-difluoro-2-(4-methoxyphenyl)-5-methylenedihydro-2H-pyran-3(4H)-one (223f) and 3,3-dihydroxy-4,4-difluoro-2-(4-methoxyphenyl)-5-methylenedihydro-2H-pyran (224f)



1,3-*bis*(2,6-diisopropylphenyl-imidazol-2-ylidene)gold(I) chloride (5 mol %, 0.031 g) and silver hexafluoroantimonate(V) (5 mol %, 0.017 g) were suspended in 2-Methyltetrahydrofuran (5.0 mL). A solution of alkyne **222f** (0.342g, 1.00 mmol) in 2-Methyltetrahydrofuran was added in a stream *via* syringe. After stirring for 21 hours at room temperature the reaction mixture was concentrated under reduced pressure to afford the crude product as a viscous dark brown oil (0.319 g). Attempted purification of the crude material by flash column chromatography (40 g silica, 3 % acetone in dichloromethane) afforded the product as a yellow gummy solid which was impure by NMR analysis.

6.3.14 Synthesis of morpholine derivative 228

Preparation of 4-fluoro-2-hexyl-5-(morpholinomethyl)-2H-pyran-3(6H)-one (228)



Ketone **228** was prepared according to the procedure of Paquin and co-workers.²⁶⁶ A solution of hydrate **224a** and ketone **223a** (0.100 g, 0.4 mmol) and morpholine (0.104 mL, 1.20 mmol) in acetonitrile (1 mL) was added *via* syringe to a stirring solution of Pd(dppf)Cl₂.CH₂Cl₂ (5 mol %, 0.016 g) in acetonitrile. The resulting mixture was stirred at 70 °C for 19 hours. After this time the reaction mixture was allowed to cool to room temperature and quenched with water (10 mL). The mixture was extracted with ethyl acetate (3 x 15 mL) and the combined organics dried (MgSO₄) and concentrated under reduced pressure to afford the crude product as a dark orange oil (0.137 g). The crude material was purified by flash column chromatography (40 g silica, 35 % diethyl ether in

petroleum ether) to afford the product as a pale yellow oil (0.032 g). The material was further purified by flash column chromatography (8 g silica, 35 % diethyl ether in petroleum ether) to afford the product as an off-white solid (0.029 g, 24 %).

$R_f = 0.26$ (30 % diethyl ether in petroleum ether);

$^1\text{H NMR}$ (400 MHz, CDCl_3): $\delta = 4.59$ (app. ddq, $^2J = 16.9$, $^4J = 6.6$, 1.0, $^4J_{\text{H-F}} = 1.0$ Hz, 1H), 4.12 (app. ddd, $^2J = 16.9$, $^4J = 6.0$, $^4J_{\text{H-F}} = 0.7$ Hz, 1H), 3.68 (t, $J = 4.7$ Hz, 4H), 2.65 (app. dt, $^2J = 12.0$, $J = 4.7$ Hz, 2H), 2.54 (app. dt, $^2J = 12.0$, $J = 4.7$ Hz, 2H), 2.00-1.85 (m, 4H), 1.63-1.51 (m, 1H), 1.44-1.10 (m, 8H), 0.88 (t, $J = 7.2$ Hz, 3H) ppm;

$^{13}\text{C NMR}$ (100 MHz, CDCl_3): $\delta = 185.8$ (d, $^2J_{\text{C-F}} = 16.2$ Hz), 147.1 (d, $^2J_{\text{C-F}} = 259.9$ Hz), 134.1 (d, $^2J_{\text{C-F}} = 8.0$ Hz), 93.5 (d, $^3J_{\text{C-F}} = 3.9$ Hz), 66.7, 61.8 (d, $^3J_{\text{C-F}} = 3.5$ Hz), 45.6, 31.1, 29.1, 27.1, 22.8, 22.0, 13.5, 10.9 (d, $^3J_{\text{C-F}} = 4.2$ Hz) ppm;

$^{19}\text{F NMR}$ (376 MHz, CDCl_3): $\delta = -141.4$ (s) ppm (the ^{19}F - ^1H splitting was not resolved in the $^{19}\text{F NMR}$ spectrum);

$\bar{\nu}$ /(neat) = 2928, 1693, 1675, 1115, 903 cm^{-1} ;

HRMS (APCI): calcd for $\text{C}_{16}\text{H}_{27}\text{F}_1\text{N}_1\text{O}_3$, 300.1969 $[\text{M}+\text{H}]^+$, found: 300.1971;

MS (EI): m/z (%): 299 (29) $[\text{M}]^+$;

t_R (GC) = 14.59 minutes.

7. References

- (1) Ghazarian, H.; Idoni, B.; Oppenheimer, S. B. *Acta Histochem.* **2011**, *113*, 236–247.
- (2) Nelson, J. M.; Beegle, F. M. *J. Am. Chem. Soc.* **1919**, *41*, 559–575.
- (3) Berg, J. M.; Tymoczko, J. L.; Stryer, L. *Biochemistry*, 5th ed.; W. H. Freeman: New York, 2002.
- (4) Lairson, L. L.; Henrissat, B.; Davies, G. J.; Withers, S. G. *Ann. Rev. Biochem.* **2008**, *77*, 521–555.
- (5) Goldstein, I. J.; So, L. L.; Yang, Y.; Callies, Q. C. *J. Immunol.* **1969**, *108*, 695–698.
- (6) Magnani, J. L. *Discov. Med.* **2009**, *8*, 247–252.
- (7) Galan, M. C.; Benito-Alifonso, D.; Watt, G. M. *Org. Biomol. Chem.* **2011**, *9*, 3598–3610.
- (8) Ernst, B.; Magnani, J. L. *Nat. Rev.* **2009**, *8*, 661–677.
- (9) Kim, C. U.; Lew, W.; Williams, M. A.; Liu, H.; Zhang, L.; Swaminathan, S.; Bischofberger, N.; Chen, M. S.; Mendel, D. B.; Tai, C. Y.; Laver, W. G.; Stevens, R. C. *J. Am. Chem. Soc.* **1997**, *119*, 681–690.
- (10) He, G.; Massarella, J.; Ward, P. *Clin Pharmacokinet* **1999**, *37*, 471–484.
- (11) Vasella, A.; Davies, G. J.; Böhm, M. *Curr. Opin. Chem. Biol.* **2002**, *6*, 619–629.
- (12) Fraser-Reid, B. O.; Tatsuta, K.; Thiem, J.; Coté, G. L.; Flitsch, S.; Ito, Y.; Kondo, H.; Nishimura, S. I.; Yu, B. *Glycoscience*, 2nd ed.; Springer: New York, 2008.
- (13) Arjona, O.; Gómez, A. M.; López, J. C.; Plumet, J. *Chem. Rev.* **2007**, *107*, 1919–2036.
- (14) Sisu, E.; Sollogoub, M.; Mallet, J.; Sinay, P. *Tetrahedron* **2002**, *58*, 10189–10196.
- (15) Bleriot, Y.; Giroult, A.; Mallet, J.; Rodriguez, E.; Vogel, P.; Sinay, P. *Tetrahedron: Asymm.* **2002**, *13*, 2553–2565.
- (16) Miller, T. W.; Arison, B. H.; Albers-Schonberg, G. *Biotechnol. Bioeng.* **1973**, *15*, 1075–1080.
- (17) McCasland, G. E.; Furuta, S.; Durham, L. J. *J. Org. Chem.* **1968**, *33*, 2835–2841.
- (18) Lillelund, V. H.; Jensen, H. H.; Liang, X.; Bols, M. *Chem. Rev.* **2002**, *102*, 515–554.
- (19) Kérourédan, E.; Percy, J. M.; Rinaudo, G.; Singh, K. *Synthesis* **2008**, 3903–3918.
- (20) Dalvit, C.; Vulpetti, A. *ChemMedChem* **2012**, *7*, 262–272.
- (21) Xu, B.; Unione, L.; Sardinha, J.; Wu, S.; Ethève-Quellejeu, M.; Pilar Rauter, A.; Blériot, Y.; Zhang, Y.; Martín-Santamaría, S.; Díaz, D.; Jiménez-Barbero, J.; Sollogoub, M. *Angew. Chem. Int. Ed. Engl.* **2014**, *53*, 9597–9602.
- (22) Leclerc, E.; Pannecoucke, X.; Ethève-Quellejeu, M.; Sollogoub, M. *Chem.*

Soc. Rev. **2013**, *42*, 4270–4283.

- (23) O'Hagan, D.; Harper, D. B. *J. Fluorine. Chem* **1999**, *100*, 127–133.
- (24) O'Hagan, D. *J. Fluorine. Chem* **2010**, *131*, 1071–1081.
- (25) Top 20 Best-Selling Drugs of 2012 <http://www.genengnews.com/insight-and-intelligence/top-20-best-selling-drugs-of-2012/77899775/?page=1>. (Date accessed March 2018)
- (26) Müller, K.; Faeh, C.; Diederich, F. *Science* **2007**, *317*, 1881–1886.
- (27) Rowley, M.; Hallett, D. J.; Goodacre, S.; Moyes, C.; Crawforth, J.; Sparey, T. J.; Patel, S.; Marwood, R.; Thomas, S.; Hitzel, L.; O'Connor, D.; Szeto, N.; Castro, J. L.; Hutson, P. H.; MacLeod, A. M. *J. Med. Chem.* **2001**, *44*, 1603–1614.
- (28) Clader, J. W. *J. Med. Chem.* **2004**, *47*, 1–9.
- (29) O'Hagan, D. *Chem. Soc. Rev.* **2008**, *37*, 308–319.
- (30) Maren, T. H.; Conroy, W. *J. Biol. Chem* **1993**, *268*, 26233–26239.
- (31) Cox, C. D.; Coleman, P. J.; Breslin, M. J.; Whitman, D. B.; Garbaccio, R. M.; Fraley, M. E.; Buser, C. A.; Walsh, E. S.; Hamilton, K.; Schaber, M. D.; Lobell, R. B.; Tao, W.; Davide, J. P.; Diehl, R. E.; Abrams, M. T.; South, V. J.; Huber, H. E.; Torrent, M.; Prueksaritanont, T.; Li, C.; Slaughter, D. E.; Mahan, E.; Fernandez-Metzler, C.; Yan, Y.; Kuo, L. C.; Kohl, N. E.; Hartman, G. D. *J. Med. Chem.* **2008**, *51*, 4239–4252.
- (32) Goncharov, N. V.; Jenkins, R. O.; Radilov, A. S. *J. Appl. Toxicol.* **2006**, *26*, 148–161.
- (33) Böhm, H.-J.; Banner, D.; Bendels, S.; Kansy, M.; Kuhn, B.; Müller, K.; Obst-Sander, U.; Stahl, M. *Chembiochem* **2004**, *5*, 637–643.
- (34) Dunitz, J. D.; Taylor, R. *Chem. Eur. J.* **1997**, *3*, 89–98.
- (35) Paulini, R.; Müller, K.; Diederich, F. *Angew. Chem. Int. Ed. Engl.* **2005**, *44*, 1788–1805.
- (36) Olsen, J. A.; Banner, D. W.; Seiler, P.; Wagner, B.; Tschopp, T.; Obst-Sander, U.; Kansy, M.; Müller, K.; Diederich, F. *Chembiochem* **2004**, *5*, 666–675.
- (37) Obst, U.; Gramlich, V.; Diederich, F.; Weber, L.; Banner, D. W. *Angew. Chem. Int. Ed.* **1995**, *34*, 1739–1742.
- (38) Olsen, J. A.; Banner, D. W.; Seiler, P.; Obst Sander, U.; D'Arcy, A.; Stihle, M.; Müller, K.; Diederich, F. *Angew. Chem. Int. Ed. Engl.* **2003**, *42*, 2507–2511.
- (39) Goldstein, D. M.; Soth, M.; Gabriel, T.; Dewdney, N.; Kuglstatter, A.; Arzeno, H.; Bingenheimer, W.; Dalrymple, S. A.; Dunn, J.; Farrell, R.; Frauchiger, S.; Fargue, J. La; Ghate, M.; Graves, B.; Hill, R. J.; Li, F.; Litman, R.; Loe, B.; Mcintosh, J.; Mcweeney, D.; Papp, E.; Park, J.; Reese, H. F.; Roberts, R. T.; Rotstein, D.; Pablo, B. S.; Sarma, K.; Stahl, M.; Sung, M.; Suttman, R. T.; Sjogren, E. B.; Tan, Y.; Trejo, A.; Welch, M.; Weller, P.; Wong, B. R.; Zecic, H. *J. Med. Chem.* **2011**, *54*, 2255–2265.
- (40) Fischer, F. R.; Schweizer, W. B.; Diederich, F. *Angew. Chemie Int. Ed.* **2007**, *46*, 8270–8273.

- (41) Thalladi, V. R.; Weiss, H.; Blaser, D.; Boese, R.; Nangia, A.; Desiraju, G. R. *J. Am. Chem. Soc.* **1998**, *120*, 8702–8710.
- (42) Parsch, J.; Engels, J. W. *J. Am. Chem. Soc.* **2002**, *124*, 5664–5672.
- (43) Thomas, P.; Bessell, E. M.; Westwood, J. H. *Biochem. J.* **1974**, *139*, 661–664.
- (44) Ioannou, A.; Cini, E.; Timofte, R. S.; Flitsch, S. L.; Turner, N. J.; Linclau, B. *Chem. Commun.* **2011**, *47*, 11228–11230.
- (45) Gelb, M. H.; Svaren, J. P.; Abeles, R. H. *Biochemistry* **1985**, *24*, 1813–1817.
- (46) Silva, A. M.; Cachau, R. E.; Sham, H. L.; Erickson, J. W. *J. Mol. Biol.* **1996**, *255*, 321–346.
- (47) Klocker, J.; Karpfen, A.; Wolschann, P. *Chem. Phys. Lett.* **2003**, *367*, 566–575.
- (48) Massa, M. A.; Spangler, D. P.; Durley, R. C.; Hickory, B. S.; Connolly, D. T.; Witherbee, B. J.; Smith, M. E.; Sikorski, J. A. *Bioorg. Med. Chem. Lett.* **2001**, *11*, 1625–1628.
- (49) Lombardo, F.; Lipinski, A.; Dominy, B. W.; Feeney, P. J. *Adv. Drug Deliv. Rev.* **1997**, *23*, 3–25.
- (50) Bégué, J. P.; Bonnet-Delpon, D. *Bioorganic and Medicinal Chemistry of Fluorine*, 1st ed.; John Wiley & Sons Inc.: Hoboken, 2008; Vol. 2.
- (51) Jacobs, R. T.; Bernstein, P. R.; Laura, A.; Buckner, C. K.; Kusnerg, E. J.; Newcomb, L. F.; Aharony, D. *J. Med. Chem.* **1994**, *37*, 1282–1297.
- (52) Tkachenko, A. N.; Mykhailiuk, P. K.; Afonin, S.; Radchenko, D. S.; Kubyshekin, V. S.; Ulrich, A. S.; Komarov, I. V. *Angew. Chem. Int. Ed. Engl.* **2013**, *52*, 1486–1489.
- (53) Thibaudeau, C.; Plavec, J.; Chattopadhyaya, J. *J. Org. Chem.* **1998**, *63*, 4967–4984.
- (54) Plavec, J.; Thibaudeau, C.; Chattopadhyaya, J. *J. Am. Chem. Soc.* **1994**, *116*, 6558–6560.
- (55) Singh, R. P.; Shreeve, J. M. *Synthesis* **2002**, 1585–1595.
- (56) Sawyer, D. A.; Potter, B. V. L. *J. Chem. Soc. Perkin. Trans 1* **1992**, 923–932.
- (57) Lichtenthaler, F. W.; Dinges, J.; Fukuda, Y. *Angew. Chem. Int. Ed.* **1991**, *30*, 1339–1343.
- (58) Gaich, T.; Baran, P. S. *J. Org. Chem.* **2010**, *75*, 4657–4673.
- (59) Gigg, J.; Gigg, R.; Payne, S.; Conant, R. *J. Chem. Soc. Perkin. Trans 1* **1987**, 1757–1762.
- (60) Ye, C.; Shreeve, J. M. *J. Fluorine. Chem.* **2004**, *125*, 1869–1872.
- (61) Shellhamer, D. F.; Briggs, A. A.; Miller, B. M.; Prince, J. M.; Scott, D. H.; Heasley, V. L. *J. Chem. Soc. Perkin. Trans 2* **1996**, 973–977.
- (62) Material safety data sheet
<https://www.sigmaaldrich.com/MSDS/MSDS/DisplayMSDSPage.do?country=GB&language=en&productNumber=494119&brand=ALDRICH&PageToGoToURL=https%3A%2F%2Fwww.sigmaaldrich.com%2Fcatalog%2Fproduct%2Faldrich%2F494119%3Flang%3Den> (accessed Mar, 2018).

- (63) Liang, T.; Neumann, C. N.; Ritter, T. *Angew. Chemie Int. Ed.* **2013**, *52*, 8214–8264.
- (64) Biggadike, K.; Borthwick, A. D.; Evans, D.; Exall, A. M.; Kirk, B. E.; Stanley, M.; Stephenson, L.; Youds, P. *J. Chem. Soc. Perkin. Trans 1* **1988**, 549–554.
- (65) L'heureux, A.; Beaulieu, F.; Bennett, C.; Bill, D. R.; Clayton, S.; Laflamme, F.; Mirmehrabi, M.; Tadayan, S.; Tovell, D.; Couturier, M. *J. Org. Chem.* **2010**, *75*, 3401–3411.
- (66) Tsegay, S.; Williams, R. J.; Williams, S. J. *Carbohydr. Res.* **2012**, *357*, 16–22.
- (67) Jiang, S.; Singh, G.; Batsanov, A. S. *Tetrahedron: Asymm.* **2000**, *11*, 3873–3877.
- (68) Seyferth, D.; Simon, R. M.; Sepelak, D. J.; Klein, H. A. *J. Am. Chem. Soc.* **1983**, *105*, 4634–4639.
- (69) Deleuze, A.; Menozzi, C.; Sollogoub, M.; Sinay, P. *Angew. Chem.* **2004**, *116*, 6848–6851.
- (70) Houlton, J. S.; Motherwell, W. B.; Ross, B. C.; Tozer, M. J.; Williams, D. J.; Slawin, A. M. Z. *Tetrahedron* **1993**, *49*, 8087–8106.
- (71) Ferrier, R. J. *J. Chem. Soc. Perkin. Trans 1* **1979**, 1455–1458.
- (72) Teobald, B. J. *Tetrahedron* **2002**, *58*, 4133–4170.
- (73) Anh, N. T.; Eisenstein, O. *Nouv. J. Chim.* **1977**, *1*, 61–70.
- (74) Sardinha, J.; Guieu, S.; Deleuze, A.; Fernández-Alonso, M. C.; Rauter, A. P.; Sinay, P.; Marrot, J.; Jiménez-Barbero, J.; Sollogoub, M. *Carbohydr. Res.* **2007**, *342*, 1689–1703.
- (75) Fritz, S. P.; West, T. H.; McGarrigle, E. M.; Aggarwal, V. K. *Org. Lett.* **2012**, *14*, 6370–6373.
- (76) Brundle, C. R.; Robin, M. B.; Kuebler, N. A.; Baschlb, H. *J. Am. Chem. Soc.* **1972**, *94*, 1451–1465.
- (77) Leroy, J.; Molines, H.; Wakselman, C. *J. Org. Chem.* **1987**, *52*, 290–292.
- (78) Arany, A.; Crowley, P. J.; Fawcett, J.; Hursthouse, M. B.; Kariuki, B. M.; Light, M. E.; Moralee, A. C.; Percy, J. M.; Salafia, V. *Org. Biomol. Chem.* **2004**, *2*, 455–465.
- (79) Crowley, P. J.; Fawcett, J.; Griffith, G. A.; Moralee, A. C.; Percy, J. M.; Salafia, V. *Org. Biomol. Chem.* **2005**, *3*, 3297–3310.
- (80) Audouard, C.; Fawcett, J.; Griffith, G. A.; Ke, E.; Miah, A.; Percy, J. M.; Yang, H. *Org. Lett.* **2004**, *6*, 4269–4272.
- (81) VanRheenen, V.; Kelly, R. C.; Cha, D. Y. *Tetrahedron Lett.* **1976**, *17*, 1973–1976.
- (82) Donohoe, T. J.; Blades, K.; Moore, P. R.; Waring, M. J.; Winter, J. J. G.; Helliwell, M.; Newcombe, N. J.; Stemp, G. *J. Org. Chem.* **2002**, *67*, 7946–7956.
- (83) Kolb, K.; Vannieuwenhze, M. S.; Sharpless, K. B. *Chem. Rev.* **1994**, *94*, 2483–2547.
- (84) Anderl, T.; Audouard, C.; Miah, A.; Percy, J. M.; Rinaudo, G.; Singh, K. *Org.*

- Biomol. Chem.* **2009**, *7*, 5200–5206.
- (85) Larrow, J. F.; Jacobsen, E. N. *Top. Organomet. Chem.* **2004**, *6*, 123–152.
- (86) Sewell, A. MChem Thesis “A Palladium Catalysed Route To Difluorinated Cycloalkenones,” University Of Strathclyde, Glasgow, 2010.
- (87) Ito, Y.; Aoyama, H.; Hirao, T.; Mochizuki, A.; Saegusa, T. *J. Am. Chem. Soc.* **1979**, *101*, 494–496.
- (88) Dénès, F.; Perez-Luna, A.; Chemla, F. *Chem. Rev.* **2010**, *110*, 2366–2447.
- (89) Toyota, M.; Wada, T.; Fukumoto, K.; Ihara, M. *J. Am. Chem. Soc.* **1998**, *120*, 4916–4925.
- (90) Toyota, M.; Ihara, M. *Synlett* **2002**, *8*, 1211–1222.
- (91) Toyota, M. *Procedia Chem.* **2014**, *13*, 3–12.
- (92) Ito, Y.; Hirao, T.; Saegusa, T. *J. Org. Chem.* **1978**, *43*, 1011–1013.
- (93) Kende, A. S.; Roth, B.; Sanfilippo, P. J.; Blacklock, T. J. *J. Am. Chem. Soc.* **1982**, *104*, 5808–5810.
- (94) Larock, R. C.; Lee, N. H. *Tetrahedron Lett.* **1991**, *32*, 5911–5914.
- (95) Larock, R. C.; Hightower, T. R. *Tetrahedron Lett.* **1995**, *36*, 2423–2426.
- (96) Steinhoff, B. A.; Stahl, S. S. *J. Am. Chem. Soc.* **2006**, *128*, 4348–4355.
- (97) Smidt, J.; Hafner, W.; Jira, R.; Sedlmeier, J.; Sieber, R.; Rutinger, R.; Kojer, H. *Angew. Chem.* **1959**, *71*, 176–182.
- (98) Smidt, J.; Hafner, W.; Jira, R.; Sieber, R.; Sedlmeier, J.; Sabel, A. *Angew. Chem. Int. Ed.* **1962**, *1*, 80–88.
- (99) Caspi, D. D.; Ebner, D. C.; Bagdanoff, J. T.; Stoltz, B. M. *Adv. Synth. Catal.* **2004**, *346*, 185–189.
- (100) Krishnan, S.; Bagdanoff, J. T.; Ebner, D. C.; Ramtohl, Y. K.; Tambar, U. K.; Stoltz, B. M. *J. Am. Chem. Soc.* **2008**, *130*, 13745–13754.
- (101) Sehnal, P.; Taylor, R. J. K.; Fairlamb, I. J. S. *Chem. Soc. Rev.* **2010**, *44*, 824–889.
- (102) Negishi, E. *Handbook of Organopalladium Chemistry For Organic Synthesis*, 1st edition.; John Wiley & Sons Inc.: New York, 2002. p4-6
- (103) Taqui Khan, M. M.; Martell, A. E. *Homogeneous Catalysis By Metal Complexes*, 2nd edition; Academic Press Inc: New York and London, 1974. p77
- (104) Kantchev, E. A. B.; O’Brien, C. J.; Organ, M. G. *Angew. Chem. Int. Ed. Engl.* **2007**, *46*, 2768–2813.
- (105) Karroumi, J. El; Haib, A. El; Manoury, E.; Benharref, A.; Daran, J. C.; Gouygou, M.; Urrutigoity, M. *J. Mol. Catal. A Chem.* **2015**, *401*, 18–26.
- (106) Stahl, S. S.; Popp, B. V. *Palladium-Catalyzed Oxidation Reactions: Comparison of Benzoquinone and Molecular Oxygen as Stoichiometric Oxidants*, 1st edition; Springer: Berlin, 2006. p86
- (107) Shi, W.; Liu, C.; Lei, A. *Chem. Soc. Rev.* **2011**, *40*, 2761–2776.
- (108) Yeung, C. S.; Dong, V. M. *Chem. Rev.* **2011**, *111*, 1215–1292.

- (109) Keith, J. A.; Nielsen, R. J.; Oxgaard, J.; Goddard, W. A. *J. Am. Chem. Soc.* **2007**, *129*, 12342–12343.
- (110) Campbell, A. N.; Stahl, S. S. *Acc. Chem. Res.* **2012**, *45*, 851–863.
- (111) Peterson, K. P.; Larock, R. C. *J. Org. Chem.* **1998**, *63*, 3185–3189.
- (112) Larock, R. C.; Hightower, T. R. *J. Org. Chem.* **1993**, *58*, 5298–5300.
- (113) Larock, R. C.; Hightower, T. R.; Hasvold, L. A.; Peterson, K. P. *J. Org. Chem.* **1996**, *61*, 3584–3585.
- (114) Diao, T.; White, P.; Guzei, I.; Stahl, S. S. *Inorg. Chem.* **2012**, *51*, 11898–11909.
- (115) Kotov, V.; Scarborough, C. C.; Stahl, S. S. *Inorg. Chem.* **2007**, *46*, 1910–1923.
- (116) Popp, B. V.; Stahl, S. S. *Chem. Eur. J.* **2009**, *15*, 2915–2922.
- (117) Stahl, S. S. *Angew. Chem. Int. Ed. Engl.* **2004**, *43*, 3400–3420.
- (118) Piera, J.; Bäckvall, J.-E. *Angew. Chem. Int. Ed. Engl.* **2008**, *47*, 3506–3523.
- (119) Grate, J. H.; Hamm, D. R.; Mahajan, S. *Catalysis Of Organic Reactions*, 1st edition; CRC Press: New York, 1993. p90
- (120) Cotton, F. A.; Wilkinson, G. *Advanced Inorganic Chemistry*, 4th edition; Wiley: New York, 1980. p132
- (121) Decharin, N.; Stahl, S. S. *J. Am. Chem. Soc.* **2011**, *2*, 5732–5735.
- (122) Michel, B. W.; Steffens, L. D.; Sigman, M. S. *J. Am. Chem. Soc.* **2011**, *133*, 8317–8325.
- (123) Muñiz, K. *Angew. Chem. Int. Ed. Engl.* **2009**, *48*, 9412–9423.
- (124) Piera, J.; Närhi, K.; Bäckvall, J.-E. *Angew. Chem.* **2006**, *118*, 7068–7071.
- (125) Lucas, M. F.; Rousseau, D. L.; Guallar, V. *Biochim. Biophys. Acta* **2011**, *1807*, 1305–1313.
- (126) Backvall, J.; Hopkins, R. B.; Grennberg, H.; Mader, M. M.; Awasthi, A. K. *J. Am. Chem. Soc.* **1990**, *112*, 5160–5166.
- (127) Deng, Y.; Persson, A. K. Å.; Bäckvall, J.-E. *Chem. Eur. J.* **2012**, *18*, 11498–11523.
- (128) Persson, A. PhD Thesis “Palladium(II)-Catalyzed Oxidative Cyclisation Strategies-Selective Formation of New C-C and C-N bonds,” Stockholm University, 2012.
- (129) Itoh, T.; Imini, T.; Ogura, H.; Kawahara, N.; Nakajima, T.; Watanabe, K. A. *Chem. Pharm. Bull.* **1985**, *33*, 1375–1379.
- (130) Bee, C.; Leclerc, E.; Tius, M. A. *Org. Lett.* **2003**, *5*, 4927–4930.
- (131) Pei, T.; Wang, X.; Widenhoefer, R. A. *J. Am. Chem. Soc.* **2003**, *125*, 648–649.
- (132) Liu, C.; Wang, X.; Pei, T.; Widenhoefer, R. A. *Chem. Eur. J.* **2004**, *10*, 6343–6352.
- (133) Burdett, J. L.; Rogers, M. T. *J. Am. Chem. Soc.* **1964**, *86*, 2105–2109.
- (134) Yip, K.-T.; Li, J.-H.; Lee, O.-Y.; Yang, D. *Org. Lett.* **2005**, *7*, 5717–5719.
- (135) Cai, Z.; Harmata, M. *Org. Lett.* **2010**, *12*, 5668–5670.

- (136) Sohn, J.; Waizumi, N.; Zhong, H. M.; Rawal, V. H. *J. Am. Chem. Soc.* **2005**, *127*, 7290–7291.
- (137) Kimbrough, R. D. *Environ. Heal. Perspect* **1976**, *14*, 51–56.
- (138) Altman, R. A.; Buchwald, S. L. *Nat. protoc.* **2007**, *2*, 3115–3121.
- (139) Patel, S. P.; Percy, J. M.; Wilkes, R. D. *Tetrahedron* **1995**, *51*, 9201–9216.
- (140) Balnaves, A. S.; Gelbrich, T.; Hursthouse, M. B.; Light, M. E.; Palmer, M. J.; Percy, J. M. *J. Chem. Soc. Perkin. Trans 1* **1999**, 2525–2535.
- (141) Kresge, J. *Acc. Chem. Res.* **1990**, *23* (2), 43–48.
- (142) Rucker, C. *Chem. Rev.* **1995**, *95*, 1009–1064.
- (143) Howarth, J.; Owton, W. M.; Percy, J. M.; Rock, M. H. *Tetrahedron* **1995**, *51*, 10289–10302.
- (144) Ripin, D. H.; Evans, D. A. http://evans.rc.fas.harvard.edu/pdf/evans_pKa_table.pdf (accessed Oct 30, 2015).
- (145) Gerig, J. T. Fluorine NMR www.biophysics.org/Portals/1/PDFs/Education/gerig.pdf (accessed Jan 1, 2015).
- (146) Feeney, J.; Sutcliffe, L. H.; Walker, S. M. *Trans. Faraday. Soc* **1966**, *62*, 2969–2979.
- (147) Fäh, C.; Hardegger, L. A.; Baitsch, L.; Schweizer, W. B.; Meyer, S.; Bur, D.; Diederich, F. *Org. Biomol. Chem.* **2009**, *7*, 3947–3957.
- (148) Guthrie, J. P. *J. Am. Chem. Soc.* **2000**, *122*, 5529–5538.
- (149) Schirlin, D.; Baltzer, S.; Altenburger, J. M.; Tarnus, C.; Remy, J. M. *Tetrahedron* **1996**, *52*, 305–318.
- (150) Han, C.; Salyer, A. E.; Kim, E. H.; Jiang, X.; Jarrard, R. E.; Powers, M. S.; Kirchho, A. M.; Salvador, T. K.; Chester, J. A.; Hockerman, G. H.; Colby, D. A. *J. Med. Chem.* **2013**, *56*, 2456–2465.
- (151) Guideline on the specification limits for residues of metal catalysts http://www.ema.europa.eu/docs/en_GB/document_library/Scientific_guideline/2009/09/WC500003587.pdf (accessed Jan 1, 2015).
- (152) Mondal, B.; Wilkes, R. D.; Percy, J. M.; Tuttle, T.; Black, R. J. G.; North, C. *Dalton Trans.* **2014**, *43*, 469–478.
- (153) Galaffu, N.; Man, S. P.; Wilkes, R. D.; Wilson, J. R. H. *Org. Process Rev. Dev.* **2007**, *11*, 406–413.
- (154) Beesley, R. M.; Ingold, C. K.; Thorpe, J. F. *J. Chem. Soc* **1915**, *107*, 1080–1106.
- (155) Nilsson, H.; Smith, L. Z. *Phys. Chem* **1933**, *166A*, 136–146.
- (156) Jung, M. E.; Piizzi, G. *Chem. Rev.* **2005**, *105*, 1735–1766.
- (157) Kirby, A. J.; Lloyd, G. J. *J. Chem. Soc. Perkin. Trans 2* **1976**, 1753–1761.
- (158) Ogura, T.; Kamimura, R.; Shiga, A.; Hosokawa, T. *Bull. Chem. Soc. Jpn.* **2005**, *78*, 1555–1557.
- (159) Ho, T.-L.; Chang, M. H.; Chen, C. *Tetrahedron Lett.* **2003**, *44*, 6955–6957.

- (160) Keith, J. A.; Henry, P. M. *Angew. Chem. Int. Ed. Engl.* **2009**, *48*, 9038–9049.
- (161) Grigor'eva, N. G.; Galyautdinova, R. R.; Vosmerikov, a. V.; Korobitsina, L. L.; Kutepov, B. I.; Dzhemilev, U. M. *Neftekhimiya* **2008**, *48*, 366–370.
- (162) Kudryashov, S. V.; Ryabov, A. Y.; Sirotkina, E. E.; Shchegoleva, G. S. *Russ. J. Appl. Chem.* **2004**, *77*, 1922–1924.
- (163) Havel, J. J. *J. Org. Chem.* **1978**, *43*, 762–763.
- (164) Clennan, E. L.; Pan, G. *Org. Lett.* **2003**, *5*, 4979–4982.
- (165) Chen, J.; Che, C.-M. *Angew. Chem. Int. Ed. Engl.* **2004**, *43*, 4950–4954.
- (166) Jiang, G.; Chen, J.; Thu, H.-Y.; Huang, J.-S.; Zhu, N.; Che, C.-M. *Angew. Chem. Int. Ed. Engl.* **2008**, *47*, 6638–6642.
- (167) Fu, Y.; Li, Z.; Liang, S.; Guo, Q.; Liu, L. *Organometallics* **2008**, *27*, 3736–3742.
- (168) Zhu, L.; Bozzelli, J. W.; Kardos, L. M. *J. Phys. Chem. A* **2007**, *111*, 6361–6377.
- (169) Zhu, B.-Z.; Zhao, H.-T.; Kalyanaraman, B.; Liu, J.; Shan, G.-Q.; Du, Y.-G.; Frei, B. *Proc. Natl. Acad. Sci.* **2007**, *104*, 3698–3702.
- (170) Liu, Q.; Dong, X.; Li, J.; Xiao, J.; Dong, Y.; Liu, H. *ACS Catal.* **2015**, *5*, 6111–6137.
- (171) Zhu, B.; Shan, G. *Chem. Res. Toxicol.* **2009**, *22*, 3698–3702.
- (172) Hamilton, D. S.; Nicewicz, D. A. *J. Am. Chem. Soc.* **2012**, *134*, 18577–18580.
- (173) Larock, R. C.; Hightower, T. R. *Tetrahedron Lett.* **1995**, *36*, 2423–2426.
- (174) Lewis, E. A.; Tolman, W. B. *Chem. Rev.* **2004**, *104*, 1047–1076.
- (175) Wickens, Z. K.; Morandi, B.; Grubbs, R. H. *Angew. Chem. Int. Ed. Engl.* **2013**, *52*, 11257–11260.
- (176) Wickens, Z. K.; Skakuj, K.; Morandi, B.; Grubbs, R. H. *J. Am. Chem. Soc.* **2014**, *136*, 890–893.
- (177) Jiang, Y.-Y.; Zhang, Q.; Yu, H.-Z.; Fu, Y. *ACS Catal.* **2015**, *5*, 1414–1423.
- (178) Ito, Y.; Nakatsuka, M.; Saegusa, T. *J. Org. Chem.* **1980**, *45*, 2022–2024.
- (179) Berenblit, B. B. *Russ. J. Org. Chem.* **1974**, *10*, 2507.
- (180) Meanwell, N. A. *J. Med. Chem.* **2011**, *54*, 2529–2591.
- (181) Vandyck, K.; Cummings, M. D.; Nyanguile, O.; Boutton, C. W.; Vendeville, S.; McGowan, D.; Devogelaere, B.; Amssoms, K.; Last, S.; Rombauts, K.; Tahri, A.; Lory, P.; Hu, L.; Beauchamp, D. A.; Simmen, K.; Raboisson, P. *J. Med. Chem.* **2009**, *52*, 4099–4102.
- (182) Overman, L. E. *Angew. Chem. Int. Ed.* **1984**, *23*, 579–586.
- (183) Kirsch, P. *Modern Fluoroorganic Chemistry: Synthesis, Reactivity, Applications*, 1st edition; Wiley: New York, 2004. p54
- (184) Hosokawa, T.; Uno, T.; Inui, S.; Murahashi, S. *J. Am. Chem. Soc.* **1981**, *103*, 2318–2323.
- (185) Hosokawa, T.; Nakahira, T.; Takano, M.; Murahashi, S. *J. Mol. Catal.* **1996**, *74*, 489–498.

- (186) Hosokawa, T.; Murahashi, S. *Acc. Chem. Res* **1990**, *23*, 49–54.
- (187) Hosokawa, T.; Takano, M.; Murahashi, S. *J. Am. Chem. Soc.* **1996**, *118*, 3990–3991.
- (188) Hosokawa, T.; Nomura, T.; Murahashi, S.-I. *J. Organomet. Chem.* **1998**, *551*, 387–389.
- (189) Hosokawa, T.; Aoki, S.; Takano, M.; Nakahira, T.; Yoshida, Y.; Murahashi, S. *J. Chem. Soc., Chem. Commun.* **1991**, 1559–1560.
- (190) Hoover, J. M.; Stahl, S. S. *J. Am. Chem. Soc.* **2011**, *133*, 16901–16910.
- (191) Hoover, J. M.; Ryland, B. L.; Stahl, S. S. *J. Am. Chem. Soc.* **2013**, *135*, 2357–2367.
- (192) Speziali, M. G.; Robles-Dutenhefner, A.; Gusevskaya, E. V. *Organometallics* **2007**, *26*, 4003–4009.
- (193) Speziali, M. G.; Costa, V.; Robles-Dutenhefner, A.; Gusevskaya, E. V. *Organometallics* **2009**, *28*, 3186–3192.
- (194) Percy, J. M.; McCarter, A. W.; Sewell, A. L.; Sloan, N.; Kennedy, A. R. *Chem. Eur. J.* **2015**, *21*, 19119–19127.
- (195) Butcher, R. J.; Overman, J. W.; Sinn, E. *J. Am. Chem. Soc.* **1980**, *102*, 3276–3278.
- (196) Patel, S. T.; Percy, J. M.; Wilkes, R. D. *Tetrahedron* **1995**, *51*, 11327–11336.
- (197) Patel, S. T.; Percy, J. M.; Wilkes, R. D. *J. Org. Chem.* **1996**, *61*, 166–173.
- (198) Griffith, G. A.; Percy, J. M.; Pintat, S.; Smith, C. A.; Spencer, N.; Uneyama, E. *Org. Biomol. Chem.* **2005**, *3*, 2701–2712.
- (199) Broadhurst, M. J.; Brown, S. J.; Percy, J. M.; Prime, M. E. *J. Chem. Soc. Perkin Trans. 1* **2000**, 3217–3226.
- (200) Griffith, G. A.; Hillier, I. H.; Percy, J. M.; Roig, R.; Vincent, M. A. *J. Org. Chem.* **2006**, *71*, 8250–8255.
- (201) Nevado, C.; Cárdenas, D. J.; Echavarren, A. M. *Chem. Eur. J.* **2003**, *9*, 2627–2635.
- (202) Backvall, J.; Vaagberg, J. O. *J. Org. Chem.* **1988**, *53*, 5695–5699.
- (203) Backvall, J.; Hopkins, R. B. *Tetrahedron Lett.* **1988**, *29*, 2885–2888.
- (204) Wang, Y.; Gao, Y.; Mao, S.; Zhang, Y.; Guo, D.; Yan, Z.; Guo, S.; Wang, Y. *Org. Lett.* **2014**, *16*, 1610–1613.
- (205) Schmidbaur, H. *Gold Bull* **2000**, *33*, 3–10.
- (206) Soriano, E.; Marco-Contelles, J. *Computational Mechanisms Of Au and Pt Catalyzed Reactions*; Springer: Berlin, 2011.
- (207) Chatt, J.; Duncanson, L. A. *J. Chem. Soc.* **1953**, 2939–2947.
- (208) Dewar, M. J. S. *Bull. Soc. Chim. Fr* **1951**, *18*, C71.
- (209) Frenking, G.; Frohlich, N. *Chem. Rev.* **2000**, *100*, 717–774.
- (210) Shapiro, N. D.; Toste, F. D. *Proc. Natl. Acad. Sci.* **2008**, *105*, 395–403.
- (211) Gorin, D. J.; Toste, F. D. *Nature* **2007**, *446*, 395–403.
- (212) Livendahl, M.; Goehry, C.; Maseras, F.; Echavarren, A. M. *Chem. Commun.*

2014, 50, 1533–1536.

- (213) Nakanishi, W.; Yamanaka, M.; Nakamura, E. *J. Am. Chem. Soc.* **2005**, *127*, 1446–1453.
- (214) Klatt, G.; Xu, R.; Pernpointner, M.; Molinari, L.; Quang Hung, T.; Rominger, F.; Hashmi, a S. K.; Köppel, H. *Chem. Eur. J.* **2013**, *19*, 3954–3961.
- (215) Malhotra, D.; Hammond, G. B.; Xu, B. *Homogeneous Gold Catalysis*; Springer, 2014.
- (216) Dorel, R.; Echavarren, A. M. *Chem. Rev.* **2015**, *115*, 9028–9072.
- (217) Krause, N.; Winter, C. *Chem. Rev.* **2011**, *111*, 1994–2009.
- (218) Chiarucci, M.; Bandini, M. *Beilstein J. Org. Chem.* **2013**, *9*, 2586–2614.
- (219) Soriano, E.; Marco-Contelles, J. *Computational Mechanisms Of Au and Pt Catalyzed Reactions*; Springer: Berlin, 2011.
- (220) Lalonde, R. L.; Brenzovich, W. E.; Benitez, D.; Tkatchouk, E.; Kelley, K.; Goddard, W. A.; Toste, F. D. *Chem. Sci.* **2010**, *1*, 226–233.
- (221) Roth, K. E.; Blum, S. A. *Organometallics* **2010**, *29*, 1712–1716.
- (222) Zhou, C.; Che, C. *J. Am. Chem. Soc.* **2007**, *129*, 5828–5829.
- (223) Xiao, Y.-P.; Liu, X.-Y.; Che, C.-M. *Angew. Chem. Int. Ed. Engl.* **2011**, *50*, 4937–4941.
- (224) Xiao, Y.-P.; Liu, X.-Y.; Che, C.-M. *Beilstein J. Org. Chem.* **2011**, *7*, 1100–1107.
- (225) Miller, D. G.; Wayner, D. D. M. *J. Org. Chem.* **1990**, *55*, 2924–2927.
- (226) Burfeindt, J.; Patz, M.; Mu, M.; Mayr, H. *J. Am. Chem. Soc.* **1998**, *7863*, 3629–3634.
- (227) Mayr, H.; Kempf, B.; Ofial, A. R. *Acc. Chem. Res.* **2003**, *36*, 66–77.
- (228) Mmutlane, E. M.; Michael, J. P.; Green, I. R.; De Koning, C. B. *Org. Biomol. Chem.* **2004**, *2*, 2461–2470.
- (229) Coverdale, A. K.; Kohnstam, G. *J. Chem. Soc.* **1960**, 3806–3811.
- (230) Chambers, R. D. *Fluorine In Organic Chemistry*; Blackwell publishing: Oxford, 1973.
- (231) Wang, W.; Hammond, G. B.; Xu, B. *J. Am. Chem. Soc.* **2012**, *134*, 5697–5705.
- (232) Staben, S. T.; Kennedy-Smith, J. J.; Huang, D.; Corkey, B. K.; Lalonde, R. L.; Toste, F. D. *Angew. Chem. Int. Ed. Engl.* **2006**, *45*, 5991–5994.
- (233) Abraham, R. J.; Edgar, M.; Griffiths, L.; Powell, R. L. *J. Chem. Soc. Perkin. Trans 2* **1995**, 561–567.
- (234) Spartan '10, Wavefunction, Irvine, CA, **2010**.
- (235) Shao, Y.; Molnar, F.; Jung, Y.; Brown, S. T.; Gilbert, A. T. B.; Slipchenko, L. V.; Levchenko, S. V; Neill, D. P. O.; Jr, A. D.; Rohini, C.; Wang, T.; Beran, G. J. O.; Besley, N. A.; John, M.; Lin, Y.; Voorhis, T. Van; Chien, H.; Sodt, A.; Steele, P.; Rassolov, V. A.; Maslen, P. E.; Korambath, P. P.; Adamson, D.; Austin, B.; Baker, J.; Byrd, E. F. C.; Dachsel, H.; Doerksen, R. J.; Dreuw, A.; Dunietz, B. D.; Dutoi, A. D.; Furlani, T. R.; Gwaltney, S. R.; Heyden, A.;

- Hirata, S.; Hsu, P.; Kedziora, G.; Khalliulin, R. Z.; Klunzinger, P.; Aaron, M.; Lee, M. S.; Liang, W.; Lotan, I.; Nair, N.; Peters, B.; Proynov, E. I.; Pieniazek, P. A.; Rhee, M.; Ritchie, J.; Sherrill, C. D.; Simmonett, A. C.; Subotnik, J. E.; Lee, H.; Iii, W.; Zhang, W.; Bell, A. T.; Chakraborty, A. K.; Daniel, M.; Keil, F. J.; Warshel, A.; Hehre, W. J.; Schaefer, H. F.; Kong, J.; Krylov, A. I.; Gill, M. W.; Head-Gordon, M. *Phys. Chem. Chem. Phys.* **2006**, *8*, 3172–3191.
- (236) Vecera, M. *Detection And Identification Of Organic Compounds*, 1st edition; Springer: New York, 1971. p46
- (237) Bonsignore, P. V; Hurwitz, M. D. *J. Org. Chem.* **1978**, *28*, 3535–3537.
- (238) Nolan, S. P. *Acc. Chem. Res.* **2011**, *44*, 91–100.
- (239) Díez-González, S.; Nolan, S. P. *Coord. Chem. Rev.* **2007**, *251*, 874–883.
- (240) Marion, N.; Nolan, S. P. *Chem. Soc. Rev.* **2008**, *37*, 1776–1782.
- (241) Dorta, R.; Stevens, E. D.; Scott, N. M.; Costabile, C.; Cavallo, L.; Hoff, C. D.; Nolan, S. P. *J. Am. Chem. Soc.* **2005**, *127*, 2485–2495.
- (242) Marion, N.; Gealageas, R.; Nolan, S. P. *Org. Lett.* **2007**, *9*, 2653–2656.
- (243) Gatling, S. C.; Jackson, J. E. *J. Am. Chem. Soc.* **1999**, *121*, 8655–8656.
- (244) Marincean, S.; Fritz, M.; Scamp, R.; Jackson, J. E. *J. Phys. Org. Chem.* **2012**, *25*, 1186–1192.
- (245) Seyden-Penne, J. *Reductions by the Alumino- and Borohydrides in Organic Synthesis*, 2nd edition; Wiley: Pittsburgh, 1997. p128
- (246) Umino, N.; Iwakuma, T.; Itoh, N. *Tetrahedron Lett.* **1976**, *17*, 2875–2876.
- (247) Kobayashi, Y.; Kumar, G. B.; Kurachi, T.; Acharya, H. P.; Yamazaki, T.; Kitazume, T. *J. Org. Chem.* **2001**, *66*, 2011–2018.
- (248) Cornforth, F. J.; Drucker, G. E.; Margolin, Z.; McCallum, R. J.; McCollum, G. J.; Vanier, N. R. *J. Am. Chem. Soc.* **1975**, *97*, 7006–7014.
- (249) Ohlinger, W. S.; Klunzinger, P. E.; Deppmeier, B. J.; Hehre, W. J. *J. Phys. Chem. A* **2009**, *113*, 2165–2175.
- (250) Robles-Machin, R.; Adrio, J.; Carretero, J. C. *J. Org. Chem.* **2006**, *71*, 5023–5026.
- (251) Collins, K. D.; Glorius, F. *Nat. Chem.* **2013**, *5*, 597–601.
- (252) Anslyn, E. V; Dougherty, D. A. *Modern Physical Organic Chemistry*, 1st edition; University Science Books: Sausalito, 2005. p232
- (253) Hornback, J. M. *Organic Chemistry*, 2nd edition; Thomson Learning: Belmont, 2006. p67
- (254) Seyden-Penne, J. *Reductions by the Alumino-and Borohydrides in Organic Synthesis*, 2nd edition; Wiley: New York, 1997. p101
- (255) Wigfield, D. C.; Phelps, D. J. *J. Org. Chem.* **1976**, *41*, 2396–2401.
- (256) Wigfield, D. C. *Tetrahedron* **1976**, *35*, 449–462.
- (257) Talhi, O.; Abdeldjebar, H.; Belmiloud, Y.; Hassaine, R.; Taibi, N.; Válega, M.; Paz, F. A. A.; Brahimi, M.; Bachari, K.; Silva, A. M. S. *New J. Chem.* **2017**, *41*, 10790–10798.

- (258) Teles, J. H.; Brode, S.; Chabanas, M. *Angew. Chemie - Int. Ed.* **1998**, *37*, 1415–1418.
- (259) Abadie, M. A.; Trivelli, X.; Medina, F.; Duhal, N.; Kouach, M.; Linden, B.; Génin, E.; Vandewalle, M.; Capet, F.; Roussel, P.; Del Rosal, I.; Maron, L.; Agbossou-Niedercorn, F.; Michon, C. *Chem. Eur. J.* **2017**, *23*, 10777–10788.
- (260) Kumar, D.; Sharma, P.; Singh, H.; Nepali, K.; Gupta, G. K.; Jain, S. K.; Ntie-Kang, F. *RSC Adv.* **2017**, *7*, 36977–36999.
- (261) Sandler, S. R.; Karo, W. *Polymer Syntheses - Volume I*, 2nd edition.; Academic Press Inc, 1991. p47
- (262) Ripin, D. H. B.; Vetelino, M. *Synlett* **2003**, 2353–2353.
- (263) Lovering, F.; Bikker, J.; Humblet, C. *J. Med. Chem.* **2009**, *52*, 6752–6756.
- (264) Hintermann, L.; Läng, F.; Maire, P.; Togni, A. *Eur. J. Inorg. Chem.* **2006**, 1397–1412.
- (265) Hazari, A.; Gouverneur, V.; Brown, J. M. *Angew. Chemie. Int. Ed.* **2009**, *48*, 1296–1299.
- (266) Pigeon, X.; Bergeron, M.; Barabé, F.; Dubé, P.; Frost, H. N.; Paquin, J. F. *Angew. Chemie. Int. Ed.* **2010**, *49*, 1123–1127.
- (267) Reich, H. J. Fluorine Shifts Overview <https://www.chem.wisc.edu/areas/reich/nmr/11-f-data.htm> (accessed Jan 18, 2018).
- (268) Choi, W. J.; Chung, H.-J.; Chandra, G.; Alexander, V.; Zhao, L. X.; Lee, H. W.; Nayak, A.; Majik, M. S.; Kim, H. O.; Kim, J.-H.; Lee, Y. B.; Ahn, C. H.; Lee, S. K.; Jeong, L. S. *J. Med. Chem.* **2012**, *55*, 4521–4525.
- (269) Zhu, C.; Yang, B.; Bäckvall, J.-E. *J. Am. Chem. Soc.* **2015**, *137*, 11868–11871.
- (270) Takagi, Y.; Nakatani, T.; Itoh, T.; Oshiki, T. *Tetrahedron Lett.* **2000**, *41*, 7889–7892.
- (271) DiMartino, G.; Hursthouse, M. B.; Light, M. E.; Percy, J. M.; Spencer, N. S.; Tolley, M. *Org. Biomol. Chem.* **2003**, *1*, 4423–4434.
- (272) Martin, S. F.; Assercq, J. M.; Austin, R. E.; Dantanarayana, A. P.; Fishpaugh, J. R.; Gluchowski, C.; Guinn, D. E.; Hartmann, M.; Tanaka, T.; Wagner, R.; White, J. B. *Tetrahedron* **1995**, *51*, 3455–3482.
- (273) Sheldrick, G. M. *Acta Crystallogr* **2008**, *A64*, 112.
- (274) Altamore, A.; Cascarano, G.; Giacobazzo, C.; Guagliardi, A.; Burla, M. C.; Polidori, G.; Camalli, M. *J. Appl. Cryst.* **1994**, *27*, 435.
- (275) Duhamel, L.; Plaquevent, J. C. *J. Organomet. Chem* **1993**, *448*, 1-3.
- (276) Breen, A. P.; Murphy, J. A. *J. Chem. Soc. Perkin. Trans 1* **1993**, 2979–2990.
- (277) Zhang, J.; Schmalz, H. G. *Angew. Chemie - Int. Ed.* **2006**, *45*, 6704–6707.
- (278) Molander, G. A.; Cameron, K. O. *J. Org. Chem.* **1993**, *58*, 5931–5943.
- (279) Rubottom, G. M.; Kim, C. W. *J. Org. Chem.* **1983**, *48*, 1550–1552.
- (280) Bilodeau, M. T.; Egbertson, M.; Green, A.; Hartnett, J. C.; Li, Y. Patent application. WO2010US50493 20100928.

- (281) Valeev, R. F.; Bikzhanov, R. F.; Miftakhov, M. S. *Russ. J. Org. Chem.* **2012**, *48*, 304–305.
- (282) Xue, F.; Seto, C. T. *J. Org. Chem.* **2005**, *70*, 8309–8321.
- (283) Matsuyama, H.; Miyazawa, Y.; Takei, Y.; Kobayashi, M. *J. Org. Chem.* **1987**, *52*, 1703–1710.
- (284) Cox, L. R.; Deboos, G. A.; Fullbrook, J. J.; Percy, J. M.; Spencer, N. S.; Tolley, M. *Org. Lett.* **2003**, *5*, 337–339.
- (285) Kobayashi, T.; Kon, Y.; Abe, H.; Ito, H. *Org. Lett.* **2014**, *16*, 6397–6399.
- (286) Fleming, I.; Kemp-Jones, A. V.; Long, W. E.; Thomas, E. J. *J. Chem. Soc. Perkin. Trans 2* **1976**, 7-14.
- (287) Warner, M. C.; Bäckvall, J. E. *European J. Org. Chem.* **2015**, 2388–2393.
- (288) Harrison, T. J.; Kozak, J. A.; Corbella-Pané, M.; Dake, G. R. *J. Org. Chem.* **2006**, *71*, 4525–4529.
- (289) Fadeeva, V. P.; Tikhova, V. D.; Nikulicheva, O. N. *J. Anal. Chem* **2008**, *63*, 1094–1106.